



universität
wien

DISSERTATION

Titel der Dissertation

„Development of novel precursors and reference compounds for PET based investigations targeting the norepinephrine transporter and monoamine oxidase B“

Verfasserin

Mag. pharm. Catharina Neudorfer

angestrebter akademischer Grad

Doktorin der Naturwissenschaften (Dr. rer. nat)

Wien, 2014

Studienkennzahl lt. Studienblatt: A 791 449

Dissertationsgebiet lt. Studienblatt: Pharmazie

Betreuer: ao. Univ.-Prof. Mag. Dr. Helmut Spreitzer

Gewidmet meinen Großvätern

Dipl.-Ing. Josef Neudorfer und

Dipl.-Ing. Herbert Polzer

Vorwort und Danksagung

Die vorliegende Arbeit wurde an der Division of Drug Synthesis/Department of Pharmaceutical Sciences der Universität Wien in Kooperation mit dem Department für Nuklearmedizin der Medizinischen Universität Wien im Zeitraum von Mai 2011 bis November 2014 durchgeführt.

Zunächst möchte ich mich von ganzem Herzen bei ao. Univ.-Prof. Mag. Dr. Helmut Spreitzer bedanken. Neben der ausgezeichneten Betreuung, gestand er mir ausreichend Freiraum beim Arbeiten zu und trug so zur Schaffung einer angenehmen Arbeitsatmosphäre bei. Zudem konnte ich durch seine Unterstützung (nicht nur) in den letzten beiden Jahren meiner Tätigkeit finanziert werden und erhielt auch die Möglichkeit, mein Zweitstudium nebenbei erfolgreich fortzuführen.

Weiterer Dank gebührt meinen KooperationskollegInnen an der Medizinischen Universität Wien, allen voran assoc. Prof. Priv.-Doz. Mag. Dr. Wolfgang Wadsak* und assoc. Prof. Priv.-Doz. Mag. Dr. Markus Mitterhauser* für ihre Unterstützung, sowie für die Bereitstellung des Themas dieser Dissertation, die damit verbundenen Herausforderungen und wissenschaftliche Inspiration. Ebenso bedanke ich mich bei Mag. Dr. Lukas Nics, Christina Rami-Mark, MSc., und Chrysoula Vraka, MSc. für ihre fachliche Hilfe und Zusammenarbeit.

Für die Möglichkeit der Durchführung von Docking-Experimenten und die Unterstützung während dieser Zeit bedanke ich mich herzlich bei Univ.-Prof. Mag. Dr. Gerhard Ecker und im Speziellen bei Mag. Andreas Jurik und Amir Seddik, MSc. für die freundschaftliche und äußerst lehrreiche Kooperation.

Ebenso zu großem Dank verpflichtet bin ich ao. Univ.-Prof. Dipl.-Ing. Dr. Wolfgang Holzer für die Aufnahme und Interpretation unzähliger NMR-Spektren sowie Univ.-Prof. Mag. Dr. Norbert Haider für seine stete Hilfsbereitschaft (nicht nur) bei sämtlichen EDV-Problemen; des Weiteren Mag. Dr. Leopold Jirovetz, Ing. Peter Unteregger, und Ing. Sandra Auernigg-Haselmaier für die Aufnahme der (hochauflösenden) Massenspektren.

Für die notwendige Abwechslung im Labor danke ich besonders Mag. Corinna Nagelreiter und Mag. Veronika Schreiber, sowie Mag. Anna Pöschl, die in jeder Situation eine wichtige Stütze waren. Ebenso danke ich meinen ArbeitskollegInnen MMag. Dr. Eva Schirmer, Dr. Theerchart Leepasert, Mag. Dr. Birgit Bornatowicz, Mag. Markus Tarnai, Laura Castoldi, MBA, MSc., Ashenafi Mamuye, MSc., Niclas Filipp, Amila Becirovic, Mag. Cornelia Joksch, und Silvia Podlipnig für die kooperative und freundschaftliche Zusammenarbeit im Labor.

Der größte Dank jedoch geht an meine Familie, die mich nicht nur in jeder Lebenslage unterstützt und mir Rückhalt gegeben hat sondern immer für mich da war und an mich geglaubt hat: Judith Neudorfer, Dipl.-Ing. Wolfgang Neudorfer, Clemens, Carolina, Christoph, und meine Omas Leopoldine Polzer und Margareta Neudorfer, sowie an meinen Freund Mag. Dr. Karem Shanab,* der mich stets motiviert und (in meiner Arbeit) bestärkt hat und mir auch in den schwierigen Phasen ausnahmslos beistand.

*Besonderer Dank für das Korrekturlesen

TABLE OF CONTENTS

Abstract

Zusammenfassung

1	INTRODUCTION.....	21
1.1	Monoamine Oxidase B	21
1.1.1	General Background.....	21
1.1.1.1	Biochemical basis.....	22
1.1.1.2	Physiological and Pathophysiological basis	23
1.1.2	Relevance	24
1.1.3	Preceding Investigations	26
1.2	Norepinephrine and the Norepinephrine Transporter	30
1.2.1	General Background and Biochemical Basis	30
1.2.1.1	The Norepinephrine Transporter	30
1.2.1.2	Norepinephrine.....	31
1.2.2	Physiological and Pathophysiological Basis	32
1.2.2.1	Attention Deficit Hyperactivity Disorder	33
1.2.2.2	Cocaine Dependence	35
1.2.2.3	Activation of Brown Adipose Tissue	37
1.2.3	Relevance	41
1.2.4	Preceding Investigations	43
1.2.4.1	Fluorine substituted 1-(3-(methylamino)-1-phenylpropyl)-3-phenyl-1,3-dihydro-2H- benzimidazol-2-one (FAPPI) derivatives	43
1.2.4.2	Substituted 1-((3S,4S)-4-phenoxy-3,4-dihydro-1H-isochromen-3-yl)methanamine (PHOXI) derivatives	45
1.3	Positron Emission Tomography	49
1.3.1	General Background.....	49
1.3.2	Physical Principles of PET Imaging and Data Acquisition	50
1.3.3	Radiopharmaceuticals	54
1.3.3.1	Prerequisites for PET Imaging Probes.....	56
1.3.3.2	Short Introduction to the Preparation of Radionuclides.....	58
1.3.3.3	Radiolabeling with ¹¹ C and ¹⁸ F.....	62
1.3.3.3.1	¹¹ C-Methylation Reactions.....	63

1.3.3.3.2	¹⁸ F Radiolabeling Reactions	64
1.3.4	Recent Advances in the Field of PET Technology	67
2	DISCUSSION	71
2.1	Aim	71
2.2	Reversible MAO-B Inhibitors	74
2.2.1	Preceding Syntheses.....	74
2.2.1.1	Preparation attempt of 5-(anthracen-9-yl)-3-phenyl-4,5-dihydro-1H-pyrazole (57)	74
2.2.1.2	Preparation attempt of 4-((2E)-3-(anthracen-9-yl)prop-2-enoyl)benzoic acid (59) and 5-((2E)-3-(anthracen-9-yl)prop-2-enoyl)thiophene-2-carboxylic acid (60)	77
2.2.1.3	Preparation attempt of methyl 4-(5-(anthracen-9-yl)-4,5-dihydro-1H-pyrazol-3-yl)benzoate (27) and methyl 5-(5-(anthracen-9-yl)-4,5-dihydro-1H-pyrazol-3-yl)thiophene-2-carboxylate (31).....	79
2.2.2	Docking Studies	83
2.2.3	Syntheses.....	87
2.2.3.1	Preparation of 1-(5-(anthracen-9-yl)-3-phenyl-4,5-dihydro-1H-pyrazol-1-yl)ethanone (68)	87
2.2.3.2	Preparation of methyl 4-(1-acetyl-5-(anthracen-9-yl)-4,5-dihydro-1H-pyrazol-3-yl)benzoate (1).....	88
2.2.3.3	Preparation of 4-(1-acetyl-5-(anthracen-9-yl)-4,5-dihydro-1H-pyrazol-3-yl)benzoic acid (2) and 2-fluoroethyl-4-(1-acetyl-5-(anthracen-9-yl)-4,5-dihydro-1H-pyrazol-3-yl)-benzoate (3) ..	92
2.2.3.4	Preparation attempt of 2-(2-(((4-methylphenyl)sulfonyl)oxy)ethoxy)ethyl 4-(1-acetyl-5-(anthracen-9-yl)-4,5-dihydro-1H-pyrazol-3-yl)benzoate (72) and 2-(2-((methylsulfonyl)oxy)ethoxy)ethyl 4-(1-acetyl-5-(anthracen-9-yl)-4,5-dihydro-1H-pyrazol-3-yl)benzoate (73)	93
2.2.3.5	Preparation of thiophene based derivatives (methyl ester 4, ethyl ester 79, carboxylic acid 5, fluoroethyl ester 6) and furan based derivatives (methyl ester 7, carboxylic acid 8, fluoroethyl ester 9)	96
2.2.3.6	Preparation attempt of methyl 4-((2E)-3-(anthracen-9-yl)prop-2-enoyl)-1H-pyrrole-2-carboxylate (85), methyl 4-((2E)-3-(anthracen-9-yl)prop-2-enoyl)-1-(phenylsulfonyl)-1H-pyrrole-2-carboxylate (86), and methyl 4-((2E)-3-(anthracen-9-yl)prop-2-enoyl)-1-methyl-1H-pyrrole-2-carboxylate (87)	100
2.2.3.7	Preparation of pyrazine based derivatives (methyl ester 10, carboxylic acid 11), preparation attempt of 2-fluoroethyl 3-(1-acetyl-5-(anthracen-9-yl)-4,5-dihydro-1H-pyrazol-3-yl)pyrazine-2-carboxylate (65).....	102
2.2.3.8	Preparation of pyridine based derivatives (methyl ester 12, carboxylic acid 13, fluoroethyl ester 14)	108

2.2.4	Comparison of Approaches and Yields	112
2.2.5	Preclinical testing	114
2.2.5.1	LogP analyses.....	115
2.2.5.2	IAM experiments	117
2.3	NET ligands	120
2.3.1	FAPPI derivatives	120
2.3.1.1	Docking studies	120
2.3.1.2	Syntheses	124
2.3.1.2.1	Preparation of 1-(3-amino-1-(4-fluorophenyl)propyl)-3-phenyl-1,3-dihydro-2H-benzimidazol-2-one (APPI:1) (109) and 1-(1-(4-fluorophenyl)-3-(methylamino)propyl)-3-phenyl-1,3-dihydro-2H-benzimidazol-2-one (FAPPI:1) (15)	124
2.3.1.2.2	Preparation of 1-(4-fluorophenyl)-3-(3-(methylamino)-1-phenylpropyl)-1,3-dihydro-2H-benzimidazol-2-one (FAPPI:2) (16) and 1-(2-fluorophenyl)-3-(3-(methylamino)-1-phenylpropyl)-1,3-dihydro-2H-benzimidazol-2-one (FAPPI:3) (17).....	126
2.3.1.3	Preclinical testing	129
2.3.1.3.1	LogP analyses.....	129
2.3.1.3.2	IAM experiments	130
2.3.2	PHOXI derivatives.....	132
2.3.2.1	Syntheses	132
2.3.2.1.1	Preparation of <i>N,N</i> -dimethyl-1-(((3 <i>S</i> ,4 <i>S</i>)-4-(2-methylphenoxy)-3,4-dihydro-1 <i>H</i> -isochromen-3-yl)methanamine (Me@PHOXI1) (18) and <i>N</i> -methyl-1-(((3 <i>S</i> ,4 <i>S</i>)-4-(2-methylphenoxy)-3,4-dihydro-1 <i>H</i> -isochromen-3-yl)methanamine (PHOXI:1) (19).....	132
2.3.2.1.2	Preparation attempt of 1-(((3 <i>S</i> ,4 <i>S</i>)-4-(2-methylphenoxy)-3,4-dihydro-1 <i>H</i> -isochromen-3-yl)methanamine (131)	134
2.3.2.1.3	Preparation of 2-fluoro- <i>N</i> -methyl- <i>N</i> -(((3 <i>S</i> ,4 <i>S</i>)-4-(2-methylphenoxy)-3,4-dihydro-1 <i>H</i> -isochromen-3-yl)methyl)ethanamine (FE@PHOXI1) (20)	136
2.3.2.1.4	Preparation of <i>N,N</i> -dimethyl-1-(((3 <i>S</i> ,4 <i>S</i>)-4-(2-(trifluoromethyl)phenoxy)-3,4-dihydro-1 <i>H</i> -isochromen-3-yl)methanamine (Me@PHOXI2) (21), <i>N</i> -methyl-1-(((3 <i>S</i> ,4 <i>S</i>)-4-(2-(trifluoromethyl)phenoxy)-3,4-dihydro-1 <i>H</i> -isochromen-3-yl)methanamine (PHOXI:2) (22) and 2-fluoro- <i>N</i> -methyl- <i>N</i> -(((3 <i>S</i> ,4 <i>S</i>)-4-(2-(trifluoromethyl)phenoxy)-3,4-dihydro-1 <i>H</i> -isochromen-3-yl)methyl)ethanamine (FE@PHOXI2) (23)	137
2.3.2.2	Preclinical testing	139
2.3.2.2.1	LogP analyses.....	139
2.3.2.2.2	IAM experiments	140
2.4	Summary and Future Perspective.....	142

3	EXPERIMENTAL	147
3.1	General.....	147
3.2	Docking Parameters	149
3.2.1	MAO-B derivatives	149
3.2.2	APPI derivatives	149
3.3	NMR Spectroscopic Investigations	150
3.4	Syntheses.....	151
3.4.1	MAO-B derivatives	151
3.4.1.1	Preparation of benzene based derivatives	151
3.4.1.1.1	(2 <i>E</i>)-3-(Anthracen-9-yl)-1-phenylprop-2-en-1-one (56)	151
3.4.1.1.2	<i>Tert</i> -butyl 5-(anthracen-9-yl)-3-phenyl-4,5-dihydro-1 <i>H</i> -pyrazole-1-carboxylate (58).....	153
3.4.1.1.3	1-(5-(Anthracen-9-yl)-3-phenyl-4,5-dihydro-1 <i>H</i> -pyrazol-1-yl)ethan-1-one (68)	154
3.4.1.1.4	Methyl 4-((2 <i>E</i>)-3-(anthracen-9-yl)prop-2-enoyl)benzoate (62)	156
3.4.1.1.5	Methyl 4-(1-acetyl-5-(anthracen-9-yl)-4,5-dihydro-1 <i>H</i> -pyrazol-3-yl)benzoate (1).....	157
3.4.1.1.6	4-(1-Acetyl-5-(anthracen-9-yl)-4,5-dihydro-1 <i>H</i> -pyrazol-3-yl)benzoic acid (2)	160
3.4.1.1.7	2-Fluoroethyl-4-(1-acetyl-5-(anthracen-9-yl)-4,5-dihydro-1 <i>H</i> -pyrazol-3-yl) benzoate (3)	162
3.4.1.1.8	2-(2-((<i>Tert</i> -butyl(diphenyl)silyl)oxy)ethoxy)ethanol (69)	164
3.4.1.1.9	2-(2-((<i>Tert</i> -butyl(diphenyl)silyl)oxy)ethoxy)ethyl 4-(1-acetyl-5-(anthracen-9-yl)-4,5- dihydro-1 <i>H</i> -pyrazol-3-yl)benzoate (70)	165
3.4.1.1.10	2-(2-Hydroxyethoxy)ethyl 4-(1-acetyl-5-(anthracen-9-yl)-4,5-dihydro-1 <i>H</i> - pyrazol-3- yl)benzoate (71).....	166
3.4.1.2	Preparation of thiophene based derivatives	168
3.4.1.2.1	Ethyl 5-acetylthiophene-2-carboxylate (74)	168
3.4.1.2.2	Ethyl 5-((2 <i>E</i>)-3-(anthracen-9-yl)prop-2-enoyl)thiophene-2-carboxylate (76)	169
3.4.1.2.3	Ethyl 5-(1-acetyl-5-(anthracen-9-yl)-4,5-dihydro-1 <i>H</i> -pyrazol-3-yl)thiophene-2- carboxylate (78).....	170
3.4.1.2.4	5-(1-Acetyl-5-(anthracen-9-yl)-4,5-dihydro-1 <i>H</i> -pyrazol-3-yl)thiophene-2- carboxylic acid (5).....	172
3.4.1.2.5	Methyl 5-acetylthiophene-2-carboxylate (63)	174
3.4.1.2.6	Methyl 5-((2 <i>E</i>)-3-(anthracen-9-yl)prop-2-enoyl)thiophene-2-carboxylate (64).....	175
3.4.1.2.7	Methyl 5-(1-acetyl-5-(anthracen-9-yl)-4,5-dihydro-1 <i>H</i> -pyrazol-3-yl)thiophene-2- carboxylate 4)	176
3.4.1.2.8	5-(1-Acetyl-5-(anthracen-9-yl)-4,5-dihydro-1 <i>H</i> -pyrazol-3-yl)thiophene-2-carboxylic acid(5) .	178
3.4.1.2.9	2-Fluoroethyl 5-(1-acetyl-5-(anthracen-9-yl)-4,5-dihydro-1 <i>H</i> -pyrazol-3-yl)thiophene-2- carboxylate (6).....	180

3.4.1.3	Preparation of furan based derivatives	182
3.4.1.3.1	Methyl 5-acetylfuran-2-carboxylate (75)	182
3.4.1.3.2	Methyl 5-((2 <i>E</i>)-3-(anthracen-9-yl)prop-2-enoyl)furan-2-carboxylate (77)	183
3.4.1.3.3	Methyl 5-(1-acetyl-5-(anthracen-9-yl)-4,5-dihydro-1 <i>H</i> -pyrazol-3-yl)furan-2-carboxylate (7)	184
3.4.1.3.4	5-(1-Acetyl-5-(anthracen-9-yl)-4,5-dihydro-1 <i>H</i> -pyrazol-3-yl)furan-2-carboxylic acid (8)	186
3.4.1.3.5	2-Fluoroethyl 5-(1-acetyl-5-(anthracen-9-yl)-4,5-dihydro-1 <i>H</i> -pyrazol-3-yl)furan-2-carboxylate (9)	188
3.4.1.4	Preparation of pyrazine based derivatives.....	190
3.4.1.4.1	Methyl pyrazine-2-carboxylate (140).....	190
3.4.1.4.2	Methyl 3-acetylpyrazine-2-carboxylate (88)	191
3.4.1.4.3	Allyl pyrazine-2-carboxylate (93)	192
3.4.1.4.4	Allyl 3-acetylpyrazine-2-carboxylate (94).....	194
3.4.1.4.5	2-Fluoroethyl pyrazine-2-carboxylate (141)	196
3.4.1.4.6	Methyl 3-((2 <i>E</i>)-3-(anthracen-9-yl)prop-2-enoyl)pyrazine-2-carboxylate (89)	198
3.4.1.4.7	Methyl 3-(1-acetyl-5-(anthracen-9-yl)-4,5-dihydro-1 <i>H</i> -pyrazol-3-yl)pyrazine-2-carboxylate (10)	199
3.4.1.4.8	Allyl 3-(1-acetyl-5-(anthracen-9-yl)-4,5-dihydro-1 <i>H</i> -pyrazol-3-yl)pyrazine-2-carboxylate (91).....	201
3.4.1.4.9	3-(1-Acetyl-5-(anthracen-9-yl)-4,5-dihydro-1 <i>H</i> -pyrazol-3-yl)pyrazine-2-carboxylic acid (11)	203
3.4.1.5	Preparation of pyridine based derivatives	205
3.4.1.5.1	Methyl 6-acetylpyridine-2-carboxylate (97)	205
3.4.1.5.2	Allyl 6-acetylpyridine-2-carboxylate (142)	206
3.4.1.5.3	Methyl 6-((2 <i>E</i>)-3-(anthracen-9-yl)prop-2-enoyl)pyridine-2-carboxylate (98).....	207
3.4.1.5.4	Methyl 6-(1-acetyl-5-(anthracen-9-yl)-4,5-dihydro-1 <i>H</i> -pyrazol-3-yl)pyridine-2-carboxylate (12)	208
3.4.1.5.5	Allyl 6-(1-acetyl-5-(anthracen-9-yl)-4,5-dihydro-1 <i>H</i> -pyrazol-3-yl)pyridine-2-carboxylate (99).....	210
3.4.1.5.6	6-(1-Acetyl-5-(anthracen-9-yl)-4,5-dihydro-1 <i>H</i> -pyrazol-3-yl)pyridine-2-carboxylic acid (13)	212
3.4.1.5.7	2-Fluoroethyl 6-(1-acetyl-5-(anthracen-9-yl)-4,5-dihydro-1 <i>H</i> -pyrazol-3-yl)pyridine-2-carboxylate (14)	214
3.4.1.6	Preparation of pyrrole derived compounds.....	216
3.4.1.6.1	1-(4-Acetyl-1 <i>H</i> -pyrrol-2-yl)-2,2,2-trichloroethanone (80).....	216
3.4.1.6.2	4-Acetyl-1 <i>H</i> -pyrrole-2-carboxylic acid (81)	217
3.4.1.6.3	Methyl 4-acetyl-1 <i>H</i> -pyrrole-2-carboxylate (82)	218
3.4.1.6.4	Methyl 4-acetyl-1-(phenylsulfonyl)-1 <i>H</i> -pyrrole-2-carboxylate (83)	219

3.4.1.6.5	Methyl 4-acetyl-1-methyl-1 <i>H</i> -pyrrole-2-carboxylate (84)	220
3.4.2	FAPPI derivatives	221
3.4.2.1	Preparation of 1-(3-Amino-1-(4-fluorophenyl)propyl)-3-phenyl-1,3-dihydro-2 <i>H</i> -benzimidazol-2-one (APPI:1) (109) and 1-(1-(4-Fluorophenyl)-3-(methylamino)propyl)-3-phenyl-1,3-dihydro-2 <i>H</i> -benzimidazol-2-one (FAPPI:1) (15)	221
3.4.2.1.1	3-Chloro-1-(4-fluorophenyl)propan-1-ol (103).....	221
3.4.2.1.2	1-(1-Bromo-3-chloropropyl)-4-fluorobenzene (104)	222
3.4.2.1.3	1-Phenyl-1,3-dihydro-2 <i>H</i> -benzimidazol-2-one (106)	223
3.4.2.1.4	1-(3-Chloro-1-(4-fluorophenyl)propyl)-3-phenyl-1,3-dihydro-2 <i>H</i> -benzimidazol-2-one (107)..	224
3.4.2.1.5	1-(1-(4-Fluorophenyl)-3-iodopropyl)-3-phenyl-1,3-dihydro-2 <i>H</i> -benzimidazol-2-one (108)	226
3.4.2.1.6	1-(3-Amino-1-(4-fluorophenyl)propyl)-3-phenyl-1,3-dihydro-2 <i>H</i> -benzimidazol-2-one (APPI:1) (109)	227
3.4.2.1.7	1-(1-(4-Fluorophenyl)-3-(methylamino)propyl)-3-phenyl-1,3-dihydro-2 <i>H</i> -benzimidazol-2-one (FAPPI:1) (15).....	229
3.4.2.2	Preparation of 1-(4-Fluorophenyl)-3-(3-(methylamino)-1-phenylpropyl)-1,3-dihydro-2 <i>H</i> -benzimidazol-2-one (FAPPI:2) (16).....	231
3.4.2.2.1	3-Chloro-1-phenylpropan-1-ol (111)	231
3.4.2.2.2	(1-Bromo-3-chloropropyl)benzene (112).....	232
3.4.2.2.3	<i>N</i> -(4-Fluorophenyl)-2-nitroaniline (116)	233
3.4.2.2.4	<i>N</i> -(4-Fluorophenyl)benzene-1,2-diamine (118)	235
3.4.2.2.5	1-(4-Fluorophenyl)-1,3-dihydro-2 <i>H</i> -benzimidazol-2-one (120).....	236
3.4.2.2.6	1-(3-Chloro-1-phenylpropyl)-3-(4-fluorophenyl)-1,3-dihydro-2 <i>H</i> -benzimidazol-2-one (122)..	238
3.4.2.2.7	1-(4-Fluorophenyl)-3-(3-iodo-1-phenylpropyl)-1,3-dihydro-2 <i>H</i> -benzimidazol-2-one (124)	240
3.4.2.2.8	1-(4-Fluorophenyl)-3-(3-(methylamino)-1-phenylpropyl)-1,3-dihydro-2 <i>H</i> -benzimidazol-2-one (FAPPI:2) (16)	242
3.4.2.3	Preparation of 1-(2-Fluorophenyl)-3-(3-(methylamino)-1-phenylpropyl)-1,3-dihydro-2 <i>H</i> -benzimidazol-2-one (FAPPI:3) (17).....	244
3.4.2.3.1	2-Fluoro- <i>N</i> -(2-nitrophenyl)aniline (117)	244
3.4.2.3.2	<i>N</i> -(2-Fluorophenyl)benzene-1,2-diamine (119)	246
3.4.2.3.3	1-(2-Fluorophenyl)-1,3-dihydro-2 <i>H</i> -benzimidazol-2-one (121)	246
3.4.2.3.4	1-(3-Chloro-1-phenylpropyl)-3-(2-fluorophenyl)-1,3-dihydro-2 <i>H</i> -benzimidazol-2-one (123) ...	248
3.4.2.3.5	1-(2-Fluorophenyl)-3-(3-iodo-1-phenylpropyl)-1,3-dihydro-2 <i>H</i> -benzimidazol-2-one (125)	250
3.4.2.3.6	1-(2-Fluorophenyl)-3-(3-(methylamino)-1-phenylpropyl)-1,3-dihydro-2 <i>H</i> -benzimidazol-2-one (FAPPI:3) (17).....	252
3.4.3	PHOXI derivatives	254

3.4.3.1	Preparation of the core structure.....	254
3.4.3.1.1	3-((Dimethylamino)methyl)-1 <i>H</i> -isochromen-4(3 <i>H</i>)-one (128)	254
3.4.3.1.2	3-((Dimethylamino)methyl)-3,4-dihydro-1 <i>H</i> -isochromen-4-ol (129).....	255
3.4.3.1.3	3-(Hydroxymethyl)-1 <i>H</i> -isochromen-4(3 <i>H</i>)-one (134).....	256
3.4.3.1.4	(4-Oxo-3,4-dihydro-1 <i>H</i> -isochromen-3-yl)methyl trifluoromethanesulfonate (135)	257
3.4.3.2	Preparation of PHOXI:1 derivatives.....	258
3.4.3.2.1	1-(3 <i>S</i> ,4 <i>S</i>)-4-(2-Bromophenoxy)-3,4-dihydro-1 <i>H</i> -isochromen-3-yl)- <i>N,N</i> - dimethylmethanamine (130)	258
3.4.3.2.2	<i>N,N</i> -Dimethyl-1-((3 <i>S</i> ,4 <i>S</i>)-4-(2-methylphenoxy)-3,4-dihydro-1 <i>H</i> -isochromen-3-yl) methanamine (Me@PHOXI1) (18).....	260
3.4.3.2.3	<i>N</i> -Methyl-1-((3 <i>S</i> ,4 <i>S</i>)-4-(2-methylphenoxy)-3,4-dihydro-1 <i>H</i> -isochromen-3-yl)methanamine (PHOXI:1) (19).....	262
3.4.3.2.4	2-Fluoro- <i>N</i> -methyl- <i>N</i> -(((3 <i>S</i> ,4 <i>S</i>)-4-(2-methylphenoxy)-3,4-dihydro-1 <i>H</i> -isochromen-3- yl)methyl)ethanamine (FE@PHOXI1) (20).....	264
3.4.3.3	Preparation of PHOXI:2 derivatives.....	266
3.4.3.3.1	<i>N,N</i> -Dimethyl-1-((3 <i>S</i> ,4 <i>S</i>)-4-(2-(trifluoromethyl)phenoxy)-3,4-dihydro-1 <i>H</i> -isochromen-3- yl)methanamine (Me@PHOXI2) (21)	266
3.4.3.3.2	<i>N</i> -Methyl-1-((3 <i>S</i> ,4 <i>S</i>)-4-(2-(trifluoromethyl)phenoxy)-3,4-dihydro-1 <i>H</i> -isochromen-3-yl) methanamine (PHOXI:2) (22)	268
3.4.3.3.3	2-Fluoro- <i>N</i> -methyl- <i>N</i> -(((3 <i>S</i> ,4 <i>S</i>)-4-(2-(trifluoromethyl)phenoxy)-3,4-dihydro-1 <i>H</i> - isochromen-3-yl)methyl)ethanamine (FE@PHOXI2) (23)	270
3.5	Preclinical Evaluation	272
3.5.1	LogP analysis	272
3.5.2	IAM chromatography.....	272
4	REFERENCES	275
5	ANNEX	301
5.1	List of Abbreviations	203
5.2	Abbreviations of FAPPI and PHOXI derivatives.....	307
5.3	Spectra.....	309
5.4	Publications.....	513
5.4.1	MAO-B.....	515
5.4.2	NET.....	523
5.5	Curriculum vitae.....	543

INDEX OF TABLES AND FIGURES

Figure 1:	Overall three-dimensional structure of human MAO-B monomeric unit.....	22
Figure 2:	Oxidative deamination of primary amines.....	23
Figure 3:	Chemical structure of L-Deprenyl and ¹¹ C radiolabeled L-Deprenyl.....	25
Figure 4:	Chemical structure of 5-(anthracen-9-yl)-3-phenyl-4,5-dihydro-1H-pyrazoles.....	27
Figure 5:	Pyrazoline derivatives docked in the MAO-B active site.....	27
Figure 6:	Topology of the norepinephrine transporter, embedded in the cytoplasmic membrane.....	31
Figure 7:	Diagram of the noradrenergic system.....	32
Figure 8:	BAT location in adults and infants.....	38
Figure 9:	BAT activation mechanism.....	39
Figure 10:	Overlay of crystal structures of (S,S) reboxetine 47, derivative 48, and compound 52.....	48
Figure 11:	Annihilation event.....	51
Figure 12:	PET-procedure.....	52
Figure 13:	PET image, MR image, PET and MR image overlay.....	54
Figure 14:	Chemical structure of reference compounds 66 and 67.....	83
Figure 15:	MAO-B binding pocket in complex with reference compounds 66 and 67 and exemplary docking poses of methyl and fluoroethyl ester derivatives.....	84
Figure 16:	Benzene based reference compounds (1, 3, and 10) and electron-deficient reference compounds (12 and 14) docked in the MAO-B active site.....	85
Figure 17:	Docking poses of electron-rich reference compounds (4, 6, 7, and 9).....	86
Figure 18:	Diagram of direct yield comparison for cyclization methods 1, 2, 5, and 6 for the preparation of compound 1.....	91
Figure 19:	Atom numbering, important HMBC correlations and NOEs of compound 4.....	99
Figure 20:	¹⁹ F-NMR spectra of compound 14.....	111
Figure 21:	Overview of the reactions and corresponding yields of MAO-B binding compounds.....	112
Figure 22:	Chemical structure of nortriptyline and ring numbering of FAPPI:1-3 (15-17).....	121
Figure 23:	Overlay of compounds 44, 45, and 15-17 in binding hypothesis 1.....	122
Figure 24:	Overlay of compounds 44, 45, and 15-17 in binding hypothesis 2 (NET).....	123
Figure 25:	Overlay of compounds 44, 45, and 15-17 in binding hypothesis 2 (SERT, DAT).....	124
Figure 26:	Illustration of the NOE of <i>cis</i> isomer 130 and its <i>trans</i> counterpart.....	133
Table 1:	Important PET radionuclides for clinical application.....	59
Table 2:	Calculated logP values of the envisaged acetyl derived pyrazoline methyl esters.....	82

Table 3:	Molecular weight, yield, melting point and calculated K_i value of methyl esters (1, 4, 7, 10, and 12) and fluoroethyl esters (3, 6, 9, and 14) as well as reference compounds (66 and 67).....	87
Table 4:	Calculated and experimental logP values of methyl ester derived references 1, 4, 7, 10, and 12.....	115
Table 5:	Calculated and experimental logP values of fluoroethyl ester derived references 3, 6, 9, and 14.....	116
Table 6:	Calculated and experimental logP values of precursors 2, 5, 8, 11, and 13.....	116
Table 7:	Membrane partition coefficient (K_m), permeability (P_m) and variation coefficient of methyl ester derived references 1, 4, 7, 10, and 12.....	117
Table 8:	Membrane partition coefficient (K_m), permeability (P_m) and variation coefficient of fluoroethyl ester derived references 3, 6, 9, and 14.....	118
Table 9:	Membrane partition coefficient (K_m), permeability (P_m) and variation coefficient of precursors 2, 5, 8, 11, and 13.....	118
Table 10:	Sequence alignment of all distinct monoamine transporter residues located in sub sites.....	122
Table 11:	Calculated and experimental logP values of FAPPI derivatives 15-17.....	129
Table 12:	Membrane partition coefficient (K_m), permeability (P_m) and variation coefficient of FAPPI derivatives 15-17.....	130
Table 13:	Calculated and experimental logP values of PHOXI derivatives 18-23.....	139
Table 14:	Membrane partition coefficient (K_m), permeability (P_m) and variation coefficient of PHOXI derivatives 18-23.....	140

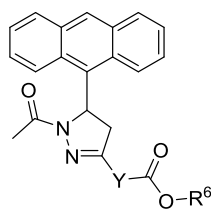
ABSTRACT

Based on the fact that the monoamine oxidase B and the norepinephrine transporter are involved in a variety of diseases, such as Alzheimer's disease, Parkinson's disease, or attention deficit hyperactivity disorder, the investigation of their underlying dysregulation mechanisms is of major interest.

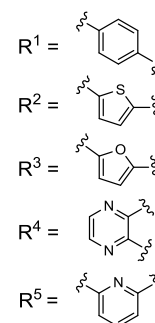
The aim of this thesis was the computational evaluation, the development of reliable syntheses and the spectroscopic characterization as well as first preclinical experiments of suitable precursors and reference compounds for the MAO-B- and NET system. These compounds serve for the development of adequate PET radiotracers, since positron emission tomography represents the most suitable and accurate technique today to gain information about enzyme/transporter abundance and density *in vivo*.

MAO-B precursors and references

- 1 Y = R¹, R⁶ = CH₃
- 2 Y = R¹, R⁶ = H
- 3 Y = R¹, R⁶ = CH₂CH₂F
- 4 Y = R², R⁶ = CH₃
- 5 Y = R², R⁶ = H
- 6 Y = R², R⁶ = CH₂CH₂F
- 7 Y = R³, R⁶ = CH₃

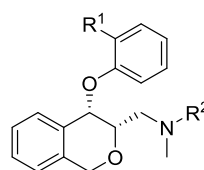
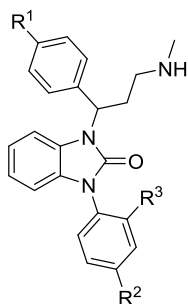


- 8 Y = R³, R⁶ = H
- 9 Y = R³, R⁶ = CH₂CH₂F
- 10 Y = R⁴, R⁶ = CH₃
- 11 Y = R⁴, R⁶ = H
- 12 Y = R⁵, R⁶ = CH₃
- 13 Y = R⁵, R⁶ = H
- 14 Y = R⁵, R⁶ = CH₂CH₂F



NET Precursoren und Referenzen

- 15 R¹ = F, R² = H, R³ = H
- 16 R¹ = H, R² = F, R³ = H
- 17 R¹ = H, R² = H, R³ = F



- 18 R¹ = CH₃, R² = CH₃
- 19 R¹ = CH₃, R² = H
- 20 R¹ = CH₃, R² = CH₂CH₂F
- 21 R¹ = CF₃, R² = CH₃
- 22 R¹ = CF₃, R² = H
- 23 R¹ = CF₃, R² = CH₂CH₂F

A total of 16 new reference compounds (1, 3, 4, 6, 7, 9, 10, 12, 14-18, 20, 21, 23) has been synthesized characterized, and evaluated *in silico/in vitro*, which will be tested regarding their affinity and selectivity towards MAO-B or NET at the Medical University of Vienna. The precursors (2, 5, 8, 11, 13, 19, 22) of the most suitable ligands will serve as starting materials for radiolabeling. In continuative studies these tracers will be subjected to biodistribution and micro-PET experiments for the investigation of MAO-B and the NET as well as for the determination of their dysregulation mechanisms in several diseases.

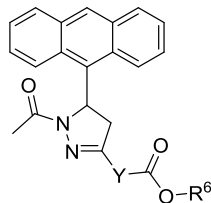
ZUSAMMENFASSUNG

Da sowohl die Monoaminoxidase B als auch der Noradrenalintransporter bei unzähligen Erkrankungen, wie etwa Alzheimer, Parkinson, oder Aufmerksamkeitsdefizitsyndrom, eine wichtige Rolle spielen, ist die Untersuchung ihres zugrundeliegenden Dysregulationsmechanismus von großem Interesse.

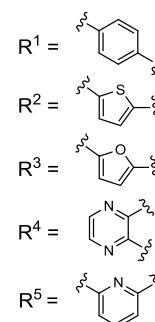
Ziel der vorliegenden Arbeit waren *in silico*-Experimente, die Entwicklung zuverlässiger Synthesewege, die Charakterisierung, und erste präklinische Tests von Precursoren und Referenzsubstanzen für das MAO-B- und NET-System. Diese Verbindungen dienen der Entwicklung von adäquaten PET Tracern, da die Positronen-Emissions-Tomographie heute eines der geeignetsten Verfahren zur Darstellung von Enzym/Transporter-Dichten und physiologischen Vorgängen *in vivo* repräsentiert.

MAO-B precursors and references

- 1 Y = R¹, R⁶ = CH₃
- 2 Y = R¹, R⁶ = H
- 3 Y = R¹, R⁶ = CH₂CH₂F
- 4 Y = R², R⁶ = CH₃
- 5 Y = R², R⁶ = H
- 6 Y = R², R⁶ = CH₂CH₂F
- 7 Y = R³, R⁶ = CH₃

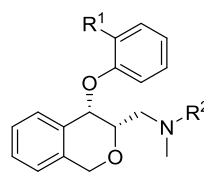
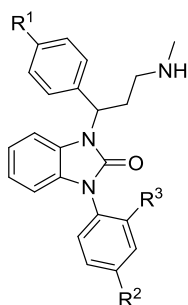


- 8 Y = R³, R⁶ = H
- 9 Y = R³, R⁶ = CH₂CH₂F
- 10 Y = R⁴, R⁶ = CH₃
- 11 Y = R⁴, R⁶ = H
- 12 Y = R⁵, R⁶ = CH₃
- 13 Y = R⁵, R⁶ = H
- 14 Y = R⁵, R⁶ = CH₂CH₂F



NET Precursoren und Referenzen

- 15 R¹ = F, R² = H, R³ = H
- 16 R¹ = H, R² = F, R³ = H
- 17 R¹ = H, R² = H, R³ = F



- 18 R¹ = CH₃, R² = CH₃
- 19 R¹ = CH₃, R² = H
- 20 R¹ = CH₃, R² = CH₂CH₂F
- 21 R¹ = CF₃, R² = CH₃
- 22 R¹ = CF₃, R² = H
- 23 R¹ = CF₃, R² = CH₂CH₂F

Insgesamt wurden 16 neue Referenzverbindungen (1, 3, 4, 6, 7, 9, 10, 12, 14-18, 20, 21, 23) synthetisiert, spektroskopisch analysiert, und *in silico/in vitro* evaluiert, welche in weiterführenden Studien an der Medizinischen Universität Wien hinsichtlich ihrer MAO-B/NET Affinität und Selektivität getestet werden. Die Precursoren (2, 5, 8, 11, 13, 19, 22) der vielversprechendsten Liganden dienen als Ausgangsmaterial für radiochemische Synthesen zur Herstellung von PET-Tracern. In anknüpfenden Biodistributions- und Mikro-PET-Studien sollen die Tracer zukünftig nicht nur Auskunft über MAO-B und NET geben, sondern auch ihre Dysregulationsmechanismen bei unterschiedlichen Erkrankungen aufzeigen.

1 INTRODUCTION

1.1 Monoamine Oxidase B

1.1.1 General Background

Monoamine oxidase (MAO) is an ubiquitous, flavin adenine dinucleotide (FAD) containing enzyme, localized in the outer mitochondrial membrane of cells in the nervous system and peripheral tissue. As it catalyzes the oxidative deamination of dietary amines and monoamine neurotransmitters, MAO is regarded as a key enzyme in the regulation of monoaminergic homeostasis and neurotransmission.^{1,2}

Currently, two distinct enzymatic isoforms of MAO have been characterized, namely MAO-A and MAO-B. Although an amino acid sequence identity of about 70% was detected by cloning the full-length cDNAs encoding for human liver MAO-A and MAO-B,³ the enzymes show diversity in their tissue distribution. In humans, both isoenzymes are described in peripheral tissues and organs. As MAO-A is mostly expressed in placental tissues and fibroblasts, MAO-B is prevalent in lymphocytes and platelets. In the human brain, MAO-A shows high levels in catecholaminergic neurons whilst MAO-B mainly predominates in serotonergic and histaminergic neurons, as well as in astrocytes.⁴

Since MAO-B is implicated in a variety of neurological disorders, such as Alzheimer's disease (AD) and Parkinson's disease (PD),⁵ its three-dimensional structure (figure 1) is of major interest:



Figure 1:⁶ (modified) Overall three-dimensional structure of a human MAO-B monomeric unit in complex with 1,4-diphenyl-2-butene; blue: FAD-binding domain, red: substrate-binding domain, green: C-terminal membrane-binding region, yellow and black ball-and-stick models: FAD cofactor and inhibitor

The enzyme is anchored in the outer mitochondrial membrane through a C-terminal polypeptide segment, which traverses the protein surface and then folds into an α -helix. Two non-polar loops, both located on different positions in the segment, form two hydrophobic areas on the protein's surface and are considered to be involved in membrane binding.⁷ Another significant feature of the MAO-B structure is the presence of two adjacent cavities in the interior of the protein. Both cavities are lined by aromatic and aliphatic residues, which create a highly non-polar environment for substrate binding. The larger cavity is directly located in front of the covalent flavin ring and forms the substrate-binding site. A substrate, entering this cavity though must first bind to an "entrance", the second cavity, which is located near the point, where the protein surface intersects with the surface of the outer mitochondrial membrane.⁸

1.1.1.1 Biochemical basis

By using oxygen as an electron acceptor, both MAO isoenzymes are involved in the oxidative degradation of primary, secondary and (some) tertiary amines to aldehydes via imine intermediates (figure 2). Thereby, the reduced FAD cofactor reacts with oxygen to generate oxidized flavin and hydrogen peroxide,⁹ which can trigger the production of

reactive oxygen species (ROS) and thus induce neuronal apoptosis and mitochondrial damage.⁴

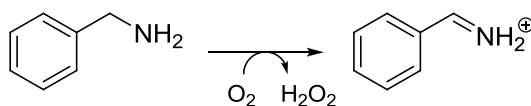


Figure 2: Oxidative deamination of primary amines

MAO-A and MAO-B have been identified on the basis of their substrate preference and inhibitory selectivity. While MAO-A displays higher affinity for indolamines (5-hydroxytryptamine, 5-HT) and catecholamines (norepinephrine, NE), MAO-B preferentially metabolizes trace amines (beta-phenylethylamine, PEA). Dopamine and monoamines like tyramine and tryptamine are degraded by both isoforms.⁴ Selective MAO-A inhibitors, such as moclobemide and clorgyline are proven beneficial for the treatment of neurological disorders, like anxiety and depression. Selective and irreversible MAO-B inhibitors, such as selegiline and rasagiline, on the other hand, are employed in the treatment of AD and PD.¹

1.1.1.2 Physiological and Pathophysiological basis

As a degradation enzyme, MAO-B is involved in a variety of neurological diseases, such as attention deficit hyperactivity disorder (ADHD), Tourette's syndrome, amyotrophic lateral sclerosis (ALS), Huntington's disease and age-related neurological disorders like PD and AD.⁴

AD is one of the most common neurodegenerative disorders, affecting more than 26.6 million people worldwide.¹¹ It is a frequent cause of dementia in the elderly, accompanied by changes in personality and progressive loss of cognition, as well as the fourth leading cause of death after heart disease, cancer and stroke.¹² As a result of the aging population incidence rates are estimated to increase. Thus, according to the United Na-

tions Population Division, the worldwide prevalence is predicted to quadruple to 106.2 million by 2050, meaning 1 in 85 persons worldwide will be living with AD.¹¹

Although the etiology of AD is not yet well established, epidemiological and molecular research suggest that both, environmental (e.g. aluminum) and genetic (e.g. mutations, susceptibility genes) factors eventually lead to deposits of beta amyloid (A β) plaques and neurofibrillary tangles (NFTs).¹³

Recent studies^{14,15} have shown that formation of A β plaques in the brain and accumulation of misfolded proteins go parallel with neuroinflammatory processes, which mostly affect the astrocytes and the microglia. Both are regarded as the main cellular elements of the brain's immune system. As a consequence of increased activation of astrocytes in AD, MAO-B, highly abundant in activated astrocytes, is up-regulated as well, especially in early stages of AD.^{14,16-18} Other studies, however, suggest that increased MAO-B levels may be associated with cholinergic disruption,¹⁹ glucocorticoid elevation²⁰ or enhanced by aluminum ions.²¹ However, alterations in MAO-B activity have been reported in several AD brain areas including the temporal lobe, white matter, frontal lobe, parietal lobe, substantia nigra and hippocampus^{14,16} as well as in platelets of Alzheimer patients.^{22,23} By using the imaging biomarker [¹¹C]-L-deprenyl, significantly higher binding in AD brains, compared to age matched control brains^{14,24} could be shown in the regions mentioned above, especially in the temporal lobe and the white matter and markedly higher binding in the hippocampus and the parietal and frontal lobes.¹⁴

1.1.2 Relevance

Today, the diagnosis of AD is based on the detection of A β plaques and NFTs in postmortem brains and on the application of SPECT (single photon emission computed tomography) and PET (positron emission tomography) tracers for A β imaging.²⁵ However, these cerebral changes seem not specific for AD, as they have also been reported in brains of cognitively unimpaired elderly individuals and in many other

chronic neurodegenerative disorders. Furthermore, the sensitivity of biomarkers, used in SPECT and PET so far, is unsatisfactory and therefore of limited value for monitoring pathological alterations in the human brain.²⁶

Since high MAO-B levels are present even in early stages of AD,^{14,16-18,22,23} the MAO-B system can be designated as an appropriate and prospective tracer target of molecular imaging biomarkers for AD.^{14,23,27,28} Although all studies have shown that MAO-B concentrations are significantly increased in lower Braak grades, compared to age matched control groups, opinions differ whether they stay the same,^{16,23} increase sharply,²⁷ or decrease^{14,22} as the disease progresses. Nevertheless, various research groups around the world (e.g. Hungary,¹⁴ California,¹⁶ Japan,¹⁷ Switzerland,¹⁸ Sweden,¹⁹ Croatia,^{22,23} Austria,²⁷ etc.) study the MAO-B system and its application in PET regarding AD, which clearly demonstrates that there is demand for new, potent and selective tracer molecules.

L-Deprenyl or selegiline (**24**) (figure 3), discovered in the seventies, was first described as a selective and irreversible MAO-B inhibitor, by covalently binding to the enzyme.¹⁴ Since then, it has been successfully employed in the treatment of early PD, 1-methyl-4-phenyl-1,2,3,6-tetrahydropyridine (MPTP)-induced parkinsonism,²⁹ and especially AD, in which it has been shown to protect neuronal cells from the consequences of oxidative stress.²

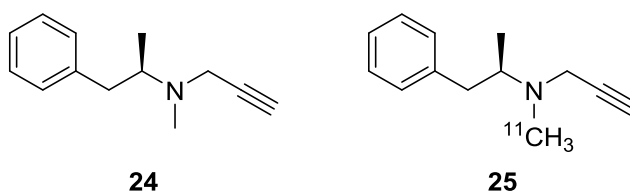


Figure 3: Chemical structure of L-Deprenyl and ¹¹C radiolabeled L-Deprenyl

Soon, the irreversible inhibitor was considered not only to be useful as an adjuvant therapeutic, but also to serve as a potential tracer for the *in vivo* investigation of MAO-B, if labeled with a suitable radionuclide. Thus, L-deprenyl has been labeled with ¹¹C (**25**) (figure 3) and studied in the human brain with PET.³⁰ Although [¹¹C]-L-deprenyl is the

most commonly used PET tracer for MAO-B studies today, its quantification of cerebral binding is rather difficult due to the fast and irreversible binding of this ligand. Therefore, several radioligands have been developed for PET MAO-B activity and density studies in the human brain: [¹¹C]-L-deprenyl and [¹¹C]pargyline are both irreversible inhibitors, whereas [¹¹C]SL25.1188 and [¹¹C]MD-230254 are reversible inhibitors of MAO-B.³¹ Since ¹¹C is a rather short-lived radionuclide (20 minutes), which can only be used in a completely equipped PET center comprising of a cyclotron, radiochemistry, and a PET scanner, ¹⁸F, featuring a half-life of 110 minutes, represents the nuclide of choice for a satellite PET center. However, only a few ¹⁸F radioligands, such as the reversible MAO-B inhibitor [¹⁸F]N-(2-aminoethyl)-5-fluoro-2-pyridinecarboxamide³⁰ and the irreversible MAO-B inhibitors ¹⁸F-FHMP³² and (S)-1-[¹⁸F]fluoro-N-4-dimethyl-N-(prop-2-ynyl)pentan-2-amines³³ have been synthesized so far. While both irreversible MAO-B inhibitors exhibit proper characteristics for a potentially useful PET radiotracer,^{32,33} the former proves to have reduced brain uptake due to high polarity of the compound.³⁰

The results of the above described investigations display the diagnostic efficacy of radiolabeled analogs of L-deprenyl in CNS diseases and especially in AD.¹⁴ As the population ages and incidence rates of AD are predicted to increase within the next 40 years, the demand for suitable molecular imaging biomarkers for the diagnosis of AD seems indispensable.

1.1.3 Preceding Investigations

On the basis of the results of Mishra *et al*,³⁴ 5-(anthracen-9-yl)-3-phenyl-4,5-dihydro-1H-pyrazoles **26** (figure 4) are highly selective and extremely potent reversible MAO-B inhibitors. *In vitro* evaluations suggest that they do not only display a superior affinity towards MAO-B, but also provide a high MAO-B/A selectivity ratio. Additionally, these compounds show superior docking scores (> - 12.5) and predicted K_i values in nanomolar

ranges for human MAO-B, what makes them at least 100 times more potent than the positive control selegiline.

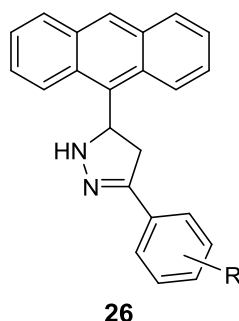


Figure 4: Chemical structure of highly potent, highly selective, and reversible MAO-B binding 5-(anthracen-9-yl)-3-phenyl-4,5-dihydro-1H-pyrazoles

As MAO-A and MAO-B differ in their active site loop conformation, the pyrazoline derivatives display higher affinity towards the compressed, spanned inside the active site, MAO-B loop. They perfectly fit into the large aromatic cavity (figure 5, pocket-1) of the active site loop due to the bulkiness of the anthracene ring and accommodate well the other hydrophobic cavity (figure 5, pocket-2) due to the molecule's benzene ring.³⁴

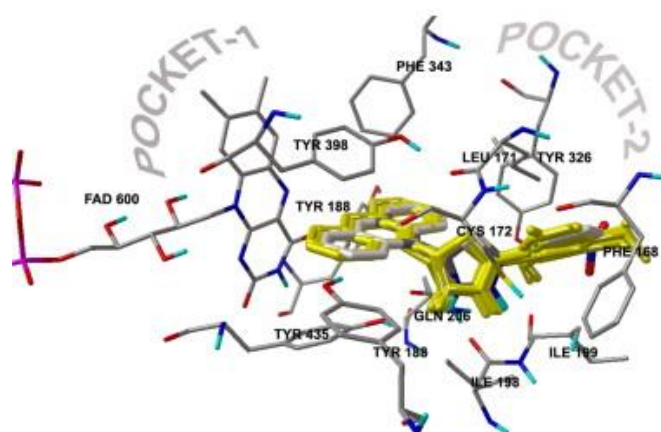


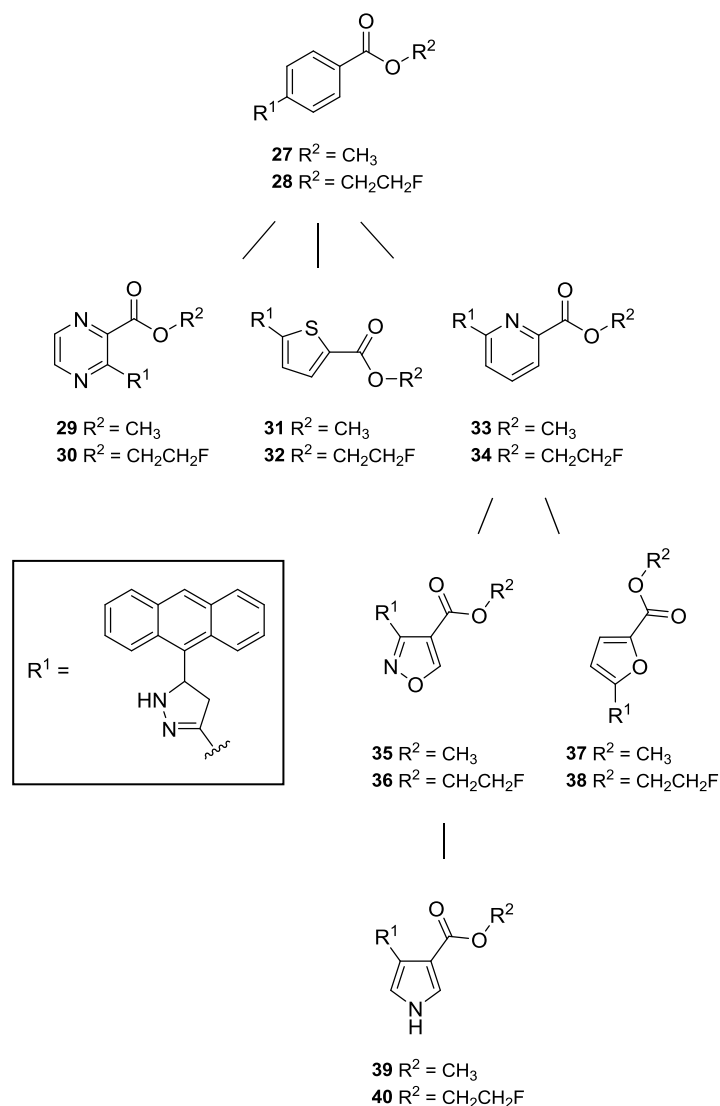
Figure 5:³⁴ Pyrazoline derivatives docked in the MAO-B active site

Since to date, there exist no proper reversible radiolabeled MAO-B inhibitors, as explained above, the present findings according to Gulyás *et al*¹⁴ and Nag *et al*³³ suggest further studies aiming at the development of more potent and preferentially ¹⁸F labeled

molecular imaging biomarkers for human diagnostic PET studies.¹⁴ Given the excellent findings of Mishra *et al*,³⁴ we hypothesized that ¹¹C and ¹⁸F labeled pyrazoline derivatives may serve as high potential and promising molecular imaging biomarkers for the diagnosis of AD, since all unlabeled compounds presented by this research group³⁴ feature excellent characteristics of selective and potent reversible MAO-B inhibitors.³⁴ Therefore, the presented PhD-thesis aimed at the synthesis of a compound library of reversible methyl and fluoroethyl substituted 5-(anthracen-9-yl)-4,5-dihydro-1H-pyrazole derivatives by applying bioisosteric principles to 5-(anthracen-9-yl)-3-phenyl-4,5-dihydro-1H-pyrazoles, which have been proven very potent towards MAO-B.

Bioisosterism is a strategy of medicinal chemistry for rational drug design, applied to a lead compound to modify its biological profil.³⁵ This principle was employed to improve compound properties of pyrazoline derivatives regarding the octanol/water partition coefficient P (logP) value, which should lie below 5 for optimal blood brain barrier (BBB) penetration of the PET tracer without excessive unspecific binding.³⁶ Since 5-(anthracen-9-yl)-3-phenyl-4,5-dihydro-1H-pyrazoles perfectly fit into the large, aromatic cavity of MAO-B due to the bulky anthracene ring, bioisosteric modifications were only conducted on the benzene ring of the molecule.

Hence, according to Lima *et al*,³⁵ modifications on the benzene ring (**27**, **28**), based on classic bioisosterism, can be carried out by substitution of a =CH- group by =N- (**29**, **30** and **33**, **34**) or -S- (**31**, **32**). Based on ring bioisosterism, pyridine (**29**, **30**) can be further replaced by isoxazole (**35**, **36**) or furan (**37**, **38**), respectively and an isoxazole (**35**, **36**) in turn can be substituted by 1H-pyrrole (**39**, **40**) (scheme 1).



Scheme 1: Bioisosteric principles applied to pyrazoline derivatives

Additionally, an ester moiety, which serves as a linker for a stable connection between the core structure and the positron emitting radionuclide, was introduced and placed exactly at the position of the molecule, where bioisosteric changes were performed, always taking into account the logP value ($\log P < 5$).

In the course of the preparation of compounds **27** and **31**, however, instability problems concerning the pyrazoline ring (cf. chapter 2.2.1) have arisen. Thus, the target compounds were modified by inserting an additional acetyl moiety at position 1 of the pyrazoline ring. Not only should this modification lead to stability of the pyrazoline ring,³⁷⁻³⁹ but moreover enhance MAO-B inhibitory activity, as described by several authors for other compounds.³⁸

1.2 Norepinephrine and the Norepinephrine Transporter

1.2.1 General Background and Biochemical Basis

1.2.1.1 The Norepinephrine Transporter

The human norepinephrine or noradrenaline transporter (NET) is a high affinity, substrate specific, sodium/chloride-dependent transporter, which belongs to the family of amino acid, monoamine and GABA transporters.⁴⁰ It is located presynaptically in the plasma membrane of noradrenergic neurons and is regulated by extrinsic signals as well as receptor- and kinase-linked pathways.⁴¹ As a key enzyme, the NET is primarily responsible for the reuptake of synaptically released norepinephrine (NE) into the presynaptic nerve terminals and is also involved in the homeostasis of NE in the nervous system.⁴² By utilizing transmembrane sodium and chloride gradients, the transporter incorporates NE accumulation into presynaptic terminals, where the neurotransmitters are either encased in storage vesicles or degraded biochemically.^{43,44} This electrogenetic process is the primary mechanism by which the biological effects of NE in the synaptic cleft are terminated. It is also regarded as a critical step, since the NET prevents the brain from excessive adrenergic neurotransmission through this process and additionally removes NE from the heart and other peripheral organs.^{45,46} Lee *et al*⁴⁷ were the first who demonstrated that the NET is up- and down-regulated in response to the availability of NE in and around the synaptic cleft. Therefore, it seems reasonable that inadequate levels of NE through changes in the levels of NET lead to a variety of neurological disorders. However, the NET is not only responsible for the reuptake of NE, but also regulates the dopamine (DA) homeostasis in the frontal cortex, whereas DA reuptake in the striatum depends primarily on the dopamine transporter (DAT).⁴⁸

The human NET is a 617 amino acid protein, which shows 66% overall identity in amino acid sequence with the human DAT and 48% identity with the human serotonin

transporter (SERT).⁴⁹ Furthermore, it consists of twelve transmembrane-spanning domains (TMDs) with a large extracellular loop between TMD 3 and 4, and comprises an intracellular NH₂- and COOH-terminus (figure 6).⁵⁰

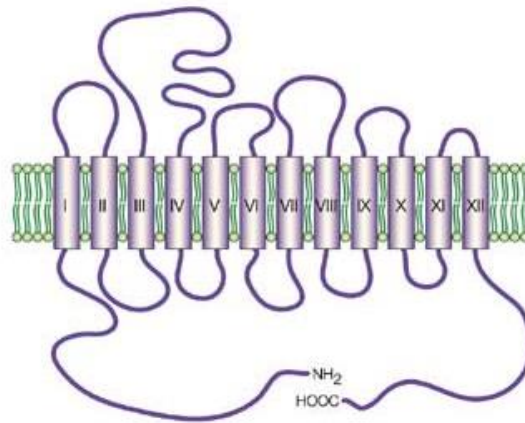


Figure 6:⁵¹ (modified) Topology of the norepinephrine transporter, embedded in the cytoplasmic membrane (green), depicting 12 transmembrane domains (light violet) connected by intracellular and extracellular loops (dark violet).

In the brain, low densities of the NET can be found in the cerebellum, the striatum and the human insular cortex, whilst the immediate region of the locus coeruleus and the dorsal raphe nuclei display NET-rich regions.⁵²⁻⁵⁹

The NET is also an important target for tricyclic antidepressants,⁴¹ various psychostimulants⁶⁰ and drugs of abuse, such as cocaine and amphetamine.⁴⁹ Like antidepressants and psychostimulants, cocaine and amphetamine interact with the NET, thereby elevating extracellular NE concentrations and potentiating the activation of postsynaptic receptors.⁶¹

1.2.1.2 Norepinephrine

NE belongs to the group of catecholamines and is a key neurotransmitter in the central as well as in the peripheral nervous system. It is biosynthesized primarily in the brainstem neurons of the locus coeruleus and subcoeruleus along an enzymatic cascade

that starts from the amino acid tyrosine.^{60,43} Once released into the synaptic cleft, NE acts through four different adrenergic receptors (α_1 , α_2 , β_1 , β_2), and is therefore regarded a crucial neurochemical messenger in the CNS (figure 7). The NET -as described above- is responsible for the reuptake of NE and thus triggers the termination of its action.⁴⁵

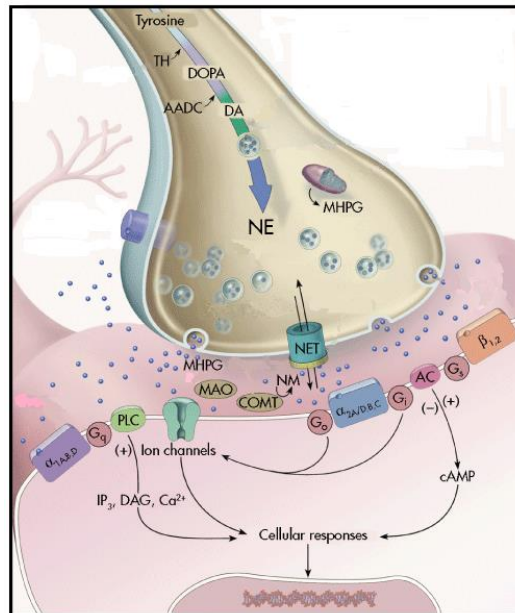


Figure 7:⁶² (modified) Diagram of the noradrenergic system

NE plays a pivotal modulatory role in physiological functions and pathological conditions.⁶¹ It is involved in processes like alertness, arousal, mood regulation, sleep regulation, and expression of behavior and has major influence on the endocrine as well as the autonomic nervous system.⁴⁵ Given the global role of NE in the nervous system, its abnormal regulation may result in various pathological conditions such as neurodegenerative, psychiatric and cardiovascular disorders.⁴²

1.2.2 Physiological and Pathophysiological Basis

Abnormal regulation of the NET or NET dysfunction, respectively, cause either increased or decreased levels of NE in the synaptic cleft. Since NE represents a fundamental neurochemical messenger, its accurate regulation is of major importance. Thus the NET,

responsible for the NE equilibrium in the synaptic cleft, is considered to be involved in a variety of neurological/psychiatric disorders,^{41,42} but also plays a pivotal role in cardiovascular,^{41,42,63} and metabolic diseases.⁶³⁻⁶⁵ Reduced NET levels go along with neurological disorders like major depression,^{49,61} PD, AD,⁴⁵⁻⁵⁶ and cardiovascular diseases such as hypertension, cardiomyopathy, and heart failure.^{51,65} Furthermore, a dysfunction of the NE system was reported in ADHD,^{46,55,66} suicide,^{41,50,67} substance abuse (cocaine dependence),⁵⁴ and schizophrenia.⁴⁷ A more recent discovery is the involvement of the NET in diseases like diabetes and obesity, due to its presence in brown adipose tissue (BAT) and the activation thereof *via* NE.^{64,65,68}

Since the Department of Biomedical Imaging and Image-guided Therapy at the Medical University of Vienna analyzes the NET in relation to brain related disorders -in particular ADHD and substance abuse (cocaine dependence)- and the activation of brown adipose tissue for the time being, the focus of this thesis will be brought especially to these fields of interest:

1.2.2.1 Attention Deficit Hyperactivity Disorder

ADHD is one of the most common cognitive, emotional, and behavioral disorders in children,^{69,70} with an estimated worldwide prevalence of 8-12%.⁷¹ According to the Diagnostic and Statistical Manual of Mental Disorders (DSM-V)⁷² it goes along with impairing and pervasive symptoms of inattention, hyperactivity, and impulsivity. These behavioral deficits arise relatively early in childhood, usually before the age of seven, and persist into adolescence in 50-80% and into adulthood in 30-50%.⁷³ Over development, ADHD is not only associated with several comorbid neuropsychiatric and neurodevelopmental disorders, such as anxiety, conduct or developmental coordination disorder,⁷⁴ but is accompanied by language, communication, and learning disorders⁷⁵ as well. This often leads to a serious financial burden to families and society,⁷⁶ which characterizes the disorder as a major public health problem.⁷⁷

Although, ADHD is one of the most thoroughly researched disorders in child psychiatry worldwide,^{70,78} its etiology and underlying mechanisms are not yet completely ascertained. Several studies^{75,79-82} suggest that genetic (especially abnormalities in genes linked to the dopaminergic and noradrenergic pathways) and environmental (e.g. stroke, traumatic brain injury, maternal smoking during pregnancy, environmental toxins) factors are involved in ADHD, thereby affecting one another and interacting with each other.^{74,83}

Neurobiological and pharmacological evidence, illustrate that a dysregulation of the central catecholaminergic system,^{74,75,84} which is responsible for the regulation of motor function, attention, and executive functions in the fronto-subcortical regulatory circuitry,^{87,88} may contribute to the underlying neurochemical pathophysiology of ADHD. In this context, the neurotransmitters DA, but especially NE^{42,66,75} gained attention over the last years, since several drugs, exhibiting noradrenergic and dopaminergic pharmacological effects, are proven beneficial for the improvement of ADHD symptoms.^{74,84} The NET, which is responsible for the NE uptake into the presynaptic terminals and the DA reuptake in the frontal cortex, turned out to play a pivotal role in the pathophysiology of ADHD. Therefore, its malfunction may lead to abnormal NE and DA levels, respectively, thereby increasing the risk for psychiatric disorders, such as ADHD.^{42,74}

Several studies and clinical observations^{74,83,85-90} pinpointed a decrease in volume and significant alterations in different brain regions of ADHD patients. Amongst them are regions where particularly high NET densities could be detected in control brains: Altered activation patterns for example could be observed in the frontostriatal circuitry,^{89,90} leading to hypoactivity in the frontal brainregions in ADHD patients. Morphological alterations were discovered in the cerebellum⁷⁴ and the dorsolateral prefrontal cortex (reductions in density)⁷³ and alterations in different phases of

information processing^{83,91} could be monitored in the fronto-subcortical regulatory circuitry.

Today the diagnosis of ADHD is based on careful examination of a patient's clinical history⁹² and documentation of the individual profile of ADHD symptoms by rating scales.⁹³ The use of imaging techniques in the diagnosis of ADHD, though, is still absent. Nevertheless, there exist several studies, which demonstrate the application of functional magnetic resonance imaging (fMRI),⁹⁴⁻⁹⁶ PET^{97,98} and diffusion tensor imaging (DTI)^{99,100} in ADHD analysis. Even though these neuroimaging techniques currently lack adequate specificity and sensitivity, they still appear beneficial for the investigation and analysis of the pathophysiology of ADHD.¹⁰¹ Thus, there still exists demand for adequate, selective, and potent molecular imaging biomarkers. Since the NET plays a fundamental role in the pathophysiological events of this disorder, it could be considered an appropriate and prospective tracer target for future analysis in PET, regarding ADHD.

1.2.2.2 Cocaine Dependence

Cocaine is one of the most strongly reinforcing drugs of abuse due to its powerful psychomotor stimulatory effects.¹⁰² Its usage does not only mediate increased locomotor activity and elevated mood with rewarding euphoria,¹⁰³ but also generates fearful and nervous aversive effects. Like other addictive drugs, cocaine induces neuroadaptations in the brain, which are presumed to play a role in the induction and persistence of drug dependence.^{104,105}

Cocaine dependence is a chronic, relapsing disorder, which goes along with somatic, psychological, socio-economic and legal complications. It is considered a significant worldwide public health problem, as major risks include infectious diseases as well as increased crime and violence rates.¹⁰⁶

Since the reinforcing effects of cocaine were traced back to its interaction with the DA system quite early,¹⁰⁷⁻¹¹⁰ much attention has been paid to elevated DAT and DA receptor levels during long-term exposure to cocaine.¹¹¹⁻¹¹⁵ Also behavioral effects, locomotor stimulation, and reward have long been thought to be mediated by the effect of cocaine on the DA-system. However, cocaine was proven not only to inhibit neurotransmitter uptake of human DAT, but of SERT and NET as well and showed ligand- and voltage-gated channel blockade with lower potencies.¹⁰²

So far, very little is known about the NET, its function and regulation in cocaine dependence. However, several studies^{47,116-120} investigated on the NET *in vitro* and *in vivo*, thereby focusing primarily on the response of NET to cocaine: Although rodent NET^{116,117} and HEK-293 cells transfected with human NET cDNA⁴⁷ seemed rather unresponsive to cocaine exposure, NET mRNA in rodents¹¹⁸ was revealed to increase in response to cocaine. Also, brain areas of non-human primates^{119,120} showed alterations in NET concentrations when exposed to cocaine. NET alterations in the human brain as a result of cocaine dependence have further been discussed: Since the bed nucleus of the stria terminalis (BNST) contains one of the highest regional densities of noradrenergic fiber inputs¹²¹ and NET binding sites,⁵⁷ several studies^{119,57} refer to the BNST as a major target in drug reinforcement processes. Also brain areas like the midbrain regions, the thalamus, and the basal ganglia as well as the occipital cortex showed cocaine-induced alterations of the NET.^{122,123}

Noradrenergic functions have also been extensively studied in the context of cocaine's aversive effects,¹²⁴⁻¹²⁶ which as well as the reinforcing/rewarding effects of the drug seem to be important parameters of cocaine self-administration,¹²⁷ as an increase of NET binding sites was determined in the brain of cocaine self-administering non-human primates.¹¹⁹ Furthermore, reinstatement of drug seeking could be mediated by NET inhibition *via* cocaine, which was demonstrated in a study using NET knockout mice.¹²⁸

Due to the lack of NET, the mice continued self-administration of cocaine, concurrently responding with increased sensitivity to the locomotor effects of the drug.⁶⁰

Although the NET is a site of action of many drugs and definitely plays an important role in cocaine dependence, knowledge of the molecular and cellular mechanisms of NET alterations caused by cocaine remain poorly understood.¹²⁹⁻¹³¹ Cocaine-induced changes in the DAT, dopamine receptors, glucose metabolism and distribution of radiolabeled cocaine, however, have been excessively analyzed in PET experiments.^{132,133} The primary reason for the lacking data regarding the human NET system in relation to cocaine dependence, is the current deficiency of adequate PET radioligands.¹³⁴ Thus, for better understanding of the function and molecular and cellular mechanisms of NET in cocaine dependence, new radiotracers need to be developed. As long term exposure to cocaine is known to cause significant changes in information perceiving and processing, and given the role of NE in arousal and attention,¹²⁰ associated NET alterations cannot be neglected and therefore require further investigation *in vivo*.

1.2.2.3 Activation of Brown Adipose Tissue

BAT is a highly metabolically active organ, which represents a unique tissue not only in humans, but in all mammals. As an extremely specialized thermogenic tissue, it is capable of oxidizing lipids and successfully transforming the resulting energy into heat.¹³⁵ Therefore, the main role of this unique organ is the regulation of body temperature in newborns and hibernating mammals. Through this process, mammals are able to be active during periods of hibernal cold, survive the cold stress of birth, and live a life despite diets low in essential macronutrients (proteins). Whilst rodents seem to maintain BAT during lifetime, it is rapidly lost postnatally in humans, but still exists in adult humans to a small percentage (figure 8).¹³⁶

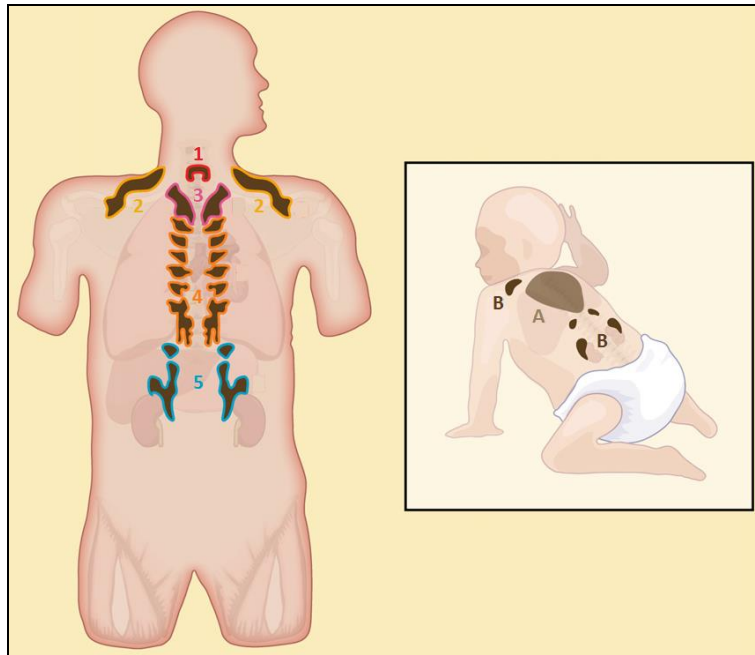


Figure 8:¹³⁵ (modified) BAT location in adults (1-5) and infants (A+B): 1) thyroid/tracheal, 2) mediastinal, 3) paracervical/supraclavicular, 4) parathoracic, 5) supra and perirenal, A) kite-shaped thin layer of BAT between shoulder blades, B) BAT deposits alongside the spine

Although, BAT and its appearance in hibernating marmots was first described by the Swiss naturalist Konrad Gessner in 1551, from the scientific point of view, this tissue is regarded a relatively new discovery, since its function and activation mechanisms were not exposed until the 20th century.¹³⁷

BAT is very rich in vascularization, highly innervated and displays a high density of mitochondria.⁹⁵ These features are not only responsible for the unique mechanism and brownish color of BAT but distinguish it from white adipose tissue (WAT) at once.¹³⁸ Whilst WAT is primarily responsible for the storage of energy, BAT burns energy for thermogenesis.¹³⁹

The heat generating process in BAT can be stimulated by pharmacological agents,¹³⁵ by hyperadrenergic stimulation in pheochromocytoma as reported by Lean *et al*,¹⁴⁰ and other tumors,¹³⁹ but most of all by acute food intake and exposure to cold environment in a process called non-shivering thermogenesis.¹³⁵ In almost all cases, the process of heat

generation is triggered by the sympathetic nervous system (figure 9). NE released from the sympathetic nerve terminals interacts with β_3 -adrenergic receptors on the surface of BAT cells and subsequently provokes a cascade of activation processes: In a cyclic adenosine monophosphate (cAMP)-mediated process, the enzyme hormone-sensitive lipase (HSL) initiates the degradation of triglycerides, thereby generating free fatty acids. These again are channeled into the mitochondria, where they are chemically altered by undergoing β -oxidation,¹⁴¹ and activate the -normally by purine nucleotides (notably ATP) inhibited-⁶⁸ uncoupling protein UCP 1. UCP 1 is a protein unique to BAT cells, which dissipates the intermembrane proton-motive force and generates heat instead of ATP.¹⁴¹

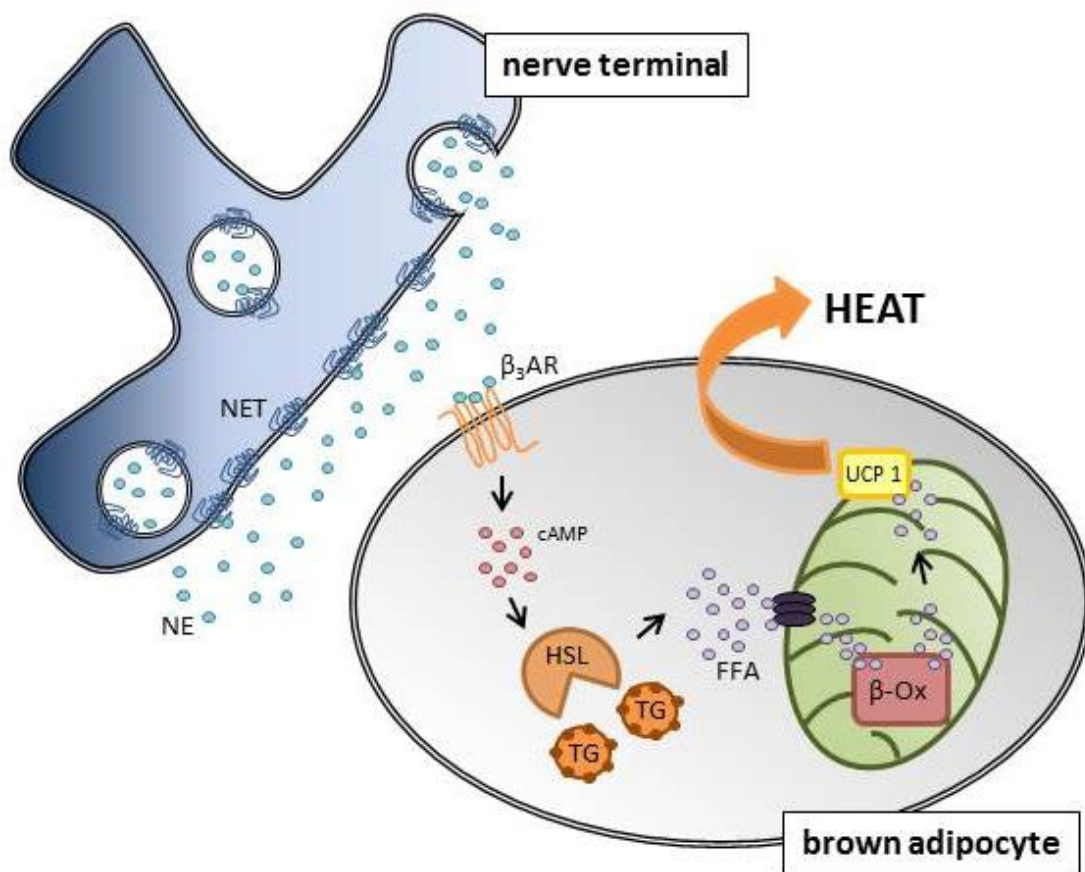


Figure 9: Norepinephrine (NE) released from the synaptic nerve terminal binds to β_3 -adrenergic receptors (β_3 AR) on the surface of BAT cells and induces cyclic adenosine monophosphate (cAMP) release. Subsequently, activated hormone sensitive lipase (HSL) transforms triglycerides (TG) into free fatty acids (FFA), which enter the mitochondria through a transporter. In the mitochondria, FFA undergo β -oxidation. The resulting substrate activates uncoupling protein UCP 1, which generates heat.

As already mentioned above, one important factor, mediating thermogenesis in BAT is acute food intake. Especially diets low in protein indicate recruitment of BAT and an increase in UCP 1.^{142,143} In this regard, questions have recently been raised, if BAT plays a role in obesity and even can be adducted a therapeutic option in the treatment of obesity and diabetes. BAT recruitment has been shown to positively correlate with the resting metabolic rate and inversely correlate with the body mass index (BMI) and fat.¹⁴⁴⁻¹⁴⁷ Furthermore, small and large population studies indicate an inverse correlation between BAT activity and obesity.¹⁴⁸⁻¹⁵⁰

The reduction of body weight by activating thermogenesis though, is not a new idea. Several drugs, affecting the sympathetic nervous system, have been developed for BAT activation over the last years. Nevertheless, their application was rather omitted, due to various side effects, which mostly affected the cardiovascular system.¹⁴¹ However, the detection of BAT activity as well as the underlying mechanism of BAT in obesity and diabetes in humans would be rather interesting, since generated data to date just apply to rodent experiments.

Since BAT activity is necessarily coupled to BAT activation *via* the sympathetic nervous system, NE, being the main trigger, represents a significant transmitter in this system. It has a primary role in the activation mechanism, as it is a key modulator for UCP 1 and therefore, an activator for the thermogenesis in BAT. It is further fundamental for the expression of the UCP 1 gene and inhibits apoptosis in brown adipocytes. In addition, NE directly regulates the proliferation of brown preadipocytes and promotes the differentiation of mature brown adipocytes.¹⁴¹

As the NET regulates synaptic NE concentrations in sympathetically innervated tissues and recycles excess NE, major attention has to be paid to the transporter in the process of BAT activation. Thus, for a better characterization and for understanding the role of NET in BAT, regarding obesity and diabetes in humans, a suitable and non-invasive imaging approach -namely PET- is required. Recent PET experiments⁶⁵ suggest the

feasibility of NET as an imaging target in BAT and since this approach is a rather new one, further studies are definitely required to gain more information about this transporter and its implication in BAT.

1.2.3 Relevance

Based on the fact that the NET is involved in a variety of diseases, such as ADHD and cocaine dependence and furthermore plays a pivotal role in the activation of BAT,^{41,42,63-65} the investigation of the underlying dysregulation-mechanism of the NE system is of major interest. For this purpose, information about the transporter abundance and density in healthy and pathological living human brains is required. The most suitable and accurate technique to gain this information is PET. As a non-invasive molecular imaging technique, it represents a suitable approach towards the collection of lacking data in the living organism and direct quantification of receptor/transporter densities *in vivo*. To fully gain insight in the molecular changes of the noradrenergic system *via* PET, however, suitable NET-PET radioligands first need to be developed.

A major problem in the context of NET-PET radiotracer production is the fact that not only the NET, but also the monoamine transporters DAT and SERT are involved in neurological, cardiovascular, and metabolic diseases.^{49,50,54,151,152} Since the NET displays high similarity to the DAT and SERT, but shows a significantly lower density in the human brain,^{57,153,154} several potential compounds for radiolabeling do not specifically bind to the NET, but to the DAT and SERT as well.⁶⁹ Therefore, selective NET radiotracers with high affinity and low unspecific binding are required. Also, considering the spatial limitations of regions such as the locus coeruleus, which is 4-8 fold richer in NET than the human insular cortex, for which a B_{\max} value of 4.4 nM for NET has been detected, the affinity of candidate NET-PET ligands must be high enough for a suitable visualization.^{53,55,57,123}

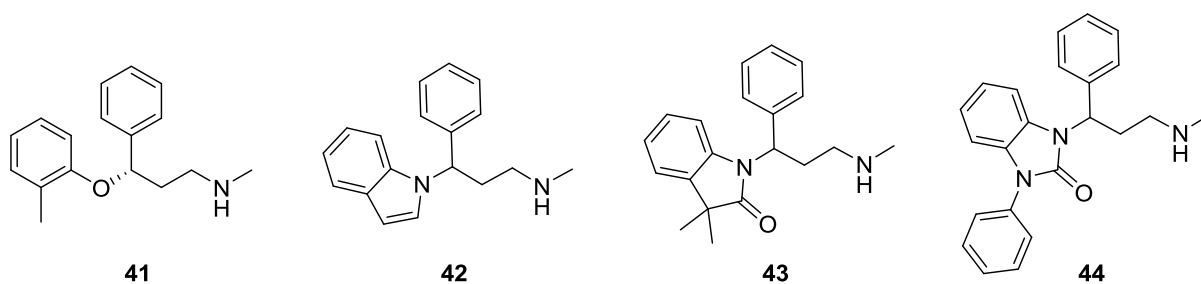
To this date, several radiotracers for the visualization of the NET have yet been established. Many of them are reboxetine analogs, since reboxetine is known for its characteristics as a selective NET-inhibitor.¹⁵⁵ ¹¹C-methylated tracer [¹¹C]-(*S,S*)-MeNER ([¹¹C]MRB, (*S,S*)-2-(α -(2-[¹¹C]methoxyphenoxy)benzyl)morpholine), for instance, was introduced in studies, examining alterations in NET concentrations due to chronic cocaine abuse.¹³⁴ Furthermore, it was employed to determine the existence of NET in BAT.⁶⁵ Also, ¹⁸F-fluoroethylated reboxetine analogs, such as (*S,S*)-[¹⁸F]FMeNER and (*S,S*)-[¹⁸F]FMeNER-D₂ have been synthesized. However, of all radiolabeled reboxetine analogs, so far, just (*S,S*)-[¹⁸F]FMeNER-D₂ showed positive preliminary results in the monkey brain.¹⁵⁶ In addition, also ¹¹C-methylated derivatives [¹¹C]nisoxetine and [¹¹C]desipramine were synthesized. [¹¹C]Nisoxetine was applied in NET distribution studies, investigating the effect of cocaine exposure in non-human primates¹²⁰ and also served as a radiomarker in interscapular BAT studies in rodents.¹⁵⁷ Whilst [¹¹C]nisoxetine only displayed moderate specific binding in mice,¹⁵⁸ [¹¹C]desipramine showed low binding in the monkey brain and thus did not allow accurate NET visualization.¹⁵⁹ Moreover, several ¹⁸F-labeled benzylguanidine analogs, such as [¹⁸F]MFBG and [¹⁸F]PFBG have been synthesized, which were tested in neuroendocrine tumors.¹⁶⁰ Further compounds for the visualization of NET are [¹²³I]iodo- and [⁷⁶Br]bromo-radiolabeled derivatives, such as (*R*)-[¹²³I]MIPP, (*S,S*)-[¹²³I]IPBM or [⁷⁶Br]MBBG, which were primarily designed for the employment in SPECT. Whereas [⁷⁶Br]MBBG showed potential for imaging NET-expressing neuroendocrine tumors, the iodo derived compounds may exhibit properties for imaging brain noradrenergic nervous functions with SPECT.¹⁶¹⁻¹⁶³ Another approach for examining the role of NET in BAT is by evaluating the uptake of 2-[¹⁸F]fluoro-2-deoxy-D-glucose ([¹⁸F]FDG) after BAT stimulation by cold exposure.^{64,164,165} Even though these experiments suggest a correlation between BAT metabolic activity, age, gender, body mass index, cold exposure, and medication, the [¹⁸F]FDG-PET approach seems not suitable for specifically imaging BAT.¹⁴⁸ Glucose is not the primary substrate for BAT heat production and thus, [¹⁸F]FDG will not address regulatory mechanisms, which are related to the specific sympathetic nervous system modulatory features of BAT.⁶⁵

Considering the fact that of all radioligands, mentioned above, only (S,S)-[¹⁸F]FMeNER-D₂ appears feasible for the investigation of NET in PET studies, the development of new, high affine, and selective NET-PET radioligands seems inevitable. Furthermore, and as already mentioned above, to this date, to the best of our knowledge, there exists no radiolabeled compound, suitable for the detection of NET concentrations in ADHD patients and also, the detection of NET in cocaine dependence and BAT activation currently lack adequacy. Thus, in order to depict the role of the NET in ADHD and cocaine dependence and fully understand the underlying mechanism of BAT regulation, new, selective and reliable NET-PET tracers need to be developed.

1.2.4 Preceding Investigations

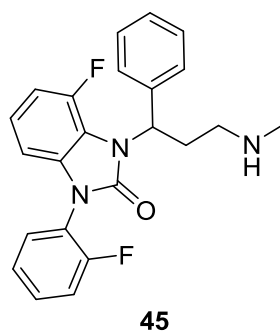
1.2.4.1 Fluorine substituted 1-(3-(methylamino)-1-phenylpropyl)-3-phenyl-1,3-dihydro-2H-benzimidazol-2-one (FAPPI) derivatives

In the context of finding new, potent monoamine transporter inhibitors with improved metabolic and pharmacological properties, Mahaney *et al*¹⁶⁶ reported the development of a series of 3-(1H-indol-1-yl)-3-arylpropan-1-amines (e.g. **42**). The series was designed on the basis of atomoxetine (**41**), a selective NE reuptake inhibitor for the treatment of ADHD, with minor modifications in the core structure. Generated candidate compounds (e.g. **42**) emerged as dual acting NE and 5-HT reuptake inhibitors. In the effort of identifying new and selective compounds for NET inhibition, Zhang *et al*¹⁶⁷ adapted the model of Mahaney *et al*, by substituting the indole ring with an oxindole or benzimidazolone ring, respectively. Whilst oxindole based propanamines (e.g. **43**) with high NET activity mostly displayed increased human serotonin transporter (hSERT) potency,¹⁶⁸ benzimidazolone derived propanamines (e.g. **44**) showed excellent NET activity and a higher selectivity of NET over SERT.¹⁶⁷



The evaluation of synthesized benzimidazolone based propanamines at the human norepinephrine transporter (hNET) *in vitro* suggested that compounds containing a phenyl moiety directly at the benzimidazolone ring (e.g. **44**) were the most potent, representing a half maximal inhibitory concentration (IC_{50}) below 10 nM ($IC_{50} < 10$ nM). Furthermore, hNET selectivity over hSERT turned out (> 300-fold) superior to those of reboxetine and atomoxetine (16- and 81-fold).¹⁶⁷

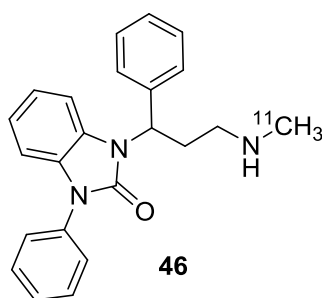
Fluorination at position 7 of the benzimidazolone core structure and position 2 of the phenyl moiety, attached to the benzimidazolone ring (**45**), indicated similar hNET potency, comparable to its non-fluorine analogs (e.g. **44**) and additionally exhibited hNET selectivity over hSERT (80-fold) similar to atomoxetine.¹⁶⁷



Both benzimidazolone derived propanamines with a phenyl moiety (e.g. **44**), as well as a fluorinated core and phenyl moiety (**45**) indicated excellent hNET selectivity over hDAT with < 50% inhibition of the cocaine analog [³H]WIN-35,428, binding to hDAT at a concentration of 10 μ M.¹⁶⁷

Given those findings, both described benzimidazolone based propanamines represent excellent candidates for selective and potent NET inhibition with high affinity and low

unspecific binding. Thus, on the basis of the results of Zhang *et al*¹⁶⁷ the methylamino moiety of core compound **44** has been radiolabeled with ¹¹C and tested by our research group.¹⁶⁹ All investigated preclinical parameters, such as affinity, BBB penetration, lipophilicity, metabolic degradation, and selectivity showed excellent results, thus suggesting excellent suitability of ¹¹C radiolabeled 1-(3-(methylamino)-1-phenylpropyl)-3-phenyl-1,3-dihydro-2H-benzimidazole-2-one (¹¹CMe@APPI) (**46**) as a NET radioligand for the employment in PET.

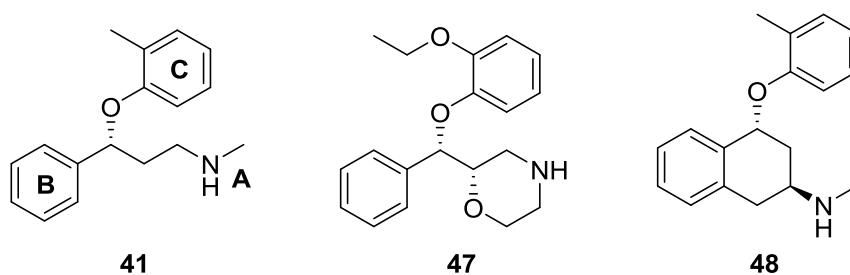


Due to successful preclinical testing of [¹¹C]Me@APPI (**46**) and given the excellent *in vitro* results of the fluorinated analog of core compound **44**, shown by Zhang *et al*,¹⁶⁷ the aim of this thesis, amongst others (cf. chapters 1.1.3. and 1.2.4.2.), were the computational evaluation and successful synthesis of several fluorinated analogs of compound **44**. In cooperation with the Medical University of Vienna, the resulting derivatives were subjected to continuative lipophilicity studies and BBB penetration experiments, for the evaluation of those compounds as suitable and future NET-PET radiotracers.

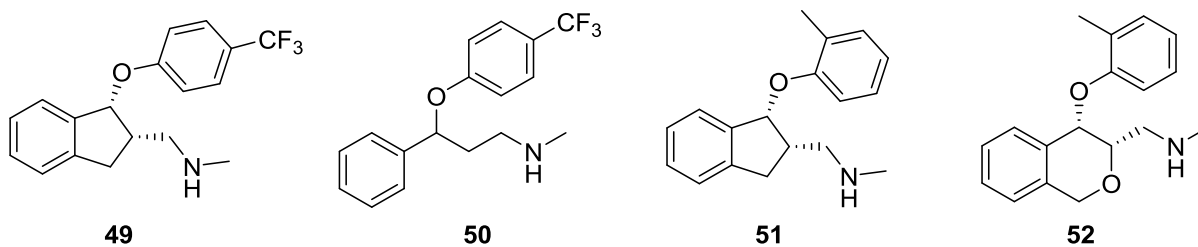
1.2.4.2 Substituted 1-((3*S*,4*S*)-4-phenoxy-3,4-dihydro-1*H*-isochromen-3-yl)methanamine (PHOXI) derivatives

Atomoxetine (**41**) and (*S,S*)-reboxetine (**47**) both feature NE reuptake inhibitory properties and can be characterized by their high affinity for the NET.^{170,171} Based on these findings, both substances often serve as model structures for the development of new NET inhibitors. In this regard, Wu *et al*¹⁷² developed a series of potent NET inhibitors (e.g. **47**), thereby applying three main structural requirements, derived from the

literature:¹⁷³ Atomoxetine (**41**) exhibits a basic site A, a secondary amine, which is responsible for the potent inhibition of the NET, and a hydrophobic site B, which forms an aromatic ring. Furthermore, it consists of an additional aromatic ring C, which -by substitution- leads to significant changes in DAT, NET, and SERT selectivity. However, the main drawback of atomoxetine is its overall molecular flexibility, resulting in metabolism and clearance impairment,^{174,175} which gave Wu *et al* reason for developing a series of improved, new compounds (e.g. **48**).



Of all compounds synthesized, isomer **48**, featured the best activity and selectivity for NET over SERT and DAT, equivalent to atomoxetine (**41**) and showed a decrease in flexibility. Additionally, it was 5-fold more potent than **41** regarding cytochrome 2D6 (CYP2D6) inhibition, which however, was also expected to cause drug-drug interactions with other CNS agents.¹⁷² In the context of improving the pharmacological properties of **48**, as well as considering already described substance **49**, which has been prepared as an analog of selective 5-HT reuptake inhibitor fluoxetine (**50**), a new series of molecules (e.g. **51**) has been developed by Hudson *et al*:¹⁷⁶ Potent and selective NET inhibitor **51** featured properties, very similar to atomoxetine (**41**) and also exhibited elevated flexibility in regard to **48**, but reduced flexibility in regard to **41**. Also, CYP2D6 inhibition and oxidative stability were similar to **41**, which led to the objective of modifying shape and geometry of **51** just enough to improve these properties, without losing potency or selectivity at the NET.¹⁷⁶



Hence, the cyclopentane ring of **51** was substituted by a cyclohexane ring or a tetrahydro-2*H*-pyran ring in order to generate the chromane or isochromane, respectively. Tetralin analogs were less potent than the similar indane and although chromane based compounds exhibited a 2-fold improvement in potency, isochromane derived compounds (e.g. **52**) trended toward higher potency,¹⁷⁶ thereby suggesting an interaction between the isochromane oxygen and the NET.¹⁷⁷ The greater potency was also correlated with the size and hydrophobicity of the aryloxy substitution, especially when a CF₃ group was substituted for the methyl moiety (**52**) at position 2 of the phenyl ring. Additional fluoro substitution at position 3, 4, 5, or 6 of the phenyl ring even led to further amplification of the effect, with single-digit nM activity for the NET.¹⁷⁶

Selectivity was discovered to be a result of fluorine positioning. Additional fluorination of **52** at position 6 of the phenyl moiety for instance, not only augmented NET affinity, but also showed a significant increase in NET selectivity over SERT and DAT. In addition, comparison of cis and trans diastereomers suggested that the cis diastereomer displayed higher affinity and selectivity towards the NET than the trans diastereomer.¹⁷⁶ Although, no improvement regarding CYP2D6 inhibition could be achieved (**52** showed similar results to **51**), in the microsomal clearance assay, **52** revealed advantageous stability compared with atomoxetine (**41**).¹⁷⁷

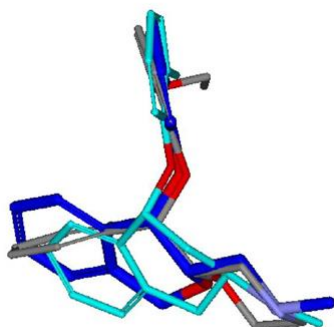


Figure 10:¹⁷⁷ (modified) Overlay of crystal structures of (S,S) reboxetine **47** (gray), derivative **48** (teal) and compound **52** (blue)

Compound **52** as well as some of its fluorinated analogs, discussed earlier, exhibit excellent properties, regarding NET affinity and selectivity. As depicted in figure 10, overall conformations of **47**, **48**, and **52** are relatively similar to each other, except for the positioning of the *N*-methyl moiety. Due to the pseudoequatorial position of aminomethyl sidechains and pseudoaxial aryloxy groups, the aryl ring as well as the amino group with its attached methyl moiety is positioned at the same distance and orientation in all compounds, which results in the complete overlap of aminopropoxyaryl chains of **47** and **52**. Furthermore, not only the second aromatic ring of **52** is in the common plane and shifted position as **48**, but also, the isochromane oxygen of **52** occupies the same space as the morpholine oxygen of **47**, assuming a specific interaction of this oxygen with the NET.¹⁷⁷

Since compound **52** and its fluorinated analogs feature excellent NET binding properties and high selectivity for NET over SERT and DAT, in addition (cf. chapters 1.1.3. and 1.2.4.1.), the aim of this thesis was the synthesis of compound **52** and several already known analogs thereof. Furthermore, an additional fluoroethyl moiety was introduced at the methylaminomethane side chain of all molecules prepared, as described in chapters 3.4.3.2.4 and 3.4.3.3.3. *N,N*-Dimethyl substituted derivatives as well as compounds featuring an *N,N*-methylfluoroethyl moiety serve as reference compounds for their later prepared ¹¹C and ¹⁸F radiolabeled analogs and underwent preclinical testing at the

Medical University of Vienna. Lipophilicity experiments and BBB penetration studies determine the suitability of these compounds for the later employment of radiolabeled analogs in PET studies, for the *in vivo* examination of the NET in ADHD, cocaine dependence, and BAT.

1.3 Positron Emission Tomography

1.3.1 General Background

PET is a powerful non-invasive imaging modality and represents an important component of molecular imaging techniques. It is the most sensitive method for the purpose of functional imaging and permits the *in vivo* measurement and quantification of molecular interaction, gene expression, signal transduction, and metabolic processes at the molecular level in the living organism.^{187,179} Therefore, it is successfully employed today as a diagnostic tool in the field of cardiology, oncology, and neurology/psychiatry, but also finds its use in research, where it serves for direct drug quantification in laboratory animals and humans.¹⁸⁰

PET comprises two main principles, the tracer principle and the tomographic principle, which have been both awarded with the Nobel Prize.¹⁸¹ The key element of PET forms the PET radiotracer, a chemical compound which is labeled with a suitable short-lived positron emitter.¹⁸² Today, ^{11}C ($t_{1/2} = 20$ min), ^{13}N ($t_{1/2} = 10$ min), and ^{15}O ($t_{1/2} = 2$ min) represent the radionuclides of choice for radiolabeling, since these isotopes are naturally occurring elements in living systems, drugs, and food ingredients. However, since there exists no positron emitting isotope of hydrogen, which is also a main constituent of molecules of biological importance, ^{18}F ($t_{1/2} = 110$ min) is commonly used to isosterically replace a hydrogen atom in a molecule.¹⁸³ Moreover, nowadays several novel drugs contain fluorine atoms, which can simply be replaced by its ^{18}F isotope without affecting

biological properties.^{184,185} The choice of the appropriate radionuclide and labeling position represent important aspects in the design of suitable and novel PET radiotracers.

Subsequent to radionuclide production, radiosynthesis, and adequate purification, the resulting radiotracer is administered to a laboratory animal or a patient. Thereby, injected quantities of the PET tracers are in the nano- or picomolar range, which enables the application of highly potent compounds without triggering any pharmacological effect.^{179,186} The fate of the emitted positron culminates with the annihilation event and the emission of gamma quanta in opposite directions, which can be detected and transformed into tomographic images using coincidence detection.

By the employment of unique data acquisition protocols, the high end technique of PET enables a wide variety of data analyses¹⁸⁷ and thus differs from other techniques used in nuclear medicine such as SPECT. PET provides a significantly higher sensitivity, which allows the acquisition of high quality 2D and 3D PET images as well as quantitative PET data.^{188,189}

Over the years, PET has become a powerful scientific and clinical tool for probing biochemical processes in the human body. Therefore, it has not only been employed in diagnostic clinical studies, basic *in vivo* research, or preclinical studies, but lately also finds its use in drug development, where PET technology assists in gaining understanding of drug actions, establishing dosage regimens or treatment strategies.¹⁹⁰

1.3.2 Physical Principles of PET Imaging and Data Acquisition

The underlying principle of PET is the β^+ decay, which naturally occurs in neutron-deficient isotopes.¹⁹¹ A PET radiotracer consists of a target specific chemical compound and such a neutron-deficient positron emitting nuclide. Its nucleus is proton rich and in the attempt of achieving stability, a proton in its core turns into a neutron by nuclear

transmutation.¹⁹² During this process, a positively charged particle, the positron (e^+), is emitted with high kinetic energy and a neutrino (ν_e) escapes, which however does not interact with the surrounding material.¹⁹³

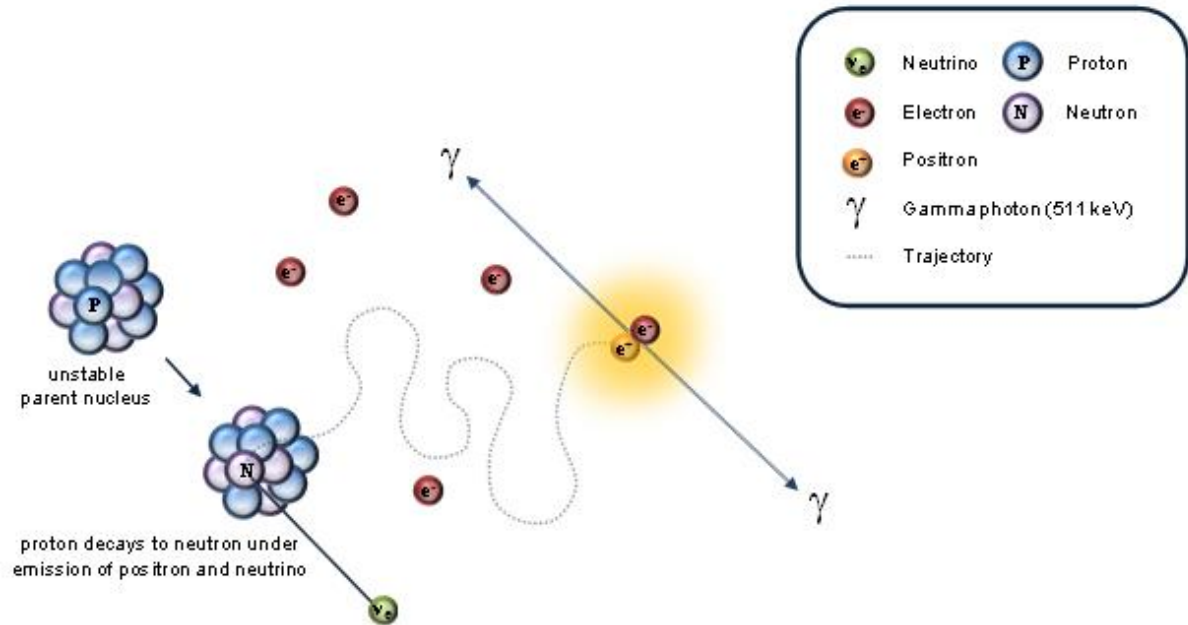


Figure 11: Annihilation event

After emission, the positron travels a short distance (also known as the positron range) and thereby loses kinetic energy by the interaction with the surrounding tissue. The complete or almost complete loss of energy results in the fusion with a free electron and thus the subsequent formation of a positronium particle. The positronium, being a short-lived positron-electron composition, is eventually annihilated, thereby converting its mass into energy in the form of two γ -rays of 511 keV. These γ -quants are simultaneously emitted in opposite directions at an angle of approximately 180 degrees (figure 11) and can be captured in coincidence by opposing detectors.^{182,193,194}

Ideally speaking, only true coincidence events should be detected by a PET scanner. These occur if both γ -rays result from one annihilation event and are detected between two parallel, opposite detectors within a narrow time window. The annihilation event is assumed to have taken place somewhere along the “line of response” (LOR) in between

the two detectors.¹⁹³ However, there also exist accidental or random events, where detectors capture γ -rays resulting from different annihilation events, and scatter coincidences, emerging from two photons being diverted from their original direction and reaching the detector to incorrectly determine the coincidence event. Since accidental events and scatter coincidences frequently occur during PET scans, causing increased background and affecting overall contrast in the final image, mathematical correction techniques are required for appropriate annihilation detection.¹⁹⁵

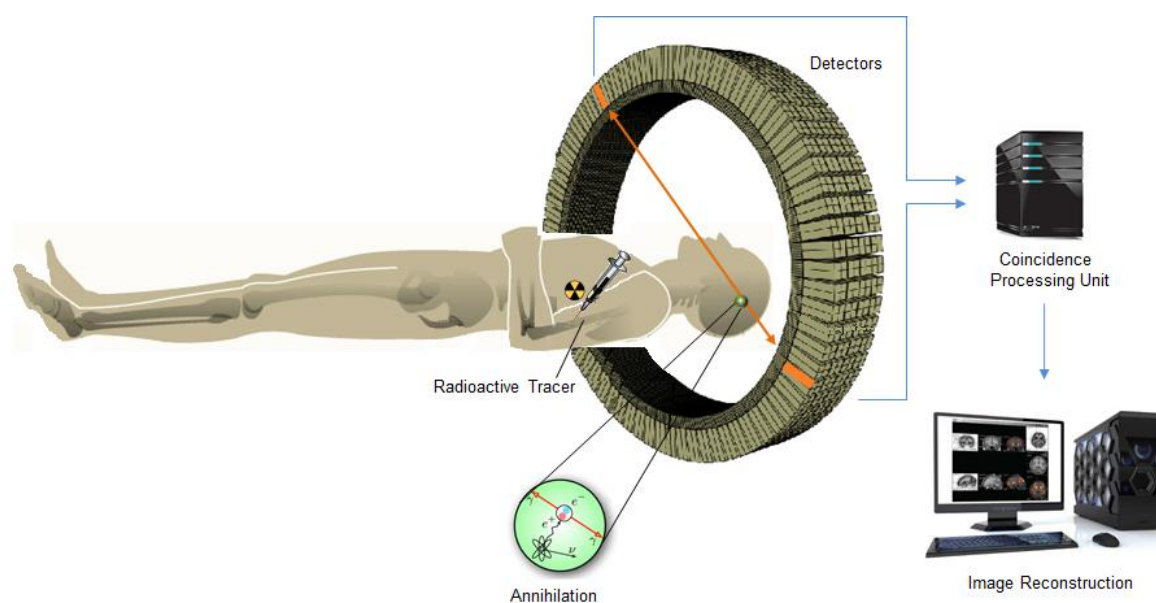


Figure 12: PET-procedure: Injection of the radiotracer into the patient, annihilation of the emitted positron with an electron and detection of the resulting γ -rays by scintillation detectors, data conversion and reconstruction of the PET image.

In a typical PET scanner hundreds of detector banks are arranged in a ring-like pattern, surrounding the laboratory animal or patient. Thus, millions of coincidence events can be detected simultaneously, as each pair of parallel and opposite detectors produces a coincidence line, which is unique in terms of location and direction. The γ -quanta, striking the scintillation detectors, which usually consist of bismuth germinate (BGO) or lutetium oxyorthosilicate (LSO), are converted into visible light. Light photons are then transformed into electronic signals by a photo detector, such as a photomultiplier tube (PMT).¹⁹⁴ The electronic signals are stored as two-dimensional matrix, also referred to as

“sinogram”, and undergo image reconstruction algorithms in order to recover the underlying radioactivity distribution and eliminate tissue alterations as well as detector non-uniformities. Today, iterative reconstruction algorithms have become the method of choice for data transformation in PET technology, since they provide superior image quality compared to traditional filtered background methods.¹⁹⁶ The fully converted two-dimensional data thus enable image reconstruction with information on the spatial distribution of radioactivity as a function of time (figure 12).¹⁹⁰

A state of the art PET system acquires coincidence data in a so-called 3D mode. Thereby, image quality is tremendously improved, even by the administration of relatively low radiopharmaceutical activities.¹⁹⁵ Furthermore, the spatial resolution of a PET scanner used in clinical practice today is between 4 and 7 mm, while micro-PET scanners offer a spatial resolution between 0.5 and 2 mm.¹⁹⁷ Amongst other factors, like positron range, detector size or noncolinearity of the annihilation photons, the spatial resolution (and therefore image quality) is influenced by the detector crystals.¹⁹⁸ Since BGO crystals meet the desired characteristics for the employment in PET, such as a high effective atomic number, high density and high stopping power, they represented the crystals of choice for the last several years. However, LSO or lutetium yttrium orthosilicate (LYSO) possess very similar properties, compared to BGO, but additionally features a higher light output and faster decay times.¹⁸⁷ The drawback of these crystals though is their high prize and the intrinsic background radioactivity, due to the occurrence of the natural isotope of lutetium (¹⁷⁶Lu) within the crystals. Despite this drawback, they are already employed in several animal PET scanners today.^{188,194}

Since PET primarily yields functional and physiological information, it is frequently combined with other non-invasive imaging modalities, such as Computed Tomography (CT) or Magnetic Resonance Imaging (MRI). CT as well as MRI provide anatomical information and thus permit accurate localization of the PET signal and allow improvement in the quantitative accuracy thereof.¹⁹⁸ Figure 13 shows a PET image, an MR image, and a combined PET/MR image.

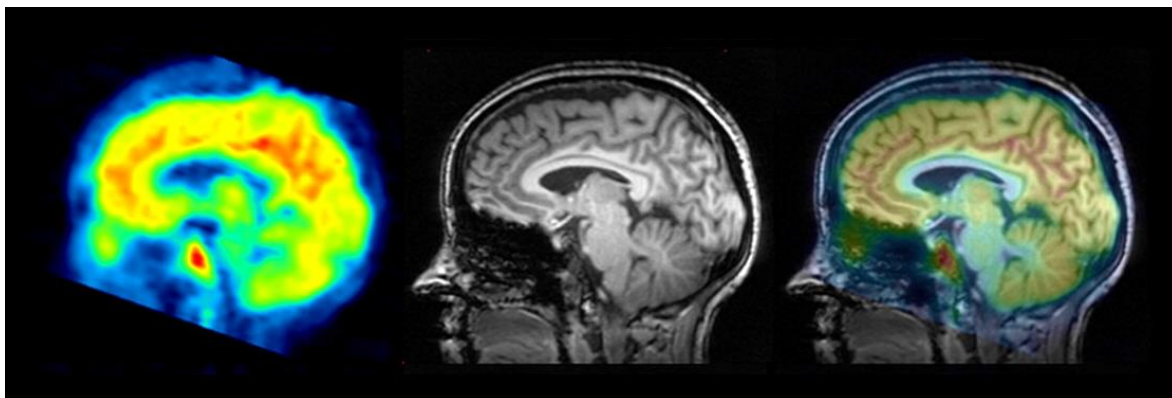


Figure 13:¹⁹⁹ (modified) From left to right: PET image of the cannabinoid CB1 receptor with ^{18}F -FMPEP-d2 in the human brain, MR image of the human brain, PET and MR image overlay.

Multimodality imaging is widely used in oncology today and enables accurate diagnosis/detection of diseases and analysis of the reconstructed simultaneous tomography.^{181,188,200} Since medicine is evolving towards personalized care, the application of combined imaging techniques is assumed to expand, not only in the field of research for the study of pharmacokinetics and pharmacodynamics of new therapeutics, but also in diagnosis and individual patient treatment.²⁰¹

1.3.3 Radiopharmaceuticals

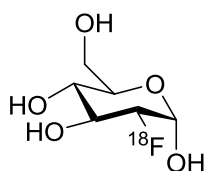
Radiopharmaceuticals are radiolabeled medicinal formulations, which are designed for the mapping of physiological function and metabolic activity *in vivo*. They consist of a molecular structure, which is responsible for the chemical and biochemical interactions and determines the fate of the radiopharmaceutical within the living organism. In addition, radiopharmaceuticals comprise a short-lived positron emitting isotope responsible for a signal, which can be detected by the use of nuclear medical methods. Often, a linker has to be introduced as a stable connection between the core structure and the positron emitting radionuclide.^{202,203}

Since a non-radioactive compound and its radioactive analog feature identical chemical properties, the living organism metabolizes them in the exact same way. Thus, radiopharmaceuticals can be employed to directly visualize functional and metabolic

processes *in vivo*, which allows the imaging of pathological changes on the molecular level long before morphological manifestation.²⁰²

In general, radiopharmaceuticals are classified by their field of application, which is either diagnosis or therapy.²⁰³ Given the growing demand for mapping biological processes in the living organism, a series of PET tracers already found their way into clinical routine. Several PET imaging agents are therefore frequently used for cardiological as well as neurological and psychiatric purposes. The main application area however is oncology.^{180,202}

One of the first radiodiagnostics, which finds its main use in the field of oncology today,²⁰⁴ is 2-[¹⁸F]fluoro-2-deoxy-D-glucose ([¹⁸F]FDG) (**53**). The molecule was first synthesized in 1978 by Ido *et al.*,²⁰⁵ but only the significant improvements made by Hamacher *et al.*²⁰⁶ at the research center Juelich (Germany) led to the continued success of this compound. Since the organism metabolizes [¹⁸F]fluoride radiolabeled glucose like the endogenous, non-radioactive analog, evaluation of the glucose metabolism can be studied easily, which makes [¹⁸F]FDG the most successful commercial PET radiopharmaceutical today. Furthermore, [¹⁸F]FDG uptake in tumor cells, due to their high glycolytic metabolic rate, was already studied in the 1980s by Di Chiro *et al.*^{207,208} These investigations indicated the increased metabolic demand of tumors for glucose and also opened the path towards precise tumor localization in initial staging and monitoring of therapy response.²⁰⁹



53

Eligible radiopharmaceuticals, like the previously discussed ¹⁸F-radiolabeled analog of glucose, are the key elements to successful molecular imaging and thus have to fulfill a number of different criteria, in order to assure accurate applicability as well as broad

availability for the employment in PET. Therefore, several prerequisites, derived from years of empirical research, are necessary, which will be discussed in the following chapter.

1.3.3.1 Prerequisites for PET Imaging Probes

The development of a useful PET imaging probe for the application in laboratory animals or patients usually represents a multistep procedure and requires interdisciplinary collaboration of radiochemists, pharmacologists, and clinicians. Thus, several prerequisites for the development and evaluation of appropriate PET radiotracers have to be considered and validated to ensure maximum reliability and efficiency thereof, in order to achieve successful *in vivo* suitability. Since no single method today can adequately predict the *in vivo* behavior of a PET radiopharmaceutical, a combination of different assays is required to evaluate a promising candidate compound.²¹⁰

Most importantly, a suitable radiopharmaceutical is characterized by its high affinity, high selectivity, and specificity towards the dedicated target site.²¹¹ Only if the site-specific radiotracer has a high affinity for its binding site, specific binding will be observed.²¹² Therefore, adequate binding affinities for PET imaging probes should lie below 10 nM or even in the subnanomolar range.¹⁹⁰

Another important factor in the development of new PET tracers is the ability of the compound to cross the blood brain barrier (BBB). The BBB is formed by a tight layer of capillary endothelial cells, which act as a physical barrier, thereby impeding the penetration of hydrophilic molecules such as peptides or proteins. Small molecules like O₂ or CO₂ as well as lipophilic compounds however are able to enter the central nervous system *via* BBB by passive diffusion.²¹³

Several methods for the prediction of a compound's suitability to penetrate the BBB are available and only a combination of different methods assures accurate prediction.

Lipinski *et al*¹³⁶ for instance, suggest the application of the “rule of 5”, which indicates several guidelines, such as a molecular weight below 500 or a $\log P < 5$, for a certain permeability of a radiopharmaceutical. Since the evaluation of the octanol/water partition coefficient P ($\log P$) is the most commonly used index of compound lipophilicity, one of the first analysis for a suitable PET radiotracer refers to the $\log P$ evaluation. However, in the literature the range assessed for the $\log P$ of appropriate PET tracer compounds varies tremendously. Therefore, the $\log P$ value is often not reliable.²¹⁴ Pike²¹⁵ for example limits the range from 2.0 to 3.5, but also refers to suitable PET tracers, which have been tested a $\log P$ over 5.0, like the radiotracer [¹¹C]MePPEP for the cannabinoid sub-type-1 (CB1) receptor, or [¹¹C]NNC 112 for the dopamine D₁ receptor. Since the $\log P$ value alone does not assure for a compound’s certain BBB penetration, further methods for BBB permeability are required. Therefore, Tavares *et al*²¹⁶ and Abraham *et al*²¹⁷ do not only include $\log P$ evaluation as a measure of lipophilicity into their experiments, but also suggest immobilized artificial membrane (IAM) HPLC experiments, which provide information on compound-membrane interactions, and plasma protein binding assays (using HSA coated HPLC columns) for determining the percentage of a molecule binding to plasma proteins, as a measure for the potential of a radioligand to penetrate the BBB.

Besides the affinity, selectivity/specificity, and the BBB permeability, a suitable radioligand is also characterized by the absence of interfering radioactive metabolites in the target tissue. Metabolization or degradation of the desired radiopharmaceutical, respectively, leads to radioactive metabolites, which can interfere with the target itself and lead to undesirable enhanced binding signals.

Furthermore, a suitable PET tracer features low non-specific binding.²¹¹ Only if a radiopharmaceutical shows low binding to plasma proteins, it is available for diffusion out of the vascular space. Moreover, merely if the non-specific binding of the radio PET

tracer is low, a high target to background ratio and consequently accurate detection of the coincidence signal can be achieved.²¹²

Another important prerequisite in PET radiotracer production is broad availability as well as reliable preparation. Therefore, several factors regarding substance planning and tracer preparation have to be taken into consideration:

Criteria for a new PET radiotracer:²¹⁸

- the expected clinical outcome of the PET study
- chemical aspects
- stereochemical aspects
- position of label
- specific radioactivity
- choice of cyclotron generated primary precursor and related online produced secondary precursor
- choice of solvent for the final formulation (physiological)

1.3.3.2 Short Introduction to the Preparation of Radionuclides

A wide range of positron emitting radionuclides for the incorporation into biomolecules is available today. However, only a few of them are actually employed in PET, since a radionuclide has to meet certain requirements, such as (1) a half-life, which allows radiotracer preparation and minimizes unnecessary radiation time on the subject of interest, or (2) reproducible production in sufficient amounts and under simple conditions.²¹⁹ The nuclides ^{11}C and ^{18}F are the most frequently employed radionuclides in PET today, since both meet the above mentioned requirements.²²⁰ Due to their favorable properties, ^{11}C as well as ^{18}F will also be used for the future radiolabeling of the precursor molecules, prepared within the scope of this thesis.

^{11}C represents an ideal radionuclide for PET, since the isotope decays rapidly and thus allows repeated investigation in the same subject within short time intervals.¹⁹⁰ ^{18}F decays almost exclusively by positron transition (97%) to the ground state of the stable daughter nuclide ^{18}O ; 3% undergo electron capture. It also provides an ideal time frame for PET investigations due to its convenient half-life (110 min) and shows excellent physical characteristics for imaging because of its low β^+ energy.²²¹ Besides ^{11}C and ^{18}F , also other radionuclides find their application in PET. Some of the most employed radionuclides in PET as well as their production methods are listed in table 1.

Nuclide	Production	Half-life
^{18}F (F^-)	^{18}O (p,n) ^{18}F	109.7 min
^{18}F (F_2)	^{20}Ne (d, α) ^{18}F	109.7 min
^{11}C	^{14}N (p, α) ^{11}C	20.4 min
^{13}N	^{16}O (p, α) ^{13}N	10.0 min
^{15}O	^{14}N (d,n) ^{15}O	2.0 min
^{64}Cu	^{64}Ni (p,n) ^{64}Cu	12.7 h
^{86}Y	^{86}Sr (p,n) ^{86}Y	14.7 h
^{76}Br	^{76}Se (p,n) ^{76}Br	16.0 h
^{68}Ga	$^{68}\text{Ge}/^{68}\text{Ga}$ generator	67.6 min

Table 1:¹⁸⁰ Important PET radionuclides for clinical application

In general, there exist three different radionuclide production methods, which include the preparation *via* generator, accelerator (cyclotron), and reactor:

- *Generator derived radionuclides*

The most convenient method is the radionuclide preparation by a generator. This technique is not only the most inexpensive but also grants ready availability of the radionuclide of choice.¹⁹¹ Generator systems include a relatively long-lived parent nuclide, attached to a matrix in a column, from which the usually much shorter-lived daughter nuclide can be eluted. Due to consecutive decay of the mother isotope a radioactive equilibrium, responsible for a gradual buildup of daughter nuclide, is reached within some time, that provides constant availability and hence immediate elution of the daughter nuclide at any time.²²² Based on the different chemical or physical state of mother and daughter isotope, separation of both radionuclides can easily be achieved. Thus, due to the longevity of the mother isotope, radionuclide generators can be transported and the daughter nuclide eluted directly at the desired location. The most common generator system is available for $^{99}\text{Mo}/^{99\text{m}}\text{Tc}$. Other systems for instance comprise ^{68}Ge , ^{81}Rb or ^{188}W as mother isotope and yield ^{68}Ga , $^{81\text{m}}\text{Kr}$, or ^{188}Re , respectively as daughter nuclide.¹⁹¹

- *Cyclotron derived radionuclides*

Particle accelerators, like cyclotrons, are the method of choice for radionuclide production and employed for the preparation of neutron-deficient radioisotopes.²²³ In the center of a cyclotron, hydrogen (H_2) or deuterium (D_2) is introduced, which is converted either into $^1\text{H}^-$ or $^2\text{H}^-$ particles, respectively. Under the effect of a strong magnetic field, $^1\text{H}^-$ or $^2\text{H}^-$ particles gain energy, which forces the anions to travel in a spiral path until they hit a stripping foil. Due to change of charge, resulting protons ($^1\text{H}^+$) or deuterons ($^2\text{H}^+$) deflect out of the acceleration chamber to collide with the target material, which can either be a gas, solid, or liquid.^{222,224} This process leads to a nuclear reaction (mostly (p,n), (d,n), (p, α) or (d, α) reactions),²²³ subsequently yielding the desired

positron-emitting radionuclide. The most common positron emitters, produced within a medical cyclotron are ^{11}C , ^{13}N , ^{15}O and ^{18}F .²²⁴

Although a wide variety of nuclear reactions is available, only one or two are employed in clinical routine. ^{11}C for instance is prepared by the $^{14}\text{N}(p,\alpha)^{11}\text{C}$ reaction *via* proton bombardment of natural nitrogen. The proton interacts with stable ^{14}N , thereby yielding ^{11}C and a neutron. Traces of oxygen in the nitrogen target material ensure conversion into $^{11}\text{C}[\text{CO}_2]$, which serves as initiator for several precursors of radiotracers.²²⁷ For ^{18}F , more than twenty nuclear reactions are known, but the most effective one is the $^{18}\text{O}(p,n)^{18}\text{F}$ reaction on ^{18}O -enriched water. ^{18}F Fluoride of high molar radioactivity can thus be produced in cyclotrons, even with low energy and within less than 1 h of irradiation time.²²⁵

- *Reactor derived radionuclides*

Since there exists a large number of currently used isotopes, that cannot be made accessible by accelerators, reactors find their application in radionuclide production. This method is generally used for radionuclide generation from stable mother isotopes and yields neutron-rich isotopes with a relatively longer half-life.²²⁶

Nuclear reactions are the key element to generate an elevated neutron flux, which leads to the production of neutrons. These are employed for the bombardment of a carrier material, placed in the reactor, which yields the desired radionuclides after the irradiation process.¹⁹¹ The standard reaction for thermal (slow) neutrons is the (n,γ) reaction, mostly generating radionuclides, which decay by β^- reaction and are therefore especially suitable for radiotherapy.^{227,228} Such radionuclides are ^{188}W resulting from ^{187}W , or ^{99}Mo produced from ^{98}Mo .¹⁹¹ However, since only a small fraction of the target atoms is activated, the material removed from the reactor will always contain stable isotopes of the nuclide, which represents the major drawback of reactor nuclides produced by neutron activation. Furthermore, natural impurities in the target material cause the

production of other radionuclides, which limits the ability to concentrate the radionuclide of interest and results in lower specific activity.^{191,227} For this reason, many of the clinically used radionuclides (e.g. ¹³¹I or ⁹⁹Mo), derived from the reactor, are instead produced by nuclear fission to maximize specific activity.²²⁷

1.3.3.3 Radiolabeling with ¹¹C and ¹⁸F

Radiolabeling standard operation techniques require viability and reproducibility of the selected production method to assure adequacy of the radiolabeled end product. Therefore, synthesis time as well as purification periods should remain as short as possible and radiolabeling strategies should aim to introduce the label in the synthetic sequence as late as possible.¹⁹⁰ A diverse array of reactions has been developed for the introduction of ¹¹C and ¹⁸F into target molecules. However, the ideal labeling technique does still not exist to accommodate all necessary requirements, since every method carries some drawbacks.¹⁸² Challenges for the incorporation of ¹¹C into the molecular target for example constitute rapid, reliable, and versatile labeling techniques, whereas incorporation of ¹⁸F isotopes into target molecules is rather challenging, due to limited chemical introduction methods in comparison to ¹¹C.²²⁰

Nevertheless, ¹¹C as well as ¹⁸F are the most widely used radionuclides in PET today.²²⁰ The employment of synthesis modules, supercritical fluids, solid-phase synthesis and automated “loop” synthesis in radiolabeling strategies with ¹¹C and ¹⁸F has enhanced the speed, safety, efficiency, and reliability of radiosyntheses, which guarantees rapid preclinical evaluation, Phase 1 studies, and possible distribution to satellite PET centers without an on-site production unit.^{220,229}

1.3.3.3.1 ^{11}C -Methylation Reactions

A relatively large quantity of ^{11}C radiolabeling precursors is available, but only a selected number finds large-scale application in routine labeling of biomolecules. Most of them can be produced directly in the target or obtained by chemical reactions from $^{11}\text{CO}_2$ or $^{11}\text{CH}_4$. With current available ^{11}C -radiolabeling techniques, $^{11}\text{CO}_2$ is by far the most versatile primary labeling precursor today.¹⁹⁰ It is commonly prepared in the cyclotron and either converted into $[^{11}\text{C}]$ methyl iodide for the further utilization in methylation reactions, transformed into $[^{11}\text{C}]\text{HCN}$, $[^{11}\text{C}]\text{COCl}_2$, and $[^{11}\text{C}]\text{CHO}$ for special applications, or directly employed in the synthesis of carbonyl or carboxyl compounds using the appropriate Grignard reactions.¹⁸⁰

$[^{11}\text{C}]$ Methyl iodide is the most widespread methylating agent and can be prepared by the reduction of $[^{11}\text{C}]\text{CO}_2$ into $[^{11}\text{C}]$ methanol via LiAlH_4 or catalytic hydrogenation and subsequent treatment with a source of HI. Separation from non-volatile impurities is easily achieved by distillation or gas chromatography, due to the volatility of the methyl halide, CO_2 , or methanol.¹⁸⁰ $[^{11}\text{C}]\text{CH}_3\text{I}$ holds the advantage of conducting relatively straightforward methylation reactions. Thereby, it is simply trapped in a solution of the target precursor and heated for a short time.²²⁰

Beside the application of $[^{11}\text{C}]$ ethyl-, $[^{11}\text{C}]$ propyl-, $[^{11}\text{C}]$ butyl- and $[^{11}\text{C}]$ benzyl-iodide^{230,231} in labeling reactions, also $[^{11}\text{C}]$ methyl triflate, represents an important methylating agent. It has gained more prominence over the recent years due to its greater reactivity and volatility,²³² which both represent ideal properties for rapid methylation reactions.²³³⁻²³⁶

Generally speaking, most methylation methods applied in basic organic chemistry can also be utilized in PET radiochemistry. Thereby, and particularly in the case of $[^{11}\text{C}]\text{CH}_3\text{I}$, amine, alcohol, or thiol groups serve as suitable precursors to form the respective amine, ether, or thioether.²²⁰ Due to impurities, such as non-radioactive CO , CO_2 , CH_4 , or other sources of carbon, the theoretical achievable maximum specific radioactivity however is

never reached. Nevertheless, attained specific radioactivity is sufficient enough for PET investigations of enzymes, receptors, or transporters in the living organism.¹⁹⁰

1.3.3.3.2 ¹⁸F Radiolabeling Reactions

Variable chemical forms of [¹⁸F]fluoride are obtained, depending on the nuclear reaction, employed for its production. Thus, several target materials find their use in [¹⁸F]fluorine labeling reactions.²³⁷ The main synthetic strategies for ¹⁸F labeling include direct fluorination, which can be subdivided into nucleophilic and electrophilic ¹⁸F-fluorination reactions, and indirect fluorination, with fluoroalkylations and fluoroethylations as the most important class thereof. Mostly, nucleophilic ¹⁸F-fluorination reactions are employed for the preparation of ¹⁸F-labeled radiopharmaceuticals, since they prove greater selectivity and capability to give compounds with high specific radioactivity.^{180,220} However, fluoroalkylations, especially fluoroethylations gained more importance over the last years, as ¹⁸F-fluoroalkylated tracers show valuable alternatives for ¹¹C-labeled compounds, with the same biologic activity.^{238,239}

- *Nucleophilic ¹⁸F-Fluorination Reactions*

In general, [¹⁸F]fluoride is employed in nucleophilic ¹⁸F-labeling reactions, which is produced according to the ¹⁸O(p,n)¹⁸F reaction and obtained from aqueous medium.¹⁹⁰ Usually, positively charged counterions, leached from the target surface during the irradiation process, form co-resident particles in the aqueous solution, beside ¹⁸F anions.²⁴⁰ Thus, ion-exchange columns are employed for the recovery of [¹⁸O]H₂O and fast separation from positively charged counterions.²²⁰ However, the aqueous fluoride obtained from the column is a poor nucleophile due to its high degree of solvation, and rather unreactive due to the high charge density of the anion.¹⁸² Therefore, [¹⁸F]fluoride ions require activation for the nucleophilic attack, before the application in radiolabeling reactions. The addition of positively charged counterions in terms of alkali salts and

cryptands before the removal of water has proven to be crucial for improving the reactivity of [^{18}F]fluoride ions for nucleophilic substitution reactions. The metal ion (Rb, Cs, K) is readily obtained from its respective carbonate, bicarbonate or hydroxide, and used in combination with a cryptand for activation. Most commonly, the aminopolyether Kryptofix 2.2.2. (4,7,13,16,21,24-Hexaoxa-1,10-diazabicyclo[8.8.8]hexacosane, K_{222}) is used as cryptand in combination with potassium carbonate, since CO_3^{2-} does not evoke base catalyzed side reactions.^{206,241} K_{222} and the potassium cation form a strong complex, which leaves the fluoride ion exposed and highly nucleophilic, when dissolved in a polar nonprotic solvent (e.g. DMF, DMSO, or acetonitrile).²²⁰ Alternatively, also tetrabutylammonium salts are employed for the activation of $^{18}\text{F}^-$, which do not only give greater yields of fluorinated products but also reduce reaction times.²⁴²

The substitution of a suitable leaving group with [^{18}F]fluoride has been proved an excellent method for the preparation of aliphatic C- ^{18}F bonds.²⁴³ Thereby, the leaving group is selected in regard to accessibility, precursor stability, reagents, solvents, method of $^{18}\text{F}^-$ separation from precursors, and formation of side products. Especially, sulfonates (mesylate, tosylate or triflate), which are particularly reactive, represent prominent leaving groups and provide excellent yields in nucleophilic [^{18}F]fluorination reactions, like in the synthesis of [^{18}F]FDG. Besides sulfonates, also halides are adequate leaving groups for aliphatic, nucleophilic substitution reactions with [^{18}F]fluoride.^{206,244,245}

Also aromatic nucleophilic substitutions are frequently employed for the preparation of biomolecules. Thereby, a proton in the aromatic ring is often substituted with a [^{18}F]fluoride atom, since fluoride and hydrogen feature a similar atom size. However, significant changes in the character of the aromatic ring system occur, due to the higher electronegativity of the fluoride atom.^{218,246}

- *Electrophilic ^{18}F -Fluorination Reactions*

$[^{18}\text{F}]\text{F}_2$ gas appeared as one of the first reagents for electrophilic fluorination and is made accessible by the bombardment of a target gas, mainly consisting of neon.²⁴⁷ Due to its high reactivity, $[^{18}\text{F}]\text{F}_2$ preparation requires extensive cooling or the utilization of highly diluted $[^{18}\text{F}]\text{fluoride}$ solutions to prevent heavy exothermic reactions. Another approach is the direct conversion of $[^{18}\text{F}]\text{F}_2$ into less reactive and more selective ^{18}F -labeled fluorination agents, such as acetyl hypofluorite,²⁴⁸ xenon difluoride,²⁴⁹ or fluorosulfonamides.²⁵⁰

Electrophilic ^{18}F -fluorination reactions give end products with rather low specific activity and low radiochemical yields in comparison to nucleophilic ^{18}F -fluorination reactions, since the reagents are prepared from carrier added (i.e. unlabeled $^{19}\text{F}_2$ gas) $^{18}\text{F}_2$.¹⁸² Nevertheless, electrophilic approaches for the radiolabeling of PET radiopharmaceuticals still represent a key method, on which the preparation of several important PET tracers, such as $[^{18}\text{F}]\text{fluoro-L-DOPA}$ ^{244,251} and 2-L- $[^{18}\text{F}]\text{fluorotyrosine}$,²⁵² relies.

- *$[^{18}\text{F}]\text{Fluoroethylation and } [^{18}\text{F}]\text{Fluoroalkylation Reactions}$*

Numerous biologically active compounds contain alkyl side chains, such as methyl and ethyl functions, which serve as basis for radiolabeling reactions. A variety of fluoroalkylating agents, such as $[^{18}\text{F}]\text{bromofluoromethane}$,^{253,254} $[^{18}\text{F}]\text{fluoroiodomethane}$,²⁵⁵ 2- $[^{18}\text{F}]\text{bromofluoroethane}$,^{256,257} 2- $[^{18}\text{F}]\text{tosyloxyfluoroethane}$,^{243,258} 3- $[^{18}\text{F}]\text{bromofluoropropane}$,²⁵⁹⁻²⁶¹ 3- $[^{18}\text{F}]\text{fluoroiodopropane}$,^{261,262} and 3- $[^{18}\text{F}]\text{tosyloxyfluoropropane}$,²⁶³ has been developed. Mostly, small alkyl chains are employed in the preparation of ^{18}F -fluoroalkylated tracers, not only to minimize structural differences in regard to the precursor molecule but also to preserve physiological parameters as well as biologic activity.^{238,239}

[¹⁸F]Fluoroethylation reactions represent the most important class amongst [¹⁸F]fluoroalkylations, since [¹⁸F]fluoroethyl groups are comparable with methyl and ethyl groups in steric and electronic properties. In addition, fluoroethylations are simple reactions, as [¹⁸F]fluoroethylating agents can be easily produced from commercially available sources.²²⁹ Usually, reagents like 2-[¹⁸F]tosyloxyfluoroethane,²⁶⁴ or 2-[¹⁸F]bromofluoroethane,²⁶⁵ which are easy to prepare, very stable, and suitable for a variety of compounds, find their use in [¹⁸F]fluoroethylation reactions. Wadsak *et al*²²⁹ describe ten different approaches for the preparation and purification of 2-[¹⁸F]bromofluoroethane and 2-[¹⁸F]tosyloxyfluoroethane, in which the combination of 2-[¹⁸F]bromofluoroethane and its purification *via* distillation proved advantageous. Targets for [¹⁸F]fluoroethylations are amine,²⁶⁶⁻²⁷¹ hydroxylic,^{272,273} mercapto,^{274,275} and carboxyl moieties.^{238,239,276-279}

1.3.4 Recent Advances in the Field of PET Technology

As PET is a relatively young discipline, numerous technical innovations have taken place over the years, not only in regard to the PET facility itself, but also in the field of radionuclide production as well as radiopharmaceutical preparation.

Increasing interest in hybrid PET/MR systems has emerged over the last few years, since the combination of MR and PET measurements provides numerous advantages: A recent report from the research institute Juelich²⁸⁰ discussed an improvement in the field strength of MRI scanners, which provides higher spatial resolution, higher functional contrast, and enhanced image contrast thus significantly facilitating structural imaging. In addition the study pointed out the advantage for PET image reconstruction and the negligible need of performing scans in two separate machines when using integrated PET/MR technology. Lately, Shah *et al*²⁸¹ also discovered a better image quality by the employment of a hybrid PET/MR system. The presence of a large static magnetic field leads to the reduction of the positron range of PET radionuclides, thereby improving PET

image resolution and contrast. Jadvar and Colletti²⁸² pinpointed the advantage of PET/MRI over PET/CT and referred to better diagnostic evaluation, clinical decision-making, as well as patient management and patient outcome by the combination of PET and MRI. In their paper²⁸² they summarize the current evidence on use of PET/MRI in several disease processes, such as neuropsychiatric, cardiac, and oncologic diseases. By providing unparalleled structural, metabolic and functional information, PET/MRI enables opportunities for novel paradigms for brain function, accurate receptor density mapping, and metabolic imaging, which according to the authors characterizes PET/MRI as the perfect tool for paving the way towards personalized care.

New developments in PET technology were made by Okamoto *et al.*²⁸³ The research group generated an animal PET scanner, using flat-panel position-sensitive PMTs, which provide high resolution as well as a large field of view (FOV). This PET scanner enables the investigation of non-human primates under conscious condition and acquires data in a 2D or 3D mode. Recently, also Lu *et al.*²⁸⁴ reported improvements in small animal PET scanners by the incorporation of Silicon Photomultipliers (SiPMs). Due to superior attributes of SiPM detectors, such as compact size, high photon detection efficiency, insensitivity to magnetic fields, and low operating voltage, they find application in compact, lightweight SiPM-based PET imaging systems.

Casella *et al.*²⁸⁵ recently reported progress in the development of novel detector systems for a high resolution Time Of Flight-PET (TOF-PET) facility. The employment of LYSO crystals together with digital Silicon Photomultipliers (dSiPMs) enables excellent intrinsic time resolution and a high level of integration, which makes this device unprecedentedly compact and particularly attractive for TOF-PET detector systems. Pizzichemi²⁸⁶ describes the development of a TOF-PET system in the context of designing a multi-modal imaging device (EndoTOFPET-US)²⁸⁷ that combines ultrasound endoscopy with TOF-PET for the detection of prostate and pancreatic cancer. Therefore, excellent spatial resolution as well as a good signal to noise ratio are required in order to detect small lesions and ensure early cancer diagnosis.

By developing a novel cyclotron, which is currently installed at the research institute Juelich, IBA Technologies recently contributed to the field of radionuclide production.²⁸⁸ Besides 30 MeV protons and 15 MeV deuterons also 30 MeV alphas can be produced, which gives the opportunity of augmenting the number of medically employed radionuclides. Additionally, the cyclotron comprises a dual-beam technique, which enables simultaneous radiation of radionuclides for radiopharmaceutical production as well as for research purposes.

Bengel *et al*²⁸⁹ recently described several newly prepared radiotracers and give an excellent overview of their application in the field of cardiology, oncology, and neurology. Within this review,²⁸⁹ also several prostate specific membrane antigen (PSMA) ligands for the imaging of prostate cancer were discussed. ⁶⁸Ga and ^{99m}Tc labeled tracers as well as ⁶⁸Ga, ¹⁷⁷Lu, and ¹³¹I labeled chelator-conjugated ligands showed high affinity for PSMA and might open new perspectives for therapeutic and diagnostic approaches in prostate cancer imaging. Bengel *et al*²⁸⁹ further described the first clinical PET results for ⁶⁸Ga-CPCR4.2, a new PET imaging agent for CXCR4. Since CXCL12/CXCR4 is involved in the signaling pathway of various pathophysiological phenomena, this novel tracer opens a new and exciting field of clinical research, as it exhibits excellent imaging characteristics, high affinity and selectivity, as well as high uptake in various tumors, and especially lymphoproliferative diseases. A new approach in the field of NET imaging was recently reported by Zhang *et al*.²⁹⁰ [¹⁸F]-MFBG was identified as a promising radiopharmaceutical for specifically imaging NET-expressing neuroblastomas. Since it showed higher sensitivity, fast pharmacokinetics, and better detection of small lesions, even with low NET expression, [¹⁸F]-MFBG is preferred over ¹³¹I/¹²³I-MIBG in NET related imaging studies.

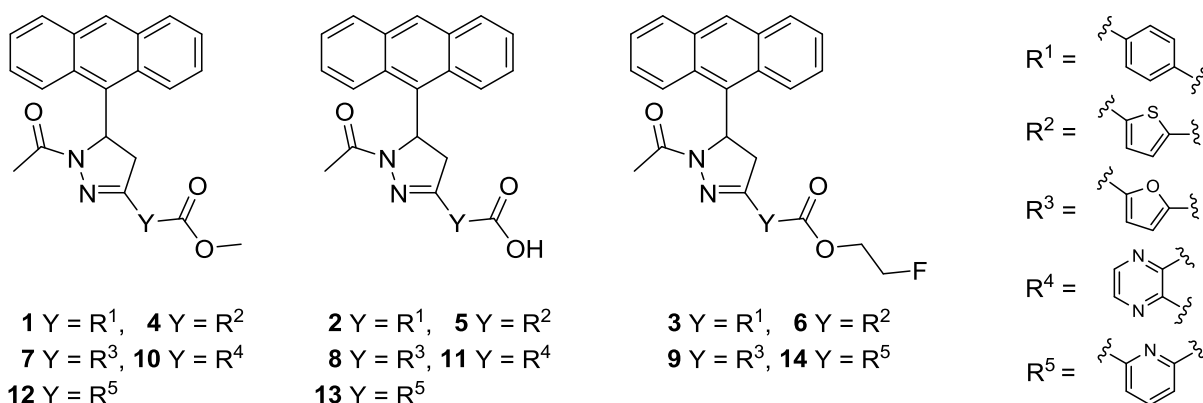
Within the scope of this organic preparative thesis, also *in silico* studies and first experiments concerning substance lipophilicity and BBB penetration were performed at the Medical University of Vienna. The described PET methods as well as methylation and

fluoroethylation radiolabeling reactions though were not part of this thesis. However, these methods, which will be used for the continuation of this project, are discussed to assure the understanding of the purpose of the presented thesis. After preclinical testing and the selection of the most potent reference compounds, their respective precursors will be radiolabeled with ^{11}C and/or ^{18}F (derived from the cyclotron) for the investigation of MAO-B and NET in the living organism *via* PET imaging.

2 DISCUSSION

2.1 Aim

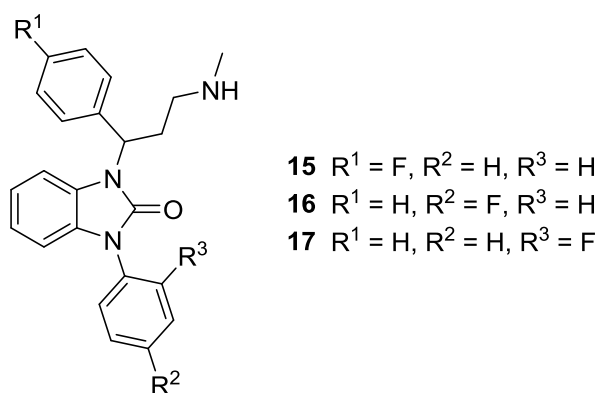
The aim of this thesis was the computational evaluation, synthesis, NMR-spectroscopic characterization, and preclinical testing of MAO-B and NET binding precursors and reference compounds for the development of ^{11}C - and ^{18}F -radiolabeled PET tracers, which allow *in vivo* investigation of MAO-B and NET related (dys)regulation mechanisms via positron emission tomography.



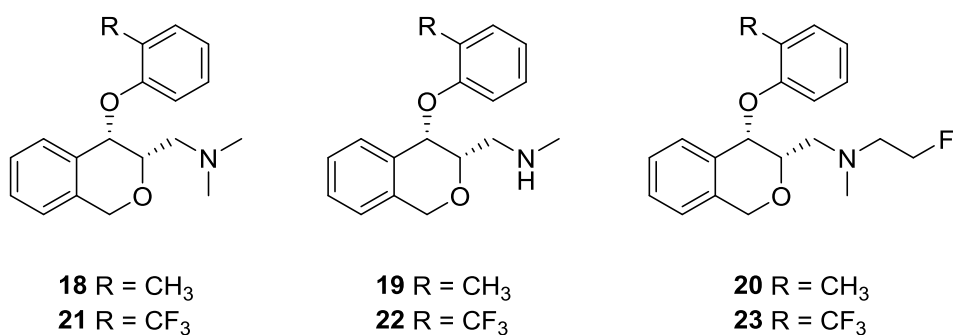
For the MAO-B system, a compound library of new, reversible PET tracer precursors (**2**, **5**, **8**, **11**, **14**) and reference compounds (**1**, **3**, **4**, **6**, **7**, **9**, **10**, **12**, **13**) should be prepared by applying principles of bioisosterism to 5-(anthracen-9-yl)-3-phenyl-4,5-dihydro-1H-pyrazole (cf. chapter 1.1.3), a compound which was recently reported a highly selective and extremely potent reversible MAO-B inhibitor.³⁴ *In silico* evaluations of the envisaged compound library should allow first conclusions to be drawn with respect to the affinity to MAO-B.

For PET based investigations of the NET, new reference compounds as well as precursors of two different substance classes should be synthesized and tested within the scope of this thesis:

Based on the previously described and evaluated NET affine derivative 1-(3-(methylamino)-1-phenylpropyl)-3-phenyl-1,3-dihydro-2H-benzimidazol-2-one (Me@APPI)^{167,169} (cf. chapter 1.2.4.1), several fluorinated analogs (FAPPI:1-3, **15-17**) should be subjected to *in silico* studies for first affinity and selectivity evaluations in respect of NET, DAT, and SERT, prior to synthesis.



Furthermore, recently reported, highly NET affine 4-phenoxy-3,4-dihydro-1H-isochromen derivatives (Me@PHOXI:1, **18**; PHOXI:1, **19**; Me@PHOXI:2, **21**; PHOXI:2, **22**)¹⁷⁶ should be made accessible as well as the fluoroethyl-methyl-amine analogs (FE@PHOXI:1, **20**; FE@PHOXI:2, **23**) thereof.



All developed precursors and references should be examined and characterized by employing spectroscopic as well as spectrometric analytical methods. In addition, they

were planned to be subjected to first preclinical studies (logP analyses and IAM experiments), which serve for the evaluation of the envisaged compounds in regard to the lipophilicity and BBB penetration potential *via* passive diffusion.

Since MAO-B (1, 3, 4, 6, 7, 9, 10, 12, and 13) and NET (15-18, 20, 21, and 23) references feature identical chemical properties in comparison to their radioactive analogs, they serve as standards for radiochemical evaluation and will be subjected to further preclinical experiments at the Medical University of Vienna. The most promising candidates among these compounds regarding their suitability as potential MAO-B or NET ligands will then be selected for further *in vivo* investigations of the MAO-B or NET system, respectively.

For this purpose, MAO-B (2, 5, 8, 11, and 14) and NET (19 and 22) precursors will be employed as starting materials for the synthesis of radiolabeled [¹¹C] and [¹⁸F] based PET tracers, respectively, which in continuative studies, will serve as probes for the visualization, detection, and investigation of MAO-B enzymes and NE transporters in the living organism.

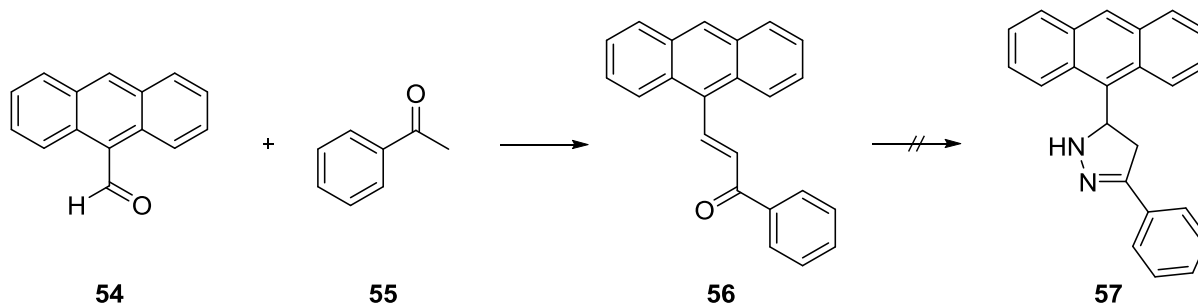
2.2 Reversible MAO-B Inhibitors

On the basis of the excellent binding properties of the highly selective and reversible MAO-B inhibitors previously described by Mishra *et al*,³⁴ a compound library of methyl- and fluoroethyl-substituted 5-(anthracen-9-yl)-4,5-dihydro-1H-pyrazole derivatives was prepared by applying principles of bioisosterism (cf. chapter 1.1.3) to the benzene ring of the molecule. After the synthesis, all compounds were subjected to lipophilicity and BBB penetration studies at the Medical University of Vienna for the determination of their suitability as future radioligands for the MAO-B system.

2.2.1 Preceding Syntheses

2.2.1.1 Preparation attempt of 5-(anthracen-9-yl)-3-phenyl-4,5-dihydro-1H-pyrazole (57)

In preparation for the development of methyl ester derived reference compounds (27, 29, 31, 33, 35, 37, and 39), the previously described reversible MAO-B inhibitor 57 should have been prepared according to the synthesis protocol of Mishra *et al*,³⁴ in order to evaluate suitability as well as applicability of the procedure.



Scheme 2

Therefore, anthracene-9-carbaldehyde (**54**) was reacted in an aldol condensation reaction with acetophenone (**55**) under mild basic conditions (scheme 2). The first step, the generation of the kinetic enolate of keton **55**, was performed by using sodium hydroxide, thus enabling the addition to anthracene-9-carbaldehyde (**54**). In the second step the resulting addition product was deprotonated at the α -carbon to form an enolate which subsequently formed an α , β -unsaturated carbonyl with the loss of hydroxide (via 1,2-elimination) to give chalcone **56**. By pouring the crude reaction product on ice and pH adjustment (pH=2) of the resulting solution, desired compound **56** was easily separated from by-products, which dissolved in the aqueous medium. Filtration and subsequent recrystallization assured high purity and excellent yields of **56**.

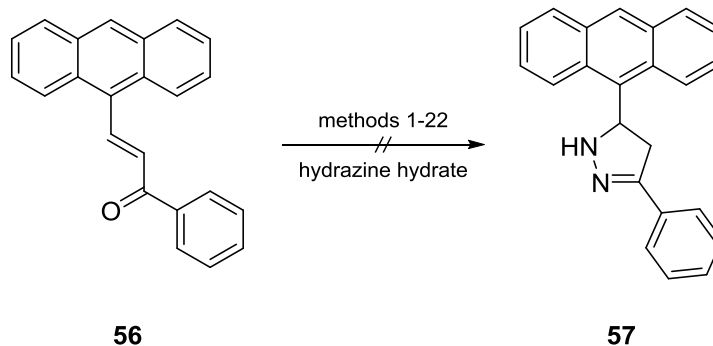
The cyclization of **56** into **57** was envisaged to be performed in one step consisting of two parts: In an aza-Michael addition, the nucleophile hydrazine monohydrate should have attached to the β -position of the α , β -unsaturated carbonyl compound (**56**). Although amines are strong nucleophiles and usually react readily with Michael acceptors without acid or base catalysis, several addition methods attempted failed, even under acidic or alkaline conditions (scheme 3).

The second part of this one step reaction would have comprised an addition-elimination reaction, where the free amine group of hydrazine monohydrate should have added intramolecularly to the carbonyl carbon in **56** and subsequent dehydration should have yielded the C=N double bond, since the elimination of oxygen in form of water is thermodynamically favored.

Although several methods for the preparation of **57** have been attempted (scheme 3) the desired product could not be obtained and it is unclear whether product formation did not occur or if the product decayed during the purification process due to instability of the pyrazoline ring.

In literature several reports refer to the stability of some pyrazoline derivatives,²⁹¹⁻²⁹³ however, several authors indicate the issue of pyrazoline instability.^{37,294} Despite untiring

efforts and numerous synthetic methods attempted derivative **57**, which was allegedly synthesized by Mishra *et al*,³⁴ could not be reproduced.



Methods 1-12, acidic reaction conditions

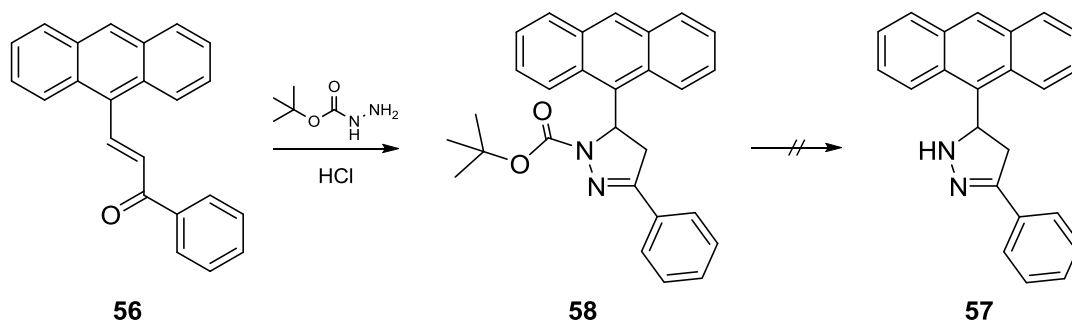
- 1.: 2N HCl, toluene, reflux, 2h
- 2.: Dean stark trap, AcOH, toluene, 4h
- 3.: Dean stark trap, AcOH, toluene, 1 drop H₂SO₄, 4h
- 4.: Microwave: MeOH, 700W, 85°C, 3min; 5min
- 5.: Microwave: EtOH, 700W, 85°C, 3min; 5min
- 6.: Microwave: MeOH, AcOH, 700W, 85°C, 7min; 8min; 15min,
- 7.: Microwave: MeOH, AcOH, 1 drop H₂SO₄, 700W, 85°C, 3min; 5min
- 8.: MeOH, AcOH, reflux, 6h
- 9.: AcOH, 1 drop H₂SO₄, reflux, 1.5h
- 10.: AcOH, 1 drop H₂SO₄, rt → 36°C, 24h
- 11.: Microwave: 2N HCl, 700W, 85°C, 5min,
- 12.: Microwave: conc. HCl, 700W, 85°C, 5min

Methods 13-22, basic and neutral reaction conditions

- 13.: MeOH, reflux, 1.5h
- 14.: Pyridine, 115°C, 45min
- 15.: Abs. EtOH, 0°C 6h → rt, 24h
- 16.: EtOH, reflux, 2.5h → ice → filtration
- 17.: abs. EtOH, reflux, argon atmosphere, 3h
- 18.: Dean stark trap, toluene, 5h
- 19.: NaOH solution in EtOH, reflux, 30min
- 20.: DMF:EtOH (1:1), 90-100°C, 4h
- 21.: Autoclave: MeOH, 80°C, 1h → over night
- 22.: EtOH, exclusion of light, argon atmosphere, reflux, 3h

Scheme 3

Neither heating under acidic (scheme 3, methods 1-12) or basic reaction conditions (scheme 3, methods 14, 19), nor microwave irradiation (scheme 3, methods 4-7, 11, 12), nor refluxing under pressure (scheme 3, method 21) led to the successful preparation of **57**. Also, exclusion of light (scheme 3, method 22), gradual removal of water (scheme 3, methods 2, 3, 18), variation of solvents, and exclusion of oxygen (scheme 3, methods 17 and 22) did not provide the desired product (**57**). Extended reaction times caused gradual decomposition but never afforded cyclization and also, the integration of a *tert*-butyloxycarbonyl protecting group at position 1 of the pyrazoline ring (**58**) followed by the subsequent cleavage thereof employing hydrochloric acid (scheme 4) was unsuccessful and did not yield desired pyrazoline derivative **57**.



Scheme 4

As compound **57** could not be made accessible by varying several methods (scheme 3), another synthetic approach had to be developed: Since Mishra *et al*³⁴ accomplished the cyclization reaction mostly with compounds, featuring strong electron withdrawing groups (e.g. NO₂) at the phenyl ring, instability of **57** may be ascribed to the bare phenyl ring. Hence, an electron withdrawing moiety was introduced at position 4 of the phenyl ring in order to acquire compound stability.

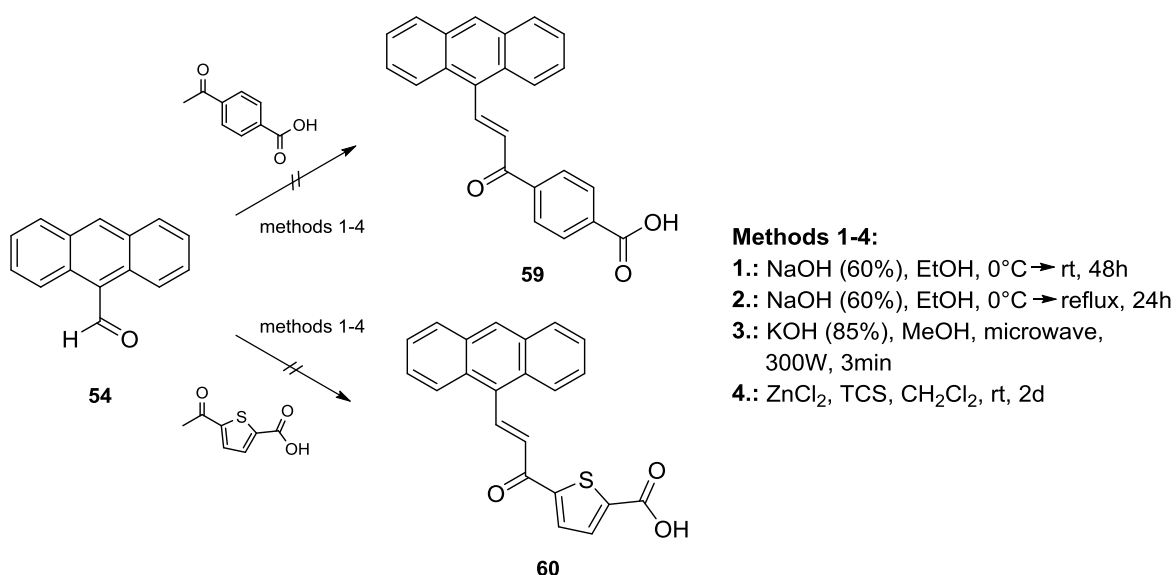
2.2.1.2 Preparation attempt of 4-((2E)-3-(anthracen-9-yl)prop-2-enoyl)benzoic acid (**59**) and 5-((2E)-3-(anthracen-9-yl)prop-2-enoyl)thiophene-2-carboxylic acid (**60**)

In the attempt of improving compound stability, a carboxylic acid group, which features strong electron withdrawing effects, was introduced at the ring where bioisosteric changes were performed (scheme 5). The introduction of this group should not only improve compound stability, but furthermore should serve as a prerequisite for later radiolabeling with ¹¹C and ¹⁸F as well as for the preparation of non-radiolabeled methyl and fluoroethyl esters.

Hence, commercially available anthracene-9-carbaldehyde (**54**) was subjected to an aldol condensation reaction with 4-acetylbenzoic acid or 5-acetylthiophene-2-carboxylic acid, respectively (scheme 5). Following the synthesis protocol of Mishra *et al*,³⁴ the reaction was carried out at 0°C, by employing an aqueous sodium hydroxide solution as base. Since however no product formation could be detected by thin-layer chromatography

(TLC) after two days, the procedure was altered (scheme 5): On the one hand, conventional refluxing was employed to achieve the conversion of **54** into **59** or **60**, and on the other hand, a microwave assisted approach in methanol was performed. Both methods however only yielded a multi-component mixture, but did not provide the desired products.

Therefore, a method of Badawy *et al*²⁹⁵ was adapted in which the binary reagent tetrachlorosilane/zinc chloride should have catalyzed the reaction of **54** with 4-acetylbenzoic acid or 5-acetylthiophene-2-carboxylic acid, respectively (scheme 5). After isolation of the formed products however, NMR (nuclear magnetic resonance) spectroscopic analysis also ruled out product formation.



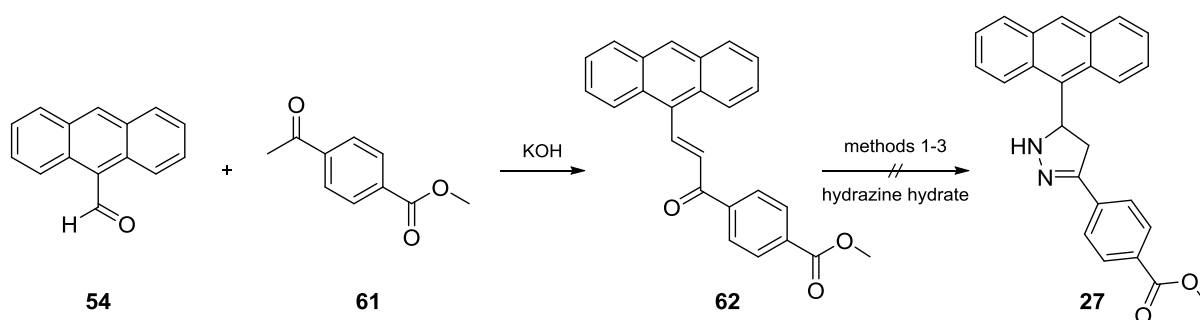
Scheme 5

Since chalcones **59** and **60** could not be made accessible by reacting anthracene-9-carbaldehyde (**54**) with the above mentioned reagents containing free carboxylic acid groups (scheme 5), another approach for the preparation of the aldol condensation products was developed, which should assure the successful conversion into the desired products.

2.2.1.3 Preparation attempt of methyl 4-(5-(anthracen-9-yl)-4,5-dihydro-1H-pyrazol-3-yl)benzoate (27) and methyl 5-(5-(anthracen-9-yl)-4,5-dihydro-1H-pyrazol-3-yl)thiophene-2-carboxylate (31)

Derivatives **61**, **63**, **74**, **75**, **88**, and **97**, bearing a methyl ester function were selected to be reacted with anthracene-9-carbaldehyde (**54**) in order to successfully prepare chalcones **62**, **64**, **76**, **77**, **89**, and **98** which represent essential intermediates for the subsequent cyclization reaction to furnish the desired methyl ester based target compounds **27**, **29**, **31**, **33**, **35**, **37**, and **39** in only two reaction steps.

For the aldol condensation, a method of Basnet *et al*²⁹⁶ was adapted, in which dropwise addition of an aqueous potassium hydroxide solution at 0°C led to deprotonation of **61** and enabled the reaction with aldehyde **54**. After 2 days of stirring at room temperature, TLC monitoring revealed almost complete conversion of **54** into desired product **62** (scheme 6). NMR spectroscopic analysis confirmed the formation of methyl 4-((2E)-3-(anthracen-9-yl)prop-2-enoyl)benzoate (**62**), which could be easily separated from its by-products by filtration and was isolated as yellow crystals.



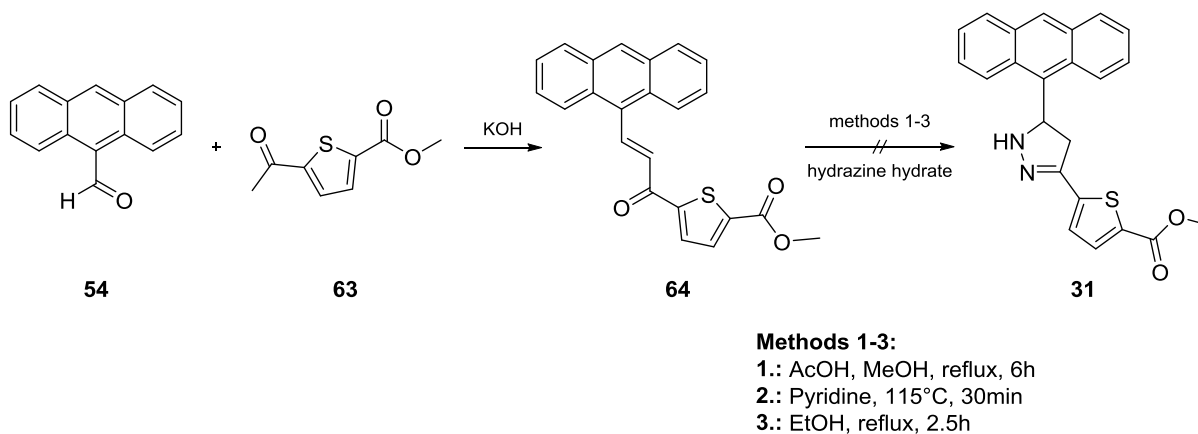
Methods 1-3:

- 1.: AcOH/1 drop H₂SO₄, reflux, 1.5h
- 2.: AcOH/1 drop H₂SO₄, toluene, reflux, 4h
- 3.: AcOH/1 drop H₂SO₄, 700W, 85°C, 5min

Scheme 6

Since 5-(anthracen-9-yl)-3-phenyl-4,5-dihydro-1*H*-pyrazole (**57**) could not be obtained by varying numerous reaction methods (schemes 3 and 4), it was investigated, if the introduction of a methyl ester moiety changed molecule properties and led to cyclization. Therefore, three different approaches (scheme 6) were selected for the formation of **27**, but neither conventional heating in acetic acid/sulfuric acid, nor refluxing in a Dean Stark trap with acetic acid/sulfuric acid, nor a microwave assisted preparation method in acetic acid yielded desired product **27**.

By analogy with **62**, also methyl 5-((*E*)-3-(anthracen-9-yl)prop-2-enoyl)thiophene-2-carboxylate (**64**) was synthesized (scheme 7). Thereby, aldehyde **54** was reacted with methyl 5-acetylthiophene-2-carboxylate (**63**), which could straightforwardly be prepared from 5-acetylthiophene-2-carboxylic acid in a simple and rapid esterification reaction with trimethylsilyldiazomethane. Chalcone **64** could be obtained in the form of yellow crystals in the same manner as **62** (scheme 6), and was attempted to be cyclized with hydrazine monohydrate by employing three different reaction methods (scheme 7).



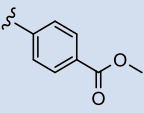
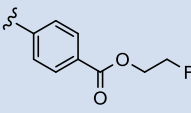
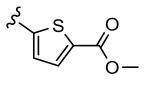
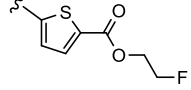
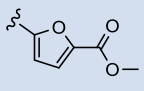
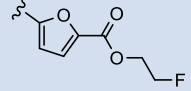
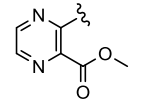
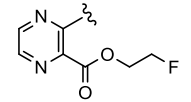
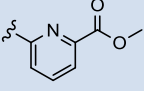
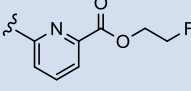
Scheme 7

Similar to the cyclization attempt of **56** and **62** to **57** and **27**, respectively (schemes 3, 4, and 6), neither acidic nor basic reaction conditions afforded the desired product **31** (scheme 7). Close TLC monitoring revealed decomposition, which was confirmed after NMR spectroscopic analysis of the isolated fractions.

In summary, it was discovered that chalcones (**62** and **64**) can be made accessible by introducing a methyl ester moiety instead of the free carboxylic acid function, which did not only allow straightforward work up due to the simple separation of by-products, but also provided the compounds (**62** and **64**) in good yields. Additionally, the introduction of the ester moiety is a crucial prerequisite, which serves as a linker for a stable connection between the core structure and the later introduced positron emitting radionuclide. The ester moiety was placed at the ring of the molecule, which was subjected to bioisosteric changes, always taking into account the logP value, which should lie below 5 for proper BBB penetration.³⁶

The preparation of cyclization products **27** and **31** however, remained unsuccessful. Thereby, it is rather unknown, whether the conversion into the desired compounds (**27** and **31**) failed or the products decomposed during the purification process.

Due to several failed cyclization attempts, which may be ascribed to the instability of the pyrazoline ring, the original compounds were altered: Since the incorporation of an acetyl moiety^{37,38,39} was reported in the literature to improve overall chemical stability of pyrazoline derivatives and additionally enhance MAO-B inhibitory activity,³⁸ the core structure of the molecules (e.g. scheme 2, compound **57**) was modified by attaching an additional acetyl moiety at position 1 of the pyrazoline ring. Table 2 lists the envisaged compound library, which depicts molecules with ester residues, featuring an acetyl group at the pyrazoline ring, and the corresponding calculated logP values.

compound	calc. logP	compound	calc. logP
 1	4.66	 3	4.85
 4	4.70	 6	4.89
 7	3.33	 9	3.52
 10	2.83	 65	3.02
 12	4.17	 14	4.36

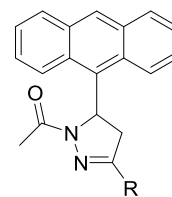


Table 2: Calculated logP values of the envisaged acetyl derived pyrazoline methyl esters (**1**, **4**, **7**, **10**, and **12**) and fluoroethyl esters (**3**, **6**, **9**, **65**, and **14**)

2.2.2 Docking Studies

Docking studies were performed in cooperation with the Pharmacoinformatics Research Group at the University of Vienna, Faculty of Life Sciences.

In order to estimate the binding affinity of the modified compounds, they were docked into the crystal structure of the human MAO-B enzyme in complex with FAD and non-covalently bound *p*-nitro-benzylamine (PDB code 2C70) (cf. chapter 3.2.1). Methyl esters (**1**, **4**, **7**, **10**, and **12**) and fluoroethyl esters (**3**, **6**, **9**, and **14**), as well as reference compounds **66** and **67** (the most active compounds in the report of Mishra *et al.*,³⁴ figure 14), were prepared for a physiological pH using LigPrep (LigPrep, version 2.5, Schrödinger, LLC, New York, NY, 2012).

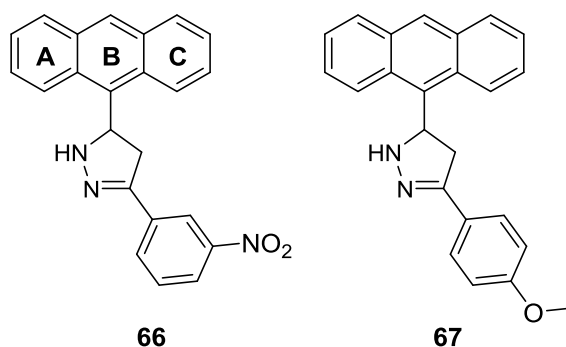


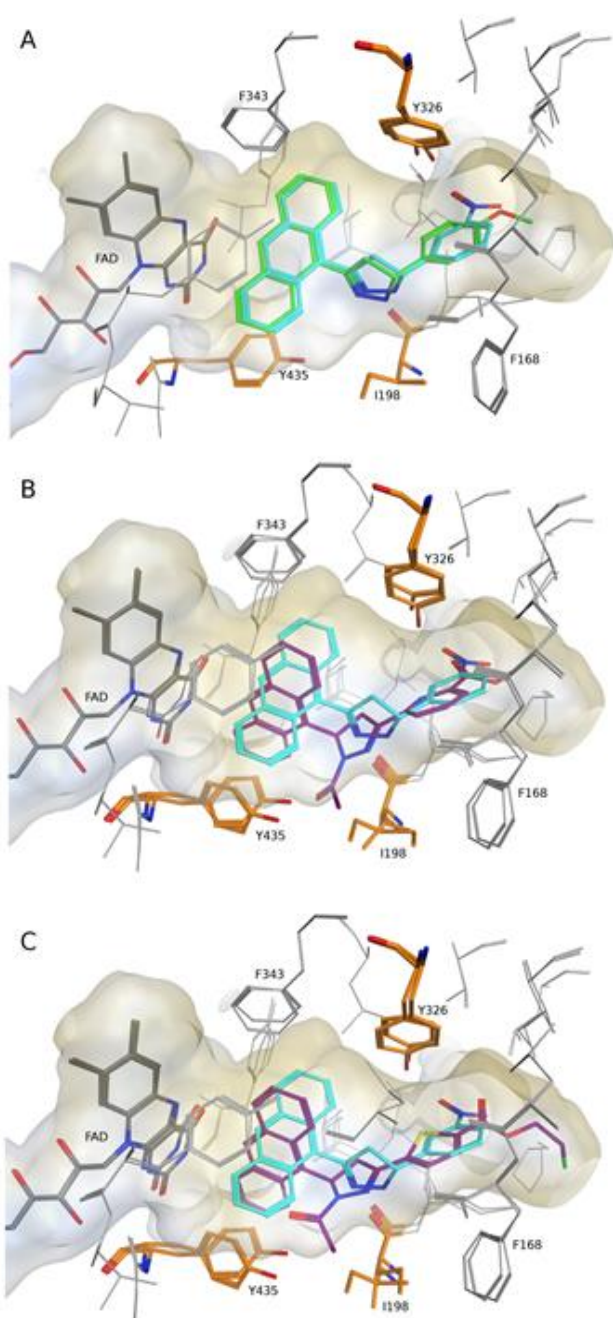
Figure 14: Chemical structure of reference compounds 5-(anthracen-9-yl)-3-(3-nitrophenyl)-4,5-dihydro-1H-pyrazole (**66**) and 5-(anthracen-9-yl)-3-(4-methoxyphenyl)-4,5-dihydro-1H-pyrazole (**67**)

As the acetyl substituent on the pyrazoline ring had to be accommodated within a relatively narrow binding pocket, side chains of the residues in the hydrophobic pocket (Ile198 and Tyr435) were allowed to take possible rotamer orientations defined within the GOLD docking software.²⁹⁷ A maximum of ten poses per ligand was allowed, primarily ranked by the default scoring function, ChemPLP.²⁹⁸ In order to reduce strain energies caused by the placement algorithm, the complexes were energy minimized using a stepwise relaxation protocol within the MOE software package (Molecular Operating Environment (MOE) version 2013.0801, Chemical Computing Group, Montreal, Canada).

Subsequently, the binding free energy of the minimized complexes was estimated by external rescoring using X-Score,²⁹⁹ as the original scoring values of ChemPLP are *per se* dimensionless. K_i values were further calculated from ΔG values of the best scored pose per ligand, using equation 1.

$$K_i = \exp\left(\frac{\Delta G}{R * T}\right)$$

Equation 1: R = 8.3144621 J/mol*K; T = 298.15 Kelvin



Analysis of the docking results indicates that the novel compounds (1, 3, 4, 6, 7, 9, 10, 12, and 14) are able to be accommodated in a similar way as described for the reference compounds 66 and 67 (figures 15, 16, and 17).

As expected, introduction of bulky groups on the central heteroaromatic linker enforced a slightly different orientation of the synthesized compounds. Figure 15 shows the most prominent interaction among the observed poses, a pi stacking interaction between Tyr435 and ring A or C of the anthracene moiety.

Figure 15: MAO-B binding pocket in complex with references (66 and 67) and exemplary docking poses of methyl and fluoroethyl ester derivatives (6 and 12). Key residues are highlighted in orange. **A:** References 66 (cyan) and 67 (green) in superposition; **B:** Docking poses of 66 (cyan) and 12 (purple); **C:** Docked complexes of 66 (cyan) and 6 (purple)

Simultaneously, the phenolic hydroxyl group of the aromatic side chain of Tyr435 was frequently observed to stabilize the substituted heteroaromatic linker (acetyl moiety).

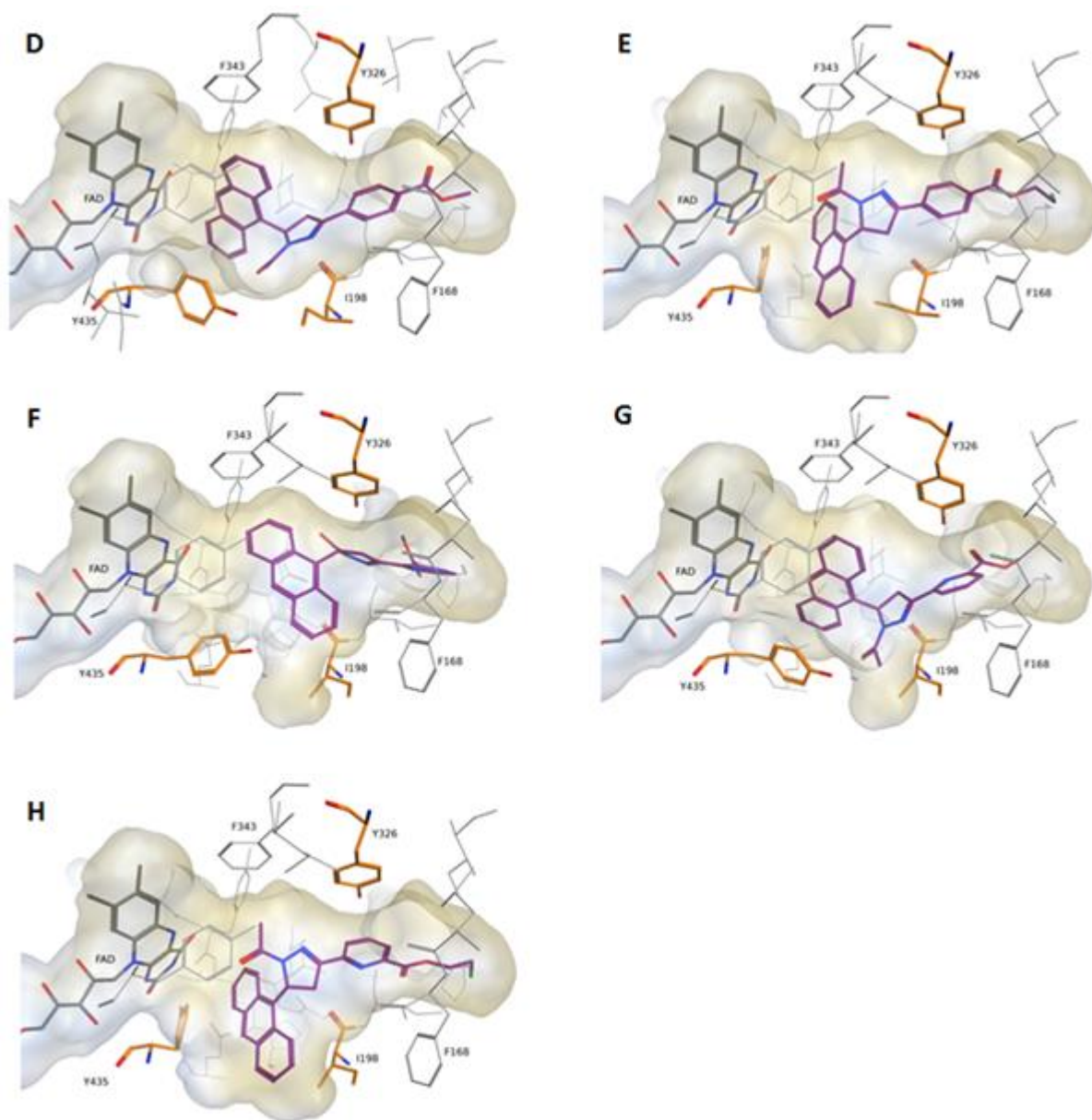


Figure 16: Benzene based reference compounds (D: **1**, E: **3**) and electron-deficient reference compounds (F: **10**, G: **12**, H: **14**) docked in the MAO-B active site

Potentially less favorable side chain orientations caused by the bulky substituents hence could be compensated. In analogy to the nitro group of compound **66**, the carbonyl oxygen of the distal ester function among the investigated molecules sporadically acted as hydrogen bond acceptor for the side chain of Tyr326. Due to the absence of an

acceptor atom in the corresponding position, reference compound **67** is unable to form this particular interaction, which could be an explanation for the inferior experimentally determined K_i value.

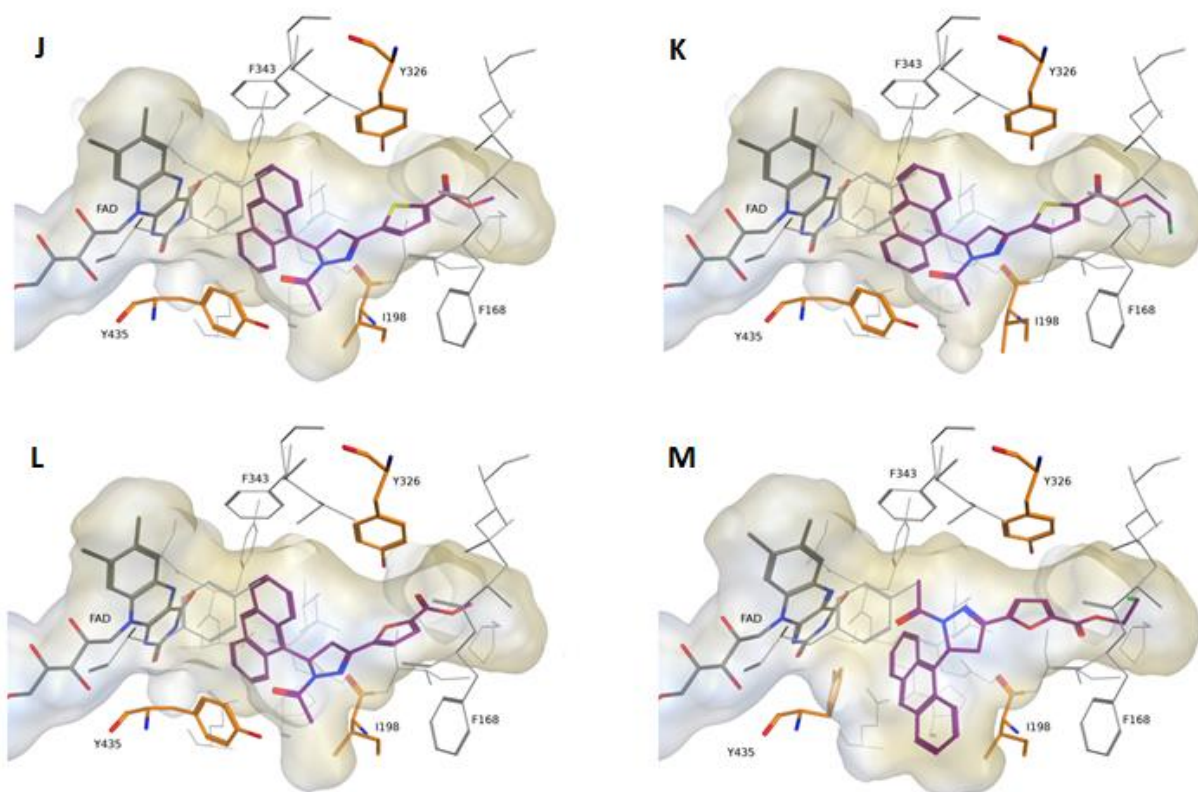


Figure 17: Docking poses of electron-rich reference compounds (J: **4**, K: **6**, L: **7**, M: **9**)

In general, the calculated K_i values were about an order of magnitude larger than the literature values of **66** and **67**. However, as demonstrated in table 3, it can be assumed that the activity of methyl esters (**1**, **4**, **7**, **10**, and **12**) and fluoroethyl esters (**3**, **6**, **9**, and **14**) is in the range of the reference compounds (**66** and **67**). As the significant activity difference between **66** and **67** was at least indicated by the calculated ΔG values, the energy estimates could as well be used for prioritizing new members of this compound class prior to *in vitro* testing.

Compound	1	3	4	6	7	9	10	12	14	66	67
calc. Ki (nM)	2.44	3.36	4.96	4.26	5.58	9.73	7.06	2.79	5.97	4.19	7.18

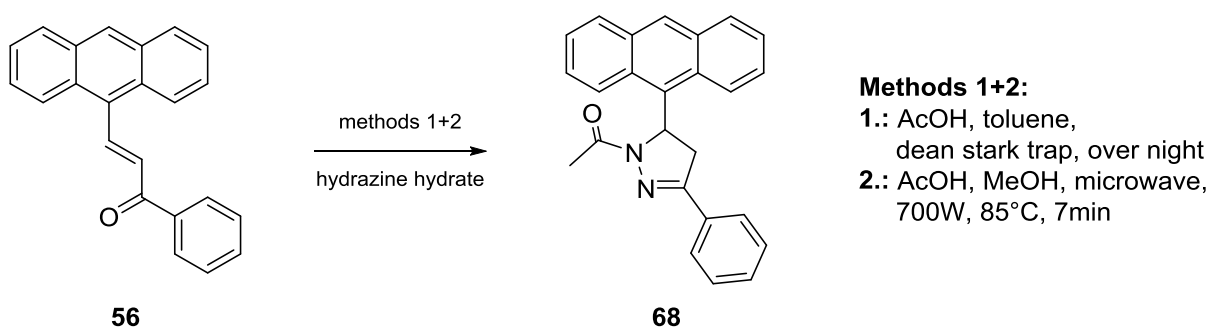
Table 3: Calculated Ki value of methyl esters (**1**, **4**, **7**, **10**, and **12**) and fluoroethyl esters (**3**, **6**, **9**, and **14**) as well as reference compounds (**66** and **67**)

2.2.3 Syntheses

2.2.3.1 Preparation of 1-(5-(anthracen-9-yl)-3-phenyl-4,5-dihydro-1H-pyrazol-1-yl)ethanone (**68**)

Since docking studies indicated potential binding of the new, envisaged compound library to MAO-B (table 3), chalcone **56** was reacted with hydrazine monohydrate and acetic acid as an experiment to verify if cyclization to **68** was possible (scheme 8).

The synthesis of this trisubstituted pyrazoline derivative was accomplished by employing two different approaches: According to the literature,^{38,39} heating is required for the preparation of pyrazoline derivatives. Thus, the first method included refluxing of **56** with acetic acid in toluene in a Dean Stark trap to remove formed water. In the following TLC, product formation could be observed as typical fluorescence at 366 nm of the aromatic system. However, emerging by-products necessitated repeated purification of **68**.



Scheme 8

The second approach was carried out by employing a microwave assisted preparation method. This kind of synthesis permits rapid heating of the reagents to 85°C in low boiling solvents like methanol and avoids the application of high boiling solvents such as *N,N*-dimethylformamide (DMF) or dimethyl sulfoxide (DMSO). As is generally known, DMF and DMSO are difficult to remove from the reaction mixture and therefore proved unsuitable for this method, especially as it was found that workup had to be conducted quickly due to rapid decomposition of **68**. Methanol was also chosen for this reaction approach due to its favorable microwave absorbing properties (loss factor ($\tan\delta$) = 0.659), which enabled efficient absorption and therefore rapid heating.³⁰⁰ Thus, the microwave assisted approach, which gave very good yields in short reaction times, was favored over the preparation by conventional heating.

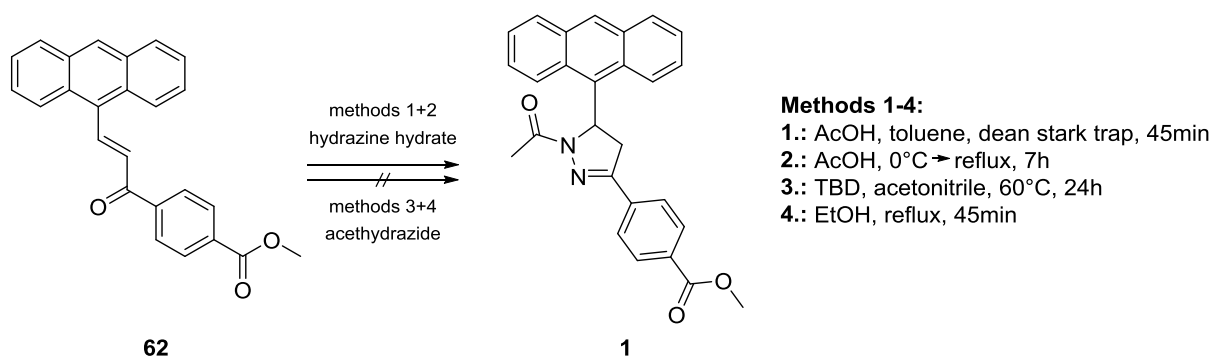
Successful synthesis and isolation of **68** demonstrated suitability of both cyclization methods, which may also serve as reliable preparation approaches for the synthesis of the envisaged methyl ester derived references (**1**, **4**, **7**, **10**, and **12**).

2.2.3.2 Preparation of methyl 4-(1-acetyl-5-(anthracen-9-yl)-4,5-dihydro-1*H*-pyrazol-3-yl)benzoate (**1**)

For the synthesis of methyl 4-(1-acetyl-5-(anthracen-9-yl)-4,5-dihydro-1*H*-pyrazol-3-yl)benzoate (**1**), several preparation approaches (schemes 9 and 10) were investigated in order to achieve maximum yields, as compound **1** represents a reference compound for MAO-B investigations and was to be employed in preclinical studies. Since methyl ester **1** was also applied as starting material for further syntheses, a larger scale production of this compound was necessary. Therefore, a simple and fast preparation route was required. Additionally, several analogs of lead compound **1** (e.g. **4**, **7**, **10**, and **12**) had to be made accessible within the scope of this thesis, thus evaluation of different preparation methods should facilitate their production and allow their synthesis in a fast and uncomplicated manner.

Since heating in a Dean Stark trap already gave 1-(5-(anthracen-9-yl)-3-phenyl-4,5-dihydro-1*H*-pyrazol-1-yl)ethanone (**68**) in moderate yields (scheme 8), the first method for the preparation of **1** was conducted by heating chalcone **62** with acetic acid in toluene (scheme 9). Although the resulting product (**1**) could be successfully separated from several by-products, it could only be obtained in poor yields, which necessitated a different preparation approach. Thus, the cyclization was carried out by combining the reactants at 0°C followed by conventional heating (scheme 9). However, this method also gave the desired compound (**1**) only in poor yields.

For the next preparation approach (scheme 9) a synthesis protocol of Mahé *et al*³⁷ was adapted, which involved the reaction of methyl 4-((2*E*)-3-(anthracen-9-yl)prop-2-enoyl)benzoate (**62**) with acethydrazide and triazabicyclo[4.4.0]dec-5-ene (TBD). As TBD selectively activates the N-H bond of acethydrazide, it catalyzes its conjugate addition of the secondary amine moiety, thereby giving rise to the formation of the cyclization product. However, after 24 h of stirring, starting material (**62**) could still be detected to a large percentage. Further refluxing neither provided the desired product but led to the formation of by-products, which proved this method unsuitable for the preparation of **1**. Also refluxing of acetylhydrazide with methyl 4-((2*E*)-3-(anthracen-9-yl)prop-2-enoyl)benzoate (**61**) in ethanol did not yield the desired product (**1**) (scheme 9).

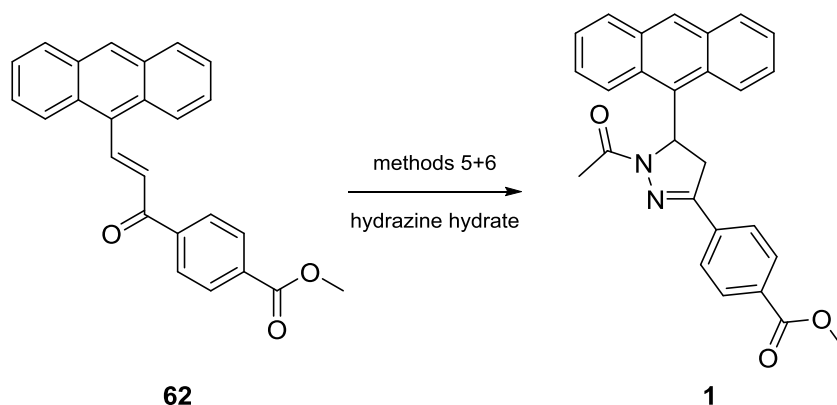


Scheme 9

Thus, the microwave assisted preparation method of **68** (scheme 8) was adapted by adding one drop of sulfuric acid as catalyst to acetic acid, which represented the solvent

and the reactant at once (scheme 10). Although, microwave absorbing properties of acetic acid ($\tan\delta = 0.174$) are inferior to those of methanol ($\tan\delta = 0.659$),³⁰⁰ this method demonstrated to improve yields of **1** in comparison to the other preparation approaches (scheme 9). After only five minutes, TLC analysis showed formation of product **1**, but unfortunately also indicated the emergence of several by-products, which had to be removed chromatographically.

In the attempt of reducing the formation of by-products and increasing yields, a last effort for the preparation of methyl 4-(1-acetyl-5-(anthracen-9-yl)-4,5-dihydro-1H-pyrazol-3-yl)benzoate (**1**) was made (scheme 10): Refluxing chalcone **62** with acetic acid in acetonitrile turned out to improve the yield by 2% in comparison to the microwave assisted method, however, a decrease in by-product formation could not be detected.



Methods 5+6:

5.: AcOH/1 drop H₂SO₄, microwave, 700W, 85°C, 5min

6.: AcOH, acetonitrile, reflux, 24h

Scheme 10

In conclusion, six different synthetic approaches were performed for the preparation of methyl 4-(1-acetyl-5-(anthracen-9-yl)-4,5-dihydro-1H-pyrazol-3-yl)benzoate (**1**). A side-by-side comparison in figure 18 demonstrates that method 5 as well as method 6 proved more suitable for the synthesis of reference compound **1** than methods 1 and 2.

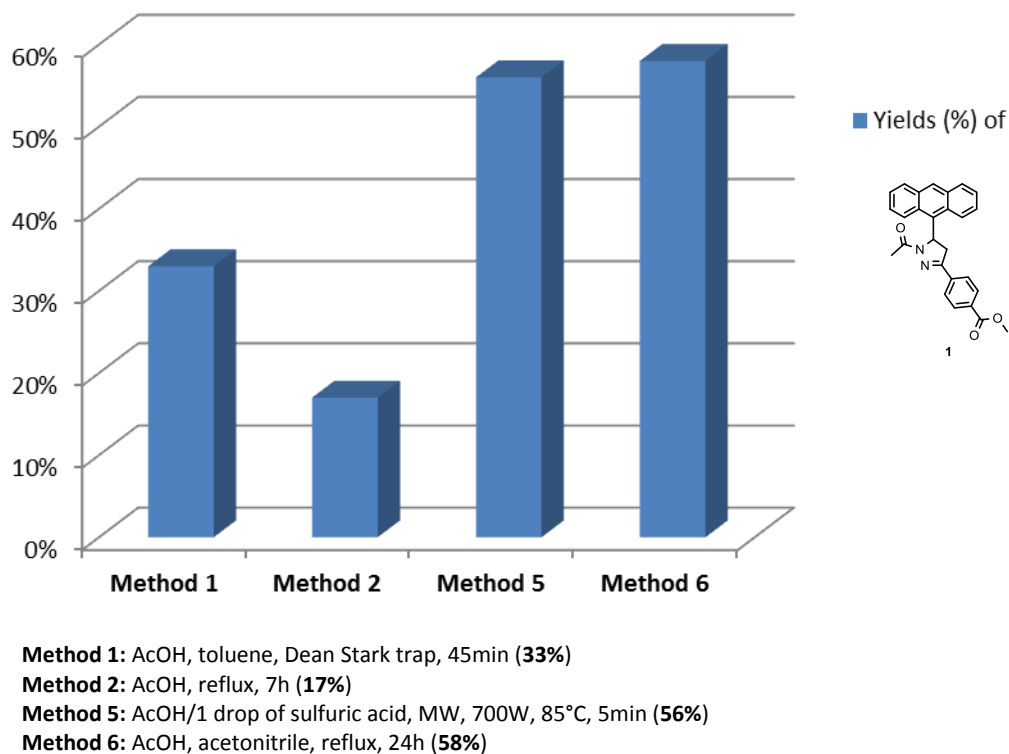
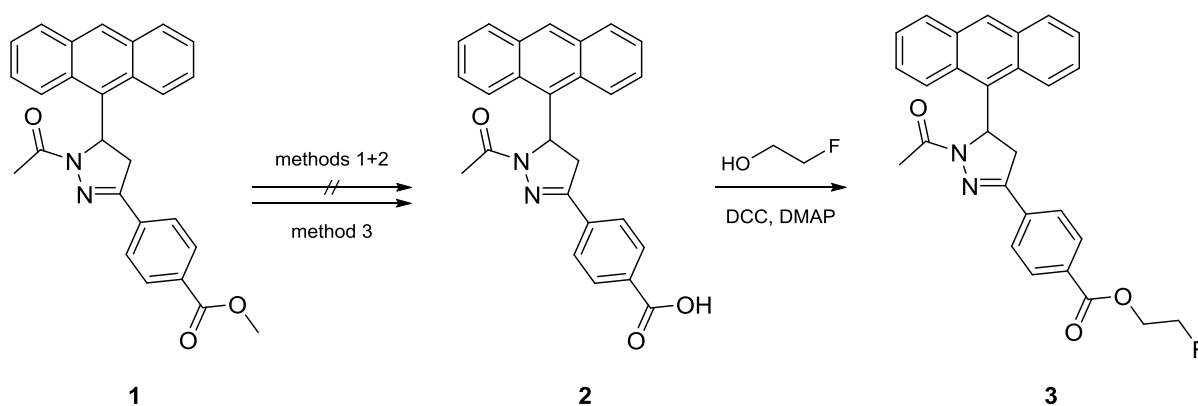


Figure 18: Diagram of direct yield comparison for cyclization methods 1, 2, 5, and 6 for the preparation of methyl 4-(1-acetyl-5-(anthracen-9-yl)-4,5-dihydro-1H-pyrazol-3-yl)benzoate (**1**)

Although refluxing of chalcone **62** with acetic acid in acetonitrile (method 6) provided **1** in higher yields (58%), the microwave assisted preparation approach (method 5) was favored for the cyclization of **62** into **1**, as only a difference of 2% in yield was determined. Since direct microwave heating reduces the reaction time from hours to minutes, increases reaction rates, and additionally improves reproducibility,^{300,301} the microwave assisted preparation approach was chosen for the larger scale synthesis of reference compound **1** as well as for the synthesis of several analogs thereof.

2.2.3.3 Preparation of 4-(1-acetyl-5-(anthracen-9-yl)-4,5-dihydro-1H-pyrazol-3-yl)benzoic acid (2) and 2-fluoroethyl-4-(1-acetyl-5-(anthracen-9-yl)-4,5-dihydro-1H-pyrazol-3-yl)-benzoate (3)

Since precursor compound **2** could not be made accessible by alkaline hydrolysis of **1** with potassium hydroxide, and also a preparation approach with lithium hydroxide monohydrate at 5°C failed to succeed, a method of Siddiqui *et al*³⁰² was adapted (scheme 11). By employing a solvent mixture of methanol/water/tetrahydrofuran and lithium hydroxide monohydrate, conversion of **1** into **2** could be detected by TLC analysis after stirring the reaction mixture for 4 h at 50°C. However, the formation of several by-products complicated purification due to their similar R_f values to **2**. Therefore, not only normal phase chromatography, but also reversed phase chromatography had to be employed several times for proper purification of compound **2**.



Methods1-3:

- 1.: KOH, MeOH/H₂O, rt, 72h
- 2.: LiOH·H₂O, MeOH/H₂O, 5°C, 24h
- 3.: LiOH·H₂O, MeOH/H₂O/THF, 50°C, 4h

Scheme 11

Fluoroethyl ester **3**, which represents a reference compound for the investigation of MAO-B, could be made accessible in a Steglich esterification in one single step under mild reaction conditions. Thereby, the conversion of the free carboxylic acid (**2**) with fluoroethanol into **3** was catalyzed by *N,N'*-dicyclohexylcarbodiimide (DCC)/4-

dimethylaminopyridine (DMAP) (scheme 11). Since workup had to be carried out rapidly due to fast decomposition of **3**, dichloromethane was chosen as a low boiling point reaction medium, which could be easily removed after completion of the reaction.

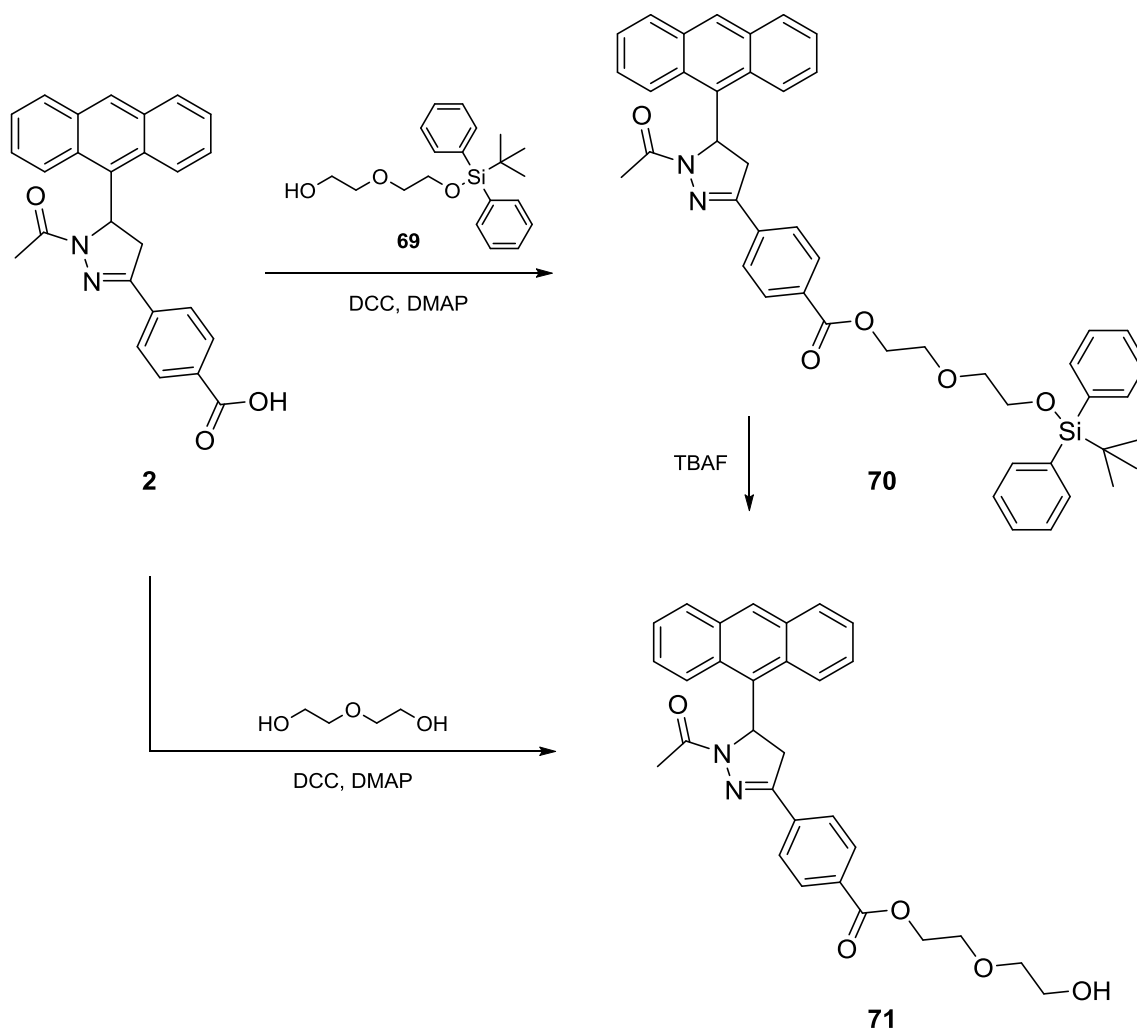
2.2.3.4 Preparation attempt of 2-(2-(((4-methylphenyl)sulfonyl)oxy)ethoxy)ethyl 4-(1-acetyl-5-(anthracen-9-yl)-4,5-dihydro-1H-pyrazol-3-yl)benzoate (**72**) and 2-(2-((methylsulfonyl)oxy)ethoxy)ethyl 4-(1-acetyl-5-(anthracen-9-yl)-4,5-dihydro-1H-pyrazol-3-yl)benzoate (**73**)

In addition to methyl 4-(1-acetyl-5-(anthracen-9-yl)-4,5-dihydro-1H-pyrazol-3-yl)benzoate (**1**) and 2-fluoroethyl-4-(1-acetyl-5-(anthracen-9-yl)-4,5-dihydro-1H-pyrazol-3-yl)benzoate (**3**), also their mesyl and tosyl polyethylene glycol analogs (**72** and **73**) should have been prepared. In the last few years, polyethylene glycol (PEG) modifications in biomolecules have been demonstrated to exhibit superior clinically useful properties in comparison to their corresponding unmodified parent molecules.³⁰³ The polymer does not only feature ideal pharmacological properties like low toxicity, reduced immunogenicity, and antigenicity, but also exhibits excellent pharmacokinetic (longer *in vivo* circulating half-lives, lower clearance, enhancing efficacy) and biodistribution behavior.^{304,305} Since several authors^{306,307} also refer to better BBB penetration by attaching a polyethylene glycol chain to a molecule, mesylate **72** and tosylate **73** should have served as starting points for methylation and fluoroethylation, respectively.

Compounds **72** and **73** should have been made accessible *via* intermediate **71**, which was prepared in two different manners (scheme 12): For the first one, derivative **69** was synthesized by deprotonation of diethylene glycol with imidazole, followed by its subsequent attack of *t*-butyl(chloro)diphenylsilane. Instead of DMF, which was employed as solvent in literature,³⁰⁸ dichloromethane was used due to its good removability.

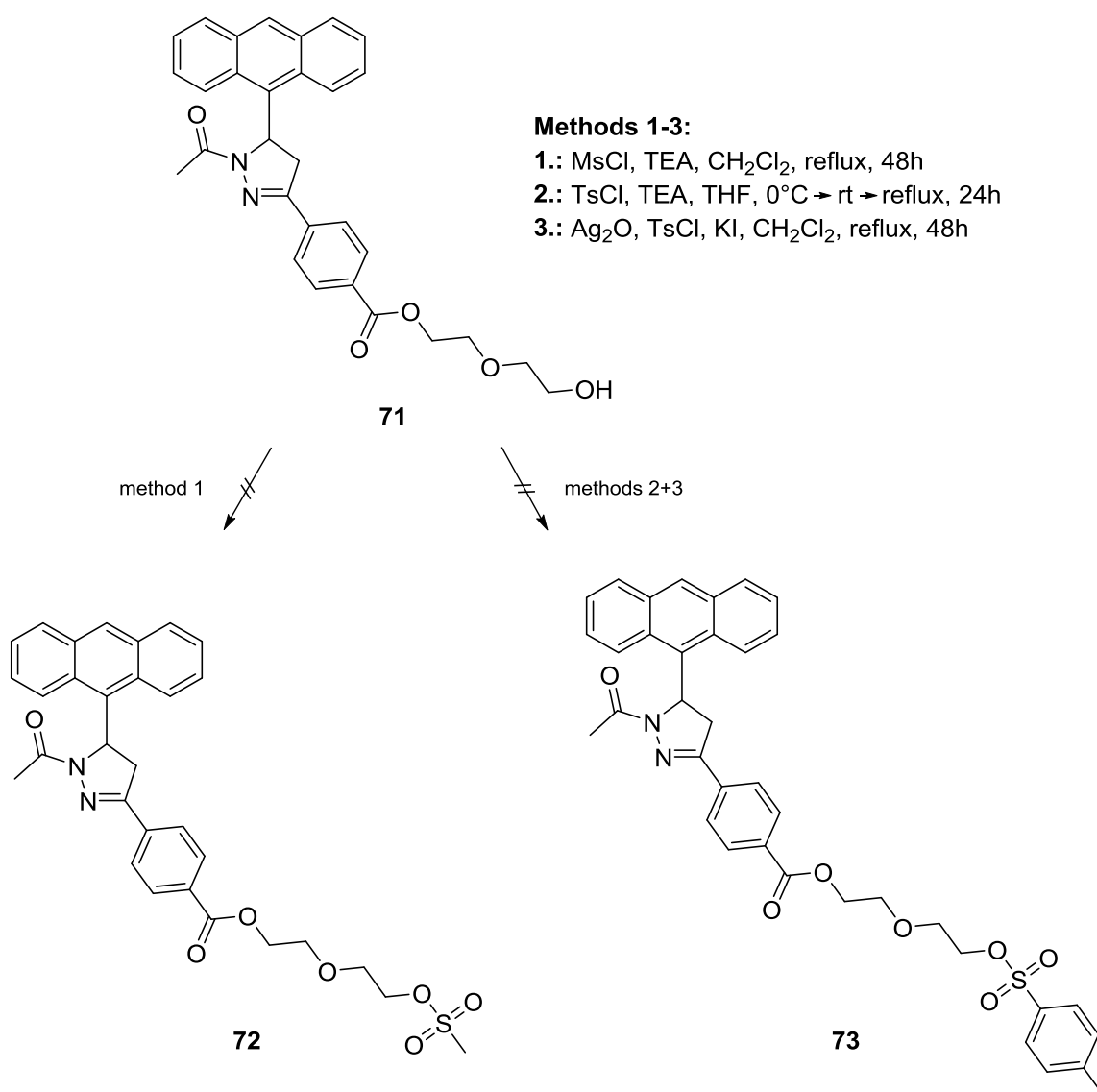
Compound **70** could then be made accessible by reacting free carboxylic acid **2** with silylether **69** in a Steglich esterification. Since mild reaction conditions (25°C) did not lead to the desired conversion, the reaction mixture was refluxed for three days.

In the next reaction step, the tetrabutylammonium salt of alcohol **71** was generated by fluoro-induced cleavage of the *t*-butyldiphenylsilyl moiety with TBAF. Final hydrolysis then provided desired alcohol **71**. Since both reaction steps resulted in rather low yields and repeated purification did not provide the desired compound (**71**) in sufficient purity due to similar R_f values of the starting material (**70**) and the product (**71**), another approach for the preparation of **71** was investigated.



Scheme 12

The second synthesis method was accomplished in one single step, by employing the unprotected diethylene glycol in the esterification reaction directly. Free carboxylic acid **2** readily underwent the conversion into alcohol **71** in 24 h under mild conditions. Similar to method 1, chromatographic purification of the target product proved to be difficult and repeated separation attempts remained unsuccessful. Although the identity of **71** could be determined by mass spectrometric analysis, the compound was used for proceeding synthetic experiments without further purification.



Scheme 13

Alcohol **71** should have been converted into mesylate **72**, which on the one hand should have served as a precursor for radioactive methylation or fluoroethylation, and on the other hand should have been employed in the further synthesis of the respective reference compounds, namely the methyl and fluoroethyl ether.

Since however, an adapted nucleophilic substitution method of Zhang *et al*³⁰⁹ did not succeed, probably due to decomposition of **72** during the purification procedure, the more stable tosylate **73** should have been synthesized (scheme 13).

Therefore, a common nucleophilic tosylation, employing triethylamine and toluene-4-sulfonyl chloride, as well as a silver oxide mediated reaction with potassium iodide and toluene-4-sulfonyl chloride,³¹⁰ were employed. Unfortunately, after purifying the crude reaction product, NMR spectroscopic analysis revealed product decomposition for both approaches.

Since the isolation of both, mesylate **72** as well as tosylate **73** could not be accomplished due to structural instability of **72** and **73**, and also milder purification methods (chromatographic purification with ALOX) did not provide the desired products, the synthesis of the pegylated analogs of compound **1** was not further pursued.

2.2.3.5 Preparation of thiophene based derivatives (methyl ester **4, ethyl ester **79**, carboxylic acid **5**, fluoroethyl ester **6**) and furan based derivatives (methyl ester **7**, carboxylic acid **8**, fluoroethyl ester **9**)**

In order to enlarge the compound library for potential MAO-B PET tracer precursors and reference compounds, also thiophene substituted pyrazoline derivatives (**4**, **5**, and **6**) and furan substituted pyrazoline derivatives (**7**, **8**, and **9**) were synthesized. Ethyl ester based thiophene derivative **78** was prepared as trial compound. All compounds were synthesized by employing the same reaction pathway, which is depicted in scheme 14.

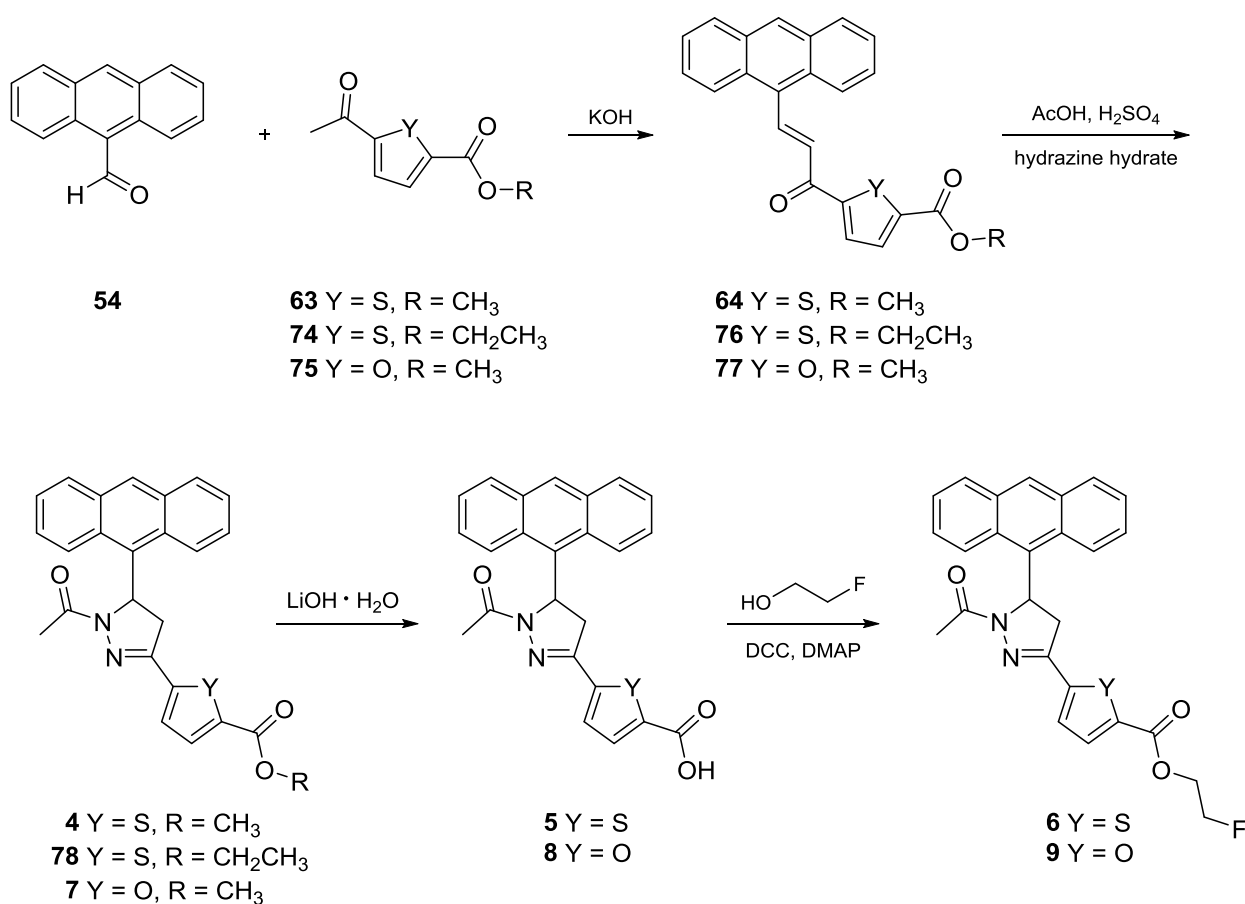
For the initial step, the synthesis of chalcones **64**, **76**, and **77**, their respective precursors, esters **63**, **74**, and **75**, first had to be made accessible. Therefore, 5-acetylthiophene-2-carboxylic acid was reacted with either ethanol in a Fischer esterification to yield ethyl ester **74** or with trimethylsilyldiazomethane, to give methyl ester **63**. Methyl 5-acetylfuran-2-carboxylate (**75**) was synthesized in an autoclave by employing the iron derivative $\text{Fe}(\text{acac})_3$ as catalyst.³¹¹

Since an aldol condensation attempt according to Aginagalde *et al*³¹² with thionyl chloride turned out unsuccessful, the potassium hydroxide based method, already described for compound **62** (scheme 6), was employed for the synthesis of chalcones **64**, **76**, and **77**. Other than ethyl ester **75**, which was purified by column chromatography, chalcones **64** and **77** could be used directly in the next reaction step after filtration, without further purification. Due to decomposition under atmospheric oxygen, however, chalcones **64**, **76**, and **77** had to be converted rapidly into their corresponding cyclization products. Therefore, the microwave assisted approach, already applied to lead compound **1** (scheme 10), proved efficient, since compounds **4**, **7**, and **78** could be made accessible in only five minutes. Interestingly, the yields of thiophene derived methyl and ethyl esters **4** and **78** were considerably lower than the one of furan based methyl ester **7**. A possible explanation for the decreased yields of **4** and **78** could be the huge atom size of the sulfur atom of the thiophene ring in comparison to the smaller oxygen atom of the furan cycle shielding the nucleophilic attack of the hydrazine molecule. However, **4** and **78** were obtained in sufficient amounts for the employment in the next reaction step.

Alkaline hydrolysis of methyl esters (**4**, **7**, and **78**) into free carboxylic acids (**5** and **8**) was achieved in the presence of lithium hydroxide monohydrate. A mixture of water/tetrahydrofuran/methanol in a ratio of 1/2/2.2 was chosen as solvent, since its use allowed almost complete conversion of the starting materials (**4**, **7**, and **78**) into desired products **5** and **8** with good to very good yields.

With the precursor compounds in hand, the reaction of **5** and **8** into the respective fluoroethyl esters (**6** and **9**) was then carried out under mild reaction conditions using DCC, DMAP, and 2-fluoroethanol. In an addition reaction, DCC binds to the carboxylic

acid and forms an *O*-acyl isourea, which features the same reactivity as the corresponding acid anhydride. In order to avoid side-product formation and increase yields, DMAP is added to the reaction. It also accelerates the reaction process by interacting with the *O*-acyl isourea thereby generating a reactive *N*-acyl pyridinium ion. This intermediate compound is unable to form intramolecular side-products, however, it reacts fast with alcohols and therefore serves as acyl transfer-reagent for the synthesis of the respective fluoroethyl esters (**6** and **9**).



Scheme 14

For model compound **4** the crucial HMBC correlations (left) as well as some important NOEs (right) are depicted in figure 19, unambiguously confirming the given structure. Full and unambiguous assignment of all ¹H, ¹³C, ¹⁵N, and ¹⁹F-NMR resonances was achieved by combining standard NMR techniques,³¹³ such as fully ¹H-coupled ¹³C-NMR spectra, APT, gs-HSQC, gs-HMBC, COSY, TOCSY, and NOESY experiments.

The location of the *N*-acetyl group and thus the position of the C=N double bond in the dihydropyrazole system is supported by HMBC correlations between pyrazole H-4 and H-4' to anthranyl C-9, from pyrazole H-5 to anthranyl C-8a, C-9, and C-9a and from thiophene H-4 to pyrazole C-3. An interesting phenomenon was observed for the 9-anthranyl system, in which corresponding positions 1 and 8, 2 and 7, 3 and 6, 8a and 9a, etc. were found to be non-equivalent. A possible explanation for this phenomenon would be restricted rotation of the anthranyl system around the pyrazole C-5 - anthranyl C-9 single bond. Thus, for instance, protons of the pyrazole system show different through-space interactions to corresponding protons of the anthranyl system: whereas a stronger NOE between pyrazole H-5 (6.88 ppm) and anthranyl H-8 (7.73 ppm) is detected, the appropriate effect is considerably smaller between pyrazole H-5 and anthranyl H-1 (8.47 ppm). Moreover, a distinct NOE between the acetyl-H protons and anthranyl H-8 is evident, in contrast, the interaction between acetyl protons and anthranyl H-1 is very small. The relatively large chemical shift difference between accordant anthranyl protons H-1 (8.47 ppm) and H-8 (7.73 ppm) can be explained by the magnetic anisotropy effect of the acetyl C=O group which obviously influences H-1 considerably more than H-8 in the preferred rotameric status at hand. In the NOESY spectrum of **4** the signals -due to anthranyl H-1 and H-8- exhibit a characteristic cross peak resulting from chemical exchange (different phase property compared to the cross peaks originating from NOEs), thus giving a hint to a slow rotation of the anthranyl unit compared to the NMR timescale.

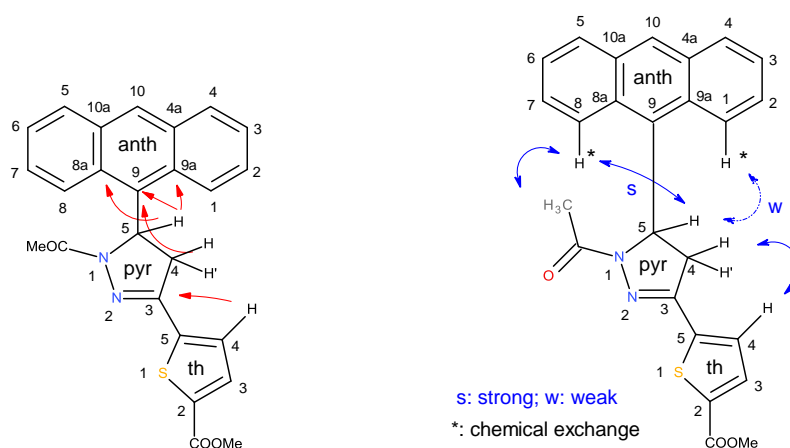


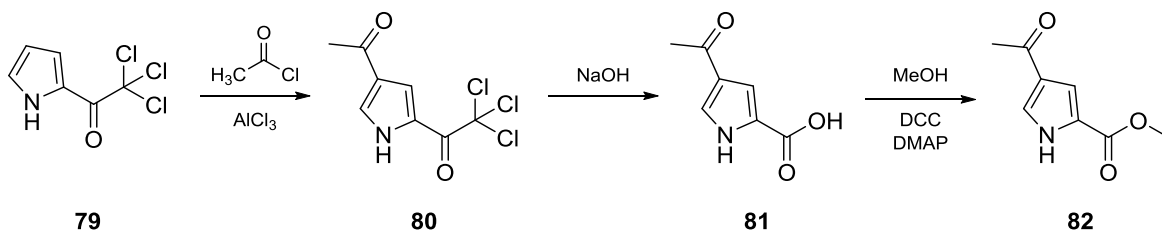
Figure 19: Atom numbering, important HMBC correlations (left), and NOEs (right) of compound **4** (in CDCl₃ solution)

Methyl esters **4** and **7** as well as fluoroethyl esters **6** and **8** will be subjected to preclinical studies and serve as references for their later prepared radiolabeled analogs. Free carboxylic acids **5** and **8** on the other hand will be object of radiochemical and nuclear medicinal investigations and are employed as starting materials for the preparation of radiolabeled ^{11}C and ^{18}F pyrazoline based MAO-B PET tracers.

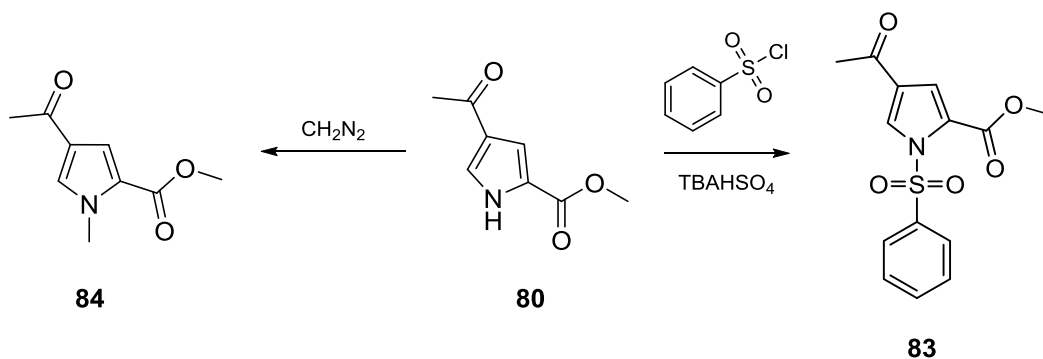
2.2.3.6 Preparation attempt of methyl 4-((2E)-3-(anthracen-9-yl)prop-2-enoyl)-1H-pyrrole-2-carboxylate (**85**), methyl 4-((2E)-3-(anthracen-9-yl)prop-2-enoyl)-1-(phenylsulfonyl)-1H-pyrrole-2-carboxylate (**86**), and methyl 4-((2E)-3-(anthracen-9-yl)prop-2-enoyl)-1-methyl-1H-pyrrole-2-carboxylate (**87**)

In order to complete the series of electron-rich heteroaromatic compounds, also pyrrole based pyrazoline derivatives should have been synthesized. Unfortunately, their preparation turned out rather difficult due to product instability and enormous by-product formation.

The original aim was to prepare methyl 4-((2E)-3-(anthracen-9-yl)prop-2-enoyl)-1H-pyrrole-2-carboxylate (**85**) (scheme 16), which should have been further reacted with hydrazine monohydrate to obtain the respective acetyl-pyrazine methyl ester. Hence, 4-acetyl-1H-pyrrole-2-carboxylic acid (**81**) was made accessible by a Friedl Crafts acylation of **79** and the subsequent transformation of acetylated intermediate **80** via alkaline treatment. Methyl ester **82** could then be obtained by employing a Steglich esterification (scheme 15).



Scheme 15



Scheme 17

Given the instability of the besylate group during the aldol condensation reaction, a last synthesis attempt was made: By using trimethylsilyldiazomethane, methyl 4-acetyl-1-methyl-1*H*-pyrrole-2-carboxylate (**84**) was prepared (scheme 17), which was reacted with anthracene-9-

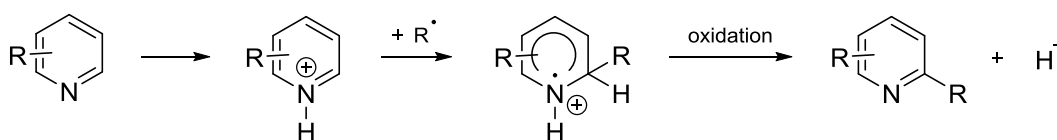
carbaldehyde (**54**) for the preparation of chalcone **87** (scheme 16). Despite *N*-methyl substitution at position 1 of the pyrrole ring, which should increase the stability of chalcone **87** during the aldol condensation, only by-product formation could be detected *via* TLC analysis. Following NMR spectroscopic analysis confirmed the failure of this procedure.

Since none of the three discussed methods provided the desired pyrrole based chalcones (**85**, **86**, and **87**), further synthesis attempts were omitted and the focus was shifted towards the preparation of electron-deficient heteroaromatic compounds.

2.2.3.7 Preparation of pyrazine based derivatives (methyl ester **10**, carboxylic acid **11**), preparation attempt of 2-fluoroethyl 3-(1-acetyl-5-(anthracen-9-yl)-4,5-dihydro-1*H*-pyrazol-3-yl)pyrazine-2-carboxylate (**65**)

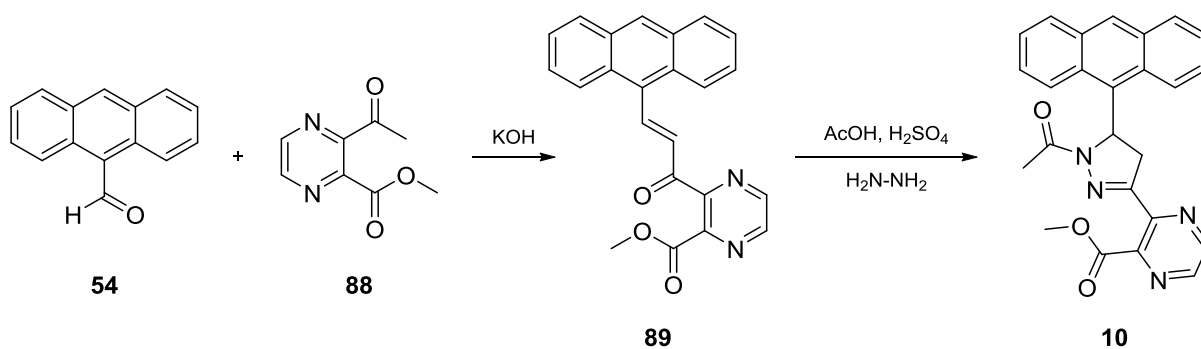
Compound **10**, which represents a bioisosteric analog of methyl 4-(1-acetyl-5-(anthracen-9-yl)-4,5-dihydro-1*H*-pyrazol-3-yl)benzoate (**1**), was synthesized in two reaction steps.

Primarily, methyl 3-acetylpyrazine-2-carboxylate (**88**) was prepared by the esterification of pyrazine-2-carboxylic acid, followed by a regioselective Minisci reaction. The latter is depicted in scheme 18 and represents a radical substitution to aromatic compounds, in particular a heteroaromatic base, which enables the introduction of alkyl as well as acyl groups,³¹⁴ by using a mixture of water, glacial acetic acid, and sulfuric acid as solvent.³¹⁵ For the Minisci reaction of methyl pyrazine-2-carboxylate into **88**, the radical was made accessible from acetaldehyde under Fenton-conditions, using *tert*-butyl hydroperoxide and iron(II)salts in an acetic acid media. Collateral *N*-protonation, which additionally increases electron-deficient effects of the heteroaromatic system, enhances the reactivity towards nucleophilic reagents, such as carbon radicals. The reaction is completed by the substitution of the radical to the protonated heteroaromatic ring, followed by subsequent rearomatization of the formed radical cation. A major drawback of the Minisci reaction however, is the formation of regioisomeric products, since several positions of the heteroaromatic ring are open to radical attack.³¹⁶ Therefore, the desired end product is often isolated only in poor yields, and also product **88** could only be obtained in 22% yield.



Scheme 18³¹⁸

Methyl 3-acetylpyrazine-2-carboxylate (**88**) was employed in an alkaline mediated aldol condensation reaction to afford chalcone **89**. This intermediate compound (**89**) was then reacted with hydrazine monohydrate in a microwave assisted reaction approach, which led to cyclization. Enormous by-product formation was detected by TLC analysis after the synthesis, which necessitated repeated purification of methyl ester **10** (scheme 19).



Scheme 19

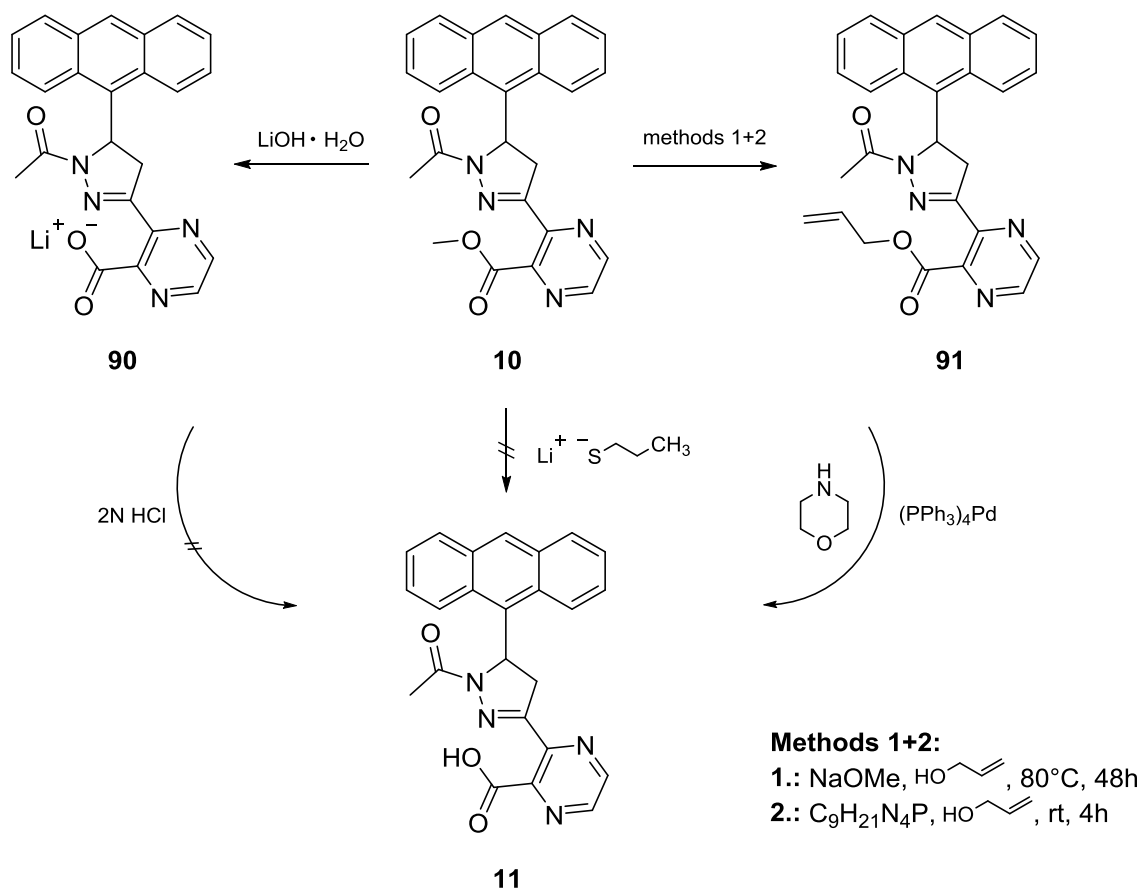
Starting from methyl 3-(1-acetyl-5-(anthracen-9-yl)-4,5-dihydro-1H-pyrazol-3-yl)pyrazine-2-carboxylate (**10**), which represents a reference compound for biological evaluation experiments, also free carboxylic acid **11** as well as fluoroethyl ester **65** should have been made accessible.

As an initial method, the preparation of 3-(1-acetyl-5-(anthracen-9-yl)-4,5-dihydro-1H-pyrazol-3-yl)pyrazine-2-carboxylic acid (**11**) was attempted in the same manner as described for electron-rich heteroaromatic compounds **5** and **8** (scheme 14), by employing lithium hydroxide monohydrate in a mixture of methanol/water/tetrahydrofuran (scheme 20). Unfortunately, after acidification of the lithium salt (**90**) and purification by column chromatography, NMR spectroscopic analysis of the isolated fractions indicated product decomposition.

Thus, a synthesis method of Bartlett and Johnson³¹⁷ was adapted, which envisaged the application of freshly prepared lithium *n*-propyl mercaptide for the alkaline hydrolysis of methyl esters (scheme 20). Although the reactants were stirred under mild conditions, also this procedure proved unsuitable for the preparation of **11**, since only side-products, but not the desired compound (**11**) could be isolated.

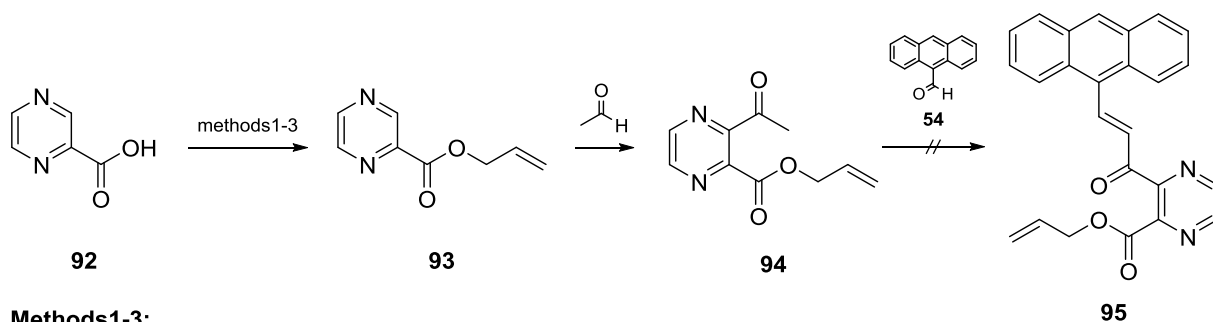
Since neither of the described methods to cleave the methyl ester proved successful for the preparation of free carboxylic acid **11**, allyl ester **91** was prepared and served as intermediate for the synthesis of **11**. The transesterification of methyl ester **10** into allyl ester **91** was performed in toluene, using sodium methoxide as catalyst (scheme 20).

Formed methanol was removed by distillation, in order to shift the reaction equilibrium towards the product (**91**), and thus achieve better yields (cf. Chooekawong³¹⁸).



Scheme 20

Since allyl ester **91** was only obtained in poor yields by employing this method, it was explored whether compound **91** could be prepared by total synthesis (scheme 21). For achieving maximum yields of **93**, pyrazine-2-carboxylic acid (**92**) was reacted by three different methods with either allyl alcohol or allyl bromide. In a radical Minisci reaction, the resulting product (**93**) was then converted into **94**, using the same reaction conditions as described for compound **88**. Allyl 3-acetylpyrazine-2-carboxylate (**94**) could only be prepared in poor yields, however the amount was sufficient for the subsequent reaction with anthracene-9-carbaldehyde (**54**). Since only side-product formation but not desired product **95** was determined by NMR spectroscopic analysis after stirring the reaction mixture for two days (cf. Chooekawong³¹⁸), the total synthesis approach of **91** was omitted for a more straightforward approach.

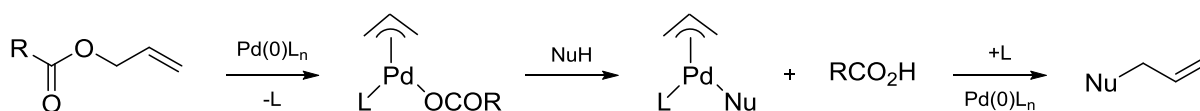
**Methods1-3:**

- 1.: SOCl_2 , $\text{HOCH}_2\text{CH}=\text{CH}_2$, reflux, 3d
- 2.: NaH , DMF, $\text{BrCH}_2\text{CH}=\text{CH}_2$, $\text{rt} \rightarrow 50^\circ\text{C}$, overnight
- 3.: CH_2Cl_2 , $\text{HOCH}_2\text{CH}=\text{CH}_2$, $0^\circ\text{C} \rightarrow \text{rt}$, overnight

Scheme 21

In the attempt of increasing the yield of allyl ester **91**, a procedure of Ilankumaran and Verkade³¹⁹ was adapted, which aimed for the transesterification of **10** by applying a nonionic superbases (scheme 20). 2,8,9-Trimethyl-2,5,8,9-tetraaza-1-phospha-bicyclo[3.3.3]undecane proved to be a suitable catalyst for transesterification processes, since its chemoselectivity is considerably higher than the one of other catalysts such as $\text{Ti}(\text{O}-i\text{Pr})_4$, DMAP, or NaOMe . Also, achievable product yields are excellent and often comparable to those obtained by conventional procedures.³¹⁹ Thus, by employing this method, not only the reaction could be carried out under milder conditions in regard to the temperature, but also the yield could be improved by 54%, compared to the approach with sodium methoxide.

For the preparation of precursor **11**, cleavage of the allyl ester function of **91** was performed selectively with tetrakis(triphenylphosphine)palladium and morpholine as nucleophile (scheme 20) (cf. Joksch³²⁰). An outline of the reaction mechanism is given in scheme 22, which shows that resonance stabilization of the carboxylate anion activates the allyl ester to nucleophilic attack by palladium catalysts. Accordingly, a π -allyl palladium complex forms, which can be trapped by mild nucleophiles, such as dimedone, barbituric acid, or morpholine and subsequently yields the free carboxylic acid.

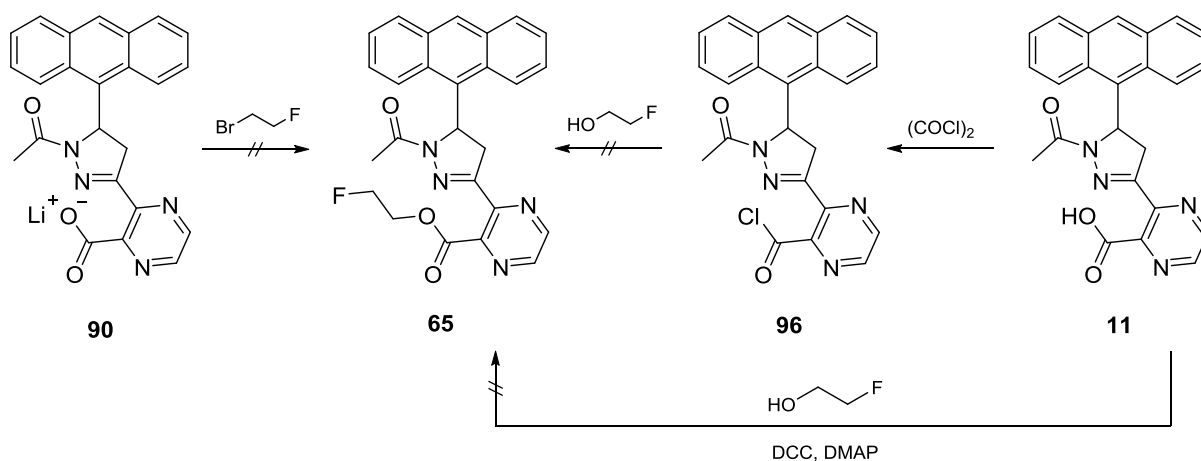
Scheme 22³²¹

Fluoroethyl ester **65** should have been made accessible, either by direct fluoroalkylation or preparation of the corresponding acid chloride and subsequent substitution thereof by 2-fluoroethanol (scheme 23):

The first synthetic approach for the preparation of **65** included a conventional Steglich esterification of **11** with 2-fluoroethanol, by employing the same reaction conditions as described for electron-rich heteroaromatic compounds **6** and **9** (scheme 14). Since Steglich esterifications are conducted under mild reaction conditions, decomposition of the molecule should have been avoided. However, after 48 h of stirring, the detection of multiple zones *via* TLC analysis forced to termination and immediate work up of the reaction. Although the crude reaction product was repeatedly purified, only by-products were detected by NMR spectroscopic analysis of the isolated fractions.

Thus, another direct fluoroalkylation method was applied, which aimed for the conversion of the lithium salt (**90**) with bromofluoroethane into **65** (scheme 23). Again, only side-product formation, but not the desired product (**65**) could be detected by NMR analysis.

Since both direct fluorination attempts failed, an indirect method *via* the preparation of acid chloride **96** was carried out in order to synthesize fluoroethyl ester **65**. Hence, a method of Cynamon and Klemens³²² was adopted, but instead of thionyl chloride, which often requires harsh reaction conditions (refluxing), a milder chlorination method was chosen. By employing oxalyl chloride, the conversion into **96** was performed at 0°C and the resulting acid chloride was directly introduced in the fluorination step without further purification. Although several spots could be detected *via* TLC analysis after the reaction, NMR spectroscopy ruled out formation of the desired product (**65**) (cf. Joksch³²⁰).



Scheme 23

Also a transesterification procedure of methyl ester **10** with sodium methoxide and fluoroethanol did not lead to the successful preparation of fluoroethyl ester **65**, and an access *via* total synthesis failed, since 2-fluoroethyl pyrazine-2-carboxylate could not be acetylated in a Minisci reaction (cf. Choekawong³¹⁸).

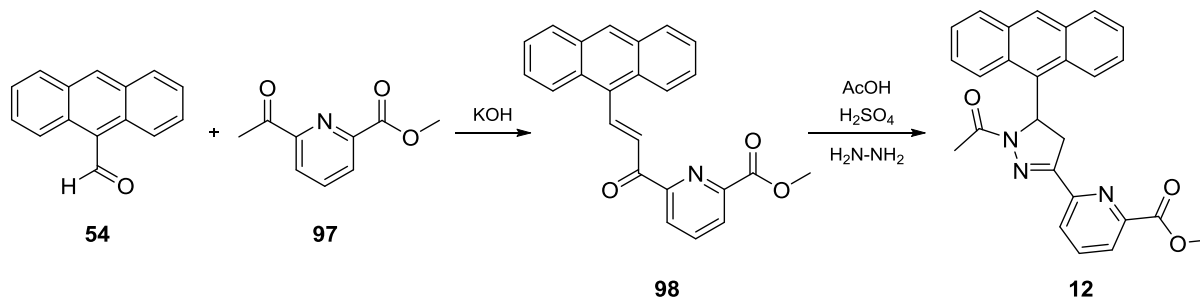
Due to the failure of all five synthetic approaches, the rather time consuming effort of the preparation of fluoroethyl ester **65** was discontinued. However, it remains unclear whether the reaction procedures were unsuccessful or the desired target compound (**65**) could not be isolated due to structural instability.

2.2.3.8 Preparation of pyridine based derivatives (methyl ester **12**, carboxylic acid **13**, fluoroethyl ester **14**)

Initial difficulties regarding the preparation of methyl 6-acetylpyridine-2-carboxylate (**97**) starting from pyridine-2,6-dicarboxylic acid and 2,6-dibromopyridine, respectively, could be overcome by employing dimethyl pyridine-2,6-dicarboxylate as precursor.

Reference compound **12** was made accessible in an aldol condensation of **54** and **97** followed by subsequent cyclization of **98** with hydrazine monohydrate (scheme 24), according to the procedure, already described for electron-rich heteroaromatic

compounds **4**, **7**, and **78** (scheme 14) and methyl 3-(1-acetyl-5-(anthracen-9-yl)-4,5-dihydro-1H-pyrazol-3-yl)pyrazine-2-carboxylate (**10**) (scheme 19).



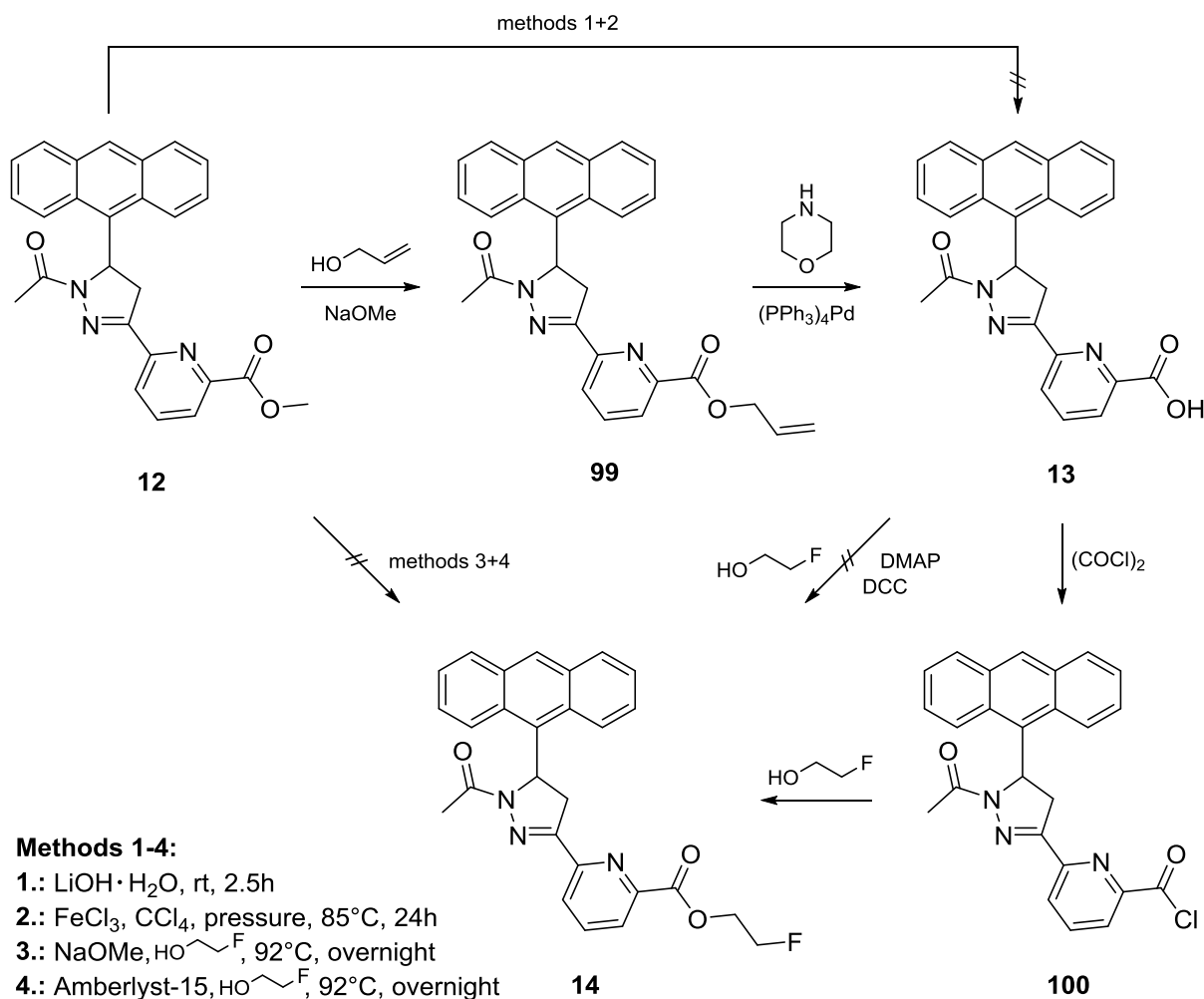
Scheme 24

Since an alkaline hydrolysis of **12** could not be performed with lithium hydroxide and also an iron(III) chloride mediated reaction in carbon tetrachloride failed, free carboxylic acid **13** had to be made accessible *via* intermediate compound **99** (scheme 25). In a sodium methoxide catalyzed transesterification reaction, **12** was reacted with allyl alcohol while formed methanol was removed by distillation, in order to shift the reaction equilibrium towards the product (**99**) (cf. Choekawong³¹⁸). As this method provided **99** only in poor yields, an attempt was carried out, in which the allyl ester (**99**) should have been synthesized *via* total synthesis. However, as allyl 6-acetylpyridine-2-carboxylate could not be reacted with anthracene-9-carbaldehyde (**54**) in an aldol condensation reaction, this preparation attempt was omitted.

In the next step, free carboxylic acid **13** was synthesized, which on the one hand represents a precursor molecule for further radiochemical syntheses and on the other hand served as starting material in the preparation of fluoroethyl ester **14**.

Cleavage of the allyl ester function of **99** to obtain free carboxylic acid **13** was conducted with tetrakis(triphenylphosphine)palladium and morpholine (scheme 25) in the same way as already described for pyrazine based carboxylic acid **11** (scheme 20). Surprisingly, the conversion of allyl ester **99** into **13** afforded better yields than the same reaction with electron deficient heteroaromatic allyl ester **91**. Additionally, remaining starting

material **99** could be readily separated from the product (**13**), which enabled its reapplication in the reaction process and therefore led to increased yields.



Scheme 25

To afford fluoroethyl ester **14**, several preparation attempts were performed (scheme 25): Starting from **13**, a Steglich esterification with fluoroethanol was carried out, which however only led to side-product formation. Thus **12** was employed as starting material and subjected to two transesterification procedures: The first one aimed for the synthesis of **14** by applying fluoroethanol and the catalyst sodium methoxide. Since only by-product formation was detected after TLC analysis, the transesterification procedure was modified by employing a macro reticular ion exchange resin, namely Amberlyst-

15.³²³ This method should have improved the yields of **14** and reduced the reaction time tremendously. However, since no conversion could be detected even after stirring the mixture for 24 h, the reaction was terminated and the focus was shifted towards another preparation approach.

Hence, 6-(1-acetyl-5-(anthracen-9-yl)-4,5-dihydro-1H-pyrazol-3-yl)pyridine-2-carbonyl chloride (**100**) was made accessible by reacting free carboxylic acid **13** under mild reaction conditions with oxalyl chloride and catalytic amounts of *N,N*-dimethylformamide. The subsequent conversion of the crude reaction product (**100**) with fluoroethanol finally led to the formation of fluoroethyl ester **14**, which was confirmed by the detection of a fluorine signal in the ¹⁹F-NMR spectrum (figure 20). Since the isolation of the obtained product turned out challenging, several purification methods had to be applied, unfortunately to the detriment of the yield.

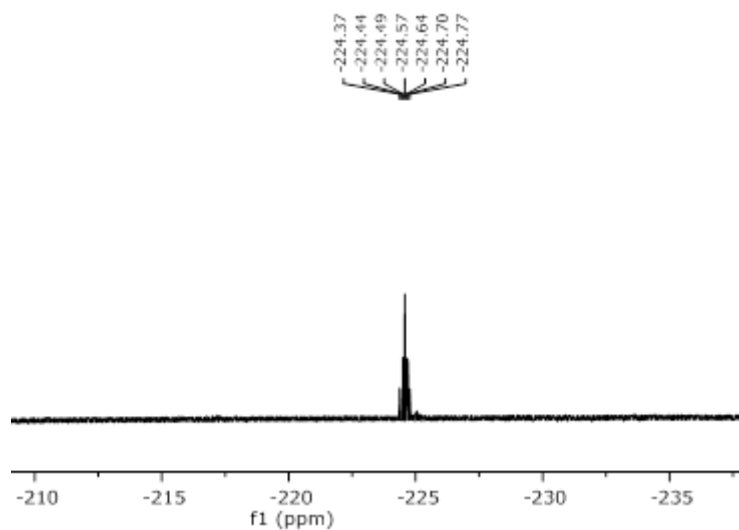


Figure 20: ¹⁹F-NMR spectrum of 2-fluoroethyl 6-(1-acetyl-5-(anthracen-9-yl)-4,5-dihydro-1H-pyrazol-3-yl)pyridine-2-carboxylate (**14**)

2.2.4 Comparison of Approaches and Yields

Figure 21 is giving an overview of the reactions and corresponding yields, whereas scheme 26 summarizes the synthesis pathway to the above discussed derivatives.

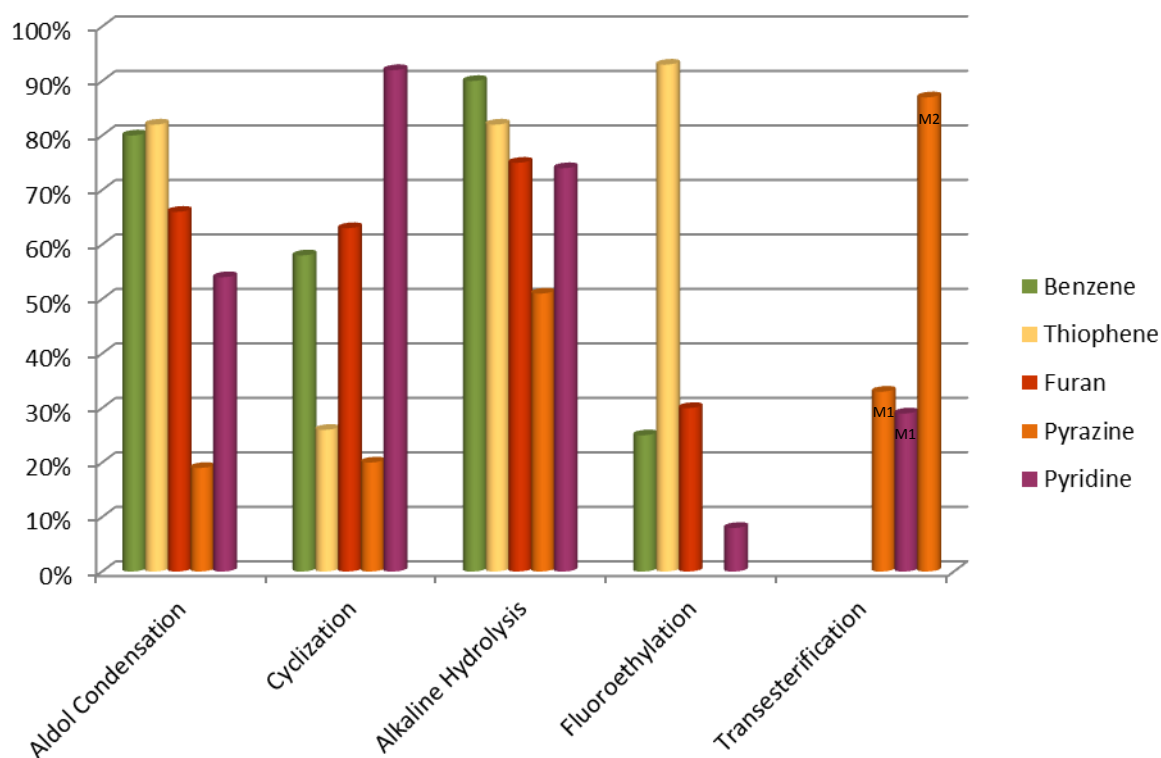
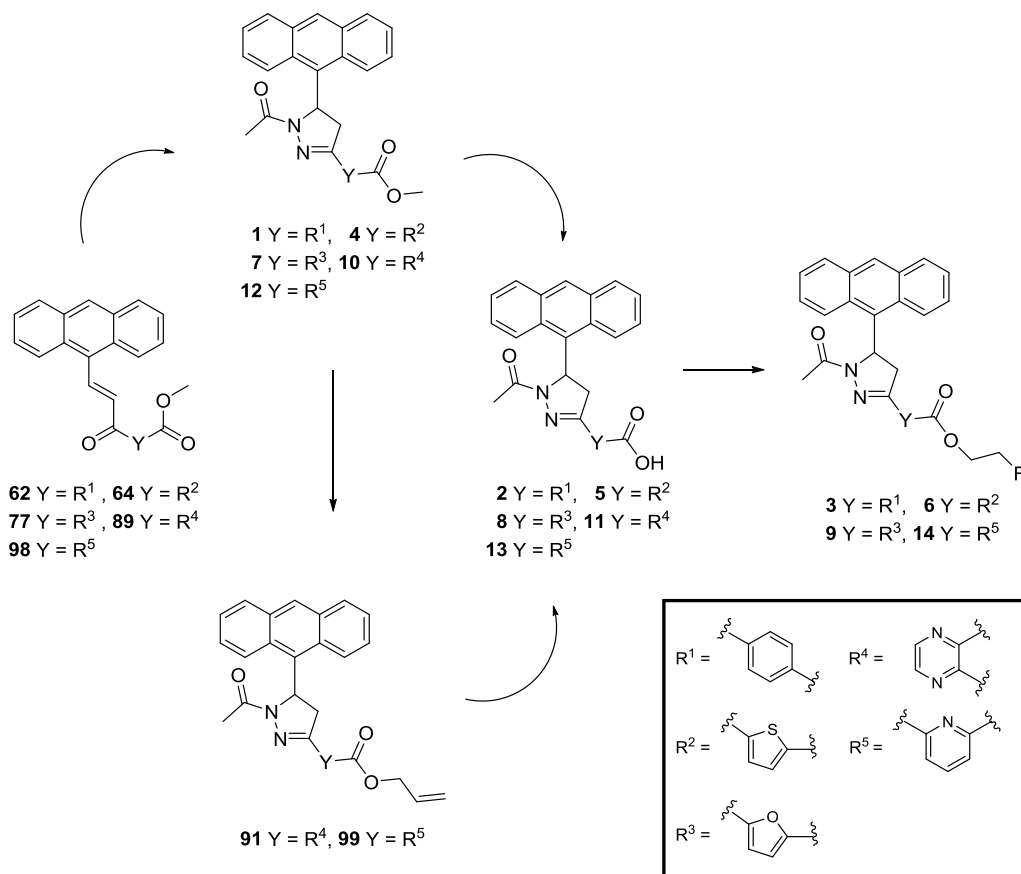


Figure 21: Overview of the reactions and corresponding yields of MAO-B binding compounds

Generally, in almost all synthesis steps, benzene based compounds (1-3) as well as electron-rich heteroaromatic derivatives (4-9) were achieved in better yields than electron-deficient heteroaromatic derivatives (10-14). Especially the preparation of benzene, thiophene, and furan based chalcones (62, 64, and 77), as well as their respective fluoroethylation products (3, 6, and 9) resulted in considerably higher yields than the preparation of electron-deficient heteroaromatic compounds (89, 98, and 14).

Since chalcones decompose relatively fast under atmospheric oxygen, they had to be converted rapidly into the corresponding cyclization products. Hence, purification by

column chromatography, which had to be performed for pyrazine based chalcone **89**, led to partial decomposition and therefore to an enormous decrease in yields.



Scheme 26

It is also interesting to note that benzene and electron-rich heteroaromatic compounds (**1-9**) could be synthesized by using the same reaction pathway (scheme 26), whereas free carboxylic acids (**11** and **13**) and the fluoroethyl ester (**14**) of electron-deficient heteroaromatic compounds had to be prepared *via* the corresponding allyl esters (**91** and **99**) or acid chloride, respectively.

Whilst the transesterification procedure of electron-deficient heteroaromatic derivatives **10** and **12** with sodium methoxide resulted in poor yields (figure 21, method 1 (M1)), the yield of pyrazine based allyl ester **91** could be enormously increased by employing the catalyst 2,8,9-trimethyl-2,5,8,9-tetraaza-1-phospha-bicyclo[3.3.3]undecane (figure 21, method 2 (M2)).

Since docking studies already indicated analogous binding of methyl esters (1, 4, 7, 10, and 12) and fluorethyl esters (3, 6, 9, and 14) in comparison to reference compounds 66 and 67,³⁴ those derivatives are promising candidates for biological testing. Thus, methyl esters (1, 4, 7, 10, and 12) and fluorethyl esters (3, 6, 9, and 14), which serve as reference compounds for their later radiolabeled analogs, as well as precursors (2, 5, 8, 11, and 13), were subjected to first preclinical investigations, which will be described in the following chapter.

2.2.5 Preclinical testing

As already discussed earlier, one of the prerequisites for a newly developed PET tracer is its ability to cross the BBB effectively. Today, there exist several *in silico*, *in vitro* and *in vivo* methods (logP evaluation,³²⁴ molecular polar surface area (PSA) investigation,³²⁵ surface tension,³²⁶ micro-dialysis,³²⁷ cerebrospinal fluid sampling,³²⁸ autoradiography,³²⁹ cultured cells applications,³³⁰⁻³³³ parallel artificial membrane assay (PAMPA)³³⁴ or immobilized artificial membrane (IAM) chromatography³³⁵) to assess the BBB penetration potential of a potential PET radiotracer. Within the scope of this PhD thesis first BBB penetration analyses were undertaken by subjecting all compounds synthesized to logP analyses as well as IAM experiments:

Although logP determination provides a measure of polarity interactions (such as lipophilicity) and hydrophobicity, it however does not reflect ionic bonding, which is involved in compound-membrane interactions as well.³³⁶⁻³³⁹ Thus, also new HPLC methods, like IAM chromatography, were employed as a prediction for BBB crossing. IAM surfaces mimic the lipid environment of fluid cell membranes on a solid matrix and hence give a more accurate prediction of passive diffusion into the brain.³⁴⁰

Lipophilicity studies and IAM experiments were performed in cooperation with the research group for Radiopharmaceutical Sciences, Department of Nuclear Medicine at the Medical University of Vienna.

2.2.5.1 LogP analyses

In order to determine the lipophilicity of the candidate compounds (**1-14**), a standardized HPLC method according to Donovan and Prescatore³⁴¹ was applied (cf. chapter 3.5.1). The obtained data were compared with those derived from DASB (logP 3.85±0.13), β-CIT (logP 3.03±0.01), PIB (logP 4.05±0.16), PE2I (logP 4.63±0.26), Raclopride (logP 1.48±0.28), and Elacridar (logP 4.85±0.30), compounds known to penetrate the blood brain barrier.³⁴²

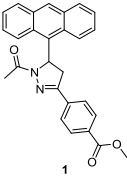
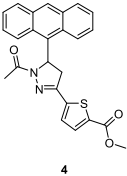
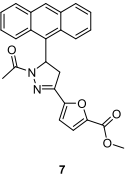
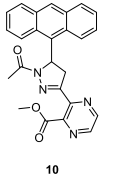
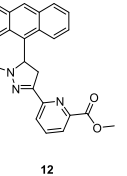
methyl esters						
compound						
	1	4	7	10	12	
calc. logP	4.66	4.70	3.33	2.83	4.17	
exp. logP	4.91±0.31	4.87±0.29	4.26±0.20	4.18±0.18	4.15±0.18	

Table 4: Calculated and experimental logP values of methyl ester derived references **1, 4, 7, 10, and 12**

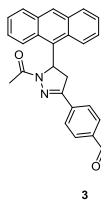
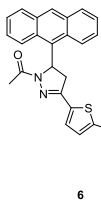
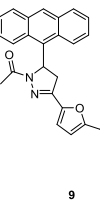
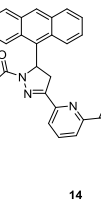
fluoroethyl esters				
compound				
calc. logP	4.85	4.89	3.52	4.36
exp. logP	4.95±0.28	4.88±0.30	4.40±0.22	4.31±0.24

Table 5: Calculated and experimental logP values of fluoroethyl ester derived references 3, 6, 9, and 14

For completeness, not only methyl and fluoroethyl derived reference compounds (1, 3, 4, 6, 7, 9, 10, 12, and 14) were subjected to logP studies (tables 4 and 5), but also precursors 2, 5, 8, 11, and 13 were evaluated for their logP values (table 6).

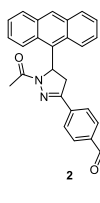
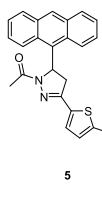
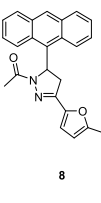
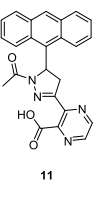
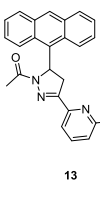
carboxylic acids					
compound					
calc. logP	4.40	4.43	3.07	2.57	3.91
exp. logP	2.22±0.15	2.24±0.15	1.86±0.21	1.80±0.22	1.69±0.24

Table 6: Calculated and experimental logP values of precursors 2, 5, 8, 11, and 13

It was determined that the lipophilicity expressed as logP for methyl and fluoroethyl esters (1, 3, 4, 6, 7, 9, 10, 12, and 14), is located between 4.15 and 4.95 (tables 4 and 5) and therefore lies in an acceptable range compared to the references. The logP values for the additionally tested free carboxylic acids (2, 5, 8, 11, and 13), which are depicted in table 6,

lie between 1.69 and 2.24 and therefore in a slightly more favorable range than the respective methyl and fluoroethyl esters.

As logP values were reported to be poor predictors for BBB penetration,³⁴³ IAM experiments were additionally performed for a more accurate prediction of BBB crossing.

2.2.5.2 IAM experiments

IAM chromatography was performed, modifying a protocol according to Taillardat-Bertschinger *et al*³⁴⁴ (cf. chapter 3.5.2). Obtained K_m values (membrane partition coefficient) and P_m values (permeability) were compared with those of external standards DASB ($K_m=71.38$, $P_m=0.25$), β -CIT ($K_m=91.34$, $P_m=0.24$), PIB ($K_m=654.05$, $P_m=2.55$), PE2I ($K_m=648.21$, $P_m=1.52$), Raclopride ($K_m=41.89$, $P_m=0.12$), and Elacridar ($K_m=2332.50$, $P_m=4.14$).³⁴²

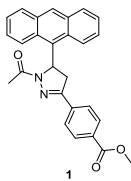
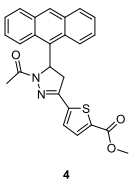
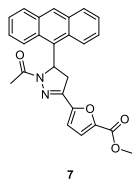
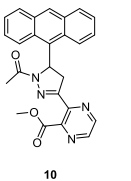
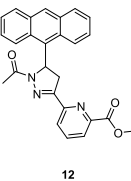
methyl esters						
compound						
K_m	38107.93	19979.60	2604.37	1986.48	1620.16	
P_m	85.04±12.00	46.63±5.18	6.31±1.90	4.68±1.26	8.22±2.17	
variation	14.11	11.10	30.08	26.90	26.37	

Table 7: Membrane partition coefficient (K_m), permeability (P_m), and variation coefficient of methyl ester derived references 1, 4, 7, 10, and 12

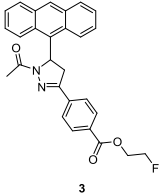
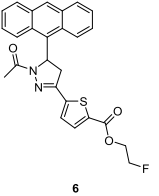
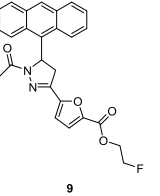
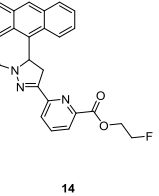
fluoroethyl esters				
compound				
K_m	19498.03	11040.94	3464.72	5395.95
P_m	42.90±9.14	23.97±4.82	7.80±2.60	11.85±2.44
variation	21.30	20.12	33.41	20.63

Table 8: Membrane partition coefficient (K_m), permeability (P_m), and variation coefficient of fluoroethyl ester derived references 3, 6, 9, and 14

In addition to methyl and fluoroethyl ester derived reference compounds (1, 3, 4, 6, 7, 9, 10, 12, and 14), IAM experiments were also performed for precursors 2, 5, 8, 11, and 13. Preliminary results of methyl esters and fluoroethyl esters are depicted in tables 7 and 8, respectively. For carboxylic acids, preliminary data are shown in table 9.

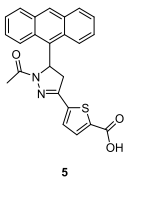
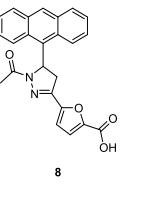
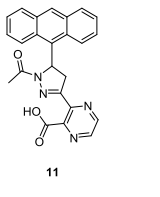
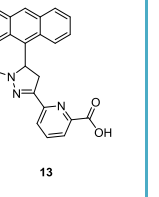
carboxylic acids				
compound				
K_m	199.96	188.43	133.82	159.66
P_m	0.48±0.08	0.38±0.06	0.33±0.03	0.39±0.06
variation	15.78	15.61	10.20	14.52

Table 9: Membrane partition coefficient (K_m), permeability (P_m), and variation coefficient of precursors 2, 5, 8, 11, and 13

Although logP studies were quite promising, IAM-chromatography experiments (n=8) revealed a rather unsatisfactory outcome for reference compounds comprising methyl and fluoroethyl esters. The P_m of derivatives **1**, **3**, **4**, **6**, and **14** is located in a much higher range than the P_m value of references **7**, **9**, **10**, and **12**. However, today to the best of our knowledge the database with the most popular tested reference compounds comprises only twenty derivatives, which range from a P_m value of 0.01 to 4.21.³⁴⁵ This database so far represents a preliminary assortment of references, which will be significantly extended in the future. Thus, the P_m range might have to be adapted. Also, considering the high variation coefficients of the investigated derivatives (**1**, **3**, **4**, **6**, **7**, **9**, **10**, **12**, and **14**), which reflect possible molecular interactions that occur in bioaffinity chromatography like IAM chromatography, BBB penetration *via* passive diffusion of compounds **7**, **9**, **10** and **12** seems not impossible.

As passive diffusion is only one mechanism for penetrating the BBB, further experiments regarding BBB crossing will definitely be performed in future. As already discussed above, there exist various other *in silico*, *in vitro*, and *in vivo* methods³²⁵⁻³³⁵ for predicting the BBB penetration behavior of a compound. Some of these approaches will be the subject of the continuing studies of the Radiopharmaceutical Sciences group at the Medical University of Vienna in order to evaluate the BBB crossing potential of methyl and fluoroethyl based pyrazoline esters (**1**, **3**, **4**, **6**, **7**, **9**, **10**, **12**, and **14**) more accurately.

In contrast to the reference compounds, precursor derivatives **2**, **5**, **8**, **11**, and **13** exhibit much better IAM-results. With a P_m ranging from 0.33 to 0.48, those substances are situated well in between of DASB ($K_m=71.38$, $P_m=0.25$) and PE2I ($K_m=648.21$, $P_m=1.52$). On the basis of these results which are suggesting only passive diffusion, a BBB penetration prediction for derivatives **2**, **5**, **8**, **11**, and **13** seems probable.

2.3 NET ligands

2.3.1 FAPPI derivatives

Given the excellent *in vitro* results of fluorinated benzimidazolone **45**, shown by Zhang *et al.*,¹⁶⁷ and also considering the positive outcome of the preclinical experiments of [¹¹C]Me@APPI (**46**)¹⁶⁹ (cf. chapter 1.2.4.1), further fluorinated NET-binding analogs of **44** were evaluated computationally, synthesized, and tested regarding their lipophilicity and BBB penetration properties.

2.3.1.1 Docking studies

Docking studies were performed in cooperation with the Pharmacoinformatics Research Group at the University of Vienna, Faculty of Life Sciences.

Since compounds **15-17** comprise a novel fluoro substitution, a computational docking study was performed to assess if these compounds still would fit in the binding site of the NET. Furthermore, a binding mode hypothesis was created which allows gaining insights into the molecular basis of binding and selectivity towards the monoamine transporters. The ligands were docked in the substrate binding site (S1) of the outward-open conformation of the transporter models (cf. chapter 3.2.2), since related inhibitors, such as nortriptyline (**101**, figure 22), sertraline, mazindol, etc. were also shown to fit in the S1 of the *Drosophila* DAT (dDAT) and the “SERT”-ized leucine transporter (“LeuBAT”) in the same protein conformation.^{346,347} Interestingly, the co-crystallized ligand in dDAT (nortriptyline **101**) has the same ranking of human NET, SERT, and DAT activity as reference compound **44**, i.e. 4.4, 18, and 1149 nM K_D vs. 9, 2995 and >10000 nM IC_{50} , respectively.^{167,348} Additionally, nortriptyline (**101**) shares important structural features

with the benzimidazolones (**15-17**), which are two aromatic moieties and an *N*-methylalkyl side chain. Therefore their binding mode can be expected to be similar.

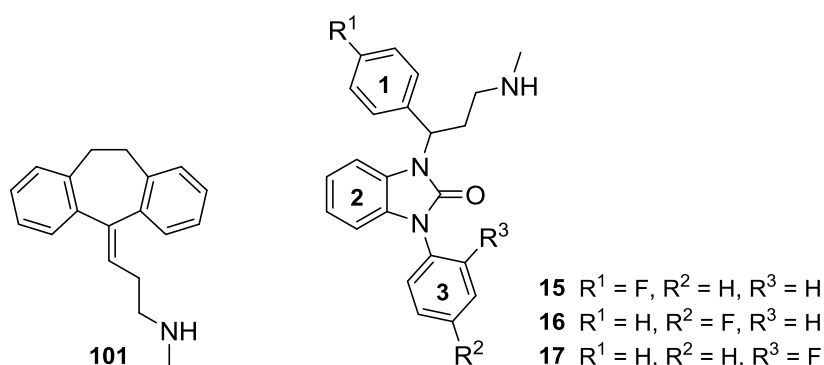


Figure 22: Chemical structure of nortriptyline (co-crystallized ligand from the template (PDB code 4M48),³⁴⁶ and assignment of ring numbers to FAPPI:1-3 (**15-17**))

Common scaffold clustering³⁴⁹ revealed two binding hypotheses (cf. chapter 3.2.2), which indicated that compounds **15-17** fit in the S1 of all three transporters. Hence, additional fluorination does not seem to cause steric clashes. In both hypotheses, the most prominent protein-ligand interaction was the cationic nitrogen atom placed in the A sub pocket,³⁵⁰ located between the central Asp75/98/79 side chain as a salt-bridge and the Phe72/95/76 side chain as a cation-*pi* interaction in NET/SERT/DAT, respectively. This is well in accordance with the X-ray structures of the templates. Additional *pi-pi* stacking interactions with Phe152/176/156 and Phe323/355/341 further promote the binding in both hypotheses obtained.

Hypothesis 1: the benzimidazolone heterocycle (ring 2) is placed in the B sub pocket and ring 3 in the C pocket, whereas ring 1 is solvent exposed (figures 22 and 23).

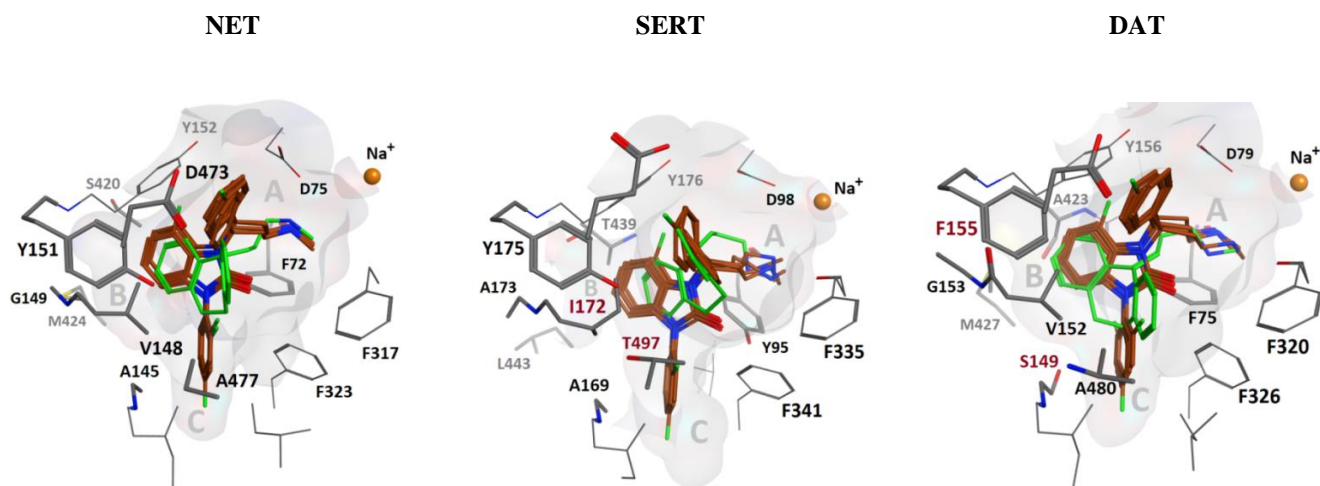


Figure 23: Overlay of compounds **44**, **45**, and **15-17** (maroon) in binding hypothesis 1 and comparison with the co-crystal pose of nortriptyline (**101**) (green). In NET, V148 allows more space than I172 in SERT. The angle between ligand ring 2 and 3 is ca. 60° in all poses. The extracellular space is located above in all figures.

Hypothesis 2: Ligand ring 1 is placed in the B pocket whereas ring 2 is placed at the same height (measured from the membrane-water interface) and both overlap with the rings of nortriptyline (**101**). The solvent exposed Tyr151/Tyr175/Phe155 in NET/SERT/DAT, respectively T-stacks with ring 2 whereas ring 3 points extracellularly (Table 10, Figure 24).

	B site			C site			Outer site		
hNET	S420	M424	G149	V148	A145	F72	D473	Y151	A477
hSERT	T439	L443	A173	I172	A177	Y95	E493	Y175	T497
hDAT	A423	M427	G153	V152	S149	F76	D476	F155	A480

Table 10: Sequence alignment of all distinct monoamine transporter residues located in sub sites in the vicinity of the docked compounds. Red: hydrophilic side chain, green: lipophilic side chain, bold: bulkier side chain.

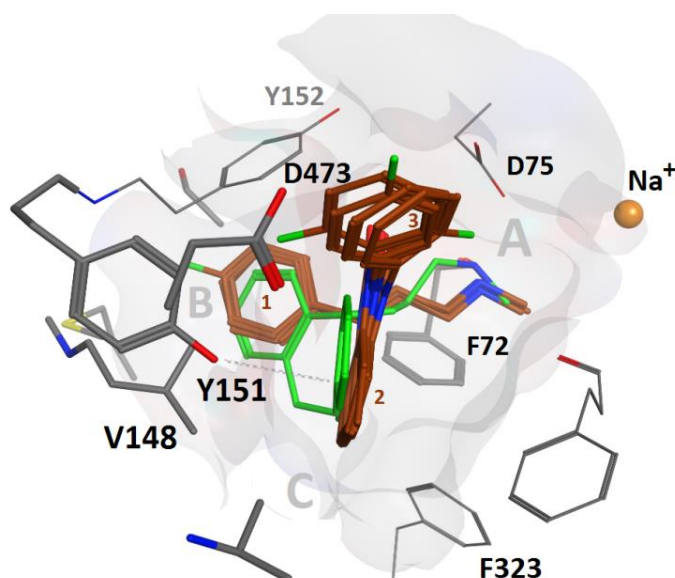


Figure 24: Overlay of compounds **44**, **45**, and **15-17** (maroon) in binding hypothesis 2 in hNET, showing agreement with the co-crystal pose of nortriptyline (**101**) (green). Val148 and Asp473 allow more space than Ile172 and Glu439 in hSERT, respectively, whereas Tyr151 might induce a more potent stacking interaction as compared to Phe155 in hDAT. The angle between ligand ring 2 and 3 is almost 90° in all poses. The extracellular space is located above.

As binding hypothesis 2 is in close agreement with the co-crystallized ligands in dDAT and LeuBAT, further analysis focused on this proposed binding mode.

Binding hypothesis 2 indicates the reason for weaker affinity of the investigated compounds (**15-17**) towards SERT and DAT than towards the NET (figures 24 and 25): lower SERT affinity may be due to Ile172 and Glu439, allowing less space for the ligand to be accommodated as compared to in NET, that comprises a valine and an aspartate at the homologous positions, respectively. Lower DAT affinity could be ascribed to weaker T stacking interactions of Phe155 as compared to Tyr151 in NET, based on previous findings that a Tyr-Phe pair has a stronger binding energy than a Phe-Phe pair.³⁵¹

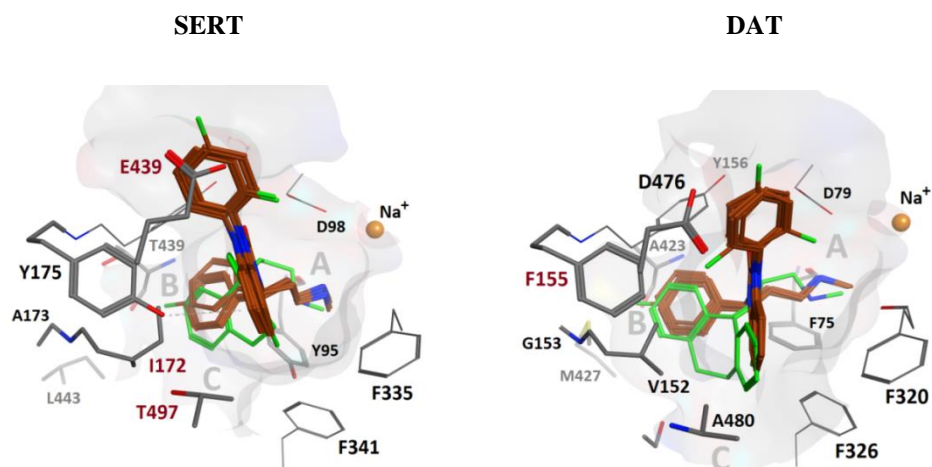


Figure 25: Overlay of compounds **44**, **45**, and **15-17** (maroon) in binding hypothesis 2 and comparison with the co-crystal pose of nortriptyline (**101**) (green). DAT lacks a more potent stacking interaction due to F155 as compared to NET[Y151] and SERT[Y175]. Binding mode 2 poses are more in agreement with the co-crystal pose. The angle between ligand ring 2 and 3 is almost 90° in all poses. The extracellular space is located above in both figures.

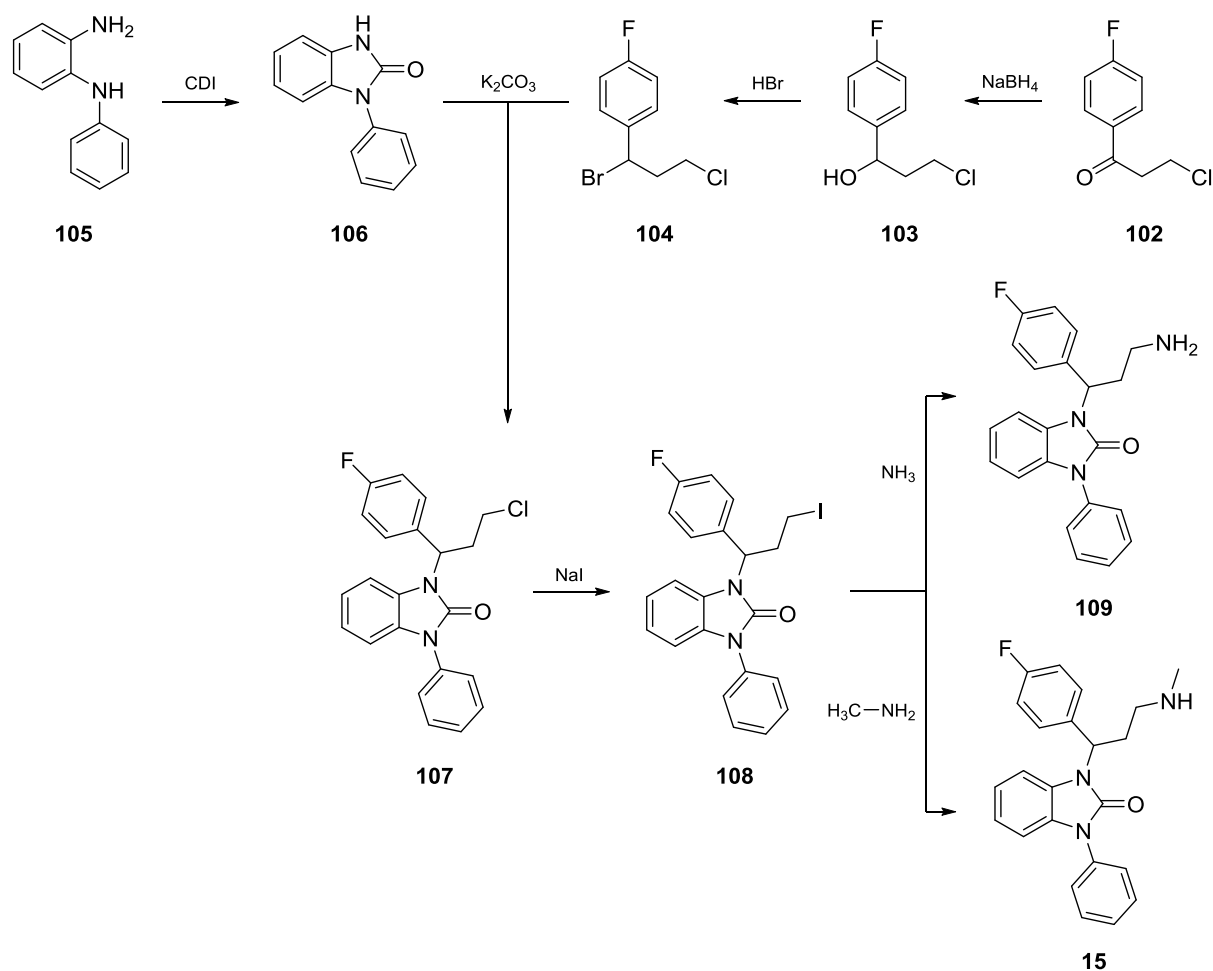
2.3.1.2 Syntheses

2.3.1.2.1 Preparation of 1-(3-amino-1-(4-fluorophenyl)propyl)-3-phenyl-1,3-dihydro-2H-benzimidazol-2-one (APPI) (**109**) and 1-(1-(4-fluorophenyl)-3-(methylamino)propyl)-3-phenyl-1,3-dihydro-2H-benzimidazol-2-one (FAPPI) (**15**)

The synthesis of precursor compound **109** (APPI:1) and reference compound **15** (FAPPI:1) was initiated by preparing side chain **104**. Therefore, commercially available 3-chloro-1-(4-fluorophenyl)-1-propanone (**102**) was reduced with sodium borohydride and the resulting alcohol (**103**) was subsequently brominated in a substitution reaction with aqueous hydrogen bromide. Since the reduction as well as the bromination afforded both products (**103** and **104**) in high purity, they could each be subjected directly to the next reaction step without further purification.

Core compound **106**, which was straightforwardly made accessible by ring closure of commercially available *N*-phenylbenzene-1,2-diamine (**105**) with 1,1'-carbonyldiimidazol, was reacted in the next step with prior synthesized side chain **104** in a nucleophilic

substitution reaction. Although complete conversion of the starting materials was detected by TLC analysis, product **107** could only be obtained in poor yields after purification, due to enormous side-product formation (scheme 27).



Scheme 27

The conversion of the chloro group of **107** into a iodo group (**108**) was carried out in a Finkelstein reaction with two equivalents of sodium iodide during 24 h of refluxing in acetone (scheme 27). Thereby, substitution of the chloroalkane side chain (**107**) led cleanly to the desired iodoalkane product (**108**), since the resulting salt was insoluble in acetone and therefore, consequently removed from the reaction equilibrium. Thus, crude iodoalkylbenzimidazolone **108** was not only obtained in high purity but also in excellent

yields, which allowed the use of **108** in the next reaction step without further purification.

Free amine **109** and secondary amine **15** were made accessible by applying the same reaction conditions (scheme 27): Compound **108** was dissolved in a solution of ammonia in isopropanol or a solution of methylamine in EtOH, respectively and heated in a sealed tube. Since starting material could still be detected by TLC in both reactions after three hours of stirring, and also by-product formation started to appear, the reactions were stopped before all of the starting material was completely consumed. Target compounds **109** and **15** were isolated and successfully separated from remaining precursor **108**, which was reused for increased yields.

2.3.1.2.2 Preparation of 1-(4-fluorophenyl)-3-(3-(methylamino)-1-phenylpropyl)-1,3-dihydro-2H-benzimidazol-2-one (FAPPI:2) (**16**) and 1-(2-fluorophenyl)-3-(3-(methylamino)-1-phenylpropyl)-1,3-dihydro-2H-benzimidazol-2-one (FAPPI:3) (**17**)

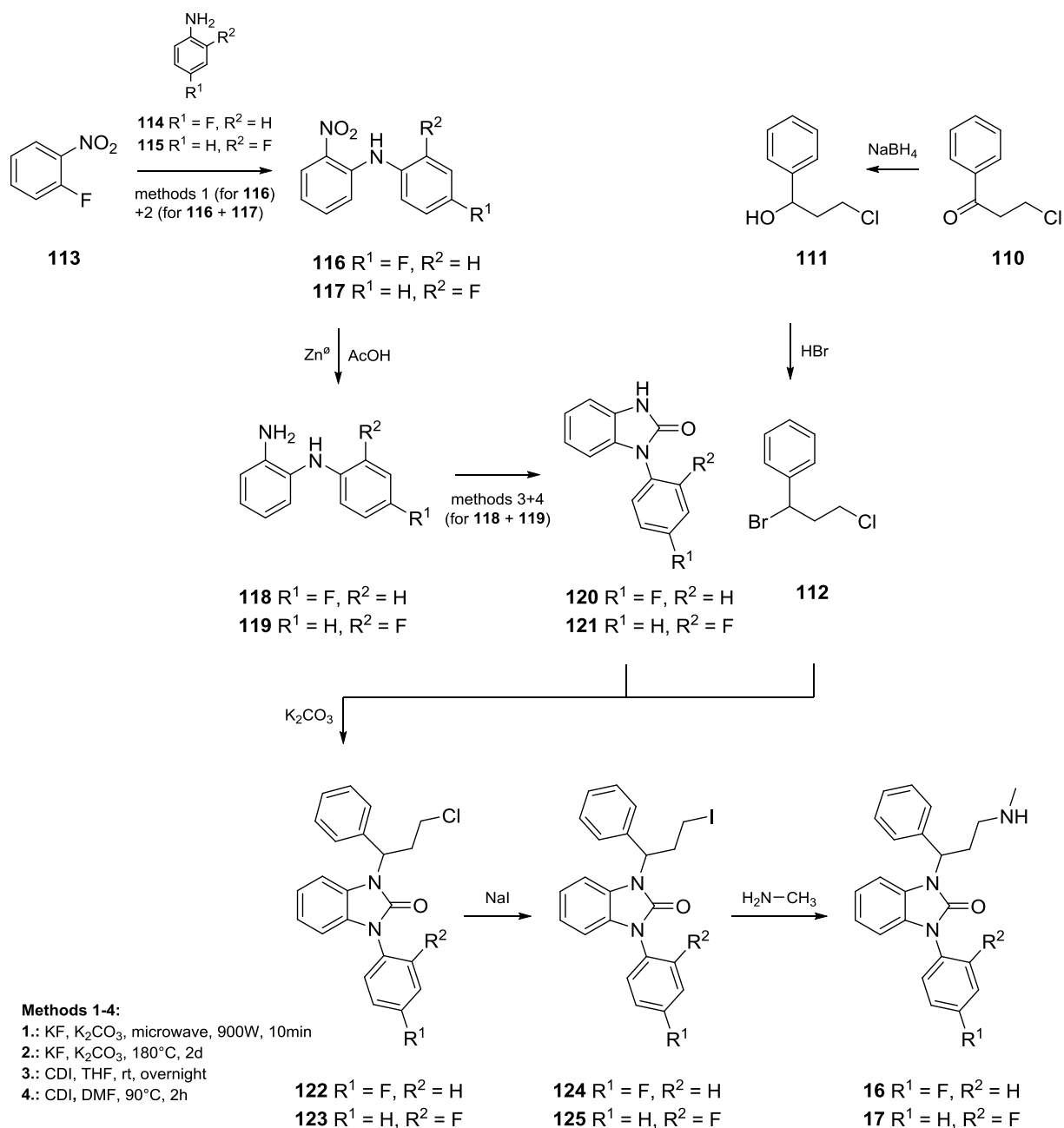
Non-radioactive reference compounds **16** (FAPPI:2) and **17** (FAPPI:3) were prepared in a similar manner to **109** and **15** (scheme 27), however, in contrast to these compounds, the fluorinated *N*-phenylbenzene-1,2-diamine core structure (**118** and **119**) had to be synthesized prior to cyclization with 1,1'-carbonyldiimidazol (scheme 28).

Initially, 1-fluoro-2-nitrobenzene (**113**) reacted with commercially available 4-fluoroaniline (**114**) in two different ways to give intermediate compound **116**. The first method involved a solvent-free microwave assisted synthesis approach with potassium fluoride and potassium carbonate for the conversion. However, since better yields were achieved by conventional heating, the second method (conventional heating) was not only selected for the larger scale synthesis of **116** but also for the preparation of **117**, which was made accessible by reacting 1-fluoro-2-nitrobenzene (**113**) with 2-fluoroaniline (**115**).

Both of the fluorinated 2-nitro-*N*-phenylanilines (**116** and **117**) were then reduced with zinc in acetic acid. Due to relatively fast oxidation of the resulting products (**118** and **119**), work up had to be carried out rapidly in order to provide the desired compounds in excellent yields.

The cyclization of **118** and **119** with 1,1'-carbonyldiimidazol was conducted in tetrahydrofuran, according to literature.¹⁶⁷ However, it was discovered that yields could be increased by 20% (for **120**) and 10% (for **121**) respectively, if compounds **118** and **119** were instead heated in *N,N*-dimethylformamide. Thus, by employing the latter cyclization procedure (heating in *N,N*-dimethylformamide), the reaction could be performed within two hours (instead of 24 h) and also work up was readily achieved: After evaporation of the solvent and addition of water, impurities dissolved and could be decanted, thereby providing the products (**120** and **121**) as brownish resin.

Side chain **112** was synthesized in the same manner as side chain **104** (scheme 27), starting from 3-chloro-1-phenylpropan-1-one (**110**). Initially, the keto group of **110** was reduced with sodium borohydride, giving intermediate alcohol **111** (scheme 28). Subsequent bromination of **111** with aqueous hydrogen bromide solution then led to the formation of **112**, which did not require purification due to its high purity after the reaction.



Scheme 28

With the key compounds in hand, benzimidazolones **120** or **121** were reacted with prior synthesized side chain **112** in a nucleophilic substitution reaction (scheme 28). Although this reaction was carried out under the same conditions for **106** (scheme 27), **120**, and **121**, the corresponding products **122** and **123**, which are bearing a fluorosubstituted phenyl moiety that is directly attached to the benzimidazolone core structure, were obtained in better yields than product **107** (scheme 27). After purification, the chloro

group of derivatives **122** and **123** was converted into a iodo group (**124** and **125**) in a Finkelstein reaction. Therefore, each **122** and **123** were refluxed for 24 h with two equivalents of sodium iodide in acetone to give compounds **124** and **125** in good yields.

Reference compounds **16** and **17** were then synthesized by dissolving **124** and **125** in a solution of methylamine in ethanol and heating the reactants in a sealed tube for 3 h. Due to by-product formation, the reactions were again terminated before all of the starting material was completely consumed. However, the yields of isolated products **16** and **17** were sufficient for further preclinical investigations.

2.3.1.3 Preclinical testing

2.3.1.3.1 LogP analyses

LogP values were determined using an HPLC based assay according to Donovan and Pescatore³⁴¹ (cf. chapter 3.5.1). Thereby, standard conditions were applied to NET affine derivatives **15-17** (FAPPI:1-3). Tracers known to penetrate the BBB (DASB, β -CIT, PIB, PE2I, Raclopride, and Elacridar)³⁴² served as external standards.

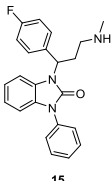
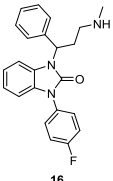
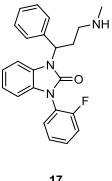
FAPPI derivatives			
compound			
	15	16	17
calc. logP	4.21	4.21	4.21
exp. logP	3.50±0.07	3.47±0.06	3.18±0.02

Table 11: Calculated and experimental logP values of FAPPI derivatives **15-17**

Resulting logP data, obtained from lipophilicity tests are depicted in table 11 and indicate lower logP values for FAPPI derivatives **15-17**, than originally predicted. In this regard, all investigated compounds are expected to penetrate the BBB in a similar way to β -CIT (logP 3.03 ± 0.01) and DASB (logP 3.85 ± 0.13), as logP values of FAPPI:1-3 (**15-17**) lie in the range of these tracers. However, to achieve more certainty about the BBB penetration behavior of **15-17**, also IAM experiments were performed.

2.3.1.3.2 IAM experiments

By adapting a protocol of Taillardat-Bertschinger *et al.*,³⁴⁴ IAM chromatography was carried out for derivatives **15-17** (cf. chapter 3.5.2). Again, known BBB penetrating tracers (DASB, β -CIT, PIB, PE2I, Raclopride, and Elacridar)³⁴² served as external standards and were compared with resulting K_m and P_m values of compounds **15-17**.

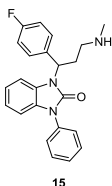
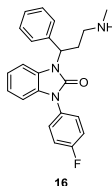
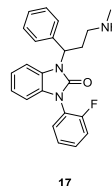
FAPPI derivatives			
compound			
K_m	273.79	1014.22	778.44
P_m	0.73 ± 0.03	2.70 ± 0.69	2.07 ± 0.37
variation	4.36	25.68	17.80

Table 12: Membrane partition coefficient (K_m), permeability (P_m), and variation coefficient of FAPPI derivatives **15-17**

IAM experiments (n=7) confirm the assumption that derivative **15** (FAPPI:1) has a high probability to penetrate the BBB *via* passive diffusion, which lipophilicity studies already

suggested. With a P_m of 0.73 (table 12), reference compound **15** is situated well in between DASB ($K_m=71.38$, $P_m=0.25$) and PE2I ($K_m=648.21$, $P_m=1.52$).

Despite acceptable lipophilicity, derivatives **16** and **17** feature higher P_m values in comparison to **15**, and also showed more interactions during the runs ($n=7$), which is expressed by a high variation coefficient. Nevertheless, with P_m values of 2.70 and 2.07 (table 12), respectively, derivatives **16** and **17** are likely to penetrate the BBB *via* passive diffusion, since also several reference compounds known to cross the BBB, which have already been tested by this method, exhibit P_m values in the range between 0.01 and 4.21.³⁴⁵

However, for more certainty regarding the BBB penetration behavior of FAPPI derivatives 1-3 (**15-17**), further experiments are planned, which will be subject of continuative studies at the Medical University of Vienna.

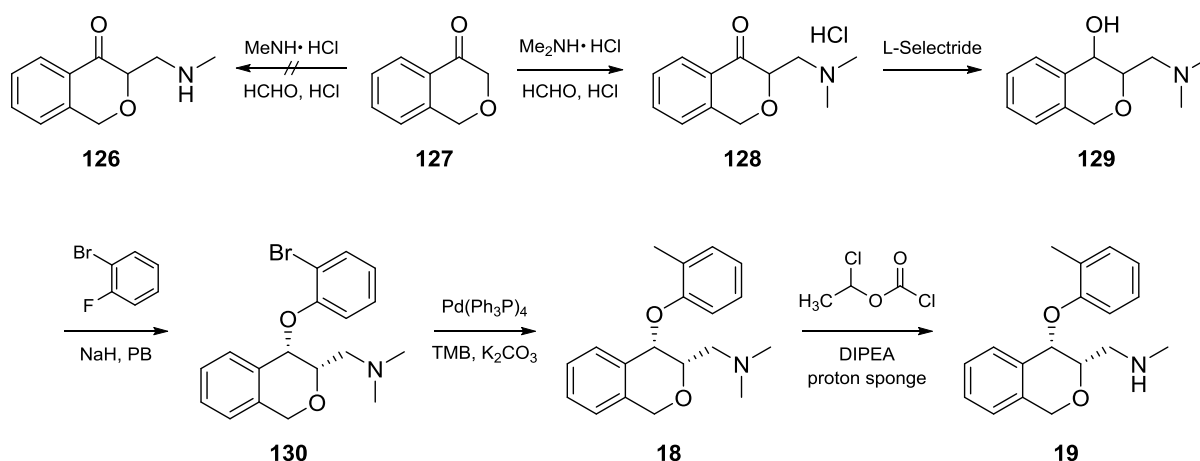
2.3.2 PHOXI derivatives

In regard to the high selectivity and excellent NET binding properties of above described compound **52** and its fluorinated analogs,^{176,177} compound **52**, several already known derivatives thereof, as well as a number of compounds with an additional *N,N*-methylfluoroethyl moiety were synthesized. All substances were subjected to lipophilicity and BBB penetration studies at the Medical University of Vienna in order to determine their suitability as future radioligands for PET based NET studies.

2.3.2.1 Syntheses

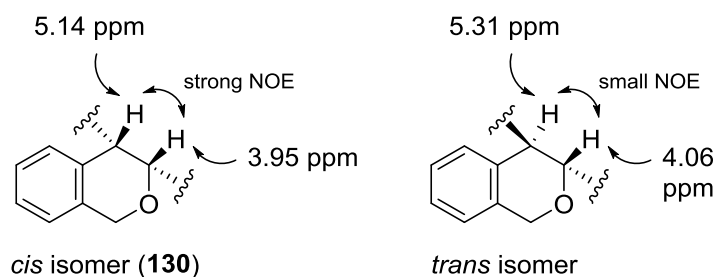
2.3.2.1.1 Preparation of *N,N*-dimethyl-1-((3*S*,4*S*)-4-(2-methylphenoxy)-3,4-dihydro-1*H*-isochromen-3-yl)methanamine (Me@PHOXI1) (**18**) and *N*-methyl-1-((3*S*,4*S*)-4-(2-methylphenoxy)-3,4-dihydro-1*H*-isochromen-3-yl)methanamine (PHOXI:1) (**19**)

Since a Mannich reaction of 1*H*-isochromen-4(3*H*)-one (**127**) with methylamine hydrochloride did not furnish desired methylamine **126**, a direct synthesis approach for the preparation of **19** could not be performed. Thus, reference compound **18** was made accessible according to the synthesis protocol of Kiankarimi *et al.*³⁵² which was then converted into precursor compound **19** (cf. Joksch³²⁰). The synthetic route towards derivative **19** is shown in scheme 29.



Scheme 29

Initially, tertiary aminoketone **128** was prepared by aminoalkylation of **127** with dimethylamine hydrochloride and paraformaldehyde in a Mannich reaction. The product (**128**) was subsequently reduced to **129** by using L-Selectride, which is a sterically hindered and therefore selective reducing agent. Amino alcohol **129** was obtained in a racemic mixture, predominantly favoring the *cis* isomer (*cis:trans* 1.4:1.0). By subjecting **129** to an S_NAr -reaction with 1-bromo-2-fluorobenzene, *cis* isomer **130** was afforded, which could be readily separated from its *trans* counterpart by chromatographic purification. *Cis* isomer **130** was distinguished from the *trans* isomer by NMR spectroscopic analysis, which indicated a stronger NOE between isochromen H-3 (3.95 ppm) and isochromen H-4 (5.14 ppm) for the *cis* isomer (**130**) than for the *trans* configuration, which featured a considerably smaller NOE effect between isochromen H-3 (4.06 ppm) and isochromen H-4 (5.31 ppm) (figure 26).

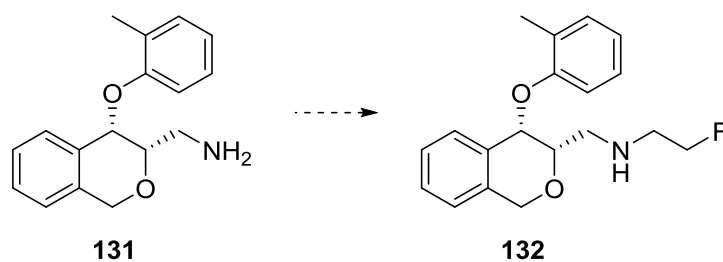
Figure 26: Illustration of the NOE of *cis* isomer 130 and its *trans* counterpart

In the next reaction step, a methyl group was substituted for the bromo group of **130** by employing palladium and trimethylboroxine. An additional celite treatment after the actual reaction allowed removal of major impurities, which proved beneficial for NMR spectroscopic analyses of **18**, since the desired product could be obtained in higher purity after chromatographic purification.

Despite the high purity of **18**, the following demethylation with 1-chloroethylchloroformate, proton sponge, and *N,N*-diisopropyl ethylamine led to enormous by-product formation, which could not be removed by extraction of the crude reaction product (**19**) in the separating funnel. Hence, not only normal phase chromatography but also reversed phase chromatography was employed for proper purification of **19**, unfortunately to the detriment of the yield.

2.3.2.1.2 Preparation attempt of 1-((3*S*,4*S*)-4-(2-methylphenoxy)-3,4-dihydro-1*H*-isochromen-3-yl)methanamine (**131**)

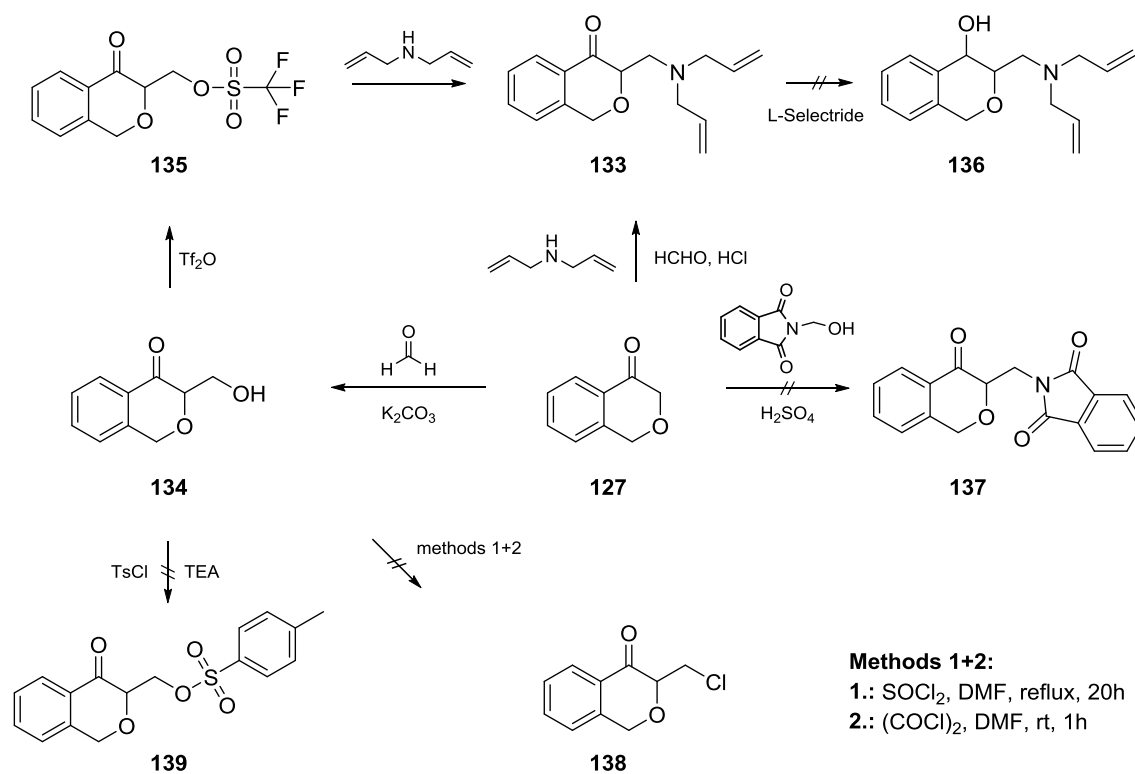
Amine **131** should have been prepared as a precursor for radiosynthesis and furthermore should have served as starting material for the preparation of fluoroethylated reference compound **132** (scheme 30).



Scheme 30

In the effort of preparing amine **131**, several synthesis strategies were developed, unfortunately none of them led to the successful formation of the desired product (scheme 31):

Initially, 3-((diallylamino)methyl)-3,4-dihydro-1*H*-isochromen-4-ol (**136**) should have been prepared, which after substitution by the methylphenyl moiety and cleavage of the *N,N*-diallyl group should have provided compound **131**. Therefore, 1*H*-isochromen-4(3*H*)-one (**127**) was reacted in a Mannich reaction with diallylamine to prepare compound **133**. However, since only poor yields were achieved by employing this method, **127** was converted into primary alcohol **134**, which was subsequently reacted with trifluoromethanesulfonic anhydride to give intermediate compound **135**. In the following step, the trifluoromethanesulfonate moiety of **135** was substituted by a diallyl moiety, thus providing **133** in better yields than the Mannich reaction. Nevertheless, the next reaction step had to be carried out with the crude reaction product (**133**) due to decomposition of **133** during the purification process. For the conversion of ketone **133** into alcohol **136**, L-Selectride was employed according to a protocol of Kiankarimi *et al.*³⁵² Although partly conversion of the starting material (**133**) was detected by TLC analysis, diallylamine **136** could not be isolated due to instability of the product and even milder reaction conditions or purification methods did not provide desired product **136**.



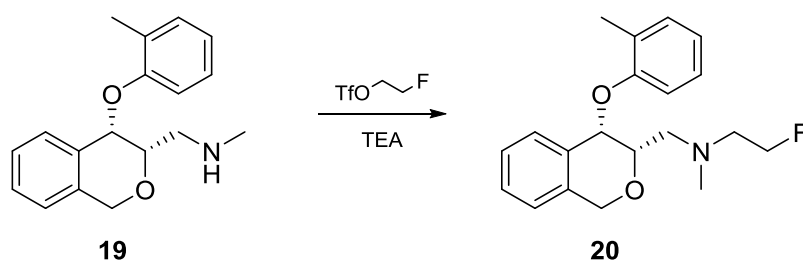
Scheme 31

Due to instability of alcohol **136**, the focus was shifted towards the preparation of 2-((4-oxo-3,4-dihydro-1*H*-isochromen-3-yl)methyl)-1*H*-isoindole-1,3(2*H*)-dione (**137**). However, it was found that neither an adapted method of Pandey³⁵³ with *N*-hydroxymethylphthalimide in sulfuric acid nor the pathway *via* chloride **138** led to the successful synthesis of **137** due to disintegration of the isochromene ring during the reaction processes. Also, an approach in which the alcohol moiety of **134** should have been converted into a tosylate group (**139**) failed, as only enormous by-product formation, but not desired product **139** was detected by NMR spectroscopic analysis.

Since several synthesis methods for the preparation of **131** were unsuccessful, the preparation of this compound (**131**) was not further pursued; instead, the focus was shifted towards the synthesis of reference compound **20**.

2.3.2.1.3 Preparation of 2-fluoro-*N*-methyl-*N*-(((3*S*,4*S*)-4-(2-methylphenoxy)-3,4-dihydro-1*H*-isochromen-3-yl)methyl)ethanamine (FE@PHOXI1) (**20**)

For the fluoroethylation of *N*-methyl-1-(((3*S*,4*S*)-4-(2-methylphenoxy)-3,4-dihydro-1*H*-isochromen-3-yl)methyl)ethanamine (**19**) a mild synthesis approach was chosen in order to avoid high temperatures (scheme 32). Thus, freshly prepared 2-fluoroethyl trifluoromethanesulfonate³⁵⁴ was reacted with the -prior activated- secondary amine (**19**) at 0°C. Due to the high reactivity of triflates, the alkylation was carried out in less than ten minutes while the temperature was slowly raised to 25°C.



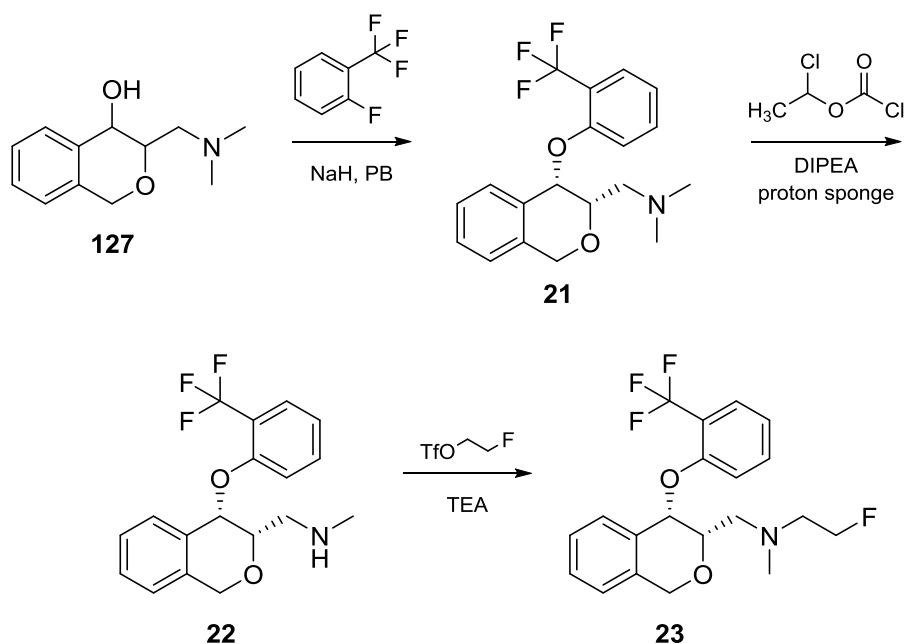
Scheme 32

After completion of the reaction, only starting material and product were detected by TLC analysis with a significant difference of R_f values, thus allowing facile separation. The preparation of **20** with 2-fluoroethyl trifluoromethanesulfonate represents an efficient fluoroalkylation technique, which, may also serve as an adequate method for the radiochemical [^{18}F]fluoroethylation of **19**, since this approach can be performed rapidly under mild reaction conditions.

2.3.2.1.4 Preparation of *N,N*-dimethyl-1-((3*S*,4*S*)-4-(2-(trifluoromethyl)phenoxy)-3,4-dihydro-1*H*-isochromen-3-yl)methanamine (Me@PHOXI2) (21**), *N*-methyl-1-((3*S*,4*S*)-4-(2-(trifluoromethyl)phenoxy)-3,4-dihydro-1*H*-isochromen-3-yl)methanamine (PHOXI:2) (**22**) and 2-fluoro-*N*-methyl-*N*-(((3*S*,4*S*)-4-(2-(trifluoromethyl)phenoxy)-3,4-dihydro-1*H*-isochromen-3-yl)methyl)ethanamine (FE@PHOXI2) (**23**)**

By analogy with references **18** and **20** and precursor **19**, also the following compounds were synthesized (scheme 33):

In a sodium hydride mediated S_NAr -reaction, racemate **127** was reacted with 2-fluorobenzotrifluoride to afford reference compound **21**. Since the yields of the *trans* isomer were extremely low, *cis* isomer **21** was straightforwardly separated from its *trans* counterpart. Furthermore, only little side-product formation was detected by TLC analysis after completion of the reaction, thus product **21** was purified without difficulty and was obtained in high purity.



Scheme 33

Dealkylation to secondary amine **22** was then achieved under alkaline conditions with catalytic amounts of proton sponge. Due to similar R_f values of formed side-products, isolation of **22** was hampered. However, by combining different purification methods (silica gel 60 and RP-18 silica gel chromatography), *N*-methylmethanamine **22** could be separated from major by-products, although to the detriment of the yield.

With precursor **22** in hand, reference compound **23** was synthesized under mild reaction conditions by employing freshly prepared 2-fluoroethyl trifluoromethanesulfonate.³²¹ Due to its favorable properties, which are good stability, wide applicability, ease of preparation, and suitability for one-pot syntheses, 2-fluoroethyl trifluoromethanesulfonate is widely used as a reagent for *O*-, *N*- and *S*-fluoroalkylations and also its ¹⁸F analog is often employed for radioactive [¹⁸F]fluoroethylation reactions.³⁵⁵ After only ten minutes completion of the reaction was determined by TLC analysis and reaction product **23** was isolated in high purity and good yields, due to its excellent separability from starting material **22**.

2.3.2.2 Preclinical testing

2.3.2.2.1 LogP analyses

Lipophilicity studies were performed according to a standardized HPLC method according to Donovan and Prescatore³⁴¹ (cf. chapter 3.5.1). DASB, β -CIT, PIB, PE2I, Raclopride, and Elacridar³⁴² are tracers known to penetrate the BBB and served as external standards.

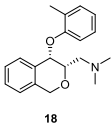
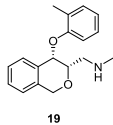
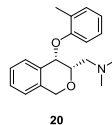
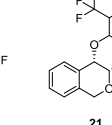
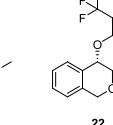
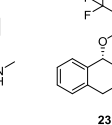
PHOXI derivatives						
compound						
calc. logP	3.63	3.25	3.82	4.06	3.69	4.25
exp. logP	3.16±0.01	n.a.	3.65±0.09	3.26±0.03	2.97±0.02	3.62±0.09

Table 13: Calculated and experimental logP values of PHOXI derivatives **18**, and **20-23**, experimental logP value for **19** is not available due to technical issues of the experimental set up, that could not be solved within the time frame of this thesis

For completeness, logP analyses were not only performed for references **18**, **20**, **21**, and **23**, but also for precursor **22**. The outcome of the lipophilicity experiments for all compounds tested (**18**, **20-23**) is shown in table 13, which indicates slightly lower logP values for PHOXI derivatives **18**, and **20-23** than originally predicted. Thus, the investigated compounds are expected to penetrate the BBB in a similar manner to β -CIT (logP 3.03±0.01) and PIB (logP 4.05±0.16), as determined logP values of **18**, and **20-23** lie in the range of these tracers. However, for a more accurate prediction of BBB crossing of **18-23** additional IAM experiments have been performed.

2.3.2.2.2 IAM experiments

For the determination of the BBB penetration behavior of derivatives **18-23**, an IAM method of Taillardat-Bertschinger *et al*³⁴⁴ was adapted (cf. chapter 3.5.2). Resulting K_m and P_m values of products **18-23** were compared with external standards (DASB, β -CIT, PIB, PE2I, Raclopride, and Elacridar),³⁴² compounds known to penetrate the BBB.

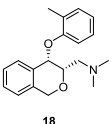
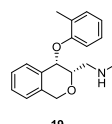
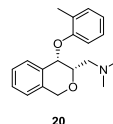
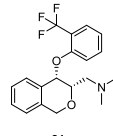
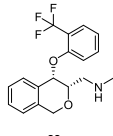
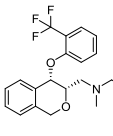
PHOXI derivatives						
compound						
K_m	367.66	756.37	1026.39	661.46	483.84	1370.42
P_m	1.24±0.15	3.17±1.94	3.12±0.71	1.88±0.16	1.43±1.01	3.57±1.99
variation	12.08	61.16	22.71	8.70	70.32	55.76

Table 14: Membrane partition coefficient (K_m), permeability (P_m), and variation coefficient of PHOXI derivatives **18-23**

IAM experiments (n=7) performed for PHOXI derivatives **18** and **22** revealed P_m values which are comparable to those of DASB ($K_m=71.38$, $P_m=0.25$) and PE2I ($K_m=648.21$, $P_m=1.52$), respectively (table 14). Accordingly, these compounds (**18** and **22**) are expected to penetrate the BBB by passive diffusion. Derivatives **19-21** and **23** however, exhibit higher P_m values and also showed more interactions during different runs (n=7), which is expressed by higher variation coefficients (table 14). Although the permeability of compounds **19-21** and **23** ranges from 1.88 to 3.57 (table 14), PHOXI:1 (**19**), FE@PHOXI1 (**20**), Me@PHOXI2 (**21**), and FE@PHOXI2 (**23**) are likely to penetrate the BBB via passive diffusion, since also several reference compounds known to cross the BBB showed P_m values in the range between 0.01 and 4.21, when tested according to this method.³⁴⁵

However, in order to gain more certainty about the BBB penetration behavior of derivatives **18-23**, further experiments will be performed in continuative studies at the Medical University of Vienna. *In silico*, continuative *in vitro*, and *in vivo* experiments³²⁵⁻³³⁵ are planned for an accurate BBB penetration prediction of **18-23**, which will reveal additional information in this regard, as passive diffusion is only one mechanism for BBB crossing.

2.4 Summary and Future Perspective

Since MAO-B as well as NET are involved in a variety of diseases, the investigation of their underlying dysregulation mechanisms *via* PET is of major interest. For this purpose, several precursors and reference compounds for both, MAO-B and NET, have been evaluated (docking studies), synthesized, characterized, and initially tested (logP analysis and IAM experiments) within the scope of this thesis.

After the performance of docking studies, a compound library of new, reversible PET tracer precursor (**2**, **5**, **8**, **11**, and **13**) and reference compounds (**1**, **3**, **4**, **6**, **7**, **9**, **10**, **12**, and **14**) was prepared for the MAO-B system by applying principles of bioisosterism to 5-(anthracen-9-yl)-3-phenyl-4,5-dihydro-1*H*-pyrazole, a compound which was reported to be a highly selective and extremely potent reversible MAO-B inhibitor.³⁴ An additional acetyl moiety, introduced at position 1 of the pyrazoline ring assured improved compound stability and additionally enhanced MAO-B inhibitory activity. Accordingly, a synthesis strategy was developed, which allowed the preparation of benzene derived MAO-B precursor (**2**) and references (**1** and **3**), electron-rich heteroaromatic compounds (**4-5** and **7-9**), and electron-deficient heterocyclic methyl ester derived references (**10** and **12**) by applying the same reaction methods. Electron-deficient heteroaromatic precursors **11** and **13** and pyridine derived fluoroethyl ester **14** however had to be made accessible *via* the respective allyl esters (**91** and **99**).

Preliminary results of logP investigations and IAM experiments of the newly synthesized compounds suggested acceptable lipophilicity of the precursors (**2**, **5**, **8**, **11**, and **13**) and references (**1**, **3**, **4**, **6**, **7**, **9**, **10**, **12**, and **14**). However, high P_m values and multiple interactions with the membrane indicated that passive diffusion through the BBB seems unlikely for reference compounds **1**, **3**, **4**, **6**, **7**, **9**, **10**, **12**, and **14**.

For PET based investigations of the NET, new reference compounds as well as precursors of two different substance classes (FAPPI derivatives, PHOXI derivatives) have been synthesized and evaluated within the scope of this thesis:

Computational evaluation of FAPPI derivatives (**15-17**) suggested similar binding of the envisaged reference compounds in comparison to previously described 1-(3-(methylamino)-1-phenylpropyl)-3-phenyl-1,3-dihydro-2H-benzimidazol-2-one (Me@APPI, **44**).¹⁶⁷ Thus, the desired references FAPPI:1-3 (**15-17**) were prepared by using the same synthesis strategies. In the course of the preparation of references **16** and **17**, different approaches for the synthesis of their intermediates were evaluated and the best methods providing the highest yields were ultimately selected for their preparation. First investigations of lipophilicity and BBB penetration behavior of the synthesized compounds (**15-17**) revealed suitable logP values and furthermore suggest likely BBB penetration by passive diffusion.

Based on the results of Hudson *et al.*,¹⁷⁶ PHOXI derivatives (**18-23**), which are highly affine and selective compounds for the NET, were synthesized within the scope of this thesis. Thereby, alcohol **129** served as starting material for the preparation of dimethyl amine derived references **18** and **21**. *Cis* isomers **130** and **21** could be successfully separated from their *trans* counterparts by chromatographic purification, and were employed for the synthesis of precursor compounds **19** and **22**. Rapid and efficient fluoroethylation of **19** and **22** then provided fluoroethyl amine derived references **20** and **23**.

Lipophilicity and IAM studies suggested suitable logP values and probable BBB penetration *via* passive diffusion for the investigated compounds (**18-23**).

Further IAM experiments as well as additional *in vitro* and *in vivo* approaches for BBB penetration prediction (co-culture models, animal models) of all precursors and references synthesized (**1-23**) will be subject of continuative studies at the Medical

University of Vienna, which will reveal more information about the BBB penetration behavior of these compounds.

In continuative studies, all newly prepared reference compounds will not only be subjected to further BBB penetration experiments, but will also be analyzed regarding their affinity and selectivity towards MAO-B or the NET. The most promising compounds regarding their suitability as potential MAO-B or NET ligands will then be selected for the development of new PET radiotracers for the MAO-B or NET system, respectively.

Accordingly, synthesized precursors will be employed as starting materials for the preparation of radiolabeled [¹¹C] and [¹⁸F] based PET tracers, which will serve for the imaging of MAO-B enzymes and NE transporters in the brain. As already discussed in chapter 1.3.3.3, there exist several [¹¹C]-methylation and [¹⁸F]-fluoroethylation methods, which will be evaluated at the Medical University of Vienna in order to standardize the most promising radiolabeling approach.

Subsequent binding studies and *in vivo* experiments as well as their interpretation and detailed evaluation will be the subject of continuative studies at the Medical University of Vienna. Additionally, micro-PET experiments, which reveal detailed information about MAO-B and NET densities *in vivo*, will be performed for the investigation of MAO-B and NET dysregulation mechanisms in the brain in different pathologies.

Docking studies as well as the organic synthesis of MAO-B (**1-14**) and FAPPI (**15-17**) derivatives have already been published in *Bioorganic & Medicinal Chemistry Letters* and *Molecules*, respectively. (cf. 5.4.1 and 5.4.2) A publication on PHOXI derivatives (**18-23**) is currently in progress and will mainly focus on the organic synthesis, enlargement of the compound library, as well as NMR based investigations of *cis/trans* isomer identification of these derivatives.

Besides BBB penetration experiments, first affinity studies are currently in progress for MAO-B and FAPPI derivatives. Inhibition assays are planned to determine MAO-B binding of the synthesized reference compounds (**1, 3, 4, 6, 7, 9, 10, 12, and 14**), whereas

membrane binding experiments are employed for FAPPI derivatives (**15-17**) as well as PHOXI derivatives (**18-23**) in order to evaluate their affinity towards the NET. The outcome of these studies will determine the suitability of the synthesized reference compounds as future MAO-B- and NET-PET radioligands.

3 EXPERIMENTAL

3.1 General

Recording of spectra:

¹H,- ¹³C,- ¹⁹F,- ¹⁵N-NMR Spectra: The NMR spectra were recorded from CDCl₃ or DMSO-*d*₆ solutions on a Bruker DPX200 spectrometer (200 MHz for ¹H, 50 MHz for ¹³C) or on a Bruker Avance III 400 spectrometer (400 MHz for ¹H, 100 MHz for ¹³C, 40 MHz for ¹⁵N, 376 MHz for ¹⁹F) at 25°C. The center of the solvent (residual) signal was used as an internal standard which was related to TMS with δ 7.26 ppm (¹H in CDCl₃), δ 2.49 ppm (¹H in DMSO-*d*₆), δ 77.0 ppm (¹³C in CDCl₃) and δ 39.5 ppm (¹³C in DMSO-*d*₆). ¹⁵N-NMR spectra (gs-HMBC, gs-HSQC) were referenced against neat, external nitromethane, ¹⁹F-NMR spectra by absolute referencing via ε ratio. Digital resolutions were 0.25 Hz/data point in the ¹H- and 0.3 Hz/data point in the ¹³C-NMR spectra. Coupling constants (*J*) are quoted in Hz. The following abbreviations were used to show the multiplicities: s: singlet, d: doublet, t: triplet, q: quadruplet, dd: doublet of doublet, m: multiplet.

Mass spectra were obtained on a Shimadzu QP 1000 instrument (EI, 70 eV)

High-resolution mass spectrometry was carried out on a Finnigan MAT 8230 (EI, 10 eV) or Finnigan MAT 900 S (ESI, 4 kV, 3 μ A, ACN/MeOH) electrospray ionization mass spectrometer with a micro-TOF analyzer.

Chromatographic purification:

Thin-layer chromatography: Merck TLC Silica Gel 60 F₂₅₄ aluminum sheets, Nr. 1.05554.0001, 0.2 mm x 20 cm x 20 cm and Merck TLC Silica Gel 60 RP-18 F_{254s} aluminum sheets, Nr. 1.05559.0001, 0.2 mm x 20 cm x 20 cm

Column chromatography: Merck Silica Gel 60 (70-230 mesh ASTM, Nr. 1.07734) or Merck LiChroprep RP-18 Silica Gel (40-63 μm)

Preclinical experiments:

Analytical HPLC was performed using an Agilent system (Boeblingen, Germany) consisting of an autosampler 1100, a quaternary pump 1200, a diode array detector 1200 (operated at 254 nm), and a lead-shielded BGO-radiodetector (Raytest).

pH measurement was carried out using a WTW inoLab 740 pH meter (WTW, Weilheim, Germany)

Other:

Melting points: were determined on a Reichert-Kofler hot-stage microscope

Microwave experiments were carried out in a Synthos 3000 microwave oven (Anton Paar, SXQ80 rotor) with an internal temperature probe.

Chemicals: Sigma Aldrich (www.sigma-aldrich.com), Acros (www.acros.com), VWR (www.vwr.com), TCI (www.tcichemicals.com)

3.2 Docking Parameters

3.2.1 MAO-B derivatives

The crystal structure of human MAO-B (PDB code 2C70) was initially prepared using the Protein Preparation Wizard embedded in the Schrödinger software package.³⁵⁶ One redundant protein chain and crystal waters were deleted, the co-factor FAD and *p*-nitrobenzylamine were kept. The protein H-Bond network was further optimized for a pH value of 7 using PROPKA. Used ligands were prepared with LigPrep in default settings.³⁵⁷ Side chains of I198 and Y435 were constrained to the internal rotamer library of GOLD,³⁵⁸ defining the coordinates of the non-covalent inhibitor as the binding site. All other settings were kept on default. After docking, the complexes were exported to MOE³⁵⁹ and energy minimized using LigX with default parameters. Subsequently, X-Score³⁶⁰ was used for rescoring of the minimized complexes.

3.2.2 APPI derivatives

The ligand structures were built in the protonated form using Molecular Operating Environment (MOE) 2013.³⁵⁹ Homology models of human NET, SERT, and DAT were obtained from the *Drosophila* dopamine transporter template (dDAT_{cryst}, PDB id 4M48³⁶¹), by selecting the model with the most favorable Discrete Optimized Protein Energy (DOPE) of 250 generated by Modeller 9.11.³⁶² The co-crystallized inhibitor nortriptyline (**101**) was retained during model generation and the compounds (**15-17**, **44**, and **45**) were docked in the same site using Genetic Optimization for Ligand Docking (GOLD) 5.2.³⁶³ One hundred poses per ligand (i.e. five hundred poses per protein target) were generated based on the GoldScore scoring function, while keeping the ligand flexible and the protein rigid.

The common chemical scaffold, i.e. the reference compound (**44**), was extracted from the resulting poses, analogous to the methods of a previous study.³⁶⁴ Cluster analysis was performed based on Euclidian distance and complete linkage of the root-mean square deviation of the ligand's heavy atoms matrix using XLStat.³⁴⁹ The dendrogram was cut at eight clusters and the ones containing all five ligands (**15-17**, **44**, and **45**) were selected.

3.3 NMR Spectroscopic Investigations

The NMR spectroscopic data of all compounds described in this study are listed in the Experimental Section. The corresponding spectra for novel compounds as well as final compounds will be displayed in the appendix.

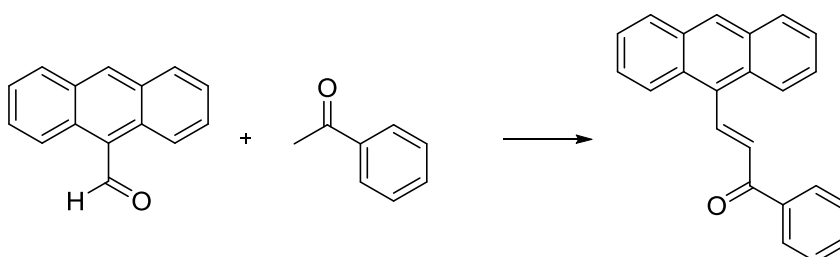
For important compounds full and unequivocal assignment of ¹H-NMR and ¹³C-NMR resonances was carried out by the combined application of various standard NMR spectroscopic techniques such as, for instance, APT (attached proton test), HSQC (heteronuclear single quantum coherence), HMBC (heteronuclear multiple bond coherence), COSY (correlated spectroscopy), TOCSY (totally correlated spectroscopy), and NOESY (nuclear overhauser enhancement spectroscopy). ¹⁵N-NMR chemical shifts were obtained *via* ¹H, ¹⁵N-HMBC and ¹H, ¹⁵N-HSQC experiments and finally referenced against external nitromethane (0 ppm). Compounds which were expected to contain fluorine atoms were additionally subjected to ¹⁹F-NMR spectroscopic measurements in order to verify the presence as well as the number of fluorine atoms.

3.4 Syntheses

3.4.1 MAO-B derivatives

3.4.1.1 Preparation of benzene based derivatives

3.4.1.1.1 (2E)-3-(Anthracen-9-yl)-1-phenylprop-2-en-1-one (56)



To a solution of acetophenone (1.00 g, 8.32 mmol) and anthracene-9-carbaldehyde (1.72 g, 8.32 mmol) in EtOH (20 ml) was added dropwise an aqueous solution of NaOH (85%, 1.11 g, 16.65 mmol) at 0°C. The mixture was stirred for 2 days, during which the temperature was allowed to rise to 25°C. Thereafter, the solution was poured into an ice bath and the pH was adjusted to a pH of 2 with 2N HCl. Prior to recrystallization from MeOH, the resulting product was filtered and evaporated to dryness.

Yield: 2.32 g (91%), yellow crystals, mp. 124°C-125°C

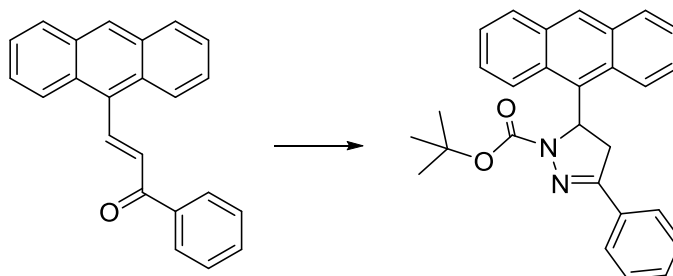
Analytical data are in complete accordance with literature values.³⁶⁵

Spectroscopic data:

¹H-NMR (200 MHz, CDCl₃): δ (ppm) 7.47-7.66 (m, 8H), 8.01-8.13 (m, 4H), 8.29-8.34 (m, 2H), 8.47 (s, 1H), 8.81 (d, *J* = 16.0 Hz, 1H)

¹³C-NMR (50 MHz, CDCl₃): δ (ppm) 125.3, 125.4, 126.4, 128.4, 128.7, 128.7, 131.0, 131.3, 133.1, 137.8, 141.9

3.4.1.1.2 *Tert*-butyl 5-(anthracen-9-yl)-3-phenyl-4,5-dihydro-1*H*-pyrazole-1-carboxylate (58)



To a cooled solution of (2*E*)-3-(anthracen-9-yl)-1-phenylprop-2-en-1-one (1.00 g, 2.63 mmol) and *tert*-butyl carbazate (0.38 g, 2.86 mmol) in THF (20 ml) was added Cs₂CO₃ (1.10 g, 3.38 mmol). After 24 h of stirring at 0°C, the mixture was warmed to room temperature, H₂SO₄ (1 drop) was added, and the solution was refluxed for another 24 h. The crude product was then purified by column chromatography (silica gel 60, PE/EtOAc 8:2).

Yield: 0.31 g (28%), yellow crystals, mp. 166°C-168°C

Spectroscopic data:

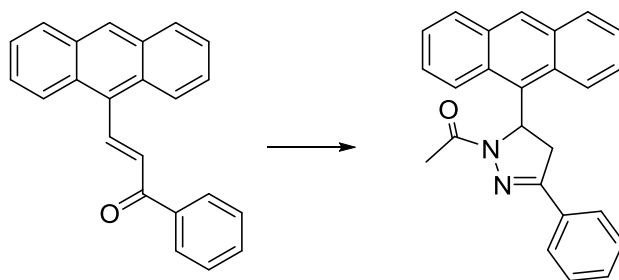
¹H-NMR (200 MHz, CDCl₃): δ (ppm) 3.72 (s, 9H), 3.53-3.67 (m, 1H), 3.85-4.00 (m, 1H), 6.69-6.81 (m, 1H), 7.33-7.59 (m, 7H), 7.86-8.06 (m, 5H), 8.35-8.46 (m, 2H)

¹³C-NMR (50 MHz, CDCl₃): δ (ppm) 27.4, 41.8, 57.2, 80.8, 122.8, 123.4, 124.7, 124.9, 126.3, 126.4, 126.8, 128.0, 128.2, 128.5, 129.3, 129.6, 129.97, 130.0, 131.1, 131.5, 131.8, 132.2, 151.8, 152.6

MS: *m/z* (%) 422 (M⁺, 2), 308 (100), 307 (56), 280 (12), 279 (36), 251 (15), 149 (10), 115 (29), 93 (13), 65 (11)

HRMS: *m/z* calculated for C₂₈H₂₆N₂O₂Na [M + Na]⁺: 445.1892. Found: 445.1890.

3.4.1.1.3 1-(5-(Anthracen-9-yl)-3-phenyl-4,5-dihydro-1H-pyrazol-1-yl)ethan-1-one (68)



- 1) Method 1: 3-(Anthracen-9-yl)-1-phenylprop-2-en-1-one (0.20 g, 0.65 mmol) was dissolved in toluene (40 ml) and to this mixture were added hydrazine monohydrate (0.32 g, 0.3 ml, 6.48 mmol) and CH_3COOH (10 ml). The solution was refluxed in a Dean-Stark trap overnight. Thereafter, the crude reaction product was evaporated *in vacuo* and purified by column chromatography (silica gel 60, PE/EtOAc 8:2).

Yield: 0.13 g (53%), orange crystals, mp. 199°C-201°C

- 2) Method 2: 3-(Anthracen-9-yl)-1-phenylprop-2-en-1-one (1.00 g, 3.24 mmol) was dissolved in MeOH (12 ml) and CH_3COOH (4 ml) and hydrazine monohydrate (0.20 g, 0.2 ml, 3.89 mmol) were added. The reaction mixture was introduced into a microwave vessel and heated in a microwave oven at 700 W and 85°C for 8 min. The resulting product was purified twice by column chromatography (silica gel 60, PE/EtOAc 9:1 and RP-18 silica gel, ACN/ H_2O 9:1).

Yield: 0.84 g (88%), orange crystals, mp. 199°C-201°C

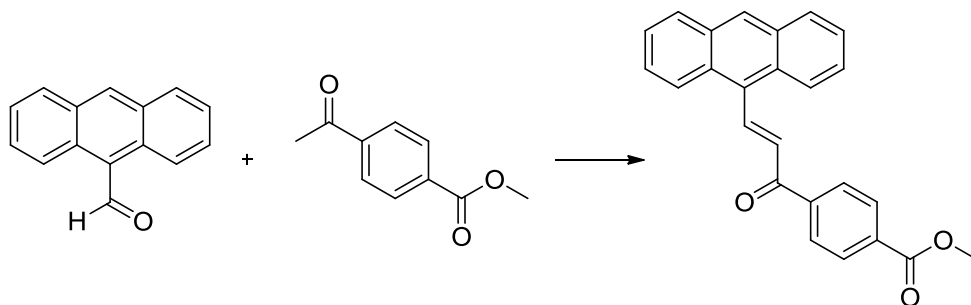
Spectroscopic data:

¹H-NMR (200 MHz, CDCl₃): δ (ppm) 2.28 (s, 3H), 3.33 (dd, *J* = 10.0 Hz and 8.0 Hz, 1H), 3.68 (dd, *J* = 14.0 Hz and 4.0 Hz, 1H), 6.95-6.77 (m, 1H), 7.25-7.47 (m, 6H), 7.70-7.83 (m, 3H), 7.87-7.93 (m, 3H), 8.32-8.37 (m, 2H)

¹³C-NMR (50 MHz, CDCl₃): δ (ppm) 21.7, 41.5, 55.9, 122.7, 123.0, 124.4, 124.7, 126.1, 126.4, 126.6, 127.8, 128.0, 128.2, 128.4, 127.7, 129.2, 130.2, 131.2, 131.3, 131.4, 131.7, 132.2

MS: *m/z* (%) 364 (M⁺, 14), 320 (12), 218 (13), 189 (27), 178 (28), 111 (27), 85 (39), 71 (68), 57 (91), 43 (100)

3.4.1.1.4 Methyl 4-((2E)-3-(anthracen-9-yl)prop-2-enoyl)benzoate (62)



To a solution of anthracene-9-carbaldehyde (3.47 g, 16.83 mmol) and methyl 4-acetylbenzoate (3.00 g, 16.83 mmol) in MeOH (50 ml) was added dropwise an aqueous solution of KOH (85%, 2.22 g, 33.65 mmol) at 0°C. The mixture was stirred for 48 h during which the temperature was allowed to rise to 25°C. Thereafter, the formed yellow crystals were filtered, washed and dried.

Yield: 4.96 g (80%), yellow powder, mp. 170°C-171°C

Spectroscopic data:

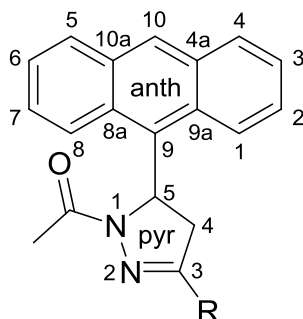
¹H-NMR (200 MHz, CDCl₃): δ (ppm) 3.94 (s, 3H), 7.46-7.55 (m, 5H), 7.97-8.02 (m, 2H), 8.07-8.18 (m, 4H), 8.24-7.29 (m, 2H), 8.43 (s, 1H), 8.79 (d, *J* = 15.9 Hz, 1H)

¹³C-NMR (50 MHz, CDCl₃): δ (ppm) 52.9, 125.6, 125.9, 127.0, 129.0, 129.2, 129.4, 130.1, 130.4, 131.1, 131.7, 134.2, 141.7, 143.3, 166.7, 189.6

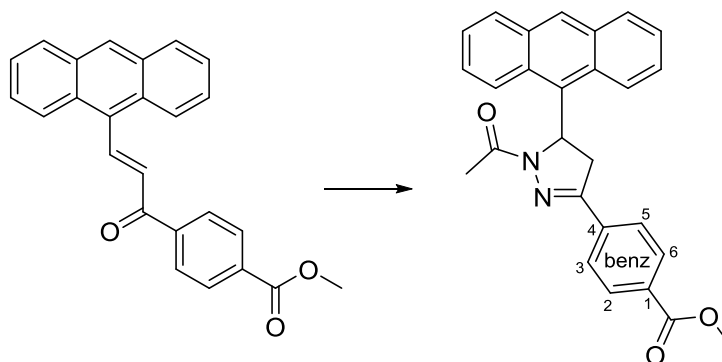
MS: *m/z* (%) 366 (M⁺, 12), 203 (100), 176 (3), 163 (35), 138 (10), 120 (3), 104 (4), 76 (6), 59 (3), 50 (3)

HRMS: *m/z* calculated for C₂₅H₁₈O₃Na [M + Na]⁺: 389.1154. Found: 389.1148.

The compound numbering depicted below was used for the signal assignment of ^1H - and ^{13}C -NMR data of compounds **1-4**, **6-14**, **78**, **91**, and **99** in the next chapters:



3.4.1.1.5 Methyl 4-(1-acetyl-5-(anthracen-9-yl)-4,5-dihydro-1H-pyrazol-3-yl)benzoate (1)



- 1) Method 1: A mixture of methyl 4-((*E*)-3-(anthracen-9-yl)prop-2-enoyl)benzoate (0.50 g, 1.36 mmol) in CH_3COOH (26 ml) was added dropwise to hydrazine monohydrate (0.14 g, 2.73 mmol) at 0°C - 5°C under stirring, and the resulting solution was refluxed for 7 h. After completion of the reaction, the mixture was poured into a saturated NaHCO_3 solution. The formed precipitate was collected by filtration, washed with H_2O , and dried. Thereafter, the crude product was purified by column chromatography (silica gel 60, PE/EtOAc 8:2 and RP-18 silica gel, ACN).

Yield: 95 mg (17%), yellow crystals, mp. 279°C - 281°C

- 2) Method 2: A solution of methyl 4-((2E)-3-(anthracen-9-yl)prop-2-enoyl)benzoate (0.50 g, 1.36 mmol), hydrazine monohydrate (0.68 g, 13.65 mmol), and CH₃COOH (12 ml) in toluene was refluxed for 45 min in a Dean-Stark trap. After the reaction, the crude product was purified by column chromatography (silica gel 60, PE/EtOAc 8:2 and RP-18 silica gel, ACN/H₂O 9:1).

Yield: 0.19 g (33%), yellow crystals, mp. 279°C-281°C

- 3) Method 3: A mixture of methyl 4-((2E)-3-(anthracen-9-yl)prop-2-enoyl)benzoate (0.50 g, 1.36 mmol), hydrazine monohydrate (0.68 g, 13.65 mmol), sulfuric acid (1 drop), and CH₃COOH (12 ml) was introduced into a microwave vessel and heated in a microwave oven at 700 W and 85°C for 5 min. After completion of the reaction, the resulting crystals were filtered, washed and dried, and then subjected to purification by column chromatography (silica gel 60, PE/EtOAc 8:2).

Yield: 0.32 g (56%), yellow crystals, mp. 279-281°C

- 4) Method 4: Hydrazine monohydrate (0.68 g, 13.65 mmol) was added dropwise to a solution of methyl 4-((2E)-3-(anthracen-9-yl)prop-2-enoyl)benzoate (0.50 g, 1.36 mmol) in CH₃COOH (7 ml)/ACN (14 ml) and the resulting mixture was refluxed for 24 h. The formed precipitate was filtered, washed several times with EtOH, and dried, prior to chromatographic purification (silica gel 60, PE/EtOAc 8:2 and RP-18 silica gel, ACN).

Yield: 0.33 g (58%), yellow crystals, mp. 279°C-281°C

Spectroscopic data:

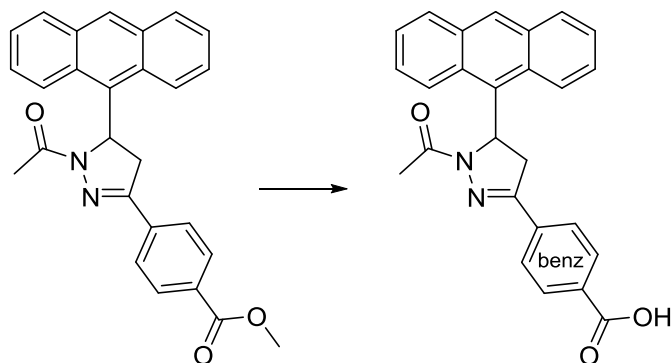
¹H-NMR (400 MHz, CDCl₃): δ (ppm) 2.38 (s, 3H, pyr NCOCH₃), 3.51 (dd, *J* = 18.1 Hz and 9.4 Hz, 1H, pyr 4-CH₂), 3.90 (dd, *J* = 18.1 Hz and 13.1 Hz, 1H, pyr 4-CH₂), 3.96 (s, 3H, benz OCH₃), 6.88 (dd, *J* = 13.1 Hz and 9.4 Hz, 1H, pyr 5-CH), 7.26-7.42 (m, 2H, anth 6-CH, anth 7-CH), 7.45-7.49 (m, 1H, anth 3-CH), 7.54-7.56 (m, 1H, anth 2-CH), 7.73-7.76 (m, 1H, anth 8-CH), 7.87-7.89 (m, 2H, benz 3-CH, benz 5-CH), 8.00-8.03 (m, 2H, anth 4-CH, anth 5-CH), 8.11-8.14 (m, 2H, benz 2-CH, benz 6-CH), 8.43 (s, 1H, anth 10-CH), 8.48-8.50 (m, 1H, anth 1-CH)

¹³C-NMR (100 MHz, CDCl₃): δ (ppm) 21.8 (pyr NCOCH₃), 41.5 (pyr 4-CH₂), 52.3 (benz OCH₃), 56.3 (pyr 5-CH), 122.6 (anth 8-CH), 123.0 (anth 1-CH), 124.6 (anth 6-CH), 124.9 (anth 3-CH), 126.2 (anth 7-CH), 126.5 (benz 3-CH, benz 5-CH), 126.6 (anth 2-CH), 128.2 (anth 8a-CH), 128.6 (anth 10-CH), 129.4 (anth 4-CH), 130.0 (benz 2-CH, benz 6-CH), 130.1 (anth 9a-CH), 130.2 (anth 5-CH), 131.1 (anth 9-CH), 131.3 (anth 4a-CH), 131.4 (benz 1-C), 131.9 (10a-CH), 135.5 (benz 4-C), 152.8 (pyr 3-C), 166.4 (benz C=O), 169.7 (pyr NCOCH₃)

MS: *m/z* (%) 422 (M⁺, 100), 379 (64), 363 (24), 349 (18), 289 (31), 276 (10), 218 (73), 203 (72), 189 (16), 178 (90), 144 (22), 43 (39)

HRMS: *m/z* calculated for C₂₇H₂₂N₂O₃Na [M + Na]⁺: 445.1528. Found: 455.1525.

3.4.1.1.6 4-(1-Acetyl-5-(anthracen-9-yl)-4,5-dihydro-1H-pyrazol-3-yl)benzoic acid (2)



Methyl 4-(1-acetyl-5-(anthracen-9-yl)-4,5-dihydro-1H-pyrazol-3-yl)benzoate (0.50 g, 1.18 mmol) and lithium hydroxide monohydrate (0.20 g, 5.92 mmol) were dissolved in a mixture of THF/MeOH/H₂O (2/3/1, 12 ml) and stirred at 50°C for 4 h. After completion of the reaction, the solution was acidified with 2N HCl and extracted with EtOAc. The combined organic layers were dried over MgSO₄ and evaporated *in vacuo*.

The reaction product was obtained in excellent yields and introduced in the next reaction step without further purification.

Yield: 0.43 g (90%), dark yellow crystals, mp. 230°C-231°C

Spectroscopic data:

¹H-NMR (200 MHz, DMSO-*d*₆): δ (ppm) 2.24 (s, 3H), 3.43 (dd, *J* = 10.0 Hz and 8.0 Hz, 1H), 4.13 (dd, *J* = 12.0 Hz and 6.0 Hz, 1H), 6.86-6.97 (m, 1H), 7.40-7.73 (m, 5H), 7.96-8.12 (m, 6H), 8.57-8.61 (m, 2H)

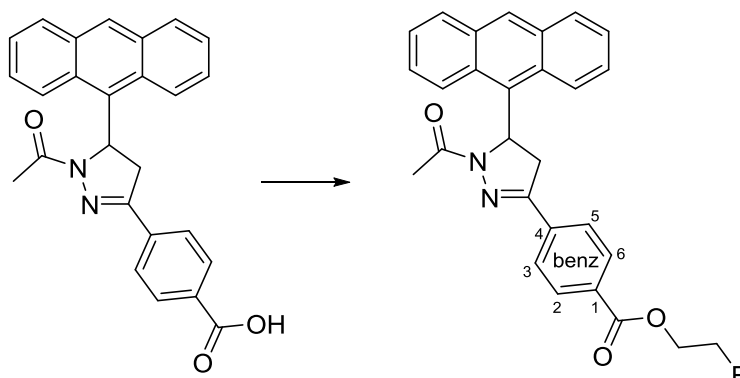
Due to limited resolution of the measuring instrument, proton benz COOHH could not be detected.

¹³C-NMR (50 MHz, DMSO-*d*₆): δ (ppm) 21.7, 41.4, 56.2, 122.5, 123.8, 124.8, 125.1, 126.2, 126.4, 126.8, 127.6, 127.8, 129.1, 129.6, 129.8, 130.0, 130.9, 131.4, 132.1, 132.3, 135.0, 135.6, 166.9, 168.2

MS: *m/z* (%) 408 (M⁺, 30), 365 (19), 289 (11), 218 (31), 203 (47), 189 (19), 178 (100), 43 (40)

HRMS: *m/z* calculated for C₂₆H₂₀N₂O₃Na [M + Na]⁺: 431.1372. Found: 431.1367.

3.4.1.1.7 2-Fluoroethyl-4-(1-acetyl-5-(anthracen-9-yl)-4,5-dihydro-1H-pyrazol-3-yl)benzoate (3)



Fluoroethanol (0.02 g, 0.25 mmol), DCC (0.06 g, 0.27 mmol), and DMAP (0.03 g, 0.27 mmol) were added to a solution of 4-(1-acetyl-5-(anthracen-9-yl)-4,5-dihydro-1H-pyrazol-3-yl)benzoic acid (0.10 g, 0.25 mmol) in absolute CH_2Cl_2 (4 ml), and the resulting reaction mixture was stirred overnight at room temperature. After completion of the reaction, the crude product was evaporated *in vacuo* and purified by column chromatography twice (silica gel 60, PE/EtOAc 6:4 and RP- silica gel, ACN/ H_2O 8:2).

Yield: 28 mg (25%), colorless crystals, mp. 214°C-215°C

Spectroscopic data:

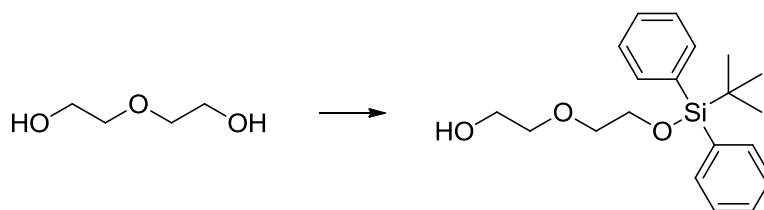
¹H-NMR (400 MHz, CDCl₃): δ (ppm) 2.39 (s, 3H, pyr NCOCH₃), 3.55 (dd, *J* = 18.1 Hz and 9.4 Hz, 1H, pyr 4-CH₂), 3.96 (dd, *J* = 18.1 Hz and 13.2 Hz, 1H, pyr 4-CH₂), 4.56-4.58 (m, 1H, benz CH₂CH₂F), 4.64-4.66 (m, 1H, benz CH₂CH₂F), 4.69-4.71 (m, 1H, benz CH₂CH₂F), 4.81-4.83 (m, 1H, benz CH₂CH₂F) 6.93 (dd, *J* = 13.2 Hz and 9.4 Hz, 1H, pyr 5-CH), 7.33-7.42 (m, 2H, anth 6-CH, anth 7-CH), 7.47-7.51 (m, 1H, anth 3-CH), 7.56-7.60 (m, 1H, anth 2-CH), 7.73-7.76 (m, 1H, anth 8-CH), 7.90-7.92 (m, 2H, benz 3-CH, benz 5-CH), 8.02-8.04 (m, 2H, anth 4-CH, anth 5-CH), 8.16-8.18 (m, 2H, benz 2-CH, benz 6-CH), 8.44 (s, 1H, anth 10-CH), 8.51-8.53 (m, 1H, anth 1-CH)

¹³C-NMR (100 MHz, CDCl₃): δ (ppm) 21.9 (pyr NCOCH₃), 41.6 (pyr 4-CH₂), 56.4 (pyr 5-CH), 64.1 (d, *J* = 20.1 Hz, benz CH₂CH₂F), 81.3 (d, *J* = 171.0 Hz, benz CH₂CH₂F), 122.7 (anth 8-CH), 123.0 (anth 1-CH), 124.6 (anth 6-CH), 124.9 (anth 3-CH), 126.3 (anth 7-CH), 126.6 (benz 3-CH, 5-CH), 126.7 (anth 2-CH), 128.3 (anth 8a-CH), 128.7 (anth 10-CH), 129.4 (anth 4-CH), 130.2 (anth 5-CH, anth 9a-CH, benz 2-CH, benz 6-CH), 130.9 (benz 1-C), 131.0 (anth 9-CH), 131.4 (anth 4a-CH), 131.9 (anth 10a-CH), 135.9 (benz 4-C), 152.7 (pyr 3-C), 165.7 (benz CO), 169.8 (NCOCH₃)

¹⁹F-NMR (471 MHz, CDCl₃): δ (ppm) -224.50 (m, benz CH₂CH₂F)

MS: *m/z* (%) 454 (M⁺, 46), 411 (26), 396 (12), 289 (15), 218 (48), 203 (63), 189 (16), 178 (100), 145 (20), 43 (33)

HRMS: *m/z* calculated for C₂₈H₂₃FN₂O₃Na [M + Na]⁺: 477.1590. Found: 477.1581.

3.4.1.1.8 2-(2-((*Tert*-butyl(diphenyl)silyl)oxy)ethoxy)ethanol (69)

Diethylene glycol (3.00 g, 28.27 mmol) and imidazole (1.90 g, 28.27 mmol) were dissolved in dry CH₂Cl₂ (44 ml) and a solution of *tert*-butylchlorodiphenylsilane (7.80 g, 28.27 mmol) in dry CH₂Cl₂ (10 ml) was added dropwise under argon atmosphere. The reaction mixture was stirred for 24 h at room temperature. After completion of the reaction, the solvent was evaporated *in vacuo* and the crude product was purified by column chromatography (silica gel 60, PE/EtOAc 9:1 → 7:3).

Yield: 3.82 g (39%), colorless oil

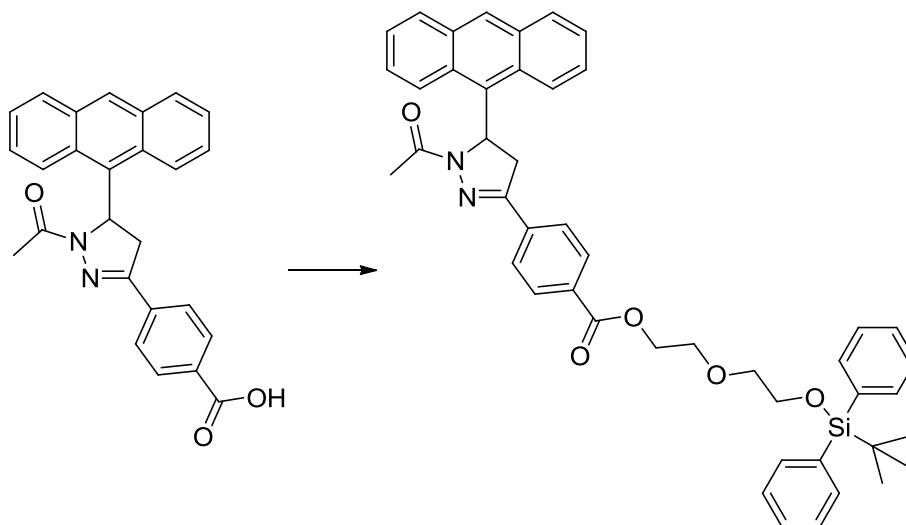
Analytical data are in complete accordance with literature values.³⁶⁶

Spectroscopic data:

¹H-NMR (200 MHz, CDCl₃): δ (ppm) 1.04 (s, 9H), 3.48-3.57 (m, 5H), 3.59-3.65 (m, 2H), 3.75-3.80 (m, 2H), 7.28-7.35 (m, 6H), 7.63-7.69 (m, 4H)

¹³C-NMR (50 MHz, CDCl₃): δ (ppm) 18.9, 26.6, 61.3, 63.2, 72.0, 72.2, 127.4, 129.4, 133.2, 135.3

3.4.1.1.9 2-(2-((*Tert*-butyl(diphenyl)silyl)oxy)ethoxy)ethyl 4-(1-acetyl-5-(anthracen-9-yl)-4,5-dihydro-1*H*-pyrazol-3-yl)benzoate (70)



4-(1-Acetyl-5-(anthracen-9-yl)-4,5-dihydro-1*H*-pyrazol-3-yl)benzoic acid (0.65 g, 1.59 mmol), DCC (0.59 g, 2.86 mmol), and DMAP (catalytic amounts) were dissolved in CH₂Cl₂ (64 ml). To this solution was added *t*-butyldiphenylsilyloxyethoxyethanol (0.55 g, 1.59 mmol) and the mixture was refluxed for 3 d. Thereafter, the resulting product was purified by column chromatography (RP-18 silica gel, MeOH/H₂O 8:2). 150 mg of the starting material could be regained.

Yield: 0.21 g (18%), yellow powder, mp. 115°C-116°C

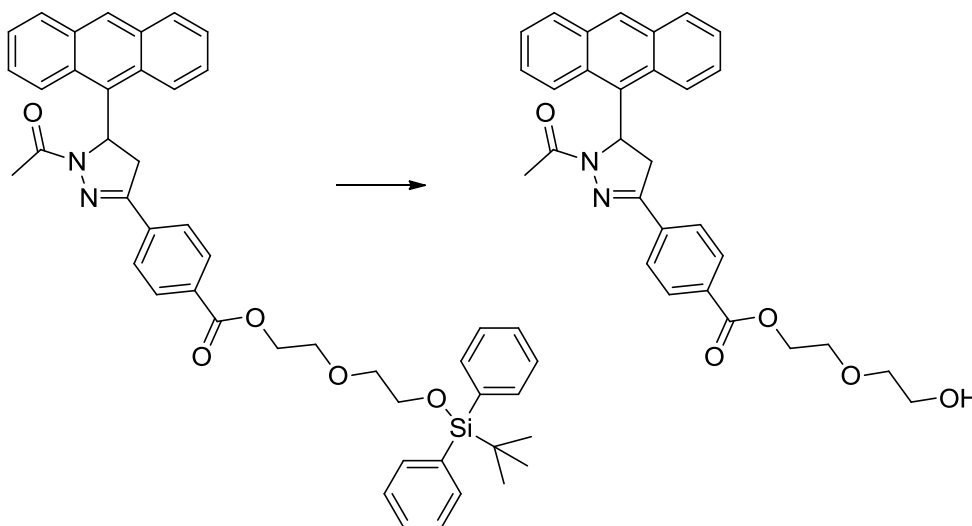
Spectroscopic data:

MS: *m/z* (%) 735 (M⁺, 2), 435 (100), 349 (13), 291 (22), 203 (54), 178 (64), 57 (29)

HRMS: *m/z* calculated for C₄₆H₄₆N₂O₅SiNa [M + Na]⁺: 757.3074. Found: 757.3070.

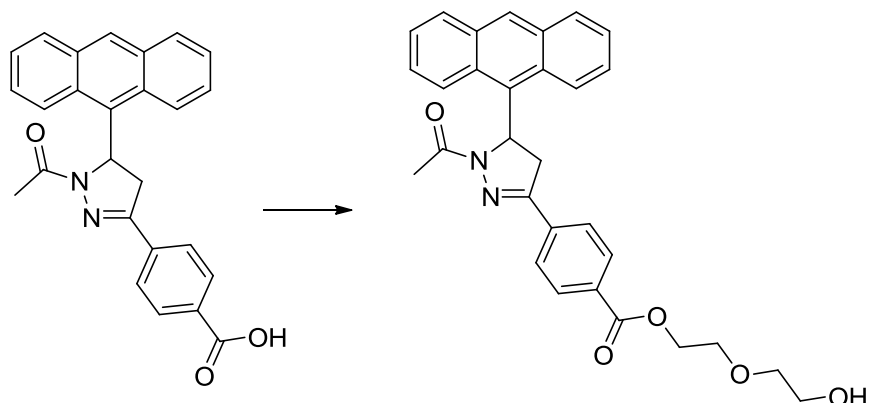
3.4.1.1.10 2-(2-Hydroxyethoxy)ethyl 4-(1-acetyl-5-(anthracen-9-yl)-4,5-dihydro-1H-pyrazol-3-yl)benzoate (71)

1) Method 1:



2-(2-((*tert*-Butyldiphenylsilyl))oxy)ethoxyethyl 4-(1-acetyl-5-(anthracen-9-yl)-4,5-dihydro-1H-pyrazol-3-yl)benzoate (0.21 g, 0.29 mmol) was dissolved in THF (4 ml) and a solution of tetra-*n*-butylammonium fluoride (1M in THF, 0.29 ml, 0.29 mmol) was added dropwise at room temperature. After stirring the mixture for 2 h at room temperature, H₂O (1 drop) was added. Evaporation afforded the crude product, which was purified repeatedly by column chromatography (RP-18 silica gel, MeOH/H₂O 7:3). Due to unsatisfactory/unsuccessful separation, the crude reaction product was directly employed in the next reaction step.

Yield: 57 mg (40%), colorless crystals, mp. n.d.

2) Method 2:

To a mixture of 4-(1-acetyl-5-(anthracen-9-yl)-4,5-dihydro-1H-pyrazol-3-yl)benzoic acid (0.10 g, 0.24 mmol) in CH_2Cl_2 (10 ml), diethylene glycol (0.02 g, 0.22 mmol), DCC (0.10 g, 0.44 mmol), and DMAP (catalytic amounts) were added and the reaction mixture was stirred overnight. Thereafter, the resulting product was purified several times by column chromatography (RP-18 silica gel, MeOH/ H_2O 8:2). Due to unsatisfactory/unsuccessful separation, the crude reaction product was directly employed in the next reaction step.

Yield: 87 mg (72%), colorless crystals, mp. n.d.

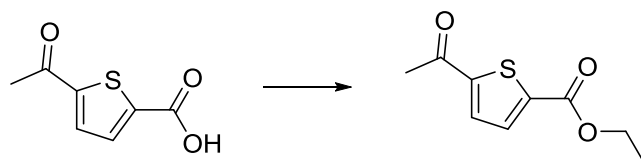
Spectroscopic data:

MS: m/z (%) 496 (M^+ , 1), 289 (1), 218 (2), 199 (100), 181 (5), 152 (6), 121 (3), 77 (12)

HRMS: m/z calculated for $\text{C}_{30}\text{H}_{28}\text{N}_2\text{O}_5\text{Na}$ [$\text{M} + \text{Na}$] $^+$: 519.1896. Found: 519.1891.

3.4.1.2 Preparation of thiophene based derivatives

3.4.1.2.1 Ethyl 5-acetylthiophene-2-carboxylate (74)



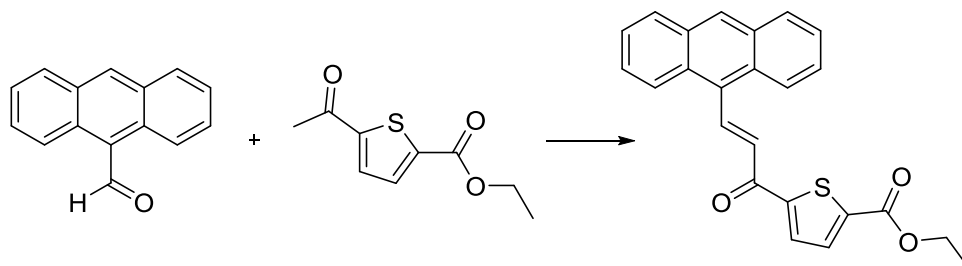
To a solution of 5-acetylthiophene-2-carboxylic acid (1.00 g, 5.88 mmol) in toluene were added EtOH (0.20 g, 4.41 mmol) and p-toluenesulfonic acid (catalytic amount). The solution was refluxed in a Dean Stark trap for 3 h. Thereafter, the crude reaction product was washed with H₂O, saturated NaHCO₃ solution, and again with H₂O. The organic layer was dried over Na₂SO₄ and evaporated to dryness to give ethyl 5-acetylthiophene-2-carboxylate in excellent yields.

Yield: 1.06 g (91%), light beige crystals, mp. 45°C-46°C

Analytical data are in complete accordance with literature values.³⁶⁷

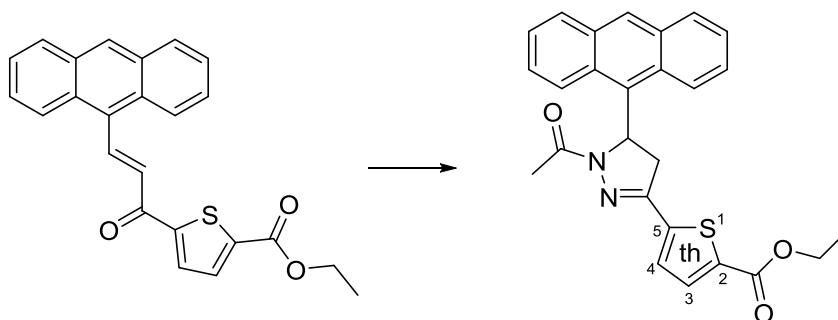
Spectroscopic data:

¹³C-NMR (50 MHz, CDCl₃): δ (ppm) 14.0, 26.7, 61.6, 131.6, 133.0, 139.9, 148.4, 161.4, 190.6

3.4.1.2.2 Ethyl 5-((2E)-3-(anthracen-9-yl)prop-2-enoyl)thiophene-2-carboxylate (76)

A mixture of anthracene-9-carbaldehyde (1.04 g, 5.04 mmol) and ethyl 5-acetylthiophene-2-carboxylate (1.00 g, 5.04 mmol) in EtOH was stirred at 0°C. An aqueous solution of NaOH (85%, 0.40 g, 10.09 mmol) was added dropwise and the mixture was stirred for 48 h, during which the temperature was allowed to rise to 25°C. Thereafter, the reaction mixture was poured into ice-cold H₂O and the pH was adjusted to pH 3 with 2N HCl. The yellow precipitate obtained was filtered, washed, and dried prior to purification by column chromatography (silica gel 60, CH₂Cl₂/MeOH 8:2). The purified product was directly employed in the next reaction step.

3.4.1.2.3 Ethyl 5-(1-acetyl-5-(anthracen-9-yl)-4,5-dihydro-1H-pyrazol-3-yl)thiophene-2-carboxylate (78)



A mixture of ethyl 5-((*E*)-3-(anthracen-9-yl)prop-2-en-1-yl)thiophene-2-carboxylate (0.27 g, 0.69 mmol), hydrazine monohydrate (0.35 g, 6.93 mmol), CH₃COOH (12 ml), and sulfuric acid (1 drop) was introduced into a microwave vessel and heated in the microwave oven at 700 W and 85°C for 5 min. The formed yellow crystals were filtered, washed several times with EtOH, and dried, prior to chromatographic separation (silica gel 60, PE/EtOAc 9:1 and RP-18 silica gel, ACN/H₂O 9:1).

Yield: 47 mg (15%), dark yellow crystals, mp. 115°C-117°C

Spectroscopic data:

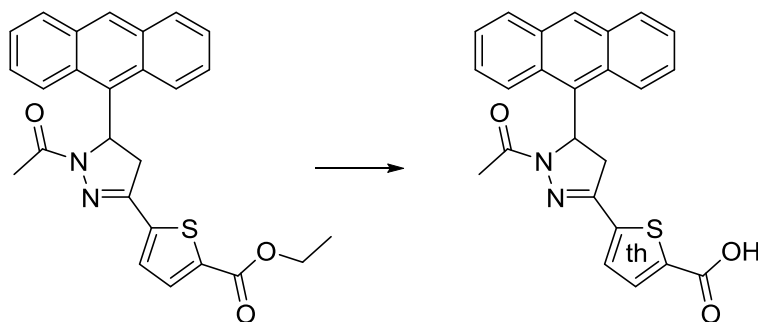
¹H-NMR (200 MHz, CDCl₃): δ (ppm) 1.42 (t, *J* = 7.2 Hz, 3H, th OCH₂CH₃), 2.32 (s, 3H, pyr NCOCH₃), 3.45 (dd, *J* = 9.5 Hz and 8.5 Hz, 1H, pyr 4-CH₂), 3.62-3.92 (m, 1H, pyr 4-CH₂), 4.41 (q, *J* = 7.0 Hz, 2H, th OCH₂CH₃), 6.84 (dd, *J* = 9.5 Hz and 3.5 Hz, 1H, pyr 5-CH), 7.14 (d, *J* = 4.0 Hz, 1H, th 4-CH), 7.35-7.59 (m, 4H, anth 7-CH, anth 6-CH, anth 3-CH, anth 2-CH), 7.71-7.75 (m, 2H, anth 8-CH, th 3-CH), 7.98-8.04 (m, 2H, anth 5-CH, anth 4-CH), 8.42-8.46 (m, 2H, anth 10-CH, anth 1-CH)

¹³C-NMR (50 MHz, CDCl₃): δ (ppm) 14.3 (th OCH₂CH₃), 21.7 (pyr NCOCH₃), 41.9 (anth 4-CH₂), 56.5 (anth 5-CH), 61.5 (th OCH₂CH₃), 122.5 (anth 8-CH), 122.9 (anth 1-CH), 124.6 (anth 6-CH), 124.9 (anth 3-CH), 126.3 (anth 7-CH), 126.7 (anth 2-CH), 128.2 (anth 8a-CH), 128.4 (th 4-CH), 128.7 (anth 10-CH), 129.4 (anth 4-CH), 130.1 (anth 9a-CH), 130.2 (anth 5-CH), 130.7 (anth 9-CH), 131.3 (anth 4a-CH), 131.8 (anth 10a-CH), 133.4 (th 3-CH), 135.7 (th 2-CH), 140.7 (th 5-CH), 148.8 (pyr 3-C), 161.8 (th CO), 169.6 (pyr NCOCH₃)

MS: *m/z* (%) 442 (M⁺, 21), 267 (100), 195 (79), 178 (40), 137 (40), 97 (46), 71 (47), 57 (75), 43 (73), 41 (60)

HRMS: *m/z* calculated for C₂₆H₂₂N₂O₃SNa [M + Na]⁺: 465.1249. Found: 465.1248.

3.4.1.2.4 5-(1-Acetyl-5-(anthracen-9-yl)-4,5-dihydro-1H-pyrazol-3-yl)thiophene-2-carboxylic acid (5)



To a mixture of ethyl 5-(1-acetyl-5-(anthracen-9-yl)-4,5-dihydro-1H-pyrazol-3-yl)thiophene-2-carboxylate (0.08 mg, 0.19 mmol) in THF/H₂O/MeOH (5/2.5/5.5, 15 ml) was added lithium hydroxide monohydrate (0.04 g, 0.92 mmol) under stirring. The resulting reaction mixture was heated to 50°C and stirred for 2 h.

Thereafter, the crude reaction product was acidified with 2N HCl and extracted with EtOAc. The combined organic layers were dried over MgSO₄, the solvent was evaporated *in vacuo* and the crude product was purified by column chromatography (RP-18 silica gel, ACN/H₂O 8:2) to give 5-(1-acetyl-5-(anthracen-9-yl)-4,5-dihydro-1H-pyrazol-3-yl)thiophene-2-carboxylic acid as colorless crystals.

Yield: 58 mg (75%), colorless crystals, mp. 280°C-281°C

Spectroscopic data:

¹H-NMR (200 MHz, DMSO-*d*₆): δ (ppm) 2.17 (s, 3H), 3.32-3.47 (m, 1H), 4.13 (dd, *J* = 12.0 Hz and 6.0 Hz, 1H), 6.91 (dd, *J* = 10.0 Hz and 2.0 Hz, 1H), 7.35 (d, *J* = 2.0 Hz, 1H), 7.41-7.51 (m, 3H), 7.54-7.63 (m, 2H), 7.71-7.76 (m, 1H), 8.09-8.14 (m, 2H), 8.59 (s, 2H)

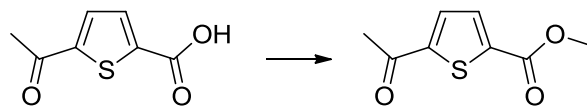
Due to limited resolution of the measuring instrument, proton th COOH could not be detected.

¹³C-NMR (50 MHz, DMSO-*d*₆): δ (ppm) 22.0, 42.4, 56.4, 122.9, 124.2, 125.2, 125.5, 126.6, 126.7, 127.9, 128.1, 129.4, 129.7, 129.9, 130.3, 130.6, 131.3, 131.8, 132.7, 136.1, 148.2, 151.1, 165.4, 168.1

MS: *m/z* (%) 414 (*M*⁺, 3), 203 (12), 84 (12), 69 (19), 57 (29), 56 (16), 55 (24), 44 (100), 43 (52), 42 (18)

HRMS: *m/z* calculated for C₂₄H₁₈N₂O₃SNa [*M* + Na]⁺: 437.0936. Found: 437.0927.

3.4.1.2.5 Methyl 5-acetylthiophene-2-carboxylate (63)



To a solution of 5-acetylthiophene-2-carboxylic acid (1.00 g, 5.52 mmol) in CH_2Cl_2 (17 ml) was added tetrafluoroboric acid (40% in H_2O , 0.49 g, 5.52 mmol) at 0°C . Thereafter, trimethylsilyldiazomethane (1.76 ml, 1.26 g, 11.04 mmol) was added dropwise in 4 portions at 0°C under stirring. The first portion was directly added after cooling to 0°C and the other 3 portions were introduced in intervals of 30 min. Stirring was continued for 30 min after the last addition. Then, the reaction mixture was extracted with $\text{CH}_2\text{Cl}_2/\text{H}_2\text{O}$, dried over MgSO_4 , and evaporated to dryness prior to purification by column chromatography (silica gel 60, PE/EtOAc 8:2).

Yield: 0.21 g (11%), light yellow crystals, mp. $127\text{--}128^\circ\text{C}$

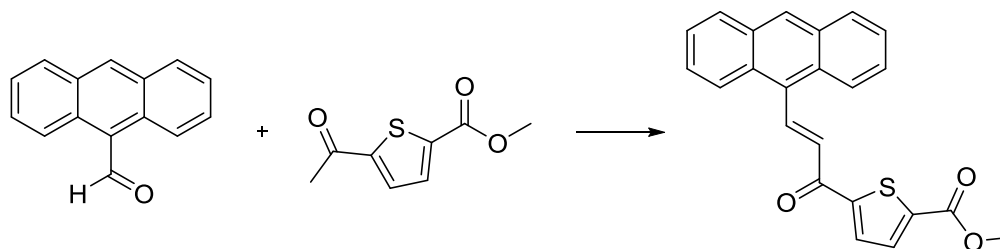
Analytical data are in complete accordance with literature values.³⁶⁸

Spectroscopic data:

$^1\text{H-NMR}$ (200 MHz, CDCl_3): δ (ppm) 2.56 (s, 3H), 3.88 (s, 3H), 7.62 (d, $J = 4.0$ Hz, 1H), 7.73 (d, $J = 4.0$ Hz, 1H)

$^{13}\text{C-NMR}$ (50 MHz, CDCl_3): δ (ppm) 26.9, 52.6, 131.6, 133.3, 139.5, 148.7, 162.0, 190.7

3.4.1.2.6 Methyl 5-((2E)-3-(anthracen-9-yl)prop-2-enoyl)thiophene-2-carboxylate (64)



To a stirred solution of anthracene-9-carbaldehyde (0.26 g, 1.25 mmol) and methyl 5-acetylthiophene-2-carboxylate (0.23 g, 1.25 mmol) in MeOH (20 ml) was added dropwise an aqueous solution of KOH (85%, 0.17 g, 2.5 mmol) at 0°C. After the addition, the reaction mixture was allowed to warm to room temperature during 48 h of stirring. The formed yellow precipitate was filtered, washed, and dried to afford the product in very good yields.

Yield: 0.38 g (82%), yellow powder, mp. 160°C-161°C

Spectroscopic data:

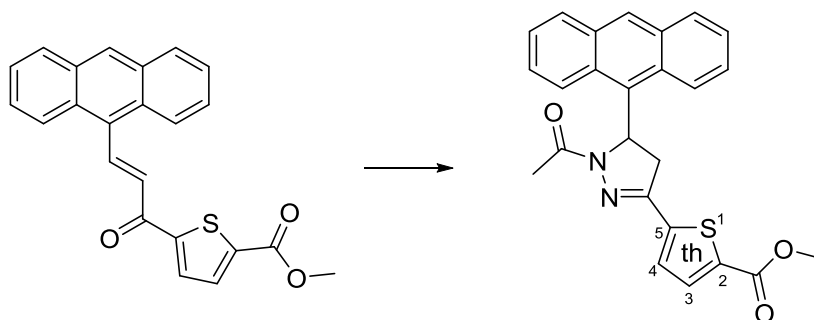
¹H-NMR (200 MHz, CDCl₃): δ (ppm) 3.93 (s, 3H), 7.36-7.56 (m, 5H), 7.73-7.80 (m, 2H), 7.99-8.04 (m, 2H), 8.25-8.29 (m, 2H), 8.46 (s, 1H), 8.85 (d, *J* = 15.8 Hz, 1H)

¹³C-NMR (50 MHz, CDCl₃): δ (ppm) 52.6, 125.0, 125.4, 126.6, 128.86, 128.93, 129.3, 129.6, 129.7, 131.2, 131.5, 133.6, 139.8, 142.4, 149.6, 162.0, 181.5

MS: *m/z* (%) 372 (M⁺, 13), 203 (100), 169 (29), 162 (3), 142 (5), 119 (3), 110 (4), 82 (5), 59 (5), 53 (5)

HRMS: *m/z* calculated for C₂₃H₁₆O₃SNa [M + Na]⁺: 395.0718. Found: 395.0716.

3.4.1.2.7 Methyl 5-(1-acetyl-5-(anthracen-9-yl)-4,5-dihydro-1H-pyrazol-3-yl)thiophene-2-carboxylate (4)



A mixture of methyl 5-((*E*)-3-(anthracen-9-yl)prop-2-enoyl)thiophene-2-carboxylate (0.50 g, 1.34 mmol), hydrazine monohydrate (0.67 g, 13.4 mmol), CH₃COOH (12 ml), and sulfuric acid (1 drop) was stirred in a microwave oven at 700 W and 85°C for 5 min. After completion of the reaction, the yellow crystals were filtered, washed, and dried prior to purification by column chromatography (silica gel 60, PE/EtOAc 8:2 and RP-18 silica gel, ACN/H₂O 9:1).

Yield: 0.15 g (26%), yellow crystals, mp. 266°C-267°C

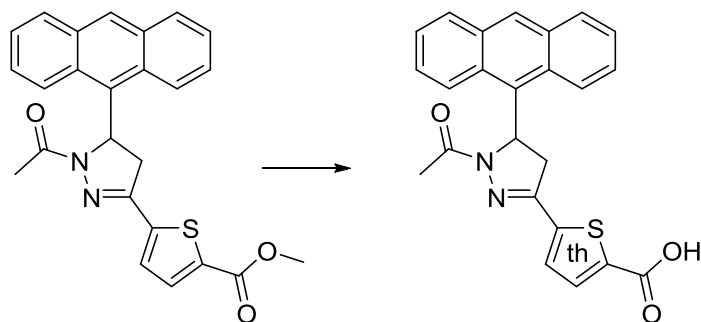
Spectroscopic data:

¹H-NMR (400 MHz, CDCl₃): δ (ppm) 2.33 (s, 3H, pyr NCOCH₃), 3.49 (dd, *J* = 18.0 Hz and 9.5 Hz, 1H, pyr 4-CH₂), 3.81 (dd, *J* = 18.0 Hz and 13.2 Hz, 1H, pyr 4-CH₂), 3.94 (s, 3H, th OCH₃), 6.88 (dd, *J* = 13.2 Hz and 9.5 Hz, 1H, anth 5-CH), 7.17 (d, *J* = 3.9 Hz, 1H, th 4-CH), 7.37-7.49 (m, 3H, anth 7-CH, anth 6-CH, anth 3-CH), 7.54-7.58 (m, 1H, anth 2-CH), 7.72-7.75 (m, 2H, anth 8-CH, th 3-CH), 7.80-8.04 (m, 2H, anth 5-CH, anth 4-CH), 8.43 (s, 1H, anth 10-CH) 8.46-8.48 (m, 1H, anth 1-CH)

¹³C-NMR (100 MHz, CDCl₃): δ (ppm) 21.8 (pyr NCOCH₃), 42.0 (pyr 4-CH₂), 52.5 (th OCH₃), 56.6 (pyr 5-CH), 122.6 (anth 8-CH), 122.9 (anth 1-CH), 124.6 (anth 6-CH), 124.9 (anth 3-CH), 126.4 (anth 7-CH), 126.7 (anth 2-CH), 128.2 (anth 8a-CH), 128.3 (th 4-CH), 128.8 (anth 10-CH), 129.4 (anth 4-CH), 130.1 (anth 9a-CH), 130.2 (anth 5-CH), 130.7 (anth 9-CH), 131.3 (anth 4a-CH), 131.9 (anth 10a-CH), 133.6 (th 3-CH), 135.2 (th 2-C), 141.0 (th 5-C), 148.7 (pyr 3-C), 162.2 (th CO), 169.6 (pyr NCOCH₃)

MS: *m/z* (%) 428 (M⁺, 97), 385 (70), 370 (33), 239 (25), 218 (59), 203 (79), 189 (22), 178 (100), 43 (50)

HRMS: *m/z* calculated for C₂₅H₂₀N₂O₃SNa [M + Na]⁺: 451.1092. Found: 451.1087.

3.4.1.2.8 5-(1-Acetyl-5-(anthracen-9-yl)-4,5-dihydro-1H-pyrazol-3-yl)thiophene-2-carboxylic acid (5)

Methyl 5-(1-acetyl-5-(anthracen-9-yl)-4,5-dihydro-1H-pyrazol-3-yl)thiophene-2-carboxylate (0.11 g, 0.27 mmol) was dissolved in a mixture of THF/H₂O/MeOH (5/2.5/5.5, 15 ml) and lithium hydroxide monohydrate (0.06 g, 1.33 mmol) was added under stirring. The reaction mixture was stirred at 50°C for 2 h. After completion of the reaction, the mixture was acidified with 2N HCl, washed with EtOAc and dried over MgSO₄. The solvent was evaporated *in vacuo* prior to purification by column chromatography (silica gel 60, CH₂Cl₂/MeOH 9:1 and RP-18 silica gel, ACN/H₂O 8:2).

Yield: 91 mg (82%), colorless crystals, mp. 280°C-281°C

Spectroscopic data:

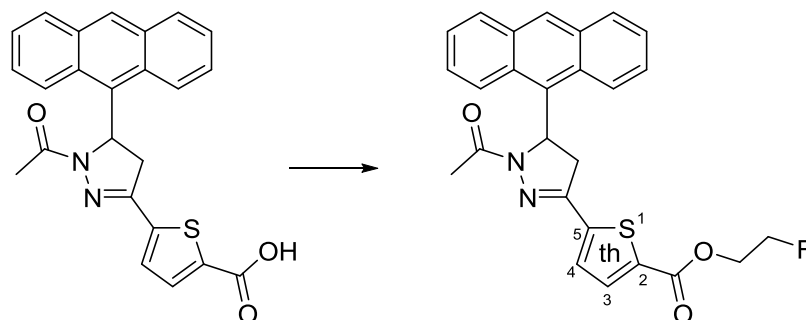
¹H-NMR (200 MHz, DMSO-*d*₆): δ (ppm) 2.17 (s, 3H), 3.32-3.47 (m, 1H), 4.13 (dd, *J* = 12.0 Hz and 6.0 Hz, 1H), 6.91 (dd, *J* = 10.0 Hz and 2.0 Hz, 1H), 7.35 (d, *J* = 2.0 Hz, 1H), 7.41-7.51 (m, 3H), 7.54-7.63 (m, 2H), 7.71-7.76 (m, 1H), 8.09-8.14 (m, 2H), 8.59 (s, 2H)

Due to limited resolution of the measuring instrument, proton th COOH could not be detected.

¹³C-NMR (50 MHz, DMSO-*d*₆): δ (ppm) 22.0, 42.4, 56.4, 122.9, 124.2, 125.2, 125.5, 126.6, 126.7, 127.9, 128.1, 129.4, 129.7, 129.9, 130.3, 130.6, 131.3, 131.8, 132.7, 136.1, 148.2, 151.1, 165.4, 168.1

MS: *m/z* (%) 414 (*M*⁺, 3), 203 (12), 84 (12), 69 (19), 57 (29), 56 (16), 55 (24), 44 (100), 43 (52), 42 (18)

HRMS: *m/z* calculated for C₂₄H₁₈N₂O₃SNa [*M* + Na]⁺: 437.0936. Found: 437.0927.

3.4.1.2.9 2-Fluoroethyl 5-(1-acetyl-5-(anthracen-9-yl)-4,5-dihydro-1H-pyrazol-3-yl)thiophene-2-carboxylate (6)

5-(1-Acetyl-5-(anthracen-9-yl)-4,5-dihydro-1H-pyrazol-3-yl)thiophene-2-carboxylic acid (0.11 g, 0.25 mmol), DCC (0.06 g, 0.28 mmol), DMAP (0.03 g, 0.28 mmol), and fluoroethanol (0.02 g, 0.25 mmol) were dissolved in absolute CH_2Cl_2 (4 ml) and stirred at room temperature for 48 h.

After completion of the reaction, the resulting crude reaction product was purified by column chromatography twice (silica gel 60, PE/EtOAc 7:3 and RP-18 silica gel, MeOH/ H_2O 8:2).

Yield: 0.11 g (93%), light yellow crystals, mp. 130°C-132°C

Spectroscopic data:

¹H-NMR (400 MHz, CDCl₃): δ (ppm) 2.33 (s, 3H, pyr NCOCH₃), 3.39 (dd, *J* = 18.0 Hz and 9.5 Hz, 1H, pyr 4-CH₂), 3.51 (dd, *J* = 18.0 Hz and 13.3 Hz, 1H, pyr 4-CH₂), 4.54-4.56 (m, 1H, th OCH₂CH₂F), 4.61-4.63 (m, 1H, th OCH₂CH₂F), 4.67-4.69 (m, 1H, th OCH₂CH₂F), 4.79-4.81 (m, 1H, th OCH₂CH₂F), 6.90 (dd, *J* = 13.3 Hz and 9.5 Hz, 1H, pyr 5-CH), 7.19 (d, *J* = 3.9 Hz, 1H, th 4-CH), 7.37-7.44 (m, 2H, anth 7-CH, anth 6-CH), 7.44-7.50 (m, 1H, anth 3-CH), 7.55-7.59 (m, 1H, anth 2-CH), 7.73 (m, 1H, anth 8-CH), 7.80 (d, *J* = 3.9 Hz, 1H, th 3-CH), 8.01-8.04 (m, 2H, anth 5-CH, anth 4-CH), 8.44 (s, 1H, anth 10-CH), 8.47-8.49 (m, 1H, anth 1-CH)

¹³C-NMR (100 MHz, CDCl₃): δ (ppm) 21.8 (pyr NCOCH₃), 42.0 (pyr 4-CH₂), 56.6 (pyr 5-CH), 64.2 (d, *J* = 20.3 Hz, th OCH₂CH₂F), 81.2 (d, *J* = 171.3 Hz, th OCH₂CH₂F), 122.5 (anth 8-CH), 122.9 (anth 1-CH), 124.6 (anth 6-CH), 124.9 (anth 3-CH), 126.4 (anth 7-CH), 126.7 (anth 2-CH), 128.3 (anth 8a-CH), 128.3 (th 4-CH), 128.8 (anth 10-CH), 129.4 (anth 4-CH), 130.1 (anth 9a-CH), 130.2 (anth 5-CH), 130.6 (anth 9-CH), 131.3 (anth 4a-CH), 131.9 (anth 10a-CH), 134.1 (th 3-CH), 134.7 (th 2-C), 141.5 (th 5-C), 148.6 (pyr 3-C), 161.5 (th CO), 169.7 (pyr NCOCH₃)

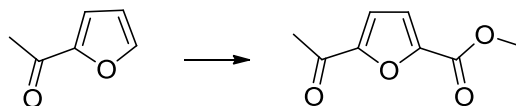
¹⁹F-NMR (471 MHz, CDCl₃): δ (ppm) -224.53 (m, th OCH₂CH₂F)

MS: *m/z* (%) 462 (M⁺, 4), 460 (34), 418 (23), 218 (37), 203 (55), 178 (85), 166 (29), 97 (28), 71 (39), 69 (65), 57 (61), 55 (54), 43 (100)

HRMS: *m/z* calculated for C₂₆H₂₁N₂O₃FSNa [M + Na]⁺: 483.1155. Found: 483.1151.

3.4.1.3 Preparation of furan based derivatives

3.4.1.3.1 Methyl 5-acetylfuran-2-carboxylate (75)



2-Acetylfuran (10.00 g, 90.82 mmol), CCl_4 (27.94 g, 181.64 mmol), and $\text{Fe}(\text{acac})_3$ (3.12 g, 9.08 mmol) were suspended in MeOH (20 ml) and heated in an autoclave to 120°C under constant stirring for 7.5 h. After completion of the reaction, the solution was cooled to room temperature and the crude reaction product pre-purified by column chromatography (silica gel 60, PE/EtOAc 9:1). Thereafter, recrystallization from diethyl ether was performed, which gave the product in poor yields.

Yield: 4.11 g (27%), light yellow crystals, mp. 100.5°C - 101°C

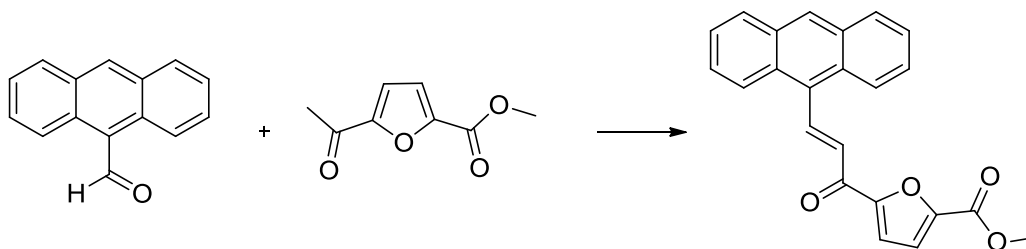
Analytical data are in complete accordance with literature values.³⁶⁹

Spectroscopic data:

$^1\text{H-NMR}$ (200 MHz, CDCl_3): δ (ppm) 2.52 (s, 3H), 3.90 (s, 3H), 7.15-7.20 (q, $J = 3.7$ Hz and 2.8 Hz, 2H)

$^{13}\text{C-NMR}$ (50 MHz, CDCl_3): δ (ppm) 26.2, 52.3, 116.5, 118.7, 146.1, 154.1, 158.4, 187.4

3.4.1.3.2 Methyl 5-((2E)-3-(anthracen-9-yl)prop-2-enoyl)furan-2-carboxylate (77)



To a solution of anthracene-9-carbaldehyde (1.23 g, 5.95 mmol) and methyl 5-acetylfuran-2-carboxylate (1.00 g, 5.95 mmol) in MeOH (120 ml) was added an aqueous solution of KOH (85%, 0.95 g, 14.43 mmol) at 0°C under continuous stirring. After the addition, the reaction mixture was allowed to warm to room temperature followed by 48 h of stirring. The resulting orange precipitate was filtered, washed, and dried to give the product in moderate yields.

Yield: 1.40 g (66%), orange crystals, mp. 198°C-200°C

Spectroscopic data:

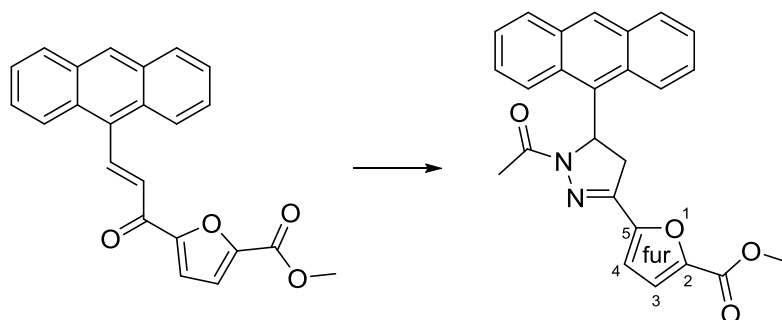
¹H-NMR (200 MHz, CDCl₃): δ (ppm) 3.91 (s, 3H), 7.30 (d, *J* = 3.7 Hz, 1H), 7.39 (d, *J* = 3.7 Hz, 1H), 7.50-7.58 (m, 5H), 8.01-8.05 (m, 2H), 8.27-8.31 (m, 2H), 8.48 (s, 1H), 8.91 (d, *J* = 16.0 Hz, 1H)

¹³C-NMR (50 MHz, CDCl₃): δ (ppm) 52.3, 117.1, 117.8, 118.8, 119.1, 125.1, 125.3, 125.4, 125.9, 126.6, 127.4, 127.4, 128.5, 128.8, 128.9, 129.6, 130.5, 131.0, 142.6, 145.7, 154.7, 158.5, 178.5

MS: *m/z* (%) 356 (M⁺, 17), 239 (9), 203 (100), 176 (4), 153 (10), 119 (10), 95 (4), 69 (9), 55 (6)

HRMS: *m/z* calculated for C₂₃H₁₆O₄Na [M + Na]⁺: 379.0946. Found: 379.0950.

3.4.1.3.3 Methyl 5-(1-acetyl-5-(anthracen-9-yl)-4,5-dihydro-1H-pyrazol-3-yl)furan-2-carboxylate (7)



Methyl 5-((*E*)-3-(anthracen-9-yl)prop-2-enyl)furan-2-carboxylate (0.30 g, 0.84 mmol), hydrazine monohydrate (0.42 g, 0.4 ml, 8.42 mmol), CH₃COOH (12 ml), and 1 drop of H₂SO₄ were introduced into a microwave vessel. The mixture was stirred in the microwave oven at 85°C and 700 W for 10 min.

After completion of the reaction, the crude product was purified several times by column chromatography (silica gel 60, PE/EtOAc 7:3 and 9:1 and RP-18 silica gel, MeOH/H₂O 7:3).

Yield: 0.44 g (63%), yellow crystals, mp. 201°C-203°C

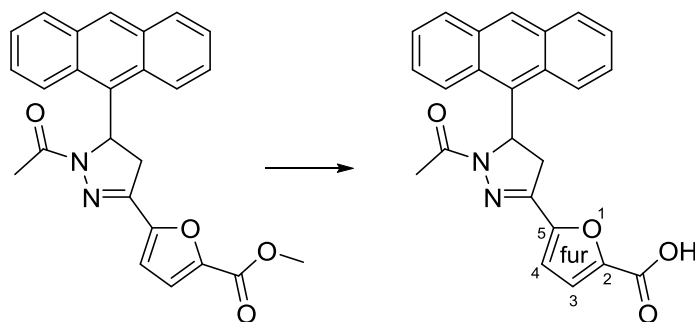
Spectroscopic data:

¹H-NMR (400 MHz, CDCl₃): δ (ppm) 2.36 (s, 3H, pyr NCOCH₃), 3.53 (dd, *J* = 18.3 Hz and 9.5 Hz, 1H, pyr 4-CH₂), 3.93 (s, 3H, fur OCH₃), 3.94 (dd, *J* = 18.3 Hz and 13.4 Hz, 1H, pyr 4-CH), 6.89 (dd, *J* = 13.4 Hz and 9.5 Hz, 1H, pyr 5-CH), 6.94 (d, *J* = 3.7 Hz, 1H, fur 4-CH), 7.30 (d, *J* = 3.7 Hz, 1H, fur 3-CH), 7.37-7.44 (m, 2H, anth 2-CH, anth 3-CH), 7.46-7.50 (m, 1H, anth 6-CH), 7.55-7.59 (m, 1H, anth 7-CH), 7.72-7.74 (m, 1H, anth 1-CH), 8.01-8.04 (m, 2H, anth 5-CH, anth 4-CH), 8.44 (s, 1H, anth 10-CH) 8.47-8.50 (m, 1H, anth 8-CH)

¹³C-NMR (100 MHz, CDCl₃): δ (ppm) 21.8 (pyr NCOCH₃), 41.2 (pyr 4-CH₂), 52.2 (fur OCH₃), 56.0 (pyr 5-CH), 112.9 (fur 4-CH), 119.4 (fur 3-CH), 122.6 (anth 1-CH), 122.9 (anth 8-CH), 124.6 (anth 3-CH), 124.9 (anth 6-CH), 126.3 (anth 2-CH), 126.7 (anth 7-CH), 128.2 (anth 9a-CH), 128.7 (anth 10-CH), 129.4 (anth 5-CH), 130.1 (anth 8a-CH), 130.2 (anth 4-CH), 130.6 (anth 9-CH), 131.3 (anth 10a-CH), 131.8 (anth 4a-CH), 144.8 (pyr 3-C), 145.4 (fur 2-C), 150.0 (fur 5-C), 158.6 (fur C=O), 169.8 (pyr NCOCH₃)

MS: *m/z* (%) 412 (M⁺, 100), 369 (70), 339 (45), 252 (60), 218 (41), 203 (77), 178 (92), 43 (56)

HRMS: *m/z* calculated for C₂₅H₂₀N₂O₄Na [M + Na]⁺: 435.1321. Found: 435.1318.

3.4.1.3.4 5-(1-Acetyl-5-(anthracen-9-yl)-4,5-dihydro-1H-pyrazol-3-yl)furan-2-carboxylic acid (8)

Methyl 5-(1-acetyl-5-(anthracen-9-yl)-4,5-dihydro-1H-pyrazol-3-yl)furan-2-carboxylate (0.37 g, 0.89 mmol) was dissolved in a mixture of MeOH/THF/H₂O (11/10/5, 26 ml) and lithium hydroxide monohydrate (0.19 g, 4.44 mmol) was added. The solution was heated to 50°C and stirred for 2 h at this temperature. After completion of the reaction the crude product was acidified with 2N HCl, extracted with EtOAc, dried over MgSO₄, and evaporated to dryness. The crude reaction product was purified twice by column chromatography (RP-18 silica gel, MeOH/H₂O 7:3 and 6:4).

Yield: 0.27 g (75%), brown crystals, mp. 287°C-288°C

Spectroscopic data:

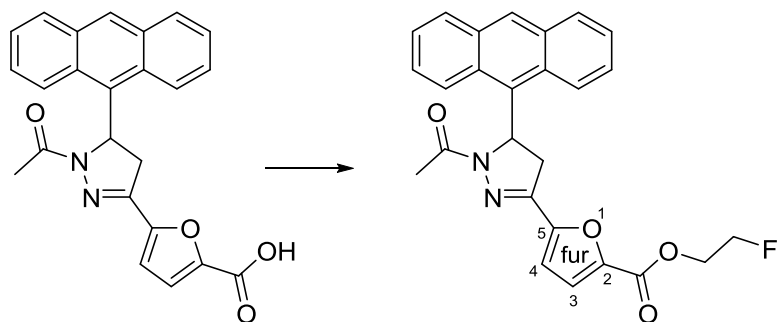
¹H-NMR (200 MHz, DMSO-*d*₆): δ (ppm) 2.21 (s, 3H, pyr NCOCH₃), 3.26-3.50 (m, 1H, pyr 4-CH₂), 4.10 (dd, *J* = 13.2 Hz and 4.8 Hz, 1H, pyr 4-CH₂), 6.91 (dd, *J* = 9.3 Hz and 3.7 Hz, 1H, pyr 5-CH), 7.12 (d, *J* = 3.5 Hz, 1H, fur 4-CH), 7.30 (d, *J* = 3.5 Hz, 1H, fur 3-CH), 7.45-7.72 (m, 5H, anth 7-CH, anth 6-CH, anth 3-CH, anth 2-CH, anth 1-CH), 8.10-8.15 (m, 2H, anth 5-CH, anth 4-CH), 8.56-8.60 (m, 2H, anth 8-CH, anth 10-CH)

Due to limited resolution of the measuring instrument, proton fur COOH could not be detected.

¹³C-NMR (50 MHz, DMSO-*d*₆): δ (ppm) 21.8 (NCOCH₃), 41.1 (pyr 4-CH₂), 55.7 (pyr 5-CH), 115.5 (fur 4-CH), 118.8 (fur 3-CH), 122.4 (anth 1-CH), 123.7 (anth 8-CH), 124.9 (anth 3-CH), 125.1 (anth 6-CH), 126.3 (anth 2-CH), 126.4 (anth 7-CH), 127.5 (anth 9a-CH), 127.9 (anth 10-CH), 129.1 (anth 5-CH), 129.6 (anth 8a-CH), 130.0 (anth 4-CH), 130.9 (anth 9-CH), 131.4 (anth 10a-CH), 131.9 (anth 4a-CH), 145.3 (pyr 3-C), 146.9 (fur 2-C), 148.6 (fur 5-C), 159.3 (fur CO), 168.2 (NCOCH₃)

MS: *m/z* (%) 398 (M⁺, 35), 252 (29), 218 (23), 203 (50), 189 (18), 178 (76), 57 (22), 43 (100)

HRMS: *m/z* calculated for C₂₄H₁₈N₂O₄Na [M + Na]⁺: 421.1164. Found: 421.1157.

3.4.1.3.5 2-Fluoroethyl 5-(1-acetyl-5-(anthracen-9-yl)-4,5-dihydro-1H-pyrazol-3-yl)furan-2-carboxylate (9)

Fluoroethanol (0.05 g, 0.77 mmol), DCC (0.17 g, 0.83 mmol), and DMAP (0.10 g, 0.83 mmol) were added to a mixture of 5-(1-acetyl-5-(anthracen-9-yl)-4,5-dihydro-1H-pyrazol-3-yl)furan-2-carboxylic acid (0.31 g, 0.77 mmol) in CH_2Cl_2 (11 ml). The reaction mixture was stirred at room temperature overnight prior to purification via column chromatography (silica gel 60, PE/EtOAc 7:3 and 9.5:0.5).

Yield: 17 mg (30%), colorless crystals, mp. 157°C-158°C

Spectroscopic data:

¹H-NMR (200 MHz, CDCl₃): δ (ppm) 2.35 (s, 3H, NCOCH₃), 3.53 (dd, *J* = 10.0 Hz and 8.0 Hz, 1H, pyr 4-CH₂), 3.95 (dd, *J* = 14.0 Hz and 4.0 Hz, 1H, pyr 4-CH₂), 4.48-4.52 (m, 1H, fur OCH₂CH₂F), 4.57-4.66 (m, 2H, fur OCH₂CH₂F, fur OCH₂CH₂F), 4.81-4.85 (m, 1H, fur OCH₂CH₂F), 6.83-6.90 (m, 1H, pyr 5-CH), 6.95-6.98 (m, 1H, fur 4-CH), 7.35-7.61 (m, 5H, anth 7-CH, anth 6-CH, anth 3-CH, anth 2-CH, fur 3-CH), 7.70-7.75 (m, 1H, anth 1-CH), 8.01-8.04 (m, 2H, anth 5-CH, anth 4-CH), 8.44-8.50 (m, 2H, anth 8-CH, anth 10-CH)

¹³C-NMR (50 MHz, CDCl₃): δ (ppm) 21.9 (pyr NCOCH₃), 41.2 (pyr 4-CH₂), 56.1 (pyr 5-CH), 64.0 (d, *J* = 20.0 Hz, fur OCH₂CH₂F), 81.1 (d, *J* = 171.0 Hz, fur OCH₂CH₂F), 112.8 (fur 4-CH), 120.1 (fur 3-CH), 122.6 (anth 1-CH), 122.9 (anth 8-CH), 124.6 (anth 3-CH), 124.9 (anth 6-CH), 126.4 (anth 2-CH), 126.7 (anth 7-CH), 128.2 (anth 9a-CH), 128.8 (anth 10-CH), 129.4 (anth 5-CH), 130.15 (anth 8a-CH), 130.2 (anth 4-CH), 130.6 (anth 9-CH), 131.3 (anth 10a-CH), 131.9 (anth 4a-CH), 144.8 (pyr 3-C), 144.9 (fur 2-C), 150.5 (fur 5-C), 157.9 (fur CO), 169.9 (pyr NCOCH₃)

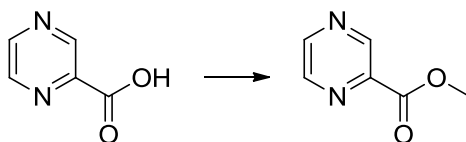
¹⁹F-NMR (471 MHz, CDCl₃): δ (ppm) -224.54 (m, fur CH₂CH₂F)

MS: *m/z* (%) 444 (M⁺, 60), 402 (42), 252 (69), 250 (25), 218 (50), 203 (82), 178 (100), 43 (89)

HRMS: *m/z* calculated for C₂₆H₂₁FN₂O₄Na [M + Na]⁺: 467.1383. Found: 467.1388.

3.4.1.4 Preparation of pyrazine based derivatives

3.4.1.4.1 Methyl pyrazine-2-carboxylate (140)^a



To a solution of 2-pyrazinecarboxylic acid (9.33 g, 75.18 mmol) in MeOH (75 ml) was added SOCl_2 (7 drops), and the resulting mixture was refluxed for 3 days. After completion of the reaction, the crude product was purified by column chromatography (silica gel 60, PE/EtOAc 7:3) to give methyl pyrazine-2-carboxylate in excellent yields.

Yield: 10.26 g (99%), colorless crystals, mp. 55-56°C

Analytical data are in complete accordance with literature values.³⁷⁰

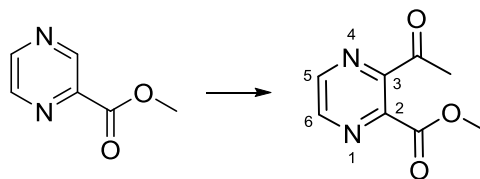
Spectroscopic data:

¹H-NMR (200 MHz, CDCl_3): δ (ppm) 3.93 (s, 3H), 8.62 (q, $J = 1.5$ Hz and 0.9 Hz, 1H), 8.68 (d, $J = 2.4$ Hz, 1H), 9.20 (d, $J = 1.4$ Hz, 1H)

¹³C-NMR (100 MHz, CDCl_3): δ (ppm) 52.9, 143.0, 144.2, 146.0, 147.5, 164.1

^acompound number not assigned in the discussion

3.4.1.4.2 Methyl 3-acetylpyrazine-2-carboxylate (88)



To a stirred solution of acetaldehyde (15.35 g, 348.42 mmol), aqueous H_2SO_4 (50%, 232 ml), CH_3COOH (99%, 232 ml), and methyl pyrazine-2-carboxylate (16.04 g, 116.14 mmol) were added an aqueous solution of *tert*- BuO_2H (70%, 31.40 g, 348.42 mmol) and a saturated $\text{FeSO}_4 \cdot 7\text{H}_2\text{O}$ solution (96.86 g, 348.42 mmol) simultaneously at -5°C . During the addition the temperature was not allowed to exceed 10°C . The resulting solution was stirred for 2 h, during which the mixture was allowed to warm to 20°C . Then, Na_2SO_3 was added in portions until a starch-iodide paper test was negative. The reaction mixture was extracted with EtOAc, the collected organic layers were dried over MgSO_4 and evaporated to dryness prior to chromatographic purification (silica gel 60, PE/EtOAc 6:4).

Yield: 4.60 g (22%), yellow crystals, mp. 136°C - 137°C

Spectroscopic data:

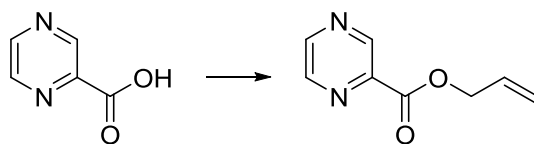
$^1\text{H-NMR}$ (200 MHz, CDCl_3): δ (ppm) 2.79 (s, 3H, COCH_3), 4.11 (s, 3H, COOCH_3), 9.35 (d, $J = 8.1$ Hz, 2H, 5- CH , 6- CH)

$^{13}\text{C-NMR}$ (50 MHz, CDCl_3): δ (ppm) 25.9 (COCH_3), 53.3 (COOCH_3), 142.8 (6- CH), 144.9 (5- CH), 145.1 (2-C), 148.9 (3-C), 163.6 (COOCH_3), 198.5 (COCH_3)

MS: m/z (%) 194 (M^+ , 1), 180 (5), 150 (7), 138 (10), 122 (11), 80 (12), 59 (7), 43 (100), 41 (5)

HRMS: m/z calculated for $\text{C}_8\text{H}_9\text{N}_2\text{O}_3$ [$\text{M} + \text{H}$] $^+$: 181.0608. Found: 181.0608.

3.4.1.4.3 Allyl pyrazine-2-carboxylate (93)



- 1) Method 1: A solution of 2-pyrazinecarboxylic acid (10.00 g, 80.58 mmol), allyl alcohol (59.50 g, 70 ml, 102.44 mmol) and SOCl_2 (10 drops) was refluxed for 3 days. After completion of the reaction, the crude reaction product was purified by column chromatography (silica gel 60, PE/EtOAc 7:3).

Yield: 3.19 g (24%), red-brownish oil

- 2) Method 2: To a suspension of NaH (0.62 g, 25.79 mmol) in DMF (42 ml) was added a solution of 2-pyrazinecarboxylic acid (2.00 g, 16.12 mmol) in DMF (28 ml). This mixture was stirred for 30 min. Thereafter, allyl bromide (2.73 g, 1.95 ml, 14.29 mmol) was introduced dropwise *via* syringe and the resulting mixture was stirred at 50°C overnight. The reaction was quenched with H_2O and the crude product purified by column chromatography (silica gel 60, PE/EtOAc 7:3).

Yield: 1.04 g (39%), red-brownish oil

- 3) Method 3: A mixture of 2-pyrazinecarboxylic acid (10.00 g, 80.58 mmol) and SOCl_2 (9.59 g, 5.8 ml, 80.58 mmol) in CH_2Cl_2 (100 ml) was refluxed for 4 h. Thereafter, pyridine (6.5 ml, 80.58 mmol) was added to the reaction mixture, which was subsequently evaporated to dryness. The obtained pyrazinoyl chloride was directly introduced into the next reaction step without further purification.

Allyl alcohol (3.89 g, 4.6 ml, 67.17 mmol) was suspended in CH_2Cl_2 (5 ml) and pyridine (6.38 g, 6.5 ml, 80.58 mmol) was added to this mixture. Thereafter, the pyrazinoyl chloride (11.49 g, 80.61 mmol) was added dropwise at 0°C. The reaction mixture was

allowed to warm to room temperature during overnight stirring. The purple mixture was extracted twice with a saturated CuSO_4 solution, once with H_2O , and twice with brine. The combined organic layers were dried over MgSO_4 and evaporated to dryness prior to purification by column chromatography (silica gel 60, PE/EtOAc 7:3).

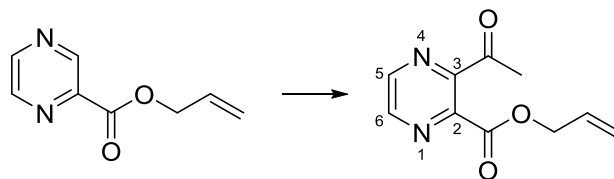
Yield: 1.14 g (9%), red-brownish oil

Spectroscopic data:

$^1\text{H-NMR}$ (200 MHz, CDCl_3): δ (ppm) 4.42 (td, $J = 2.0$ Hz, 2.0 Hz, and 2.0 Hz, 2H), 4.86 (dq, $J = 2.0$ Hz, 8.0 Hz, 14.0 Hz, and 16.0 Hz, 2H), 5.46-5.66 (m, 1H), 8.25-8.33 (m, 2H), 8.77 (s, 1H)

$^{13}\text{C-NMR}$ (50 MHz, CDCl_3): δ (ppm) 65.4, 118.0, 130.5, 142.2, 143.4, 145.0, 146.8, 162.3

3.4.1.4.4 Allyl 3-acetylpyrazine-2-carboxylate (94)



To a solution of allyl pyrazine-2-carboxylate (1.90 g, 11.57 mmol) and acetaldehyde (1.53 g, 34.71 mmol) in CH_3COOH (99%, 12 ml), an aqueous solution of H_2SO_4 (50%, 12 ml) was slowly added under stirring. After cooling the mixture to -5°C , an aqueous solution of *tert*- BuO_2H (70%, 3.13 g, 34.71 mmol) and a saturated $\text{FeSO}_4 \cdot 7\text{H}_2\text{O}$ solution (9.65 g, 34.71 mmol) were added simultaneously to the reaction mixture. During the addition, the temperature was not allowed to exceed 10°C . The mixture was stirred for 2 h, during which the temperature was allowed to rise to 20°C . After 2 h, Na_2SO_3 was added in portions to the reaction mixture until a starch-iodide paper test was negative.

Thereafter, the crude reaction product was extracted several times with EtOAc, the combined organic layers were dried over MgSO_4 and evaporated to dryness. Purification by column chromatography (silica gel 60, PE/EtOAc 8:2) afforded the reaction product in poor yields.

Yield: 0.22 g (9%), yellow-brownish oil

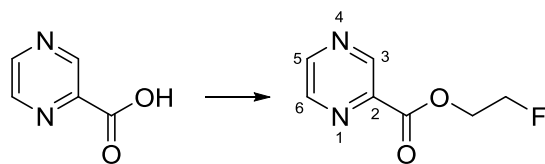
Spectroscopic data:

¹H-NMR (200 MHz, CDCl₃): δ (ppm) 2.67 (s, 3H, COCH₃), 4.88 (d, *J* = 4.0 Hz, 2H, allyl-CH₂CHCH₂), 5.25-5.43 (m, 2H, allyl-CH₂CHCH₂), 5.89-6.10 (m, 1H, allyl-CH₂CHCH₂), 9.24 (d, *J* = 10.0 Hz, 2H, 6-CH, 5-CH)

¹³C-NMR (50 MHz, CDCl₃): δ (ppm) 25.8 (COCH₃), 66.9 (allyl-CH₂CHCH₂), 119.7 (allyl-CH₂CHCH₂), 130.9 (allyl-CH₂CHCH₂), 142.7 (6-CH), 144.8 (5-CH), 145.2 (2-C), 148.8 (3-C), 162.8 (COO), 198.3 (COCH₃)

MS: *m/z* (%) 206 (M⁺, 2), 161 (5), 150 (16), 136 (7), 122 (49), 79 (9), 66 (5), 43 (100), 41 (68)

HRMS: *m/z* calculated for C₁₀H₁₀N₂O₃Na [M + Na]⁺: 229.0589. Found: 229.0586.

3.4.1.4.5 2-Fluoroethyl pyrazine-2-carboxylate (141)^b

- 1) Method 1: To a solution of 2-pyrazinecarboxylic acid (2.00 g, 16.11 mmol) in CH₂Cl₂ (50 ml) were added DCC (3.60 g, 17.57 mmol), DMAP (2.14 g, 17.57 mmol), and fluoroethanol (1.03 g, 0.9 ml, 16.11 mmol). The mixture was stirred for 24 h at room temperature and thereafter purified by column chromatography (silica gel 60, PE/EtOAc 4:6).

Yield: 1.95 g (71%), light yellow resin

- 2) Method 2: To a solution of 2-pyrazinecarboxylic acid (2.00 g, 16.11 mmol) in CH₂Cl₂ (70 ml) was added SOCl₂ (1.92 g, 1.17 ml, 16.11 mmol), and the mixture was refluxed for 2 h. Thereafter, the solvent was evaporated *in vacuo* and the residue was dissolved in CH₂Cl₂ (20 ml) again. To this mixture, fluoroethanol (1.70 g, 1.54 ml, 26.50 mmol) and TEA (1.63 g, 2.23 ml, 16.11 mmol) were slowly added at 0°C. Stirring was further continued for 30 min during which the reaction mixture was allowed to warm to room temperature. After completion of the reaction, the crude product was extracted with H₂O three times, dried over MgSO₄, and evaporated to dryness prior to purification *via* column chromatography (silica gel 60, PE/EtOAc 7:3).

Yield: 1.88 g (69%), light yellow resin

^bcompound number not assigned in the discussion

Spectroscopic data:

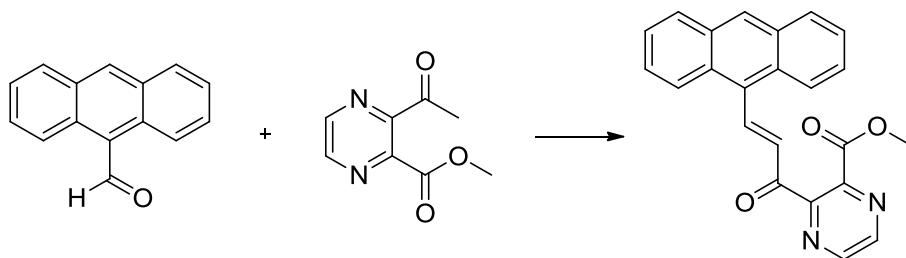
¹H-NMR (200 MHz, CDCl₃): δ (ppm) 4.42-4.61 (m, 3H), 4.61-4.75 (m, 1H), 8.57-8.63 (m, 2H), 9.13 (s, 1H)

¹³C-NMR (50 MHz, CDCl₃): δ (ppm) 64.5 (dd, *J* = 20.0 Hz, OCH₂CH₂F), 80.6 (dd, *J* = 170.0 Hz, OCH₂CH₂F), 142.5 (2-C), 144.2 (3-C), 145.9 (5-CH), 147.5 (6-CH), 163.2 (COO)

MS: *m/z* (%) 170 (M⁺, 1), 108 (32), 95 (0.5), 80 (93), 57 (2), 52 (100), 41 (2)

HRMS: *m/z* calculated for C₇H₇FN₂O₂Na [M + Na]⁺: 193.0389. Found: 193.0388.

3.4.1.4.6 Methyl 3-((2E)-3-(anthracen-9-yl)prop-2-enoyl)pyrazine-2-carboxylate (89)



An aqueous solution of KOH (85%, 0.95 g, 14.43 mmol) was added to a mixture of anthracene-9-carbaldehyde (1.49 g, 7.22 mmol) and methyl 3-acetylpyrazine-2-carboxylate (1.30 g, 7.22 mmol) in MeOH (100 ml) at 0°C. The reaction mixture was allowed to warm to room temperature during 48 h of stirring. The formed dark orange precipitate was evaporated *in vacuo* and purified by column chromatography (silica gel 60, PE/EtOAc 6:4 and RP-18 silica gel, ACN/H₂O 8:2).

Yield: 0.49 g (19%), orange crystals, mp. 150°C-151°C

Spectroscopic data:

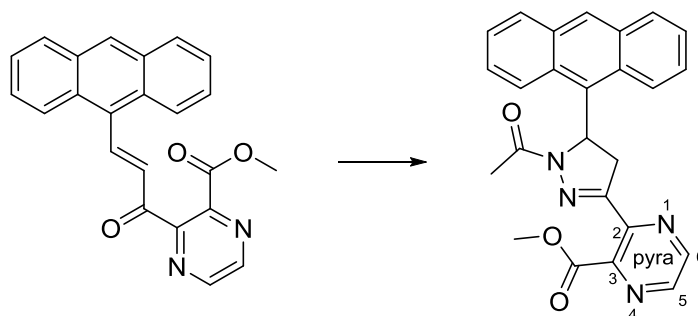
¹H-NMR (200 MHz, CDCl₃): δ (ppm) 4.07 (s, 3H), 7.49-7.57 (m, 4H), 8.00-8.04 (m, 2H), 8.12-8.20 (m, 1H), 8.30-8.35 (m, 2H), 8.46 (s, 1H), 9.01 (d, *J* = 16.0 Hz, 1H), 9.29 (s, 1H), 9.52 (s, 1H)

¹³C-NMR (50 MHz, CDCl₃): δ (ppm) 53.4, 125.1, 125.4, 126.7, 128.9, 129.0, 129.3, 129.4, 129.8, 131.3, 143.7, 144.3, 150.0, 163.8, 187.5

MS: *m/z* (%) 368 (M⁺, 13), 231 (8), 203 (100), 154 (11), 138 (12), 101 (4), 88 (3)

HRMS: *m/z* calculated for C₂₃H₁₆N₂O₃Na [M + Na]⁺: 391.1059. Found: 391.1048.

3.4.1.4.7 Methyl 3-(1-acetyl-5-(anthracen-9-yl)-4,5-dihydro-1H-pyrazol-3-yl)pyrazine-2-carboxylate (10)



Methyl 3-((*E*)-3-(anthracen-9-yl)prop-2-en-1-yl)pyrazine-2-carboxylate (0.20 g, 0.54 mmol) was introduced into a microwave vessel and suspended in CH₃COOH (5 ml). Hydrazine monohydrate (0.27 g, 0.3 ml, 5.43 mmol) as well as H₂SO₄ (1 drop) were added to the slurry and the suspension was subsequently heated in the microwave oven at 700 W and 85°C for 5 min. The resulting crude reaction product was purified by column chromatography (silica gel 60, PE/EtOAc 6:4 and RP-18 silica gel, ACN/H₂O 7:3).

Yield: 46 mg (20%), yellow crystals, mp. 244°C-246°C

Spectroscopic data:

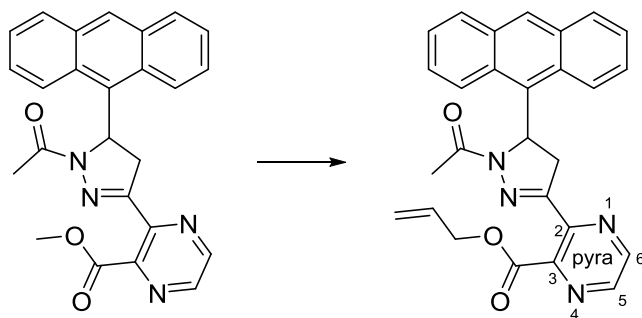
¹H-NMR (400 MHz, CDCl₃): δ (ppm) 2.41 (s, 3H, NCOCH₃), 3.66 (dd, *J* = 19.1 Hz and 9.8 Hz, 1H, pyr 4-CH₂), 4.08 (s, 3H, pyra OCH₃), 4.10 (m, 1H, pyr 4-CH₂), 6.95 (dd, *J* = 13.6 Hz and 9.8 Hz, 1H, pyr 5-CH), 7.34-7.43 (m, 2H, anth 6-CH, anth 7-CH), 7.48-7.52 (m, 1H, anth 3-CH), 7.57-7.61 (m, 1H, anth 2-CH), 7.67 (d, *J* = 8.7 Hz, 1H, anth 8-CH), 8.03-8.05 (m, 2H, anth 4-CH, anth 5-CH), 8.46 (s, 1H, anth 10-CH), 8.50 (d, *J* = 9.0 Hz, 1H, 1-CH), 9.26 (d, *J* = 1.5 Hz, 1H, pyra 6-CH), 9.60-9.61 (m, 1H, pyra 5-CH)

¹³C-NMR (100 MHz, CDCl₃): δ (ppm) 21.9 (pyr NCOCH₃), 41.0 (pyr 4-CH₂), 53.3 (pyra OCH₃), 56.9 (pyr 5-CH), 122.4 (anth 8-CH), 122.9 (anth 1-CH), 124.6 (anth 6-CH), 125.0 (anth 3-CH), 126.3 (anth 7-CH), 126.8 (anth 2-CH), 128.3 (anth 8a-C), 128.9 (anth 10-CH), 129.5 (anth 4-CH), 130.2 (anth 9a-C), 130.3 (anth 5-CH), 130.5 (anth 9-C), 131.4 (anth 4a-C), 131.9 (anth 10a-C), 142.2 (pyra 2-C), 142.5 (pyra 5-CH), 145.5 (pyra 6-CH), 149.1 (pyra 3-C), 152.4 (pyr 3-C), 164.3 (pyra CO), 170.0 (NCOCH₃)

MS: *m/z* (%) 424 (M⁺, 30), 381 (30), 215 (60), 203 (41), 189 (23), 178 (48), 57 (15), 43 (100)

HRMS: *m/z* calculated for C₂₅H₂₀N₄O₃Na [M + Na]⁺: 447.1433. Found: 447.1431.

3.4.1.4.8 Allyl 3-(1-acetyl-5-(anthracen-9-yl)-4,5-dihydro-1H-pyrazol-3-yl)pyrazine-2-carboxylate (91)



- 1) Method 1: To a solution of methyl 3-(1-acetyl-5-(anthracen-9-yl)-4,5-dihydro-1H-pyrazol-3-yl)pyrazine-2-carboxylate (0.40 g, 0.10 mmol) in toluene (50 ml) were added allyl alcohol (5.80 mg, 0.10 mmol) and NaOMe (0.50 mg, 0.01 mmol). The mixture was stirred for 2 days at 80°C and thereafter, evaporated to dryness prior to purification by column chromatography (silica gel 60, PE/EtOAc 8:2).

Yield: 15 mg (33%), yellow crystals, mp. 183°C-185°C

- 2) Method 2: To a stirred solution of 2,8,9-trimethyl-2,5,8,9-tetraaza-1-phosphabicyclo[3.3.3]undecane (2.72 mg, 0.01 mmol) in allyl alcohol (4.25 g, 5 ml, 73.17 mmol) was added methyl 3-(1-acetyl-5-(anthracen-9-yl)-4,5-dihydro-1H-pyrazol-3-yl)pyrazine-2-carboxylate (0.04 g, 0.10 mmol) at room temperature. The mixture was stirred for 4 h at room temperature prior to evaporation of the solvent and chromatographic purification (silica gel 60, PE/EtOAc 7:3).

Yield: 38 mg (87%), yellow crystals, mp. 183°C-185°C

Spectroscopic data:

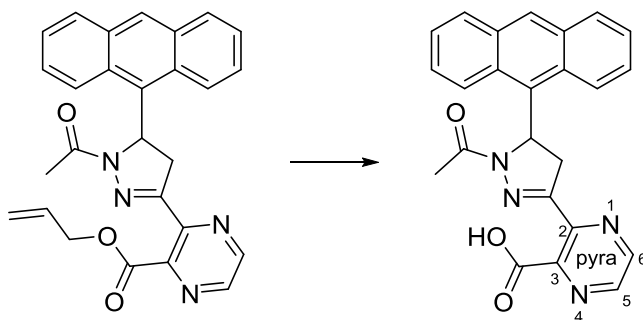
¹H-NMR (200 MHz, CDCl₃): δ (ppm) 2.40 (s, 3H, pyr NCOCH₃), 3.58-3.73 (m, 1H, pyr 4-CH₂), 4.01-4.17 (m, 1H, pyr 4-CH₂), 4.96-5.00 (m, 2H, pyra allyl-CH₂CHCH₂), 5.29-5.53 (m, 2H, pyra allyl-CH₂CHCH₂), 6.00-6.20 (m, 1H, pyra allyl-CH₂CHCH₂), 6.94 (dd, *J* = 10.0 Hz and 4.0 Hz, 1H, pyr 5-CH), 7.29-7.69 (m, 5H, anth 8-CH, anth 7-CH, anth 6-CH, anth 3-CH, anth 2-CH), 8.02-8.06 (m, 2H, anth 5-CH, anth 4-CH), 8.46-8.52 (m, 2H, anth 10-CH, anth 1-CH), 9.27 (d, *J* = 2.0 Hz, 1H, pyra 6-CH), 9.59 (m, 1H, pyra 5-CH)

¹³C-NMR (50 MHz, CDCl₃): δ (ppm) 21.9 (pyr NCOCH₃), 40.9 (pyr 4-CH₂), 56.8 (pyr 5-CH₃), 66.9 (pyra allyl-CH₂CHCH₂), 119.8 (pyra allyl-CH₂CHCH₂), 122.4 (anth 8-CH), 122.9 (anth 1-CH), 124.6 (anth 6-CH), 125.0 (anth 3-CH), 126.3 (anth 7-CH), 126.8 (anth 2-CH), 128.3 (anth 8a-C), 128.9 (anth 10-CH), 129.5 (anth 4-CH), 130.2 (anth 9a-C), 130.3 (anth 5-CH), 130.5 (anth 9-C), 131.3 (pyra allyl-CH₂CHCH₂), 131.4 (anth 4a-C), 131.9 (anth 10a-C), 142.3 (pyra 2-C), 142.5 (pyra 5-CH), 145.5 (pyra 6-CH), 149.0 (pyra 3-C), 152.4 (pyr 3-C), 163.4 (pyra CO), 169.9 (pyr NCOCH₃)

MS: *m/z* (%) 450 (M⁺, 80), 407 (71), 313 (71), 239 (41), 215 (100), 203 (85), 178 (60), 43 (75)

HRMS: *m/z* calculated for C₂₇H₂₂N₄O₃Na [M + Na]⁺: 473.1590. Found: 473.1577.

3.4.1.4.9 3-(1-Acetyl-5-(anthracen-9-yl)-4,5-dihydro-1H-pyrazol-3-yl)pyrazine-2-carboxylic acid (11)



To a solution of allyl 3-(1-acetyl-5-(anthracen-9-yl)-4,5-dihydro-1H-pyrazol-3-yl)pyrazine-2-carboxylate (0.08 g, 0.18 mmol) in THF (15 ml) were added $(PPh_3)_4Pd$ (0.03 g, 0.02 mmol) and morpholine (0.19 g, 0.18 ml, 2.12 mmol) under argon atmosphere. The mixture was stirred for 3.5 h at room temperature and thereafter, evaporated to dryness. The crude reaction product was purified by column chromatography twice (RP-18 silica gel, MeOH/H₂O 7:3 and 6:4).

Yield: 38 mg (51%), yellow crystals, mp. n.d.

Spectroscopic data:

¹H-NMR (200 MHz, DMSO-*d*₆): δ (ppm) 2.25 (s, 3H, pyr NCOCH₃), 3.48 (dd, *J* = 14.0 Hz and 4.0 Hz, 1H, pyr 4-CH₂), 4.22 (dd, *J* = 14.0 Hz and 4.0 Hz, 1H, pyr 4-CH₂), 6.90-7.01 (m, 1H, pyr 5-CH), 7.41-7.71 (m, 5H, anth 8-CH, anth 7-CH, anth 6-CH, anth 3-CH, anth 2-CH), 8.10-8.14 (m, 2H, anth 5-CH, anth 4-CH), 8.60 (s, 2H, anth 10-CH, anth 1-CH), 9.13 (s, 1H, pyra 6-CH), 9.37 (s, 1H, pyra 5-CH)

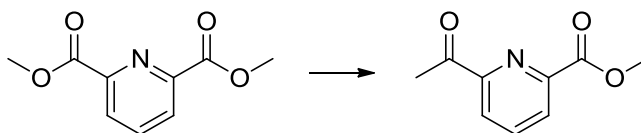
Due to limited resolution of the measuring instrument, proton pyra COOH could not be detected.

¹³C-NMR (50 MHz, DMSO-*d*₆): δ (ppm) 21.7 (pyr NCOCH₃), 42.8 (pyr 4-CH₂), 56.2 (pyr 5-CH), 122.4 (anth 8-CH), 123.8 (anth 1-CH), 124.8 (anth 6-CH), 125.1 (anth 3-CH), 126.3 (anth 7-CH), 126.4 (anth 2-CH), 127.5 (anth 8a-C), 127.9 (anth 10-CH), 129.1 (anth 4-CH), 129.7 (anth 9a-C), 130.0 (anth 5-CH), 130.9 (anth 9-C), 131.4 (anth 4a-C), 131.9 (anth 10a-C), 144.4 (pyra 2-C), 144.7 (pyra 5-CH), 147.6 (pyra 6-CH), 153.2 (pyra 3-C), 155.5 (pyr 3-C), 165.9 (pyra C=O), 168.5 (pyr NCOCH₃)

HRMS: *m/z* calculated for C₂₄H₁₇N₄O₃ [M - H]: 409.1306. Found: 409.1306.

3.4.1.5 Preparation of pyridine based derivatives

3.4.1.5.1 Methyl 6-acetylpyridine-2-carboxylate (97)



Dimethyl pyridine-2,6-dicarboxylate (1.00 g, 5.12 mmol) and NaOMe (0.30 g, 5.63 mmol) were introduced into a two-neck flask. EtOAc (4 ml) followed by MeOH (8 ml) were slowly added to the mixture and the resulting slurry was refluxed for 12 h under argon atmosphere. Concentrated HCl (2 ml) was added dropwise and the mixture was refluxed for another 6 h. Thereafter, the reaction was stopped by the addition of H₂O (5 ml) and the mixture was extracted with CH₂Cl₂ (4 x 25 ml). The combined organic layers were washed with an aqueous Na₂CO₃ solution (5%, 20 ml), dried over Na₂SO₄, filtered, and evaporated to dryness prior to purification by column chromatography (silica gel 60, PE/EtOAc 9:1).

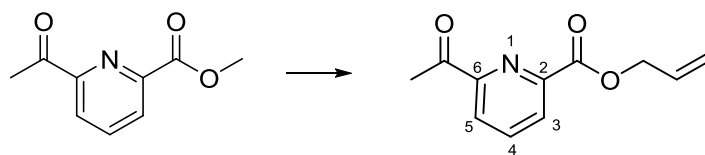
Yield: 0.43 g (47%), colorless crystals, mp. 50°C-51.5°C

Analytical data are in complete accordance with literature values.³⁷¹

Spectroscopic data:

¹H-NMR (200 MHz, CDCl₃): δ (ppm) 2.75 (s, 3H), 3.99 (s, 3H), 7.91-7.99 (m, 1H), 8.14-8.26 (m, 2H)

¹³C-NMR (50 MHz, CDCl₃): δ (ppm) 25.5, 52.9, 124.4, 128.1, 137.9, 147.4, 153.5, 165.1, 199.4

3.4.1.5.2 Allyl 6-acetylpyridine-2-carboxylate (142)^c

Allyl alcohol (0.32 g, 0.38 ml, 5.58 mmol) was slowly added to a mixture of methyl 6-acetylpyridine-2-carboxylate (1.00 g, 5.58 mmol) and NaOMe (0.03 g, 0.56 mmol) in toluene (20 ml). The resulting solution was stirred at 70°C for 48 h in a two-neck round bottom flask provided with a distillation condenser to remove formed MeOH. The reaction was terminated after 48 h and the crude product was purified by column chromatography (silica gel 60, PE/EtOAc 9.5:0.5). 0.36 g of the starting material could be recovered and recycled in a new reaction.

Yield: 0.50 g (44%), yellow oil

Spectroscopic data:

¹H-NMR (200 MHz, CDCl₃): δ (ppm) 2.56 (s, 3H, COCH₃), 4.68-4.72 (m, 2H, allyl-CH₂CHCH₂), 5.08-5.33 (m, 2H, allyl-CH₂CHCH₂), 5.81-5.97 (m, 1H, allyl-CH₂CHCH₂), 7.76-7.84 (m, 1H, 5-CH), 7.92-8.07 (m, 2H, 3-CH, 4-CH)

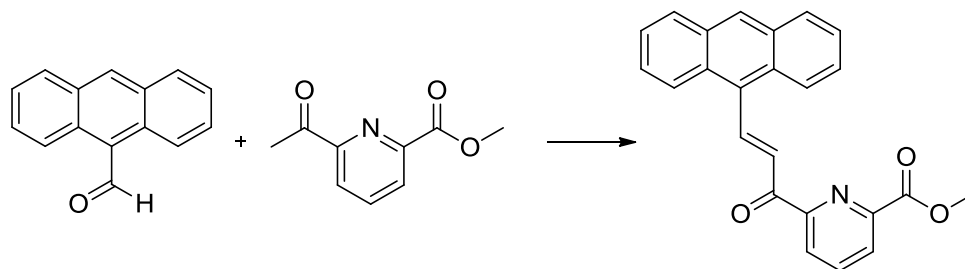
¹³C-NMR (50 MHz, CDCl₃): δ (ppm) 25.1 (COCH₃), 63.8 (allyl-CH₂CHCH₂), 118.2 (allyl-CH₂CHCH₂), 123.9 (5-CH), 127.7 (3-CH), 131.3 (allyl-CH₂CHCH₂), 137.6 (4-CH), 147.0 (2-C), 153.0 (6-C), 163.7 (COO), 198.8 (12-COCH₃)

MS: m/z (%) 205 (M⁺, 27), 162 (25), 148 (7), 121 (37), 105 (12), 77 (15), 43 (100), 41 (49)

HRMS: m/z calculated for C₁₁H₁₁NO₃Na [M + Na]⁺: 228.0637. Found: 228.0632.

^ccompound number not assigned in the discussion

3.4.1.5.3 Methyl 6-((2E)-3-(anthracen-9-yl)prop-2-enoyl)pyridine-2-carboxylate (98)



To a solution of anthracene-9-carbaldehyde (1.15 g, 5.58 mmol) and methyl 6-acetylpyridine-2-carboxylate (1.00 g, 5.58 mmol) in MeOH (200 ml) was added an aqueous KOH solution (85%, 0.70 g, 11.16 mmol) at 0°C. The reaction mixture was allowed to warm to room temperature and stirred further for 48 h. Thereafter, the resulting product was filtered, washed and dried. The reaction product was used in the next step without further purification.

Yield: 1.11 g (54%), orange crystals, mp. 189°C-190°C

Spectroscopic data:

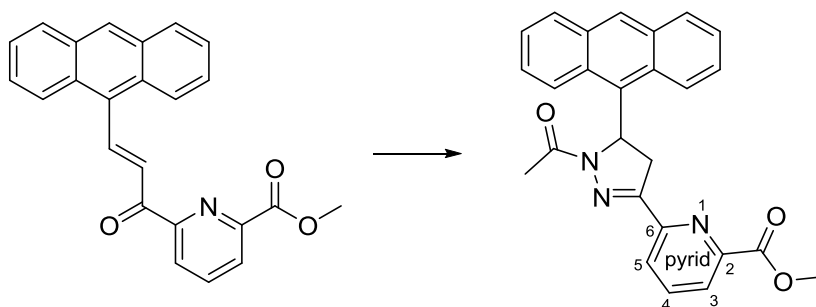
¹H-NMR (200 MHz, CDCl₃): δ (ppm) 3.95 (s, 3H), 7.46-7.57 (m, 4H), 7.99-8.09 (m, 3H), 8.21-8.47 (m, 6H), 8.99 (d, *J* = 16.0 Hz, 1H)

¹³C-NMR (50 MHz, CDCl₃): δ (ppm) 52.8, 125.3, 125.4, 126.0, 126.3, 128.0, 128.6, 128.8, 129.7, 130.0, 130.1, 131.2, 138.1, 142.7, 147.4, 154.1, 165.2, 188.5

MS: *m/z* (%) 367 (M⁺, 19), 307 (7), 278 (14), 203 (100), 137 (74), 101 (32), 77 (12), 59 (8)

HRMS: *m/z* calculated for C₂₄H₁₇NO₃Na [M + Na]⁺: 390.1106. Found: 390.1106.

3.4.1.5.4 Methyl 6-(1-acetyl-5-(anthracen-9-yl)-4,5-dihydro-1H-pyrazol-3-yl)pyridine-2-carboxylate (12)



Methyl 6-((*E*)-3-(anthracen-9-yl)prop-2-enoyl)pyridine-2-carboxylate (0.30 g, 0.82 mmol), hydrazine monohydrate (0.4 ml, 8.17 mmol), CH₃COOH (24 ml), and H₂SO₄ (2 drops) were introduced into a microwave vessel. The mixture was heated in the microwave oven at 85°C and 700 W for 5 min. Thereafter, the crude reaction product was evaporated to dryness and purified by column chromatography (silica gel 60, PE/EtOAc 8:2 and 6:4).

Yield: 0.32 g (92%), light yellow crystals, mp. 154°C-155°C

Spectroscopic data:

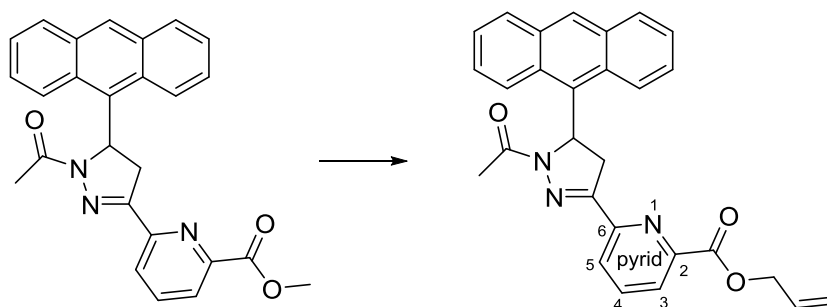
¹H-NMR (400 MHz, CDCl₃): δ (ppm) 2.38 (s, 3H, pyr NCOCH₃), 3.75 (dd, *J* = 19.3 Hz and 9.8 Hz, 1H, pyr 4-CH₂), 3.92 (s, 3H, pyrid OCH₃), 4.23 (dd, *J* = 19.3 Hz and 13.3 Hz, 1H, pyr 4-CH₂), 6.92 (dd, *J* = 13.3 Hz and 9.8 Hz, 1H, pyr 5-CH), 7.31-7.5 (m, 1H, anth 7-CH), 7.37-7.41 (m, 1H, anth 6-CH), 7.47-7.50 (m, 1H, anth 3-CH), 7.55-7.59 (m, 1H, anth 2-CH), 7.76-7.78 (m, 1H, anth 8-CH), 7.97 (‘t’, *J* = 7.8 Hz, 1H, pyrid 4-CH), 8.02 (d, *J* = 8.3 Hz, 1H, anth 5-CH), 8.03 (d, *J* = 8.4, 1H, anth 4-CH), 8.16 (d, *J* = 7.7 Hz, 1H, pyrid 3-CH), 8.43 (s, 1H, anth 10-CH), 8.45 (d, *J* = 7.9 Hz, 1H, pyrid 5-CH), 8.50 (d, *J* = 9.2 Hz, 1H, anth 1-CH)

¹³C-NMR (100 MHz, CDCl₃): δ (ppm) 21.6 (pyr NCOCH₃), 41.6 (pyr 4-CH₂), 52.8 (pyrid OCH₃), 56.8 (pyr 5-CH), 122.9 (anth 8-CH), 123.0 (anth 1-CH), 124.3 (pyr 5-CH), 124.5 (anth 6-CH), 124.9 (anth 3-CH), 125.7 (pyrid 3-CH), 126.0 (anth 7-CH), 126.6 (anth 2-CH), 128.3 (anth 8a-C), 128.6 (anth 10-CH), 129.4 (anth 4-CH), 130.1 (anth 9a-C), 130.1 (anth 5-CH), 131.2 (anth 9-C), 131.4 (anth 4a-C), 131.9 (anth 10a-C), 137.3 (pyrid 4-CH), 148.1 (pyrid 2-C), 151.1 (pyrid 6-C), 155.0 (pyr 3-C), 165.4 (pyrid C=O), 169.8 (pyr NCOCH₃)

MS: *m/z* (%) 423 (M⁺, 81), 380 (69), 320 (39), 292 (100), 218 (58), 203 (61), 178 (47), 43 (85)

HRMS: *m/z* calculated for C₂₆H₂₁N₃O₃Na [M + Na]⁺: 446.1481. Found: 446.1490.

3.4.1.5.5 Allyl 6-(1-acetyl-5-(anthracen-9-yl)-4,5-dihydro-1H-pyrazol-3-yl)pyridine-2-carboxylate (99)



Methyl 6-(1-acetyl-5-(anthracen-9-yl)-4,5-dihydro-1H-pyrazol-3-yl)pyridine-2-carboxylate (0.20 g, 0.47 mmol) was dissolved in toluene (15 ml) and to this solution were added allyl alcohol (0.03 g, 0.47 mmol) and NaOMe (0.003 g, 0.05 mmol). This reaction was carried out by stirring the mixture at 80°C for 24 h, using a Liebig condenser to remove formed MeOH.

The crude product was purified by column chromatography (silica gel 60, PE/EtOAc 9.5:0.5). 69 mg of the starting material could be recovered and recycled in a new reaction.

Yield: 62 mg (29%), colorless to light yellow crystals, mp. 194°C-195°C

Spectroscopic data:

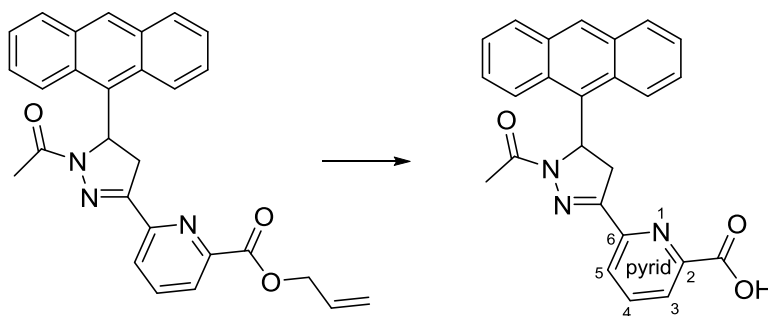
¹H-NMR (200 MHz, CDCl₃): δ (ppm) 2.38 (s, 3H, pyr NCOCH₃), 3.65-3.81 (m, 1H, anth 4-CH₂), 4.07-4.37 (m, 1H, anth 4-CH₂), 4.80-4.84 (m, 2H, pyrid allyl-CH₂CHCH₂), 5.21-5.43 (m, 2H, pyrid allyl-CH₂CHCH₂), 5.89-6.09 (m, 1H, pyrid allyl-CH₂CHCH₂), 6.93 (dd, *J* = 10.0 Hz and 2.0 Hz, 1H, pyr 5-CH), 7.29-7.62 (m, 4H, anth 7-CH, anth 6-CH, anth 3-CH, anth 2-CH), 7.75-7.80 (m, 1H, anth 8-CH), 7.93-8.05 (m, 3H, pyrid 4-CH, anth 5-CH, anth 4-CH), 8.17 (dd, *J* = 6.0 Hz and 2.0 Hz, 1H, pyrid 3-CH), 8.44-8.53 (m, 3H, pyrid 5-CH, anth 10-CH, anth 1-CH)

¹³C-NMR (50 MHz, CDCl₃): δ (ppm) 21.9 (pyr NCOCH₃), 41.5 (pyr 4-CH₂), 56.8 (pyr 5-CH), 66.3 (pyrid allyl-CH₂CHCH₂), 118.9 (pyrid allyl-CH₂CHCH₂), 122.9 (anth 8-CH), 123.0 (anth 1-CH), 124.3 (pyrid 5-CH), 124.5 (anth 6-CH), 124.9 (anth 3-CH), 125.7 (pyrid 3-CH), 126.0 (anth 7-CH), 126.6 (anth 2-CH), 128.3 (anth 8a-C), 128.6 (anth 10-CH), 129.4 (anth 4-CH), 130.1 (anth 5-CH), 131.2 (anth 9-CH), 131.4 (anth 4a-C), 131.6 (pyrid allyl-CH₂CHCH₂), 131.9 (anth 10a-C), 137.2 (pyrid 4-CH), 148.1 (pyrid 2-C), 151.2 (pyrid 6-C), 155.1 (pyr 3-C), 164.5 (pyrid C=O), 169.8 (pyr NCOCH₃)

Due to limited resolution of the measuring instrument, quaternary carbon anth 9a-C could not be detected.

MS: *m/z* (%) 449 (M⁺, 35), 406 (26), 291 (76), 218 (42), 203 (54), 189 (20), 178 (26), 43 (100)

HRMS: *m/z* calculated for C₂₈H₂₃N₃O₃Na [M + Na]⁺: 472.1637. Found: 472.1638.

3.4.1.5.6 6-(1-Acetyl-5-(anthracen-9-yl)-4,5-dihydro-1H-pyrazol-3-yl)pyridine-2-carboxylic acid (13)

To a mixture of allyl 6-(1-acetyl-5-(anthracen-9-yl)-4,5-dihydro-1H-pyrazol-3-yl)pyridine-2-carboxylate (0.20 g, 0.44 mmol) in THF (5 ml) were added $(\text{PPh}_3)_4\text{Pd}$ (0.06 g, 0.05 mmol) and morpholine (0.45 g, 0.45 ml, 5.18 mmol) under argon atmosphere. The mixture was stirred at room temperature for 2 h. Thereafter, the crude product was evaporated *in vacuo* and purified three times by column chromatography (RP-18 silica gel, MeOH/ H_2O 8:2, 7:3, and 6:4).

Yield: 0.14 g (74%), yellow crystals, mp. 279°C-281°C

Spectroscopic data:

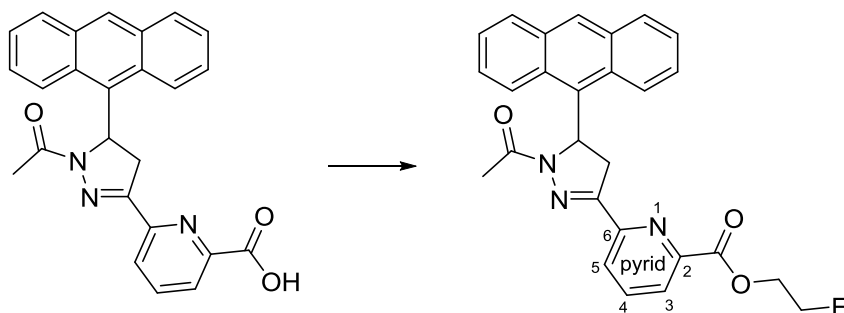
¹H-NMR (200 MHz, DMSO-*d*₆): δ (ppm) 2.22 (s, 3H), 3.43-3.53 (m, 1H), 4.24 (dd, *J* = 12.0 Hz and 4.0 Hz, 1H), 6.88 (dd, *J* = 8.0 Hz and 4.0 Hz, 1H), 7.34-7.61 (m, 4H), 7.70-7.75 (m, 1H), 7.82-8.02 (m, 3H), 8.09-8.13 (m, 2H), 8.55-8.58 (m, 2H)

Due to limited resolution of the measuring instrument, proton pyrid COOH could not be detected.

¹³C-NMR (50 MHz, DMSO-*d*₆): δ (ppm) 21.8, 41.3, 56.2, 121.6, 122.6, 123.8, 124.6, 124.8, 125.1, 126.1, 126.3, 127.5, 127.7, 129.0, 129.5, 129.9, 130.9, 131.4, 132.4, 137.2, 148.4, 155.7, 167.4, 168.3

HRMS: *m/z* calculated for C₂₅H₁₈N₃O₃Na [M + Na]⁺: 408.1354. Found: 408.1352.

3.4.1.5.7 2-Fluoroethyl 6-(1-acetyl-5-(anthracen-9-yl)-4,5-dihydro-1H-pyrazol-3-yl)pyridine-2-carboxylate (14)



Oxalyl chloride (0.02 g, 0.17 mmol) and DMF (3 drops) were added dropwise to a solution of 6-(1-acetyl-5-(anthracen-9-yl)-4,5-dihydro-1H-pyrazol-3-yl)pyridine-2-carboxylic acid (0.05 g, 0.13 mmol) in CH_2Cl_2 (10 ml) at 0°C . The mixture was allowed to warm to room temperature and was stirred overnight. The resulting yellow solution was evaporated to dryness and directly used in the next reaction step without further purification.

6-(1-acetyl-5-(anthracen-9-yl)-4,5-dihydro-1H-pyrazol-3-yl)pyridine-2-carbonyl chloride (0.05 g, 0.13 mmol) was dissolved in CH_2Cl_2 (10 ml) and fluoroethanol (0.008 g, 0.13 mmol) was added dropwise to the solution. The mixture was stirred for 24 h at room temperature after which the resulting product was purified several times by column chromatography (PE/EtOAc 6:4, 7:3 and RP-18 silica gel, MeOH/ H_2O 8:2).

Yield: 5 mg (8%), brown resin

Spectroscopic data:

¹H-NMR (400 MHz, CDCl₃): δ (ppm) 2.38 (s, 3H, pyr NCOCH₃), 3.71-3.74 (m, 1H, pyr 4-CH₂), 4.23 (dd, *J* = 19.4 Hz and 13.3 Hz, 1H, pyr 4-CH₂), 4.53-4.55 (m, 1H, pyrid OCH₂CH₂F), 4.60-4.64 (m, 2H, pyrid OCH₂CH₂F), 4.73-4.76 (m, 1H, pyrid OCH₂CH₂F), 6.92 (dd, *J* = 13.3 Hz and 9.8 Hz, 1H, pyr 5-CH), 7.31-7.35 (m, 1H, anth 7-CH), 7.37-7.41 (m, 1H, anth 6-CH), 7.47-7.51 (m, 1H, anth 3-CH), 7.56-7.60 (m, 1H, anth 2-CH), 7.75-7.78 (m, 1H, anth 8-CH), 7.99 (t, *J* = 7.8 Hz, 1H, pyrid 4-CH), 8.01-8.04 (m, 2H, anth 5-CH, anth 4-CH), 8.18 (dd, *J* = 7.8 Hz and 1.0 Hz, 1H, pyrid 3-CH), 8.43 (s, 1H, anth 10-CH), 8.48 (dd, *J* = 7.8 Hz and 1.0 Hz, 1H, pyrid 5-CH), 8.50-8.52 (m, 1H, anth 1-CH)

¹³C-NMR (100 MHz, CDCl₃): δ (ppm) 21.9 (pyr NCOCH₃), 41.6 (pyr 4-CH₂), 56.8 (pyr 5-CH), 64.5 (d, *J* = 20.4 Hz, pyrid OCH₂CH₂F), 81.1 (d, *J* = 171.2 Hz, pyrid OCH₂CH₂F), 122.9 (anth 8-CH), 123.0 (anth 1-CH), 124.5 (anth 6-CH, pyrid 5-CH), 124.9 (anth 3-CH), 125.8 (pyrid 3-CH), 126.0 (anth 7-CH), 126.6 (anth 2-CH), 128.3 (anth 8a-CH), 128.6 (anth 10-CH), 129.4 (anth 4-CH), 130.1 (anth 9a-CH), 130.2 (anth 5-CH), 131.2 (anth 9-CH), 131.4 (anth 4a-CH), 131.9 (anth 10a-CH), 137.3 (pyrid 4-CH), 147.6 (pyrid 2-C), 151.3 (pyrid 6-C), 155.1 (pyr 3-C), 164.6 (pyrid C=O), 169.8 (pyr NCOCH₃)

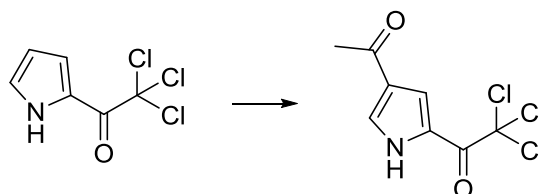
¹⁹F-NMR (471 MHz, CDCl₃): δ (ppm) -224.56 (m, pyrid CH₂CH₂F)

MS: *m/z* (%) 455 (M⁺, 37), 412 (31), 320 (26), 292 (90), 236 (21), 218 (53), 203 (58), 189 (21), 178 (32), 144 (37), 71 (23), 57 (33), 43 (100)

HRMS: *m/z* calculated for C₂₇H₂₂N₃O₃FNa [M + Na]⁺: 478.1543. Found: 478.1554.

3.4.1.6 Preparation of pyrrole based compounds

3.4.1.6.1 1-(4-Acetyl-1H-pyrrol-2-yl)-2,2,2-trichloroethanone (80)



To a solution of 2-(trichloroacetyl)pyrrole (3.00 g, 14.12 mmol) and AlCl_3 (2.32 g, 17.48 mmol) in nitromethane (15 ml) and CH_2Cl_2 (15 ml) was added a mixture of acetyl chloride (1.37 g, 17.42 mmol) in dry CH_2Cl_2 (5 ml) at -20°C . The resulting solution was stirred for 18 h at -20°C . Thereafter, the crude reaction product was poured on ice-water and the aqueous layer was extracted several times with diethyl ether. The combined organic extracts were dried over Na_2SO_4 and subsequently evaporated to dryness. The residue was then recrystallized from 30-50 ml of EtOH.

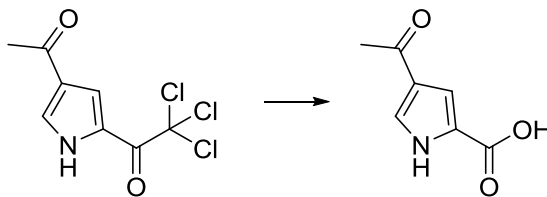
Yield: 2.43 g (81%), colorless crystals, mp. 188°C - 189°C

Analytical data are in complete accordance with literature values.³⁷²

Spectroscopic data:

$^1\text{H-NMR}$ (200 MHz, $\text{DMSO-}d_6$): δ (ppm) 1.25 (s, 3H), 7.33 (s, 2H)

3.4.1.6.2 4-Acetyl-1H-pyrrole-2-carboxylic acid (81)



After slowly adding 1-(4-acetyl-1H-pyrrol-2-yl)-2,2,2-trichloroethanone (2.43 g, 9.55 mmol) to a solution of NaOH (20% in H₂O, 40 ml), the mixture was refluxed for 1 h. Then, the solution was cooled and adjusted to pH 2 with 6N HCl. The crude reaction product was extracted repeatedly with diethyl ether. The collected organic layers were evaporated to dryness to subsequently accomplish purification by reversed phase column chromatography (RP-18 silica gel, ACN).

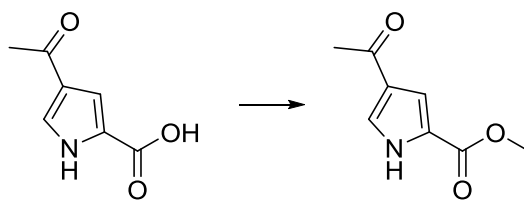
Yield: 1.54 g (63%), light yellow crystals, mp. 213°C-214°C

Analytical data are in complete accordance with literature values.³⁷²

Spectroscopic data:

¹H-NMR (200 MHz, DMSO-*d*₆): δ (ppm) 2.46 (s, 3H), 7.63 (q, *J* = 1.3 Hz and 0.9 Hz, 1H), 8.10 (q, *J* = 1.3 Hz and 2.1 Hz, 1H), 13.05 (s, 1H)

¹³C-NMR (50 MHz, DMSO-*d*₆): δ (ppm) 27.4, 119.5, 122.7, 127.2, 132.3, 173.0, 192.4

3.4.1.6.3 Methyl 4-acetyl-1H-pyrrole-2-carboxylate (82)

To a solution of 4-acetyl-1H-pyrrole-2-carboxylic acid (1.82 g, 11.85 mmol) in CH_2Cl_2 (7 ml) were added DCC (2.74 g, 13.27 mmol), DMAP (0.07 g, 0.59 mmol), and MeOH (18 ml). The mixture was stirred overnight at room temperature. Thereafter, the crude reaction product was extracted with $\text{CH}_2\text{Cl}_2/\text{H}_2\text{O}$, dried over MgSO_4 , and evaporated to dryness prior to purification *via* column chromatography (silica gel 60, PE/EtOAc 7:3).

Yield: 1.78 g (90%), light yellow crystals, mp. 118°C-120°C

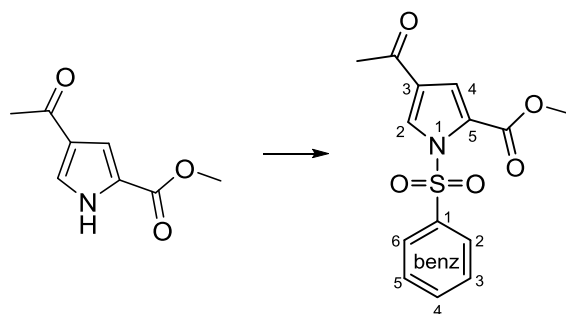
Analytical data are in complete accordance with literature values.³⁷³

Spectroscopic data:

$^1\text{H-NMR}$ (200 MHz, CDCl_3): δ (ppm) 2.48 (s, 3H), 3.91 (s, 3H), 7.33 (d, $J = 2.0$ Hz, 1H), 7.62 (d, $J = 2.0$ Hz), 10.62 (br s, 1H)

$^{13}\text{C-NMR}$ (50 MHz, CDCl_3): δ (ppm) 27.3, 51.8, 115.1, 123.8, 126.9, 127.0, 161.5, 193.7

3.4.1.6.4 Methyl 4-acetyl-1-(phenylsulfonyl)-1H-pyrrole-2-carboxylate (83)



To a solution of methyl 4-acetyl-1H-pyrrole-2-carboxylate (1.00 g, 5.98 mmol) in CH_2Cl_2 (10 ml) were added TBAHSO_4 (0.20 g, 0.57 mmol) and aqueous NaOH (50%, 4.26 g, 5.98 mmol) under argon atmosphere. Then, a solution of benzenesulfonyl chloride (1.15 g, 0.83 ml, 6.52 mmol) in dry CH_2Cl_2 (5 ml) was added dropwise to the mixture under intense stirring. After 40 min, the solution was washed with H_2O and the organic layers were dried over MgSO_4 and evaporated to dryness.

Yield: 1.50 g (82%), yellow-brownish crystals, mp. 126°C-128°C

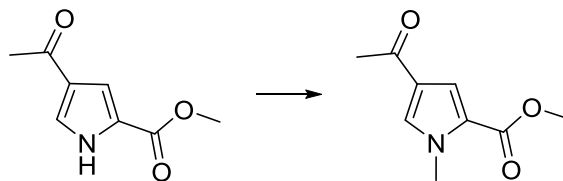
Spectroscopic data:

$^1\text{H-NMR}$ (200 MHz, CDCl_3): δ (ppm) 2.51 (s, 3H, COCH_3), 3.77 (s, 3H, COOCH_3), 7.41 (d, $J = 2.0$ Hz, 1H, 4-CH) 7.54-7.74 (m, 3H, benz 3-CH, benz 4-CH, benz 5-CH), 8.03-8.08 (m, 2H, benz 2-CH, benz 6-CH), 8.29 (d, $J = 2.0$ Hz, 1H, 2-CH)

$^{13}\text{C-NMR}$ (50 MHz, CDCl_3): δ (ppm) 27.2, 52.0, 121.2, 125.6, 125.9, 125.9, 128.4, 128.9, 134.4, 137.6, 158.6, 192.6

MS: m/z (%) 307 (M^+ , 35), 292 (26), 228 (8), 141 (48), 120 (56), 77 (100), 51 (14)

3.4.1.6.5 Methyl 4-acetyl-1-methyl-1H-pyrrole-2-carboxylate (84)



Methyl 4-acetyl-1H-pyrrole-2-carboxylate (0.50 g, 2.99 mmol) was dissolved in CH_2Cl_2 (20 ml) and cooled to 0°C . Trimethylsilyldiazomethane (1.08 g, 1.5 ml, 9.43 mmol) was added dropwise and the resulting solution was stirred for 2 days at room temperature. Thereafter, the reaction mixture was evaporated to dryness and the crude reaction product was purified by column chromatography (PE/EtOAc 7:3).

Yield: 0.14 g (26%), light yellow oil

Spectroscopic data:

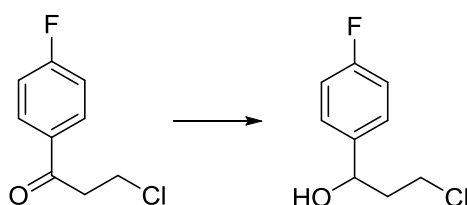
$^1\text{H-NMR}$ (200 MHz, CDCl_3): δ (ppm) 2.37 (s, 3H), 3.81 (s, 3H), 3.92 (s, 3H), 7.28 (d, $J = 2.0$ Hz, 1H), 7.37 (d, $J = 2.0$ Hz, 1H)

$^{13}\text{C-NMR}$ (50 MHz, CDCl_3): δ (ppm) 26.8, 37.2, 51.2, 117.6, 123.4, 124.2, 132.0, 161.0, 192.7

3.4.2 FAPPI derivatives

3.4.2.1 Preparation of 1-(3-Amino-1-(4-fluorophenyl)propyl)-3-phenyl-1,3-dihydro-2H-benzimidazol-2-one (APPI:1) (109) and 1-(1-(4-Fluorophenyl)-3-(methylamino)propyl)-3-phenyl-1,3-dihydro-2H-benzimidazol-2-one (FAPPI:1) (15)

3.4.2.1.1 3-Chloro-1-(4-fluorophenyl)propan-1-ol (103)



EtOH (30 ml) was introduced into a solution of 3-chloro-1-(4-fluorophenyl)-1-propanone (5.00 g, 26.79 mmol) in THF (30 ml). The mixture was cooled to -10°C and NaBH_4 (1.06 g, 28.13 mmol) was slowly added to the mixture at this temperature. The solution was stirred at -5°C for 10 min and thereafter, poured into a mixture of saturated aqueous ammonium chloride solution (80 ml) and ice (40 g). The product was extracted with diethyl ether, dried over Na_2SO_4 , and evaporated to dryness. The crude product was employed directly in the subsequent reaction step without further purification.

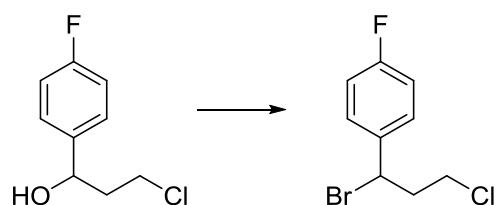
Yield: 4.78 g (95%), light yellow oil

Analytical data are in complete accordance with literature values.³⁷⁴

Spectroscopic data:

$^1\text{H-NMR}$ (200 MHz, CDCl_3): δ (ppm) 1.96 (d, $J = 4.0$ Hz, 1H), 2.02-2.27 (m, 2H), 3.52-3.58 (m, 1H), 3.71-3.77 (m, 1H), 4.95 (m, 1H), 7.03-7.36 (m, 4H)

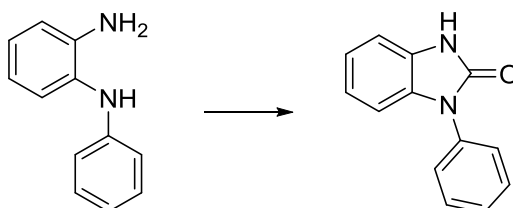
$^{13}\text{C-NMR}$ (50 MHz, CDCl_3): δ (ppm) 41.6, 41.7, 70.9, 115.6 (d, $J = 20.6$ Hz), 127.6 (d, $J = 8.0$ Hz), 139.6 (d, $J = 4.1$ Hz), 162.5 (d, $J = 244.3$ Hz)

3.4.2.1.2 1-(1-Bromo-3-chloropropyl)-4-fluorobenzene (104)

To 3-chloro-1-(4-fluorophenyl)propan-1-ol (4.78 g, 25.34 mmol) was added an aqueous HBr solution (48%, 80 ml) and the mixture was stirred for 3 h at room temperature. Thereafter, the solution was poured into a mixture of K_2CO_3 (22 g) and ice (140 g). Additional K_2CO_3 was added for neutralization (pH 7). The crude reaction product was extracted with diethyl ether, the combined organic layers were dried over MgSO_4 and evaporated to dryness. The resulting product was employed directly in the subsequent reaction step without further purification.

Yield: 4.10 g (64%), light yellow oil

Analytical data are in complete accordance with literature values.³⁷⁵

3.4.2.1.3 1-Phenyl-1,3-dihydro-2H-benzimidazol-2-one (106)

N-Phenylbenzene-1,2-diamine (1.00 g, 5.43 mmol) and 1,1-carbonyldiimidazol (1.23 g, 7.60 mmol) were dissolved in THF (10 ml) and stirred under argon atmosphere overnight at 25°C. After evaporation of the solvent, the crude reaction product was purified by column chromatography (silica gel 60, PE/EtOAc 1:1).

Yield: 0.85 g (74%), pink crystals, mp. 201°C-202°C

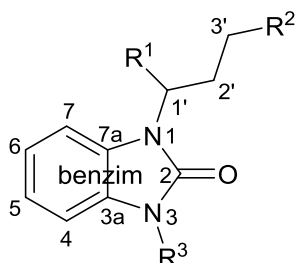
Analytical data are in complete accordance with literature values.³⁷⁶

Spectroscopic data:

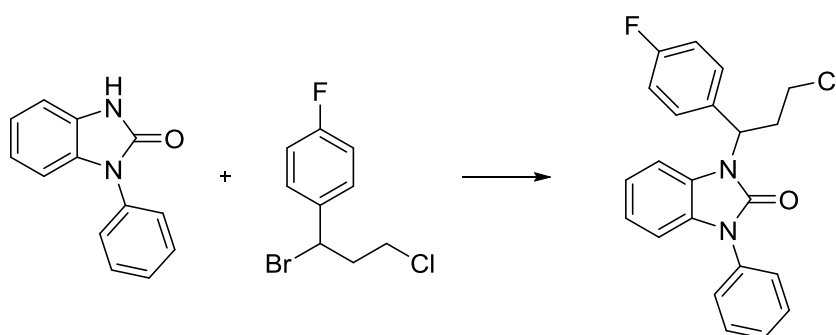
¹H-NMR (200 MHz, DMSO): δ (ppm) 6.85-7.17 (m, 2H), 7.34-7.45 (m, 2H), 7.43-7.69 (m, 5H), 11.16 (br s, 1H)

¹³C-NMR (50 MHz, DMSO): δ (ppm) 108.2, 109.2, 121.0, 121.9, 126.0, 127.4, 128.5, 129.5, 130.1, 134.6, 153.3

The compound numbering depicted below was used for the signal assignment of ^1H - and ^{13}C -NMR data of compounds **15-17**, **109**, and **122-125** in the next chapters:



3.4.2.1.4 1-(3-Chloro-1-(4-fluorophenyl)propyl)-3-phenyl-1,3-dihydro-2H-benzimidazol-2-one (107)



1-Phenyl-1,3-dihydro-2H-benzimidazol-2-one (2.28 g, 10.85 mmol) and K_2CO_3 (3.00 g, 21.69 mmol) were suspended in DMF (15 ml) and stirred at 25°C for 30 min. 1-(1-Bromo-3-chloropropyl)-4-fluorobenzene (4.09 g, 16.27 mmol) was then added and the solution was stirred at room temperature overnight. To the mixture were added EtOAc and H_2O . The aqueous layer was extracted with EtOAc and the combined organic layers were washed with brine, dried over MgSO_4 , and evaporated to dryness. Thereafter, the crude reaction product was purified by column chromatography (silica gel 60, PE/EtOAc 8:2).

Yield: 1.31 g (32%), colorless oil

Spectroscopic data:

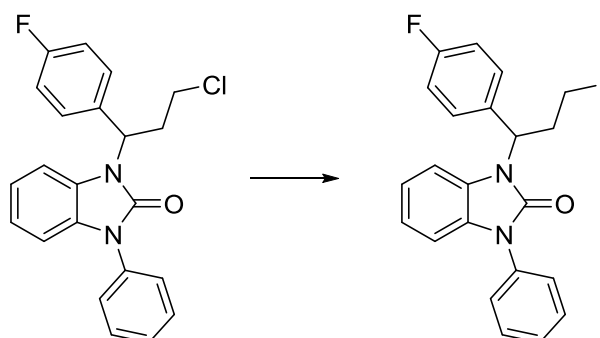
¹H-NMR (200 MHz, CDCl₃): δ (ppm) 2.70-2.87 (m, 1H), 3.12-3.30 (m, 1H), 3.60-3.66 (m, 2H), 5.73 (m, 1H), 7.00-7.11 (m, 6H), 7.38-7.57 (m, 7H)

¹³C-NMR (50 MHz, CDCl₃): δ (ppm) 34.3, 42.0, 53.8, 108.7, 109.0, 115.5, 115.9, 121.7, 122.0, 126.0, 127.8, 129.2, 129.4, 129.5

MS: m/z (%) 380 (M⁺, 21), 210 (100), 181 (8), 167 (12), 135 (9), 115 (5), 109 (58), 77 (12)

HRMS: m/z calculated for C₂₂H₁₈ClFN₂ONa [M + Na]⁺: 403.0989. Found: 403.0989.

3.4.2.1.5 1-(1-(4-Fluorophenyl)-3-iodopropyl)-3-phenyl-1,3-dihydro-2H-benzimidazol-2-one (108)



A solution of 1-(3-chloro-1-(4-fluorophenyl)propyl)-3-phenyl-1,3-dihydro-2H-benzimidazol-2-one (1.31 g, 3.39 mmol) and NaI (1.03 g, 6.89 mmol) in acetone (25 ml) was refluxed for 24 h. The precipitate formed was filtered and the solvent was removed *in vacuo*. The resulting product did not require purification and thus, was employed directly in the next reaction step.

Yield: 1.34 g (82%), yellow resin

Spectroscopic data:

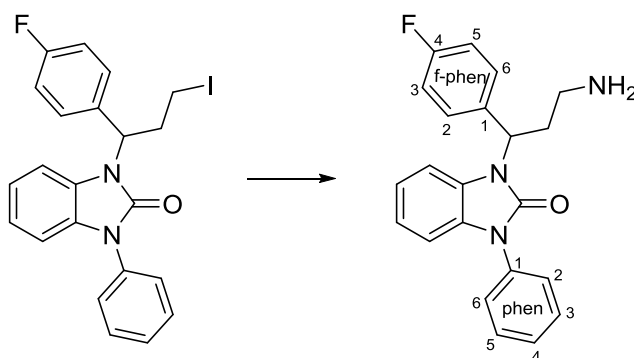
¹H-NMR (200 MHz, CDCl₃): δ (ppm) 2.77-2.92 (m, 1H), 3.14-3.31 (m, 3H), 5.63-5.70 (m, 1H), 7.01-7.10 (m, 6H), 7.36-7.56 (m, 7H)

¹³C-NMR (50 MHz, CDCl₃): δ (ppm) 2.3, 35.3, 57.0, 108.8, 108.9, 115.5, 115.9, 121.6, 122.0, 126.0, 127.7, 128.5, 129.1, 129.3, 129.4, 134.0, 134.1, 134.3, 153.0, 159.9, 164.8

MS: m/z (%) 472 (M⁺, 32), 210 (100), 181 (11), 167 (23), 135 (43), 109 (34), 77 (15)

HRMS: m/z calculated for C₂₂H₁₈FIN₂ONa [M + Na]⁺: 495.0346. Found: 495.0353.

3.4.2.1.6 1-(3-Amino-1-(4-fluorophenyl)propyl)-3-phenyl-1,3-dihydro-2H-benzimidazol-2-one (APPI:1) (109)



1-(1-(4-Fluorophenyl)-3-iodopropyl)-3-phenyl-1,3-dihydro-2H-benzimidazol-2-one (0.26 g, 0.55 mmol) was suspended in a solution of NH_3 in isopropanol (2 M, 22.0 ml) and the resulting mixture was heated in a sealed tube for 3 h at 80°C . After evaporation of the solvent, the crude reaction product was purified by column chromatography (silica gel 60, $\text{CH}_2\text{Cl}_2/\text{MeOH}$ 9:1).

Yield: 0.10 g (50%), light brown crystals, mp. 87°C - 88°C

Spectroscopic data:

¹H-NMR (400 MHz, CDCl₃): δ (ppm) 2.74-2.84 (m, 3H, 2'-CH₂, 3'-CH₂), 2.98-3.04 (m, 1H, 3'-CH₂), 5.74-5.78 (m, 1H, 1'-CH), 6.79-6.81 (m, 1H, benzim 7-CH), 6.96-7.01 (m, 5H, benzim 4-CH, benzim 5-CH, benzim 6-CH, f-phen 3-CH, f-phen 5-CH), 7.30-7.33 (m, 1H, phen 4-CH), 7.40-7.48 (m, 4H, f-phen 2-CH, f-phen 6-CH, phen 3-CH, phen 5-CH), 7.52-7.54 (m, 2H, phen 2-CH, phen 6-CH)

Due to limited resolution of the measuring instrument, protons NH₂ could not be detected.

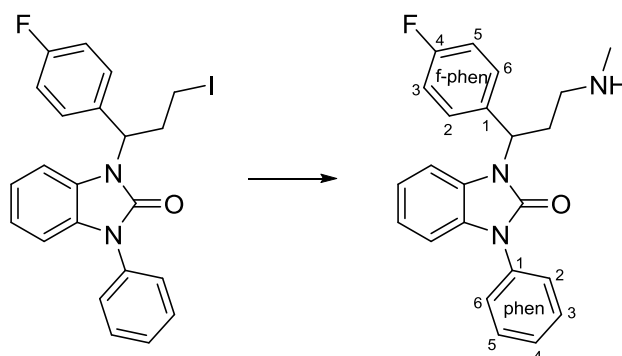
¹³C-NMR (100 MHz, CDCl₃): δ (ppm) 30.3 (2'-CH₂), 37.8 (3'-CH₂), 52.7 (1'-CH), 109.2 (benzim 4-CH), 110.0 (benzim 7-CH), 115.7 (d, *J* = 21.5 Hz, f-phen 3-CH), 115.7 (d, *J* = 8.2 Hz, f-phen 5-CH), 122.0 (benzim 5-CH), 122.3 (benzim 6-CH), 126.4 (phen 2-CH), 126.4 (phen 6-CH), 127.5 (benzim 7a-C), 128.1 (phen 4-CH), 129.2 (d, *J* = 8.2 Hz, f-phen 2-CH), 129.2 (d, *J* = 8.2 Hz, f-phen 6-CH), 129.5 (benzim 3a-C), 129.7 (phen 3-CH), 129.7 (phen 5-CH), 133.3 (d, *J* = 3.2 Hz, f-phen 1-C), 134.0 (phen 1-CH), 153.8 (benzim 2-CO), 162.3 (d, *J* = 247.4 Hz, f-phen 4-CF)

¹⁹F-NMR (471 MHz, CDCl₃): δ (ppm) -113.68 (m, f-phen CF)

MS: *m/z* (%) 361 (M⁺, 17), 210 (100), 181 (15), 167 (16), 149 (29), 128 (17), 77 (19), 57 (20)

HRMS: *m/z* calculated for C₂₂H₂₁FN₃O [M + H]⁺: 362.1669. Found: 362.1674.

3.4.2.1.7 1-(1-(4-Fluorophenyl)-3-(methylamino)propyl)-3-phenyl-1,3-dihydro-2H-benzimidazol-2-one (FAPPI:1) (15)



1-(1-(4-Fluorophenyl)-3-iodopropyl)-3-phenyl-1,3-dihydro-2H-benzimidazol-2-one (0.20 g, 0.42 mmol) was dissolved in a solution of methylamine in EtOH (8 M, 5.3 ml) and the resulting mixture was heated in a sealed tube for 3 h at 80°C. After evaporation of the solvent, the crude reaction product was purified by column chromatography twice (silica gel 60, CH₂Cl₂/MeOH 9:1 and CH₂Cl₂/EtOAc/MeOH 7:2:1).

Yield: 77 mg (48%), light orange resin

Spectroscopic data:

¹H-NMR (400 MHz, CDCl₃): δ (ppm) 2.42 (s, 3H, NHCH₃), 2.57-2.74 (m, 4H, 2'-CH₂, 3'-CH₂), 3.15 (br s, 1H, NHCH₃), 5.76-5.79 (m, 1H, 1'-CH), 6.88-6.90 (m, 1H, benzim 7-CH), 6.97-7.05 (m, 4H, benzim 5-CH, benzim 6-CH, f-phen 3-CH, f-phen 5-CH), 7.07-7.10 (m, 1H, benzim 4-CH), 7.39-7.43 (m, 1H, phen 4-CH), 7.46-7.57 (m, 6H, f-phen 2-CH, f-phen 6-CH, phen 2-CH, phen 3-CH, phen 5-CH, phen 6-CH)

¹³C-NMR (100 MHz, CDCl₃): δ (ppm) 30.6 (2'-CH₂), 35.9 (NHCH₃), 48.3 (3'-CH₂), 53.1 (1'-CH), 108.9 (benzim 4-CH), 109.5 (benzim 7-CH), 115.5 (d, *J* = 21.5 Hz, f-phen 3-CH), 115.5 (d, *J* = 21.5 Hz, f-phen 5-CH), 121.4 (benzim 5-CH), 121.8 (benzim 6-CH), 126.0 (phen 2-CH), 126.0 (phen 6-CH), 127.7 (phen 4-CH), 128.0 (benzim 7a-C), 129.0 (d, *J* = 8.1 Hz, f-phen 2-CH), 129.0 (d, *J* = 8.1 Hz, f-phen 6-CH), 129.4 (benzim 3a-C), 129.5 (phen 3-CH), 129.5 (phen 5-CH), 134.4 (phen 1-CH), 134.6 (d, *J* = 3.4 Hz, f-phen 1-CH), 153.5 (benzim 2-CO), 162.1 (d, *J* = 246.7 Hz, f-phen 4-CF)

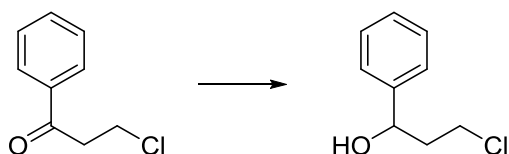
¹⁹F-NMR (471 MHz, CDCl₃): δ (ppm) -114.36 (m, f-phen 4-CF)

MS: *m/z* (%) 375 (M⁺, 16), 210 (57), 167 (12), 109 (22), 97 (16), 71 (27), 57 (78), 44 (100)

HRMS: *m/z* calculated for C₂₃H₂₃FN₃O [M + H]⁺: 376.1825. Found: 376.1821.

3.4.2.2 Preparation of 1-(4-Fluorophenyl)-3-(3-(methylamino)-1-phenylpropyl)-1,3-dihydro-2H-benzimidazol-2-one (FAPP1:2) (16)

3.4.2.2.1 3-Chloro-1-phenylpropan-1-ol (111)



A solution of 3-chloro-1-phenylpropan-1-one (4.49 g, 26.60 mmol) in THF (25 ml) was diluted with EtOH (35 ml). The solution was cooled to -10°C and NaBH_4 (1.06 g, 27.93 mmol) was added in portions. After stirring the mixture for additional 10 min at -5°C , it was allowed to warm to room temperature. The solution was poured into a mixture of saturated NH_4Cl solution (82 ml) and ice (42 g) and the product was extracted with diethyl ether. The combined organic layers were dried over Na_2SO_4 and evaporated to dryness.

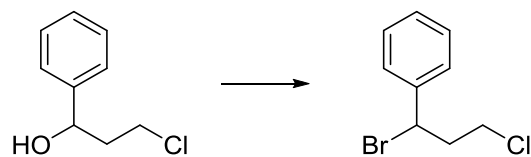
Yield: 4.61 g (99%), light yellow oil

Analytical data are in complete accordance with literature values.³⁷⁷

Spectroscopic data:

$^1\text{H-NMR}$ (200 MHz, CDCl_3): δ (ppm) 2.04-2.35 (m, 2H), 3.40 (br s, 1H), 3.52-3.63 (m, 1H), 3.70-3.82 (m, 1H), 3.91-3.77 (m, 1H), 4.98 (dd, $J = 6.0$ Hz and 2.0 Hz, 1H), 7.37-7.51 (m, 5H)

$^{13}\text{C-NMR}$ (50 MHz, CDCl_3): δ (ppm) 41.4, 41.7, 71.3, 125.7, 127.9, 128.6, 143.7

3.4.2.2.2 (1-Bromo-3-chloropropyl)benzene (112)

A mixture of 3-chloro-1-phenylpropan-1-ol (4.81 g, 28.19 mmol) in aqueous HBr (48%, 92 ml) was stirred for 3 h at room temperature and then poured into a mixture of saturated K₂CO₃ solution (11 ml) and ice (72 g). The pH of the solution was adjusted to pH 7 by adding further K₂CO₃ to the mixture. Thereafter, the product was extracted with diethyl ether, dried over MgSO₄, and evaporated to dryness. The crude reaction product was employed directly in the next reaction step without further purification.

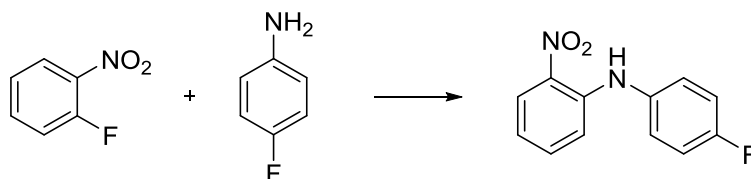
Yield: 5.64 g (86%), yellow oil

Analytical data are in complete accordance with literature values.³⁷⁷

Spectroscopic data:

¹H-NMR (200 MHz, CDCl₃): δ (ppm) 2.41-2.58 (m, 1H), 2.65-3.82 (m, 1H), 3.54-3.81 (m, 2H), 5.24 (dd, *J* = 4.0 Hz and 4.0 Hz, 1H), 7.32-7.46 (m, 5H)

¹³C-NMR (50 MHz, CDCl₃): δ (ppm) 41.8, 42.5, 51.3, 127.1, 128.5, 128.6, 140.6

3.4.2.2.3 *N*-(4-Fluorophenyl)-2-nitroaniline (116)

- 1) Method 1: Anhydrous KF (4.13 g, 70.87 mmol), and K_2CO_3 (9.81 g, 70.87 mmol) were well powdered with a mortar and a pestle and added to 4-fluoroaniline (7.89 g, 70.87 mmol). Then, 1-fluoro-2-nitrobenzene (10.00 g, 70.87 mmol) was added and the mixture was irradiated in the microwave oven (900 W, 10 min). Thereafter, H_2O (20 ml) and CH_2Cl_2 (20 ml) were added and the organic layer was washed with 10% HCl (10 ml) and brine (10 ml). The combined organic layers were dried over Na_2SO_4 and evaporated to dryness prior to purification by column chromatography (silica gel 60, PE/EtOAc 9.5:0.5).

Yield: 9.51 g (58%), dark orange crystals, mp. 82°C-83°C

- 1) Method 2: Anhydrous KF (4.28 g, 73.70 mmol), and K_2CO_3 (10.18 g, 73.70 mmol) were well powdered with a mortar and a pestle and added to 4-fluoroaniline (8.19 g, 73.70 mmol). Then, 1-fluoro-2-nitrobenzene (10.40 g, 73.70 mmol) was added and the mixture was stirred for 2 days at 180°C. Thereafter, H_2O (20 ml) and CH_2Cl_2 (20 ml) were added and the organic layer was washed with 10% HCl (10 ml) and brine (10 ml). The combined organic layers were dried over Na_2SO_4 and evaporated to dryness prior to purification by column chromatography (silica gel 60, PE/EtOAc 9:1 and RP-18 silica gel, MeOH/ H_2O 7:3).

Yield: 11.59 g (68%), dark orange crystals, mp. 82°C-83°C

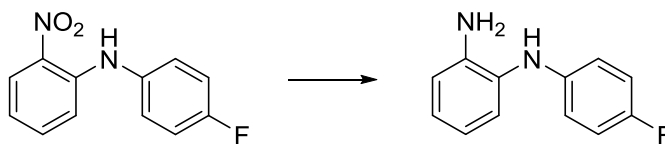
Analytical data are in complete accordance with literature values.³⁷⁸

Spectroscopic data:

¹H-NMR (200 MHz, CDCl₃): δ (ppm) 6.73-6.77 (m, 1H), 6.78-7.42 (m, 6H), 8.18-8.23 (m, 1H), 9.41 (br s, 1H)

¹³C-NMR (50 MHz, CDCl₃): δ (ppm) 115.6, 116.3, 116.8, 117.4, 126.6, 126.8, 127.0, 134.5, 135.7, 143.5, 158.1, 163.0

MS: m/z (%) 233 (M⁺, 1), 141 (100), 111 (21), 95 (58), 83 (50), 75 (86), 69 (26), 57 (24), 50 (23)

3.4.2.2.4 *N*-(4-Fluorophenyl)benzene-1,2-diamine (118)

To a solution of *N*-(4-fluorophenyl)-2-nitroaniline (2.17 g, 9.34 mmol) in abs. CH₂Cl₂ (15 ml) were added glacial acetic acid (8 ml) and Zn⁰ (8.39 g, 128.89 mmol) at 0°C under argon atmosphere. After the addition, the mixture was allowed to warm to room temperature and was stirred for 2 h. Zn⁰ was filtered off and the pH of the solution was adjusted to pH 9 with 2N NaOH. Thereafter, the aqueous layer was extracted three times with CH₂Cl₂, the combined organic layers were dried over MgSO₄, evaporated to dryness, and purified by column chromatography (silica gel 60, PE/EtOAc 9:1).

Yield: 1.75 g (93%), dark orange-reddish oil

Analytical data are in complete accordance with literature values.³⁷⁹

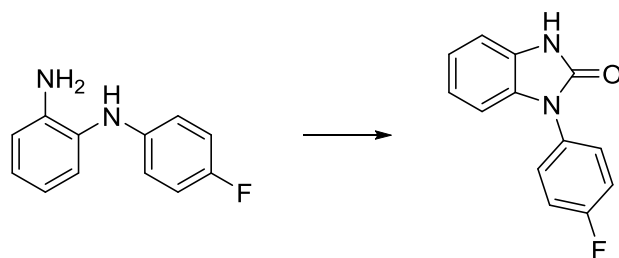
Spectroscopic data:

¹H-NMR (200 MHz, CDCl₃): δ (ppm) 3.68 (br s, 2H), 5.13 (br s, 1H), 6.65-7.10 (m, 8H)

¹³C-NMR (50 MHz, CDCl₃): δ (ppm) 116.0, 116.5, 116.7, 117.2, 117.4, 119.7, 124.3, 125.9, 129.8, 141.8, 141.8, 155.0, 159.7

MS: m/z (%) 202 (M⁺, 100), 187 (13), 181 (9), 154 (5), 139 (6), 100 (5), 80 (5), 53 (5), 43 (7)

3.4.2.2.5 1-(4-Fluorophenyl)-1,3-dihydro-2H-benzimidazol-2-one (120)



- 1) Method 1: To a solution of *N*-(4-fluorophenyl)benzene-1,2-diamine (4.50 g, 22.25 mmol) in THF (25 ml) was added 1,1'-carbonyldiimidazole (5.05 g, 31.22 mmol) under argon atmosphere and the mixture was stirred at room temperature overnight. Column filtration was carried out to separate major impurities. Thereafter, the product was employed directly in the next reaction step. A small sample was subjected to further purification by column chromatography (silica gel 60, PE/ethyl acetate 9:1) for spectroscopic analysis.

Yield: 3.12 g (61%), brown resin

- 2) Method 2: *N*-(4-Fluorophenyl)benzene-1,2-diamine (0.54 g, 2.69 mmol) was dissolved in DMF (10 ml) and a solution of 1,1'-carbonyldiimidazole (1.75 g, 10.78 mmol) in DMF (10 ml) was slowly added under argon atmosphere. The resulting mixture was stirred at 90°C for 2 h. Thereafter, the crude reaction product was evaporated to dryness, taken up in H₂O, filtered and dried. The product was obtained in sufficient purity and did not require further purification.

Yield: 0.49 g (80%), brown resin

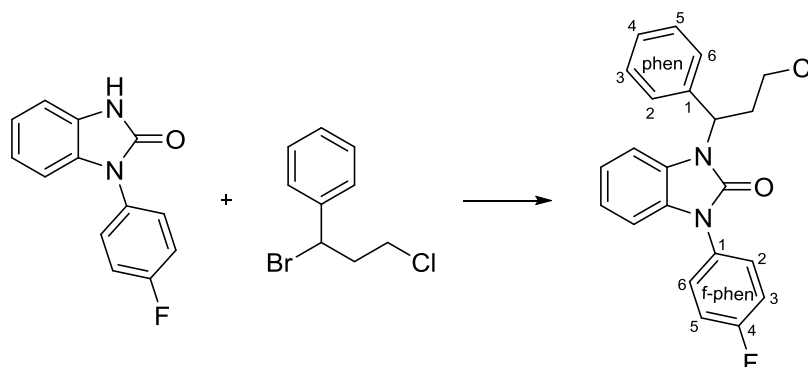
Spectroscopic data:

¹H-NMR (200 MHz, CDCl₃): δ (ppm) 6.74-6.81 (m, 2H), 6.89-7.11 (m, 2H), 7.14-7.23 (m, 2H), 7.48-7.59 (m, 1H), 7.73-7.78 (m, 1H), 9.03 (br s, 1H)

¹³C-NMR (50 MHz, CDCl₃): δ (ppm) 108.5, 110.0, 116.3, 116.8, 121.4, 121.7, 122.3, 128.0, 128.2, 130.4, 135.1, 155.1, 159.3, 164.2

MS: m/z (%) 228 (M⁺, 100), 199 (31), 172 (8), 114 (9), 95 (10), 75 (17), 51 (10)

HRMS: m/z calculated for C₁₃H₁₀FN₂O [M + H]⁺: 229.0772. Found: 229.0769.

3.4.2.2.6 1-(3-Chloro-1-phenylpropyl)-3-(4-fluorophenyl)-1,3-dihydro-2H-benzimidazol-2-one (122)

A solution of 1-(4-fluorophenyl)-1,3-dihydro-2H-benzimidazol-2-one (0.69 g, 3.01 mmol) and K_2CO_3 (0.83 g, 6.03 mmol) in DMF (5 ml) was stirred for 30 min at room temperature. Thereafter, a solution of (1-bromo-3-chloropropyl)benzene (1.05 g, 4.52 mmol) in DMF (0.5 ml) was slowly added and the resulting mixture was stirred at room temperature overnight. EtOAc (10 ml) and H_2O (10 ml) were added and the organic layer was separated from the aqueous layer. The aqueous layer was extracted another three times with EtOAc, and the combined organic layers were washed with a saturated NaCl solution, dried over $MgSO_4$, and evaporated to dryness prior to purification by column chromatography (silica gel 60, PE/EtOAc 9:1 and RP-18 silica gel, MeOH).

Yield: 0.72 g (63%), dark orange resin

Spectroscopic data:

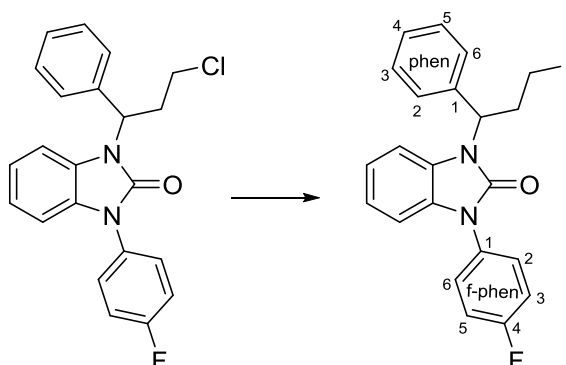
¹H-NMR (400 MHz, CDCl₃): δ (ppm) 2.80-2.88 (m, 1H, 2'-CH₂), 3.17-3.26 (m, 1H, 2'-CH₂), 3.62-3.70 (m, 2H, 3'-CH₂), 5.79 (dd, *J* = 10.0 Hz and 5.6 Hz, 1H, 1'-CH), 7.04-7.09 (m, 4H, benzim 4-CH, benzim 5-CH, benzim 6-CH, benzim 7-CH), 7.21-7.26 (m, 2H, f-phen 3-CH, f-phen 5-CH), 7.31-7.33 (m, 1H, phen 4-CH), 7.36-7.40 (m, 2H, phen 3-CH, phen 5-CH), 7.52-7.56 (m, 4H, f-phen 2-CH, f-phen 6-CH, phen 2-CH, phen 6-CH)

¹³C-NMR (100 MHz, CDCl₃): δ (ppm) 34.1 (2'-CH₂), 42.0 (3'-CH₂), 54.4 (1'-CH), 108.6 (benzim 4-CH), 109.0 (benzim 7-CH), 116.4 (d, *J* = 22.9 Hz, f-phen 3-CH), 116.4 (d, *J* = 22.9 Hz, f-phen 5-CH), 121.6 (benzim 5-CH), 122.1 (benzim 6-CH), 127.4 (phen 2-CH), 127.4 (phen 6-CH), 127.9 (d, *J* = 8.6 Hz, f-phen 2-CH), 127.9 (d, *J* = 8.6 Hz, f-phen 6-CH), 128.1 (phen 4-CH), 128.7 (benzim 7a-C), 128.8 (phen 3-CH), 128.8 (phen 5-CH), 129.4 (benzim 3a-C), 130.3 (d, *J* = 3.1 Hz, f-phen 1-C), 138.4 (phen 1-C), 153.2 (benzim 2-CO), 161.6 (d, *J* = 247.7 Hz, f-phen 4-CF)

¹⁹F-NMR (471 MHz, CDCl₃): δ (ppm) -113.31 (m, f-phen 5-CF)

MS: *m/z* (%) 380 (M⁺, 2), 228 (100), 199 (11), 185 (16), 153 (6), 117 (14), 91 (73), 75 (8)

HRMS: *m/z* calculated for C₂₂H₁₉ClFN₂O [M + H]⁺: 381.1170. Found: 381.1176.

3.4.2.2.7 1-(4-Fluorophenyl)-3-(3-iodo-1-phenylpropyl)-1,3-dihydro-2H-benzimidazol-2-one (124)

To a solution of 1-(3-chloro-1-phenylpropyl)-3-(4-fluorophenyl)-1,3-dihydro-2H-benzimidazol-2-one (0.60 g, 1.59 mmol) in acetone (12 ml) was added NaI (0.48 g, 3.18 mmol), and the mixture was refluxed for 24 h. The resulting precipitate was filtered and the crude reaction product was evaporated *in vacuo* prior to purification by column chromatography (silica gel 60, PE/EtOAc 9:1).

Yield: 0.56 g (76%), yellow crystals, mp. 39°C-41°C

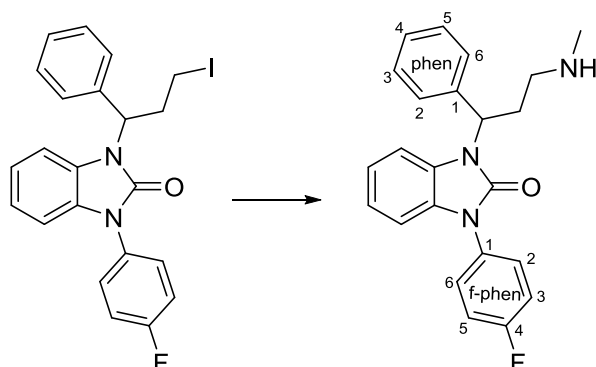
Spectroscopic data:

¹H-NMR (200 MHz, CDCl₃): δ (ppm) 2.81-2.99 (m, 1H, 2'-CH₂), 3.11-3.35 (m, 3H, 2'-CH₂, 3'-CH₂), 5.70 (dd, *J* = 6.0 Hz and 2.0 Hz, 1H, 1'-CH), 7.04-7.09 (m, 4H, benzim 4-CH, benzim 5-CH, benzim 6-CH, benzim 7-CH), 7.17-7.42 (m, 5H, f-phen 3-CH, f-phen 5-CH, phen 4-CH, phen 2-CH, phen 5-CH), 7.51-7.57 (m, 4H, f-phen 2-CH, f-phen 6-CH, phen 2-CH, phen 6-CH)

¹³C-NMR (50 MHz, CDCl₃): δ (ppm) 2.4 (2'-CH₂), 35.2 (3'-CH₂), 57.6 (1'-CH), 108.6 (benzim 4-CH), 109.2 (benzim 7-CH), 116.4 (d, *J* = 23.0 Hz, f-phen 3-CH), 116.4 (d, *J* = 23.0 Hz, f-phen 5-CH), 121.6 (benzim 5-CH), 122.1 (benzim 6-CH), 127.3 (phen 2-CH), 127.3 (phen 6-CH), 127.8 (phen 4-CH), 128.1 (d, *J* = 5.0 Hz, f-phen 2-CH), 128.1 (d, *J* = 5.0 Hz, f-phen 6-CH), 128.5 (benzim 7a-C), 128.8 (phen 3-CH), 128.8 (phen 5-CH), 129.4 (benzim 3a-C), 130.3 (d, *J* = 3.0 Hz, f-phen 1-C), 138.1 (phen 1-C), 153.2 (benzim 2-CO), 161.6 (d, *J* = 247.0 Hz, f-phen 4-CF)

MS: *m/z* (%) 472 (M⁺, 13), 317 (5), 228 (100), 185 (15), 117 (47), 103 (2), 91 (40), 75 (8), 55 (5)

HRMS: *m/z* calculated for C₂₂H₁₉FIN₂O [M + H]⁺: 473.0526. Found: 473.0506.

3.4.2.2.8 1-(4-Fluorophenyl)-3-(3-(methylamino)-1-phenylpropyl)-1,3-dihydro-2H-benzimidazol-2-one (FAPP1:2) (16)

1-(4-Fluorophenyl)-3-(3-iodo-1-phenylpropyl)-1,3-dihydro-2H-benzimidazol-2-one (0.29 g, 0.62 mmol) was dissolved in a solution of methylamine in EtOH (8 M, 7.8 ml) and the resulting mixture was stirred in a sealed vessel at 80°C for 3 h. After evaporation of the solvent, the crude reaction product was purified by column chromatography (silica gel 60, CH₂Cl₂/MeOH 9:1 and RP-18 silica gel MeOH/H₂O 9:1 and 7:3).

Yield: 68 mg (29%), light yellow crystals, mp. 100°C-102°C

Spectroscopic data:

¹H-NMR (200 MHz, CDCl₃): δ (ppm) 2.53 (s, 3H, NHCH₃), 3.13 (br s, 4H, 2'-CH₂, 3'-CH₂), 5.77-5.81 (m, 1H, 1'-CH), 6.96-7.03 (m, 4H, benzim 4-CH, benzim 5-CH, benzim 6-CH, benzim 7-CH), 7.16-7.34 (5H, f-phen 3-CH, f-phen 5-CH, phen 4-CH, phen 2-CH, phen 5-CH), 7.49-7.56 (m, 4H, f-phen 2-CH, f-phen 6-CH, phen 2-CH, phen 6-CH)

Due to limited resolution of the measuring instrument, proton NHCH₃ could not be detected.

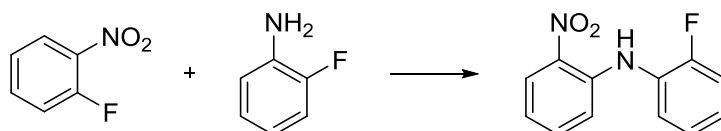
¹³C-NMR (50 MHz, CDCl₃): δ (ppm) 27.6 (2'-CH₂), 33.1 (NHCH₃), 47.0 (3'-CH₂), 54.2 (1'-CH), 108.8 (benzim 4-CH), 109.9 (benzim 7-CH), 116.6 (d, J = 23.0 Hz, f-phen 3-CH), 116.6 (d, J = 23.0 Hz, f-phen 5-CH), 122.1 (benzim 5-CH), 122.6 (benzim 6-CH), 127.2 (phen 2-CH), 127.2 (phen 6-CH), 127.7 (phen 4-CH), 128.3 (d, J = 6.0 Hz, f-phen 2-CH), 128.3 (d, J = 6.0 Hz, f-phen 6-CH), 128.4 (benzim 7a-C), 128.9 (phen 3-CH), 128.9 (phen 5-CH), 129.2 (benzim 3a-C), 129.7 (d, J = 3.0 Hz, f-phen 1-C), 136.9 (phen 1-C), 153.4 (benzim 2-CO), 161.7 (d, J = 248.0 Hz, f-phen 4-CF)

MS: m/z (%) 375 (M⁺, 11), 228 (50), 185 (9), 147 (17), 128 (26), 91 (13), 58 (34), 44 (100)

HRMS: m/z calculated for C₂₃H₂₃FN₃O [M + H]⁺: 376.1825. Found: 376.1828.

3.4.2.3 Preparation of 1-(2-Fluorophenyl)-3-(3-(methylamino)-1-phenylpropyl)-1,3-dihydro-2H-benzimidazol-2-one (FAPPI:3) (17)

3.4.2.3.1 2-Fluoro-N-(2-nitrophenyl)aniline (117)



After the addition of well powdered anhydrous KF (2.06 g, 35.44 mmol), and K_2CO_3 (4.90 g, 35.44 mmol) to 2-fluoroaniline (3.94 g, 35.44 mmol), 1-fluoro-2-nitrobenzene (5.00 g, 35.44 mmol) was added and the mixture was refluxed for 2 days at 180°C. Thereafter, H_2O (10 ml) and CH_2Cl_2 (10 ml) were added and the organic layer was washed with 10% HCl (5 ml) and brine (5 ml). The combined organic layers were dried over Na_2SO_4 and evaporated to dryness prior to purification by column chromatography (silica gel 60, PE/EtOAc 9:1).

Yield: 4.36 g (52%), orange crystals, mp. 79°C-80°C

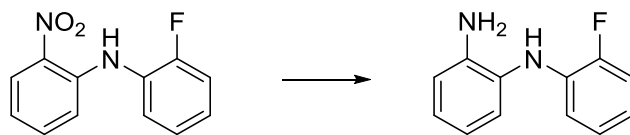
Analytical data are in complete accordance with literature values.³⁸⁰

Spectroscopic data:

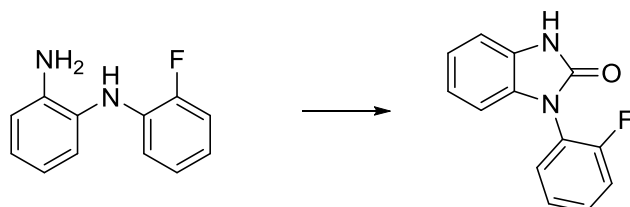
¹H-NMR (200 MHz, CDCl₃): δ (ppm) 6.83 (ddd, *J* = 7.2 Hz, 7.0 Hz, and 1.2 Hz, 1H), 7.08 (dt, *J* = 2.9 Hz, 1.5 Hz, and 1.4 Hz, 1H), 7.24-7.18 (m, 3H), 7.44-7.37 (m, 2H), 8.21 (dd, *J* = 8.7 Hz and 1.5 Hz, 1H), 9.30 (br s, 1H)

¹³C-NMR (50 MHz, CDCl₃): δ (ppm) 115.9, 115.9, 116.4, 116.8, 118.0, 124.6, 124.7, 125.8, 125.8, 126.4, 126.7, 126.9, 133.7, 135.7, 142.2, 154.1, 159.0

MS: *m/z* (%) 232 (M⁺, 100), 215 (18), 198 (18), 185 (77), 167 (15), 75 (26), 57 (33), 50 (24)

3.4.2.3.2 *N*-(2-Fluorophenyl)benzene-1,2-diamine (119)

To a solution of 2-fluoro-*N*-(2-nitrophenyl)aniline (2.50 g, 10.76 mmol) in abs. CH₂Cl₂ (15 ml) were added glacial acetic acid (5 ml) and Zn⁰ (9.71 g, 148.48 mmol) at 0°C under argon atmosphere. After the addition, the mixture was stirred for 2 h during which the temperature was allowed to warm to 25°C. Zn⁰ was filtered off and the pH of the solution was adjusted to pH 9 with 2N NaOH. Thereafter, the aqueous layer was extracted with CH₂Cl₂, the combined organic layers were dried over MgSO₄ and evaporated to dryness. The crude reaction product was directly used in the next reaction step without further purification.

3.4.2.3.3 1-(2-Fluorophenyl)-1,3-dihydro-2*H*-benzimidazol-2-one (121)

- 1) Method 1: To a solution of *N*-(4-fluorophenyl)benzene-1,2-diamine (1.74 g, 8.60 mmol) in THF (20 ml) was added 1,1'-carbonyldiimidazole (1.95 g, 12.05 mmol) under argon atmosphere and the mixture was stirred at room temperature overnight. Thereafter, the crude reaction product was purified by column chromatography (silica gel 60, PE/EtOAc 9:1).

Yield: 1.35 g (69%), brown resin

- 2) Method 2: A solution of 1,1'-carbonyldiimidazole (8.09 g, 49.98 mmol) in DMF (20 ml) was slowly added to a mixture of *N*-(4-fluorophenyl)benzene-1,2-diamine (2.53 g, 12.51 mmol) in DMF (20 ml) under argon atmosphere. The resulting solution was stirred at 90°C for 2 h. After completion of the reaction, the solvent was evaporated *in vacuo*, the slurry was taken up in H₂O, filtered, and dried. The resulting product was obtained in sufficient purity and did not require further purification.

Yield: 2.30 g (80%), brown resin

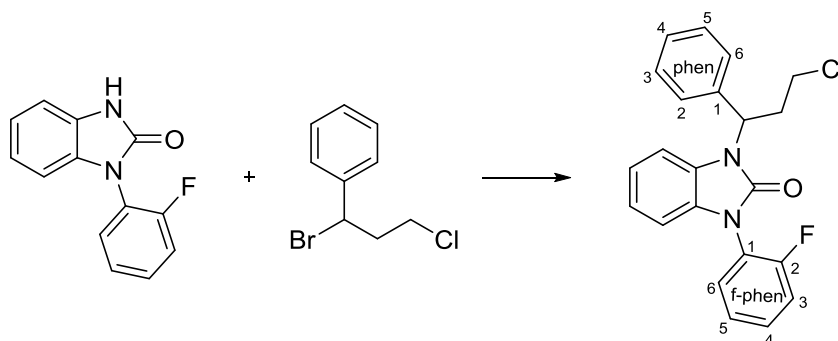
Spectroscopic data:

¹H-NMR (200 MHz, CDCl₃): δ (ppm) 6.82-6.85 (m, 1H), 7.00-7.19 (m, 3H), 7.26-7.88 (m, 2H), 7.43-7.60 (m, 2H), 10.54 (br s, 1H)

¹³C-NMR (50 MHz, CDCl₃): δ (ppm) 108.9, 110.1, 117.0, 117.4, 121.5, 121.9, 122.4, 124.9, 125.0, 128.2, 129.6, 130.4, 154.8, 155.4, 160.5

MS: *m/z* (%) 228 (M⁺, 33), 199 (9), 181 (15), 149 (17), 111 (22), 97 (20), 71 (41), 69 (100)

HRMS: *m/z* calculated for C₁₃H₉FN₂NaO [M + Na]⁺: 251.0597. Found: 251.0592.

3.4.2.3.4 1-(3-Chloro-1-phenylpropyl)-3-(2-fluorophenyl)-1,3-dihydro-2H-benzimidazol-2-one (123)

To a solution of 1-(2-fluorophenyl)-1,3-dihydro-2H-benzimidazol-2-one (1.00 g, 4.38 mmol) in DMF (5 ml) was added K_2CO_3 (1.21 g, 8.76 mmol). This mixture was stirred for 30 min at room temperature. Thereafter, a solution of (1-bromo-3-chloropropyl)benzene (1.53 g, 6.57 mmol) in DMF (0.5 ml) was slowly added and the resulting mixture was stirred overnight at room temperature. After completion of the reaction, H_2O (5 ml) was added and the aqueous layer was extracted with EtOAc three times. The combined organic layers were washed with a saturated NaCl solution, dried over $MgSO_4$, evaporated to dryness, and purified by column chromatography (silica gel 60, PE/EtOAc 9:1).

Yield: 0.82 g (55%), orange resin

Spectroscopic data:

¹H-NMR (400 MHz, CDCl₃): δ (ppm) 2.78-2.86 (m, 1H, 2'-CH₂), 3.23 (br s, 1H, 2'-CH₂), 3.64-3.68 (m, 2H, 3'-CH₂), 5.79 (br s, 1H, 1'-CH), 6.85-6.87 (m, 1H, benzim 4-CH) 7.05-7.06 (m, 3H, benzim 5-CH, benzim 6-CH, benzim 7-CH), 7.28-7.40 (m, 5H, f-phen 3-CH, f-phen 6-CH, phen 3-CH, phen 4-CH, phen 5-CH), 7.43-7.48 (m, 1H, f-phen 4-CH), 7.52-7.56 (m, 3H, f-phen 5-CH, phen 2-CH, phen 6-CH)

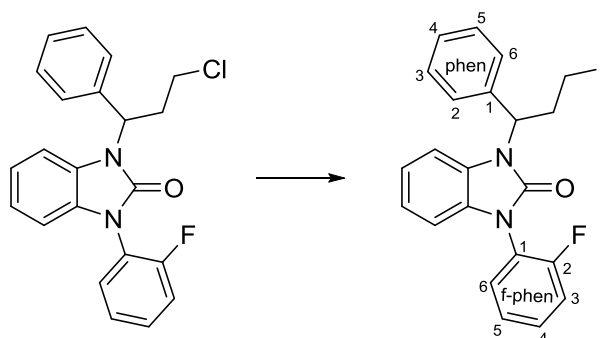
¹³C-NMR (100 MHz, CDCl₃): δ (ppm) 34.2 (2'-CH₂), 41.9 (3'-CH₂), 54.5 (1'-CH), 108.8 (d, *J* = 1.7 Hz, benzim 4-CH), 109.0 (benzim 7-CH), 117.1 (d, *J* = 19.5 Hz, f-phen 3-CH), 121.6 (benzim 5-CH), 121.9 (f-phen 1-C), 122.0 (benzim 6-CH), 124.8 (d, *J* = 3.9 Hz, f-phen 6-CH), 127.3 (phen 2-CH), 127.3 (phen 6-CH), 128.1 (phen 4-CH), 128.8 (phen 3-CH), 128.8 (phen 5-CH), 129.4 (benzim 3a-C), 129.5 (f-phen 5-CH), 130.2 (d, *J* = 7.8 Hz, f-phen 4-CH), 138.4 (phen 1-C), 153.0 (benzim 2-CO), 157.9 (d, *J* = 253.2 Hz, f-phen 2-CF)

Due to limited resolution of the measuring instrument, quaternary carbon benzim 7a-C could not be detected.

¹⁹F-NMR (471 MHz, CDCl₃): δ (ppm) -118.39 (m, f-phen 2-CF)

MS: *m/z* (%) 380 (M⁺, 12), 228 (100), 199 (5), 153 (3), 117 (7), 91 (49), 75 (5)

HRMS: *m/z* calculated for C₂₂H₁₉ClFN₂O [M + H]⁺: 381.1170. Found: 381.1164.

3.4.2.3.5 1-(2-Fluorophenyl)-3-(3-iodo-1-phenylpropyl)-1,3-dihydro-2H-benzimidazol-2-one (125)

NaI (0.66 g, 4.40 mmol) was added to a solution of 1-(3-chloro-1-phenylpropyl)-3-(2-fluorophenyl)-1,3-dihydro-2H-benzimidazol-2-one (0.84 g, 2.20 mmol) in acetone (15 ml) and the resulting mixture was refluxed for 24 h. Thereafter, the formed precipitate was filtered and the crude reaction product was evaporated *in vacuo* prior to chromatographic purification (silica gel 60, PE/EtOAc 9:1).

Yield: 0.55 g (53%), yellow crystals, mp. 38°C-39°C

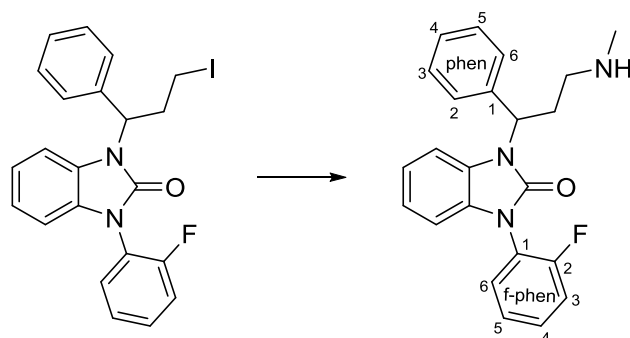
Spectroscopic data:

¹H-NMR (200 MHz, CDCl₃): δ (ppm) 2.80-2.98 (m, 1H, 2'-CH₂), 3.13-3.36 (m, 3H, 2'-CH₂, 3'-CH₂), 5.67-5.74 (m, 1H, 1'-CH), 6.85-6.88 (m, 1H, benzim 4-CH) 6.99-7.07 (m, 3H, benzim 5-CH, benzim 6-CH, benzim 7-CH), 7.26-7.45 (m, 5H, f-phen 3-CH, f-phen 6-CH, phen 3-CH, phen 4-CH, phen 5-CH), 7.47-7.58 (m, 4 H, f-phen 4-CH, f-phen 5-CH, phen 2-CH, phen 6-CH)

¹³C-NMR (50 MHz, CDCl₃): δ (ppm) 2.3 (2'-CH₂), 35.4 (3'-CH₂), 57.6 (1'-CH), 108.9 (d, J = 1.5 Hz, benzim 4-CH), 109.1 (benzim 7-CH), 117.1 (d, J = 19.0 Hz, f-phen 3-CH), 121.6 (benzim 5-CH), 121.9 (f-phen 1-C), 122.0 (benzim 6-CH), 124.8 (d, J = 3.5 Hz, f-phen 6-CH), 127.3 (phen 2-CH), 127.3 (phen 6-CH), 128.1 (phen 4-CH), 128.8 (phen 3-CH), 128.8 (phen 5-CH), 129.5 (f-phen 5-CH), 130.2 (d, J = 8.0 Hz, f-phen 4-CH), 138.2 (phen 1-C), 153.0 (benzim 2-CO), 157.8 (d, J = 251.5 Hz, f-phen 2-CF)

MS: m/z (%) 472 (M⁺, 9), 317 (5), 241 (4), 228 (100), 199 (5), 185 (10), 117 (37), 91 (29), 75 (7)

HRMS: m/z calculated for C₂₂H₁₉FIN₂O [M + H]⁺: 473.0526. Found: 473.0532.

3.4.2.3.6 1-(2-Fluorophenyl)-3-(3-(methylamino)-1-phenylpropyl)-1,3-dihydro-2H-benzimidazol-2-one (FAPPI:3) (17)

1-(2-Fluorophenyl)-3-(3-iodo-1-phenylpropyl)-1,3-dihydro-2H-benzimidazol-2-one (0.30 g, 0.64 mmol) was dissolved in a solution of methanamine in EtOH (8 M, 8.0 ml) and the resulting mixture was stirred in a sealed vessel for 3 h at 80°C. After completion of the reaction, the crude product was evaporated *in vacuo* and purified by column chromatography (silica gel 60, CH₂Cl₂/MeOH 9:1 and RP-18 silica gel MeOH/H₂O 9:1 and 7:3).

Yield: 73 mg (30%), yellow crystals, mp. 92°C-93°C

Spectroscopic data:

¹H-NMR (200 MHz, CDCl₃): δ (ppm) 2.57 (s, 3H, NHCH₃), 3.01-3.15 (m, 4H, 2'-CH₂, 3'-CH₂), 5.75-5.86 (m, 1H, 1'-CH), 6.83-6.87 (m, 1H, benzim 4-CH) 6.98-7.05 (m, 3H, benzim 5-CH, benzim 6-CH, benzim 7-CH), 7.25-7.42 (m, 5H, f-phen 3-CH, f-phen 6-CH, phen 3-CH, phen 4-CH, phen 5-CH), 7.48-7.61 (m, 4H, f-phen 4-CH, f-phen 5-CH, phen 2-CH, phen 6-CH)

Due to limited resolution of the measuring instrument, proton NHCH₃ could not be detected.

¹³C-NMR (50 MHz, CDCl₃): δ (ppm) 27.7 (2'-CH₂), 33.2 (NHCH₃), 46.9 (3'-CH₂), 53.5 (1'-CH), 109.0 (benzim 4-CH), 110.1 (benzim 7-CH), 117.1 (d, J = 19.5 Hz, f-phen 3-CH), 122.2 (benzim 5-CH), 122.7 (benzim 6-CH), 125.1 (d, J = 3.0 Hz, f-phen 6-CH), 127.3 (phen 2-CH), 127.1 (phen 6-CH), 128.3 (phen 4-CH), 128.9 (phen 3-CH), 128.9 (phen 5-CH), 129.5 (f-phen 5-CH), 130.7 (d, J = 4.5 Hz, f-phen 4-CH), 136.5 (phen 1-C), 153.6 (benzim 2-CO), 157.6 (d, J = 250.5 Hz, f-phen 2-CF)

Due to limited resolution of the measuring instrument, quaternary carbon f-phen 1-C could not be detected.

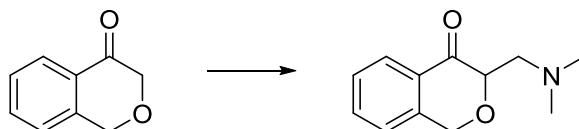
MS: m/z (%) 375 (M⁺, 17), 318 (10), 228 (82), 147 (16), 128 (35), 91 (20), 58 (43), 44 (100)

HRMS: m/z calculated for C₂₃H₂₃FN₃O [M + H]⁺: 376.1825. Found: 376.1822.

3.4.3 PHOXI derivatives

3.4.3.1 Preparation of the core structure

3.4.3.1.1 3-((Dimethylamino)methyl)-1*H*-isochromen-4(3*H*)-one (128)



To a solution of 1*H*-isochromen-4(3*H*)-one (5.00 g, 33.75 mmol) in EtOH (22 ml) were added paraformaldehyde (2.03 g, 67.50 mmol), dimethylamine hydrochloride (3.03 g, 37.13 mmol), and aqueous HCl (37%, 2.9 ml). The resulting mixture was refluxed for 6 h. The crystals formed were isolated by suction and the crude reaction product was recrystallized from isopropyl alcohol twice.

Yield: 2.58 g (32%), colorless crystals

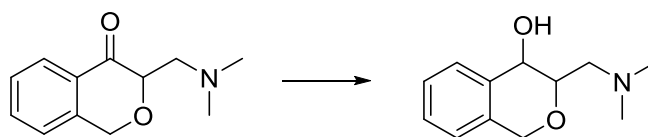
¹H-NMR data are in complete accordance with literature values.³⁵³

Spectroscopic data:

¹H-NMR (200 MHz, CDCl₃): δ (ppm) 2.85 (s, 6H), 3.38-3.50 (m, 1H), 3.76 (dd, *J* = 2.0 Hz, and 2.0 Hz, 1H), 4.97-5.17 (m, 3H), 7.40-7.52 (m, 2H), 7.66-7.74 (m, 1H), 7.90 (d, *J* = 8.0 Hz, 1H), 10.97 (br s, 1H)

¹³C-NMR (50 MHz, CDCl₃): δ (ppm) 43.0, 55.4, 66.2, 76.3, 125.1, 126.0, 127.9, 128.2, 134.8, 142.0, 192.0

3.4.3.1.2 3-((Dimethylamino)methyl)-3,4-dihydro-1H-isochromen-4-ol (129)



To a solution of 3-((dimethylamino)methyl)-1H-isochromen-4(3H)-one (2.58 g, 10.67 mmol) in THF (57 ml), L-Selectride (1.0 M in THF, 21.3 ml, 21.34 mmol) was added dropwise over an hour at -30°C . Thereafter, the solution was allowed to warm to 0°C and was diluted with EtOAc (48 ml). The organic layer was washed with a 10% NaOH solution (48 ml), H_2O (48 ml) and brine (48 ml), followed by extraction with 1N HCl (2 x 48 ml). The combined HCl extracts were taken to pH 9 with an aqueous NaOH solution (50% in H_2O) and were washed with EtOAc (4 x 24 ml). The combined organic layers were dried over Na_2SO_4 , filtered, and concentrated *in vacuo*. The resulting product was obtained in sufficient purity and did not require further purification.

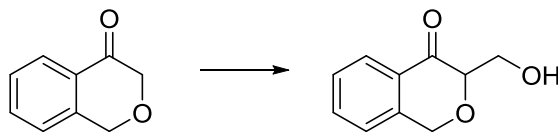
Yield: 1.23 g (58%), colorless crystals

$^1\text{H-NMR}$ data are in complete accordance with literature values.³⁵³

Spectroscopic data:

$^1\text{H-NMR}$ (200 MHz, CDCl_3): δ (ppm) 2.39 (s, 6H), 2.72-2.86 (m, 2H), 3.74-3.80 (m, 1H), 4.57-4.86 (m, 3H), 6.97-7.06 (m, 1H), 7.19-7.34 (m, 2H), 7.59-7 (m, 1H)

MS: m/z (%) 207 (M^+ , 1), 179 (1), 145 (1), 132 (2), 119 (2), 104 (1), 91 (4), 77 (2), 58 (100)

3.4.3.1.3 3-(Hydroxymethyl)-1H-isochromen-4(3H)-one (134)

To a solution of 1H-isochromen-4(3H)-one (0.50 g, 3.37 mmol) in MeOH (10 ml) were added H₂O (2 ml), an aqueous formaldehyde solution (35%, 0.32 ml, 4.05 mmol), and K₂CO₃ (0.05 g, 0.34 mmol) to stir the resulting mixture for 2.5 h at 40°C. H₂O (30 ml) was added to complete the reaction and the product was extracted three times with EtOAc (50 ml). The combined organic layers were dried over Na₂SO₄ and evaporated to dryness prior to purification by column chromatography (silica gel 60, PE/EtOAc 7:3).

Yield: 82 mg (14 %), light yellow oil

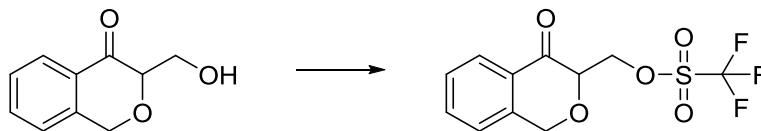
Spectroscopic data:

¹H-NMR (200 MHz, CDCl₃): δ (ppm) 2.90 (br s, 1H), 4.08-4.15 (m, 2H), 4.25-4.30 (m, 1H), 4.99 (s, 1H), 7.18-7.30 (m, 1H), 7.38-7.46 (m, 1H), 7.55-7.63 (m, 1H), 8.04 (d, *J* = 8.0 Hz, 1H)

¹³C-NMR (50 MHz, CDCl₃): δ (ppm) 61.9, 67.0, 81.8, 124.4, 126.5, 127.8, 129.4, 134.2, 141.7

MS: *m/z* (%) 178 (M⁺, 1), 160 (27), 148 (80), 118 (65), 90 (100), 77 (12)

3.4.3.1.4 (4-Oxo-3,4-dihydro-1*H*-isochromen-3-yl)methyl trifluoromethanesulfonate (135)



To a solution of 3-(hydroxymethyl)-1*H*-isochromen-4(3*H*)-one (0.07 g, 0.40 mmol) in CH_2Cl_2 (4 ml), trifluoromethanesulfonic anhydride (0.16 ml, 0.96 mmol) was added dropwise at 0°C under argon atmosphere. The resulting reaction mixture was stirred for 50 min at 0°C . Thereafter, the reaction was completed by the addition of saturated Na_2CO_3 solution (5 ml). The product was extracted three times with CH_2Cl_2 , the organic layers were dried over Na_2SO_4 and evaporated to dryness prior to purification by column chromatography (silica gel 60, PE/EtOAc 1:1).

Yield: 72 mg (58%), brown oil

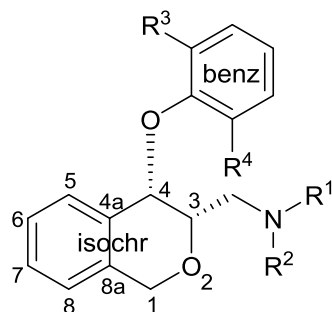
Spectroscopic data:

$^1\text{H-NMR}$ (200 MHz, CDCl_3): δ (ppm) 4.52-4.56 (m, 1H), 4.91-4.94 (m, 1H), 4.97-5.11 (m, 3H), 7.25-7.29 (m, 1H), 7.43-7.50 (m, 1H), 7.60-7.68 (m, 1H), 8.06 (d, $J = 8.0$ Hz, 1H)

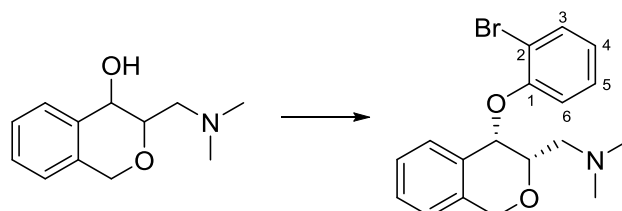
$^{13}\text{C-NMR}$ (50 MHz, CDCl_3): δ (ppm) 67.2, 74.3, 79.1, 121.7, 124.6, 126.9, 128.1, 128.7, 134.9, 141.4, 190.6

3.4.3.2 Preparation of PHOXI:1 derivatives

The compound numbering depicted below was used for the signal assignment of ^1H - and ^{13}C -NMR data of compounds **18-23**, and **30** in the next chapters:



3.4.3.2.1 1-(3*S*,4*S*)-4-(2-Bromophenoxy)-3,4-dihydro-1*H*-isochromen-3-yl)-*N,N*-dimethylmethanamine (**130**)



To a solution of NaH (0.17 g, 7.23 mmol) in dry DMSO (16 ml) was added (3*S*,4*S*)-3-((dimethylamino)methyl)-3,4-dihydro-1*H*-isochromen-4-ol (1.00 g, 4.82 mmol) to stir the solution at room temperature for 15 min. Thereafter, potassium benzoate (0.77 g, 4.82 mmol) was added and the mixture was stirred for additional 15 min. 1-Bromo-2-fluorobenzene (1.69 g, 1.10 ml, 9.64 mmol) was added after 15 min and the resulting mixture was stirred at 65°C overnight. The mixture was diluted with EtOAc (66 ml) and washed with a saturated NaHCO₃ solution (39 ml) and brine (39 ml). The combined organic layers were dried over Na₂SO₄, filtered, and evaporated to dryness prior to purification by column chromatography (silica gel 60, 3% MeOH in CH₂Cl₂).

Yield: 0.85 g (49%), yellow oil

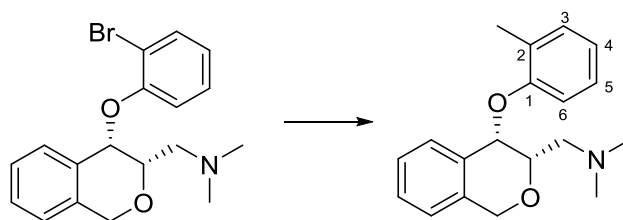
$^1\text{H-NMR}$ data are in complete accordance with literature values.³⁵³

Spectroscopic data:

$^1\text{H-NMR}$ (400 MHz, CDCl_3): δ (ppm) 2.25 (s, 6H, $\text{CH}_2\text{NC}_2\text{H}_6$), 2.77-2.79 (m, 2H, $\text{CH}_2\text{NC}_2\text{H}_6$), 3.94-3.97 (m, 1H, isochr 3- CH), 4.78 (d, $J = 15.4$ Hz, AB-system, 1H, isochr 1- CH_2), 4.96 (d, $J = 15.4$ Hz, AB-system, 1H, isochr 1- CH_2), 5.14 (d, $J = 2.0$ Hz, 1H, isochr 4- CH), 6.76-6.82 (m, 2H, benz 4- CH , isochr 5- CH), 6.96-6.99 (m, 3H, isochr 6- CH , benz 6- CH , isochr 8- CH), 7.09-7.14 (m, 1H, benz 5- CH), 7.15-7.19 (m, 1H, isochr 7- CH), 7.38-7.40 (m, 1H, benz 3- CH)

$^{13}\text{C-NMR}$ (100 MHz, CDCl_3): δ (ppm) 45.8 ($\text{CH}_2\text{NC}_2\text{H}_6$), 59.5 ($\text{CH}_2\text{NC}_2\text{H}_6$), 67.4 (isochr 1- CH_2), 74.5 (isochr 4- CH), 74.7 (isochr 3- CH), 115.0 (benz 2- CBr), 119.6 (benz 6- CH), 123.3 (benz 4- CH), 124.0 (isochr 8- CH), 126.1 (isochr 6- CH), 128.0 (benz 5- CH), 128.5 (isochr 7- CH), 129.2 (isochr 5- CH), 131.0 (isochr 4a-C), 133.1 (benz 3- CH), 134.9 (isochr 8a-C), 154.2 (benz 1-C)

3.4.3.2.2 *N,N*-Dimethyl-1-((3*S*,4*S*)-4-(2-methylphenoxy)-3,4-dihydro-1*H*-isochromen-3-yl)methanamine (Me@PHOXI1) (18)



To a solution of 1-((3*S*,4*S*)-4-(2-bromophenoxy)-3,4-dihydro-1*H*-isochromen-3-yl)-*N,N*-dimethylmethanamine (0.50 g, 1.38 mmol) in dioxane (4 ml) were added trimethylboroxine (50% in THF, 0.38 ml, 1.52 mmol) and K_2CO_3 (0.52 g, 3.75 mmol). The mixture was degassed with argon for 15 min. Thereafter, $(PPh_3)_4Pd$ (0.12 g, 0.10 mmol) was added and the mixture was degassed with argon for another 15 min. Then, the reaction mixture was heated in a sealed vessel at 110°C for 2 h. After cooling, the crude reaction product was filtered through a plug of celite and washed with EtOH (3 x 9 ml). The filtrate was concentrated *in vacuo* and dissolved in a mixture of 20% EtOAc in hexane. The resulting precipitate was removed by filtration and the filtrate was evaporated to dryness prior to purification by column chromatography (silica gel 60, 30% THF in PE containing 2% triethylamine).

Yield: 0.21 g (52%), yellow oil

¹H-NMR data are in complete accordance with literature values.³⁵³

Spectroscopic data:

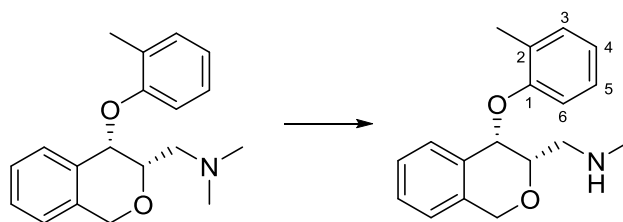
¹H-NMR (200 MHz, CDCl₃): δ (ppm) 1.93 (s, 3H, benz CH₃), 2.31 (s, 6H, CH₂NC₂H₆), 2.74-2.79 (m, 2H, CH₂NC₂H₆), 3.96-4.03 (m, 1H, isochr 3-CH), 4.86 (d, J = 14.0 Hz, AB-system, 1H, isochr 1-CH₂), 5.05 (d, J = 16.0 Hz, AB-system, 1H, isochr 1-CH₂), 5.15 (s, 1H, isochr 4-CH), 6.85-6.96 (m, 2H, isochr 5-CH, benz 4-CH), 7.03-7.09 (m, 3H, isochr 8-CH, isochr 6-CH, benz 6-CH), 7.16-7.28 (m, 3H, isochr 7-CH, benz 5-CH, benz 3-CH)

¹³C-NMR (50 MHz, CDCl₃): δ (ppm) 16.1 (benz CH₃), 46.1 (CH₂NC₂H₆), 59.8 (CH₂NC₂H₆), 67.6 (isochr 1-CH₂), 73.9 (isochr 4-CH), 75.1 (isochr 3-CH), 116.4 (benz 6-CH), 121.6 (benz 4-CH), 124.0 (isochr 8-CH), 126.2 (isochr 6-CH), 126.6 (benz 5-CH), 128.2 (isochr 7-CH), 128.7 (isochr 5-CH), 129.4 (benz 2-C), 130.7 (benz 3-CH), 132.4 (isochr 4a-C), 134.8 (isochr 8a-C), 156.4 (benz 1-C)

MS: m/z (%) 297 (M⁺, 1), 205 (2), 190 (1), 132 (3), 115 (2), 104 (4), 91 (3), 77 (3), 58 (100)

HRMS: m/z calculated for C₁₉H₂₄NO₂ [M + H]⁺: 298.1802. Found: 298.1754.

3.4.3.2.3 *N*-Methyl-1-((3*S*,4*S*)-4-(2-methylphenoxy)-3,4-dihydro-1*H*-isochromen-3-yl)methanamine (PHOXI:1) (19)



N,N-Diisopropyl ethylamine (0.31 g, 0.2 ml, 2.36 mmol), proton sponge (catalytic amount), and 1-chloroethylchloroformate (0.34 g, 0.2 ml, 2.36 mmol) were added to a solution of *N,N*-dimethyl-1-((3*S*,4*S*)-4-(2-methylphenoxy)-3,4-dihydro-1*H*-isochromen-3-yl)methanamine (0.35 g, 1.18 mmol) in 1,2-dichloroethane (5 ml). The mixture was heated for 1 h at 40°C and after cooling to room temperature, the mixture was evaporated to dryness. The residue was redissolved in MeOH (5 ml) and stirred for 2 h at room temperature. The reaction mixture was concentrated *in vacuo* again and the residue dissolved in CH₂Cl₂ (25 ml). This solution was washed with a saturated NaHCO₃ solution (6 ml) and brine (6 ml). The organic layer was dried over Na₂SO₄, filtered, and evaporated to dryness. The crude reaction product was purified by column chromatography (silica gel 60, 7% MeOH in CH₂Cl₂ and RP-18 silica gel, MeOH/H₂O 7:3).

Yield: 80 mg (24%), yellow oil

¹H-NMR data are in complete accordance with literature values.³⁵³

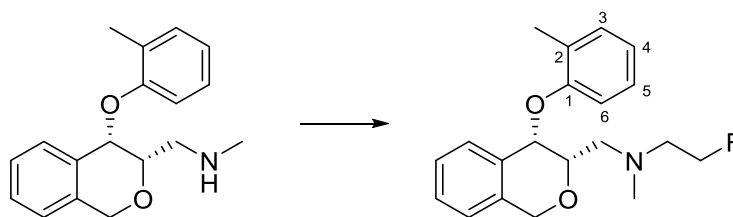
Spectroscopic data:

¹H-NMR (400 MHz, CDCl₃): δ (ppm) 1.97 (s, 3H, benz CH₃), 2.52 (s, 3H, CH₂NHCH₃), 2.85 (br s, 1H, CH₂NHCH₃), 2.98 (dd, *J* = 12.5 Hz and 8.8 Hz, 1H, CH₂NHCH₃), 3.17 (dd, *J* = 12.5 Hz and 8.8 Hz, 1H, CH₂NHCH₃), 4.09 (ddd, *J* = 8.8 Hz, 3.8 Hz, and 2.3 Hz, 1H, isochr 3-CH), 4.86 (d, *J* = 15.2 Hz, AB-system, 1H, isochr 1-CH₂), 5.03 (d, *J* = 15.2 Hz, AB-system, 1H, isochr 1-CH₂), 5.17 (d, *J* = 2.2 Hz, 1H, isochr 4-CH), 6.90-6.98 (m, 2H, isochr 5-CH, benz 4-CH), 7.06-7.11 (m, 4H, isochr 8-CH, isochr 6-CH, benz 6-CH, benz 3-CH), 7.16-7.20 (m, 1H, benz 5-CH), 7.25-7.29 (m, 1H, isochr 7-CH)

¹³C-NMR (100 MHz, CDCl₃): δ (ppm) 16.2 (benz CH₃), 36.4 (CH₂NHCH₃), 52.1 (CH₂NHCH₃), 67.7 (isochr 1-CH₂), 73.6 (isochr 4-CH), 76.4 (isochr 3-CH), 116.0 (benz 6-CH), 121.8 (benz 4-CH), 124.1 (isochr 8-CH), 126.4 (isochr 6-CH), 126.7 (benz 5-CH), 128.4 (isochr 7-CH), 129.0 (isochr 5-CH), 129.5 (benz 2-C), 131.0 (benz 3-CH), 132.3 (isochr 4a-C), 134.8 (isochr 8a-C), 156.3 (benz 1-C)

MS: *m/z* (%) 283 (M⁺, 1), 177 (2), 151 (5), 132 (16), 104 (4), 77 (5), 65 (2), 44 (100)

HRMS: *m/z* calculated for C₁₈H₂₂NO₂ [M + H]⁺: 284.1645. Found: 284.1621.

3.4.3.2.4 2-Fluoro-N-methyl-N-(((3S,4S)-4-(2-methylphenoxy)-3,4-dihydro-1H-isochromen-3-yl)methyl)ethanamine (FE@PHOXI1) (20)

To a suspension of N-methyl-1-(((3S,4S)-4-(2-methylphenoxy)-3,4-dihydro-1H-isochromen-3-yl)methanamine (0.07 g, 0.26 mmol) in dry ACN (10 ml) was added triethylamine (0.05 ml, 0.33 mmol) under argon atmosphere. The reaction mixture was cooled to 0°C and 2-fluoroethyl trifluoromethanesulfonate (0.04 ml, 0.31 mmol) was slowly added to the mixture. Thereafter, the solution was stirred for 10 min, during which the mixture was allowed to warm to room temperature. The crude reaction product was evaporated *in vacuo* and purified by column chromatography (silica gel 60, 7% MeOH in CH₂Cl₂).

Yield: 15 mg (17%), yellow oil

Spectroscopic data:

¹H-NMR (400 MHz, CDCl₃): δ (ppm) 1.91 (s, 3H, benz CH₃), 2.56 (s, 3H, CH₂NCH₃CH₂CH₂F), 2.84-3.07 (m, 2H, CH₂NCH₃CH₂CH₂F), 3.04-3.13 (m, 2H, CH₂NCH₃CH₂CH₂F), 4.22 (m, 1H, isochr 3-CH), 4.60 (t, *J* = 4.8 Hz, 1H, CH₂NCH₃CH₂CH₂F), 4.71 (t, *J* = 4.8 Hz, 1H, CH₂NCH₃CH₂CH₂F), 4.90 (d, *J* = 15.2 Hz, AB-system, 1H, isochr 1-CH₂), 5.04 (d, *J* = 15.2 Hz, AB-system, 1H, isochr 1-CH₂), 5.19 (d, *J* = 2.1 Hz, 1H, isochr 4-CH), 6.90-6.91 (m, 1H, isochr 5-CH), 6.92-6.94 (m, 1H, benz 4-CH), 7.04-7.06 (m, 1H, isochr 6-CH), 7.07 (m, 1H, isochr 8-CH), 7.08-7.09 (m, 1H, benz 3-CH), 7.15-7.19 (m, 2H, benz 5-CH, benz 6-CH), 7.25-7.29 (m, 1H, isochr 7-CH)

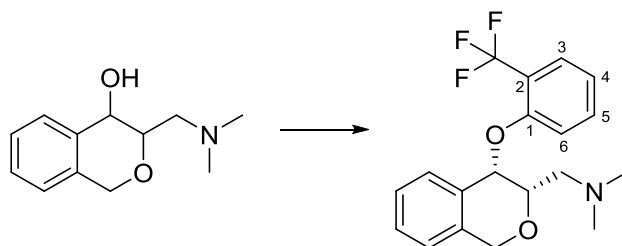
¹³C-NMR (100 MHz, CDCl₃): δ (ppm) 16.2 (benz CH₃), 43.1 (CH₂NCH₃CH₂CH₂F), 57.7 (d, *J* = 19.8 Hz, CH₂NCH₃CH₂CH₂F), 58.3 (CH₂NCH₃CH₂CH₂F), 67.7 (isochr 1-CH₂), 73.6 (isochr 4-CH), 74.9 (isochr 3-CH), 81.4 (d, *J* = 168.0 Hz, CH₂NCH₃CH₂CH₂F), 116.0 (benz 6-CH), 122.0 (benz 4-CH), 124.2 (isochr 8-CH), 126.4 (isochr 6-CH), 126.8 (benz 5-CH), 128.6 (isochr 7-CH), 129.1 (isochr 5-CH), 129.8 (benz 2-C), 130.9 (benz 3-CH), 132.0 (isochr 4a-C), 134.6 (isochr 8a-C), 156.2 (benz 1-C)

MS: *m/z* (%) 329 (M⁺, 1), 222 (1), 188 (1), 132 (2), 115 (2), 104 (3), 90 (100), 77 (2), 44 (4)

HRMS: *m/z* calculated for C₂₀H₂₅FNO₂ [M + H]⁺: 330.1864. Found: 330.1831.

3.4.3.3 Preparation of PHOXI:2 derivatives

3.4.3.3.1 *N,N*-Dimethyl-1-((3*S*,4*S*)-4-(2-(trifluoromethyl)phenoxy)-3,4-dihydro-1*H*-isochromen-3-yl)methanamine (Me@PHOXI2) (21)



To a suspension of NaH (0.09 g, 3.62 mmol) in dry DMSO (8 ml) was added 3-((dimethylamino)methyl)-3,4-dihydro-1*H*-isochromen-4-ol (0.50 g, 2.41 mmol) and the mixture was stirred for 15 min. Potassium benzoate (0.39 g, 2.41 mmol) was added in portions and the resulting slurry was stirred for another 15 min. Then, 2-fluorobenzotrifluoride (0.79 g, 0.6 ml, 4.82 mmol) was added and the mixture was heated at 65°C overnight. After completion of the reaction, the solution was diluted with EtOAc (33 ml) and washed with a saturated NaHCO₃ solution (20 ml) and brine (20 ml). The organic layer was dried over Na₂SO₄, filtered, and evaporated to dryness prior to purification by column chromatography (silica gel 60, 3% MeOH in CH₂Cl₂).

Yield: 0.37 g (44%), colorless crystals, mp. 85°C-87°C

Spectroscopic data:

¹H-NMR (200 MHz, CDCl₃): δ (ppm) 2.34 (s, 6H, CH₂NC₂H₆), 2.74-2.77 (m, 2H, CH₂NC₂H₆), 4.09-4.16 (m, 1H, benz 3-CH), 4.88 (d, J = 16.0 Hz, AB-system, 1H, isochr 1-CH₂), 5.08 (d, J = 16.0 Hz, AB-system, 1H, isochr 1-CH₂), 5.47 (d, J = 2.0 Hz, 1H, isochr 4-CH), 7.00-7.14 (m, 4H, benz 4-CH, isochr 8-CH, isochr 6-CH, isochr 5-CH), 7.24-7.37 (m, 2H, benz 6-CH, isochr 7-CH), 7.46-7.58 (m, 2H, benz 5-CH, benz 3-CH)

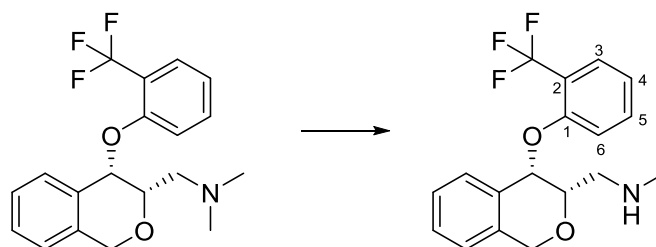
¹³C-NMR (50 MHz, CDCl₃): δ (ppm) 46.1 (CH₂NC₂H₆), 59.0 (CH₂NC₂H₆), 67.1 (isochr 1-CH₂), 73.3 (isochr 4-CH), 74.4 (isochr 3-CH), 116.5 (benz 6-CH), 120.8 (benz 2-C), 121.3 (benz 4-CH), 124.2 (isochr 8-CH), 126.5 (isochr 6-CH), 127.1 (q, J = 5 Hz, benz 3-CH), 128.6 (isochr 7-CH), 128.8 (isochr 5-CH), 131.3 (isochr 4a-C), 132.9 (benz 5-CH), 135.3 (isochr 8a-C)

Due to limited resolution of the measuring instrument, quaternary carbon benz 1-C and benz CF₃ could not be detected.

MS: m/z (%) 351 (M⁺, 1), 219 (1), 132 (3), 115 (2), 104 (4), 91 (2), 77 (3), 58 (100), 42 (3)

HRMS: m/z calculated for C₁₉H₂₁F₃NO₂ [M + H]⁺: 352.1519. Found: 352.1480.

3.4.3.3.2 N-Methyl-1-((3*S*,4*S*)-4-(2-(trifluoromethyl)phenoxy)-3,4-dihydro-1*H*-isochromen-3-yl)methanamine (PHOXI:2) (22)



To a solution of *N,N*-dimethyl-1-((3*S*,4*S*)-4-(2-(trifluoromethyl)phenoxy)-3,4-dihydro-1*H*-isochromen-3-yl)methanamine (0.19 g, 0.54 mmol) in 1,2-dichloroethane (3 ml), *N,N*-diisopropylethylamine (0.14 g, 0.1 ml, 1.08 mmol), proton sponge (catalytic amount), and 1-chloroethylchloroformate (0.15 g, 0.1 ml, 1.08 mmol) were added. The mixture was heated for 1 h at 40°C. After cooling to room temperature, the solution was concentrated *in vacuo* and the residue was redissolved in MeOH (3 ml). The mixture was stirred for 2 h at room temperature and thereafter, evaporated to dryness. The resulting residue was dissolved in CH₂Cl₂ (13 ml) and washed with a NaHCO₃ solution (3 ml) and brine (3 ml). The organic layer was dried over Na₂SO₄, filtered, and evaporated to dryness. Then, the crude reaction product was repeatedly purified by column chromatography (silica gel 60, 7% MeOH in CH₂Cl₂, and 2% MeOH in CH₂Cl₂ and RP-18 silica gel, MeOH/H₂O 8:2).

Yield: 22 mg (12%), yellow oil

Spectroscopic data:

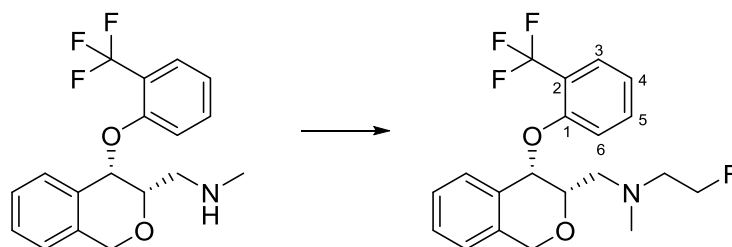
¹H-NMR (400 MHz, CDCl₃): δ (ppm) 2.51 (s, 3H, CH₂NHCH₃), 2.60 (br s, 1H, CH₂NHCH₃), 2.93-2.97 (m, 1H, CH₂NHCH₃), 3.07-3.12 (m, 1H, CH₂NHCH₃), 4.15-4.18 (m, 1H, isochr 3-CH), 4.85 (d, *J* = 15.3 Hz, AB-system, 1H, isochr 1-CH₂), 5.03 (d, *J* = 15.3 Hz, AB-system, 1H, isochr 1-CH₂), 5.43 (d, *J* = 2.2 Hz, 1H, isochr 4-CH), 7.01-7.12 (m, 4H, benz 4-CH, isochr 8-CH, isochr 6-CH, isochr 5-CH), 7.21-7.30 (m, 2H, benz 6-CH, isochr 7-CH), 7.44-7.48 (m, 1H, benz 5-CH), 7.53-7.56 (m, 1H, benz 3-CH)

¹³C-NMR (100 MHz, CDCl₃): δ (ppm) 36.3 (CH₂NHCH₃), 51.3 (CH₂NHCH₃), 67.0 (isochr 1-CH₂), 73.1 (isochr 4-CH), 75.6 (isochr 3-CH), 116.5 (benz 6-CH), 120.8 (q, *J* = 30.6 Hz, benz 2-C), 121.0 (benz 4-CH), 123.5 (q, *J* = 272.6 Hz, benz CF₃), 124.2 (isochr 8-CH), 126.6 (isochr 6-CH), 127.3 (q, *J* = 5.1 Hz, benz 3-CH), 128.7 (isochr 7-CH), 128.9 (isochr 5-CH), 131.0 (isochr 4a-C), 132.9 (benz 5-CH), 135.2 (isochr 8a-C), 155.6 (q, *J* = 1.3 Hz, benz 1-C)

¹⁹F-NMR (471 MHz, CDCl₃): δ (ppm) -61.8 (m, benz CF)

MS: *m/z* (%) 338 (M⁺, 1), 205 (3), 145 (2), 132 (34), 115 (2), 104 (7), 91 (2), 77 (4), 44 (100)

HRMS: *m/z* calculated for C₁₈H₁₉F₃NO₂ [M + H]⁺: 338.1362. Found: 338.1344.

3.4.3.3.3 2-Fluoro-N-methyl-N-(((3S,4S)-4-(2-(trifluoromethyl)phenoxy)-3,4-dihydro-1H-isochromen-3-yl)methyl)ethanamine (FE@PHOXI2) (23)

To a suspension of *N*-methyl-1-((3*S*,4*S*)-4-(2-(trifluoromethyl)phenoxy)-3,4-dihydro-1*H*-isochromen-3-yl)methanamine (0.07 g, 0.22 mmol) in dry ACN (5 ml) was added triethylamine (0.05 ml, 0.33 mmol) under argon atmosphere. After cooling the mixture to 0°C, 2-fluoroethyl trifluoromethanesulfonate (0.03 ml, 0.26 mmol) was slowly added. The solution was stirred for 10 min during which the temperature was allowed to warm to 20°C. After evaporation of the solvent, the crude reaction product was purified by column chromatography (silica gel 60, 7% MeOH in CH₂Cl₂).

Yield: 55 mg (65%), light yellow oil

Spectroscopic data:

¹H-NMR (400 MHz, CDCl₃): δ (ppm) 2.42 (s, 3H, CH₂NCH₃CH₂CH₂F), 2.73-2.75 (m, 1H, CH₂NCH₃CH₂CH₂F), 2.85 (dd, *J* = 13.3 Hz and 6.6 Hz, 1H, CH₂NCH₃CH₂CH₂F), 2.88-2.91 (m, 1H, CH₂NCH₃CH₂CH₂F) 2.98 (dd, *J* = 13.3 Hz and 6.4 Hz, 1H, CH₂NCH₃CH₂CH₂F), 4.12 (dt, *J* = 2.3 Hz and 6.5 Hz, 1H, isochr 3-CH), 4.46 (t, *J* = 4.9 Hz, 1H, CH₂NCH₃CH₂CH₂F), 4.58 (t, *J* = 4.9 Hz, 1H, CH₂NCH₃CH₂CH₂F), 4.87 (d, *J* = 15.3 Hz, AB-system, 1H, isochr 1-CH₂), 5.05 (d, *J* = 15.3 Hz, AB-system, 1H, isochr 1-CH₂), 5.50 (d, *J* = 2.3 Hz, 1H, isochr 4-CH), 7.00-7.04 (m, 1H, benz 4-CH), 7.07-7.12 (m, 3H, isochr 8-CH, isochr 5-CH, isochr 6-CH), 7.26-7.30 (m, 1H, isochr 7-CH), 7.35-7.37 (m, 1H, isochr-6-CH), 7.46-7.51 (m, 1H, benz 5-CH), 7.52-7.54 (m, 1H, benz 3-CH)

¹³C-NMR (100 MHz, CDCl₃): δ (ppm) 43.4 (CH₂NCH₃CH₂CH₂F), 57.4 (CH₂NCH₃CH₂CH₂F), 57.9 (d, *J* = 19.8 Hz, CH₂NCH₃CH₂CH₂F), 67.3 (isochr 1-CH₂), 72.7 (isochr 4-CH), 74.6 (isochr 3-CH), 81.8 (d, *J* = 167.8 Hz, CH₂NCH₃CH₂CH₂F), 116.4 (benz 6-CH), 120.6 (q, *J* = 30.5 Hz, benz 2-C), 120.8 (benz 4-CH), 123.5 (q, *J* = 272.6 Hz, benz CF₃), 124.3 (isochr 8-CH), 126.5 (isochr 6-CH), 127.2 (q, *J* = 5.3 Hz, benz 3-CH), 128.7 (isochr 7-CH), 128.9 (isochr 5-CH), 131.2 (isochr 4a-C), 132.9 (benz 5-CH), 135.3 (isochr 8a-C), 155.9 (q, *J* = 1.7 Hz, benz 1-C)

¹⁹F-NMR (471 MHz, CDCl₃): δ (ppm) -61.8 (s, benz CF), -219.3 (m, CH₂NCH₃CH₂CH₂F)

MS: *m/z* (%) 383 (M⁺, 1), 350 (1), 322 (1), 218 (1), 175 (1), 132 (4), 115 (3), 104 (4), 90 (100)

HRMS: *m/z* calculated for C₂₀H₂₂F₄NO₂ [M + H]⁺: 384.1581. Found: 384.1532.

3.5 Preclinical Evaluation

3.5.1 LogP analysis

In order to determine the lipophilicity of the test compounds, a standardized HPLC method according to Donovan and Prescatore³⁴⁴ was applied. Briefly, two internal standards (toluene and triphenylene) with known logP values were mixed with the analytes and 3 μ l were injected onto a short polymeric octadecyl-polyvinyl alcohol column (Shodex[®], Showa Denko Europe GmbH, Munich, Germany). A linear gradient from 10% methanol and 90% 25 mM phosphate buffer to 100% methanol was used as the eluent in 9.4 min, at a constant flow of 1.5 ml/min. Detection was performed at 260 nm and 285 nm. Equilibration time between the runs was 4 min. From the retention times of the known standard compounds and the target molecules, respectively, the so-called $_{\text{HPLC}}\log\text{P}$ was determined. The measurements were performed in triplicates from at least 2 different mixtures. For calculating the experimental logP values, the literature logP value, the logP* value from the Pomona College Database,³⁸¹⁻³⁸⁴ and the $_{\text{HPLC}}\log\text{P}$ value were averaged.

3.5.2 IAM chromatography

IAM chromatography was performed varying a protocol according to Taillardat-Bertschinger *et al.*,³⁴⁷ thereby using a RegisTech IAM.PC.DD2 (Regis Technologies Inc., Morton Grove, USA) column (15 cm x 4.6 mm). For compound analysis, 0.01 M phosphate buffer and acetonitrile (in ratios of 35:65, 40:60, 45:55, and 50:50) were used as mobile phase at a flow rate of 1ml/min. The pH adjustment to pH 7 of the mobile phase was carried out after mixing of acetonitrile and phosphate buffer, to mimic nearly physiological conditions. References as well as precursors were injected onto the IAM column. Thereby the duration of the runs was variable (3-30 min) and adjusted to the

compound and solvent ratios, respectively. By implying a correction factor, K_m values (membrane partition coefficient) were determined (V_s and V_m), which served for the calculation of the P_m values (permeability). Obtained P_m values were compared with known BBB penetrating compounds,³⁴⁸ as external standards.

4 REFERENCES

- 1) Chimenti, F.; Maccioni, E.; Secci, D.; Bolasco, A.; Chimenti, P.; Granese, A.; Befani, O.; Turini, P.; Alcaro, S.; Ortuso, F.; Cardia, M. C.; Distinto, S. *J. Med. Chem.*, **2007**, 50, 707
- 2) Chimenti, F.; Fioravanti, R.; Bolasco, A.; Manna, F.; Chimenti, P.; Secci, D.; Rossi, F.; Turini, P.; Ortuso, F.; Alcaro, S.; Cardia M. C. *Eur. J. Med. Chem.*, **2008**, 43, 2262
- 3) Shih, J. C.; Chen, K.; Ridd, M. J. *Annu. Rev. Neurosci.*, **1999**, 22, 197
- 4) Bortolato, M.; Chen, K.; Shih, J. C. *Adv. Drug Deliv. Rev.*, **2008**, 60, 1527
- 5) Chimenti, F.; Secci, D.; Bolasco, A.; Chimenti, P.; Granese, A.; Carradori, S.; Yanez, M.; Orallo, F.; Sanna, M. L.; Gallinella, B.; Cirilli, R. *J. Med. Chem.*, **2010**, 53, 6516
- 6) Binda, C.; Li, M.; Hubálek, F.; Restelli, N.; Edmondson, D. E.; Mattevi, A. *PNAS*, **2003**, 100, 9750
- 7) Cesura, A. M.; Pletscher, A. *Prog. Drug Res.*, **1992**, 38, 171
- 8) Binda, C.; Mattevi, A.; Edmondson, D. E. *J. Biol. Chem.*, **2002**, 277, 23973
- 9) Edmondson, D.E.; Mattevi, A.; Binda, C.; Li, M.; Hubálek, F. *Curr. Med. Chem.*, **2004**, 11, 1983
- 10) Matos, M. J.; Vina, D.; Janeiro, P.; Borges, F.; Santana, L.; Uriarte, E. *Bioorg. Med. Chem. Lett.*, **2010**, 20, 5157
- 11) Brookmeyer, R.; Johnson, E.; Ziegler-Graham, K.; Arrighi, H. M. *Alzheimers Dement.*, **2007**, 3, 186
- 12) Lendon, C. L.; Ashall, F.; Goate, A. M. *JAMA*, **1997**, 277, 825
- 13) Gökhan-Kelekc, N.; Yabanoglu, S.; Küpeli, E.; Salgin, U.; Özgen, Ö.; Ucar, G.; Yesilada, E.; Kendi, E.; Yesilada, A.; Bilgin, A. A. *Bioorg. Med. Chem.*, **2007**, 15, 5775
- 14) Gulyás, B.; Pavlova, E.; Kása, P.; Gulya, K.; Bakota, L.; Várszegi, S.; Keller, É.; Horváth, M. C.; Nag, S.; Hermeicz, I.; Magyar, K.; Halldin, C. *Neurochem. Int.*, **2011**, 58, 60

- 15) Pugliese, M.; Rodriguez, M. J.; Gimeno-Bayon, J.; Pujadas, L.; Billett, E. E.; Wells, C.; Mahy, N. *J. Neurosci. Res.*, **2010**, 88, 2588
- 16) Kennedy, B. P.; Ziegler, M. G.; Alford, M.; Hansen, L. A.; Thal, L. J.; Masliah, E. *J. Neural Transm.*, **2003**, 110, 789
- 17) Nakamura, S.; Kawamata, T.; Akiguchi, I.; Kameyama, M.; Nakamura, N.; Kimura, H. *Acta Neuropathologica*, **1990**, 80, 419
- 18) Saura, J.; Luque, J. M.; Cesura, A. M.; Da Prada, M.; Chan-Palay, V.; Huber, G.; Löffler, J.; Richards, J.G. *Neurosci.*, **1994**, 62, 15
- 19) Jossan, S. S.; Gillberg, P. G.; Gottfries, C. G.; Karlsson, I.; Oreland, L. *Neurosci.*, **1991**, 45, 1
- 20) Giubilei, F.; Patacchioli, F. R.; Antonini, G.; Sepe, M. M.; Tisei, P.; Bastianello, S.; Monnazzi, P.; Angelucci, L. *Neurosci. Res.*, **2001**, 66, 262
- 21) Lovell, M. A.; Ehmann, W. D.; Markesbery, W. R. *Ann. Neurol.*, **1993**, 33, 36
- 22) Mück-Seler, D.; Presecki, P.; Mimica, N.; Mustapic, M.; Pivac, N.; Babic, A.; Nedic, G.; Folnegovic-Smalc, V. *Progress in Neuro-Psychopharmacology & Biological Psychiatry*, **2009**, 33, 1226
- 23) Mimica, N.; Mück-Seler, D.; Pivac, N.; Mustapic, M.; Dezeljin, M.; Stipcevic, T.; Presecki, P.; Radonic, E.; Folnegovic-Smalc, V. *Coll. Antropol.*, **2008**, 32, 119
- 24) Jossan, S. S.; d'Argy, R.; Gillberg, P. G.; Aquilonius, S. M.; Langström, B.; Halldin, C.; Bjurling, P.; Stalnacke, C. G.; Fowler, J.; MacGregor, R. *Journal of Neural Transmission*, **1989**, 77, 55
- 25) Valotassiou, V.; Archimandritis, S.; Sifakis, N.; Papatriantafyllou, J.; Georgoulas, P. *Curr. Alzheimer Res.*, **2010**, 7, 477
- 26) Korolainen, M. A.; Nyman, T. A.; Aittokallio, T.; Pirttilä, T. *J. Neurochem.*, **2010**, 112, 1386
- 27) Zellner, M.; Baureder, M.; Rappold, E.; Bugert, P.; Kotzailias, N.; Babeluk, R.; Baumgartner, R.; Attems, J.; Gerner, C.; Jellinger, K.; Roth, E.; Oehler, R.; Umlauf, E. *Journal of Proteomics*, **2012**, 75, 2080

- 28) Holland, J. P.; Liang, S. H.; Rotstein, B. H.; Collier, T. L.; Stephenson, N. A.; Greguric, I.; Vasdev, N. *J. of Labelled Compounds and Radiopharmaceutics*, **2014**, 57 (4), 323
- 29) Fowler, J. S.; MacGregor, R. R.; Wolf, A. P.; Arnett, C. D.; Dewey, S. L.; Schlyer, D.; Christman, D.; Logan, J.; Smith, M.; Sachs, H.; Aquilonius, S. M.; Bjurling, P.; Halldin, C.; Hartvig, P.; Leenders, K. L.; Lundqvist, H.; Oreland, L.; Stalnacke, C. G.; Langström, B. *Science*, **1987**, 235, 481
- 30) Bläuenstein, P.; Rémy, N.; Buck, A.; Ametamey, S.; Häberli, M.; Schubiger, P. A. *Nucl. Med. Biol.*, **1998**, 25, 472
- 31) Saba, W.; Valette, H.; Peyronneau, M. A.; Bramoullé, Y.; Coulon, C.; Curet, O.; George, P.; Dollé, F.; Bottlaender, M. *Synapse*, **2010**, 64, 131
- 32) Mukherjee, J.; Yang, Z. Y.; Lew, R. *Nucl. Med. Biol.*, **1999**, 26, 111
- 33) Nag, S.; Kettschau, G.; Heinrich, T.; Varrone, A.; Lehmann, L.; Gulyás, B.; Thiele, A.; Keller, E.; Halldin, C. *Bioorg. Med. Chem.*, **2013**, 21, 186
- 34) Mishra, N.; Sasmal, D. *Bioorg. Med. Chem. Lett.*, **2011**, 21, 1969
- 35) Lima, L. M.; Barreiro, E. J. *Curr. Med. Chem.*, **2005**, 12, 23
- 36) Lipinski, C. A.; Lombardo, F.; Dominy, B. W.; Feeney, P. J. *Advanced Drug Delivery Reviews*, **2001**, 46, 3
- 37) Mahé, O.; Frath, D.; Dez, I.; Marsais, F.; Levacher, V.; Brière, J. F. *Org. Biomol. Chem.*, **2009**, 7, 3648
- 38) Lévai, A.; Jekö, J. *J. Heterocyclic Chem.*, **2006**, 43, 111
- 39) Lévai, A.; Jekö, J.; Brahmabhatt, D. I. *J. Heterocyclic Chem.*, **2005**, 42, 1231
- 40) Uhl, G.R.; Johnson P. S. *J. exp. Biol.*, **1994**, 196, 229
- 41) Sung, U.; Apparsundram, S.; Galli, A.; Kahlig, K. M.; Savchenko, V.; Schroeter, S.; Quick, M. W.; Blakely, R. D. *J. Neurosci*, **2003**, 23 (5), 1697
- 42) Kim, C. H.; Hahn, M. K.; Joung, Y.; Anderson, S. L.; Steele, A. H.; Mazei-Robinson, M. S.; Gizer, I.; Teicher, M. H.; Cohen, B. M.; Robertson, D.; Walman, I. D.; Blakely, R. D.; Kim, K. S. *PNAS*, **2006**, 103 (50), 19164
- 43) Ressler, K. J.; Nemoeroff, C. B. *Biol. Psychiatry*, **1999**, 46, 1219

- 44) Melikian, H. E.; Ramamoorthy, S.; Tate, C. G.; Blakely, R. D. *Molecular Pharmacology*, **1996**, 50, 266
- 45) Tellioglu, T.; Robertson, D. *Exp. Rev. Mol. Med.*, **2001**, 1
- 46) Blakely, R. D.; Bauman, A. L. *Curr. Opin. Neurobiol.*, **2000**, 10, 328
- 47) Zhu, M. Y.; Shamburger, S.; Li, J.; Ordway, G. A. *Journal of Pharmacology and Experimental Therapeutics*, **2000**, 295 (3), 951
- 48) Moron, J. A.; Grockington, A.; Wise, R. A.; Rocha, B. A.; Hope, B. T. *J. Neurosci.*, **2002**, 22, 386
- 49) Stöber, G.; Nöthen, M. M.; Pörzgen, P.; Brüß, M.; Bönisch, H.; Knapp, M.; Beckmann, H.; Propping, P. *American Journal of Medical Genetics (Neuropsychiatric Genetics)*, **1996**, 67, 523
- 50) Schroeter, S.; Apparsundaram, S.; Wiley, R. G.; Miner, L. H.; Sesack, S. R.; Blakely, R. D. *The Journal of comparative neurology*, **2000**, 420, 211
- 51) Torres, G. E.; Gainetdinov, R. R.; Caron, M. G. *Nature Reviews Neuroscience*, **2003**, 4, 13
- 52) Ordway, G. A.; Stockmeier, C. A.; Cason, G. W.; Klimek, V. J. *J. Neurosci.*, **1997**, 17, 1710
- 53) Smith, H. R.; Beveridge, T. J. R.; Porrino, L. J. *J. Neurosci.*, **2006**, 138, 703
- 54) Zhou, J. *Drugs Future*, **2004**, 29, 1235
- 55) Curatolo, P.; D'Agati, E.; Moavero, R. *Ital. J. Pediatr.*, **2010**, 36, 79
- 56) Mash, D. C.; Ouyang, Q.; Qin, Y.; Pablo, J. *J. Neurosci. Methods*, **2005**, 143, 79
- 57) Tejani-Butt, S. M. *J. Pharmacol. Exp. Ther.*, **1992**, 260, 427
- 58) Donnan, G. A.; Kaczmarczyk, S. J.; Paxinos, G.; Chilco, P. J.; Kalnins, R. M.; Woodhouse, D. G.; Mendelsohn, F. A. O. *Comp. Neurol.*, **1991**, 304, 419
- 59) Bäckström, I. T.; Marcusson, J. O. *Neuropsychobiology*, **1990**, 23, 68
- 60) Xu, R.; Gainetdinov, R. R.; Wetsel, W. C.; Jones, S. R.; Bohn, L. M.; Miller, G. W.; Wang, Y. M.; Caron, M. G. *Nature Neuroscience*, **2000**, 3 (5), 465
- 61) Young, J. B.; Landsberg, L. *Catecholamines and the adrenal medulla*. In: Williams Textbook of Endocrinology, 9th Ed., Wilson, J. D., Foster, D. W. (Eds.), W. B. Saunders Co., Philadelphia, **1998**, 680

- 62) Szabo, S. T.; Gould, T. D.; Manji, H. K. *Neurotransmitters, Receptors, Signal Transduction and Second Messengers in Psychiatric Disorders*. In: Textbook of Psychopharmacology, 4th Ed., Schatzberg, A. F.; Nemeroff, C. B., The American Psychiatric Publishing, Virginia, **2009**
- 63) Hahn, M. K.; Robertson, D.; Blakely, R. D. *J. Neurosci.*, **2003**, 23 (11), 4470
- 64) Mirbolooki, M. R.; Upadhyay, S. K.; Constantinescu, C. C.; Pan, M. L.; Mukherjee, J. *Nucl. Med. Biol.*, **2014**, 41, 10
- 65) Lin, S. L.; Fan, X.; Yeckel, C. W.; Weinzimmer, D.; Mulnix, T.; Gallezot, J. D.; Carson, R. E.; Sherwin, R. S.; Ding, Y. S. *Nucl. Med. Biol.*, **2012**, 39, 1081
- 66) Barr, C. L.; Kroft, J.; Feng, Y.; Wigg, K.; Roberts, W.; Malone, M.; Ickowicz, A.; Schachar, R.; Tannock, R.; Kennedy, J. L. *American Journal of Medical Genetics (Neuropsychiatric Genetics)*, **2002**, 114, 255
- 67) Klimek, V.; Stockmeier, C.; Overholser, J.; Meltzer, H. Y.; Kalka, S.; Dilley, G.; Ordway, G. A. *J. Neurosci.*, **1997**, 17 (21), 8451
- 68) Nedergaard, J.; Cannon, B. *Cell Metabolism*, **2010**, 11 (4), 268
- 69) Jensen, P.; Kettle, L.; Roper, M. T.; Sloan, M. T.; Dulcan, M. K.; Hoven, C.; Bird, H. R.; Baumeister, J. J.; Payne, J. D. *J. Am. Acad. Child. Adolesc. Psychiatry*, **1999**, 38, 797
- 70) Goldman, L.; Genel, M.; Bezman, R.; Slanetz, P. *JAMA*, **1998**, 279, 1100
- 71) Faraone, S.; Sergeant, J.; Gillberg, C.; Biederman, J. *World Psychiatry*, **2003**, 2, 104
- 72) American Psychiatric Association: Diagnostic and Statistical Manual of Mental Diseases (DSM-V), 5th Ed., American Psychiatric Publishing, Washington, DC, **2013**
- 73) Barkley, R. A. *Psychological Bulletin*, **1997**, 121 (1), 65
- 74) Cortese, S. *Eur. J. Paediatr. Neurol.*, **2012**, 16 (5), 422
- 75) Kim, J. W.; Biederman, J.; McGarh, C. L.; Doyle, A. E.; Mick, E.; Fagerness, J.; Purcell, S.; Smoller, J. W.; Sklar, P.; Faraone, S. V. *Molecular Psychiatry*, **2007**, 1
- 76) National Institutes of Health: National Institutes of Health Consensus Development Conference Statement: diagnosis and treatment of attention-deficit/hyperactivity disorder (ADHD). *J. Am. Acad. Child. Adolesc. Psychiatry*, **2000**, 39, 182

- 77) Visser, S. N.; Lesesne, C. A. *MMWR*, **2005**, 54 (34), 842
- 78) Wolraich, M. L. *Ment. Retard. Dev. Disabil. Res. Rev.*, **1999**, 5, 163
- 79) Faraone, S. V.; Biederman, J. *Biol. Psychiatry*, **1998**, 44 (10), 951
- 80) Rappley, M. D. *N. Engl. J. Med.*, **2005**, 352, 165
- 81) Faraone, S. V.; Perlis, R. H.; Doyle, A. E.; Smoller, J. W.; Goralnick, J. J.; Holmgren, M. A.; Sklar, P. *Biol. Psychiatry*, **2005**, 57, 1313
- 82) Castellanos, F. X.; Tannock, R. *Nature Reviews Neuroscience*, **2002**, 3 (8), 617
- 83) Millenet, S.; Hohmann, S.; Poustka L.; Petermann, F.; Banaschewski, T. *Kindheit und Entwicklung*, **2013**, 22 (4), 201
- 84) Ramoz, N.; Boni, C.; Downing, A. C. M.; Close, S. L.; Peters, S. L.; Prokop, A. M.; Allen, A. J.; Hamon, M.; Purper-Quakil, D.; Gorwood, P. *Neuropsychopharmacology*, **2009**, 34, 2135
- 85) Arnsten, A. F. *Journal of Clinical Psychiatry*, **2006**, 67 (Suppl. 8), 7
- 86) Sagvolden, T.; Johansen, E. B.; Aase, H.; Russell, V. A. *Behavioral and Brain Sciences*, **2005**, 28 (3), 397
- 87) Seidman, L. J.; Valera, E. M.; Makris, N. *Biological Psychiatry*, **2005**, 57, 1263
- 88) Valera, E. M.; Faraone, S. V.; Murray, K. E.; Seidman, L. J. *Biological Psychiatry*, **2007**, 61, 1361
- 89) Bush, G.; Valera, E. M.; Seidman, L. J. *Biological Psychiatry*, **2005**, 57, 1273
- 90) Dickstein, S. G.; Bannon, K.; Castellanos, F. X.; Milham, M. P. *Journal of Child Psychology and Psychiatry and Allied Disciplines*, **2006**, 47, 1051
- 91) Banaschewski, T.; Brandeis, D. *Journal of Child Psychology and Psychiatry and Allied Disciplines*, **2007**, 48, 415
- 92) Barkely, R. *Attention-Deficit/Hyperactivity Disorder: A Handbook for Diagnosis and Treatment*, 2nd Ed.; Guilford Press, New York, **1998**
- 93) Spencer, T. J.; Biederman, J.; Mick, E. *Journal of Pediatric Psychology*, **2007**, 32 (6), 631
- 94) Cubillo, A.; Halari, R.; Ecker, C.; Giampietro, V.; Taylor, E.; Rubia, K. *Journal of Psychiatric Research*, **2010**, 44 (10), 629

- 95) DePue, B. E.; Burgess, G. C.; Willcutt, E. G.; Ruzik, L.; Banich, M. T. *Neuropsychologia*, **2010**, 48 (13), 3909
- 96) Durston, S.; Tottenham, N. T.; Thomas, K. M.; Davidson, M. C.; Eigsti, I. M.; Yang, Y.; Casey, B. J. *Biological Psychiatry*, **2003**, 53, 871
- 97) Lou, H. C.; Henriksen, L.; Bruhn, P. *Archives of Neurology*, **1984**, 41, 825
- 98) Zimmer, L. *Neuropharmacology*, **2009**, 57, 601
- 99) Ashtari, M.; Kumra, S.; Bhaskar, S. L.; Clarke, T.; Thaden, E.; Cervellione, K. L.; Ardekani, B. A. *Biological Psychiatry*, **2005**, 57 (5), 448
- 100) Cao, Q.; Sun, L.; Gong, G.; Lv, Y.; Cao, X.; Shuai, L.; Wang, Y. *Brain Research*, **2010**, 1310, 171
- 101) Weyandt, L.; Swentosky, A.; Gudmundsdottir B. G. *Developmental Neuropsychology*, **2013**, 38 (4), 211
- 102) Kuhar, M. J.; Ritz, M. C.; Boja, J. W. *Trends Neurosci.*, **1991**, 14, 299
- 103) Johanson, C. E.; Fischman, M. W. *Pharmacol. Rev.*, **1989**, 41, 3
- 104) McClung, C. A.; Nestler, E. J. *Nat. Neurosci.*, **2003**, 6, 1208
- 105) Zhang, L.; Lou, D.; Jiao, H.; Zhang, D.; Wang, X.; Xia, Y.; Zhang, J.; Xu, M. *J. Neurosci.*, **2004**, 24, 3344
- 106) Laurent, K.; Gorelick, D.; Weinstein, A.; Noble, F.; Benyamina, A.; Coscas, S.; Blecha, L.; Lowenstein, W.; Martinot, J. L.; Reynaud, M.; Lépine, J. P. *International Journal of Neuropsychopharmacology*, **2008**, 11, 425
- 107) Roberts, D. C.; Koob, G. F.; Klonoff, P.; Fibiger, H. C. *Pharmacol. Biochem. Behav.*, **1980**, 12, 781
- 108) Goeders, N. E.; Smith, J. E. *Science*, **1983**, 221, 773
- 109) Ritz, M. C.; Lamb, R. J.; Goldberg, S. R.; Kuhar, M. J. *Science*, **1987**, 237, 1219
- 110) Giros, B.; Jaber, M.; Jones, S. R.; Wightman, R. M.; Caron, M. G. *Nature*, **1996**, 379, 606
- 111) Farfel, G. M.; Kleven, M. S.; Woolverton, W. L.; Seiden, L. S.; Perry, B. D. *Brain Res.*, **1992**, 578, 235

- 112) Volkow, N. D.; Fowler, J. S.; Wang, G. J.; Hitzemann, R.; Logan, J.; Schlyer, D. J.; Dewey, S. L.; Wolf, A. P. *Synapse*, **1993**, 14, 169
- 113) Volkow, N. D.; Fowler, J. S.; Wang, G. J. *Psychopharmacol.*, **1999**, 13, 337
- 114) Letchworth, S. R.; Nader, M. A.; Smith, H. R.; Friedman, D. P.; Porrino, L. J. *J. Neurosci.*, **2001**, 21, 2799
- 115) Nader, M. A.; Daunais, J. B.; Moore, T.; Nader, S. H.; Moore, R. J.; Smith, H. R.; Friedman, D. P.; Porrino, L. J. *Neuropsychopharmacology*, **2002**, 27, 35
- 116) Belej, T.; Manij, D.; Sioutis, S.; Barros, H. M.; Nobrega, J. N. *Brain Res.*, **1996**, 736, 287
- 117) Benmansour, S.; Tejani-Butt, S. M.; Hauptmann, M.; Brunswick, D. J. *Psychopharmacology*, **1992**, 106, 459
- 118) Burchett, S. A.; Bannon, M. J. *Brain Res. Mol. Brain Res.*, **1997**, 49, 95
- 119) Macey D. J.; Smith, H. R.; Nader, M. A.; Porrino, L. J. *J. Neurosci.*, **2003**, 23, 12
- 120) Beveridge, T. J. R.; Smith, H. R.; Nader, M. A.; Porrino, L. J. *Psychopharmacology*, **2005**, 180, 781
- 121) Brownstein, M. J.; Palkovits, M. *Classical transmitters in the CNS, Pt 1*. In: Handbook of chemical neuroanatomy, Vol 2, Bjorklund A., Hokfelt T. (Eds.) Elsevir, Amsterdam, **1984**
- 122) Ghose, S.; Fujita, M.; Morrison, P.; Uhl, G.; Murphy, D. L.; Mozley, P. D.; Schou, M.; Halldin, C.; Innis, R. *Synapse*, **2005**, 56, 100
- 123) Logan, J.; Wang, G. J.; Telang, F.; Fowler, J. S.; Alexoff, D.; Zabroski, J.; Jayne, M.; Hubbard, B.; King, P.; Carter, P.; Shea, C.; Xu, Y.; Muench, L.; Schlyer, D.; Learned-Coughlin, S.; Cosson, V.; Volkow, N. D.; Ding, Y. S. *Nucl. Med. Biol.*, **2007**, 34, 667
- 124) McDougle, C. J.; Black, J. E.; Malison, R. T.; Zimmermann, R. C.; Kosten, T. R.; Heninger, G. R.; Price, L. H. *Arch. Gen. Psychiatry*, **1994**, 51, 713
- 125) Rothman, R. B.; Baumann, M. H.; Dersch, C. M.; Romero, D. V.; Rice, K. C.; Carroll, F. I.; Partilla, J. S. *Synapse*, **2001**, 39, 32
- 126) Schank, J.; Ventura, R.; Puglisi-Allegra, S.; Alcaro, A.; Cole, C.; Liles, L.; Seeman, P.; Weinshenker, D. *Neuropsychopharmacology*, **2006**, 31, 2221
- 127) Freeman, K. B.; Verendejev, A.; Riley, A. L. *Pharmacol. Biochem. Behav.*, **2008**, 88, 523

- 128) Platt, D. M.; Rowlett, J. K.; Spealman, R. D. *J. Pharmacol. Exp. Ther.*, **2007**, 322, 894
- 129) Vocci, F.; Elkashef, A. *Curr. Opin. Psychiatry*, **2005**, 18, 265
- 130) Weinshenker, D.; Schroeder, J. P. *Neuropsychopharmacology*, **2007**, 32, 1433
- 131) Hall, F. S.; Li, X. F.; Sora, I.; Xu, F.; Caron, M.; Lesch, K. P.; Murphy, D. L.; Uhl, G. R. *Neurosci.*, **2002**, 115, 153
- 132) Martinez, D.; Kim, J. H.; Krystal, J.; Abi-Dargham, A. *Neuroimaging Clin. N. Am.*, **2007**, 17, 537
- 133) Volkow, N. D.; Wang, G. J.; Fowler, J. S.; Franceschi, D.; Thanos, P. K.; Wong, C.; Gatley, S. J.; Ding, Y. S.; Molina, P.; Schlyer, D.; Alexoff, D.; Hitzemann, R.; Pappas, N. *Life Sci.*, **2000**, 66, PL161
- 134) Ding, Y. S.; Singhal, T.; Planeta-Wilson, B.; Gallezot, J. D.; Nabulsi, N.; Labaree, D.; Ropchan, J.; Henry, S.; Williams, W.; Carson, R. E.; Neumeister, A.; Malison, R. T. *Synapse*, **2010**, 64, 30
- 135) Cypess, A. M.; Chen, Y. C.; Sze, C.; Wang, K.; English, J.; Chan, O.; Holman, A. R.; Tal, I.; Palmer, M.; Kolodny, G. M.; Kahn, R. *PNAS*, **2012**, 109 (25), 10001
- 136) Nedergaard, J.; Bengtsson, T.; Cannon, B. *Am. J. Physiol. Endocrinol. Metab.*, **2007**, 293, E444
- 137) Enerbäck, S. *Cell Metabolism*, **2010**, 11, 248
- 138) Weber, W. A. *J. Nucl. Med.*, **2004**, 45 (7), 1101
- 139) Cypess, A. M.; Kahn, C. R. *Curr. Opin. Endocrinol. Diabetes Obes.*, **2010**, 17 (2), 143
- 140) Lean, M. E.; James, W. P.; Jennings, G.; Trayhurn, P. *Int. J. Obes.*, **1986**, 10, 219
- 141) Cannon, B.; Nedergaard, J. *Physiol. Rev.*, **2004**, 84, 277
- 142) Rothwell, N. J.; Stock, M. J. *Nature*, **1979**, 281, 31
- 143) Mercer, S. W.; Trayhurn, P. *J. Nutr.*, **1987**, 117, 2147
- 144) van Marken Lichtenbelt, W. D.; Vanhommerig, J. W.; Smulders, N. M.; Drossaerts, J. M.; Kemerink, G. J.; Bouvy, N. D.; Schrauwen, P.; Jaap Teule, G. J. *N. Engl. J. Med.*, **2009**, 360, 1500

- 145) Virtanen, K. A.; Lidell, M. E.; Orava, J.; Heglind, M.; Westergren, R.; Niemi, T.; Taittonen, M.; Laine, J.; Savisto, N. J.; Enerbäck, S.; Nuutila, P. *N. Engl. J. Med.*, **2009**, 360, 1518
- 146) Zingaretti, M. C.; Crosta, F.; Vitali, A.; Guerrieri, M.; Frontini, A.; Cannon, B.; Nedergaard, J.; Cinti, S. *FASEB J.*, **2009**, 23, 3113
- 147) Yoneshiro, T.; Aita, S.; Matsushita, M.; Kameya, T.; Nakada, K.; Kawai, Y.; Saito, M. *Obesity (Silver Spring)*, **2011**, 19, 13
- 148) Cypess, A. M.; Lehman, S.; Williams, G.; Tal, I.; Rodman, D.; Goldfine, A. B.; Kuo, F. C.; Palmer, E. L.; Tseng, Y. H.; Doria, A.; Kolodny, G. M.; Kahn, C. R. *N. Engl. J. Med.*, **2009**, 360, 1509
- 149) Saito, M.; Okamatsu-Ogura, Y.; Matsushita, M.; Watanabe, K.; Yoneshiro, T.; Nio-Kobayashi, J.; Iwanaga, T.; Miyagawa, M.; Kameya, T.; Nakada, K.; Kawai, Y.; Tsujisaki, M. *Diabetes*, **2009**, 58, 1526
- 150) Pfannenbergl, C.; Werner, M. K.; Ripkens, S.; Stef, I.; Deckert, A.; Schmadl, M.; Reimold, M.; Häring, H. U.; Claussen, C. D.; Stefan, N. *Diabetes*, **2010**, 59, 1789
- 151) Logan, J.; Ding, Y. S.; Lin, K. S.; Pareto, D.; Fowler, J.; Biegol, A. *Nuclear Medicine and Biology*, **2005**, 32, 531
- 152) Belmaker, R. H.; Agam, G. *N. Engl. J. Med.*, **2008**, 358, 55
- 153) Fowler, J. S.; Volkow, N. D.; Wang, G. J.; Gatley, S. J.; Logan, J. *Nucl. Med. Biol.*, **2001**, 28, 561
- 154) Pristupa, Z. B.; Wilson, J. M.; Hoffman, B. J.; Kish, S. J.; Niznik, H. B. *Mol. Pharmacol.*, **1994**, 45, 125
- 155) Wong, E. H. F.; Sonders, M. S.; Amara, S. G.; Tinholt, P. M.; Piercey, M. F. P.; Hoffmann, W. P.; Hyslop, D. K.; Franklin, S.; Porsolt, R. D.; Bonsignori, A.; Carfagna, N.; McArthur, R. A. *Biological Psychiatry*, **2000**, 47 (9), 818
- 156) Schou, M.; Halldin, C.; Sovago, J.; Pike, V. W.; Hall, K.; Gulyás, B.; Mozley, D.; Dobson, D.; Shchukin, E.; Innis, R. B.; Farde, L. *Synapse*, **2004**, 53, 57
- 157) King, V. L.; Dwoskin, L. P.; Cassis, L. A. *American Journal of Physiology*, **1999**, 276, R143

- 158) Haka, M. S.; Kilbourn, M. R. *Nucl. Med. Biol.*, **1989**, 16, 771
- 159) Schou, M.; Halldin, C.; Pike, V.; Sovago, J.; Gulyás, B.; Innis, B.; Farde, L. *Eur. J. Nucl. Med. Mol. Imag.*, **2000**, 29, 59
- 160) Zhang, H.; Huang, R.; Pillarsetty, N. V. K.; Thorek, D. L. J.; Vaidyanathan, G.; Serganova, I.; Blasberg, R. G.; Lewis, J. S. *Eur. J. Nucl. Med. Mol. Imag.*, **2014**, 41 (2), 322
- 161) Watanabe, S.; Hanaoka, H.; Liang, J. X.; Iida, Y.; Endo, K.; Ishioka, N. S. *The Journal of Nuclear Medicine*, **2010**, 51 (9), 1472
- 162) Kiyono, Y.; Kanegawa, N.; Kawashima, H.; Kitamura, Y.; Iida, Y.; Saji, H. *Nucl. Med. Biol.*, **2004**, 31, 147
- 163) Kanegawa, N.; Kiyono, Y.; Kimura, H.; Sugita, T.; Kajiyama, S.; Kawashima, H.; Ueda, M.; Kuge, Y.; Saji, H. *Eur. J. Nucl. Med. Mol. Imag.*, **2006**, 33 (6), 639
- 164) Tatsumi, M.; Engles, J. M.; Ishimori, T.; Nicely, O. B.; Cohade, C.; Wahl, R. L. *J. Nucl. Med.*, **2004**, 45, 1189
- 165) Mirbolooki, M. R.; Constantinescu, C. C.; Pan, M. L.; Mukherjee, J. *Synapse*, **2013**, 67, 79
- 166) Mahaney, P. E.; Vu, A. T.; McComas, C. C.; Zhang, P.; Nogle, L. M.; Watts, W. L.; Sarkahian, A.; Leventhal, L.; Sullivan, N. R.; Uveges, A. J.; Trybulski, E. J. *Bioorg. Med. Chem.*, **2006**, 14, 8455
- 167) Zhang, P.; Terefenko, E. A.; McComas, C. C.; Mahaney, P. E.; Vu, A.; Trybulski, E.; Koury, E.; Johnston, G.; Bray, J.; Deecher, D. *Bioorg. Med. Chem. Lett.*, **2008**, 18, 6067
- 168) McComas, C. C.; Vu, A. T.; Mahaney, P. E.; Cohn, S. T.; Fensome, A.; Marella, M. A.; Nogle, L.; Trybulski, E. J.; Ye, F.; Zhang, P.; Alfinito, P.; Bray, J.; Johnston, G.; Koury, E.; Deecher, D. C. *Bioorg. Med. Chem. Lett.*, **2008**, 18, 4929
- 169) Mark, C.; Bornatowicz, B.; Mitterhauser, M.; Hendl, M.; Nics, L.; Haeusler, D.; Lanzenberger, R.; Berger, M. L.; Spreitzer, H.; Wadsak, W. *Nucl. Med. Biol.*, **2013**, 40, 295

- 170) Ding, Y. S.; Naganawa, M.; Gallezot, J. D.; Nabulsi, N.; Lin, S. F.; Ropchan, J.; Weinzimmer, D.; McCarthy, T. J.; Carson, R. E.; Huang, Y.; Laruelle, M. *NeuroImage*, **2014**, 86, 164
- 171) Eyding, D.; Lelgemann, M.; Grouven, U.; Härter, M.; Kromp, M.; Kaiser, T.; Kerekes, M. F.; Gerken, M.; Wieseler, B. *BMJ*, **2010**, 341, c4737
- 172) Wu, D.; Pontillo, J.; Ching, B.; Hudson, S.; Gao, Y.; Fleck, B. A.; Gogas, K.; Wade, W. S. *Bioorg. Med. Chem. Lett.*, **2008**, 18, 4224
- 173) Maxwell, R. A.; White, H. L. *Handbook Psychopharmacol.*, **1978**, 14, 83
- 174) Sauer, J. M.; Ring, B. J.; Witcher, J. W. *Clin. Pharmacokinet.*, **2005**, 44, 571
- 175) Bymaster, F. P.; Lee, T. C.; Knadler, M. P.; Detke, M. J.; Iyengar, S. *Curr. Pharm. Des.*, **2005**, 11, 1475
- 176) Hudson, S.; Kiankarimi, M.; Eccles, W.; Mostofi, Y. S.; Genicot, M. J.; Dwight, W.; Fleck, B. A.; Gogas, K.; Wade, W. S. *Bioorg. Med. Chem. Lett.*, **2008**, 18, 4495
- 177) Hudson, S.; Kiankarimi, M.; Eccles, W.; Dwight, W.; Mostofi, Y. S.; Genicot, M. J.; Fleck, B. A.; Gogas, K.; Aparicio, A.; Wang, H.; Wen, J.; Wade, W. S. *Bioorg. Med. Chem. Lett.*, **2008**, 18, 4491
- 178) Wüst, F. R. *Trends in Organic Chemistry*, **2003**, 10, 61
- 179) Schlyer, D. J. *Ann. Acad. Med. Singapore*, **2004**, 33, 146
- 180) Mitterhauser, M.; Wadsak, W. [¹⁸F]fluoroethylated and [¹¹C]methylated PET tracers for research and routine diagnosis. In: *Trends in Radiopharmaceuticals (ISTR-2005): Proceedings of an International Symposium organized by the International Atomic Energy Agency and held in Vienna (Austria) 14-18 November, 2005*. Wien, IAEA, **2007**, 2, 161
- 181) Ludqvist, H.; Lubberink, M.; Tolmachev, V. *Eur. J. Phys.*, **1998**, 19, 537
- 182) Li, Y. *Sci. China Chem.*, **2013**, 56, 12
- 183) Paans, A. M. J.; Vaalburg, W. *Current Pharmaceutical Design*, **2000**, 6, 1583
- 184) Ismail, F. M. D. J. *Fluorine Chem.*, **2002**, 18, 27
- 185) Park, B. K.; Kitteringham, N. R.; O'Neill, P. M. *Annu. Rev. Pharmacol. Toxicol.*, **2001**, 41, 443

- 186) Ishiwata, K.; Kimura, Y.; De Vries, E. F. J.; Elsinga, P. H. *Central Nervous System Agents in Med. Chem.*, **2007**, 7 (1), 57
- 187) Paans, A. M. J.; van Waarde, A.; Elsinga, P. H.; Willemsen, A. T. M.; Vaalburg, W. *Methods*, **2002**, 27, 195
- 188) Weber, W. A. *Journal of Clinical Oncology*, **2006**, 24 (20), 3282
- 189) Pichler, B. J.; Wehrl, H. F.; Judenhofer, M. S. *J. Nucl. Med.*, **2008**, 49, 5S
- 190) Ametamey, S. M.; Honer, M.; Schubiger, P. A. *Chem. Rev.*, **2008**, 108, 1501
- 191) Wadsak, W. *Medizinische Radiochemie I*, Lecture at the Medicinal University of Vienna, WS **2013/14**
- 192) Townsend, D. W. *Ann. Acad. Med. Singapore*, **2004**, 33 (2), 133
- 193) Basu, S.; Kwee, T. C.; Surti, S.; Akin, E. A.; Yoo, D.; Alavi, A. *Ann. N. Y. Acad. Sci.*, **2011**, 1228, 1
- 194) Shan, B.; Chai, P.; Zhang, Z. *Positron Emission Tomography*. In: *Molecular Imaging, Fundamentals and Applications*, Tian, J. (Ed.), Springer-Verlag, Berlin Heidelberg, **2013**, 241
- 195) Shukla, A. K.; Kumar, U. *Journal of Medical Physics*, **2006**, 31 (1), 13
- 196) Ziegler, S. I. *Nuclear Physics A*, **2005**, 752, 679c
- 197) Shanab, K. *Synthese von Precursoren von A₃-Adenosin-Rezeptor PET-Tracern – Im Dienste der Nuklearmedizin*. Vdm Verlag Dr. Müller, Wien, **2008**
- 198) Zaidi, H.; Del Guerra, A. *Medical Physics*, **2011**, 38 (10), 5667
- 199) Terry, G. E.; Hirvonen, J.; Liow, J. S.; Zoghbi, S. S.; Gladding, R.; Tauscher, J. T.; Schaus, J. M.; Phebus, L.; Felder, C. C.; Morse, C. L.; Donohue, S. R.; Pike, V. W.; Halldin, C.; Innis, R. B. *Nucl. Med. Biol.*, **2010**, 51, 112
- 200) Alberini, J. L.; Edeline, V.; Giraudet, A. L.; Champion, L.; Paulmier, B.; Madar, O.; Poinsignon, A.; Bellet, D.; Pecking, A. P. *Journal of Surgical Oncology*, **2011**, 103, 602
- 201) Catana, C.; Procissi, D.; Wu, Y.; Judenhofer, M. S.; Qi, J.; Pichler, B. J.; Jacobs, R. E.; Cherry, S. R. *PNAS*, **2008**, 105 (10), 3705
- 202) Wadsak, W.; Mitterhauser, M. *European Journal of Radiology*, **2010**, 73, 461

- 203) http://www.iaea.org/About/Policy/GC/GC51/GC51InfDocuments/English/gc51inf-3-att2_en.pdf (accessed 22.4.2014)
- 204) Cao, Q.; Hersl, J.; La, H.; Smith, M.; Jenkins, J.; Goloubeva, O.; Dilsizian, V.; Tkaczuk, K.; Chen, W.; Jones, L. *BMC Cancer*, **2014**, 14, 126
- 205) Ido, T.; Won, C. N.; Casella, V.; Fowler, J.; Wolf, A. P.; Reivich, M.; Kuhl, D. E. *J. Label. Compd. Radiopharm.*, **1978**, 14, 175
- 206) Hamacher, K.; Coenen, H. H.; Stöcklin, G. *J. Nucl. Med.*, **1986**, 27, 235
- 207) Di Chiro, G. *Invest. Radiol.*, **1987**, 22, 360
- 208) Di Chiro, G.; Oldfield, E.; Bairamian, D.; Brooks, R. A.; Patronas, N. J.; Mansi, L.; Kornblith, P. L.; Smith, B. H.; Sank, V. J.; Margolin, R. A. *In vivo glucose utilization of tumors of the brain stem and spinal cord*. In: Positron Emission Tomography, Greitz T.; Ingvar D.H; Widen L. (Eds.) Raven Press, New York, **1985**, 351-361
- 209) Kostakoglu, L.; Goldsmith, S. J. *J. Nucl. Med.*, **2003**, 44 (2), 224
- 210) Bergström, M.; Awad, R.; Estrada, S.; Mälman, J.; Lu, L.; Lendvai, G.; Bertström-Pettermann, E.; Längström, B. *Mol. Imag. Biol.*, **2003**, 5 (6), 390
- 211) Haeusler, D.; Mitterhauser, M.; Mien, L. K.; Shanab, K.; Lanzenberger, R. R.; Schirmer, E.; Ungersboeck, J.; Nics, L.; Spreitzer, H.; Viernstein, H.; Dudczak, R.; Kletter, K.; Wadsak, W. *Radiochim. Acta*, **2009**, 97, 753
- 212) Gibson, R. E.; Burns, H. D.; Hamill, T. G.; Eng, W.; Francis, B. E.; Ryan, C. *Current Pharmaceutical Design*, **2000**, 6, 973
- 213) Abbott, N. J.; Rönnbäck, L.; Hansson, E. *Nature Reviews Neuroscience*, **2006**, 7, 41
- 214) Schubiger, P. A. *Molecular Imaging with PET-Open Questions*. In: PET Chemistry – The Driving Force in Molecular Imaging, Schubiger, P. A.; Lehmann, L.; Friebe, M. (Eds.) Springer-Verlag, Berlin Heidelberg, **2007**
- 215) Pike, V. W. *Trends in Pharmacological Sciences*, **2009**, 30 (8), 431
- 216) Tavares, A. A. S.; Lewsey, J.; Dewar, D.; Pimlott, S. L. *Nucl. Med. Biol.*, **2012**, 39, 127
- 217) Abraham, M. H.; Acree Jr. W. E.; Fahr, A.; Liu, X. *Journal of Chromatography A*, **2013**, 1298, 44

- 218) Mien, L. K. *About the radiosynthesis and preclinical evaluation of innovative PET-tracers labelled with fluorine-18 and carbon-11 for neuroimaging*. Dissertation, University of Vienna, Vienna, **2007**
- 219) Vallabhajosula, S. *Semin. Nucl. Med.*, **2007**, 37, 400
- 220) Miller, P. W.; Long, N. J.; Vilar, R.; Gee, A. D. *Angew. Chem. Int. Ed.*, **2008**, 47, 8998
- 221) Mikolajczak, R.; Staniszewska, J.; Mikolajewski, S.; Rurarz, E. *Nukleonika*, **2002**, 47 (1), 13
- 222) Gillings, N. *Magn. Reson. Mater. Phy.*, **2013**, 26, 149
- 223) <http://www.radiopharmaceutical-sciences.net/media/downloads/category/3-radiopharmazie> (accessed 2.5.2014)
- 224) Jacobson, M. S.; Steichen, R. A.; Peller, P. J. *PET Radiochemistry and Radiopharmacy*. In: *PET-CT and PET-MRI in Oncology*, Peller, P.; Subramaniam, R.; Guermazi, A. (Eds.) Springer-Verlag, Berlin Heidelberg, **2012**
- 225) Coenen, H. H. *Fluorine-18 Labeling Methods: Features and Possibilities of Basic Reactions*. In: *PET Chemistry – The Driving Force in Molecular Imaging*, Schubiger, P. A.; Lehmann, L.; Friebe, M. (Eds.) Springer-Verlag, Berlin Heidelberg, **2007**
- 226) Mushtaq, A. *Ann. Nucl. Med.*, **2010**, 24, 759
- 227) Bushberg, J. T.; Seibert, J. A.; Leidholdt, E. W.; Boone, J. M. *Radionuclide Production, Radiopharmaceuticals, and Internal Dosimetry*. In: *The Essential of Physics of Medical Imaging*, 3rd Ed., Mitchell, C. W. (Ed.), Wolters Kluwer, Philadelphia, **2012**
- 228) Qaim, S. M. *Radiochim. Acta*, **2012**, 100, 635
- 229) Wadsak, W.; Mien, L. K.; Ettliger, D. E.; Eidlerr, H.; Haeusler, D.; Sindelar, K. M.; Keppler, B. K.; Dudczak, R.; Kletter, K.; Mitterhauser, M. *Nucl. Med. Biol.*, **2007**, 34, 1019
- 230) Langstrom, B.; Antoni, G.; Gullberg, P.; Halldin, C.; Nagren, K.; Rimland, A.; Svard, H. *Appl. Radiat. Isot.*, **1986**, 37, 1141
- 231) Antoni, G.; Langstrom, B. *J. Labelled Compd. Radiopharm.*, **1987**, 24, 125
- 232) Jewett, D. M. *Appl. Radiat. Isot.*, **1992**, 43, 1383

- 233) Tominiaux, C.; Dolle, F.; James, M. L.; Bramouille, Y.; Boutin, H.; Besret, L.; Gregoire, M. C.; Valette, H.; Bottlaender, M.; Tavitian, B.; Hantraye, P.; Selleri, S.; Kassiou, M. *Appl. Radiat. Isot.*, **2006**, 64, 570
- 234) Dolle, F.; Emond, P.; Mavel, S.; Demphel, S.; Hinnen, F.; Mincheva, Z.; Saba, W.; Valette, H.; Chalon, S.; Halldin, C.; Helfenbein, J.; Legaillard, J.; Madelmont, J. C.; Deloye, J. B.; Bottlaender, M.; Guilloteau, D. *Bioorg. Med. Chem.*, **2006**, 14, 1115
- 235) Wilson, A. A.; Garcia, A.; Chestakova, A.; Kung, H.; Houle, S. J. *Labelled Compd. Radiopharm.*, **2004**, 47, 679
- 236) Kawamura, K.; Ishiwata, K. *Ann. Nucl. Med.*, **2004**, 18, 165
- 237) Qaim, S. M.; Clark, J. C.; Crouzel, C.; Guillaume, M.; Helmeke, H. J.; Nebeling, B.; Pike, V. W.; Stöcklin, G. *PET Radionuclide Production*. In: *Radiopharmaceutical for Positron Emission Tomography-Methological Aspects*, Stöcklin, G.; Pike, V. W. (Eds.), Kluwer, Dordrecht, **1993**, 1
- 238) Mitterhauser, M.; Wadsak, W.; Wabnegger, L.; Sieghart, W.; Viernstein, H.; Kletter, K.; Dudczak, R. *Eur. J. Nucl. Med. Mol. Imaging*, **2003**, 30 (10), 1398
- 239) Mitterhauser, M.; Wadsak, W.; Wabnegger, L.; Mien, L. K.; Tögel, S.; Langer, O.; Sieghart, W.; Viernstein, H.; Kletter, K.; Dudczak, R. *Nucl. Med. Biol.*, **2004**, 31 (2), 291
- 240) Nickles, R. J.; Gatley, S. J.; Votaw, J. R.; Korngut, M. L. *Appl. Radiat. Isot.*, **1986**, 37, 649
- 241) Coenen, H. H.; Klatte, B.; Knöchel, A.; Schüller, M.; Stöcklin, G. *Labelled Compd. Radiopharm.*, **1986**, 23, 455
- 242) Sun, H.; DiMagno, S. G. *Chem. Commun.*, **2007**, 65, 682
- 243) Block, D.; Coenen, H. H.; Stöcklin, G. *J. Nucl. Med.*, **1987**, 24, 1029
- 244) Dolle, F.; Demphel, S.; Hinnen, F.; Fournier, D.; Vaufrey, F.; Crouzel, C. *J. Labell. Compd. Radiopharm.*, **1998**, 41, 105
- 245) Liu, C.; Jiang, S. *Sci. China Chem.*, **2009**, 52, 2199
- 246) Kilbourn, M. R. *National Acad. Press, Nucl. Sci. Series*, **1990**, NAS-NS-3203
- 247) Casella, V.; Ido, T.; Wolf, A. P.; Fowler, J. S.; MacGregor, R. R.; Ruth, T. J. *J. Nucl. Med.*, **1980**, 21, 750

- 248) Shiue, C. Y.; Salvadori, P. A.; Wolf, A. P.; Fowler, J. S.; MacGregor, R. R. *J. Nucl. Med.*, **1982**, 23, 899
- 249) Chirakal, R.; Firnau, G.; Schrobigen, G. J.; MacKay, J.; Garnett, E. S. *Appl. Radiat. Isot.*, **1984**, 35, 401
- 250) Satyamurthy, N.; Bida, G. T.; Phelps, M. E.; Barrio, J. R. *Appl. Radiat. Isot.*, **1990**, 41, 733
- 251) Forsback, S.; Eskola, O.; Haarparanta, M.; Bergman, J.; Solin, O. *Radiochim. Acta*, **2008**, 96, 845
- 252) Hess, E.; Sichler, S.; Kluge, A.; Coenen, H. H. *Appl. Radiat. Isot.*, **2002**, 57, 185
- 253) Coenen, H. H.; Colosimo, M.; Schüller, M.; Stöcklin, G. J. *Label. Compd. Radiopharm.*, **1986**, 23, 587
- 254) Bergman, J.; Eskola, O.; Lehtikoinen, P.; Solin, O. *Appl. Rad. Isot.*, **2001**, 54, 927
- 255) Zheng, L.; Berridge, M. S. *Appl. Rad. Isot.*, **2000**, 52, 55
- 256) Elsinga, P. H.; Kawamura, K.; Kobayashi, T.; Tsukada, H.; Senda, M.; Vaalburg, W.; Ishiwata, K. *J. Label. Compd. Radiopharm.*, **2001**, 44 (Suppl. 1), S4
- 257) Wilson, A. A.; Da Silva, J. N.; Houle, S. *Nucl. Med. Biol.*, **1996**, 23, 487
- 258) Skaddan, M. B.; Kilbourn, M. R.; Snyder, S. E.; Sherman, P. S.; Desmond, T. J.; Frey, K. A. *J. Med. Chem.*, **2000**, 43, 4552
- 259) Oh, S. J.; Choe, Y. S.; Chi, D. Y.; Kim, S. E.; Choi, Y.; Lee, K. H.; Ha, H. J.; Kim, B. T. *Appl. Rad. Isot.*, **1999**, 51, 293
- 260) Lundkvist, C.; Halldin, C.; Ginovart, N.; Swahn, C. G.; Farde, L. *Nucl. Med. Biol.*, **1997**, 24, 621
- 261) Chesis, P. L.; Welsh, M. J. *Appl. Rad. Isot.*, **1990**, 41, 259
- 262) Zijlstra, S.; De Groot, T. J.; Kok, L. P.; Visser, G. M.; Vaalburg, W. *J. Org. Chem.*, **2000**, 43, 4552
- 263) De Groot, T. J.; Elsinga, P. H.; Visser, G. M.; Vaalburg, W. *Appl. Rad. Isot.*, **1992**, 43, 1335
- 264) Chin, F. T.; Musachio, J. L.; Cai, L.; Pike, V. W. *J. Label. Compds. Radiopharm.*, **2003**, 46, S172

- 265) Zhang, M. R.; Furutsuka, K.; Yoshida, A.; Suzuki, K. *J. Label. Comp. Radiopharm.*, **2003**, 46, 587
- 266) Gründer, G.; Siessmeier, T.; Lange-Asschenfeldt, C.; Vernaleken, I.; Buchholz, H. G.; Stoeter, P.; Drzezga, A.; Lüddens, H.; Rösch, F.; Bartenstein, P. *Eur. J. Nucl. Med.*, **2001**, 28, 1463
- 267) Satyamurthy, N.; Barrio, J. R.; Bida, G. T.; Huang, S. C.; Mazziotta, J. C.; Phelps, M. E. *Appl. Radiat. Isot.*, **1990**, 41, 113
- 268) Satyamurthy, N.; Bida, G. T.; Barrio, J. R.; Luxen, A.; Mazziotta, J. C.; Huang, S. C.; Phelps, M. E. *Int. J. Radiat. Appl. Instrum., Part B*, **1986**, 13 (6), 617
- 269) Chi, D. Y.; Kilbourn, M. R.; Katzenellenbogen, J. A.; Brodack, J. W.; Welch, M. J. *Appl. Radiat. Isot.*, **1986**, 37, 1173
- 270) Goodman, M. M.; Kilts, C. D.; Keil, R.; Shi, B.; Martarello, L.; Xing, D.; Votaw, J.; Ely, T. D.; Lambert, P.; Owens, M. J.; Camp, V. M.; Malveaux, E.; Hoffman, J. M. *Nucl. Med. Biol.*, **2000**, 27 (1), 1
- 271) Zijlstra, S.; Visser, G. M.; Korf, J.; Vaalburg, W. *Appl. Radiat. Isot.*, **1993**, 44, 651
- 272) Wester, H. J.; Willoch, F.; Tölle, T. R.; Munz, F.; Herz, M.; Oye, I.; Schadrack, J.; Schwaiger, M.; Bartenstein, P. *J. Nucl. Med.*, **2000**, 41, 1279
- 273) Hamacher, K.; Coenen, H. H. *Appl. Radiat. Isot.*, **2002**, 57, 853
- 274) Suehiro, M.; Greenberg, J. H.; Shiue, C. Y.; Gonzales, C.; Dembowski, B.; Reivich, M. *Nucl. Med. Biol.*, **1996**, 23, 407
- 275) Tang, G.; Wang, M.; Tang, X.; Luo, L.; Gan, M. *Appl. Radiat. Isot.*, **2003**, 58, 219
- 276) Wilson, A. A.; Da Silva, J. N.; Houle, S. *Appl. Radiat. Isot.*, **1995**, 46 (8), 765
- 277) Wadsak, W.; Mitterhauser, M. *J. Label. Compd. Radiopharm.*, **2003**, 46, 1229
- 278) Wadsak, W.; Mitterhauser, M.; Mien, L. K.; Toegel, S.; Keppler, B.; Dudczak, R.; Kletter, K. *J. Label. Compd. Radiopharm.*, **2003**, 30, 1398
- 279) Mitterhauser, M.; Wadsak, W.; Mien, L. K.; Hoepfing, A.; Viernstein, H.; Dudczak, R.; Kletter, K. *Synapse*, **2005**, 55, 73

- 280) Shah, N. J.; Mauler, J.; Neuner, I.; Oros-Peusquens, A. M.; Romanzetti, S.; Vahedipour, K.; Felder, J.; Celik, A.; Iida, H.; Langen, K. J.; Herzog, H. *Nuclear Instruments and Methods in Physics Research A*, **2013**, 702, 16
- 281) Shah, N. J.; Herzog, H.; Weirich, C.; Tellman, L.; Kaffanke, J.; Caldeira, L.; Rota Kops, E.; Qaim, S. M.; Coenen, H. H.; Iida, H. *PLOS ONE*, **2014**, 9 (4), e95250
- 282) Jadvar, H.; Colletti, P. M. *European Journal of Radiology*, **2014**, 83, 84
- 283) Okamoto, T.; Ote, K.; Sakai, K.; Noda, A.; Shimizu, K.; Masuda, K.; Ohmura, T.; Watanabe, M. *Ann. Nucl. Med.*, **2014**, 28, 74
- 284) Lu, Y.; Yang, K.; Zhou, K.; Zhang, Q.; Pang, B.; Ren, Q. *Nuclear Instruments and Methods in Physics Research A*, **2014**, 743, 30
- 285) Casella, C.; Heller, M.; Joram, C.; Schneider, T. *Nuclear Instruments and Methods in Physics Research A*, **2014**, 736, 161
- 286) Pizzichemi, M. *Development of EndoTOFPET-US, a multi-modal endoscope for ultrasound and time of flight positron emission tomography: 13th topical seminar on innovative particle and radiation detectors and held in Siena (Italy) 7-10 October, 2013*. JINST, **2014**, 9, C02002
- 287) <http://endotofpet-us.web.cern.ch/endotofpet-us/> (accessed 16.5.2014)
- 288) http://www.fz-juelich.de/inm/inm-5/DE/Home/_Fokus/projekte2.html (accessed 16.5.2014)
- 289) Bengel, F.; Bonfiglioli, R.; Fanti, S. *Eur. J. Nucl. Med. Mol. Imaging*, **2014**, 41, 792
- 290) Zhang, H.; Huang, R.; Cheung, N. K. V.; Guo, H.; Zanzonico, P. B.; Thaler, H. T.; Lewis, J. S.; Blasberg, R. G. *Clin. Cancer Res.*, **2014**, 20 (8), 2182
- 291) Amir, M.; Kumar, H.; Khan, S. A. *Bioorg. Med. Chem. Lett.*, **2008**, 18, 918
- 292) Lévai, A.; *J. Heterocyclic Chem.*, **2002**, 39, 1
- 293) Mamolo, M. G.; Zampieri, D.; Falagiani, V.; Vio, L.; Banfi, E. *Il Farmaco*, **2001**, 56, 593
- 294) Bauer, U.; Egner, B. J.; Nilsson, I.; Berghult, M. *Tetrahedron Letters*, **2000**, 41, 2713
- 295) Badawy, D. S.; Abdel-Galil, E.; Kandeel, E. M.; Basyouni, W. M.; Khatab, T. K. *Phosphorus, Sulfur, and Silicon*, **2009**, 184, 2799

- 296) Basnet, A.; Thapa, P.; Karki, R.; Na, Y.; Jahng, Y.; Jeong, B. S.; Cheon Jeong, T.; Lee, C. S.; Lee, E. S. *Bioorg. Med. Chem.*, **2007**, 15, 4351
- 297) Verdonk, M. L.; Cole, J. C.; Hartshorn, M. J.; Murray, C. W.; Taylor, R. D. *Proteins*, **2003**, 52, 609
- 298) Korb, O.; Stützle, T.; Exner, T. E. *J. Chem. Inf. Model.*, **2009**, 49, 84
- 299) Wang, R.; Lai, L.; Wang, S. *J. Comput. Aided Mol. Des.*, **2002**, 16, 11
- 300) Kappe, C. O. *Angew. Chem. Int. Ed.*, **2004**, 43, 6250
- 301) Chemat, F.; Esveld, E. *Chem. Eng. Technol.*, **2001**, 24, 7
- 302) Siddiqui, M. A.; Nan, Y.; Patel, M. F.; Reddy, P. A. P.; Mansoor, U. F.; Meng, Z.; Vitharana, L. D.; Zhao, L.; Mandal, A. K.; Liu, D.; Tang, S.; Mccriner, A.; Belanger, D. B.; Curran, P. J.; Dai, C.; Angeles, A. R.; Yang, L.; Daniels, M. H. *PCT Int. Appl.*, **2011**, WO 2011090935 A1 20110728, 1ff.
- 303) Bailon, P.; Palleroni, A.; Schaffer, C. A.; Spence, C. L.; Fung, W. J.; Porter, J. E. *Bioconjugate Chem.*, **2001**, 12, 195
- 304) Malik, F.; Delgado, C.; Knusli, C.; Irvine, A.E.; Fisher, D.; Francis, G.E. *Experimental Hematology*, **1992**, 20 (8), 1028
- 305) Zalipsky, S. *Advanced Drug Delivery Reviews*, **1995**, 16, 157
- 306) Patel, M. M.; Goyal, B. R.; Bhadada, S. V.; Bhatt, J. S.; Amin, A. F. *CNS Drugs*, **2009**, 23 (1), 35
- 307) Garcia-Garcia, E.; Andrieux, K.; Gil, S.; Couvreur, P. *International Journal of Pharmaceutics*, **2005**, 298, 274
- 308) Kniess, T.; Spies, H.; Santos, I.; Zablotska, A. *J. Label. Compds. Radiopharm.*, **2002**, 45, 629
- 309) Zhang, W.; Oya, S.; Kung, M. P.; Hou, C.; Maier, D. L.; Kung, H. F. *Nucl. Med. Biol.*, **2005**, 32, 799
- 310) Bouzide, A.; LeBerre, N.; Saufé, G. *Tetrahedron Lett.*, **2001**, 42, 8781
- 311) Khusnutdinov, R. I.; Baiguzina, A. R.; Mukminov, R. R.; Dzhemilev, U. M. *Russian Journal of Applied Chemistry*, **2009**, 82 (2), 340

- 312) Aginagalde, M.; Bello, T.; Masdeu, T.; Vara, Y.; Arrieta, A.; Cossio, F. P. *J. Org. Chem.*, **2010**, 75, 7435
- 313) Braun, S.; Kalinowski, O. O.; Berger, S. *150 and More Basic NMR Experiments: A Practical Course – Second Expanded Edition*, Wiley-VCH, Weinheim, **1998**
- 314) Duncton, M. A. *J. Med. Chem. Comm.*, **2011**, 2, 1135
- 315) Minisci, F. *Synthesis*, **1973**, 1
- 316) Kürti, L.; Czakó, B. *Strategic Applications of Named Reactions in Organic Synthesis: Background and Detailed Mechanisms*, Elsevier Academic Press, **2005**, 290
- 317) Bartlett, P. A.; Johnson, W. S. *Tetrahedron Letters*, **1970**, 11 (51), 4459
- 318) Chooekawong, K., *Synthesis of pyrazoline based derivatives for the application as MAO-B inhibitors*. Bachelor Thesis, University of Vienna, Vienna, **2013**
- 319) Ilankumaran, P.; Verkade, J. G. *J. Org. Chem.*; **1999**, 64, 3086
- 320) Jochsch, C., *Noradrenalin-Wiederaufnahme-Hemmer mit Imidazolstrukturen als PET-Precursor*. Diplomarbeit, Universität Wien, Wien, **2014**
- 321) Kocienski, P. J. *Protecting Groups*. 3rd Ed., Georg Thieme Verlag, Stuttgart-New York, **2005**, 417 ff.
- 322) Cynamon, M. H.; Klemens, S. P. *J. Med. Chem.*, **1992**, 35 (7), 1212
- 323) Chavan, S. P.; Subbarao, Y. T.; Dantale, S. W.; Sivappa, R. *SYNTHETIC COMMUNICATIONS*, **2001**, 31 (2), 289
- 324) Pardridge, W. M. *Advanced drug delivery reviews*, **1995**, 15, 5
- 325) Clark, D. E. *Journal of pharmaceutical sciences*, **1999**, 88 (8), 807
- 326) Suomalainen, P.; Johans, C.; Soderlund, T.; Kinnunen, P. K. *Journal of medicinal chemistry*, **2004**, 47 (7), 1783
- 327) Mano, Y.; Higuchi, S.; Kamimura, H. *Biopharmaceutics & drug disposition*, **2002**, 23 (9), 351
- 328) Shen, D. D.; Artru, A. A.; Adkison, K. K. *Advanced drug delivery reviews*, **2004**, 56 (12), 1825
- 329) Ross, T. M.; Martinez, P. M.; Renner, J. C.; Thorne, R. G.; Hanson, L. R.; Frey, W. H. *Journal of neuroimmunology*, **2004**, 151 (1-2), 66

- 330) Otis, K. W.; Avery, M. L.; Broward-Partin, S. M.; Hansen, D. K.; Behlow, H. W. Jr.; Scott, D. O.; Thompson, T. N. *Journal of pharmacological and toxicological methods*, **2001**, 45 (1), 71
- 331) Yamazaki, M.; Terasaki, T.; Yoshioka, K.; Nagata, O.; Kato, H.; Ito, Y., Tsuji, A. *Pharmaceutical research*, **1994**, 11 (7), 975
- 332) Murakami, H.; Sawada, N.; Koyabu, N.; Ohtani, H.; Sawada, Y. *Pharmaceutical research*, **2000**, 17 (12), 1526
- 333) Faassen, F.; Vogel, G.; Spanings, H.; Vromans, H. *International journal of pharmaceutics*, **2003**, 263 (1-2), 113
- 334) Di, L.; Kerns, E. H.; Fan, K.; McConnell, O. J.; Carter, G. T. *European journal of medicinal chemistry*, **2003**, 38 (3), 223
- 335) Dash, A. K.; Elmquist, W. F. *Journal of chromatography B, Analytical technologies in the biomedical and life sciences*, **2003**, 797 (1-2), 241
- 336) Giaginis, C.; Tsantili-Kakoulidou, A. *Journal of Pharmaceutical Sciences*, **2008**, 97 (8), 2984
- 337) Giaginis, C.; Tsantili-Kakoulidou, A. *J. Liq. Chromatogr. Related Technol.*, **2008**, 31, 79
- 338) Ong, S.; Liu, H.; Pidgeon, C. *J. Chromatogr. A*, **1996**, 728(1-2), 113
- 339) Yang, C.; Cai, S. R.; Lui, H.; Pidgeon, C. *Advanced drug delivery reviews*, **1996**, 23, 229
- 340) Ong, S.; Liu, H.; Pidgeon, C. *J. Chromatogr. A*, **1996**, 728 (1-2), 113
- 341) Donovan, S. F.; Pescatore, M. C. *J. Chromatogr. A*, **2002**, 952, 47
- 342) Vraka, C. unpublished data
- 343) Naik, P.; Cucullo, L. *J. Pharm. Sci.*, **2012**, 101, 1337
- 344) Taillardat-Bertschinger, A.; Carrupt, P. A.; Barbato, F.; Testa, B. *J. Med. Chem.*, **2003**, 46 (5), 655
- 345) Vraka, C.; Nics, L.; Weiss, V.; Wagner, K. H.; Hacker, M.; Wadsak, W.; Mitterhauser, M. *Eur. J. Nucl. Med. Mol. Imaging*, **2014**, 41, 442
- 346) Penmatsa, A.; Wang, K. H.; Gouaux, E. *Nature*, **2013**, 503, 85
- 347) Wang, H.; Goehring, A.; Wang, K. H.; Penmatsa, A.; Ressler, R.; Gouaux, E. *Nature*, **2013**, 503, 141

- 348) Tatsumi, M.; Groshan, K.; Blakely, R. D.; Richelson, E. *European Journal of Pharmacology*, **1997**, 340, 249
- 349) Richter, L.; de Graaf, C.; Sieghart, W.; Varagic, Z.; Morzinger, M.; de Esch, I. J.; Ecker, G. F.; Ernst, M., *Nature chemical biology*, **2012**, 8, 455
- 350) Andersen, J.; Olsen, L.; Hansen, K. B.; Taboureau, O.; Jorgensen, F. S.; Jorgensen, A. M.; Bang-Andersen, B.; Egebjerg, J.; Stromgaard, K.; Kristensen, A. S. *The Journal of biological chemistry*, **2010**, 285, 2051
- 351) Chelli, R.; Gervasio, F. L.; Procacci, P.; Schettino, V. *J. Am. Chem. Soc.*, **2002**, 124, 6133
- 352) Kiankarimi, M.; Hudson, S.; Dwight, W. J.; Wesley, J.; Wade, W. S. *U.S. Pat. Appl. Publ.*, **2006**, US 20060252818 A1 20061109, 1 ff.
- 353) Pandey, V. K. *Current Science*, **1981**, 50 (15), 678
- 354) Claremon, D. A., Zhuang, L.; Leftheris, K.; Tice, C. M.; Xu, Z.; Ye, Y.; Singh, S. B.; Cacatian, S.; Zhao, W.; Himmelsbach, F.; Eckhardt, M. *PCT Int. Appl.*, **2009**, WO 2009134392 A1, 1ff
- 355) Lu, S. Y.; Chin, F. T.; McCarron, J. A.; Pike, V. W. *J. Label. Compd. Radiopharm.*, **2001**, 47, 289
- 356) Schrödinger Suite 2013 Protein Preparation Wizard; Epik version 2.6, Schrödinger, LLC, New York, NY, 2013; Impact version 6.1, Schrödinger, LLC, New York, NY, 2013; Prime version 3.3, Schrödinger, LLC, New York, NY, **2013**
- 357) LigPrep, version 2.5, Schrödinger, LLC, New York, NY, **2012**
- 358) Verdonk, M. L.; Cole, J. C.; Hartshorn, M. J.; Murray, C. W.; Taylor, R. D. *Proteins*, **2003**, 52, 609
- 359) Molecular Operating Environment (MOE), C. C. G. I., 1010 Sherbooke St. West, Suite #910, Montreal, QC, Canada, H3A 2R7, **2013**
- 360) Wang, R.; Lai, L.; Wang, S. *J. Comput. Aided Mol. Des.*, **2002**, 16, 11
- 361) Penmatsa, A.; Wang, K. H.; Gouaux, E. *Nature*, **2013**, 503, 85
- 362) Sali, A.; Potterton, L.; Yuan, F.; van Vlijmen, H.; Karplus, M. *Proteins*, **1995**, 23, 318
- 363) Jones, G.; Willett, P.; Glen, R. C.; Leach, A. R.; Taylor, R. *Journal of Molecular Biology*, **1997**, 267, 727

- 364) Addinsoft Inc., N. Y., NY. USA
- 365) Becker, H. D.; Andersson, K. *J. Org. Chem.*, **1983**, 48, 4542
- 366) Hawker, C. J.; Chu, F.; Pomery, P. J.; Hill, D. J. T. *Macromolecules*, **1996**, 29, 3831
- 367) Noyce, D. S.; Lipinski, C. A.; Nichols, R. W. *J. Org. Chem.*, **1972**, 37 (16), 2615
- 368) Blackburn, C.; Gigstad, K. M.; Xu, H. *PCT Int. Appl.*, **2011**, WO 2011106627, 140 ff.
- 369) Khusnutdinov, R. I.; Baiguzina, A. R.; Mukminov, R. R.; Dzhemilev, U. M. *Russian Journal of Applied Chemistry*, **2009**, 82 (2), 340
- 370) Bettle, P. J.; Dawe, L. N.; Anwar, M. Wu.; Thompson L. K. *Eur. J. Inorg. Chem.*, **2011**, 5036
- 371) Zhang, W.; Sun, W.; Wu, B.; Zhang, S.; Ma, H.; Li, Y.; Chen, J.; Hao, P. *Journal of Organometallic Chemistry*, **2006**, 691 (22), 4759
- 372) Garrido, D. O. A.; Buldain, G.; Ojea, M. I.; Frydman, B. *J. Org. Chem.*, **1988**, 53, 403
- 373) Muratake, H.; Matsumura N.; Natsume, M. *Chem. Pharm. Bull.*, **1998**, 46 (4), 559
- 374) Yu, F.; Zhou, J. N.; Zhang, X. C.; Sui, Y. Z.; Wu, F. F.; Xie, L. J.; Chan, A. S. C.; Wu, J. *Chemistry - A European Journal*, **2011**, 17 (50), 14234
- 375) La Regina, G.; Diodata D'Auria, F.; Tafi, A.; Piscitelli, F.; Olla, S.; Caporuscio, F.; Nencioni, L.; Cirilli, R.; La Torre, F.; Rodrigues De Melo, N.; Kelly, S. L.; Lamb, D. C.; Artico, M.; Botta, M.; Palamara, A. T.; Silvestri, R. *J. Med. Chem.*, **2008**, 51, 3841
- 376) Liu, P.; Wang, Z.; Hu, X. *European Journal of Organic Chemistry*, **2012**, 10, 1994
- 377) Varney, M. D.; Romines, W. H.; Boritzki, T.; Margosiak, S. A.; Barlett, C.; Howland, E. J. *J. Heterocyclic Chem.*, **1995**, 32 (5), 1493
- 378) Xu, Z. B.; Lu, Y.; Guo, Z. R. *Synlett*, **2003**, 4, 564
- 379) Wang, X. J.; Xi, M. Y.; Fu, J. H.; Zhang, F. R.; Cheng, G. F.; Yin, D. L.; You, Q. D. *Chinese Chemical Letters*, **2012**, 23, 707
- 380) Panagopoulos, A. M.; Steinman, D.; Goncharenko, A.; Geary, K.; Schleisman, C.; Spaargaren, E.; Zeller, M.; Becker, D. P. *JOC*, **2013**, 78, 3532
- 381) Medchem Project logP database, available through Biobyte, Claremont CA. (<http://www.biobyte.com/>)

- 382) Hansch, C.; Leo, A. J.; Hoekman, D. *Exploring QSAR; Hydrophobic, Electronic, and Steric Constants* (ACS Professional Reference Book), American Chemical Society, Washington, DC, **1995**
- 383) Hansch, C.; Leo, A. J. *Substituent Constants for Correlation Analysis in Chemistry and Biology*, Wiley, New York, **1979**
- 384) Leo, A. J.; Hansch, C.; Elkins, D. *Chem. Rev.*, **1971**, 71, 525

5.1 List of Abbreviations

A β	beta amyloid	cAMP	cyclic adenosine mono
ACN	acetonitrile		phosphate
AcOH	acetic acid	CB1 receptor	cannabinoid 1 receptor
AD	Alzheimer's disease	CDI	1, 1'-
ADHD	attention deficit hyper-		carbonyldiimidazole
	activity disorder	cDNA	complementary deoxy
ALOX	aluminum oxide		ribonucleic acid
ALS	amyotrophic lateral	cf.	confer
	sclerosis	CNS	central nervous system
anth	anthracene	COSY	correlation spectroscopy
APT	attached proton test	CT	computed tomography
AR	adrenergic receptor	CXCL12	C-X-C motif chemokine
Asp	asparagine		12
ATP	adenosine triphosphate	CXCR4	C-X-C chemokine recep-
BAT	brown adipose tissue		tor type 4
BBB	blood brain barrier	CYP2D6	cytochrome 2D6
benz	benzene	d	deuterium
benzim	benzimidazolone	D ₂	deuterium
β -CIT	2beta-carbomethoxy-	2D	two-dimensional
	3beta-(4'-iodo-	3D	three-dimensional
	phenyl)tropane	DA	dopamine
BGO	bismuth germinate	DASB	3-amino-4-(2-dimethyl-
B _{max}	maximum of drug spe-		aminomethyl-phenyl-
	cifically binding to re-		sulfanyl)benzonitrile
	ceptor	DAT	dopamine transporter
BMI	body mass index	DCC	N,N'-
BNST	bed nucleus of the stria		dicyclohexylcarbodi-
	terminalis		imide
ca.	circa	dDAT	drosophila dopamine
calc.	calculated		transporter

ΔG	Gibbs free energy	gs-HMBC	gradient-selected heteronuclear multiple bond correlation
DIPEA	<i>N,N</i> -Diisopropylethylamine		
DMAP	dimethylaminopyridine	gs-HSQC	gradient-selected heteronuclear single quantum coherence
DMF	dimethylformamid		
DMSO	dimethylsulfoxid		
DOPA	dihydroxyphenylalanine	h	hour(s)
DSM	Diagnostic and Statistical Manual	hDAT	human dopamine transporter
DTI	diffusion tensor imaging	HEK	human embryonic kidney
e^+	positron		
e^-	electron	hNET	human norepinephrine transporter
e.g.	exempli gratia		
<i>et al</i>	et alii	HPLC	high performance liquid chromatography
etc.	etcetera		
exp	exponential function	HSA	human serum albumin
exp	experimental	hSERT	human serotonin transporter
FAD	flavin adenin dinucleotide	HSL	hormone-sensitive lipase
[^{18}F]FDG	2-[^{18}F]-fluoro-D-deoxy-D-glucose	5-HT	5-Hydroxytryptamine
$\text{Fe}(\text{acac})_3$	Tris(acetylacetonato)iron(III)	IAM	immobilized artificial membrane
FFA	free fatty acids	IC_{50}	inhibitory concentration
fig.	figure	i.e.	id est
fMRI	functional magnetic resonance imaging	Ile	isoleucine
FOV	field of view	isochr	4,3-dihydro-1 <i>H</i> -isochromene
fur	furan	K_{222}	Kryptofix 2.2.2.
GABA	gamma-Aminobutyric acid	K_D	dissociation constant
Glu	glutamic acid	keV	kiloelectron volt
		K_i	inhibition constant

K_m	membrane partition coefficient	n n.a.	neutron not available
L	ligand	NaOMe	sodium methoxide
LeuBAT	“SERT”-ized leucine transporter	n.d. NE	not detectable norepinephrine
logP	partition-coefficient	NET	norepinephrine trans- porter
LOR	line of response		
LSO	lutetium oxyorthosili- cate	NFTs nM	neurofibrillary tangles nanomolar
LYSO	lutetium yttrium ortho- silicate	NMR	Nuclear Magnetic Reso- nance
M	molar	NOE	nuclear overhouser effect/enhancement
MAO	monoamine oxidase		
MeV	megaelectron volt	NOESY	nuclear overhauser enhancement spectros- copy
min	minutes		
ml	millilitre		
μ l	microlitre	Nu	nucleophile
mm	millimeters	NuH	protonated nucleophile
mM	millimolar	p	proton
μ M	micromolar	PAMPA	parallel artificial membrane assay
MOE	Molecular Operating Environment	PB	potassium benzoate
mp.	melting point	PD	Parkinson’s disease
MPTP	1-methyl-4-phenyl- 1,2,3,6- tetrahydropyridine	PDB Pd(0) L_n	Protein Data Bank palladium(0)-ligand- complex
MR	magnet resonance	PE	petroleum ether
MRI	magnetic resonance imaging	PE2I	N-(3-iodopro-2E-enyl)- 2beta-carbomethoxy- 3beta-(4'-methylphenyl)
mRNA	messenger ribonucleic acid		nortropane
MW	microwave	PEA	beta-phenylethylamine

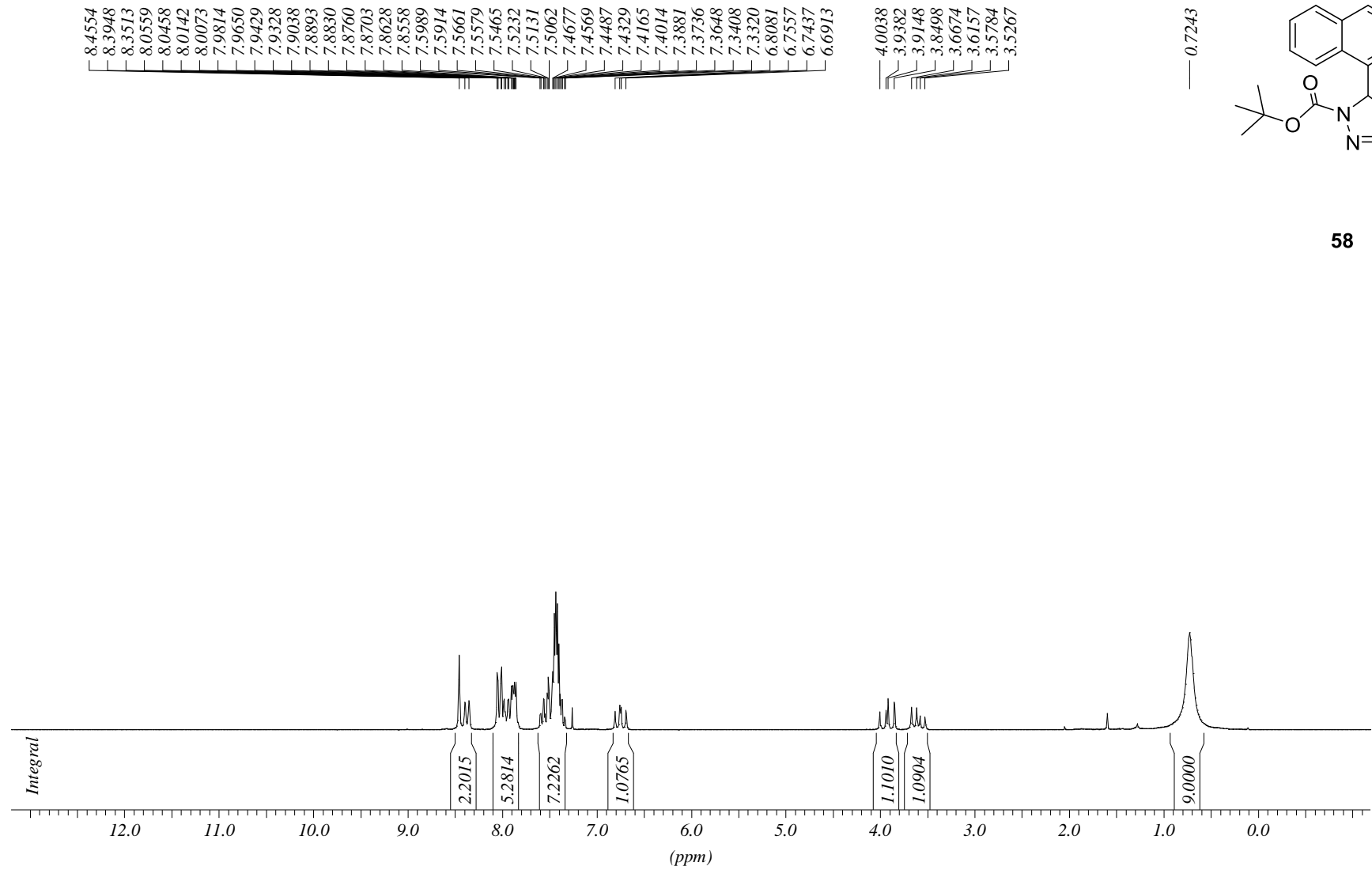
PEG	polyethylene glycole	TBAF	tetra- <i>n</i> -butylammonium fluoride
PET	positron emission tomography	TBD	triazabicyclo[4.4.0]dec-5-ene
pH	potentia/pondus hydrogenii	TCS	tetrachlorosilane
PhD	Doctor of Philosophy	TEA	triethylamine
Phe	phenylalanine	TG	triglycerides
phen	phenyl	th	thiophene
PIB	Pittsburgh compound B	Ti(O- <i>i</i> Pr) ₄	titanisopropoxid
PKa	scale of acidity	TLC	thin-layer chromatography
P _m	permeability	TMB	trimethylboroxine
PMT(s)	photomultiplier tube(s)	TMD(s)	transmembrane-spanning domain(s)
ppm	pars per million	TOCSY	total correlated spectroscopy
PSA	polar surface area	TOV	time of flight
PSMA	prostate specific membrane antigen	TsCl	tosyl chlorid
pyr	pyrazole	Tyr	tyrosine
pyra	pyrazine	UCP	uncoupling protein
pyrid	pyridine	v _e	neutrino
R	gas constant (J mol ⁻¹ K ⁻¹)	V _m	mobile phase volume
R _f	retardation factor	V _s	stationary phase volume
ROS	reactive oxygen species	W	Watt
rt	room temperature	WAT	white adipose tissue
SERT	serotonin transporter	Y	yield
SiPM(s)	silicon photomultiplier(s)		
SPECT	single photon emission computed tomography		
t _{1/2}	half-life		
tanδ	loss factor		
T	temperature (°C or K)		

5.2 Abbreviations of FAPPI and PHOXI derivatives

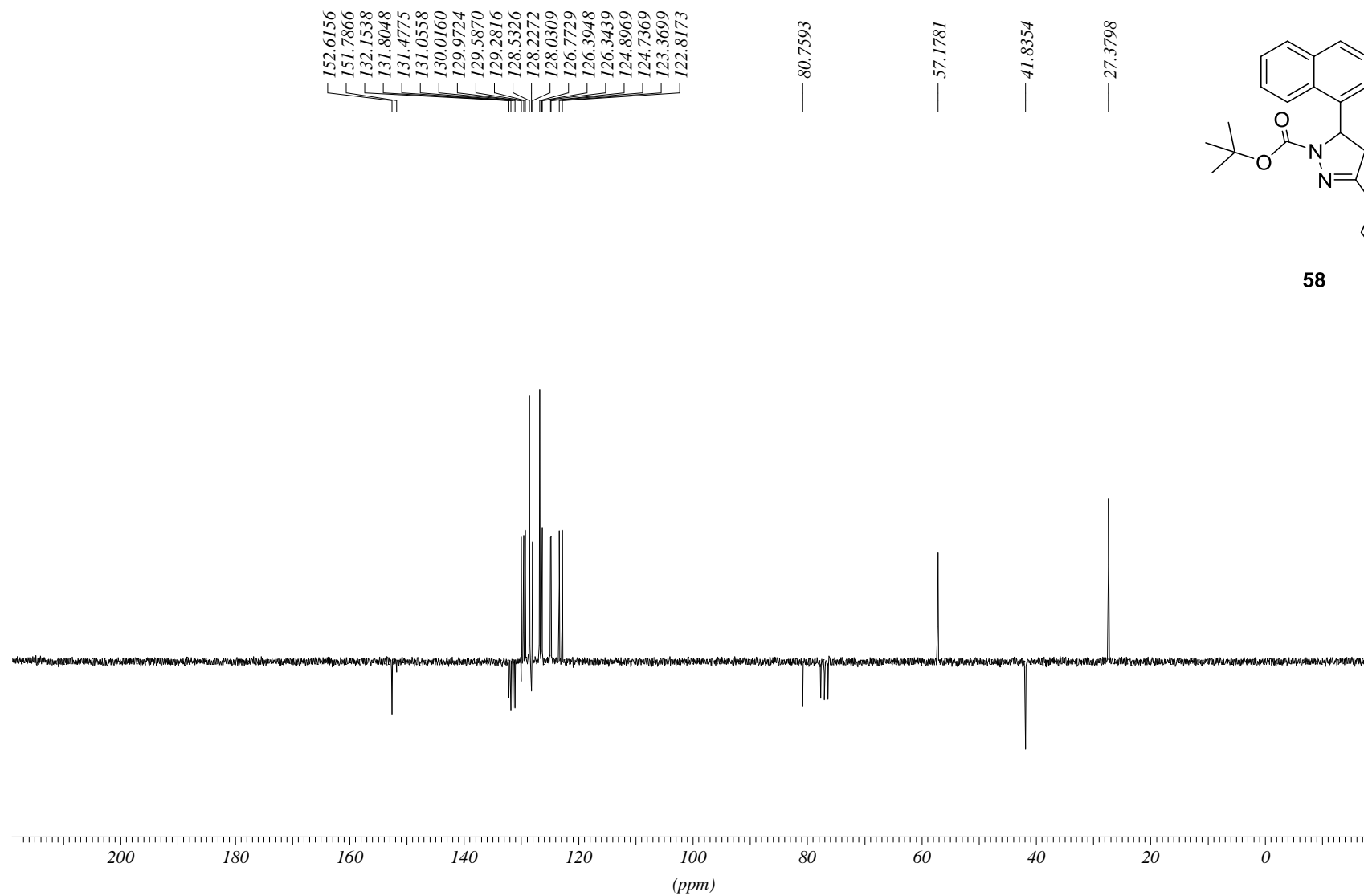
APPI:1	1-(3-Amino-1-(4-fluorophenyl)propyl)-3-phenyl-1,3-dihydro-2 <i>H</i> -benzimidazol-2-one
FAPPI:1	1-(1-(4-Fluorophenyl)-3-(methylamino)propyl)-3-phenyl-1,3-dihydro-2 <i>H</i> -benzimidazol-2-one
FAPPI:2	1-(4-Fluorophenyl)-3-(3-(methylamino)-1-phenylpropyl)-1,3-dihydro-2 <i>H</i> -benzimidazol-2-one
FAPPI:3	1-(2-Fluorophenyl)-3-(3-(methylamino)-1-phenylpropyl)-1,3-dihydro-2 <i>H</i> -benzimidazol-2-one
Me@PHOXI1	<i>N,N</i> -Dimethyl-1-((3 <i>S</i> ,4 <i>S</i>)-4-(2-methylphenoxy)-3,4-dihydro-1 <i>H</i> -isochromen-3-yl)methanamine
PHOXI:1	<i>N</i> -Methyl-1-((3 <i>S</i> ,4 <i>S</i>)-4-(2-methylphenoxy)-3,4-dihydro-1 <i>H</i> -isochromen-3-yl)methanamine
FE@PHOXI1	2-Fluoro- <i>N</i> -methyl- <i>N</i> -(((3 <i>S</i> ,4 <i>S</i>)-4-(2-methylphenoxy)-3,4-dihydro-1 <i>H</i> -isochromen-3-yl)methyl)ethanamine
Me@PHOXI2	<i>N,N</i> -Dimethyl-1-((3 <i>S</i> ,4 <i>S</i>)-4-(2-(trifluoromethyl)phenoxy)-3,4-dihydro-1 <i>H</i> -isochromen-3-yl)methanamine
PHOXI:2	<i>N</i> -Methyl-1-((3 <i>S</i> ,4 <i>S</i>)-4-(2-(trifluoromethyl)phenoxy)-3,4-dihydro-1 <i>H</i> -isochromen-3-yl)methanamine
FE@PHOXI2	2-Fluoro- <i>N</i> -methyl- <i>N</i> -(((3 <i>S</i> ,4 <i>S</i>)-4-(2-(trifluoromethyl)phenoxy)-3,4-dihydro-1 <i>H</i> -isochromen-3-yl)methyl)ethanamine

5.3 SPECTRA

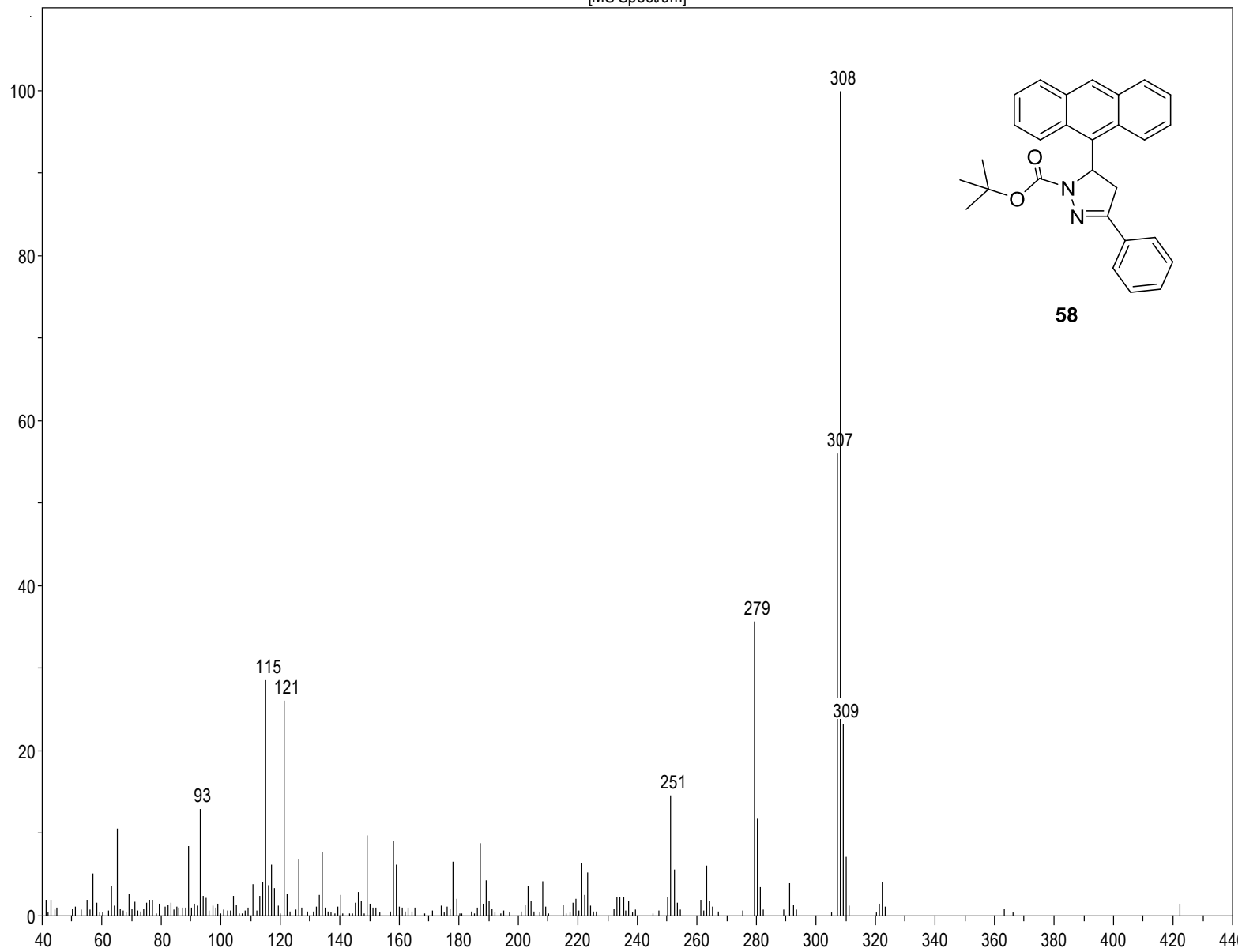
PROTON CDCl3 opt/xwinnmr neudorfer 36

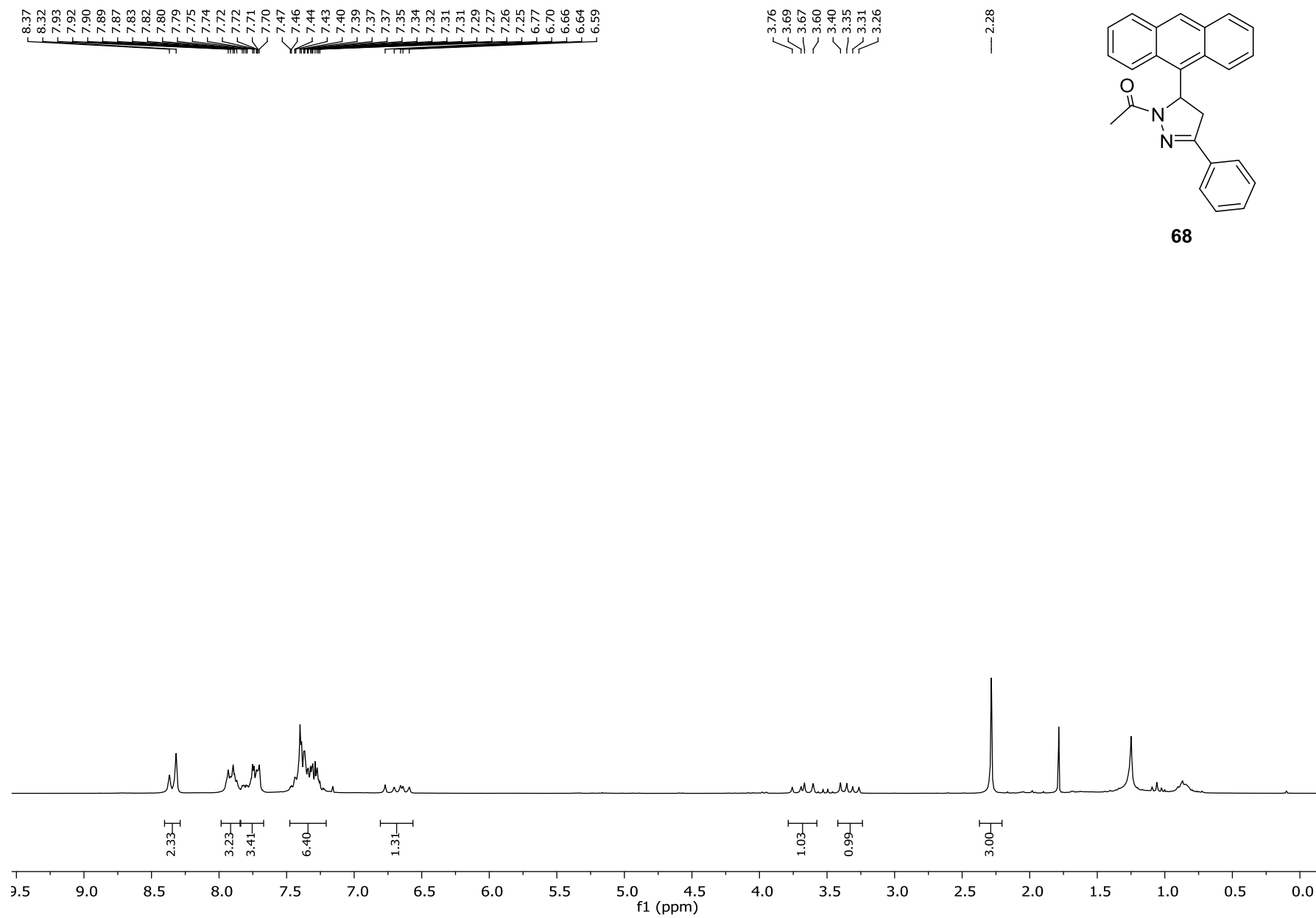


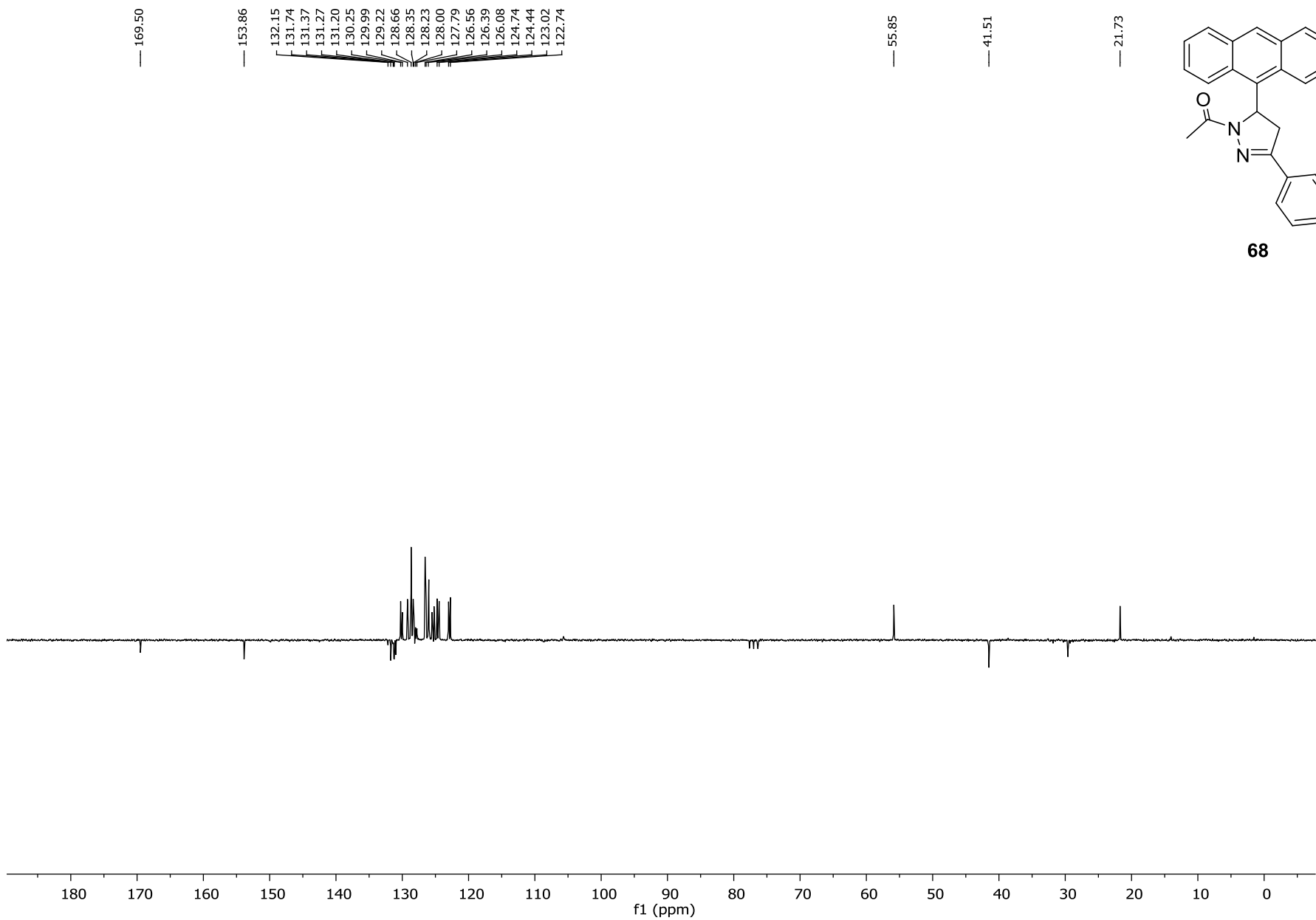
C13APT CDCl3 opt/xwinmmr neudorfer 36



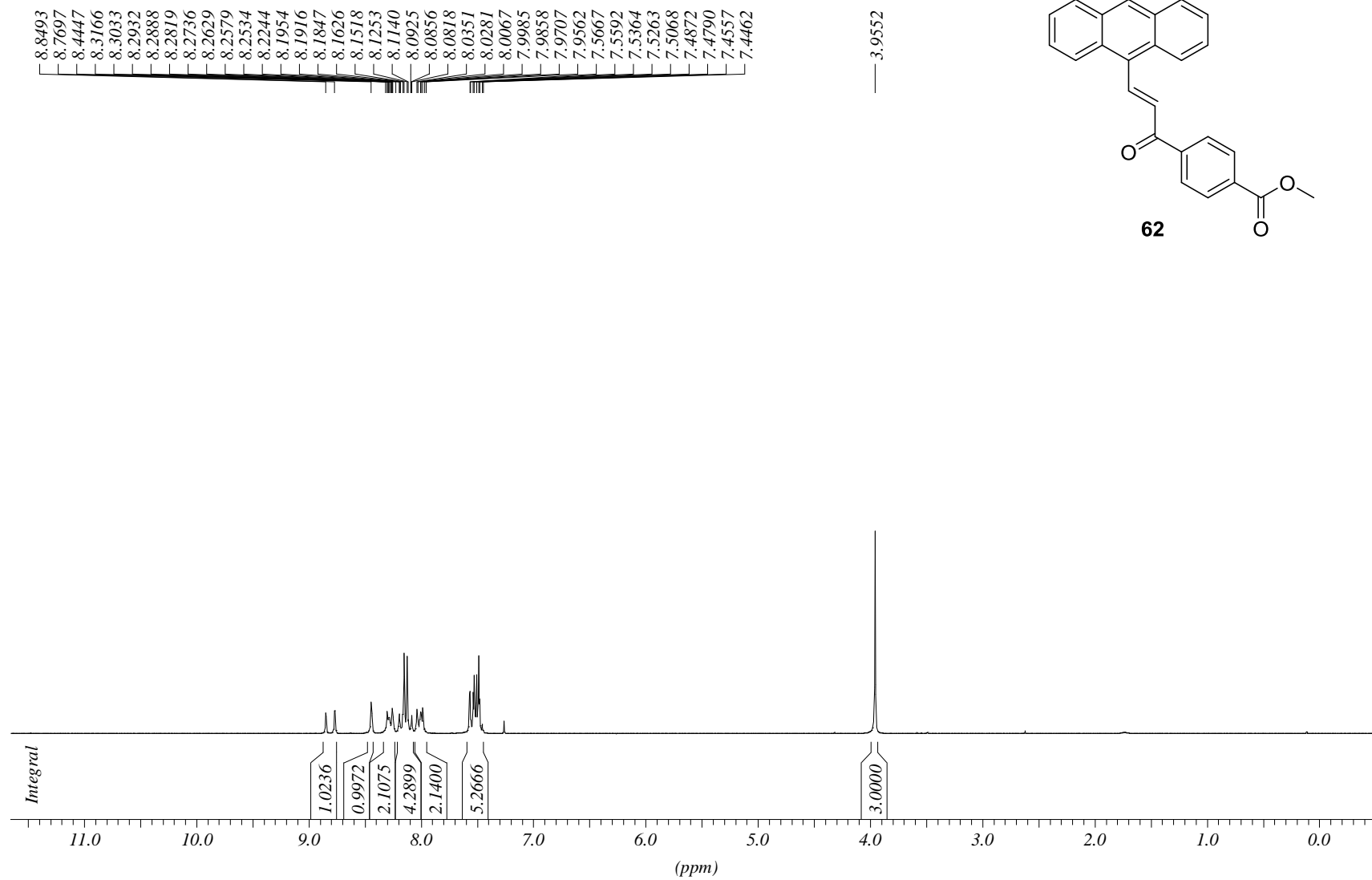
[MS Spectrum]



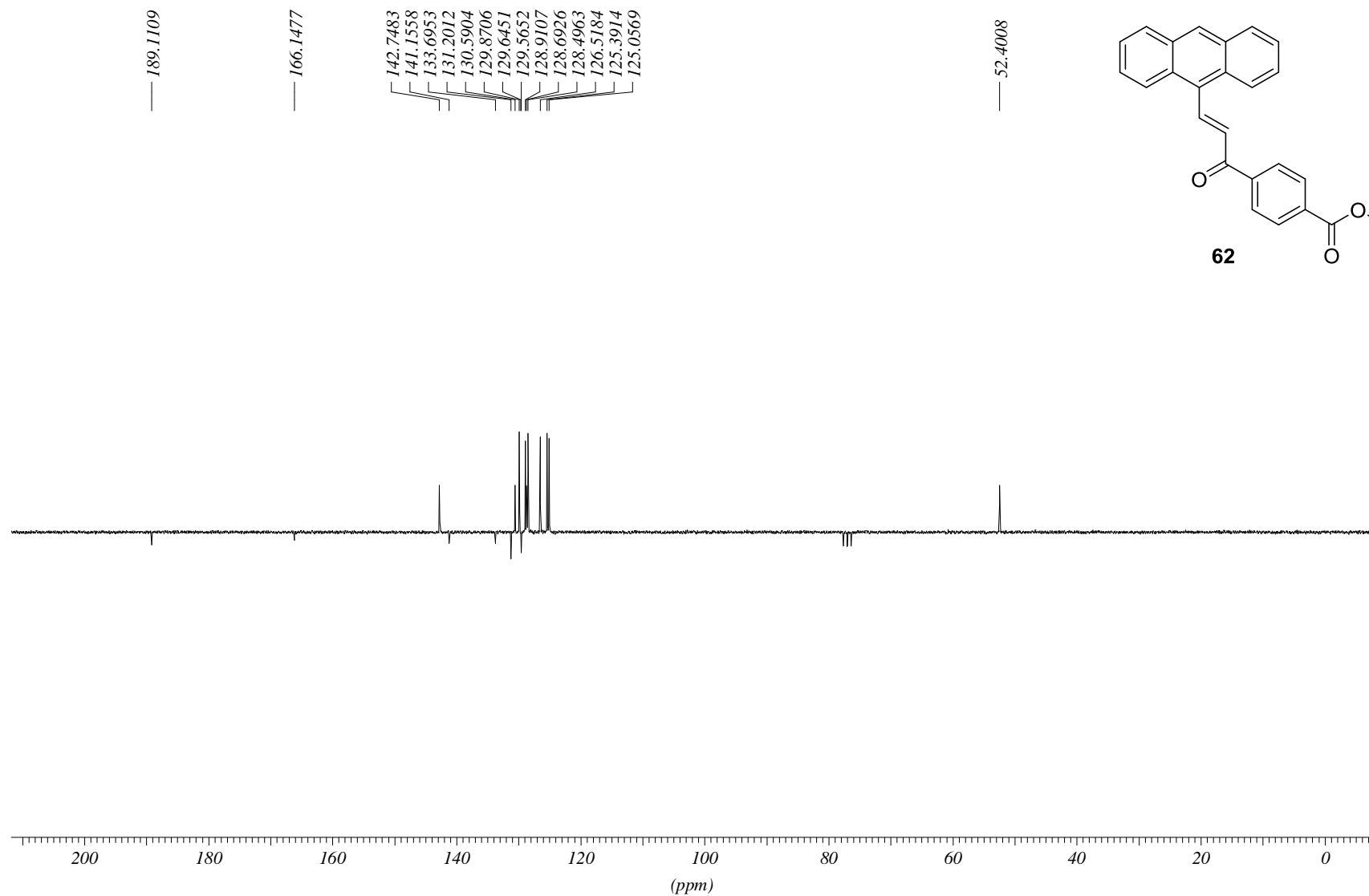


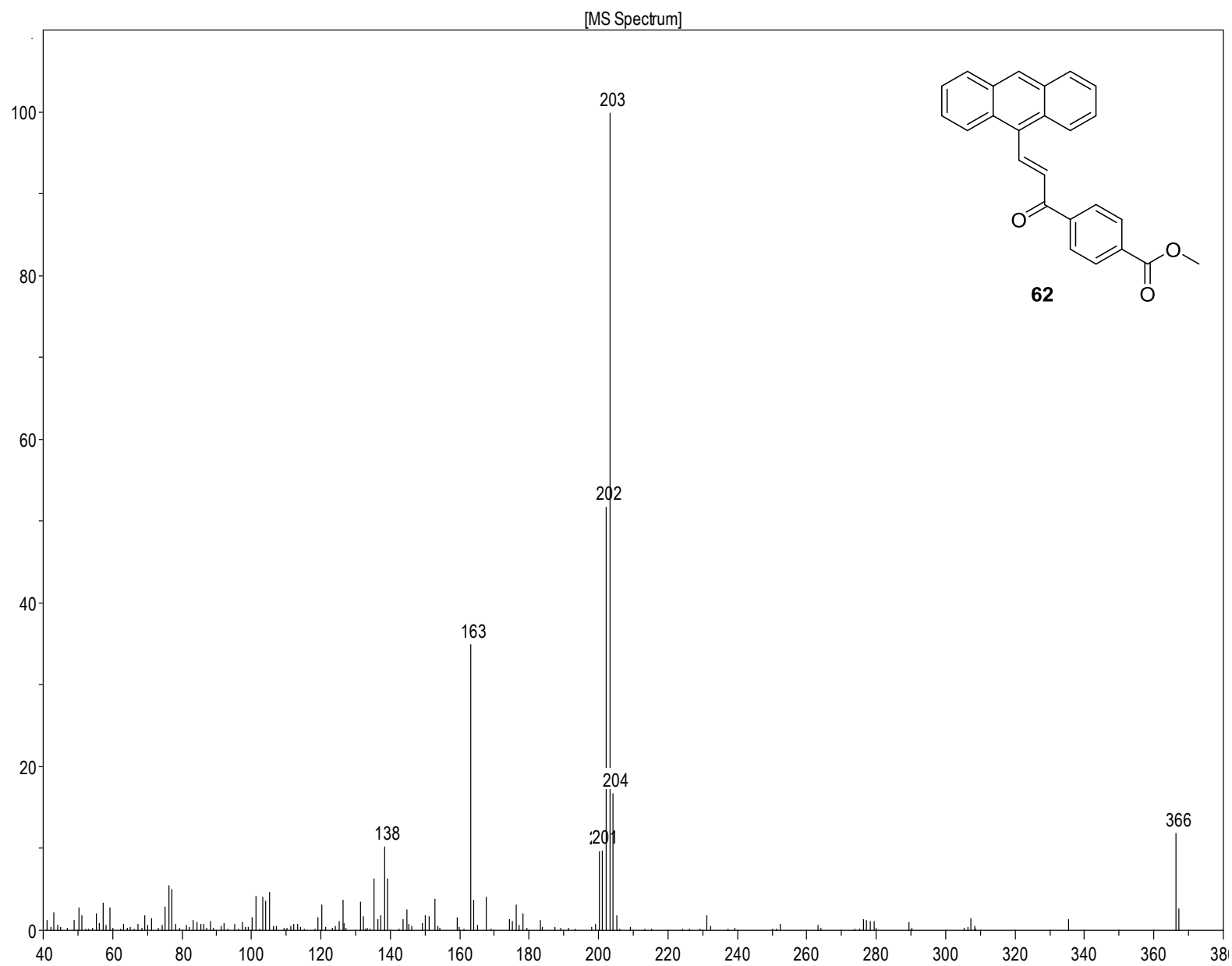


PROTON CDCl3 opt/xwinnmr neudorfer 33

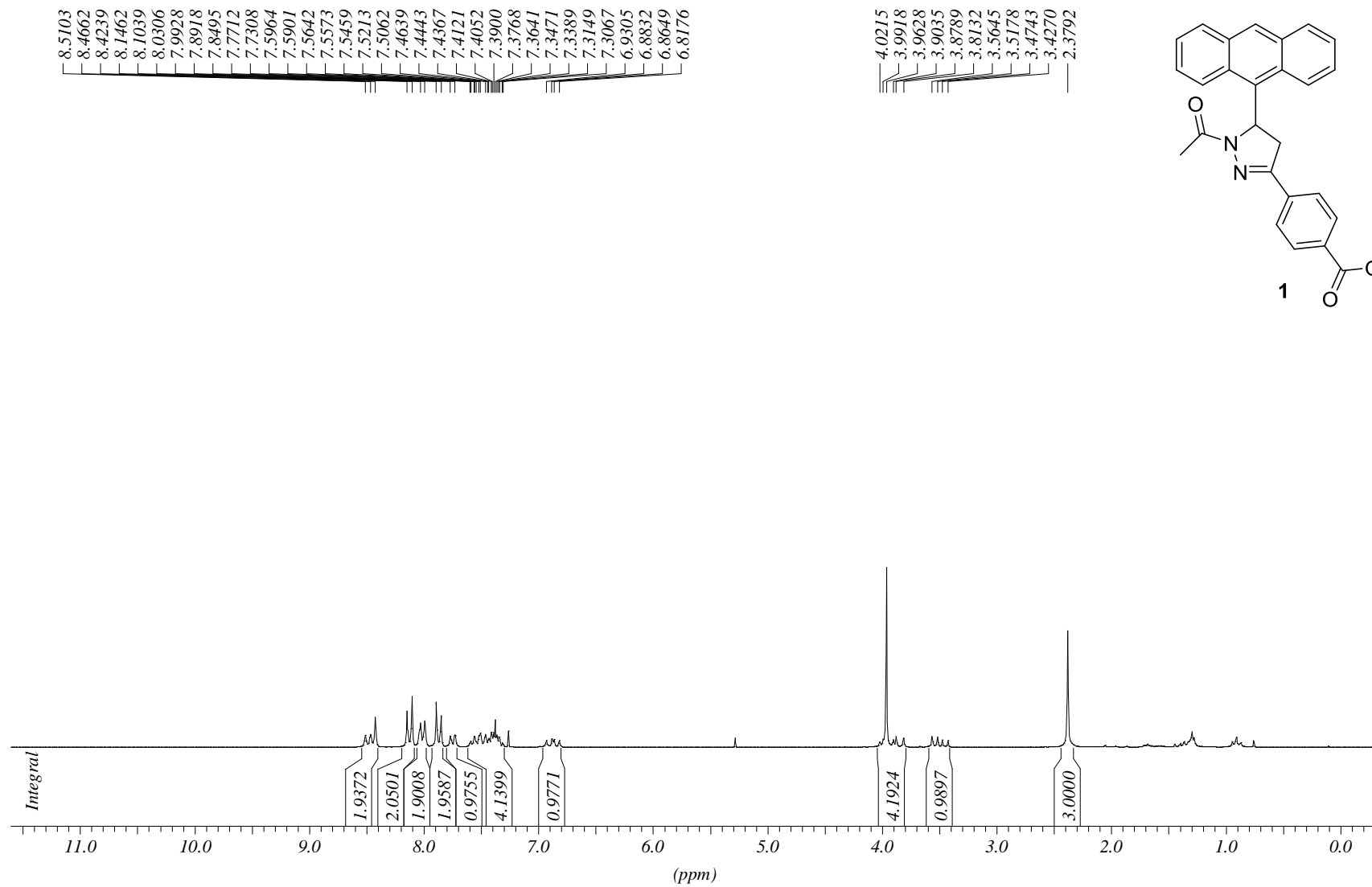


C13APT CDCl3 opt/xwinmr neudorfer 33

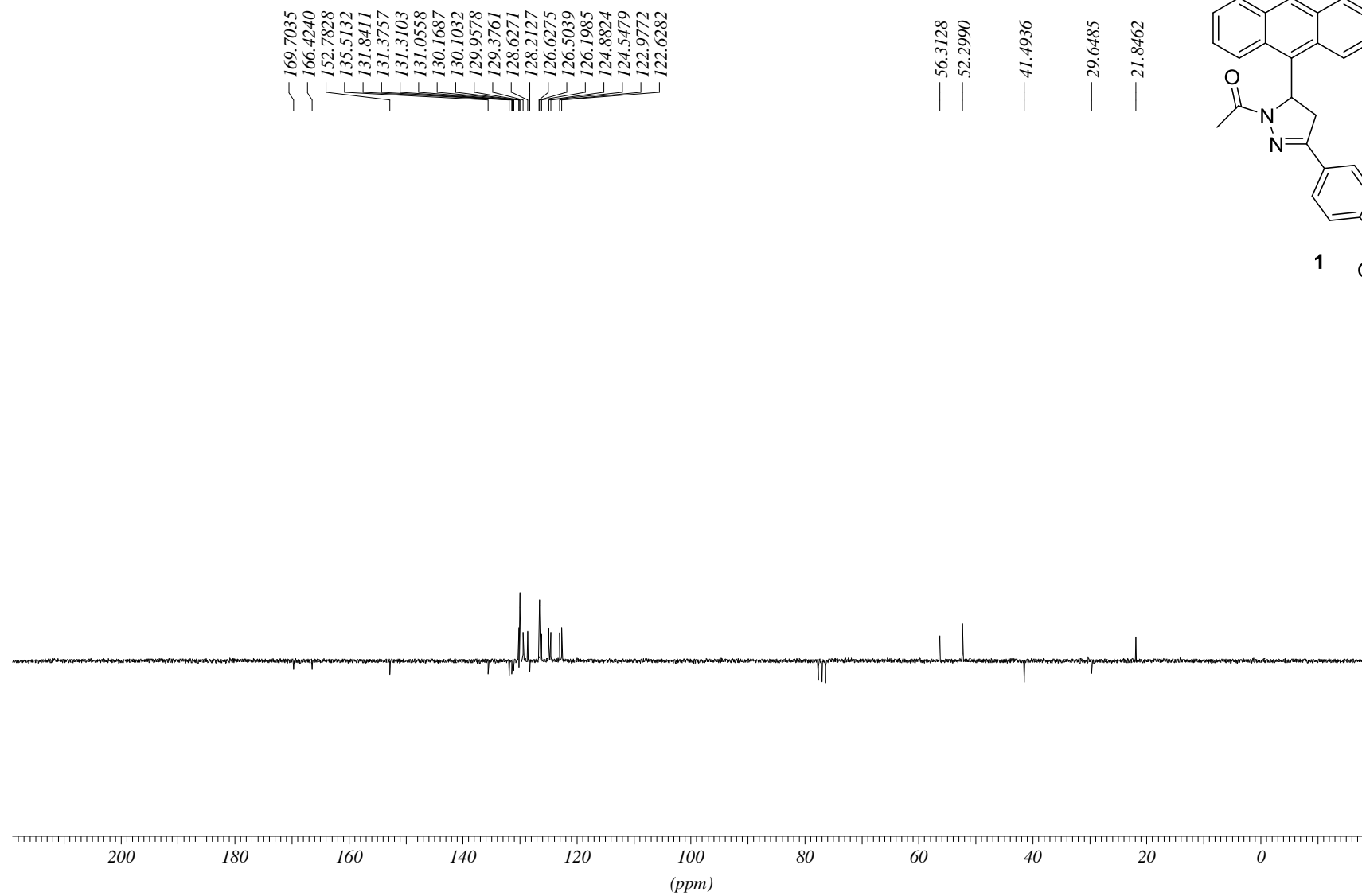




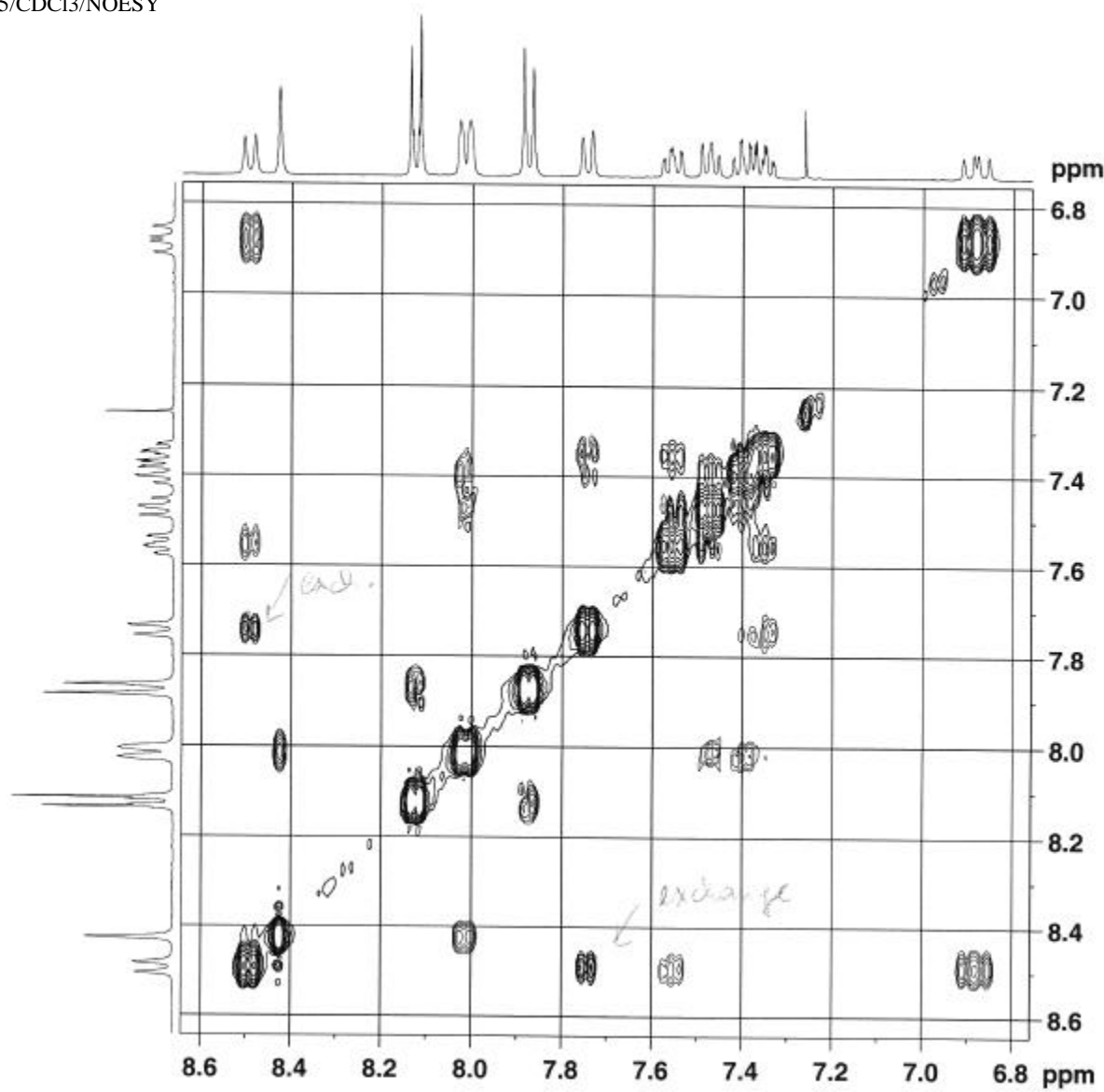
PROTON CDCl3 opt/xwinmr neudorfer 9



C13APT CDCl3 opt/xwinnmr neudorfer 12



accyc5/CDC13/NOESY



Current Data Parameters
NAME KN_accyc5
EXPNO 5
PROCNO 1

F2 - Acquisition Parameters
Date_ 20131025
Time 12.38
INSTRUM spect
PROBHD 5 mm PABBO BB/
PULPROG noesypph
TD 2048
SOLVENT CDC13
NS 8
DS 8
SWH 4000.000 Hz
FIDRES 1.953125 Hz
AQ 0.2560500 sec
RG 256
DW 125.000 usec
DE 10.00 usec
TE 297.3 K
D0 0.00010901 sec
D1 2.00000000 sec
D8 0.80000001 sec
D16 0.00020000 sec
INO 0.00024985 sec

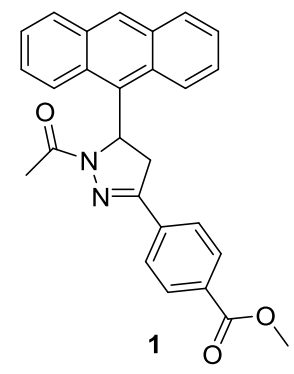
===== CHANNEL f1 =====
NUC1 1H
P1 12.50 usec
P2 25.00 usec
PLW1 16.00000000 W
SFO1 400.2318829 MHz

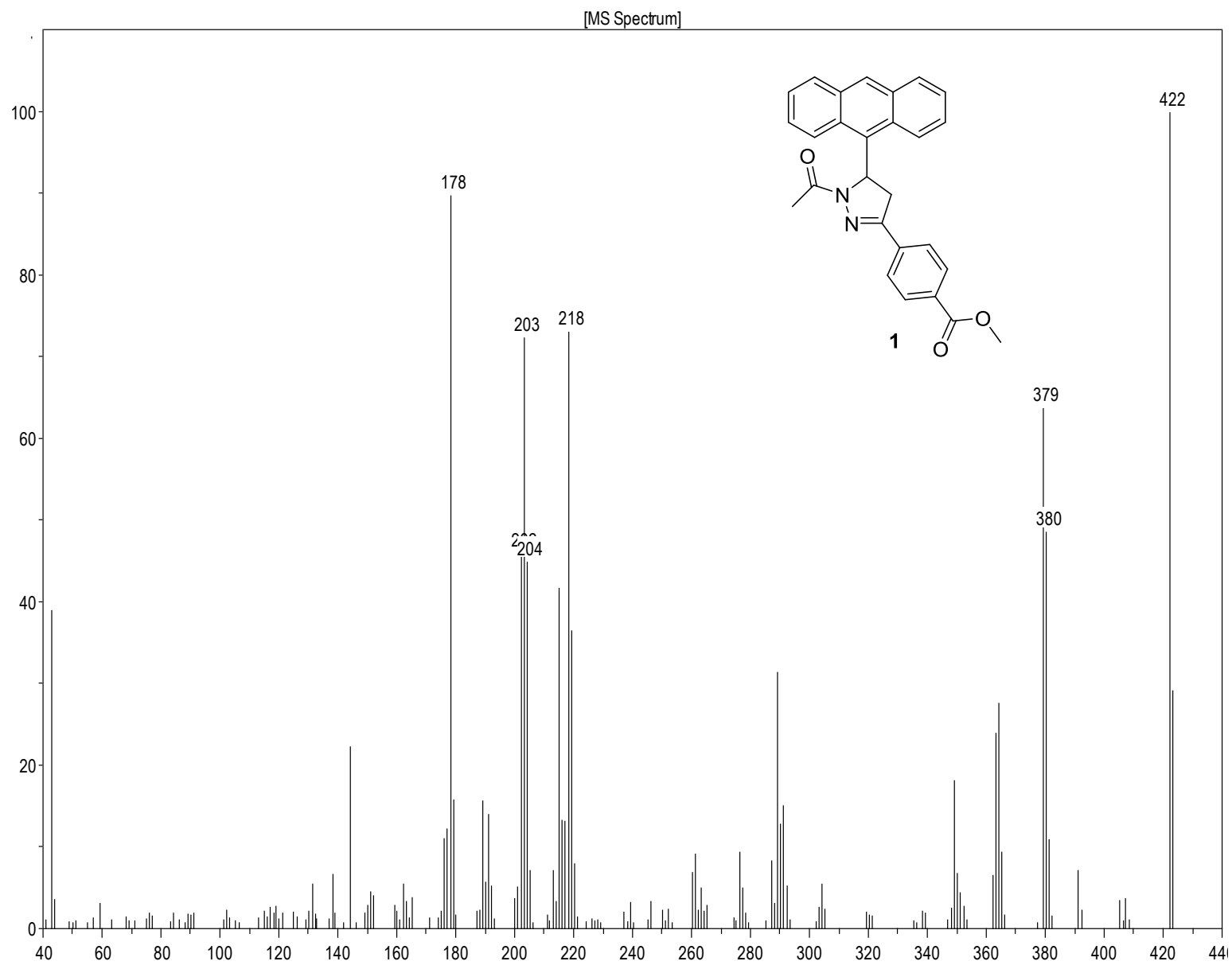
===== GRADIENT CHANNEL =====
GPMAM1 SMSQ10.100
GP21 40.00 %
P16 1000.00 usec

F1 - Acquisition parameters
TD 256
SFO1 400.2319 MHz
FIDRES 15.634058 Hz
SW 10.000 ppm
FhMODE States-TPPI

F2 - Processing parameters
SI 2048
SF 400.2300123 MHz
WDW QSIINE
SSB 2
LB 0 Hz
GB 0
PC 1.00

F1 - Processing parameters
SI 2048
MC2 States-TPPI
SF 400.2300123 MHz
WDW States-TPPI
SSB 2
LB 0 Hz
GB 0





MassenspektrometrieZentrum FakultätChemieUniWien

Analysis Info

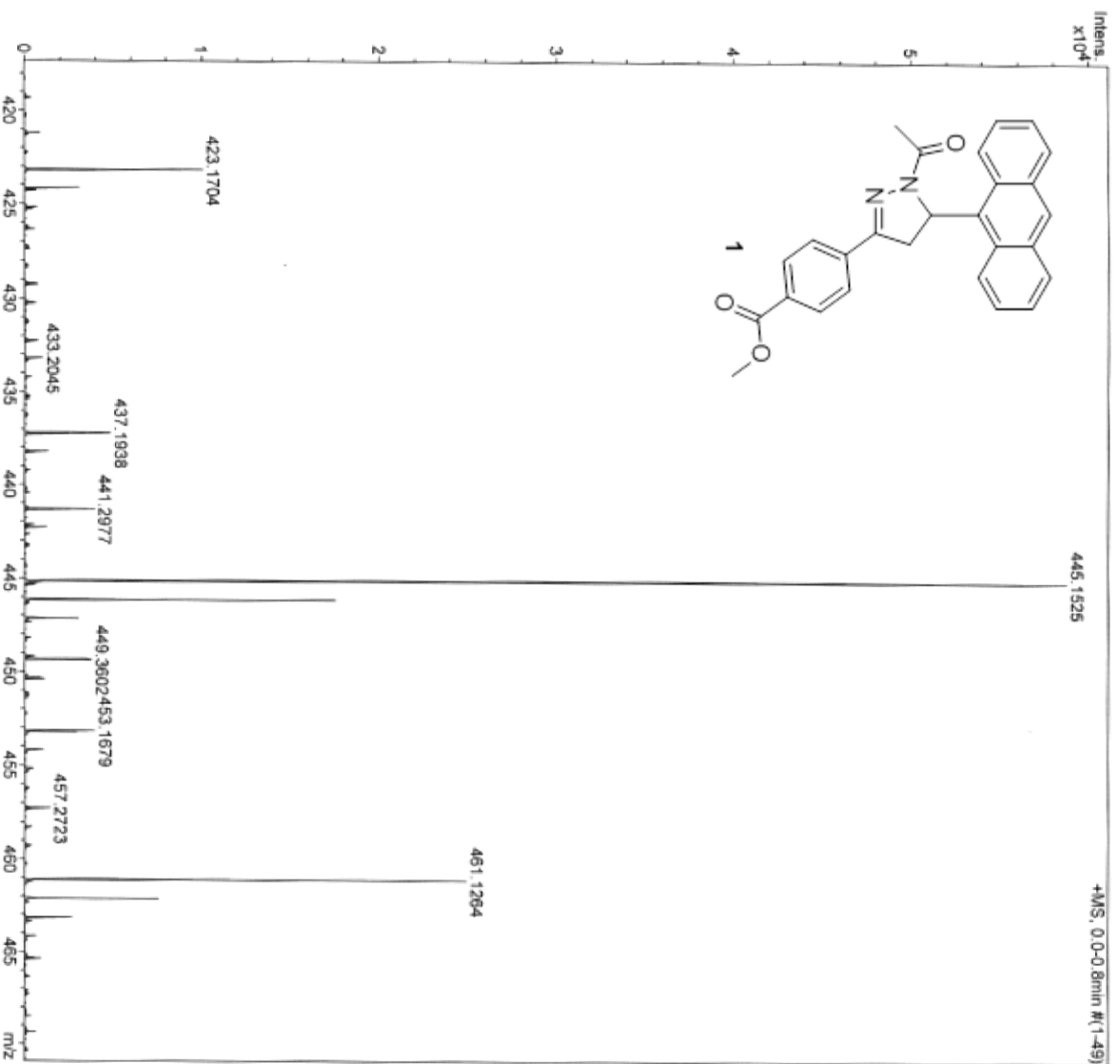
Analysis Name D:\Data\MS_MessService\38816000001.d
Method Nanomate infusion training01.m
Sample Name accyc5
Auftraggeber/Com Neudorfer/Spreitzer

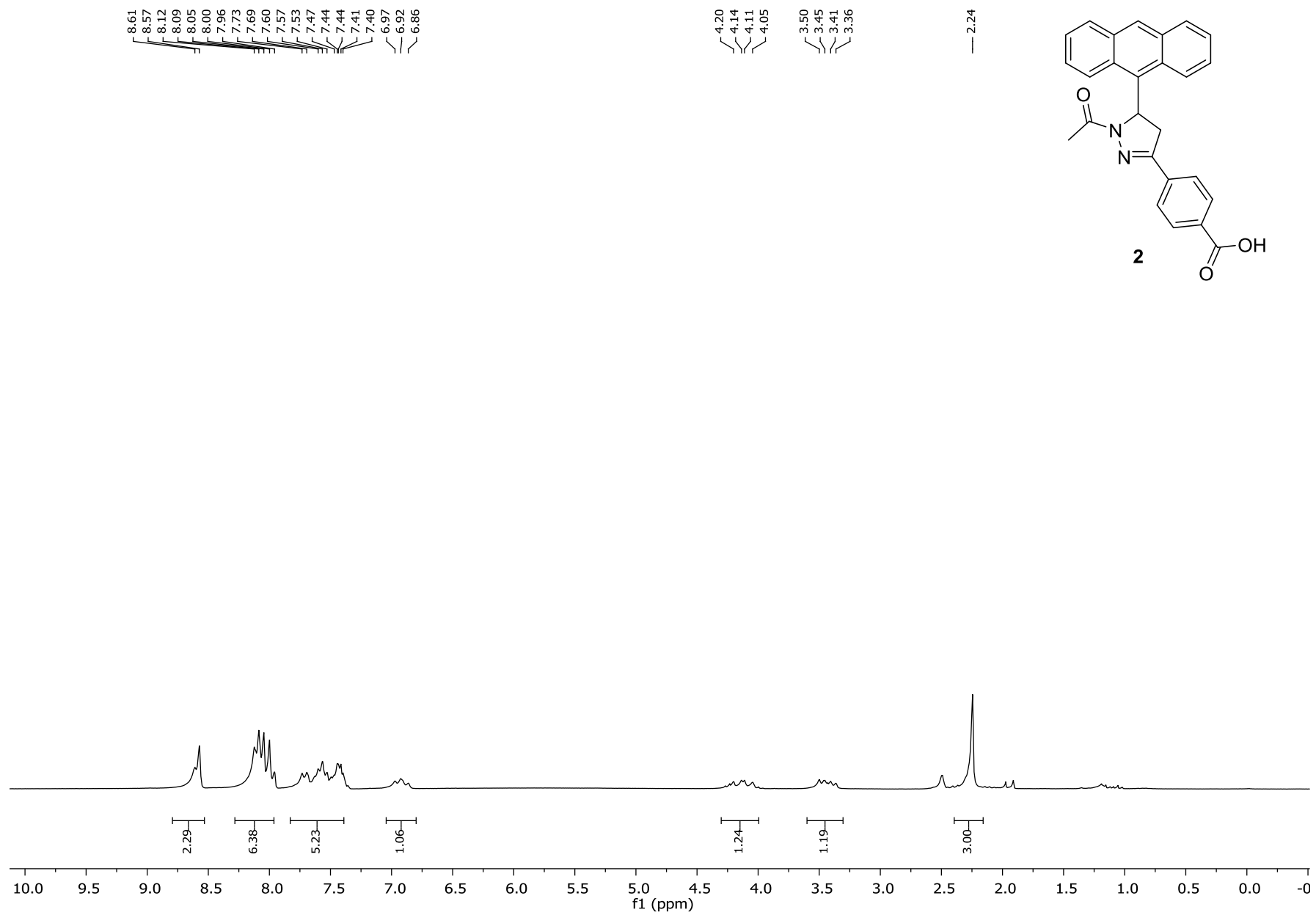
Acquisition Date 9/12/2012 10:34:39 AM

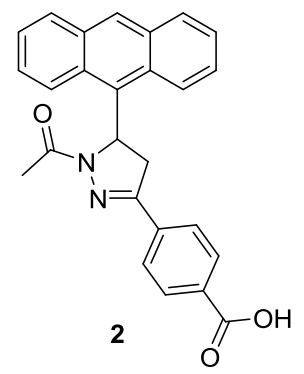
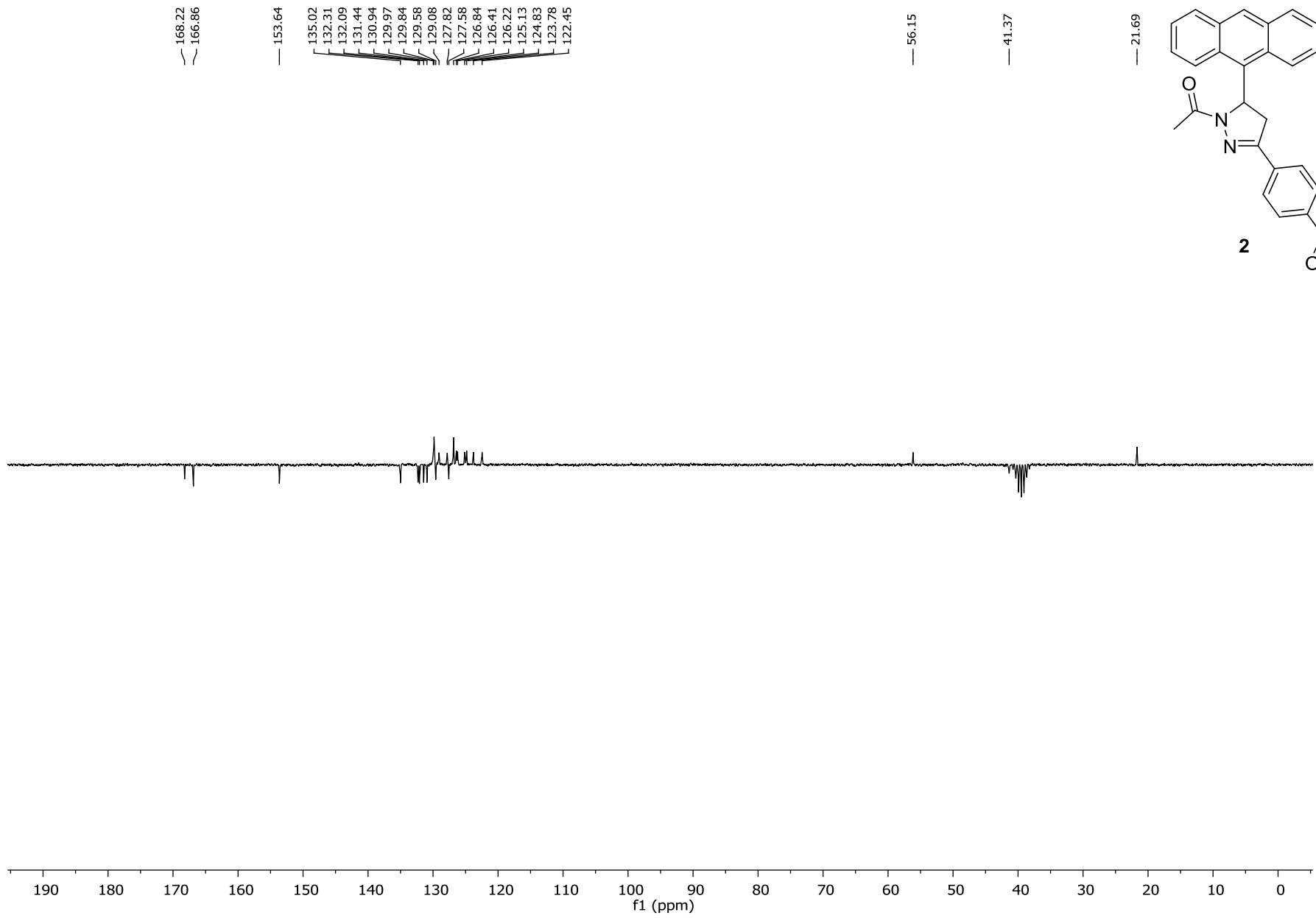
Operator phu
Instrument maxis

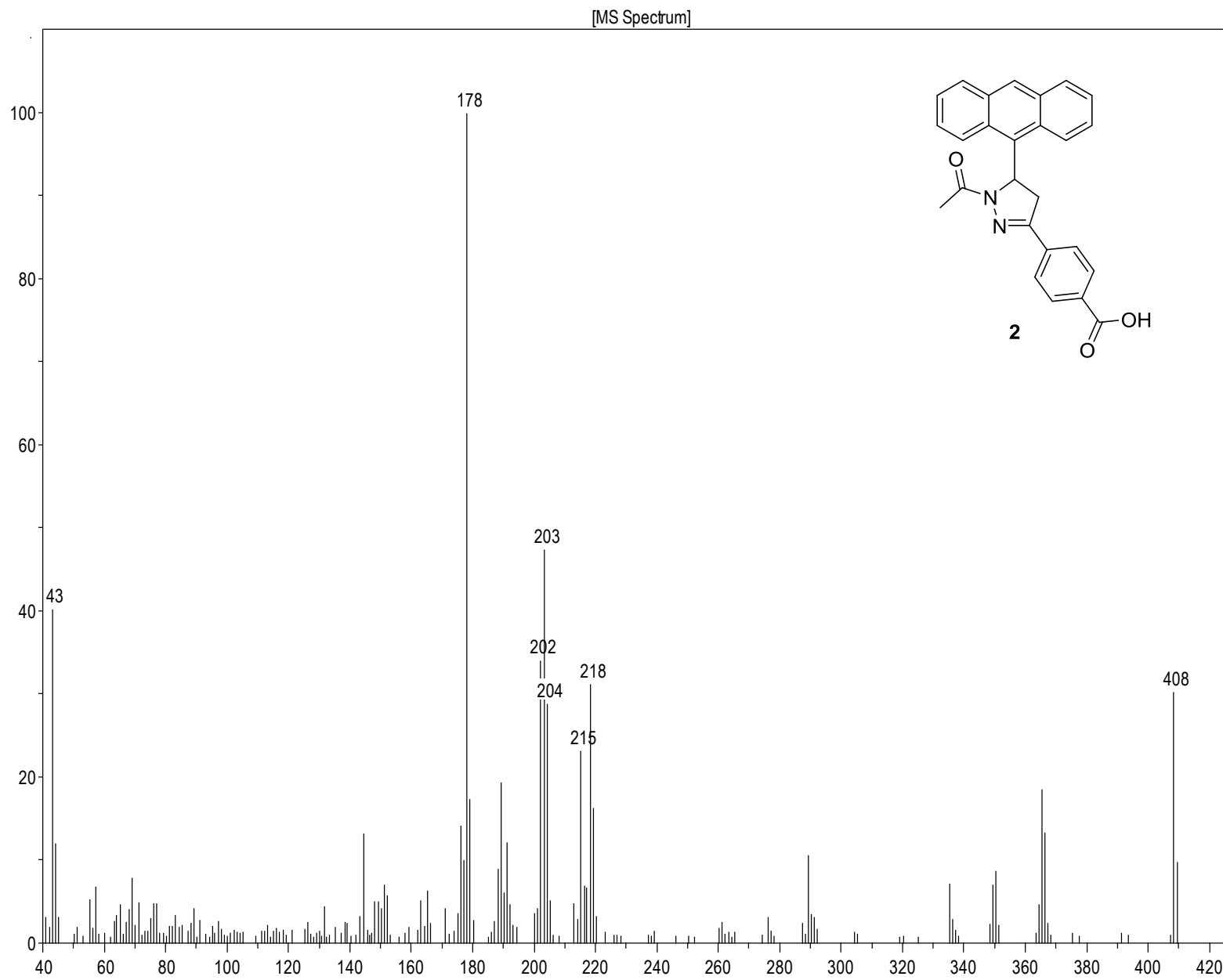
Ergebnis: +/- 5 ppm

MeOH/ACN



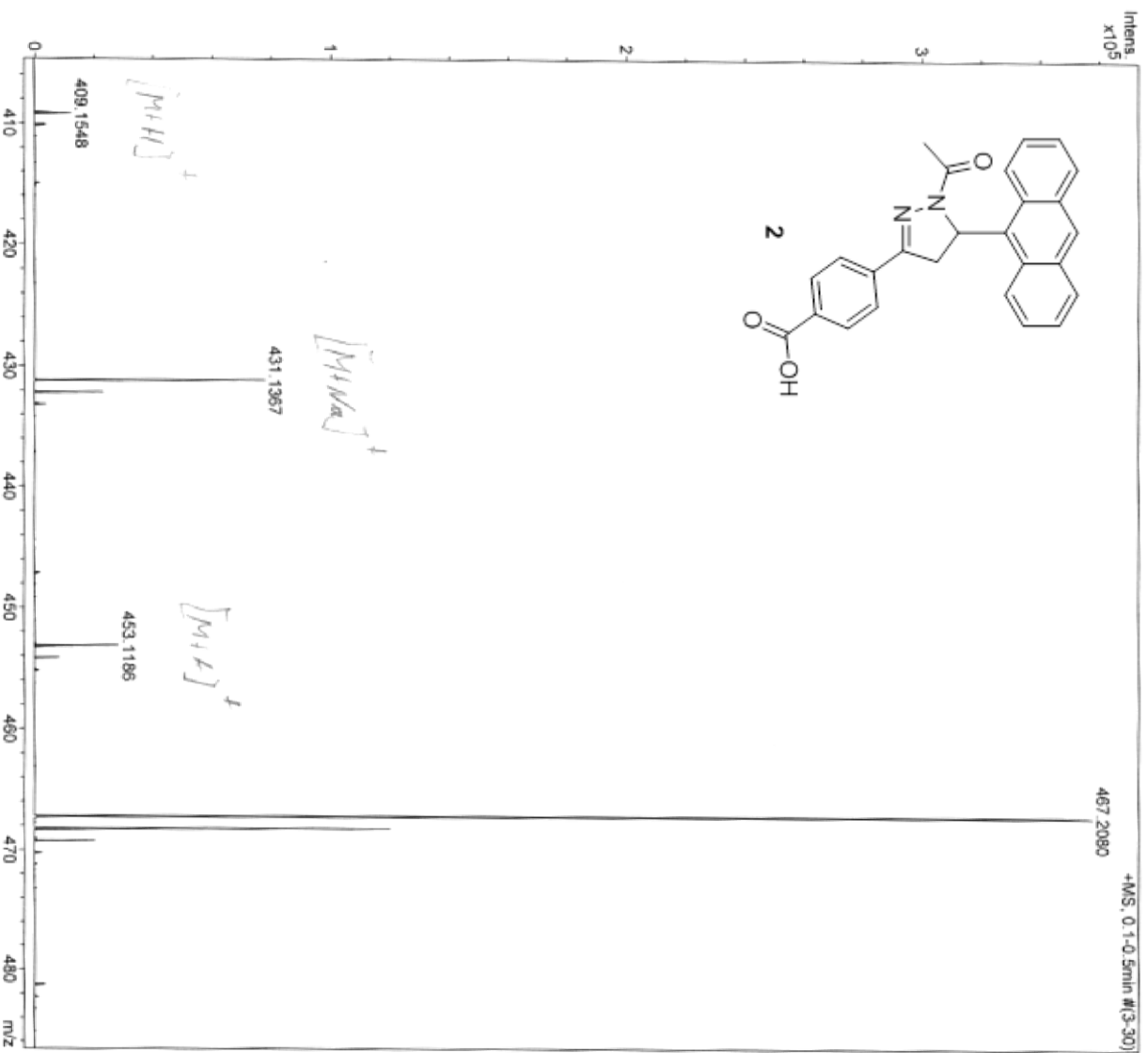
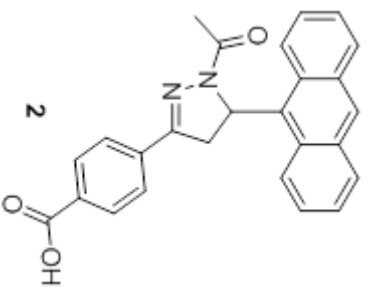


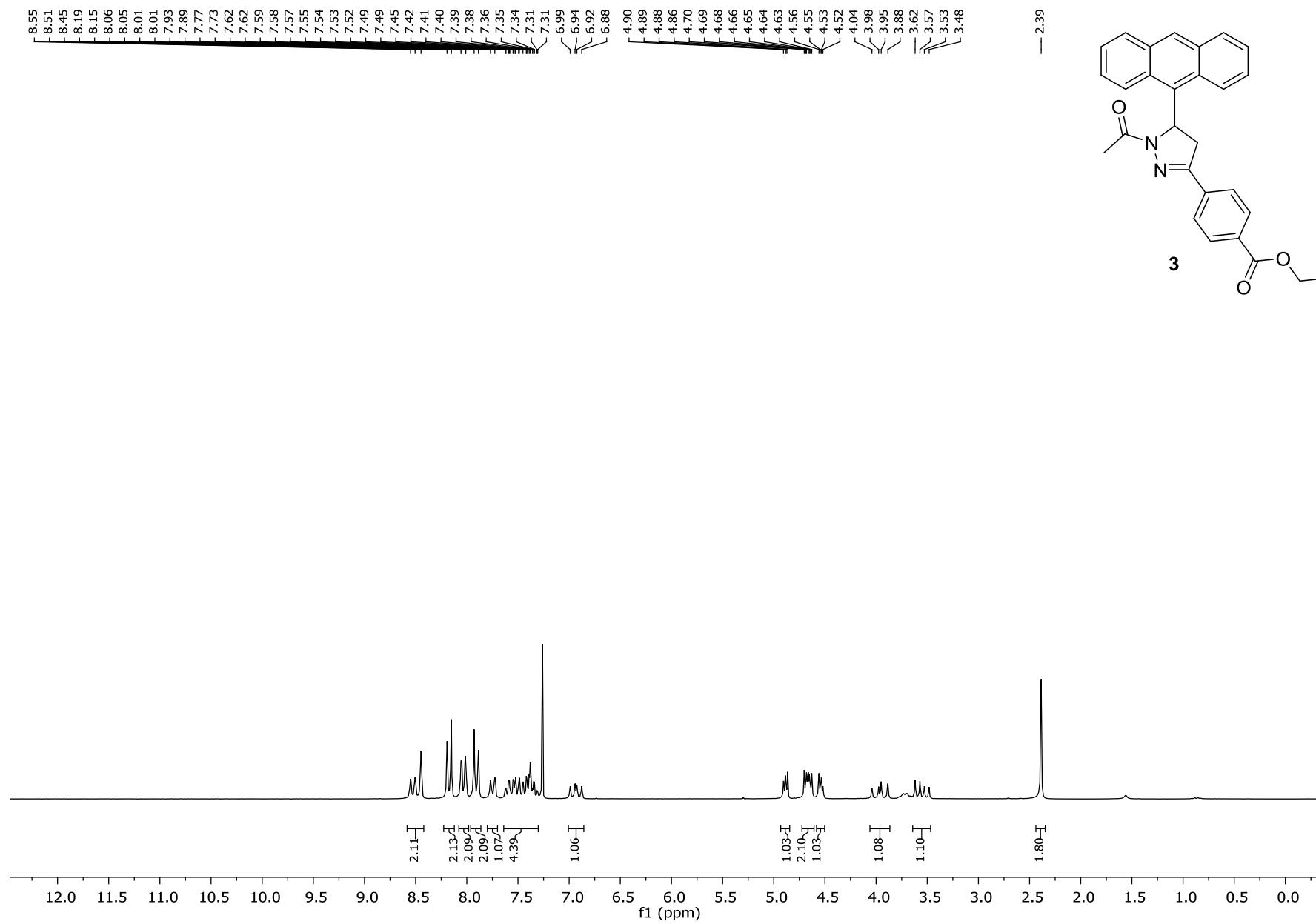




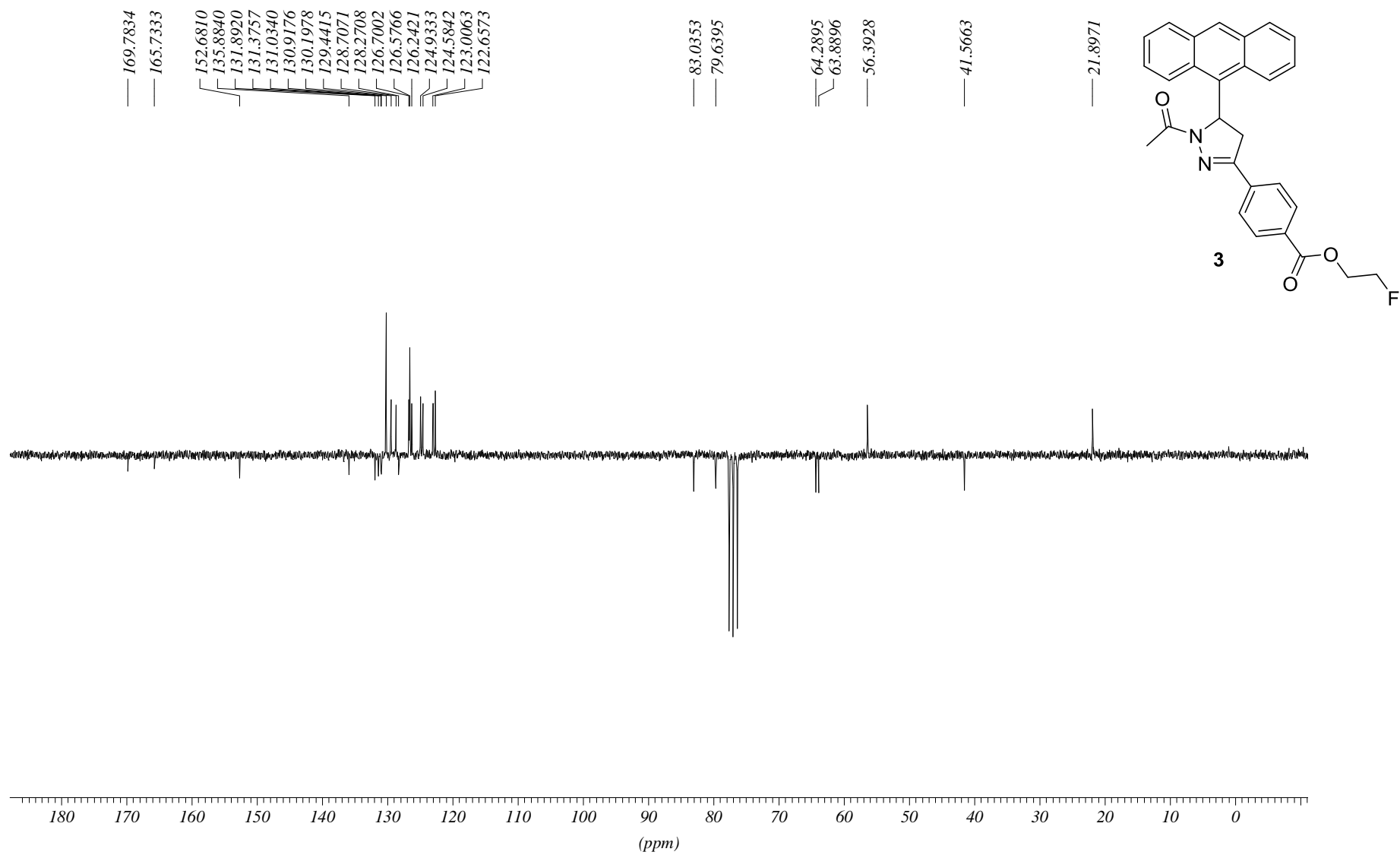
MassenspektrometrieZentrum FakultätChemieUniWien

Analysis Info
Analysis Name D:\Data\MS_MessService\38969000001.d Acquisition Date 10/18/2012 11:27:53 AM
Method tune_low_nach_Quadropol.m Operator phu
Sample Name III Instrument maxis
Auftragegeber/Com Neudorfer/Spreitzer Ergebnis: +/-5 ppm
ACN/MeOH

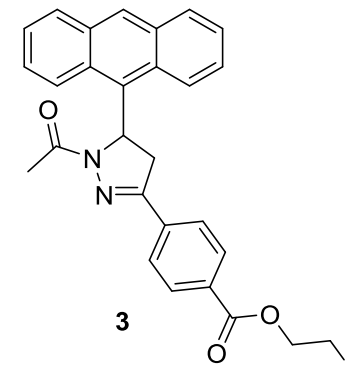
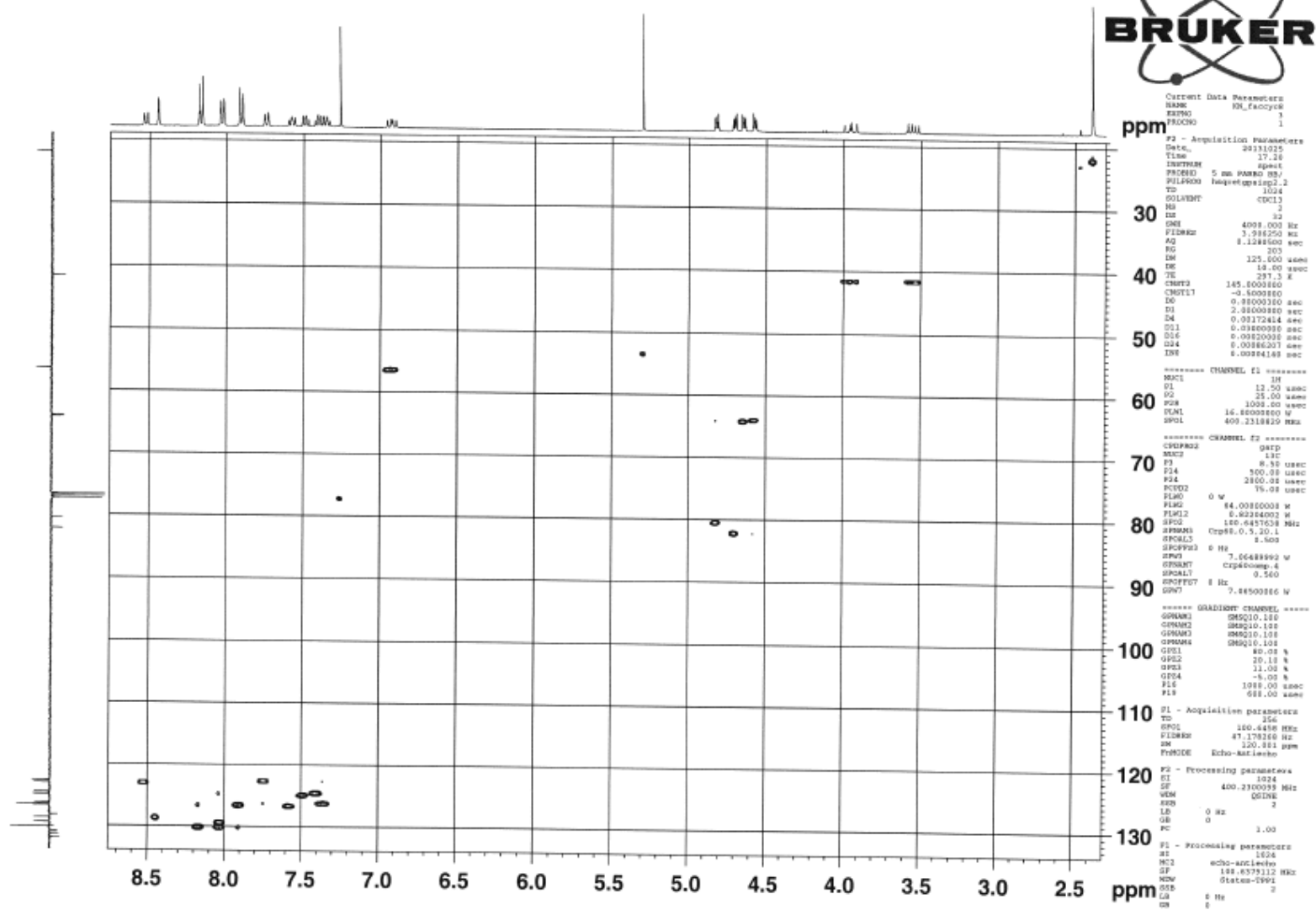




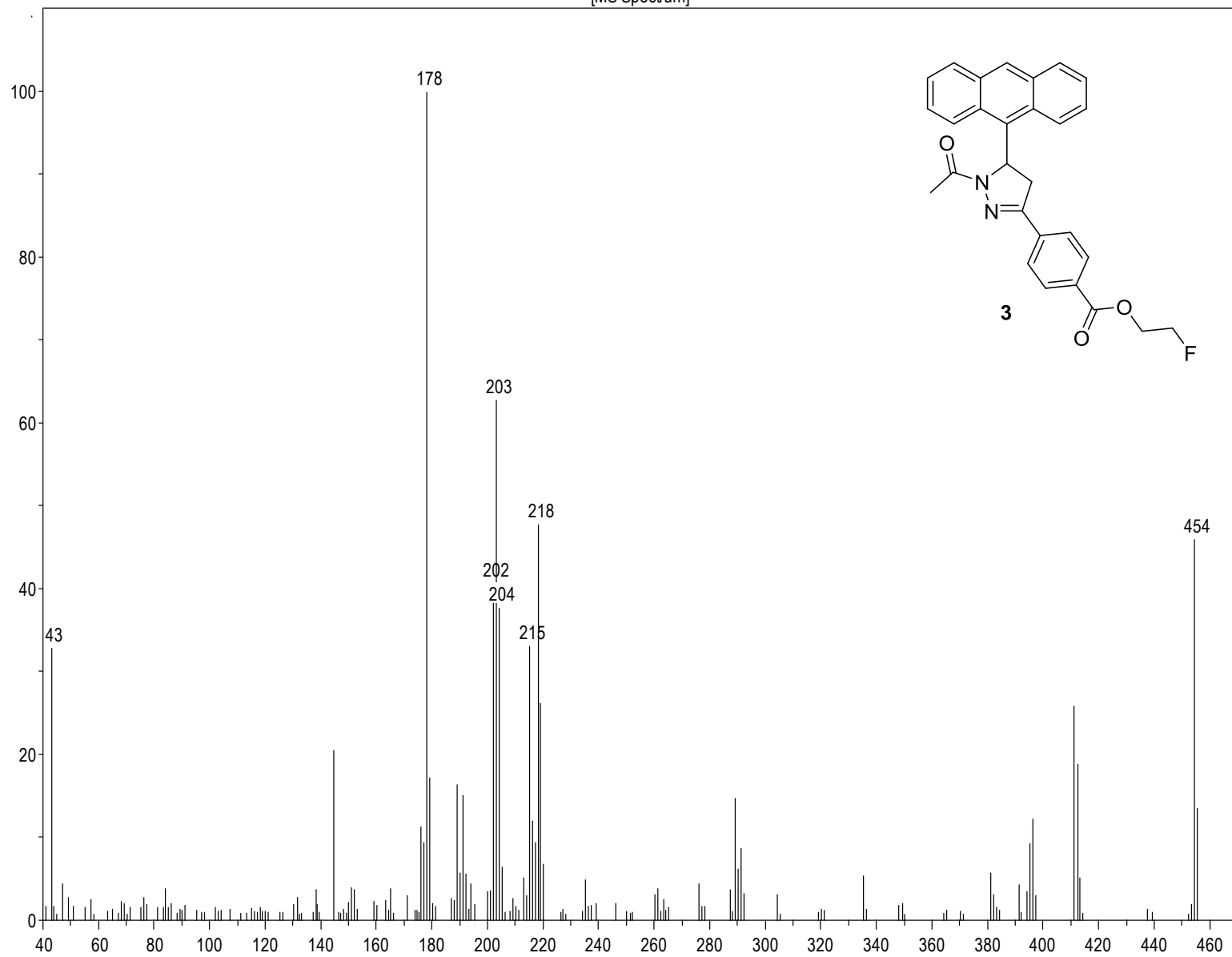
C13APT CDCl3 opt/xwinnmr neudorfer 36



faccyc9/CDC13/HSQC



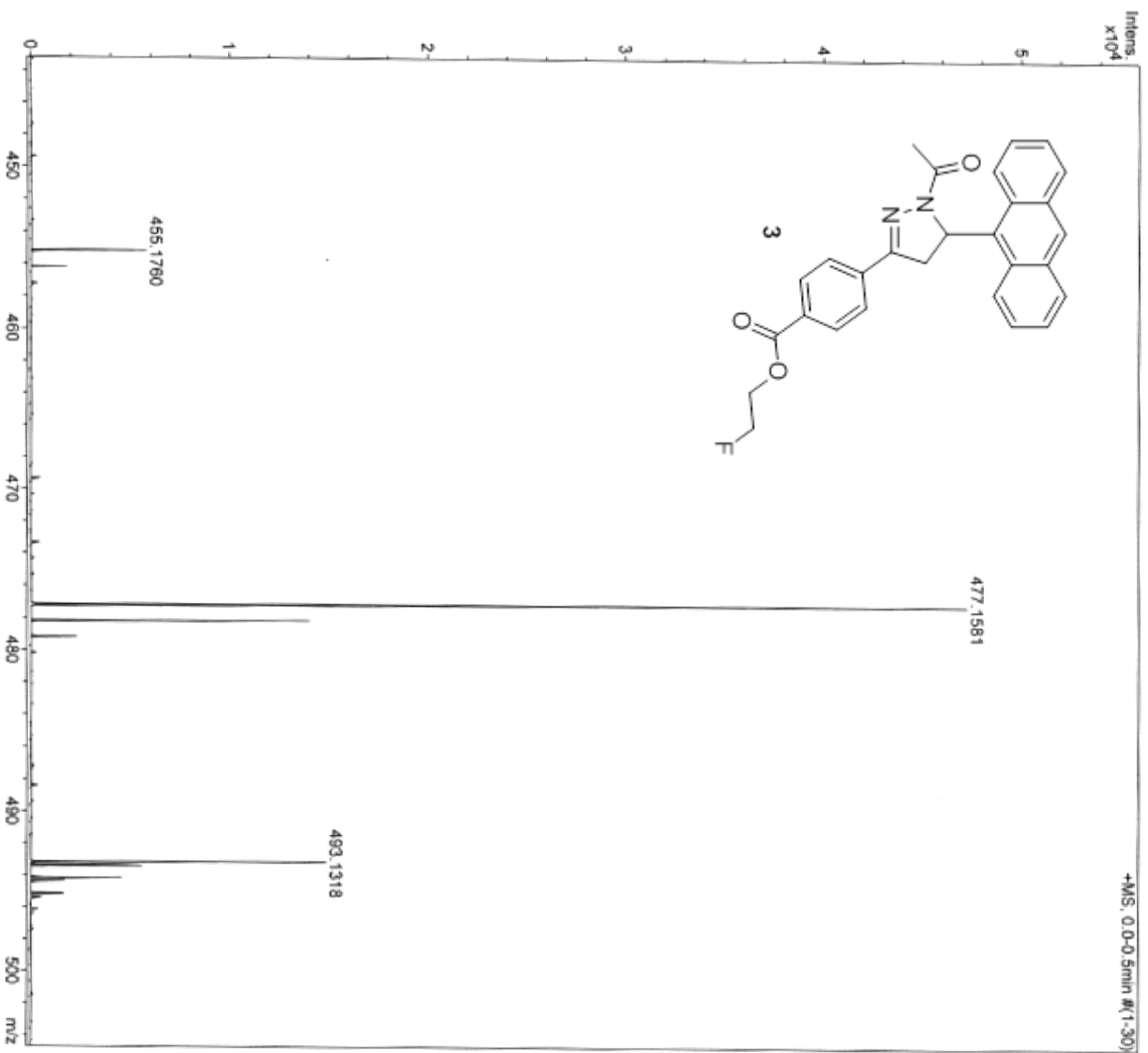
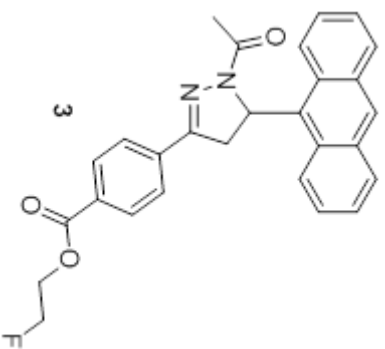
[MS Spectrum]



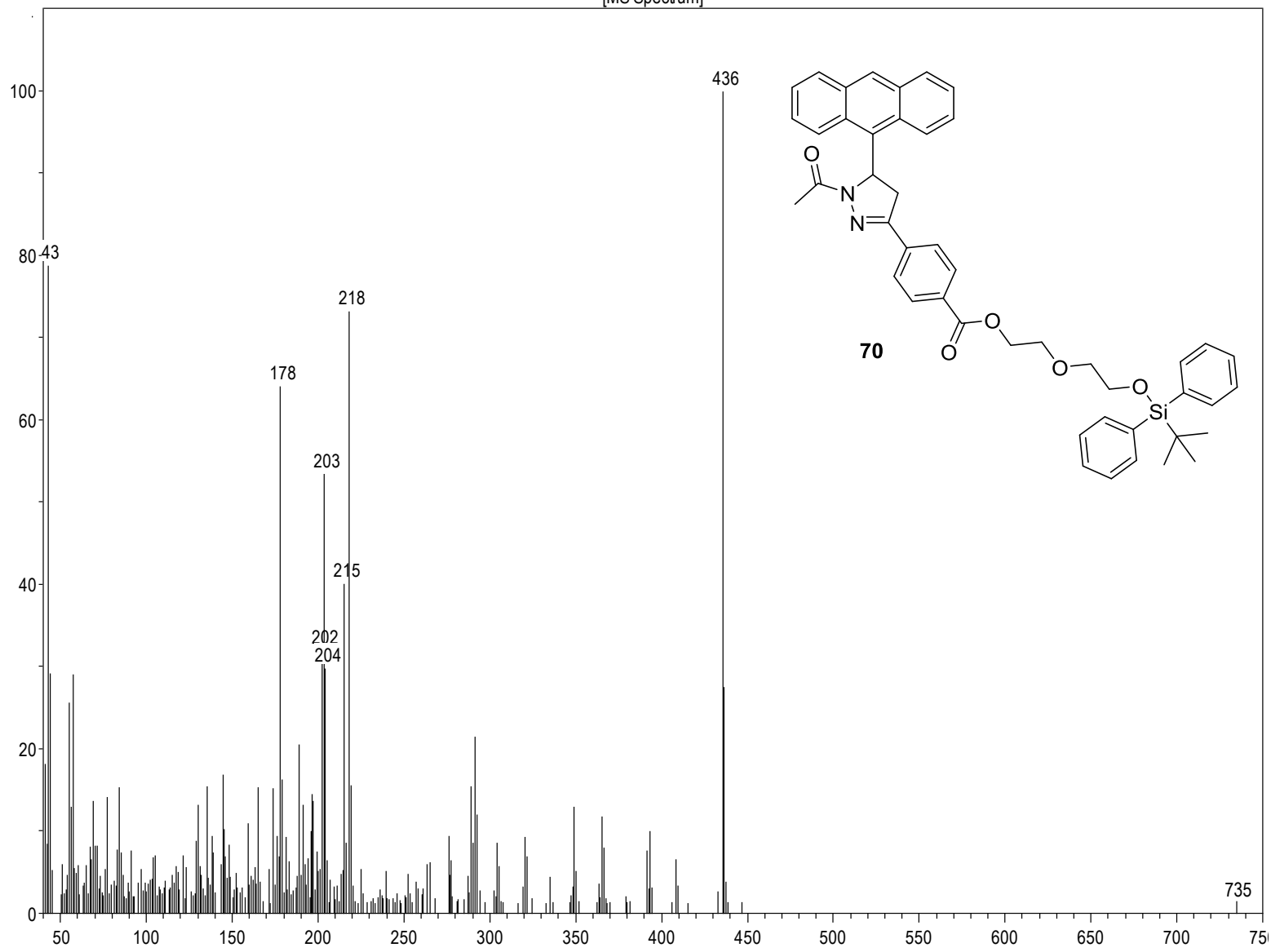
MassenspektrometrieZentrum FakultätChemieUniWien

Analysis Info
Analysis Name D:\Data\MS_MessService\39132000001.d
Method tune_low_nach_Quadropol.m
Sample Name facyc7
Auftraggeber/Com Neudorfer/Spreitzer/Pharm
Ergebnis: +/- 5 ppm
ACN/MeOH

Acquisition Date 12/14/2012 2:09:59 PM
Operator phu
Instrument maxis



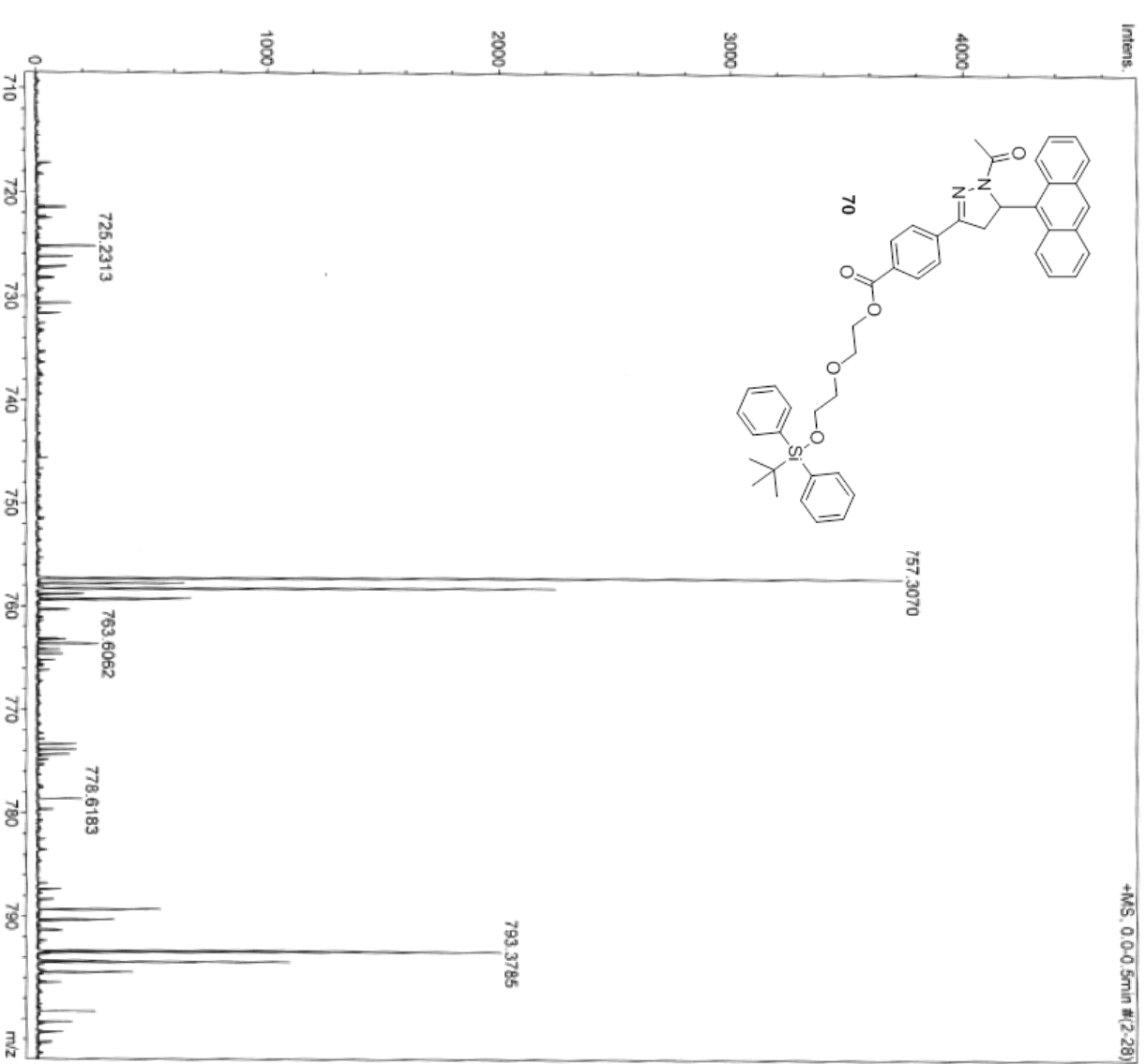
[MS Spectrum]



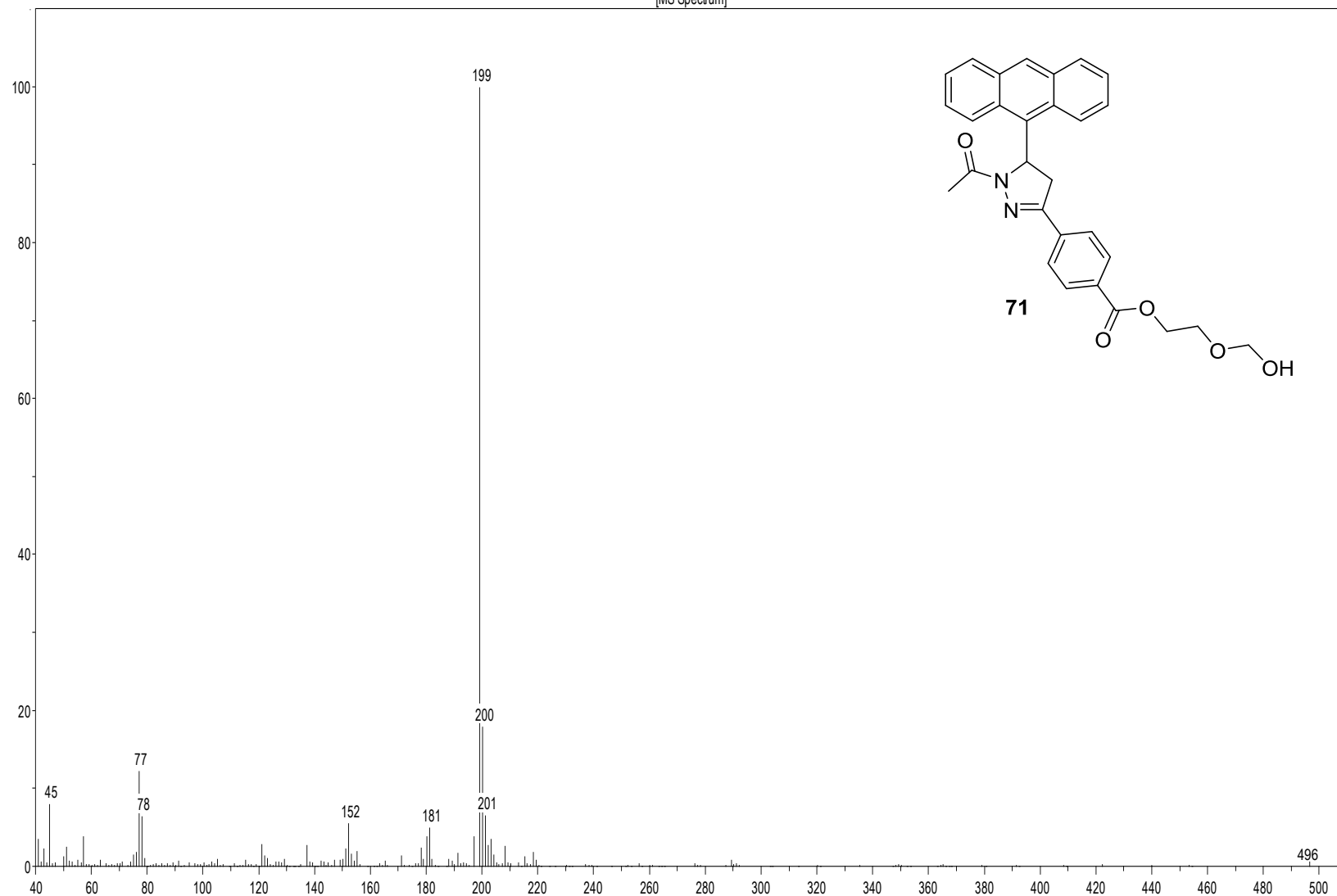
MassenspektrometrieZentrum FakultätChemieUniWien

Analysis Info
 Analysis Name D:\Data\MS_MessService\139722000001.d
 Method tune_low_MS_Service_07_13.m
 Sample Name pegs 2
 Auftraggeber/Com Neudorfer/Spreitzer
 Ergebnis: +/- 5ppm
 ACN/MeOH 1%/H2O

Acquisition Date 7/16/2013 9:15:17 AM
 Operator phu
 Instrument maxIs



[MS Spectrum]

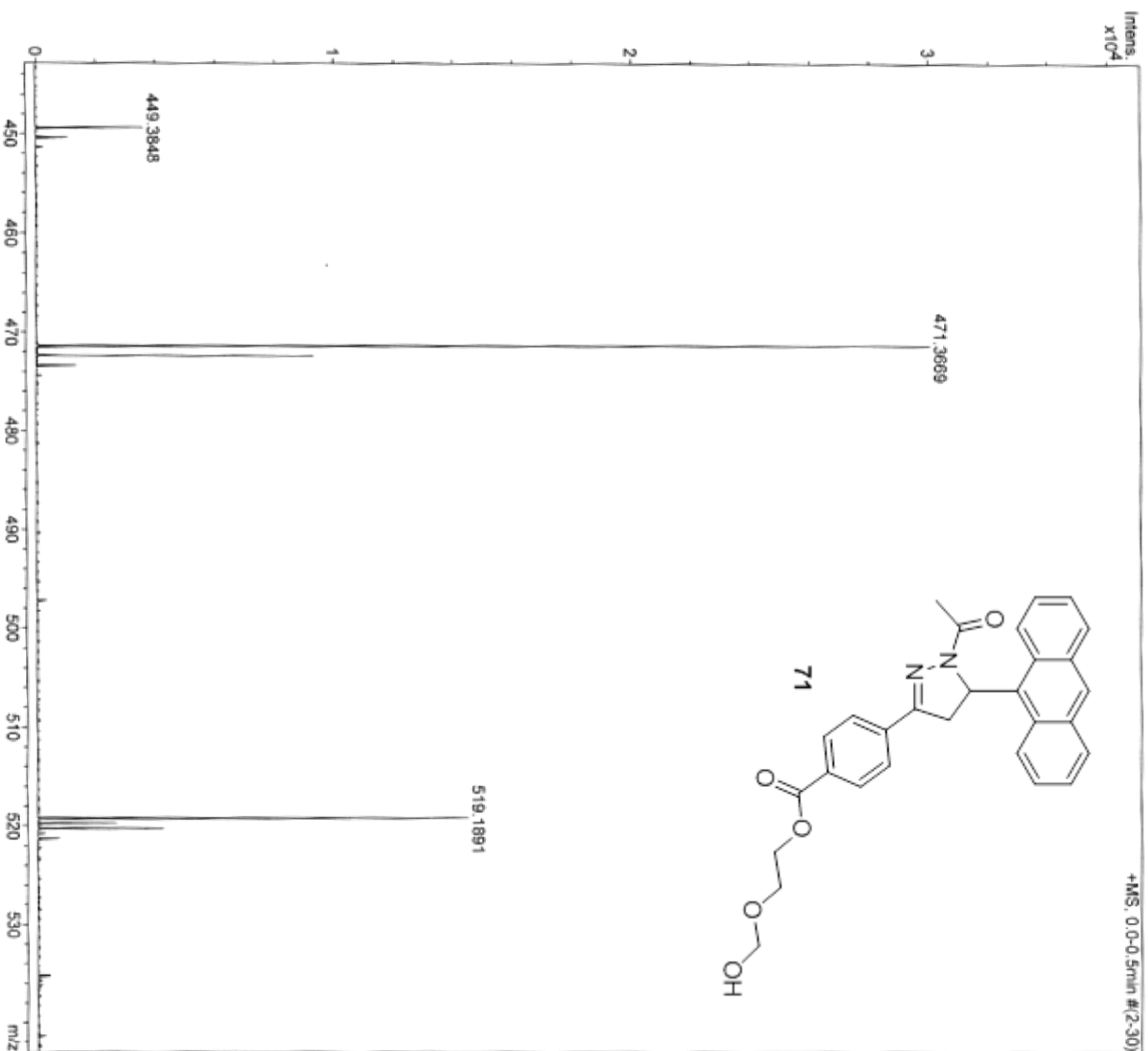
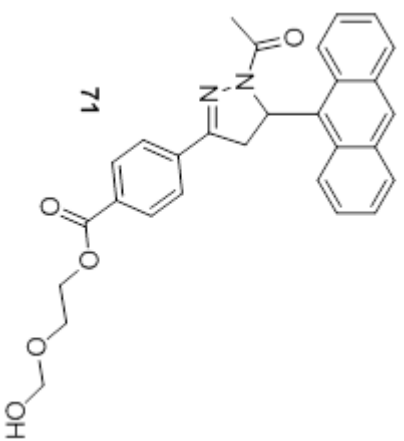


MassenspektrometrieZentrum FakultätChemieUniWien

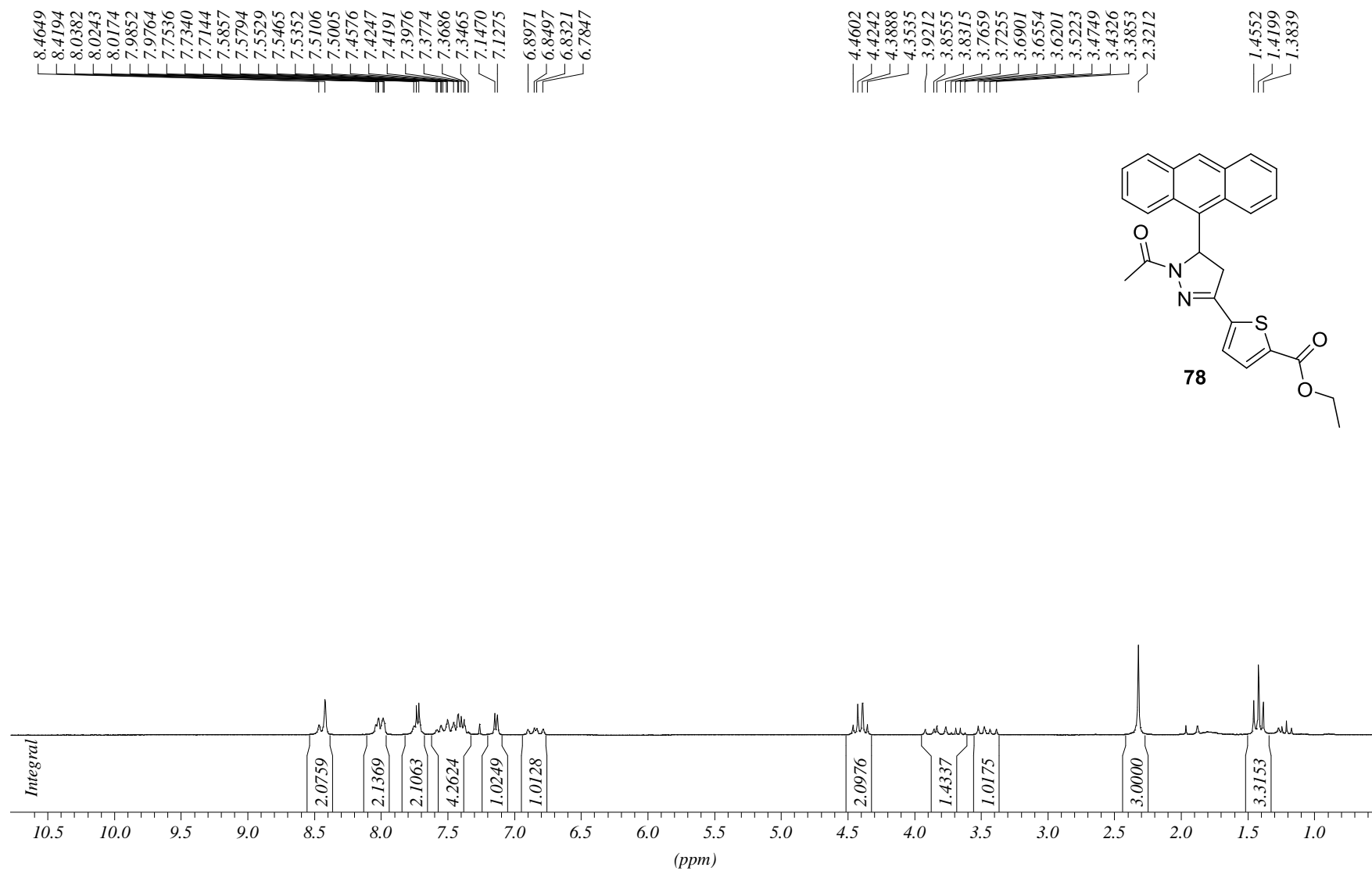
Analysis Info

Analysis Name D:\Data\MS_MessService\39579000001.d
Method tune_low_MS_Service_05_13.m
Sample Name peg1
Auftragegeber/Com Neudorfer/Spreitzer
Ergebnis: +/- 5ppm
ACN/MeOH 1%/H2O

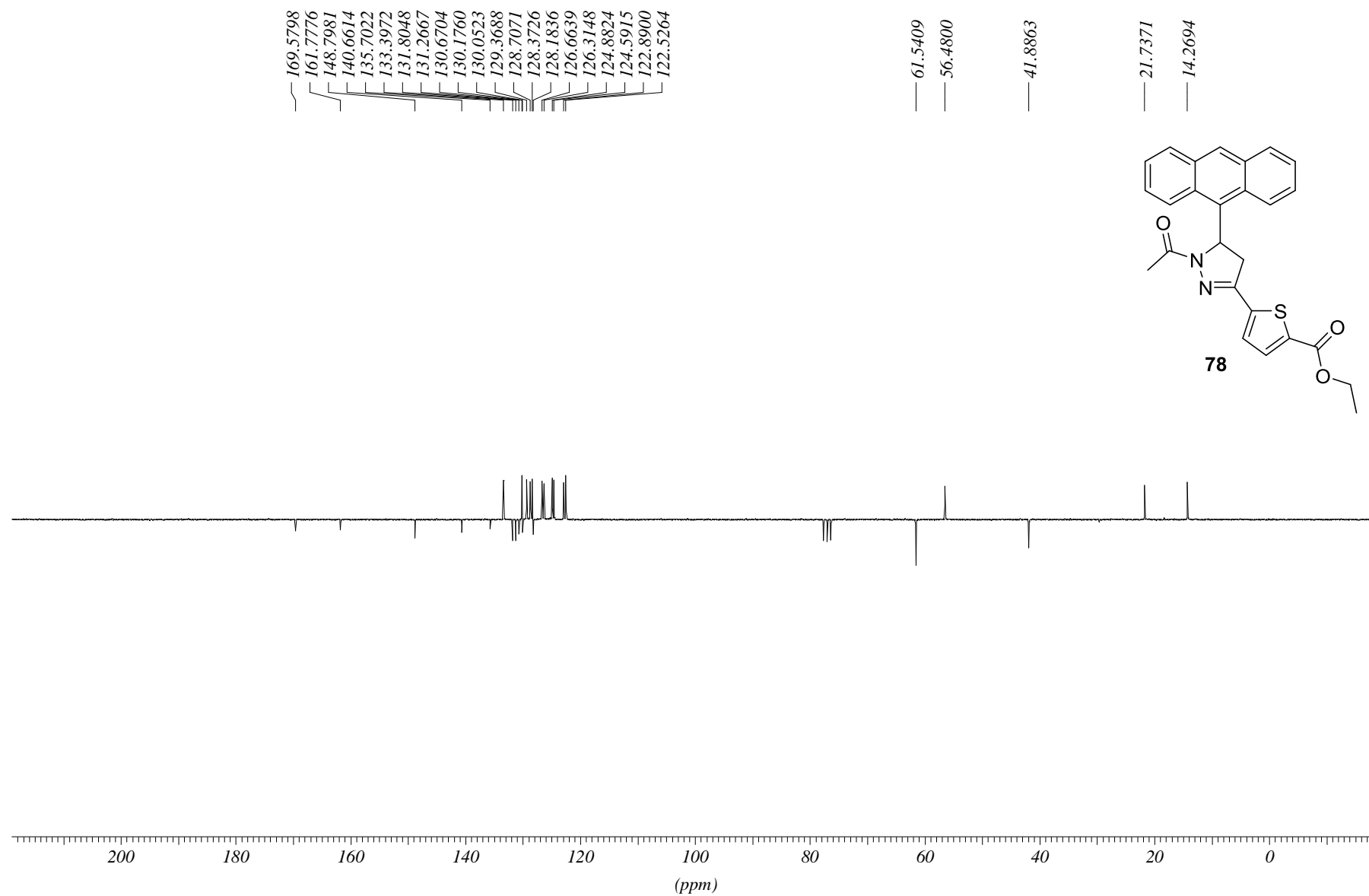
Acquisition Date 5/27/2013 10:48:39 AM
Operator phu
Instrument maxIs

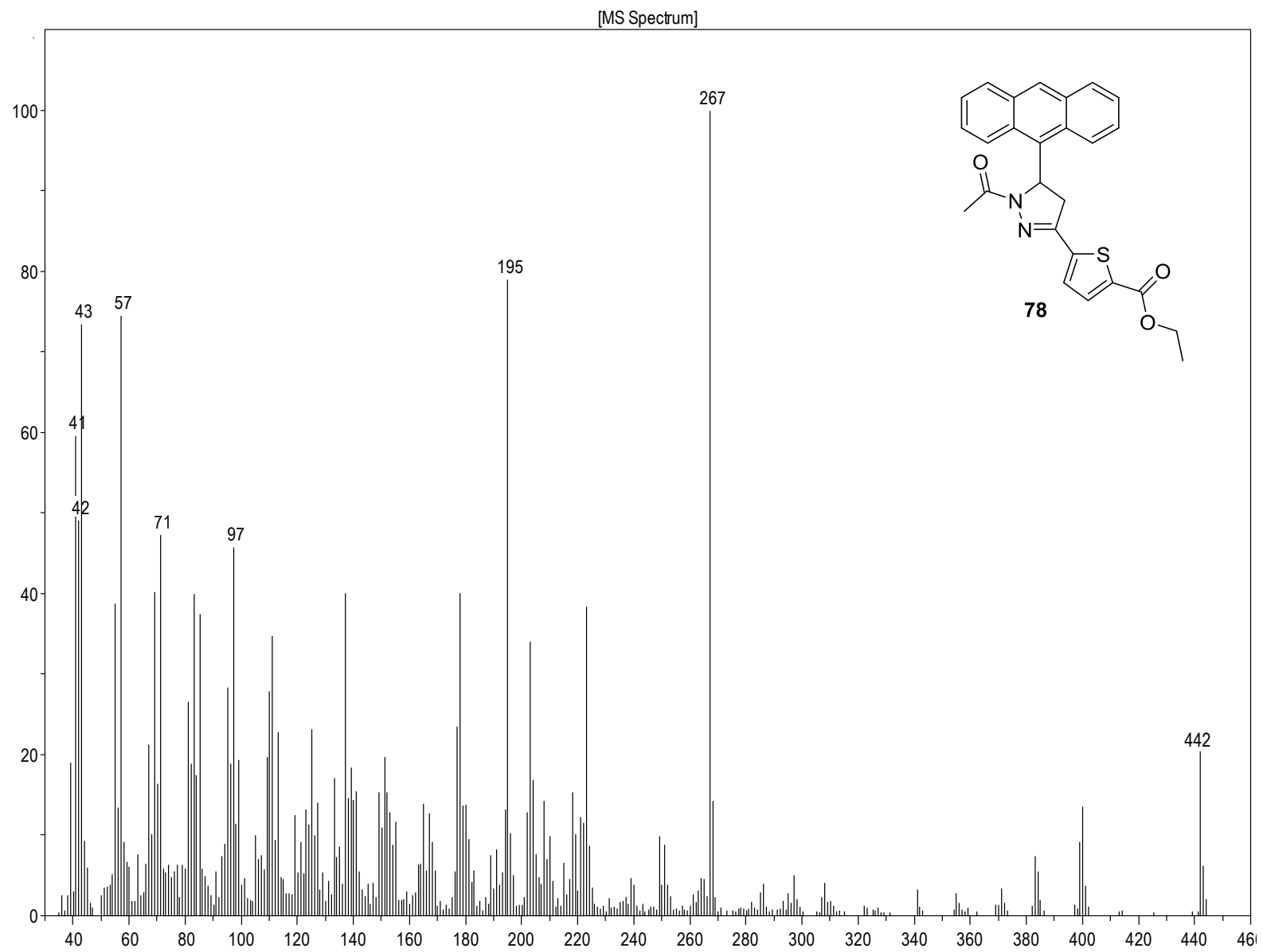


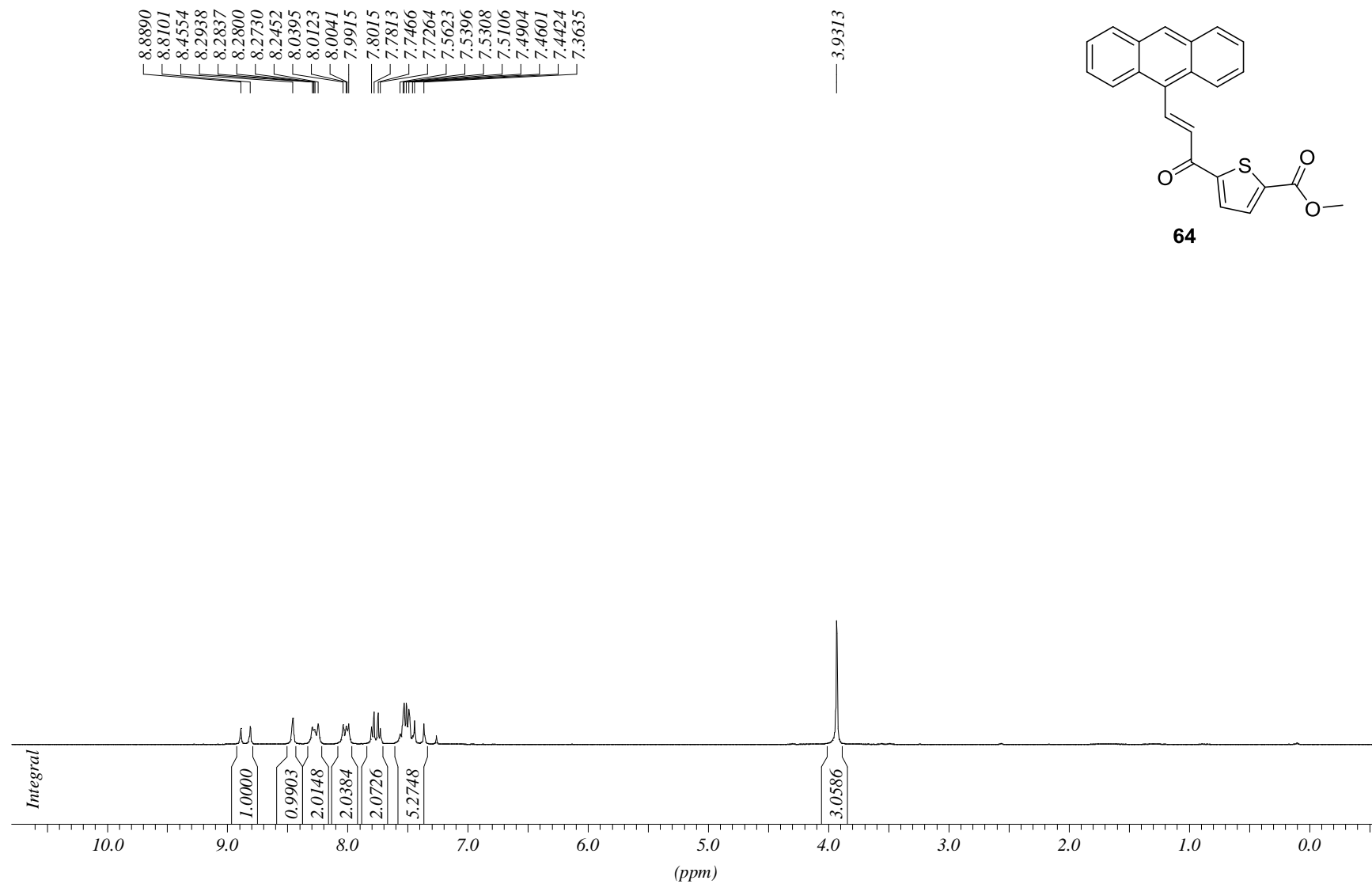
PROTON CDCl3 opt/xwinmr neudorfer 34



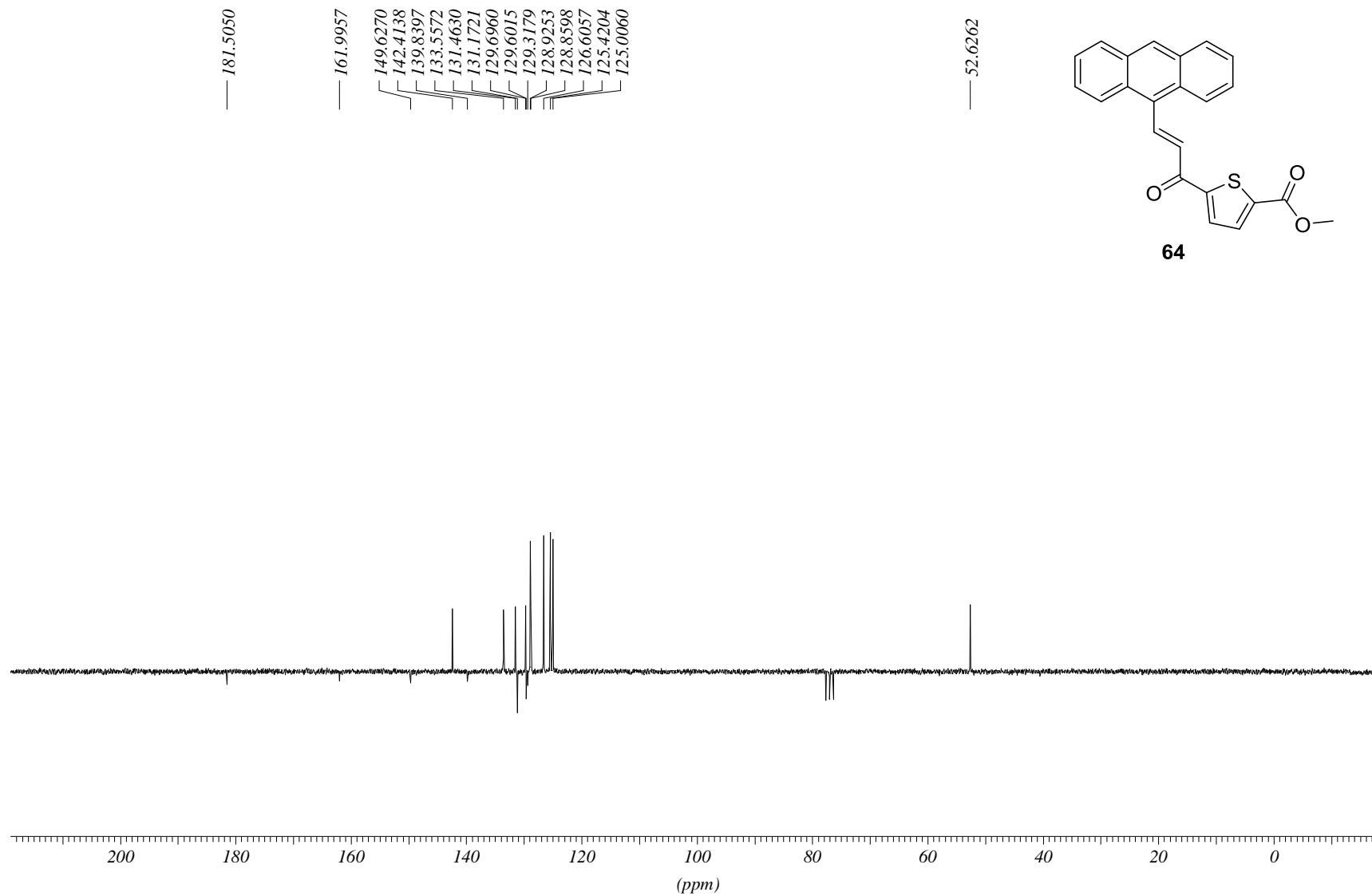
C13APT CDCl3 opt/xwinnmr neudorfer 34

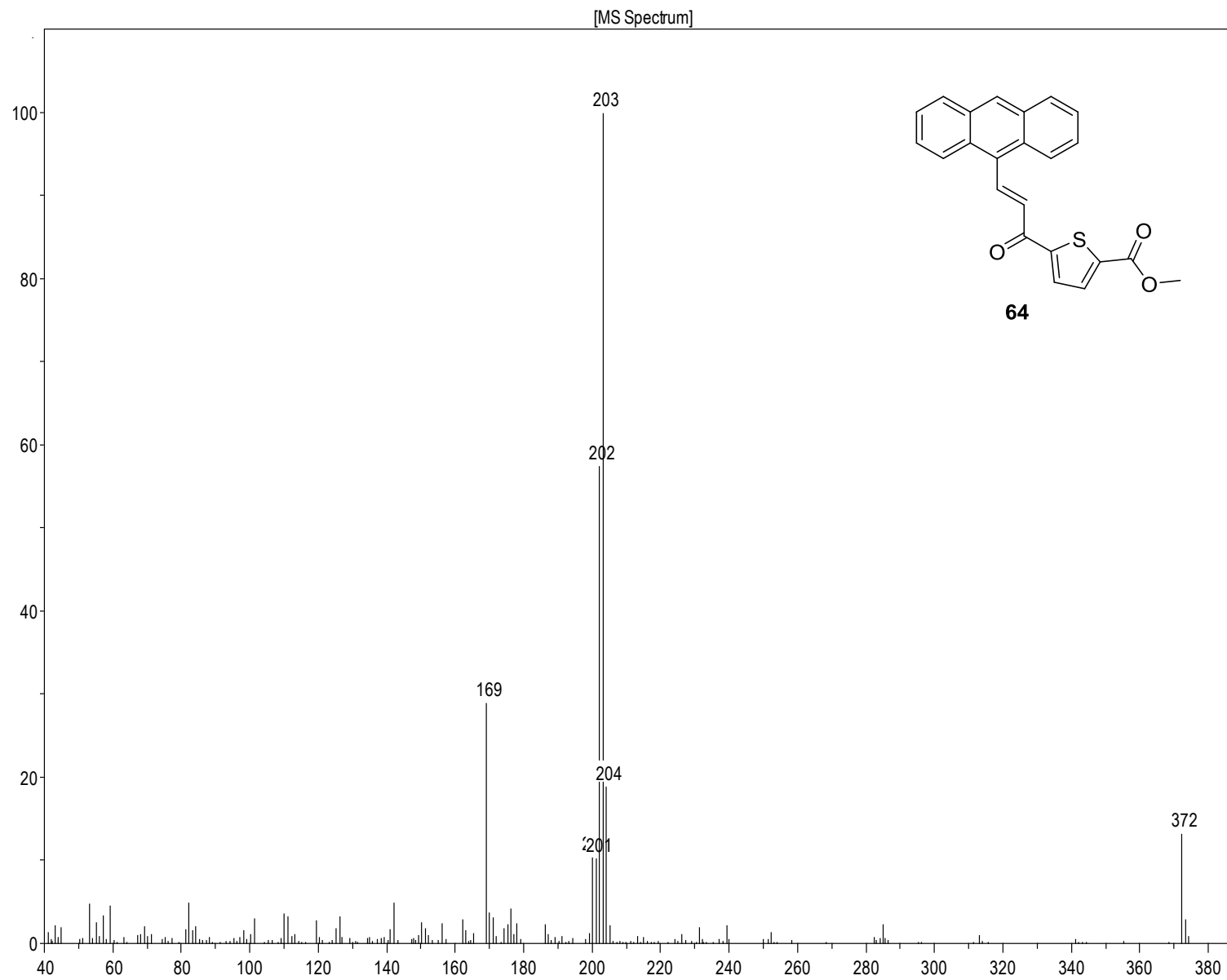


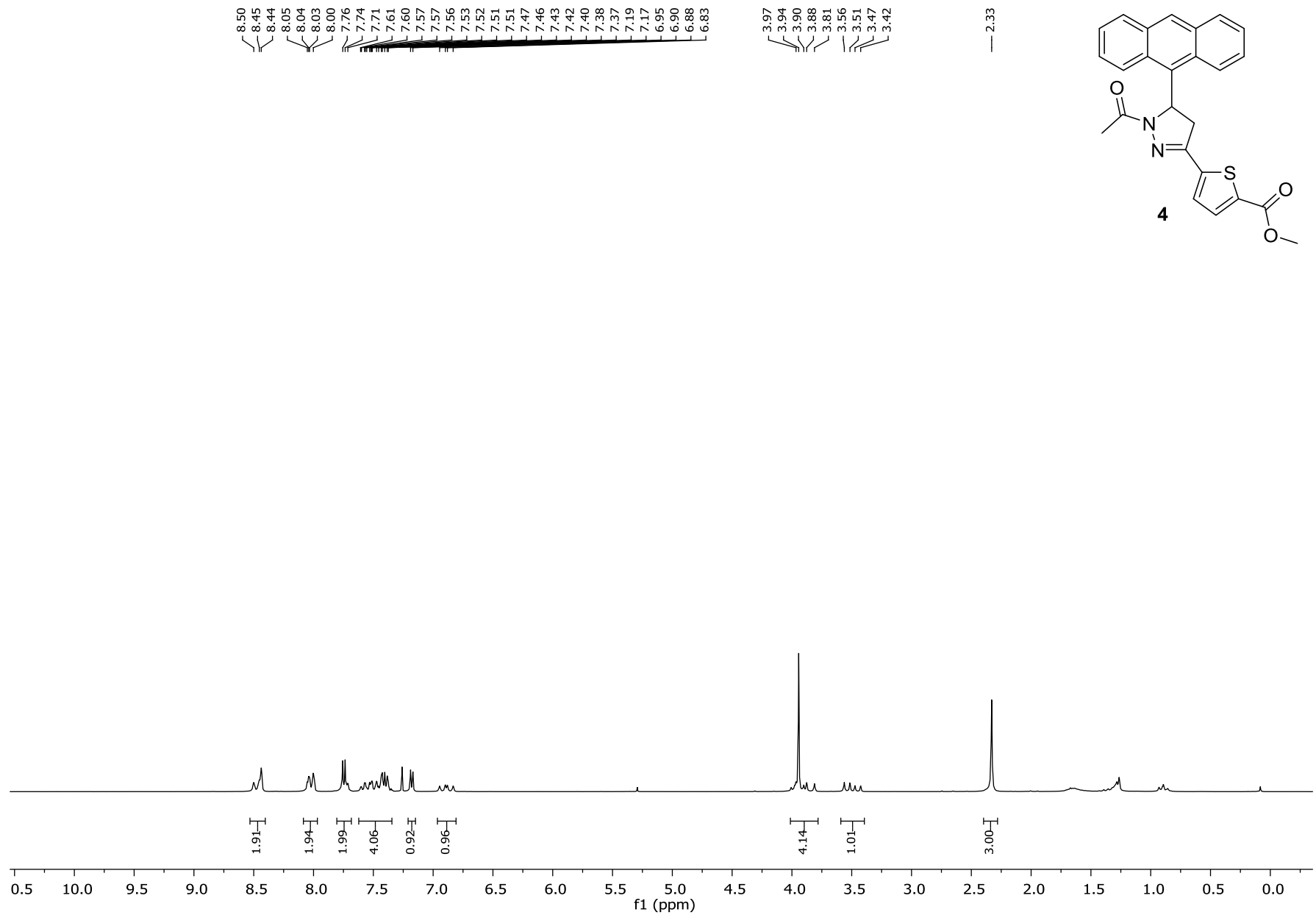


PROTON CDCl₃ opt/xwinmr neudorfer 38

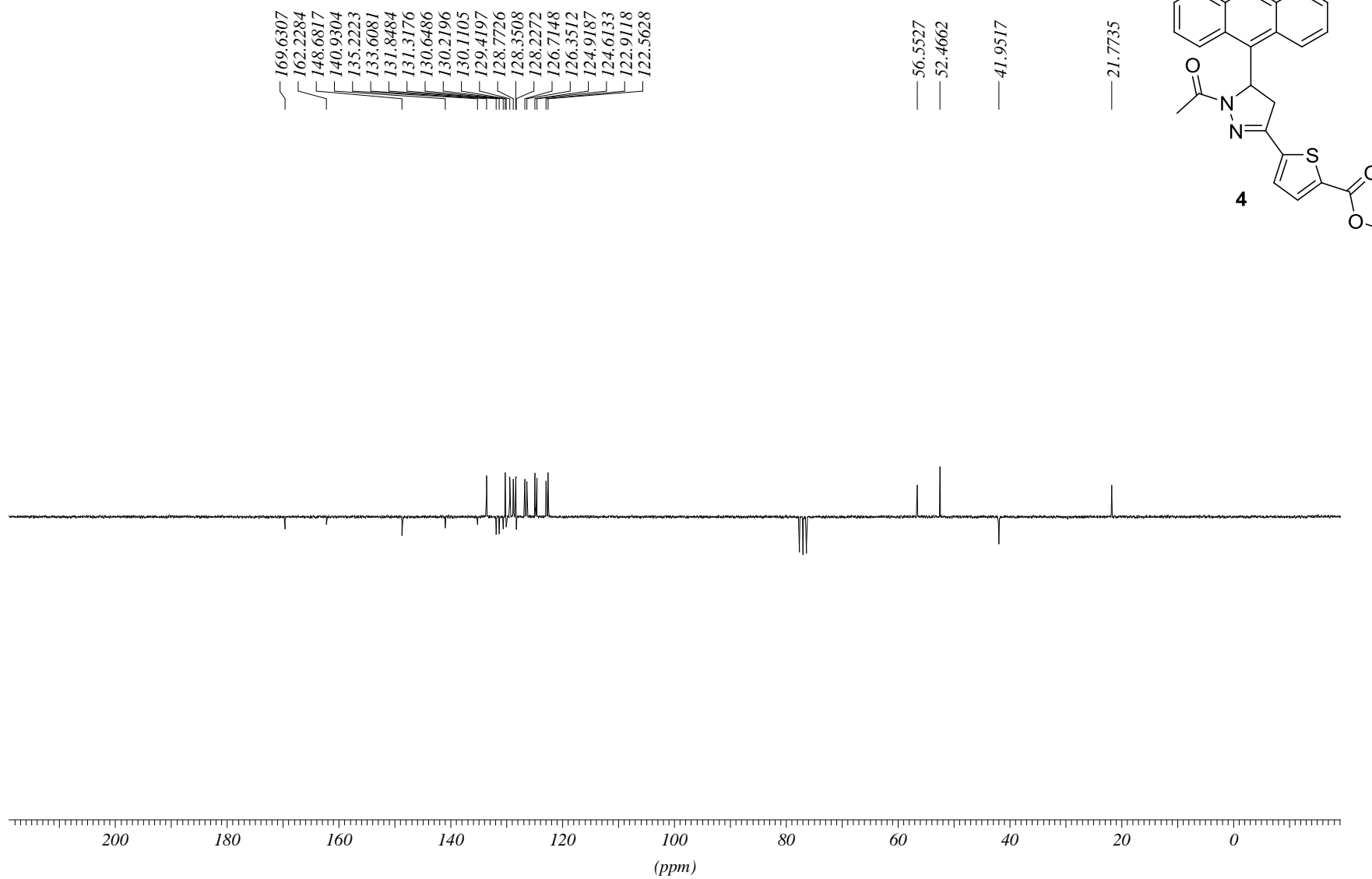
C13APT CDCl3 opt/xwinmr neudorfer 38



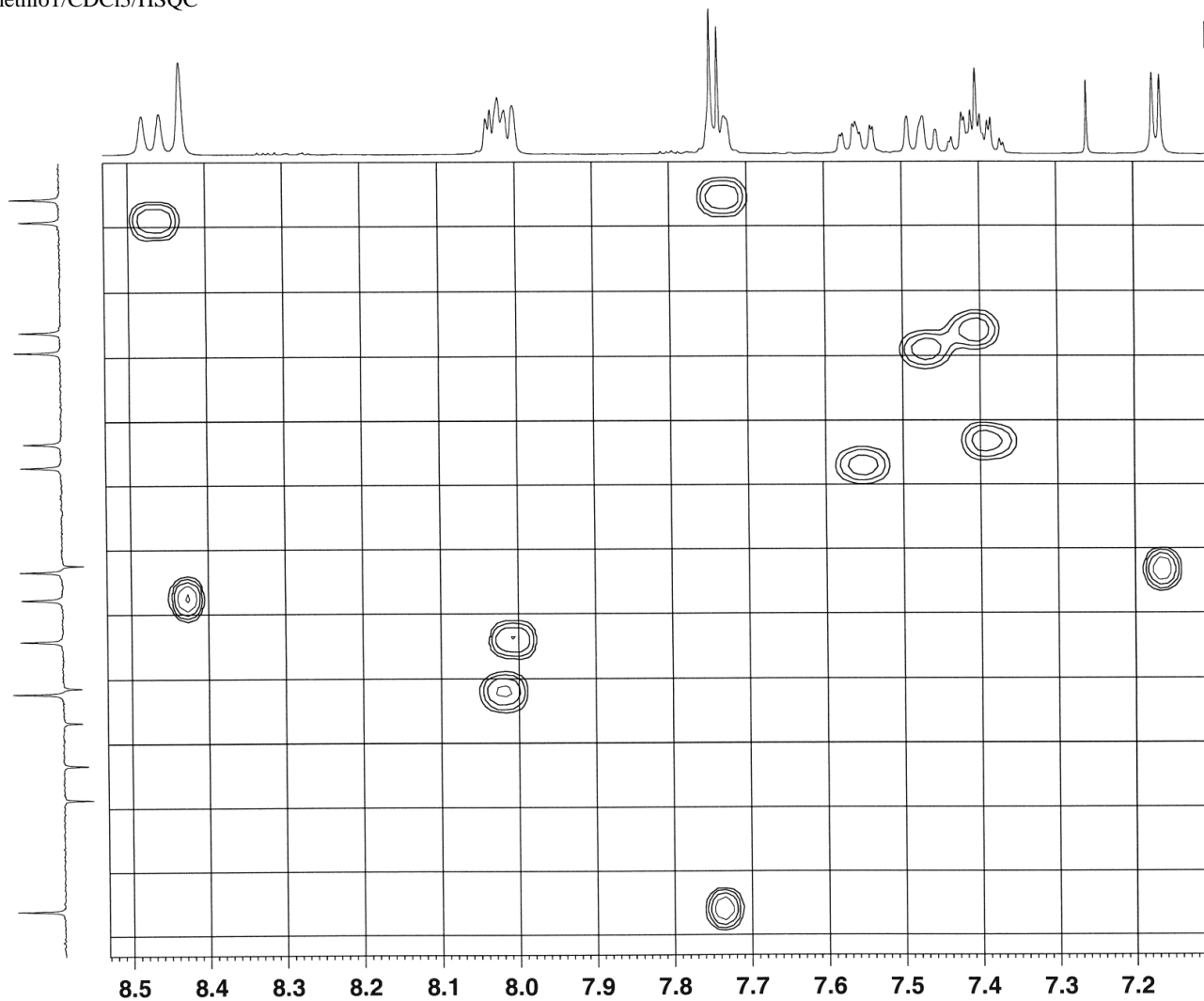




C13APT CDCl3 opt/xwinmr neudorfer 43

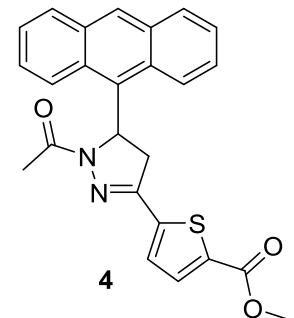


methio1/CDC13/HSQC

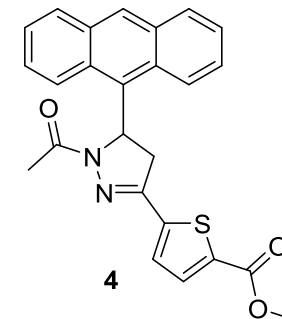
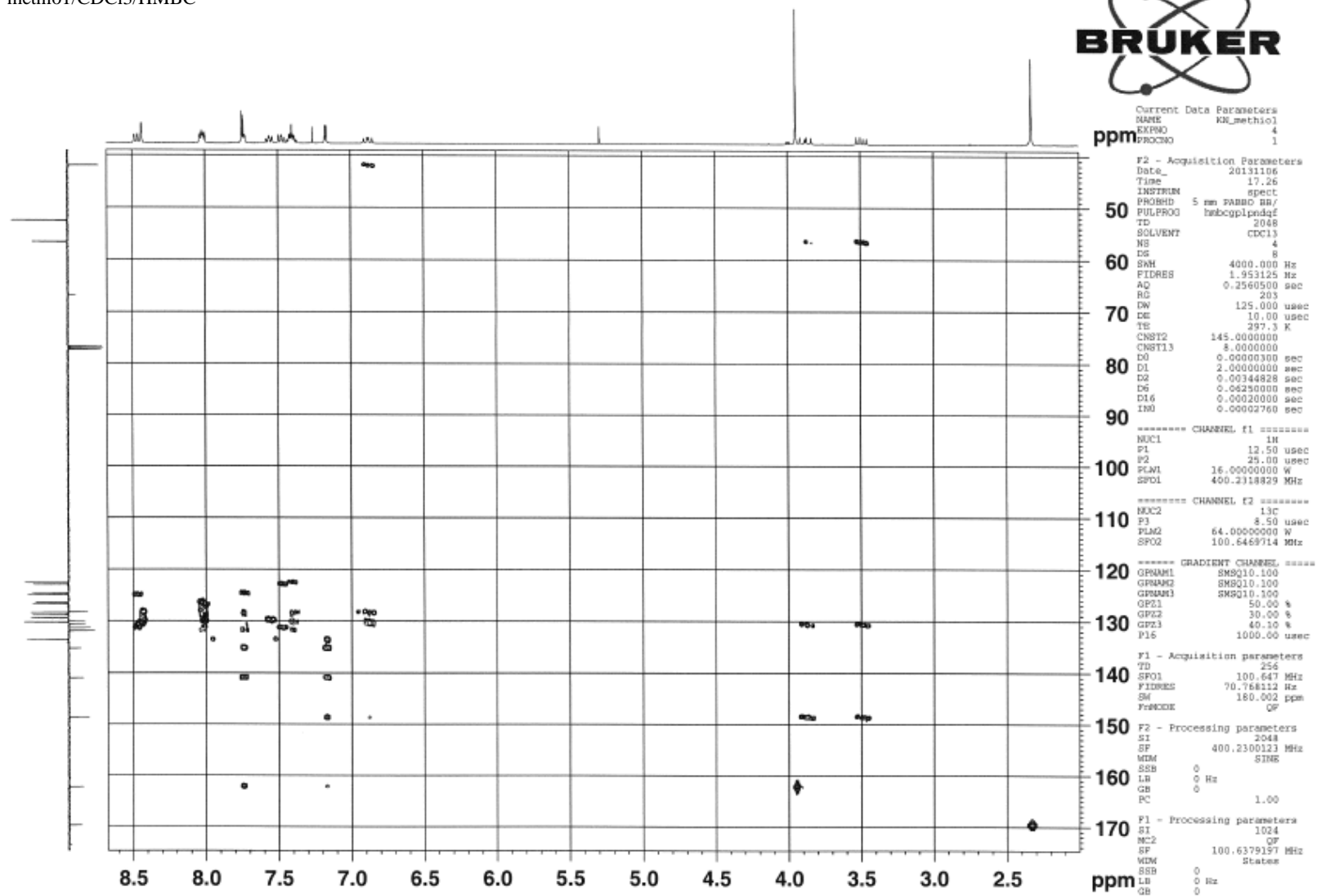


```

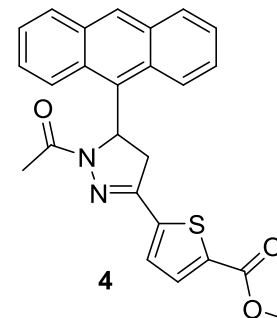
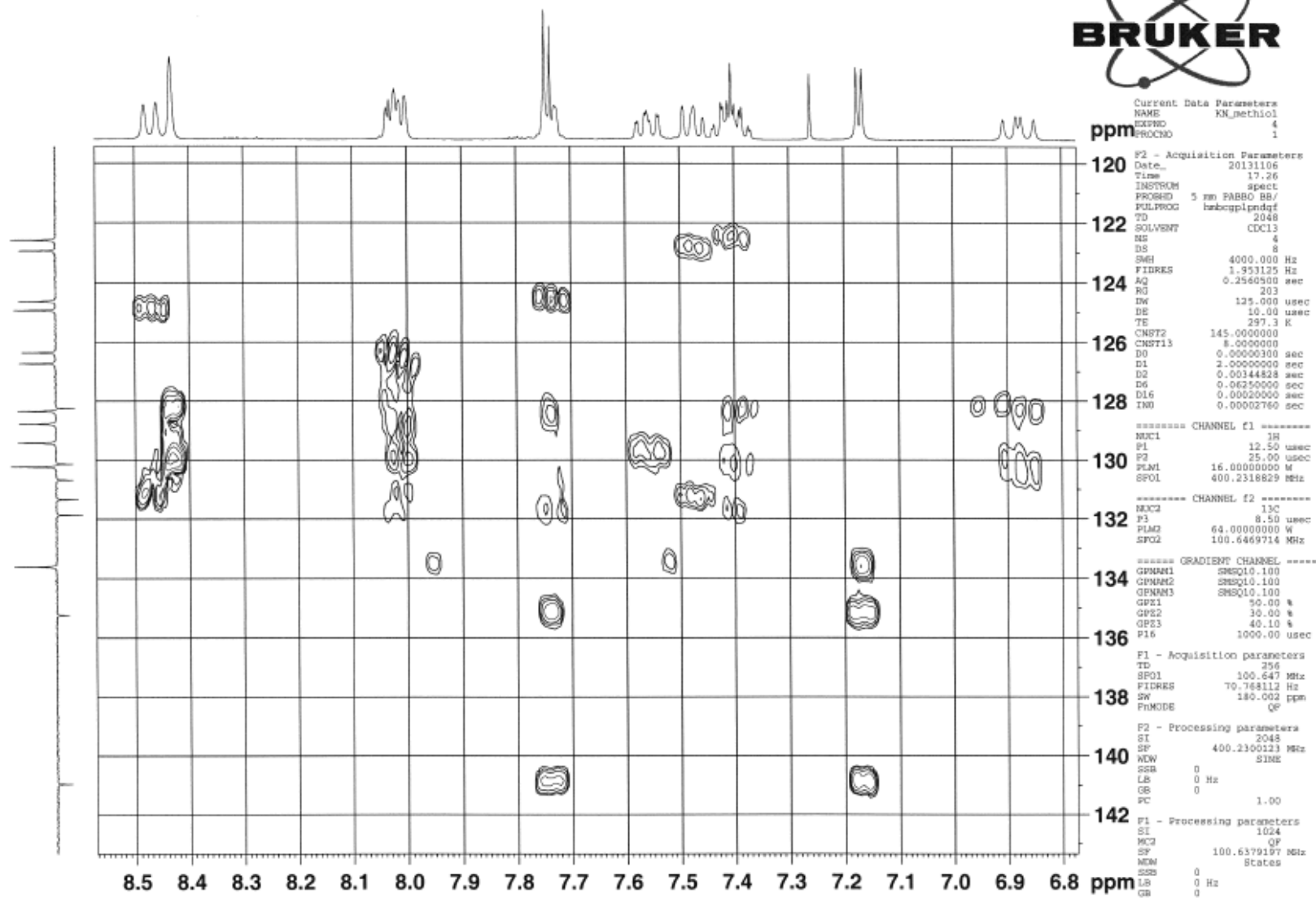
Current Data Parameters
NAME          rx_methio1
EXPNO        3
PROCNO       1
-----
F2 - Acquisition Parameters
Date_        2011106
Time         17.06
INSTRUM      spect
PROBHD       5 mm PABBO BB/
PULPROG      zgpg30
TD           1024
SOLVENT      CDC13
NS           2
DS           32
SWH          4000.000 Hz
FIDRES       3.906250 Hz
AQ           0.1280500 sec
RG           203
DM           125.000 usec
DE           10.00 usec
TE           297.3 K
CNSR2        145.000000
CNSR17       -0.500000
DO           0.00000300 sec
DL           2.00000000 sec
D4           0.00172414 sec
DL1          0.03000000 sec
DL6          0.00020000 sec
D24          0.00086207 sec
IN0          0.00004970 sec
-----
***** CHANNEL E1 *****
NUC1         1H
P1           12.50 usec
P2           25.00 usec
P28          1000.00 usec
PLM1         16.00000000 W
SFO1         400.2318829 MHz
-----
***** CHANNEL E2 *****
CPOPRG2     gpcp
NUC2         13C
P3           8.50 usec
P14          500.00 usec
P24          2000.00 usec
PCPD2       75.00 usec
PLM0         0 W
PLM2         64.00000000 W
PLM12        0.82204002 W
SFO2         100.6469714 MHz
SFOA3        Crp60.0.S.20.1
SFOA13       0.500
SFOA33       0 Hz
SFOA37       7.06489992 W
SFOA39       Crp60.comp.4
SFOA7        0.500
SFOA377      0 Hz
SFOA77       7.06500006 W
-----
***** GRADIENT CHANNEL *****
GPNAM1      SMSQ10.100
GPNAM2      SMSQ10.100
GPNAM3      SMSQ10.100
GPNAM4      SMSQ10.100
GP21        80.00 %
GP22        20.10 %
GP23        11.00 %
GP24        -5.00 %
P16         1000.00 usec
P19         600.00 usec
-----
F1 - Acquisition parameters
TD           256
SFO1         100.647 MHz
FIDRES       39.314751 Hz
SW           99.999 ppm
FNUCDE      Echo-Antiecho
-----
F2 - Processing parameters
SI           1024
SF           400.2300123 MHz
WDW          GAUSS
SBB          2
LB           0 Hz
GB           0
PC           1.00
-----
F1 - Processing parameters
SI           1024
MC2          echo-antiecho
SF           100.6379197 MHz
WDW          States-TPP1
SBB          2
LB           0 Hz
GB           0
  
```



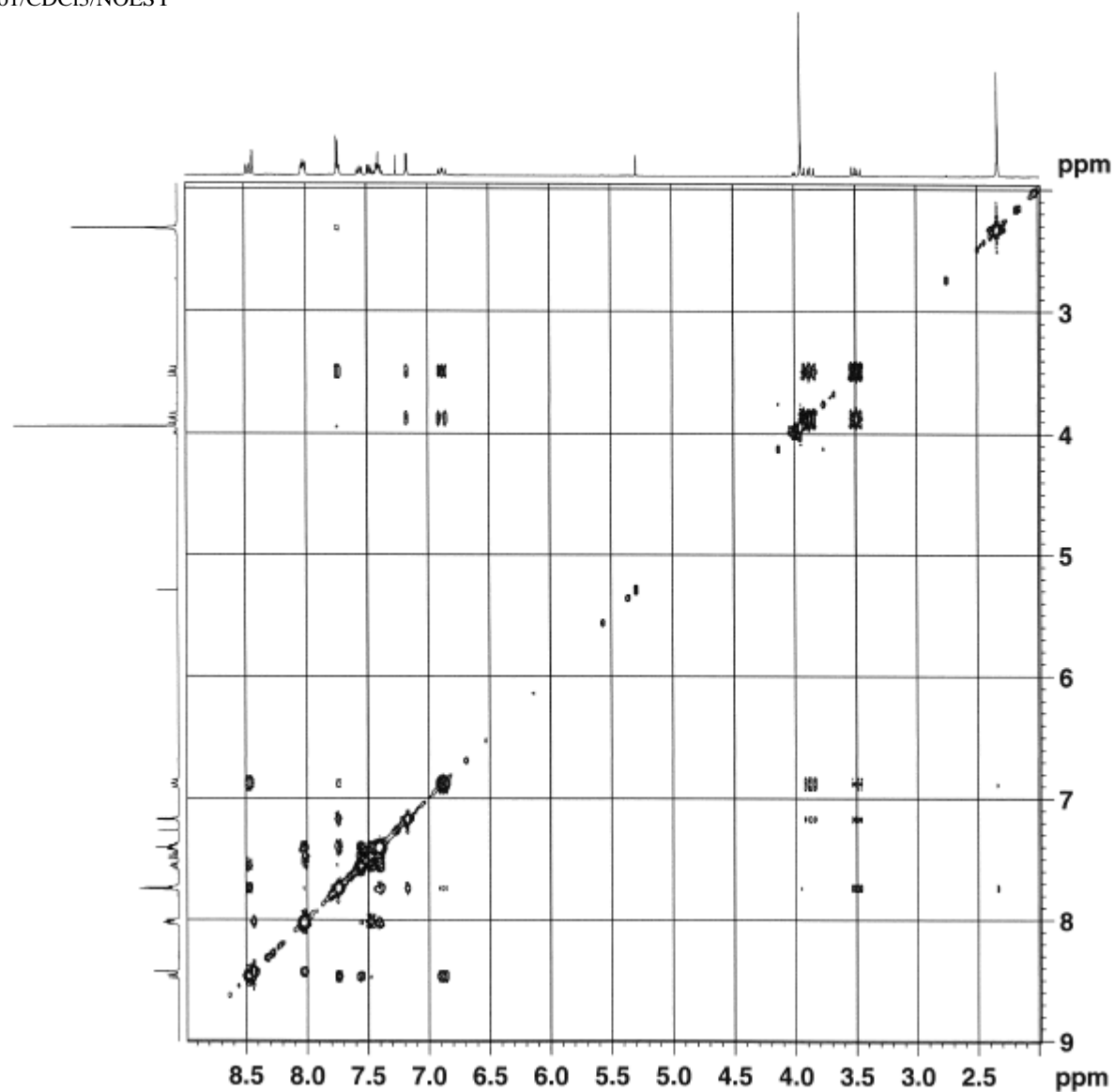
methio1/CDC13/HMBC



methio1/CDC13/HMBC



methio1/CDC13/NOESY



Current Data Parameters
 NAME KM_methiol
 EXPNO 5
 PROCNO 1

F2 - Acquisition Parameters
 Date_ 2011106
 Time_ 18.07
 INSTRUM spect
 PROBRD 5 mm PABBO BB/
 PULPROG noesyppgh
 TD 2048
 SOLVENT CDC13
 NS 8
 DS 8
 SWH 4000.000 Hz
 FIDRES 1.953125 Hz
 AQ 0.2560500 sec
 RG 362
 IW 125.000 usec
 DE 10.00 usec
 TE 297.3 K
 D0 0.00010901 sec
 D1 2.0000000 sec
 D8 0.80000001 sec
 D16 0.00020000 sec
 INO 0.00024985 sec

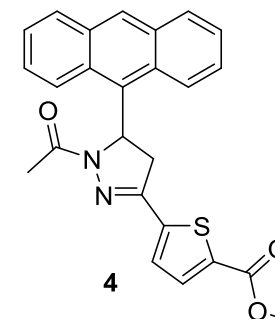
----- CHANNEL f1 -----
 MUC1 ih
 P1 12.50 usec
 P2 25.00 usec
 PLW1 16.0000000 W
 SFO1 400.2318829 MHz

----- GRADIENT CHANNEL -----
 GPNAM1 SMSQ10.100
 GPZ1 40.00 %
 P16 1000.00 usec

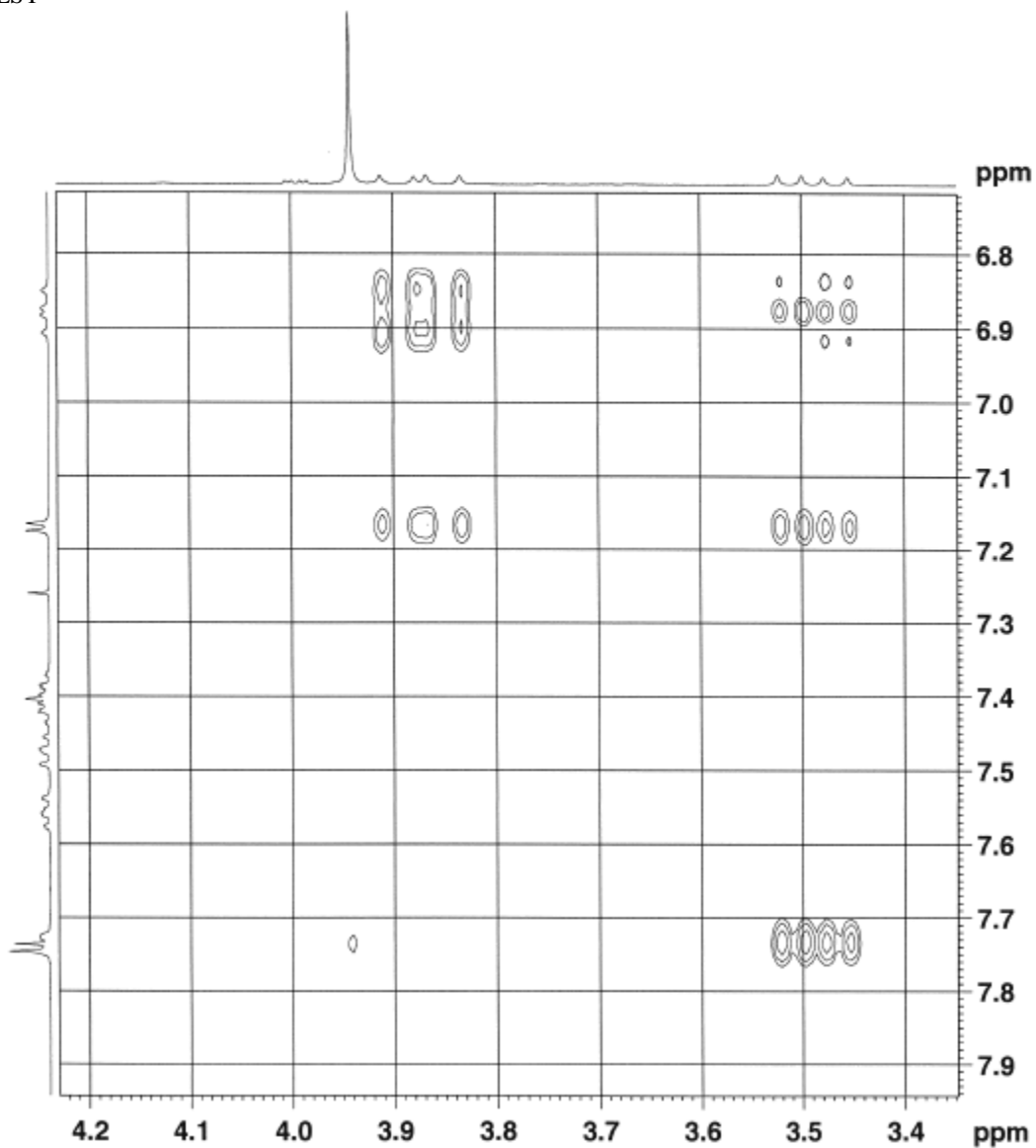
F1 - Acquisition parameters
 TD 256
 SFO1 400.2319 MHz
 FIDRES 15.634058 Hz
 SW 10.000 ppm
 FwMODE States-TPPI

F2 - Processing parameters
 SI 2048
 SF 400.2300123 MHz
 WDW QSINE
 SSB 2
 LB 0 Hz
 GB 0
 PC 1.00

F1 - Processing parameters
 SI 2048
 MC2 States-TPPI
 SF 400.2300123 MHz
 WDW States-TPPI
 SSB 2
 LB 0 Hz
 GB 0



methio1/CDC13/NOESY



Current Data Parameters
NAME KN_methio1
EXPNO 5
PROCNO 1

F2 - Acquisition Parameters
Date_ 20131106
Time 18.07
INSTRUM spect
PROBHD 5 mm PABBO BB/
PULPROG ncesypph
TD 2048
SOLVENT CDC13
NS 8
DS 8
SWH 4000.000 Hz
FIDRES 1.953125 Hz
AQ 0.2560500 sec
RG 362
DM 125.000 usec
DE 10.00 usec
TE 297.3 K
D0 0.00010901 sec
D1 2.00000000 sec
D8 0.80000001 sec
D16 0.00020000 sec
INO 0.00024985 sec

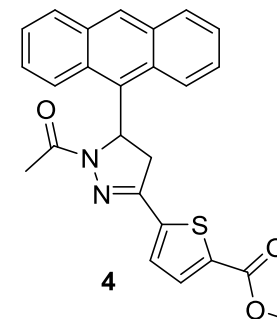
***** CHANNEL f1 *****
NUC1 1H
P1 12.50 usec
P2 25.00 usec
PLW1 16.00000000 W
SFO1 400.2318829 MHz

***** GRADIENT CHANNEL *****
GPNAM1 SMSQ10.100
GPZ1 40.00 %
P16 1000.00 usec

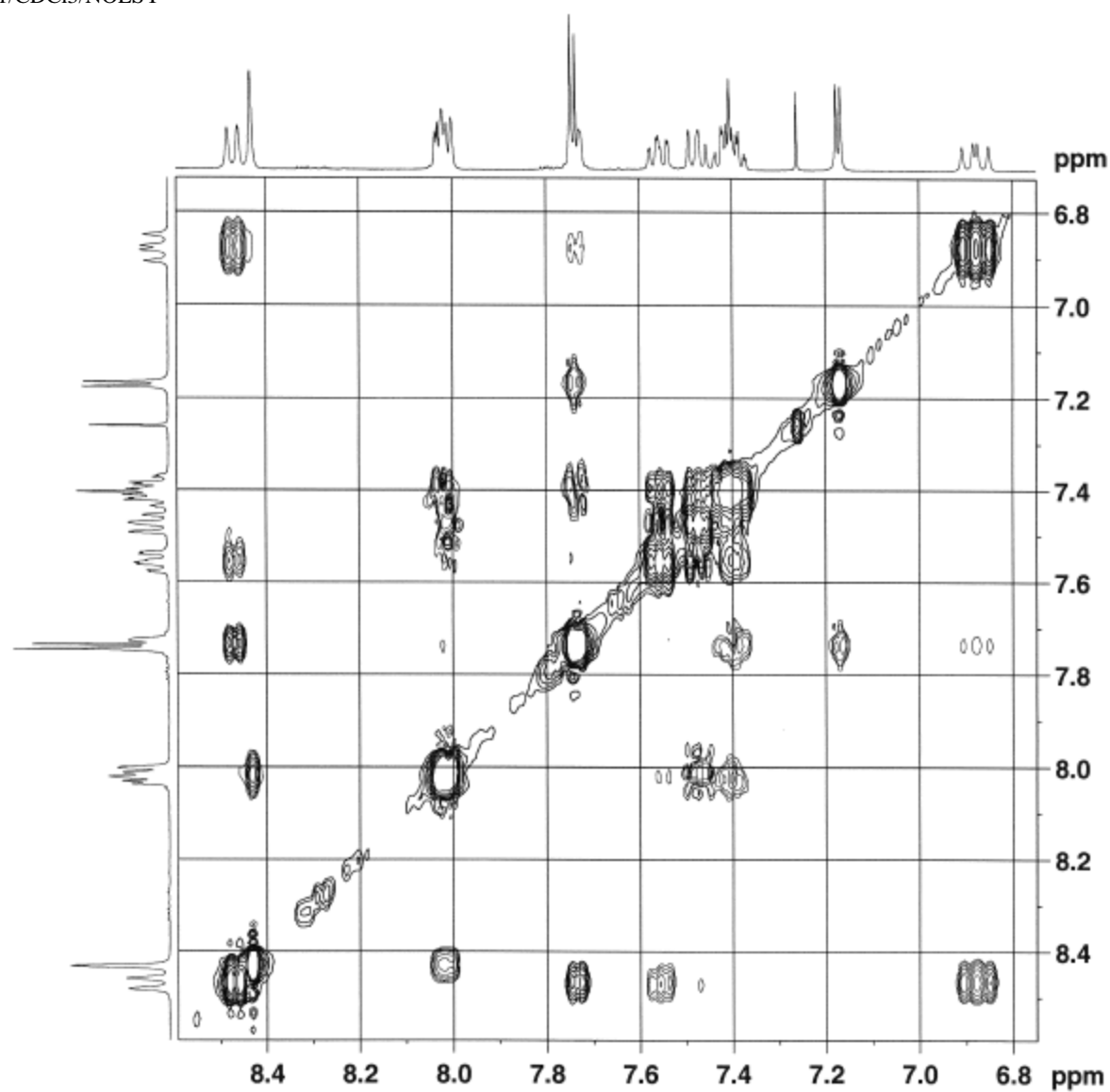
F1 - Acquisition parameters
TD 256
SFO1 400.2319 MHz
FIDRES 15.634058 Hz
SW 10.000 ppm
FhMODE States-TPPI

F2 - Processing parameters
SI 2048
SP 400.2300123 MHz
MDW QSINE
SSB 2
LB 0 Hz
GB 0
PC 1.00

F1 - Processing parameters
SI 2048
MC2 States-TPPI
SP 400.2300123 MHz
MDW States-TPPI
SSB 2
LB 0 Hz
GB 0



methio1/CDC13/NOESY



Current Data Parameters
 NAME KN_methio1
 EXPNO 5
 PROCNO 1

F2 - Acquisition Parameters
 Date_ 20131106
 Time 18.07
 INSTRUM spect
 PROBHD 5 mm PABBO BB/
 PULPROG noesypph
 TD 2048
 SOLVENT CDCl3
 NS 8
 DS 8
 SMH 4000.000 Hz
 FIDRES 1.953125 Hz
 AQ 0.2560500 sec
 RG 362
 DW 125.000 usec
 DE 10.00 usec
 TE 297.3 K
 D0 0.00010901 sec
 D1 2.00000000 sec
 D8 0.80000001 sec
 D16 0.00020000 sec
 IN0 0.00024985 sec

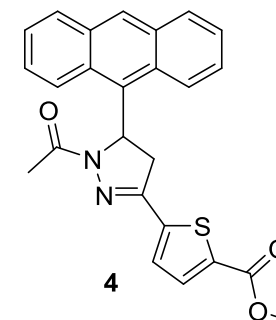
***** CHANNEL f1 *****
 NUC1 1H
 P1 12.50 usec
 P2 25.00 usec
 PLM1 16.00000000 W
 SF01 400.231829 MHz

***** GRADIENT CHANNEL *****
 GPNAM1 SMSQ10.100
 GPZ1 40.00 %
 P16 1000.00 usec

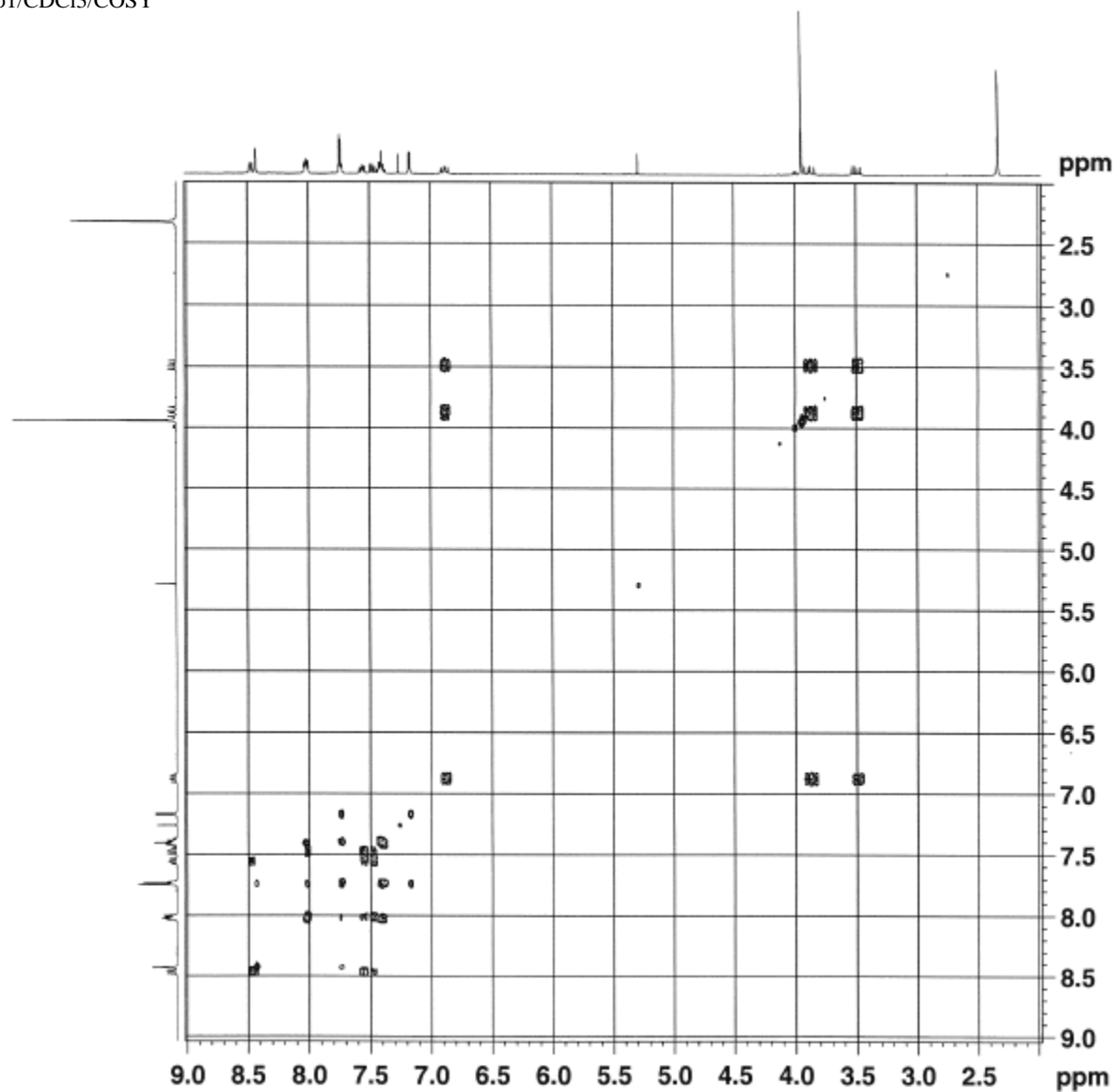
F1 - Acquisition parameters
 TD 256
 SF01 400.2319 MHz
 FIDRES 15.634058 Hz
 SW 10.000 ppm
 PnMODE States-TPPI

F2 - Processing parameters
 SI 2048
 SF 400.2300123 MHz
 WDW QSINE
 SSB 2
 LB 0 Hz
 GB 0
 FC 1.00

F1 - Processing parameters
 SI 2048
 MC2 States-TPPI
 SF 400.2300123 MHz
 WDW States-TPPI
 SSB 2
 LB 0 Hz
 GB 0



methio1/CDC13/COSY



Current Data Parameters
NAME KM_methiol
EXPRNO 7
PROCNO 1

F2 - Acquisition Parameters
Date_ 20131105
Time 21.16
INSTRUM spect
PROBHD 5 mm PABBO BB/
PULPROG cosypppqf
TD 2048
SOLVENT CDC13
NS 2
DS 8
SWH 2802.691 Hz
FIDRES 1.368501 Hz
AQ 0.3654132 sec
RG 181
TM 10.00 usec
DE 178.400 usec
TE 297.3 K
DO 0.00000300 sec
D1 2.00000000 sec
D11 0.03000000 sec
D12 0.00002000 sec
D13 0.00000400 sec
D16 0.00020000 sec
IN0 0.00035695 sec

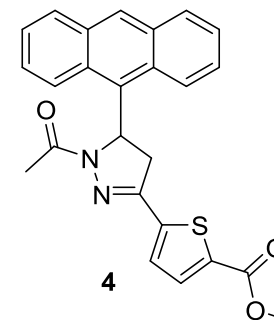
==== CHANNEL f1 =====
NUC1 1H
P0 12.50 usec
P1 12.50 usec
P17 2500.00 usec
PLW1 15.0000000 W
PLW10 2.40150003 W
SP01 400.2324014 MHz

===== GRADIENT CHANNEL =====
GPNAM1 SMSQ10.100
GPZ1 20.00 %
P16 1000.00 usec

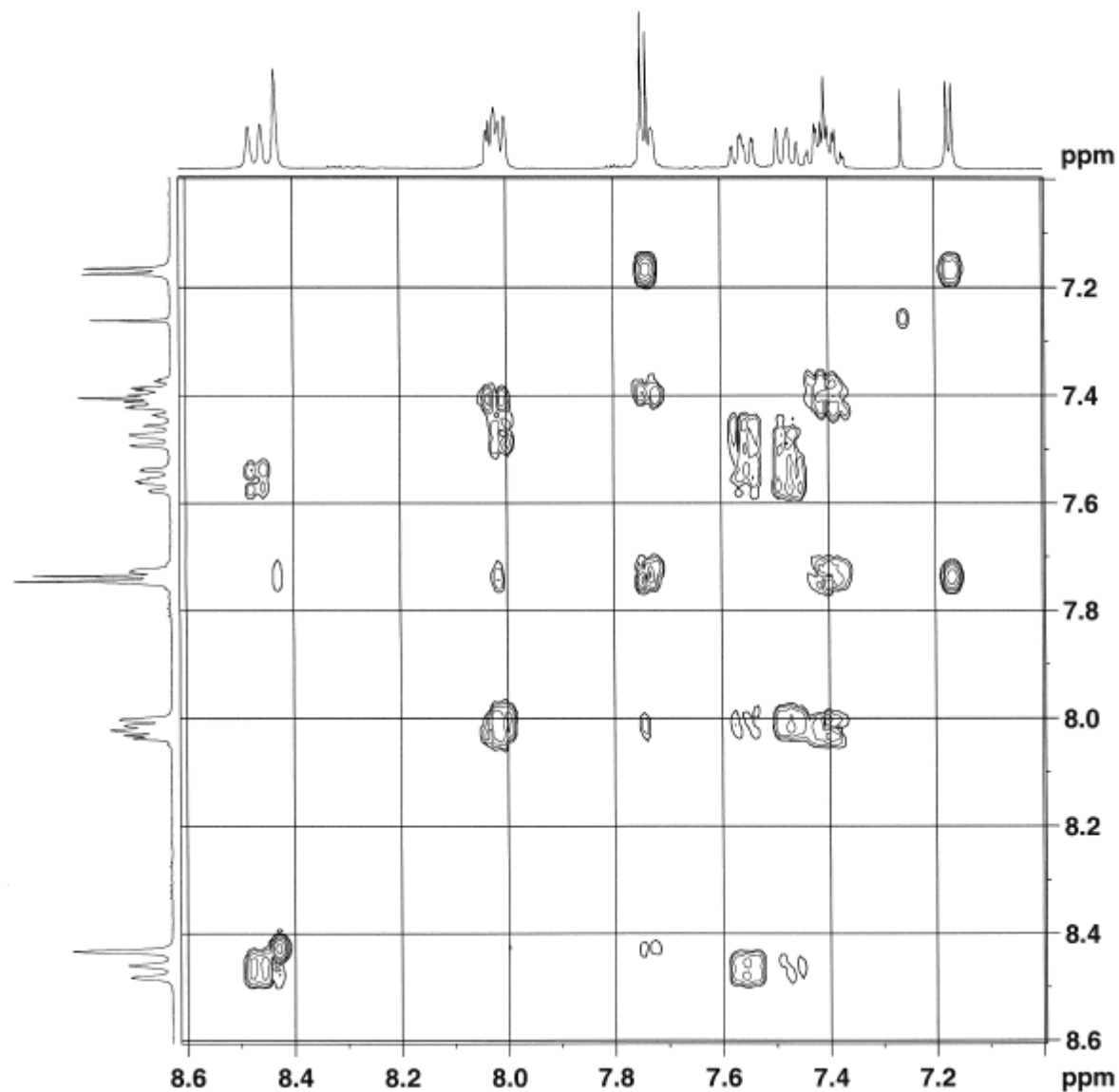
F1 - Acquisition parameters
TD 256
SP01 400.2324 MHz
FIDRES 10.943841 Hz
SW 7.000 ppm
PnMODE QF

F2 - Processing parameters
SI 1024
SF 400.2300123 MHz
MDM QSINE
SBB 0
LB 0 Hz
GB 0
PC 1.00

F1 - Processing parameters
SI 1024
MC2 QF
SF 400.2300123 MHz
MDM States-TPPI
SBB 0
LB 0 Hz
GB 0



methio1/CDC13/COSY



Current Data Parameters
 NAME EN_methiol
 EXPNO 7
 PROCNO 1

F2 - Acquisition Parameters
 Date_ 20131106
 Time 21.16
 INSTRUM spect
 PROBHD 5 mm PABBO BB/
 PULPROG cosygpppqf
 TD 2048
 SOLVENT CDC13
 NS 2
 DS 8
 SMH 2802.691 Hz
 FIDRES 1.368501 Hz
 AQ 0.3654132 sec
 RG 181
 DM 178.400 usec
 DE 10.00 usec
 TE 297.3 K
 D0 0.00000300 sec
 D1 2.00000000 sec
 D11 0.03000000 sec
 D12 0.00002000 sec
 D13 0.00004000 sec
 D16 0.00020000 sec
 INO 0.00035695 sec

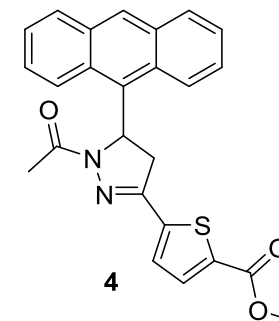
***** CHANNEL f1 *****
 NUC1 1H
 P0 12.50 usec
 P1 12.50 usec
 P17 2500.00 usec
 PLW1 16.00000000 W
 PLW10 2.60150003 W
 SFO1 400.2324014 MHz

***** GRADIENT CHANNEL *****
 GPNAM1 SMSQ10.100
 GPE1 20.00 %
 P16 1000.00 usec

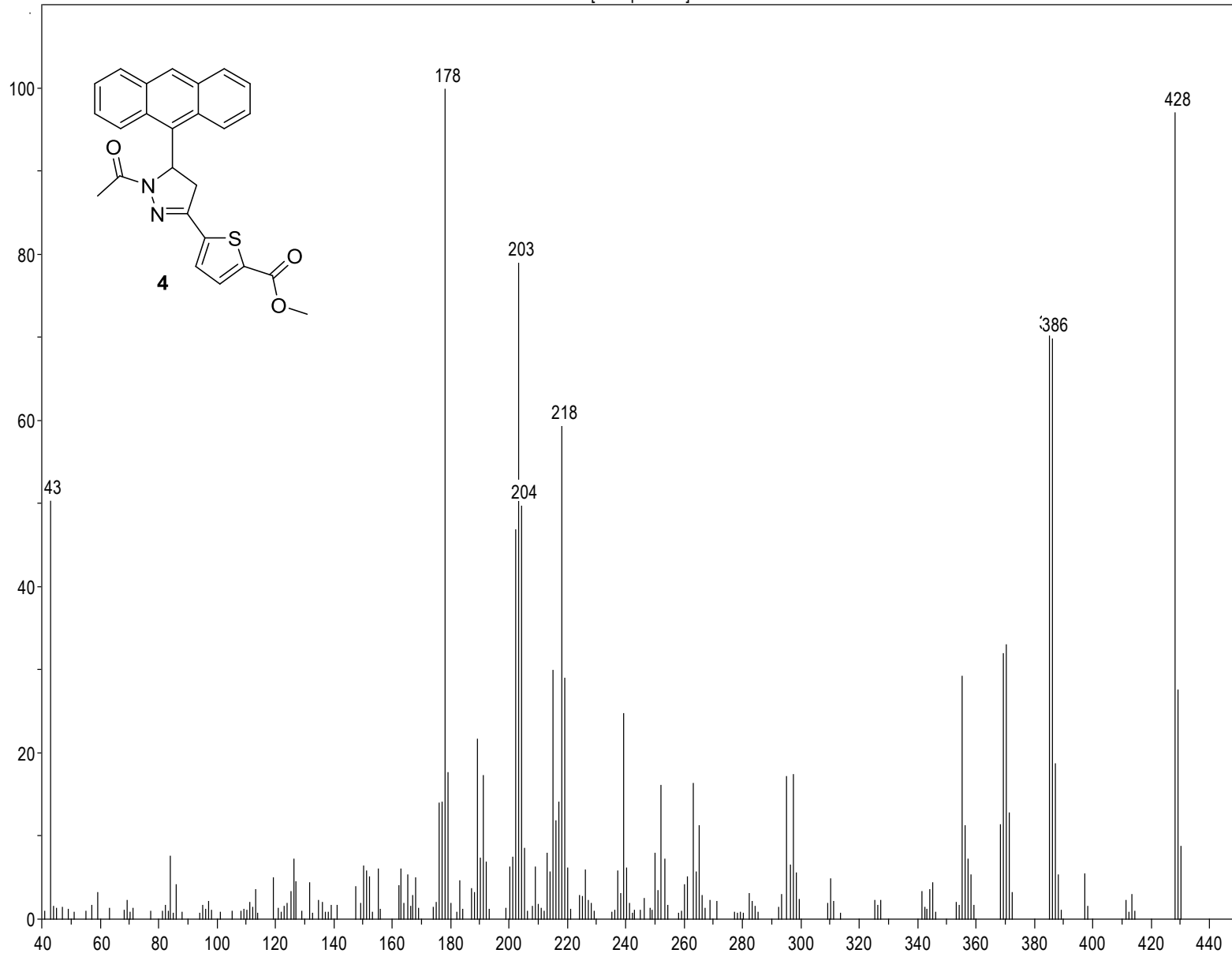
F1 - Acquisition parameters
 TD 256
 SFO1 400.2324 MHz
 FIDRES 10.943841 Hz
 SW 7.000 ppm
 FhMODE QF

F2 - Processing parameters
 SI 1024
 SF 400.2300123 MHz
 MDM QSINE
 SSB 0
 LB 0 Hz
 GB 0
 PC 1.00

F1 - Processing parameters
 SI 1024
 MC2 QF
 SF 400.2300123 MHz
 WDW States-TPPI
 SSB 0
 LB 0 Hz
 GB 0



[MS Spectrum]



MassenspektrometrieZentrum FakultätChemieUniWien

Analysis Info

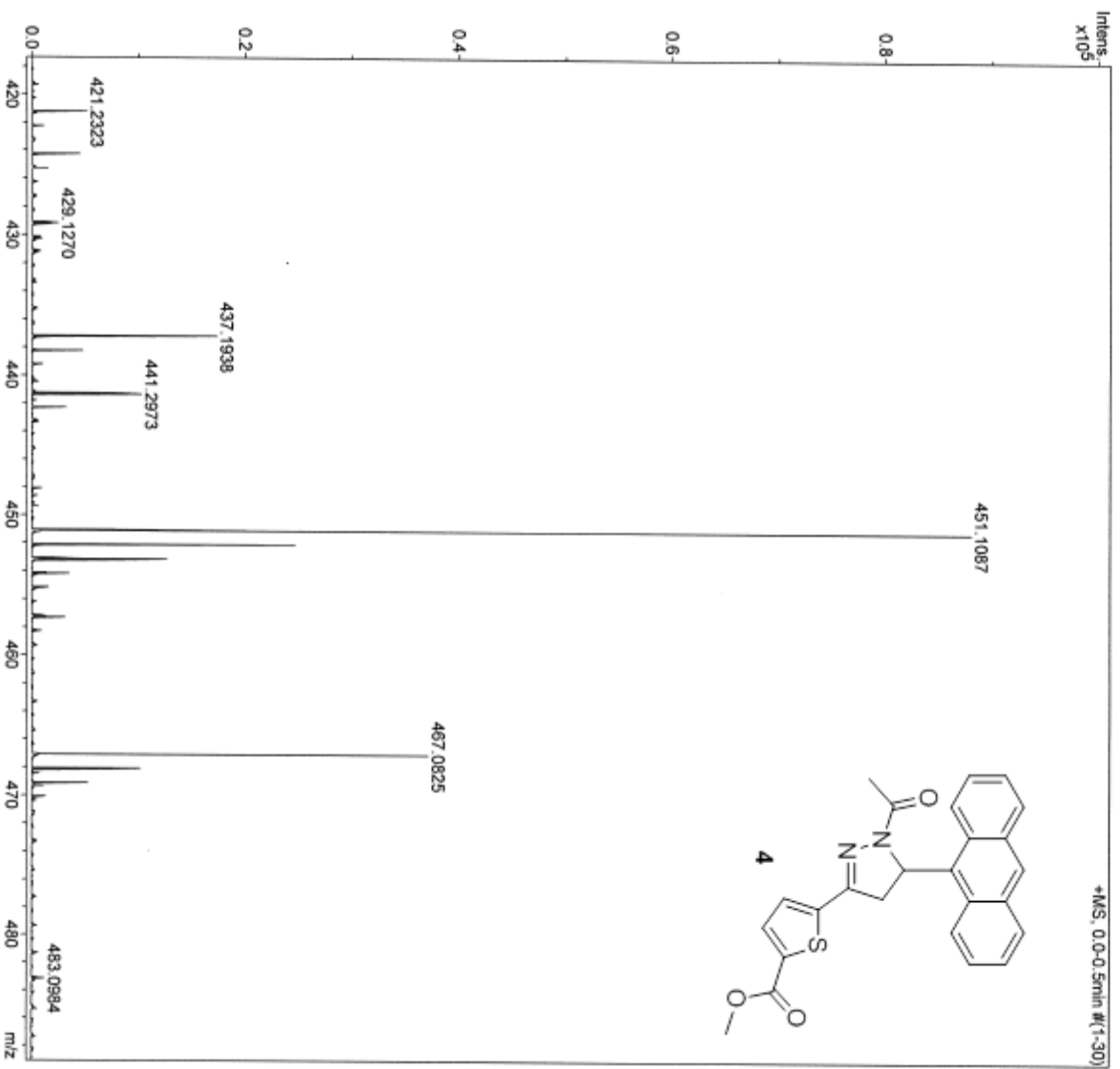
Analysis Name D:\Data\MS_MessService\38817000001.d
 Method Nanomate infusion training01.m
 Sample Name Tpyc6
 Auftraggeber/Com Neudorfer/Spreitzer

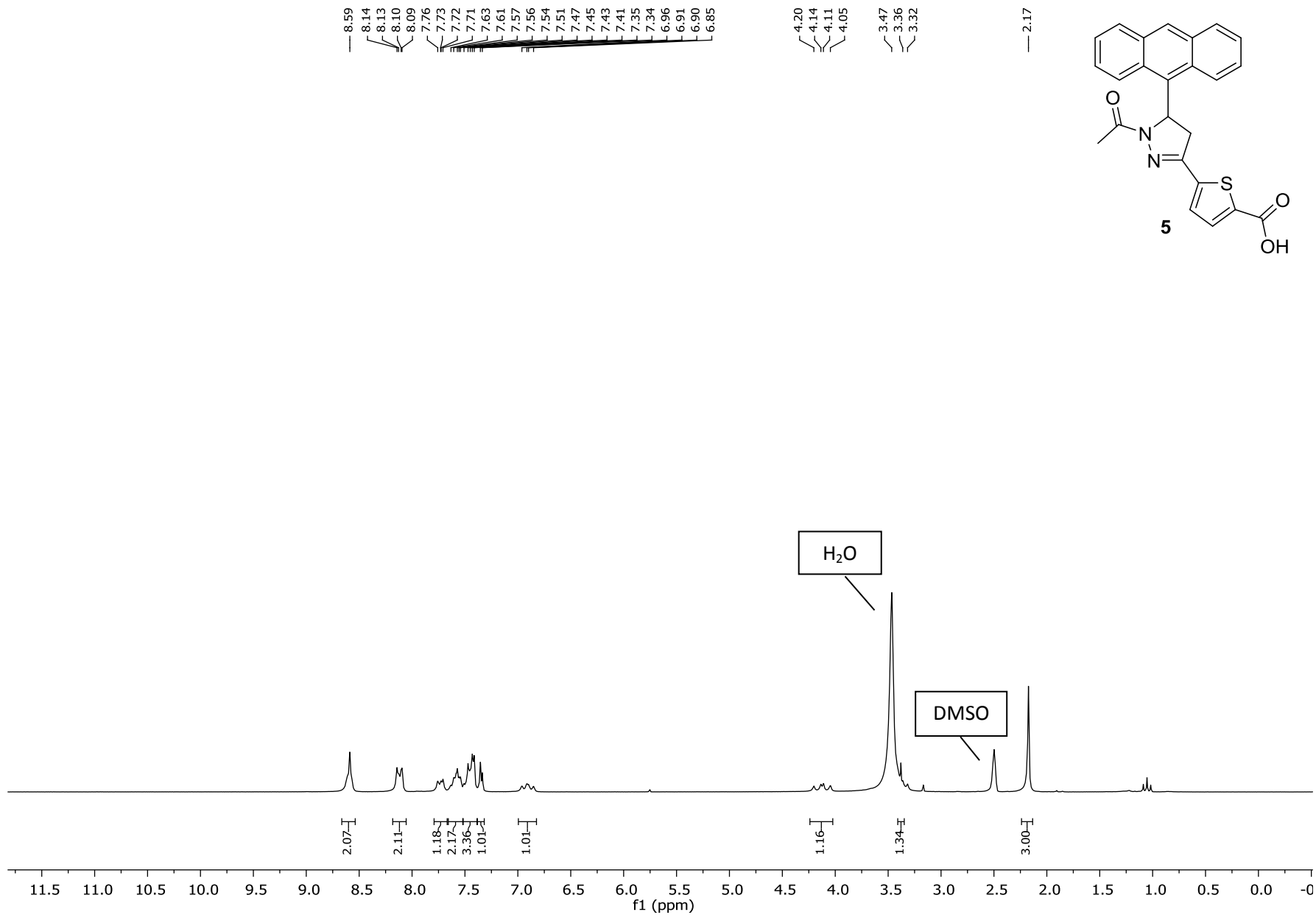
Acquisition Date 9/12/2012 11:24:06 AM

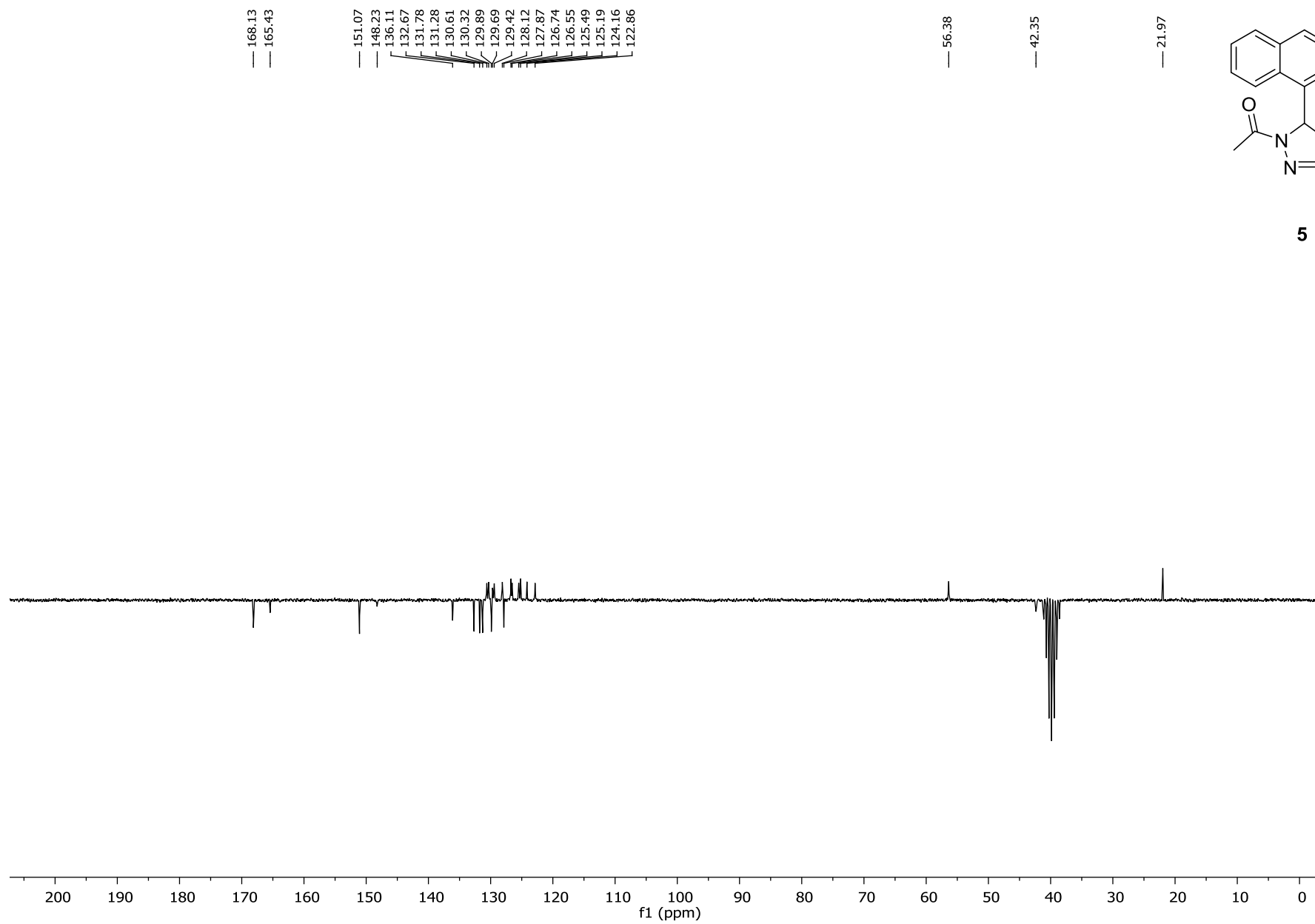
Operator phu
 Instrument maxis

Ergebnis: +/- 5 ppm

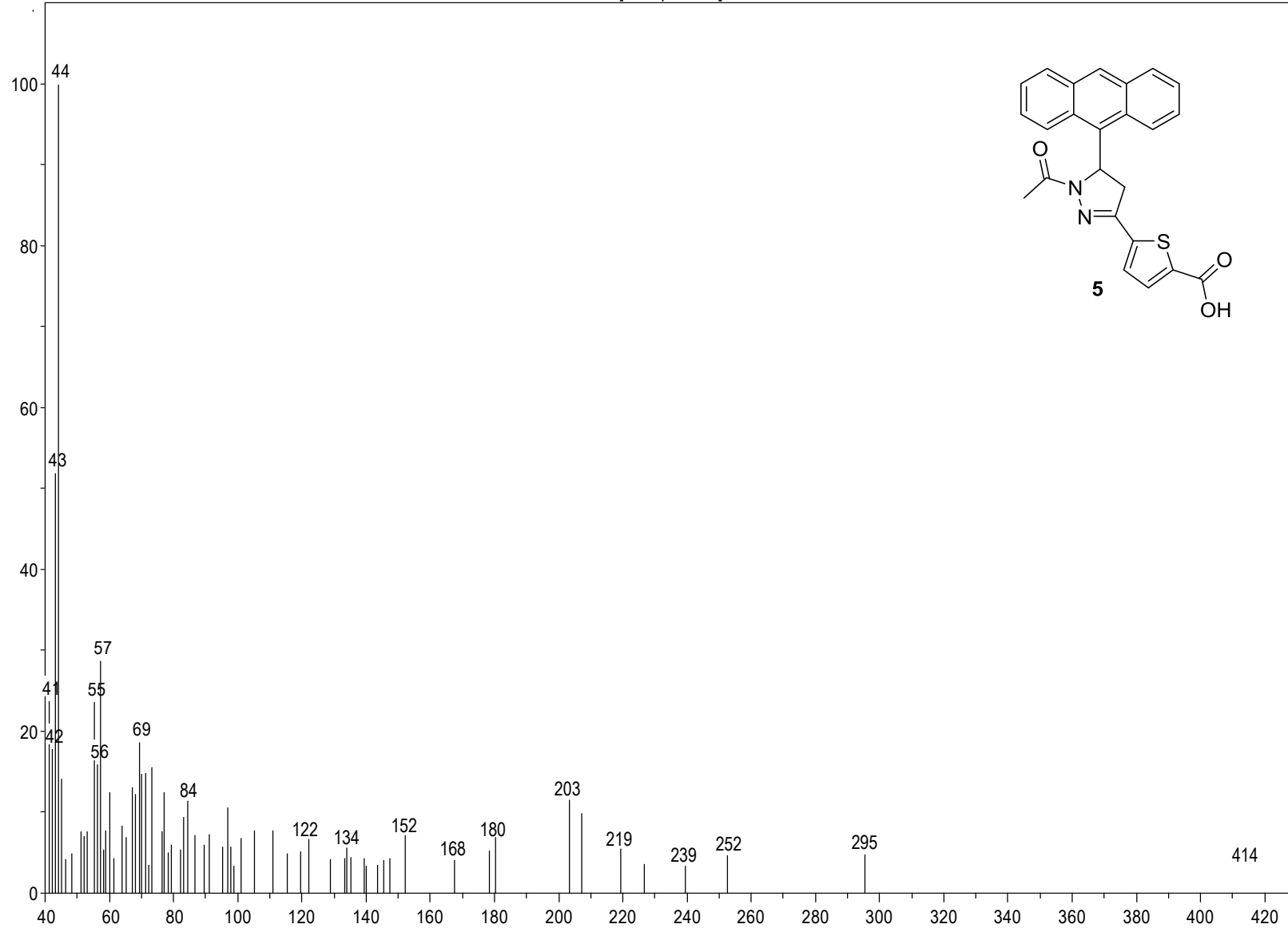
MeOH/ACN







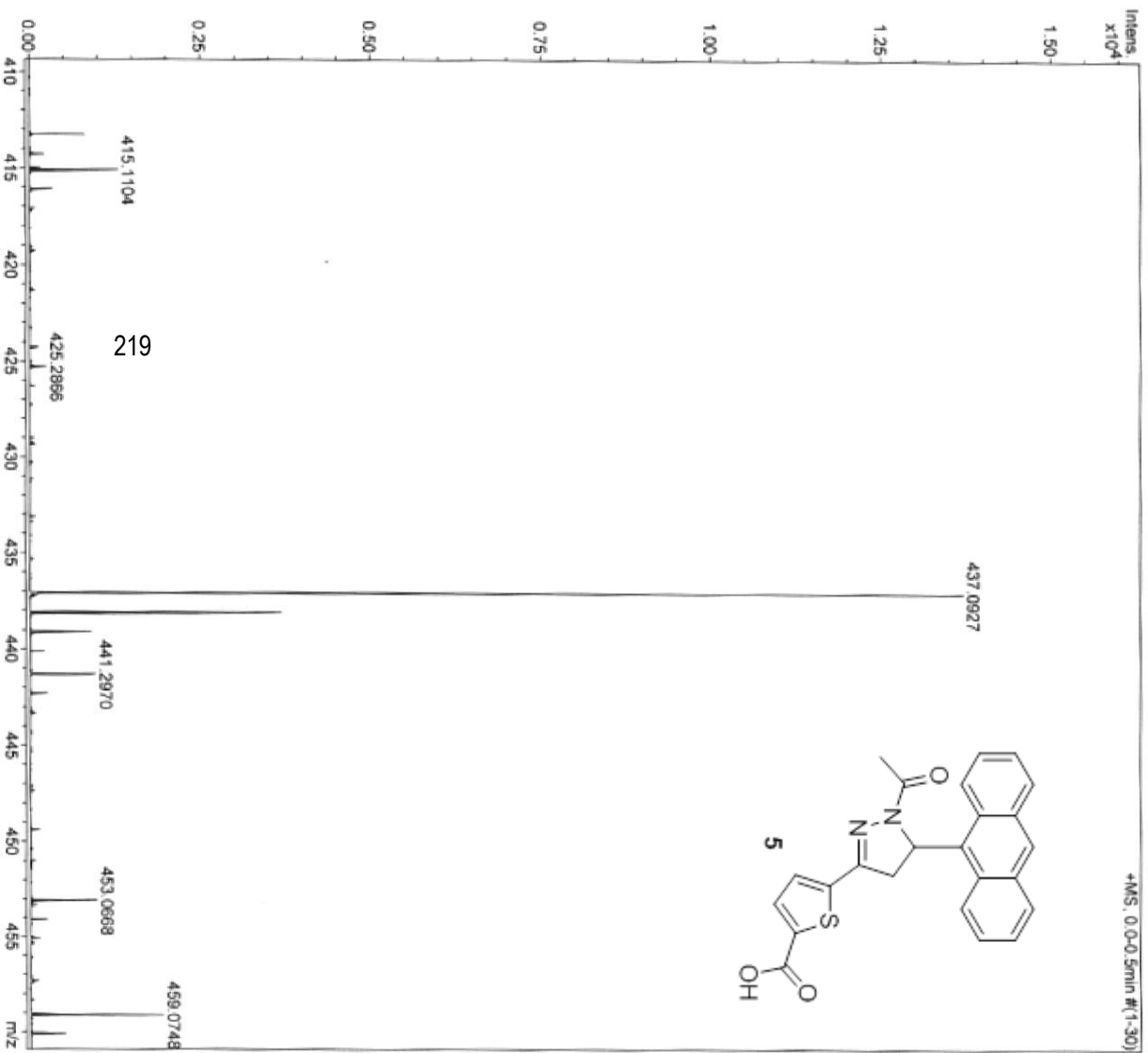
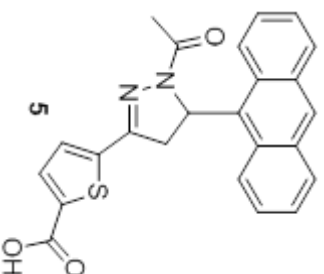
[MS Spectrum]

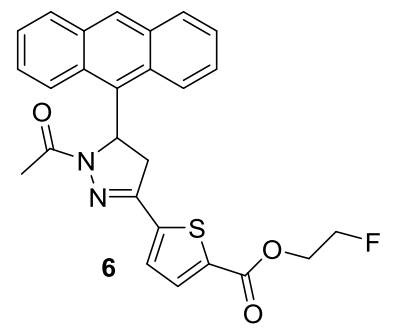
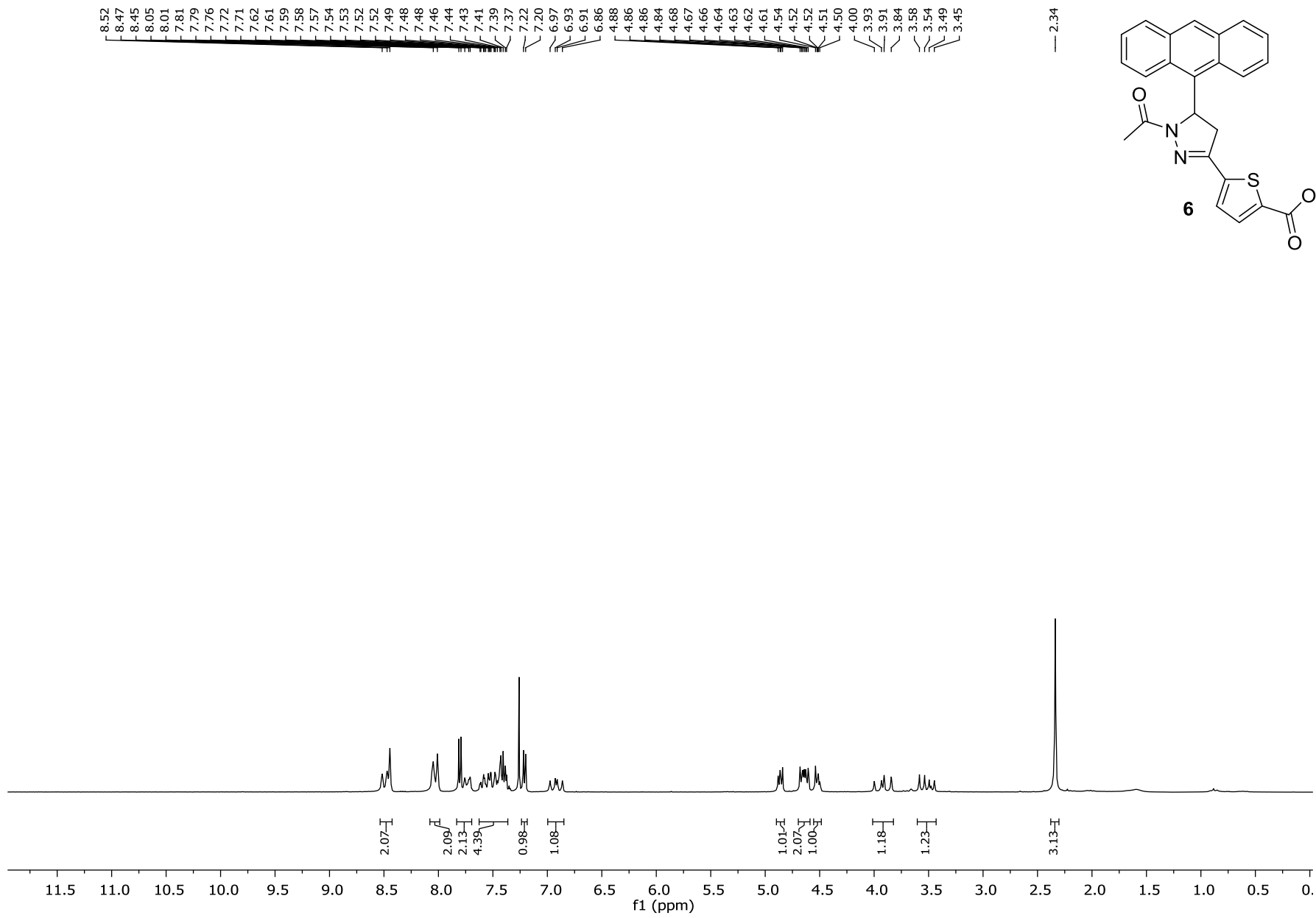


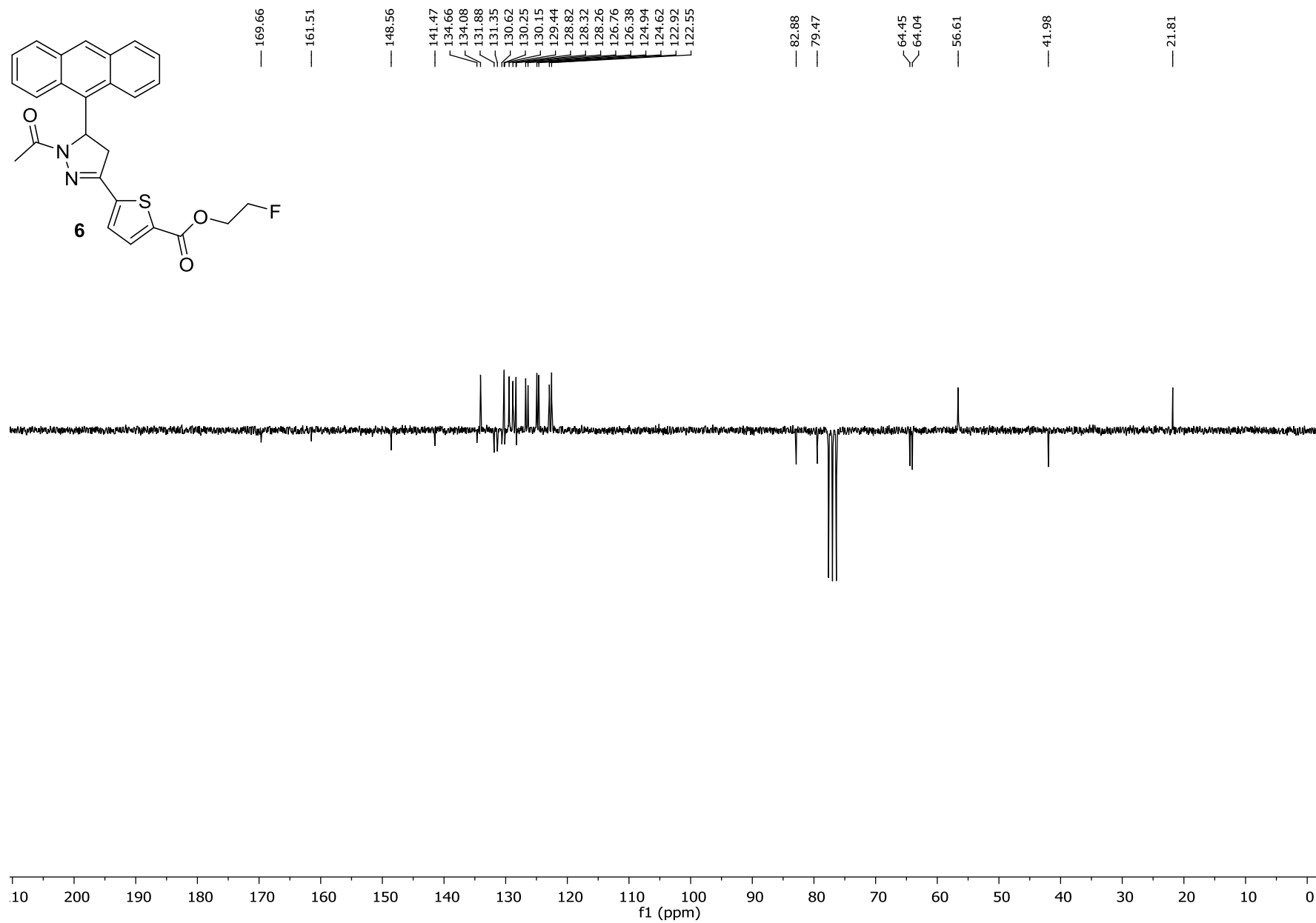
MassenspektrometrieZentrum FakultätChemieUniWien

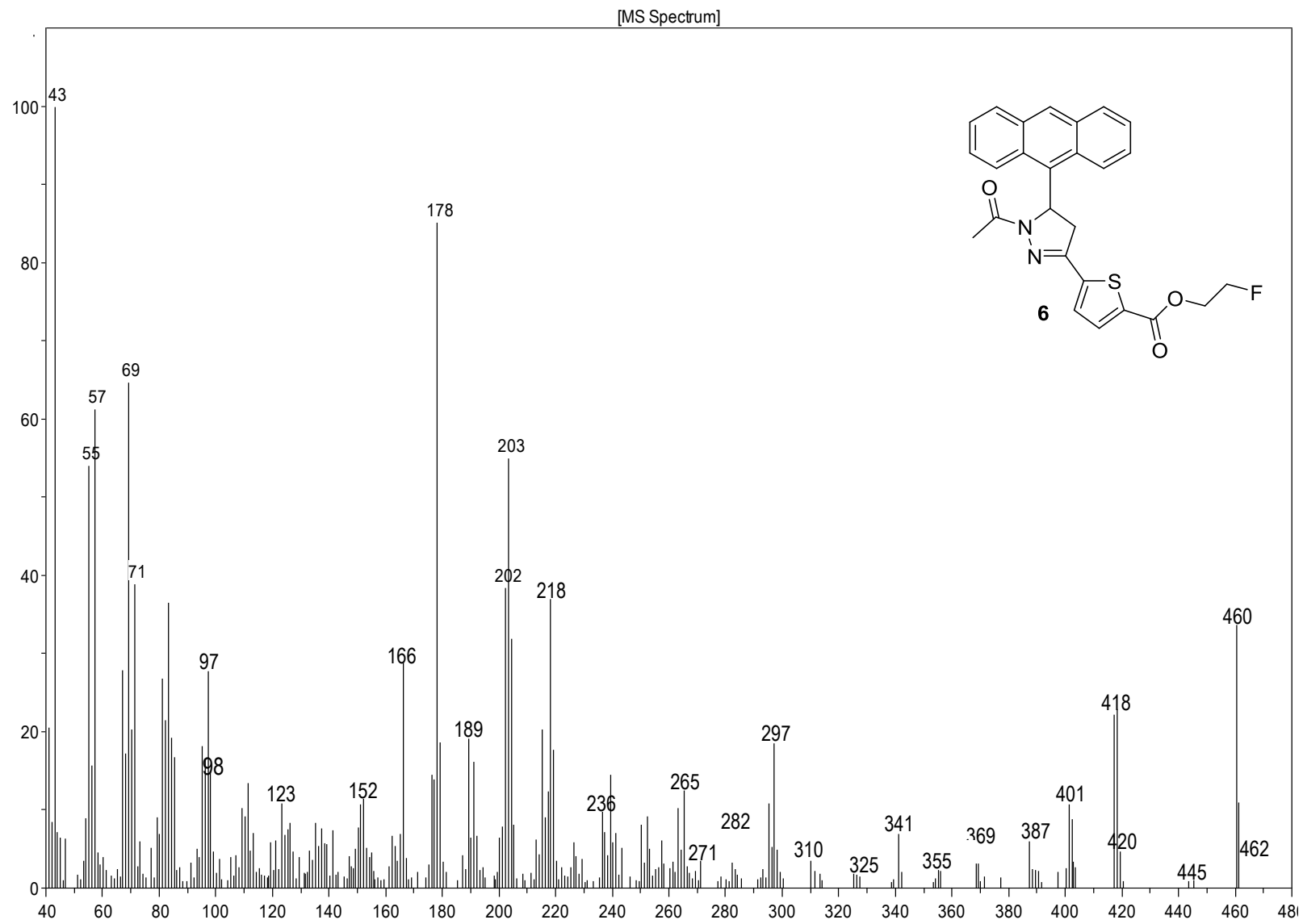
Analysis Info
 Analysis Name D:\Data\MS_MessService\39131000001.d
 Method tune_low_nach_Quadropol.m
 Sample Name achsr1
 Auftraggeber/Com Neudorfer/Spreitzer/Pharm
 Ergebnis: +/- 5 ppm
 ACN/MeOH

Acquisition Date 12/14/2012 2:03:59 PM
 Operator phu
 Instrument maxis





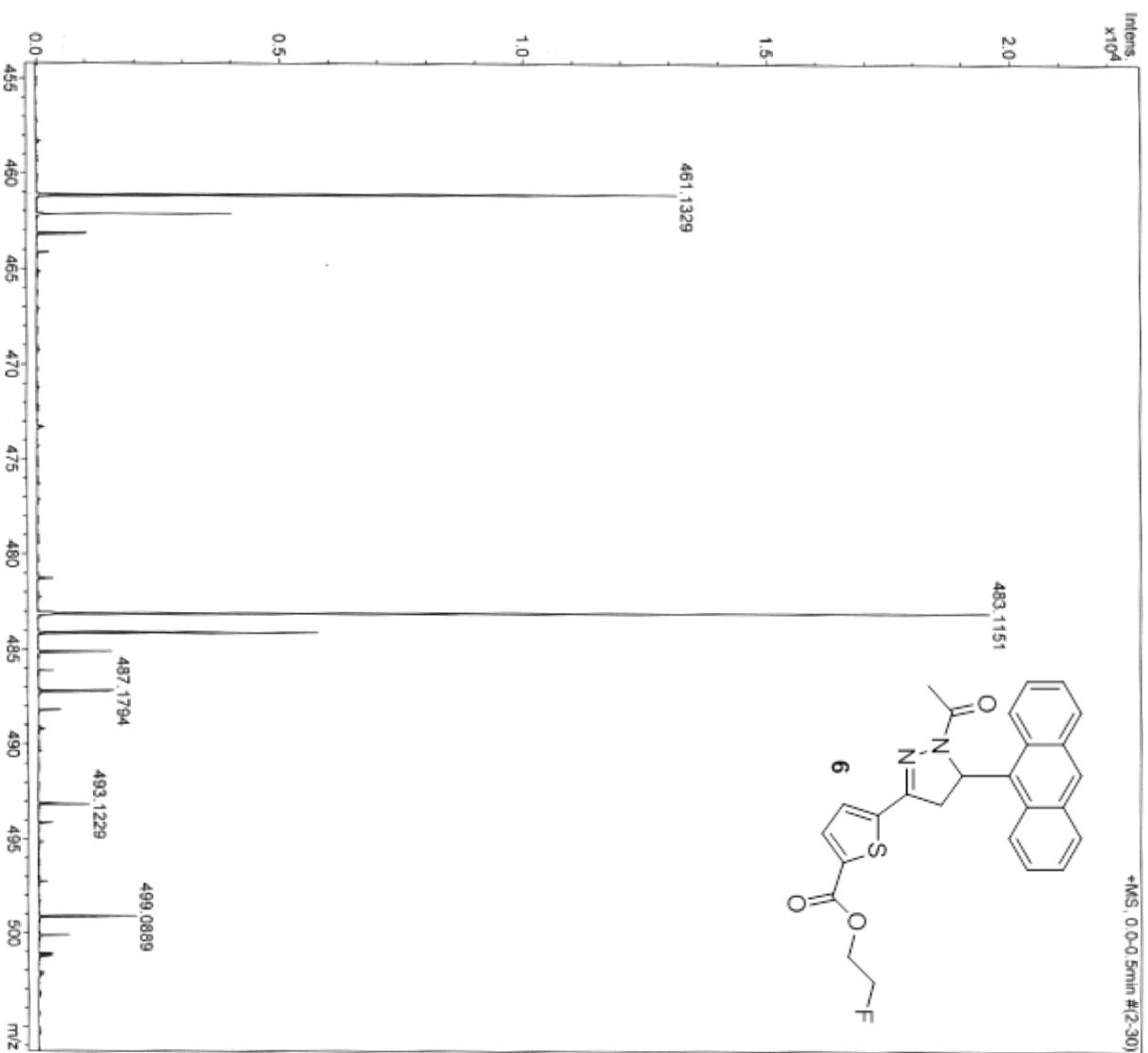
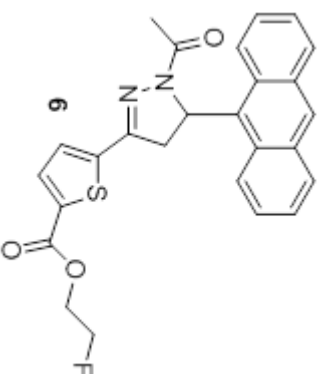




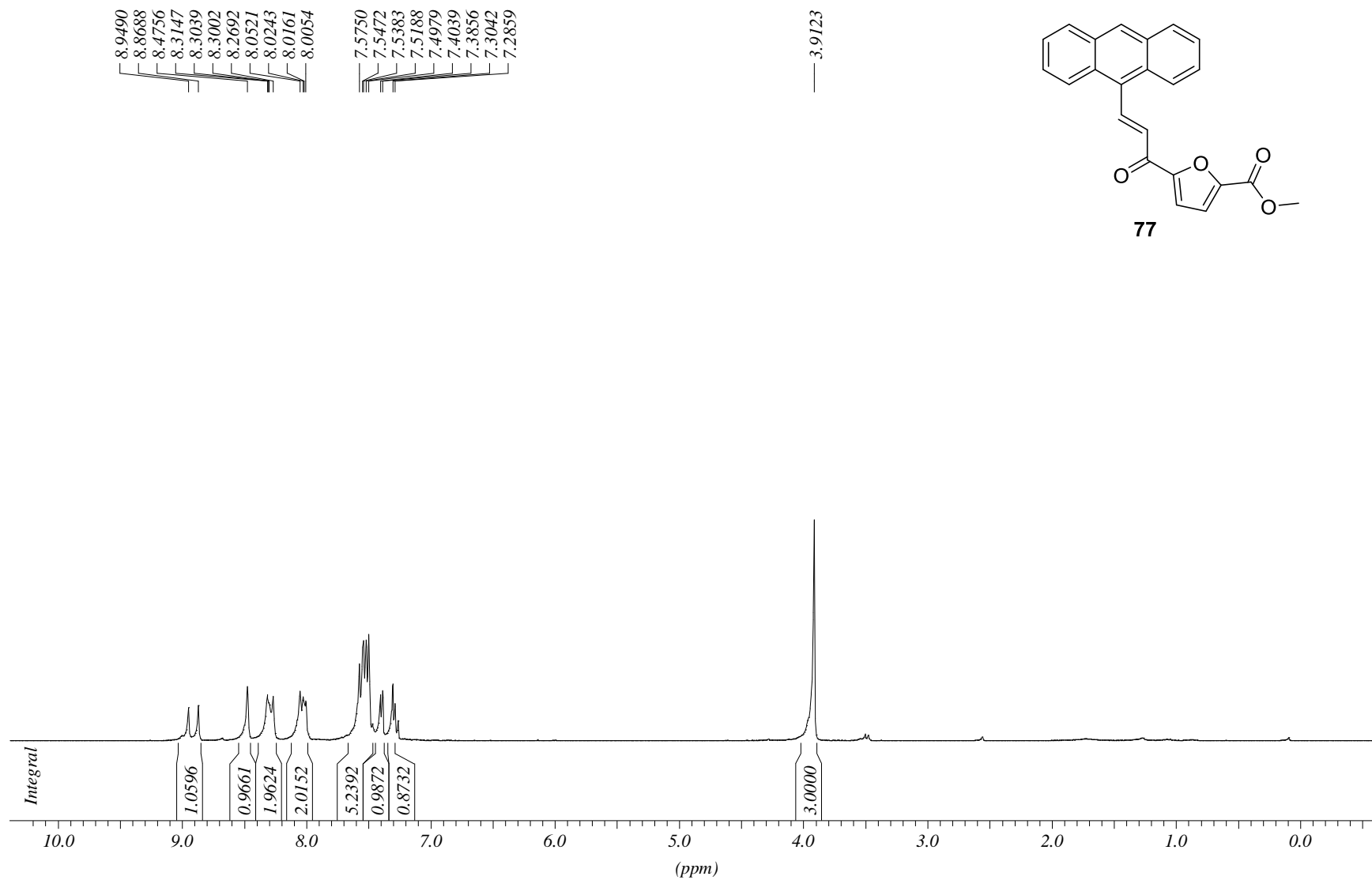
MassenspektrometrieZentrum FakultätChemieUniWien

Analysis Info
 Analysis Name D:\Data\MS_MessService\396333000001.d
 Method tune_low_MS_Service_06_13.m
 Sample Name thiol 4
 Auftraggeber/Com Neudorfer/Spreitzer
 Ergebnis: +/- 5ppm
 ACN/MeOH 1%/H2O

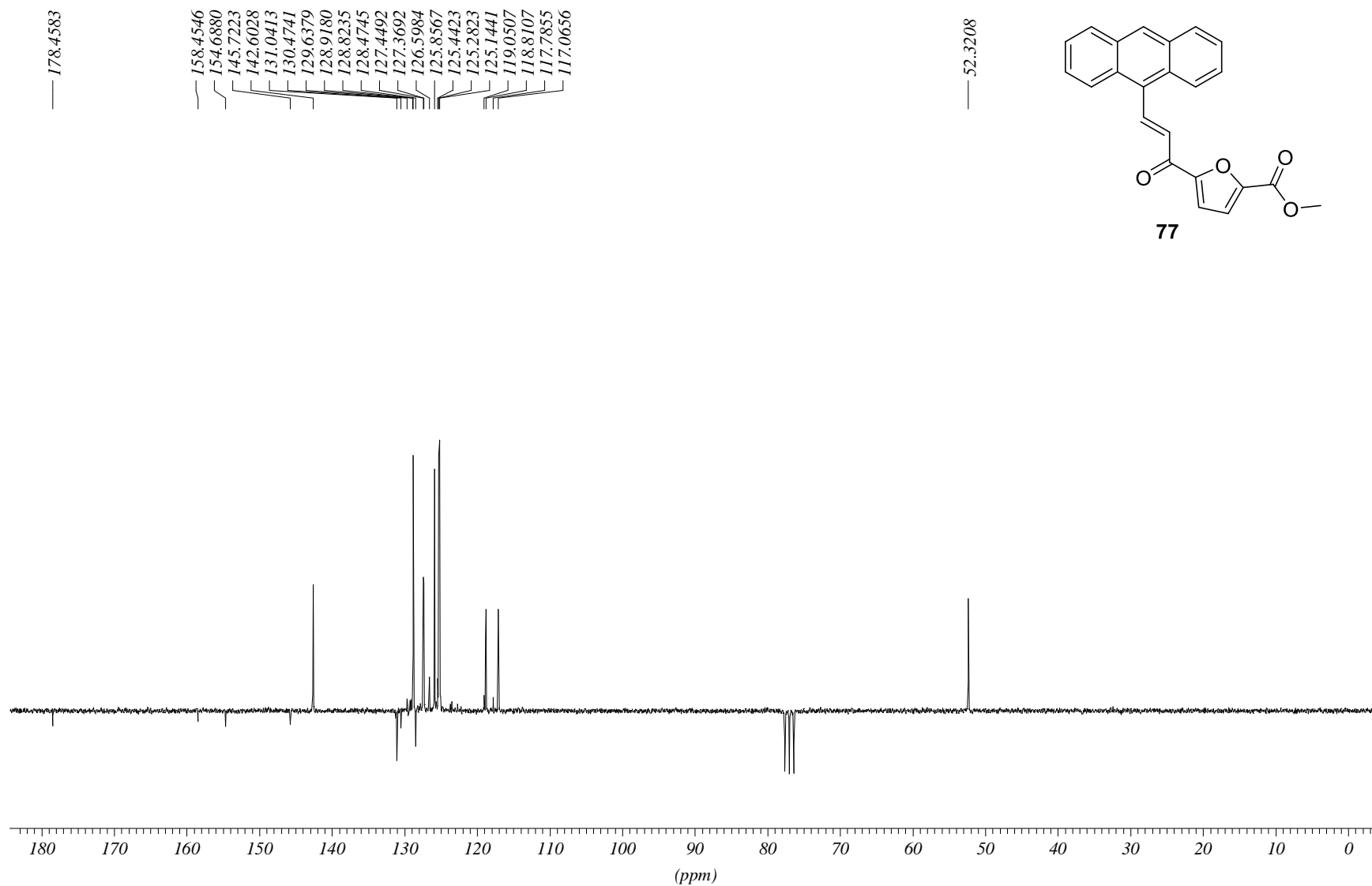
Acquisition Date 6/14/2013 1:09:06 PM
 Operator phu
 Instrument maxis

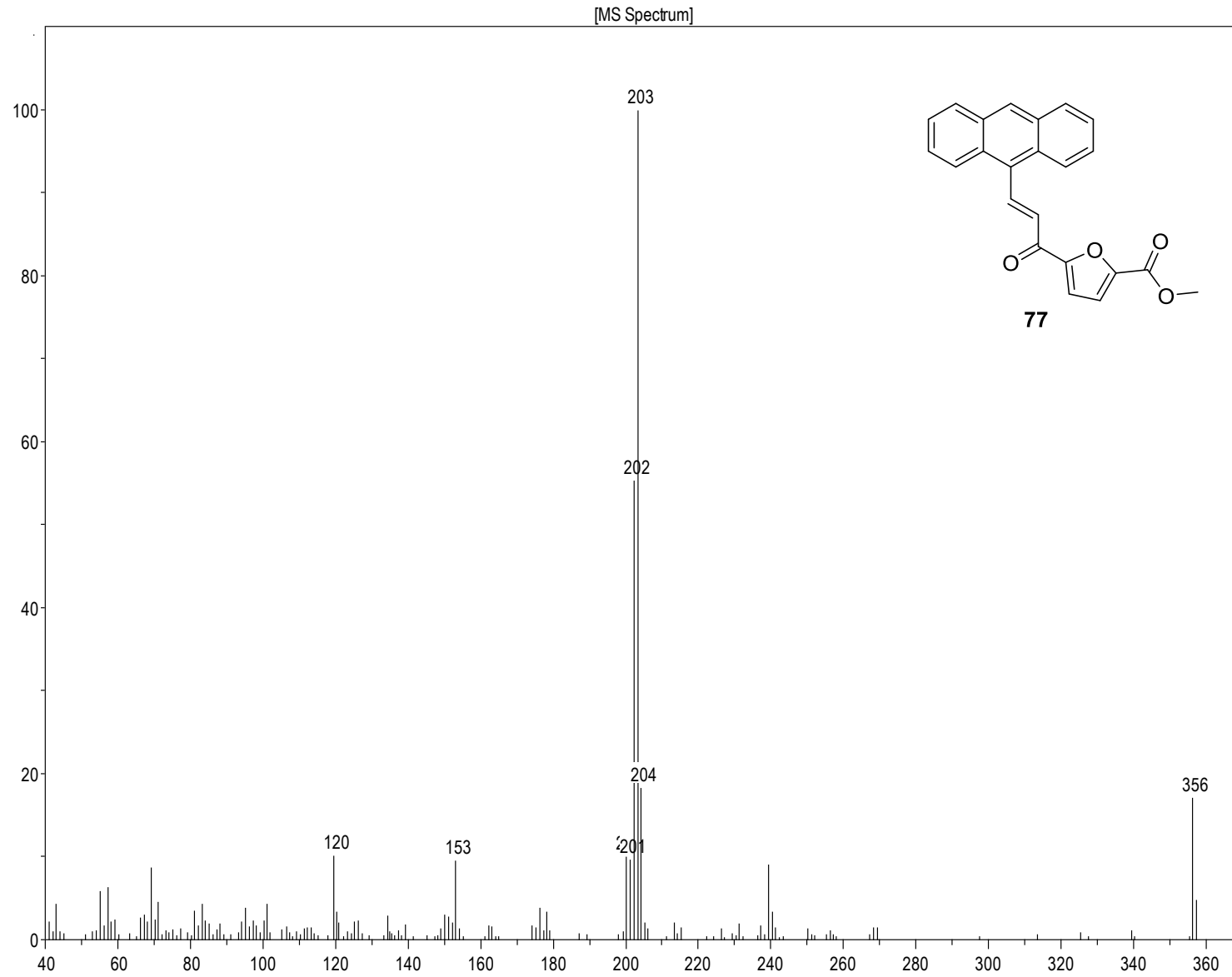


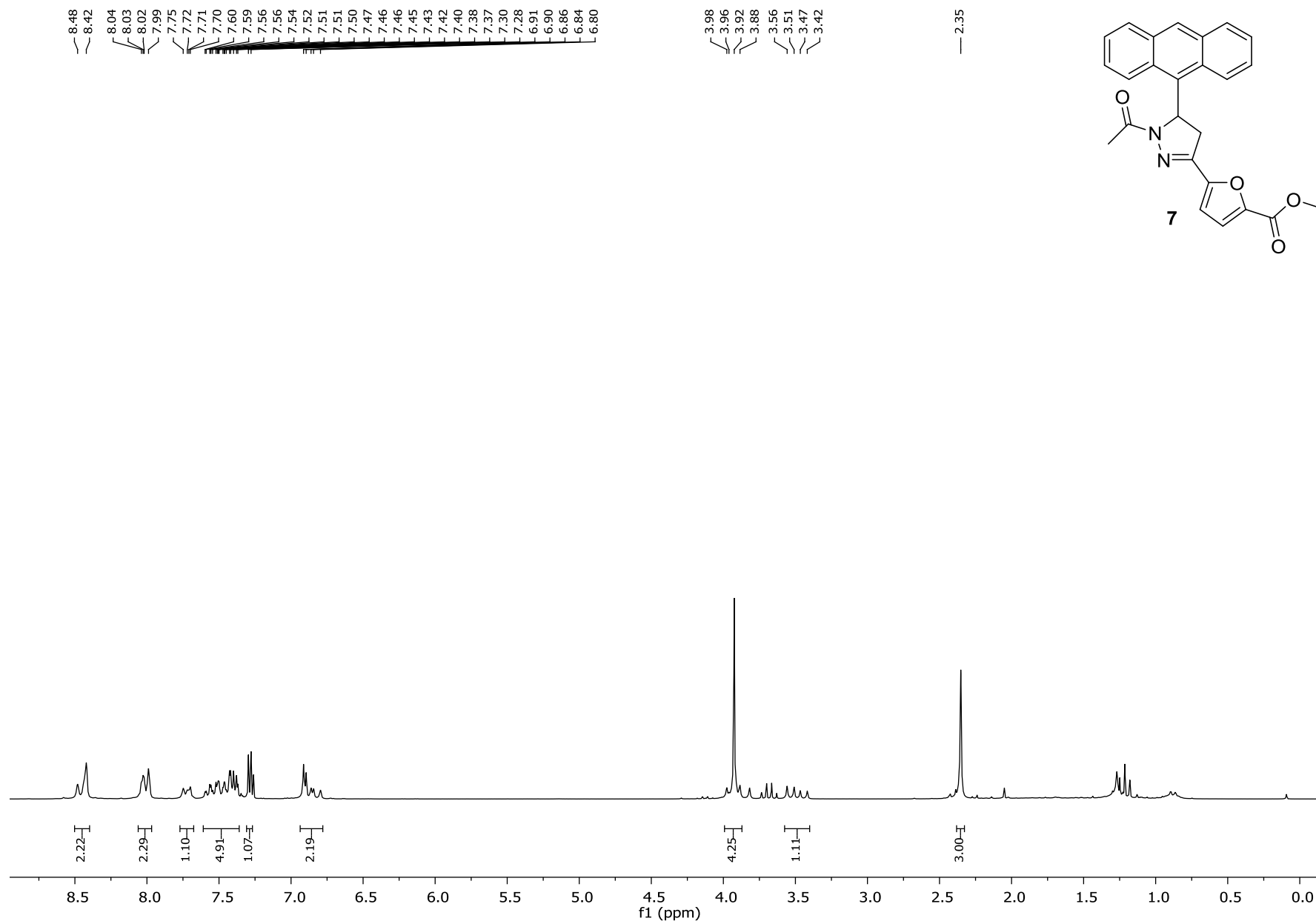
PROTON CDCl3 opt/xwinmr neudorfer 19

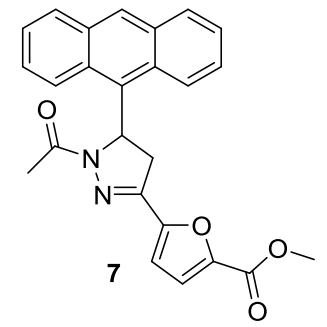
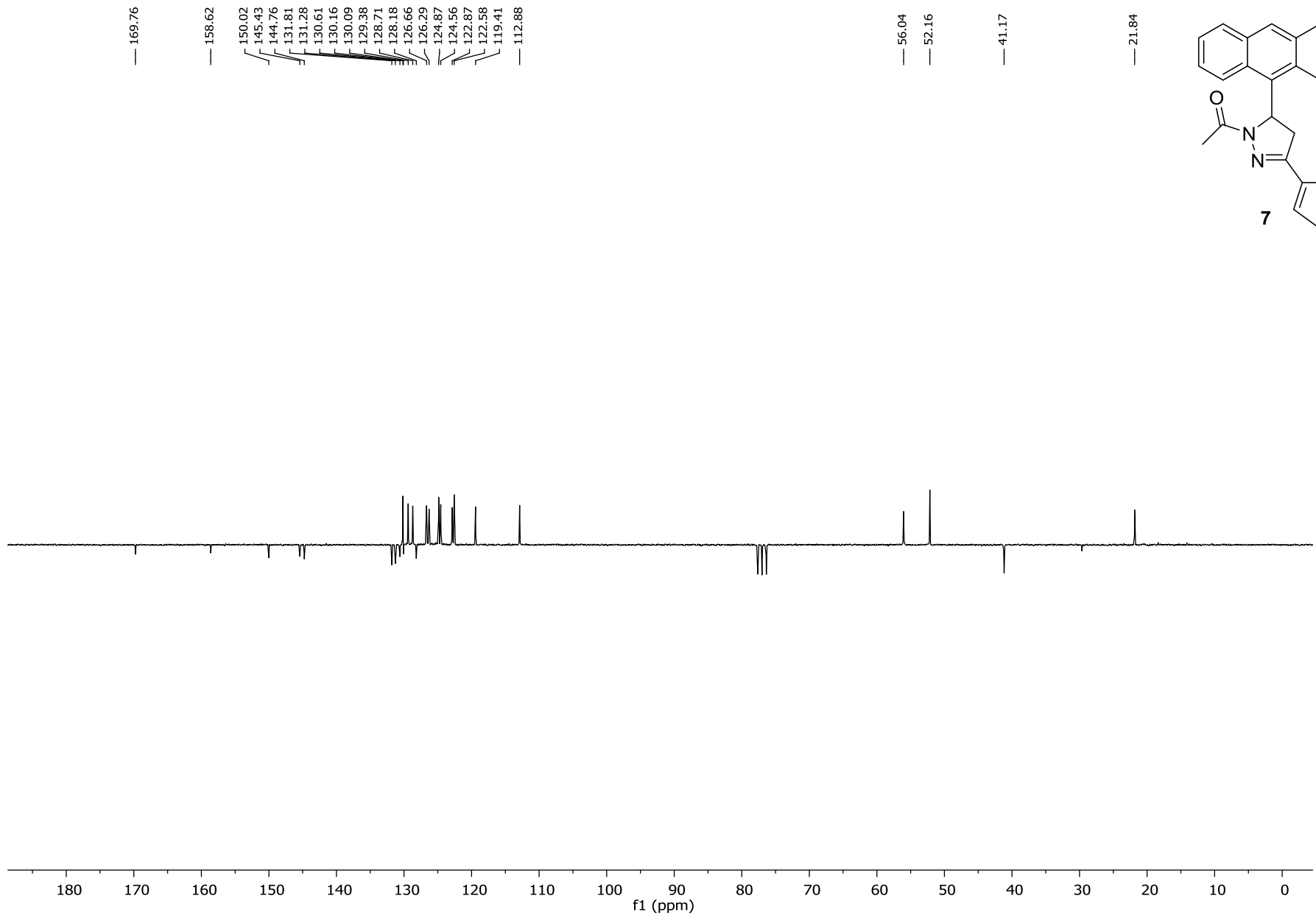


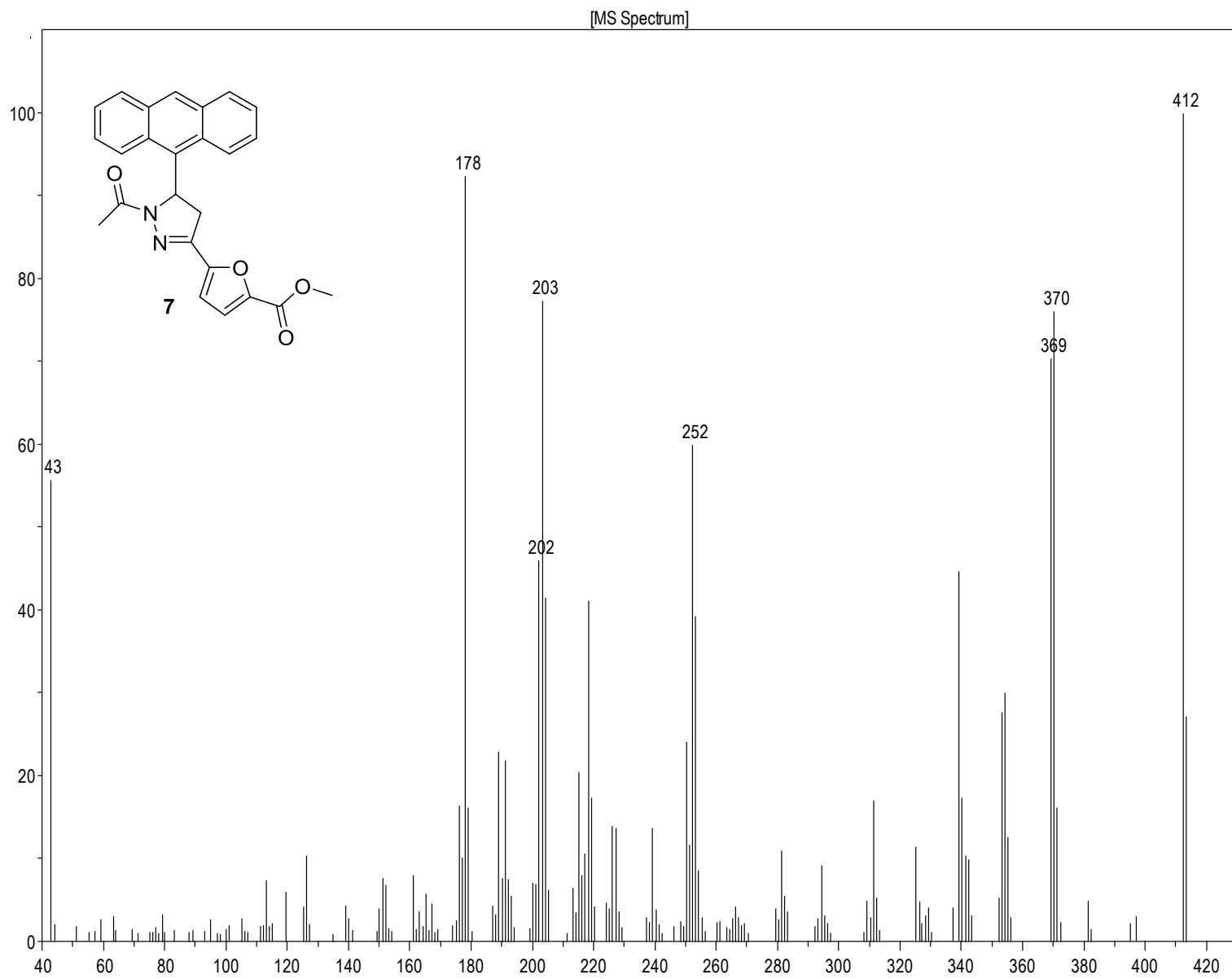
C13APT CDCl3 opt/xwinmr neudorfer 31





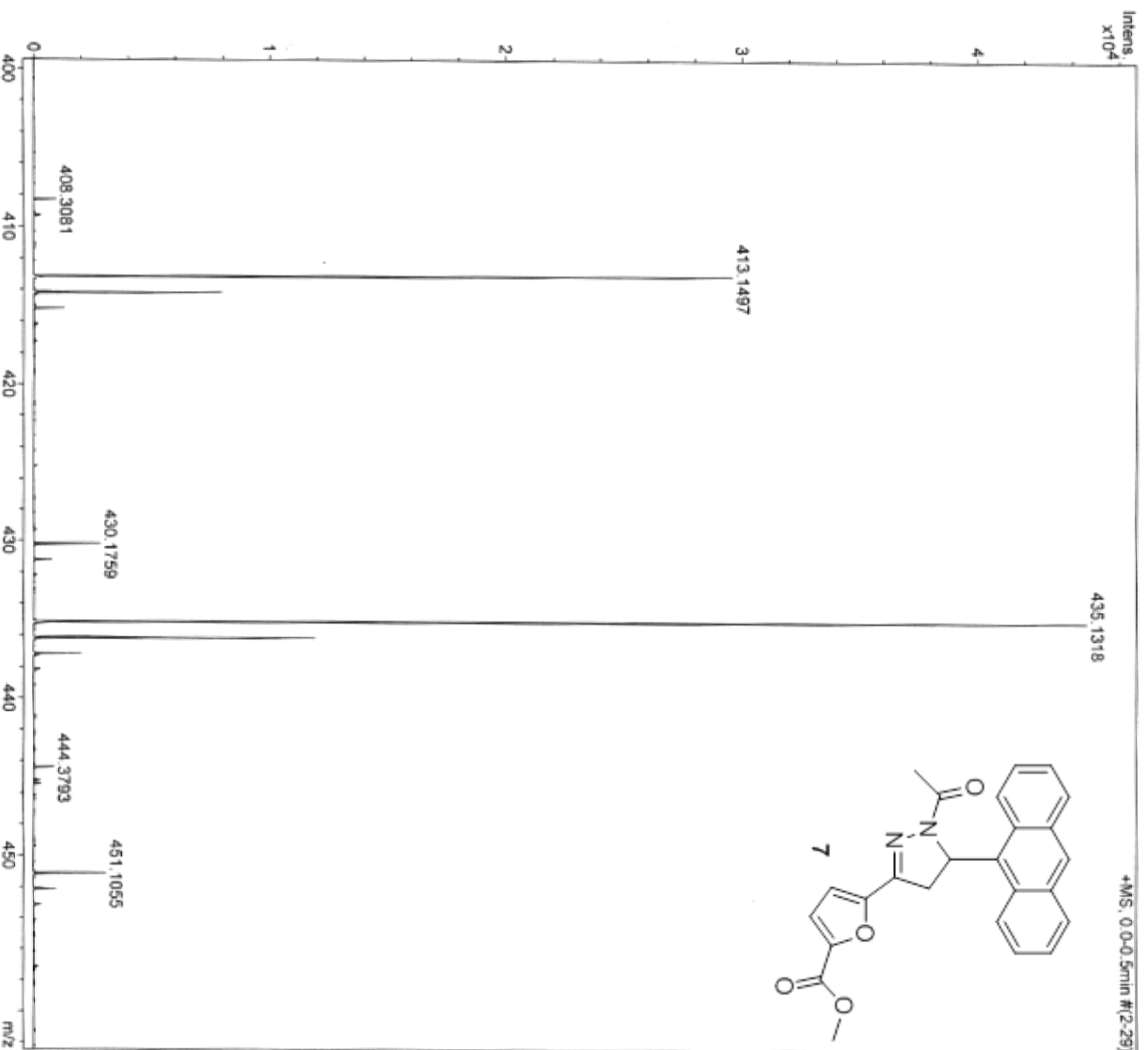


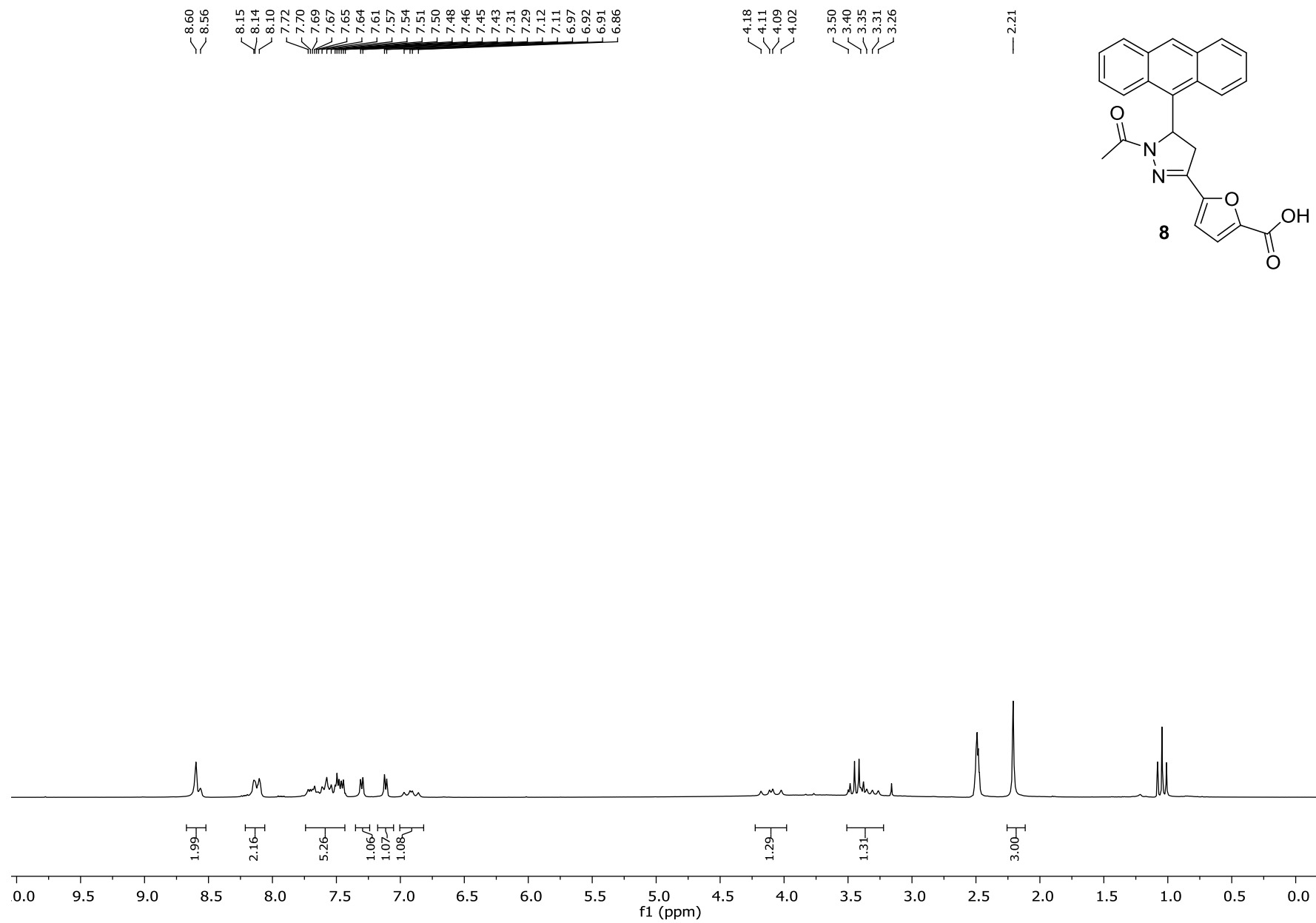


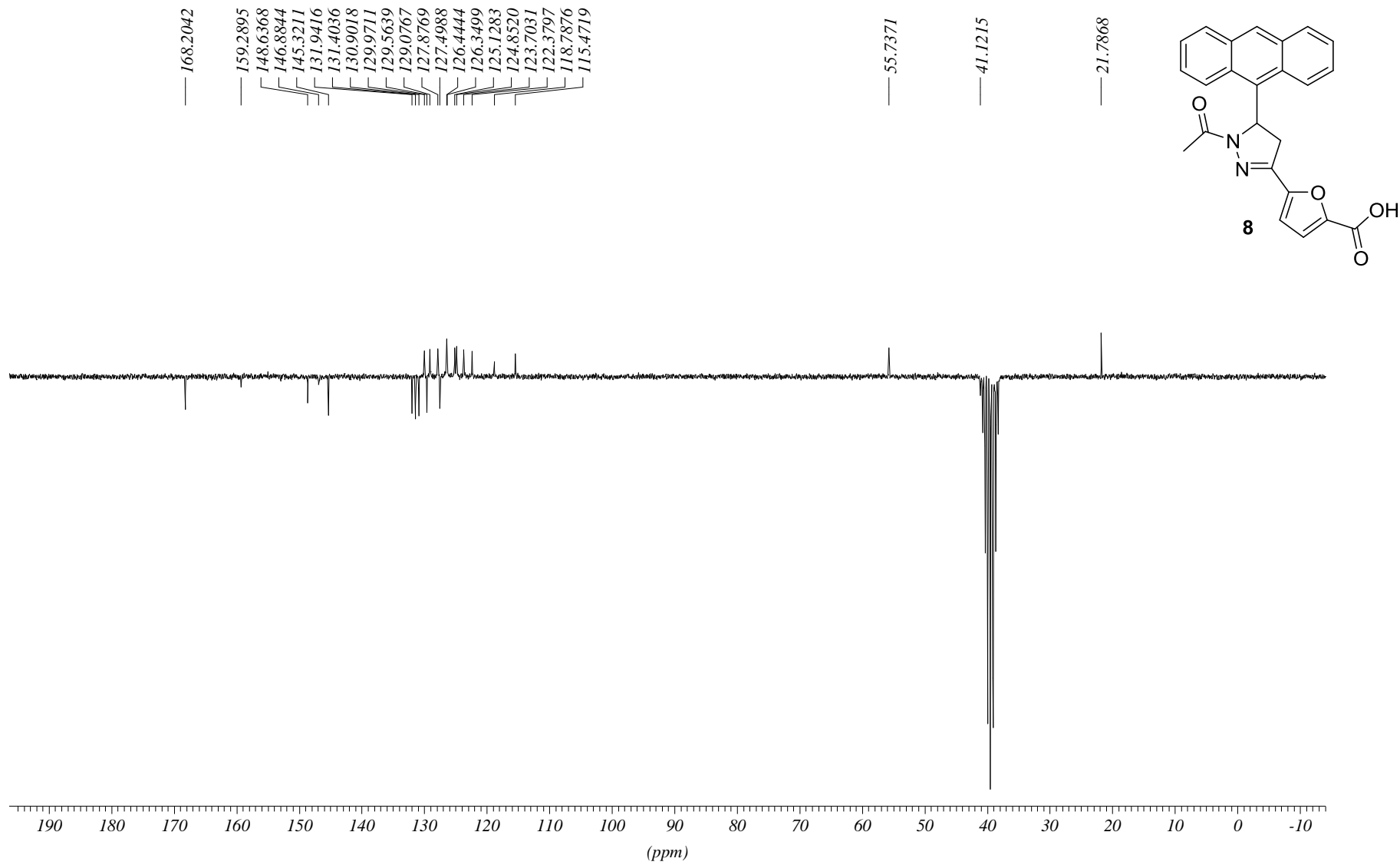


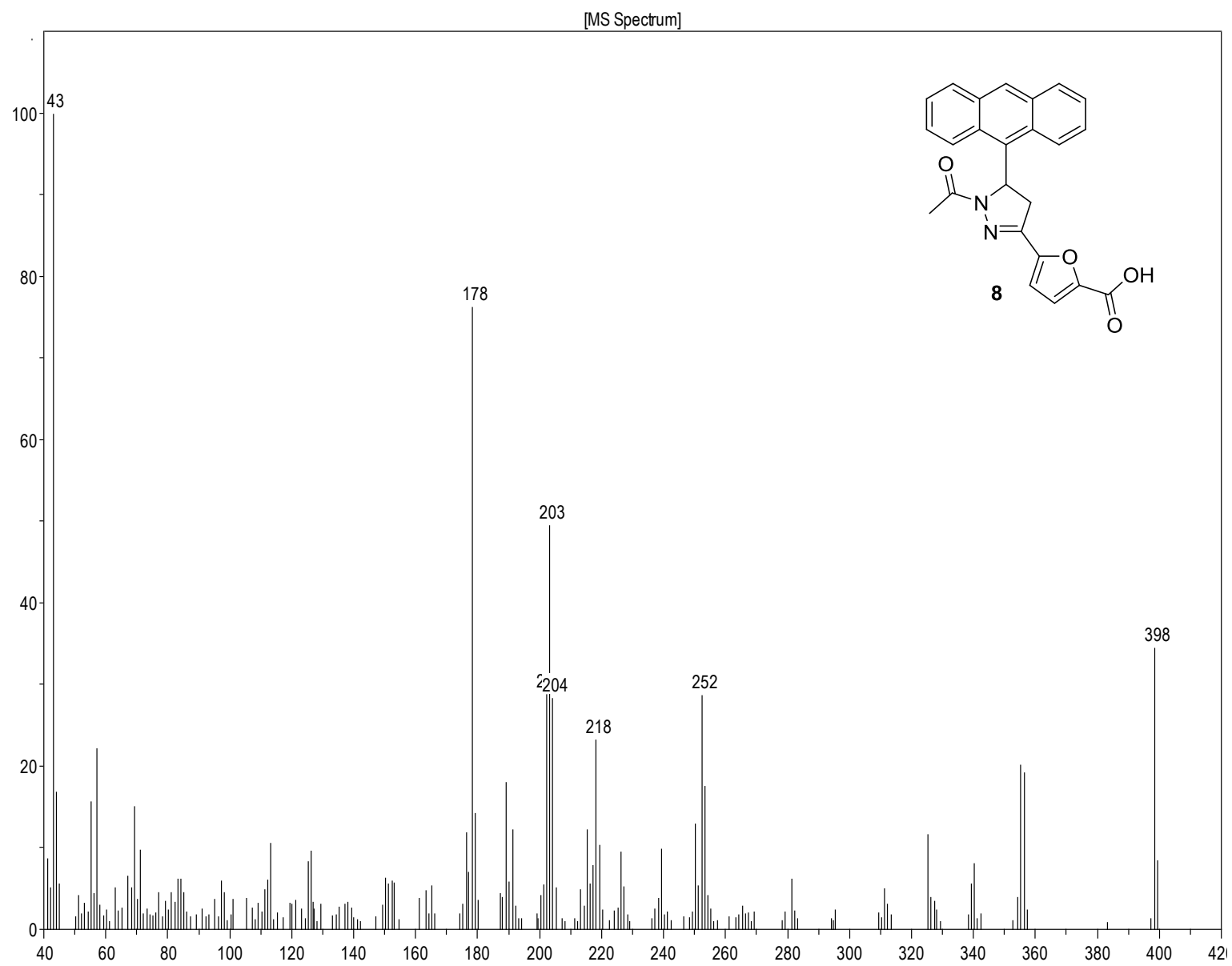
MassenspektrometrieZentrum FakultätChemieUniWien

Analysis Info Acquisition Date 6/14/2013 1:03:24 PM
Analysis Name D:\Data\Ms_MessService\39632000001.d Operator phu
Method tune_low_MS_Service_06_13.m Instrument maxis
Sample Name turoyc 2
Auftragneber/Com Neudorfer/Spreitzer
Ergebnis: +/- 5ppm
ACN/MeOH 1%/H2O









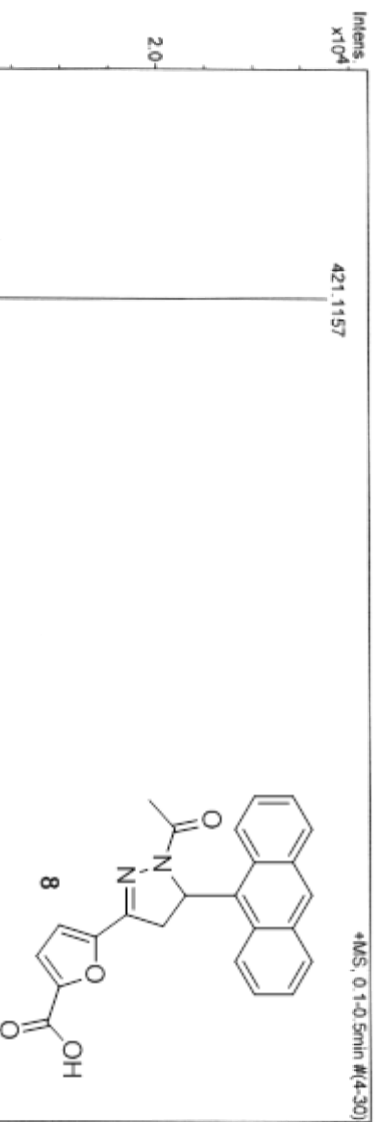
MassenspektrometrieZentrum FakultätChemieUniWien

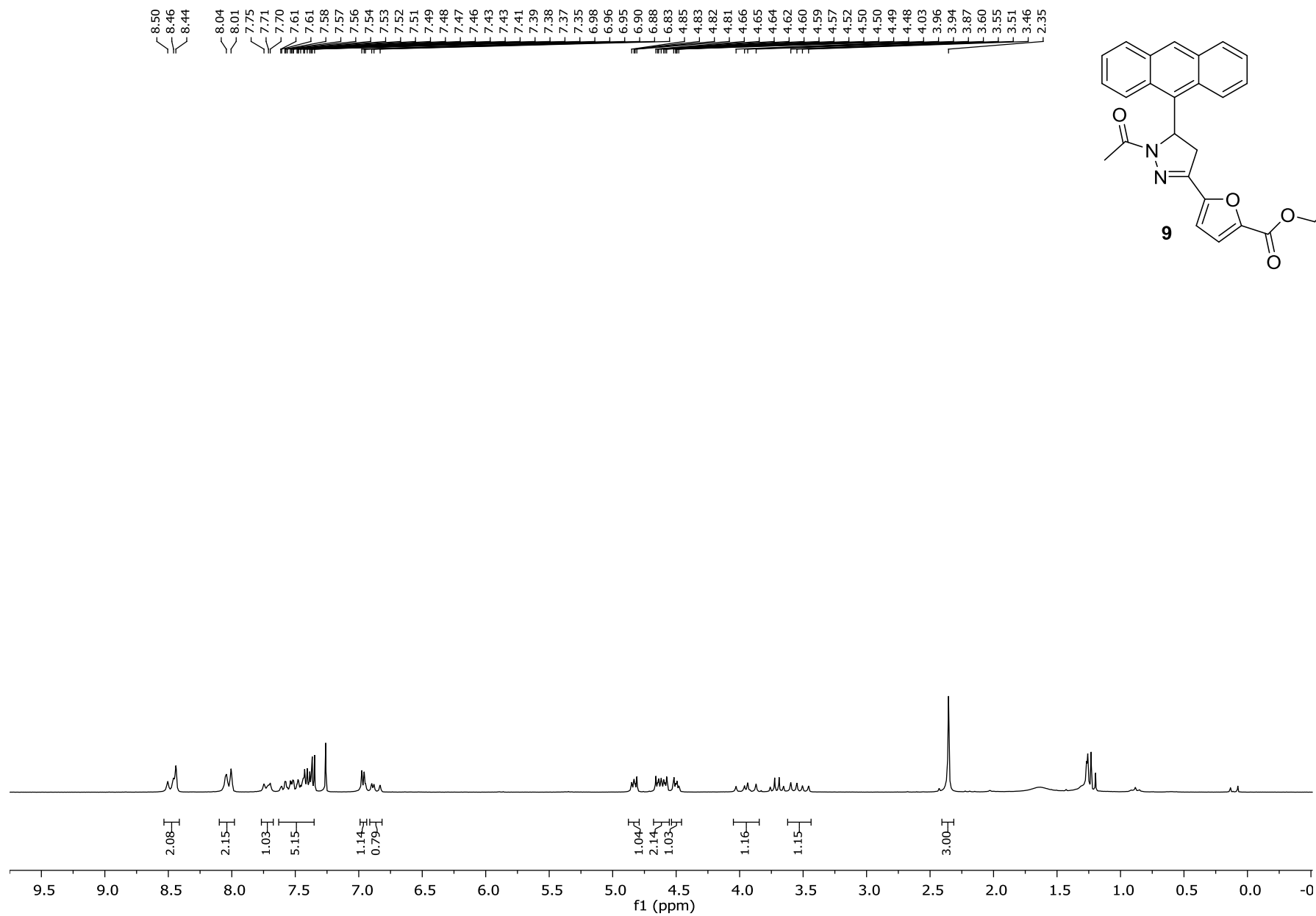
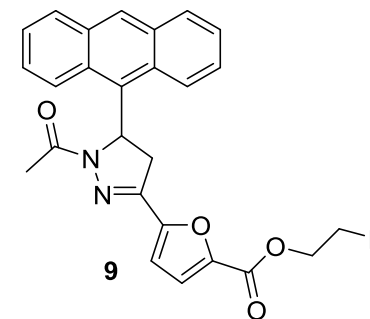
Analysis Info

Analysis Name D:\Data\MS_MessService\39580000001.d
Method tune_low_MS_Service_05_13.m
Sample Name fursre_4
Auftraggeber/Com Neudorfer/Spreitzer
Ergebnis: +/- 5ppm
ACN/MeOH 1%/H2O

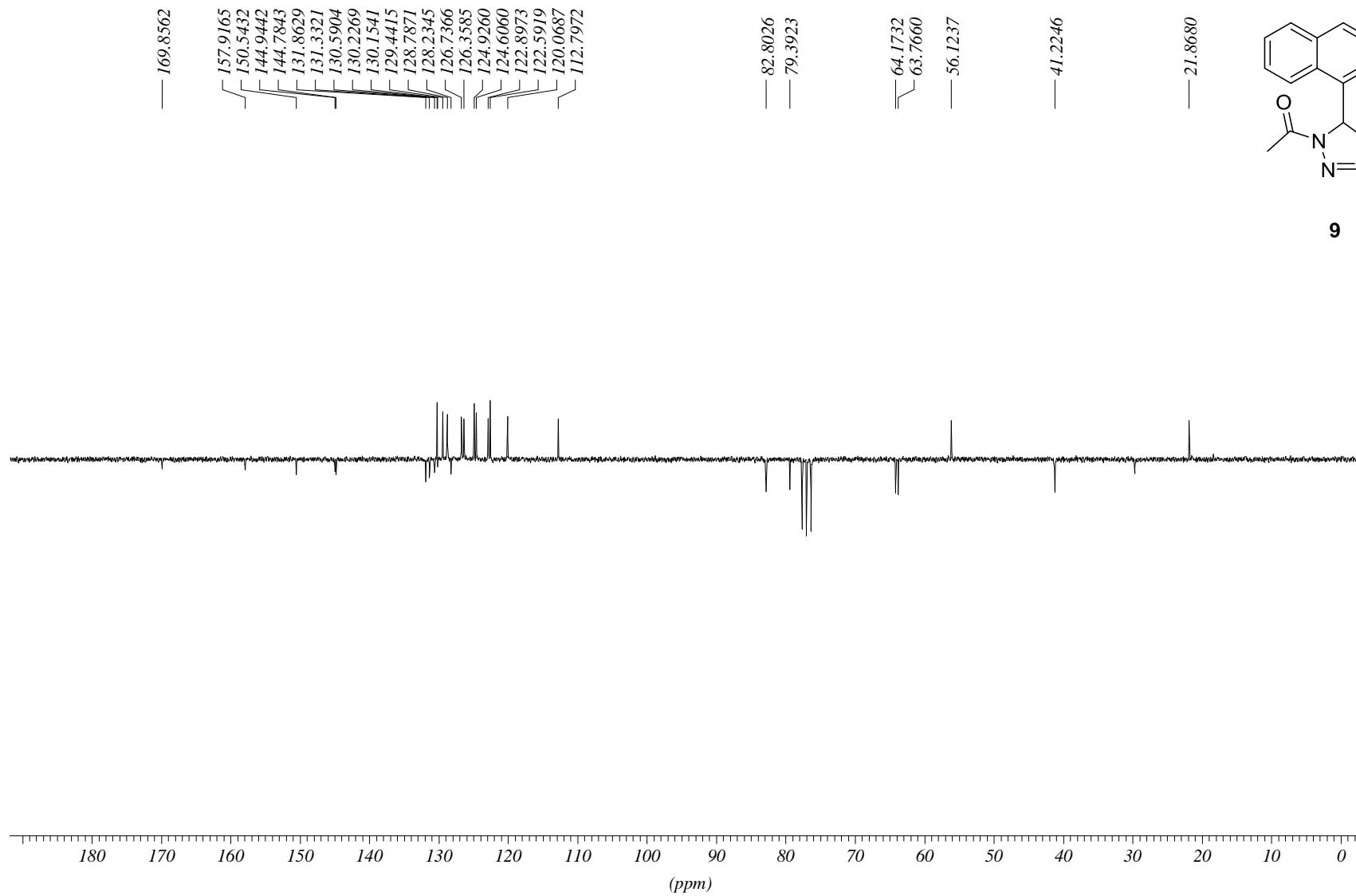
Acquisition Date 5/27/2013 10:56:43 AM

Operator phu
Instrument maxis

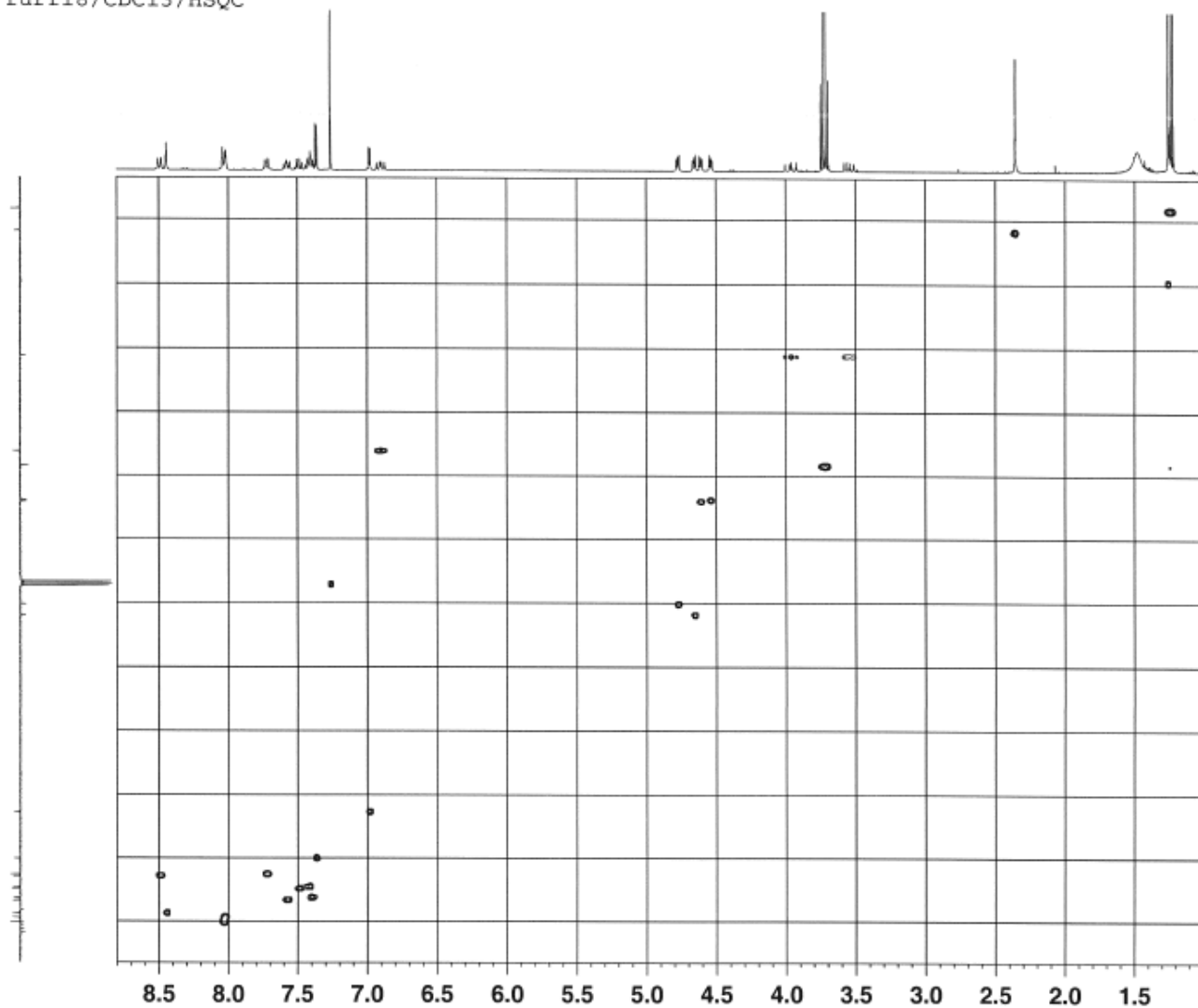




C13APT CDCl3 opt/xwinnmr neudorfer 51



furfi8/CDC13/HSQC



Current Data Parameters
NAME: furfi8
EXPNO: 1
PROCNO: 1

F2 - Acquisition Parameters
Date_ : 20130823
Time : 15.17
INSTRUM : spect
PROBHD : 5 mm BBBO-1H
PULPROG : zgpg30
TD : 1324
SOLVENT : CDC13
NS : 8
DS : 2
SWH : 4800.860 Hz
FIDRES : 3.906250 Hz
AQ : 0.1280160 sec
RG : 283
DQ : 125.000 usec
DE : 10.00 usec
TE : 297.2 K
CNS23 : 145.860000
CMT17 : -0.500000
D9 : 0.0000000 sec
D1 : 2.0000000 sec
D4 : 0.00172414 sec
D14 : 0.0000000 sec
D16 : 0.0000000 sec
D24 : 0.0006287 sec
D30 : 0.0000149 sec

***** CHANNEL F1 *****
NUC1 : 13C
P1 : 12.50 usec
F2 : 25.00 usec
F2B : 1600.00 usec
FLM1 : 16.0000000 M
SFO1 : 400.2118219 MHz

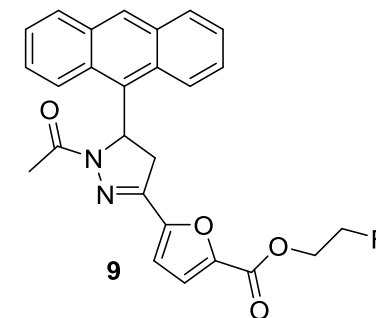
***** CHANNEL F2 *****
CPDPRG2 : gpcp
NUC2 : 1H
P2 : 8.50 usec
F4 : 500.00 usec
F4B : 2000.00 usec
PCPD2 : 75.00 usec
FLM2 : 0 W
FLM3 : 64.0000000 M
FLM4 : 0.0000000 M
SFO2 : 100.6457618 MHz
SFO3 : Ccp40.9.5.23.1
SFOAL3 : 0.500
SFOF33 : 0 Hz
SFO4 : 7.06489882 M
SFO47 : Ccp40comp.4
SFO47 : 0.500
SFOF57 : 0 Hz
SFO7 : 7.06500000 M

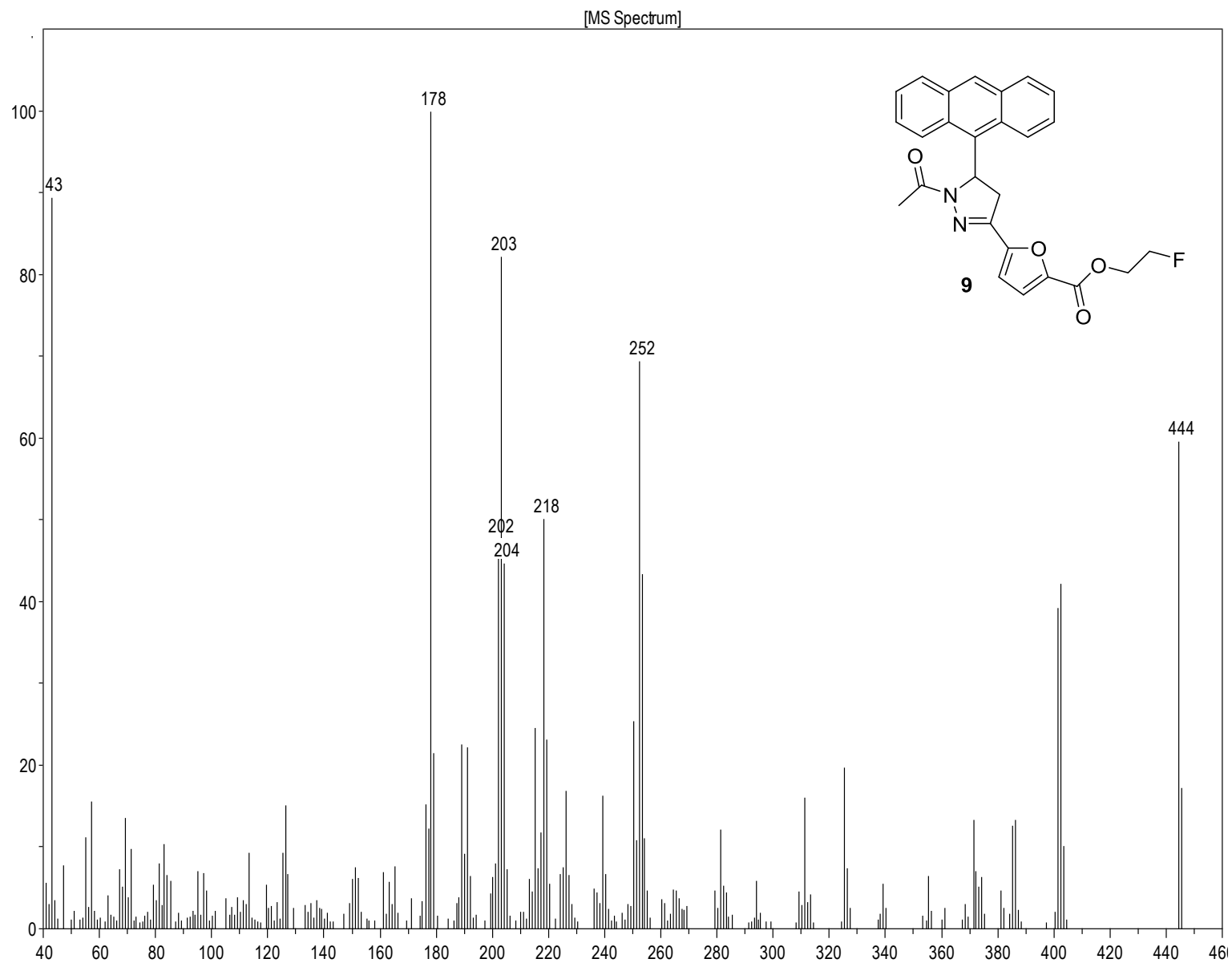
***** GRADIENT CHANNEL *****
GPM1 : 0.0000000 M
GPM2 : 0.0000000 M
GPM3 : 0.0000000 M
GPM4 : 0.0000000 M
GPE1 : 00.00 %
GPE2 : 20.00 %
GPE3 : 11.00 %
GPE4 : -5.00 %
PL1 : 1800.00 usec
PL2 : 600.00 usec

F1 - Acquisition parameters
TD : 216
SFO1 : 180.6458 MHz
SFO2 : 42.809600 Hz
NUC1 : 140.016 ppm
PULPROG : Echo-ant1echo

F2 - Processing parameters
SI : 1324
SF : 400.2100138 MHz
WDW : GEMME
SSB : 2
LB : 0 Hz
GB : 0
PC : 1.00

F1 - Processing parameters
SI : 1324
SF : Echo-ant1echo
WDW : EM
SSB : 2
LB : 0 Hz
GB : 0

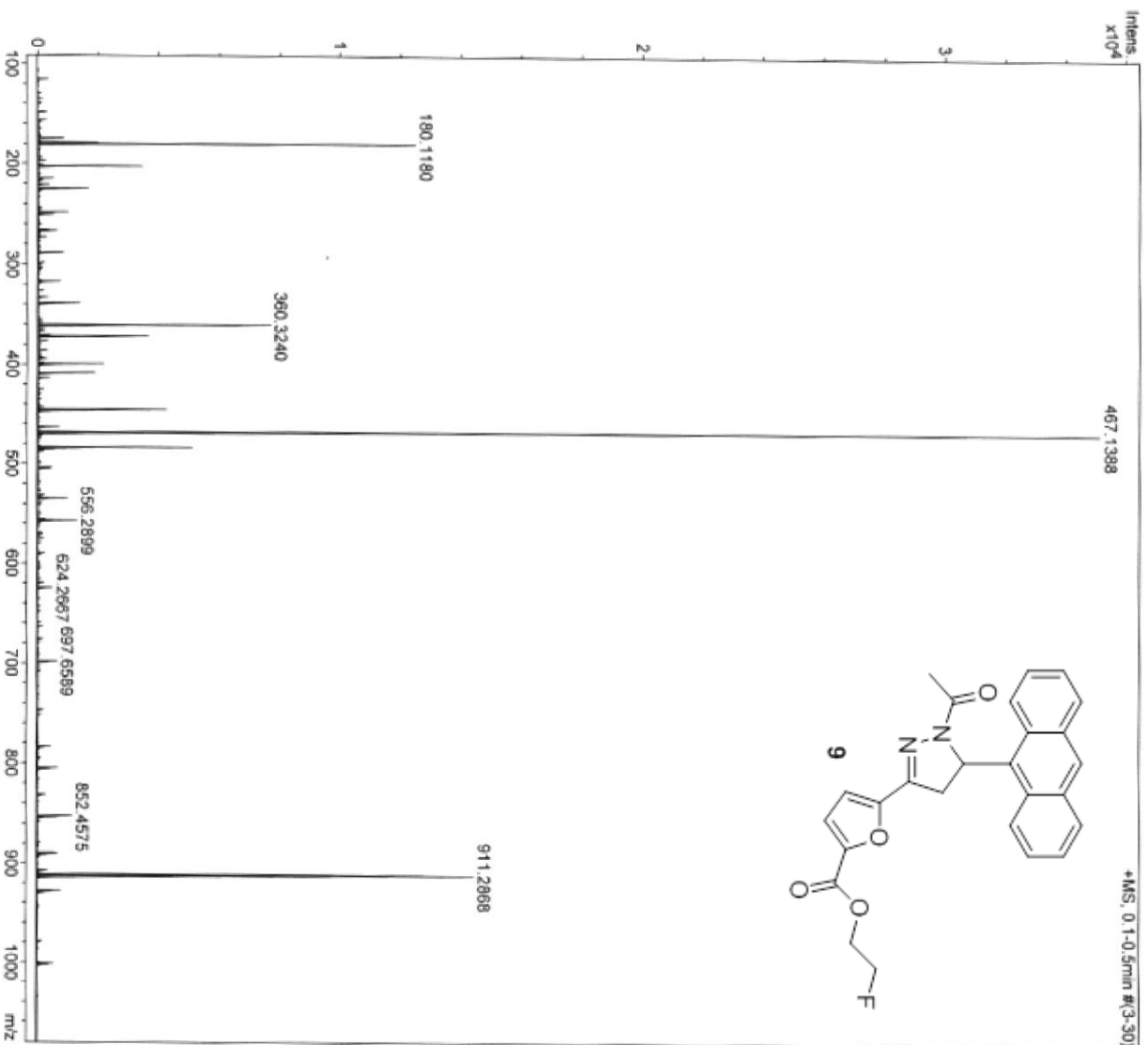
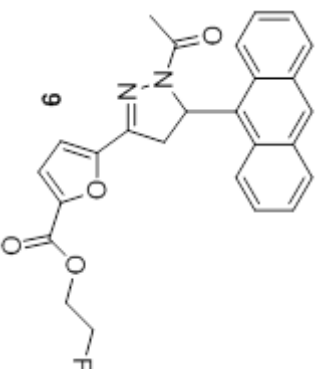




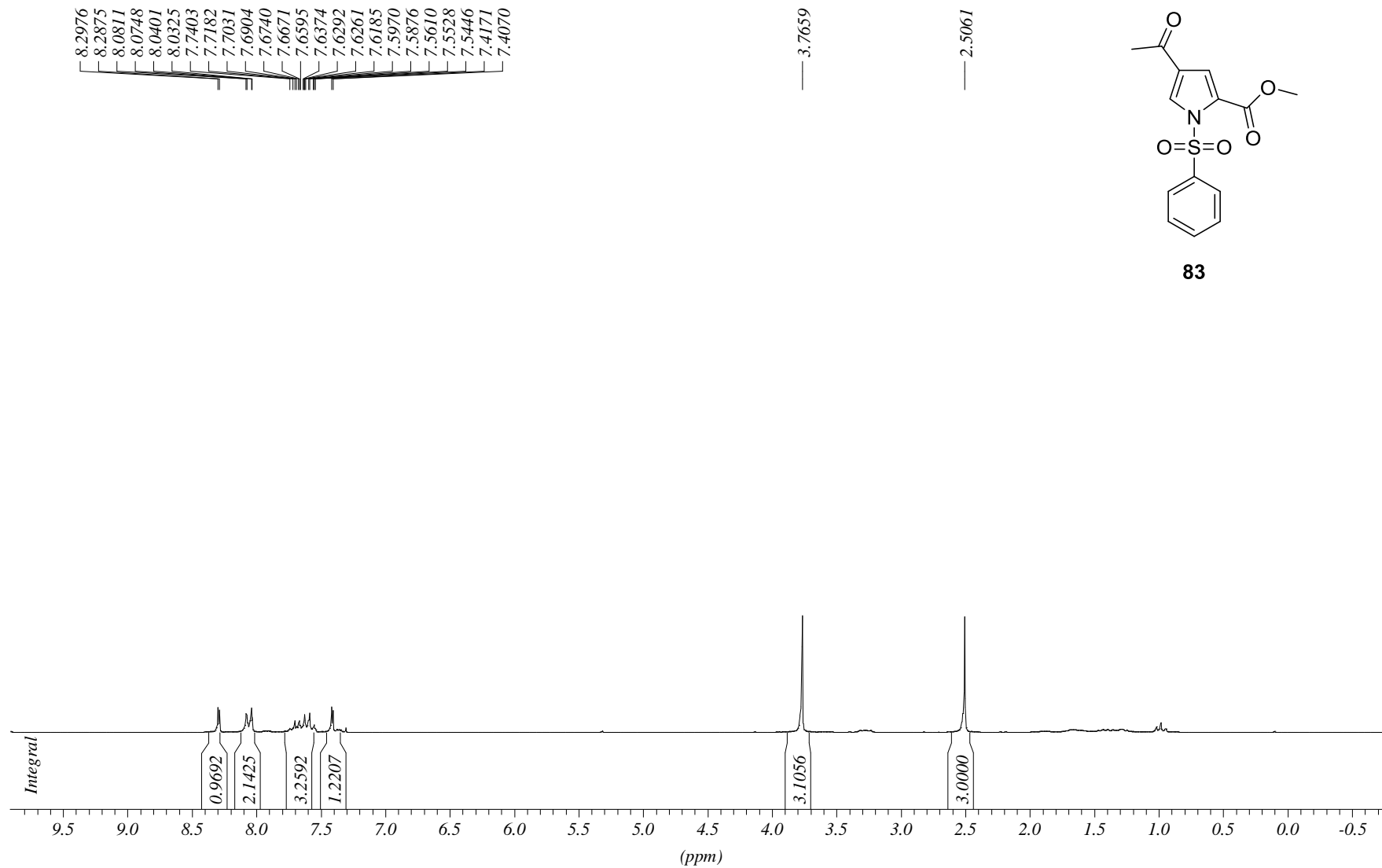
MassenspektrometrieZentrum FakultätChemieUniWien

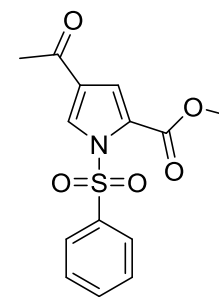
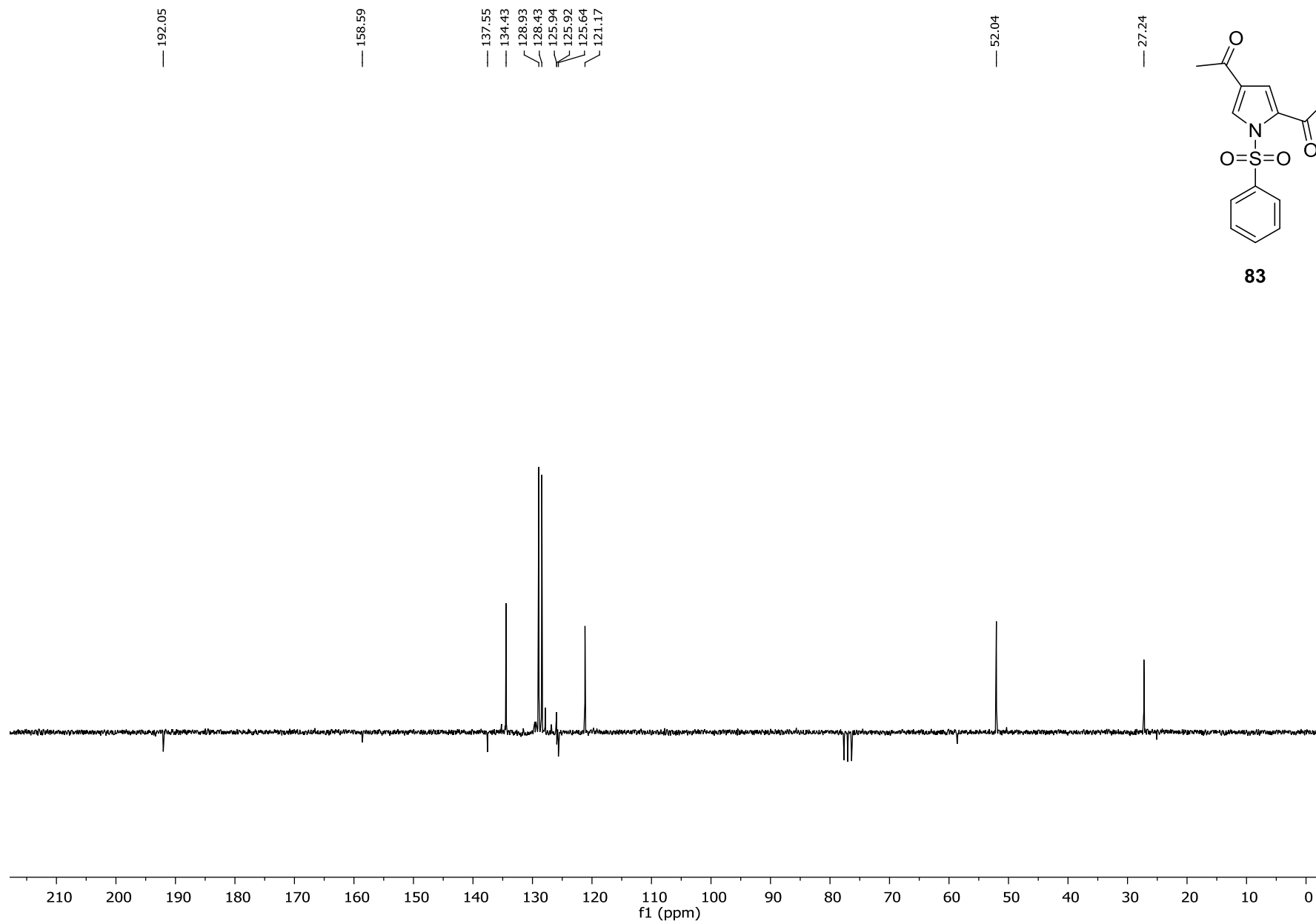
Analysis Info
 Analysis Name D:\Data\MS_MessService\39605000001.d
 Method tune_low_MS_Service_06_13.m
 Sample Name turfi7
 Auftraggeber/Com Neudorfer/Spreitzer
 Ergebnis: +/- 5ppm
 ACN/MeOH 1%/H2O

Acquisition Date 6/7/2013 8:53:03 AM
 Operator phu
 Instrument maxis

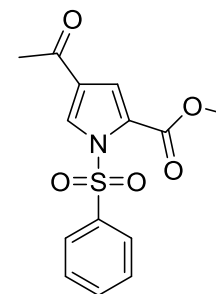
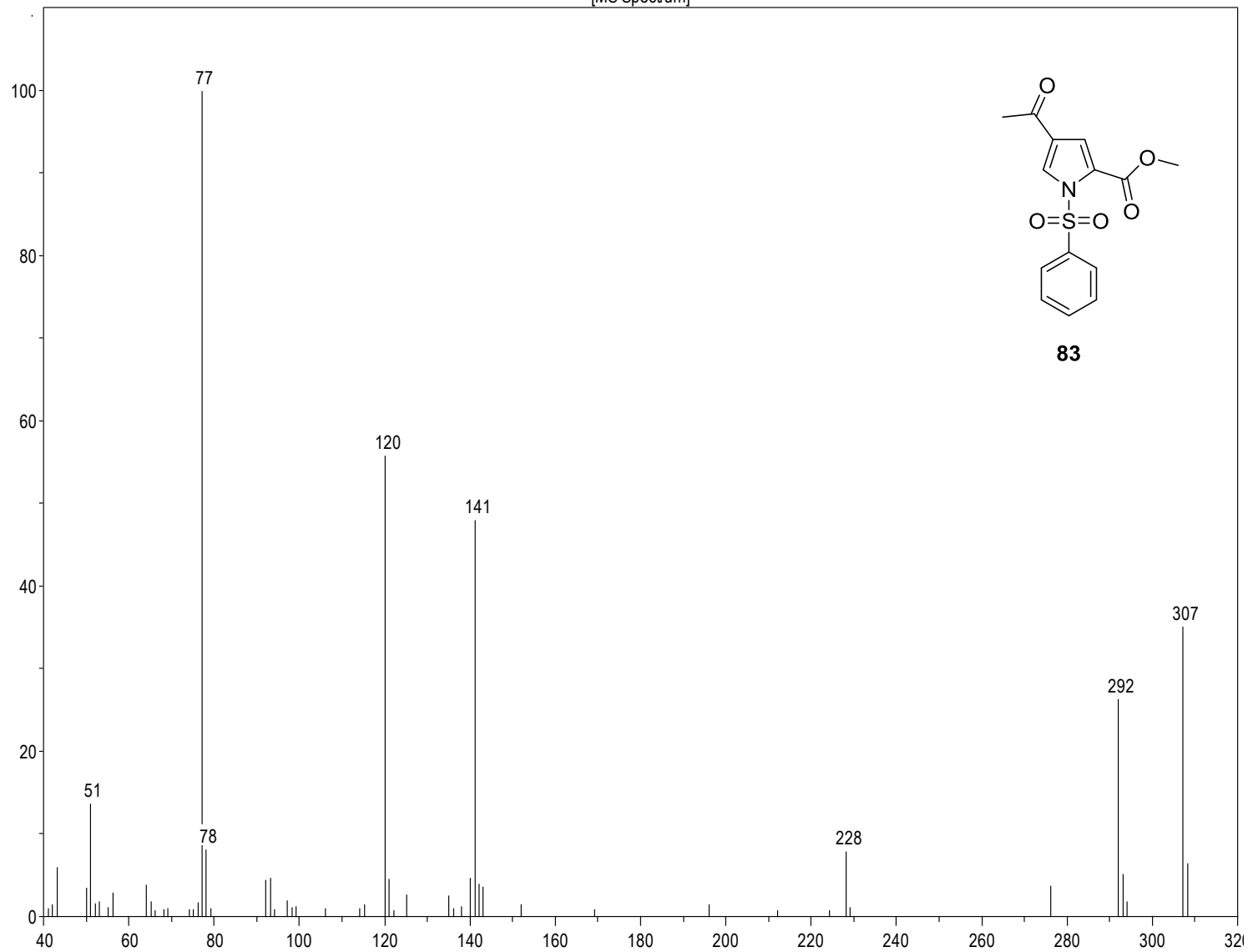


PROTON CDCl3 opt/xwinmr neudorfer 14

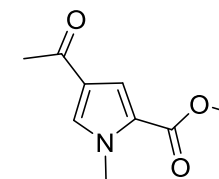
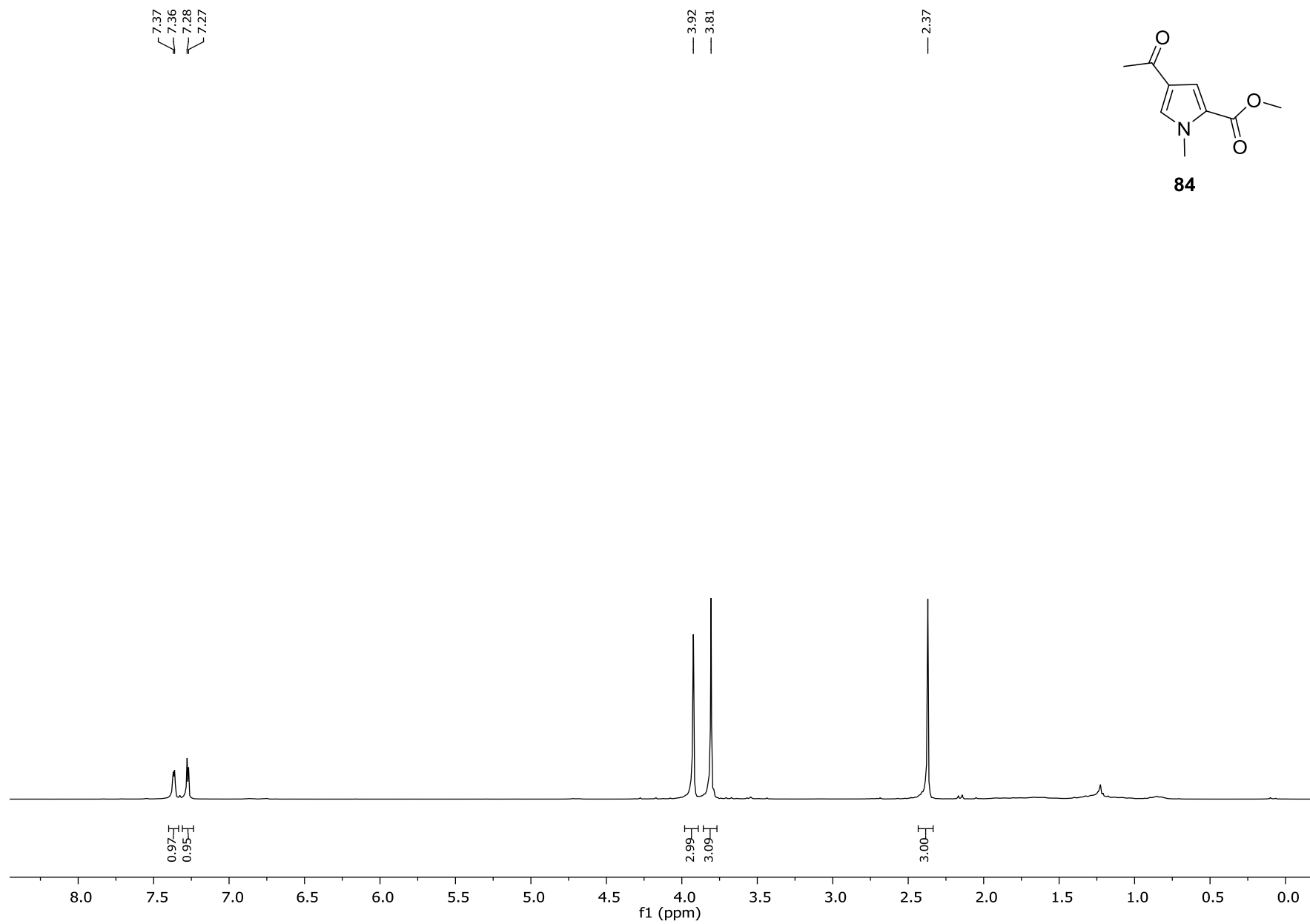


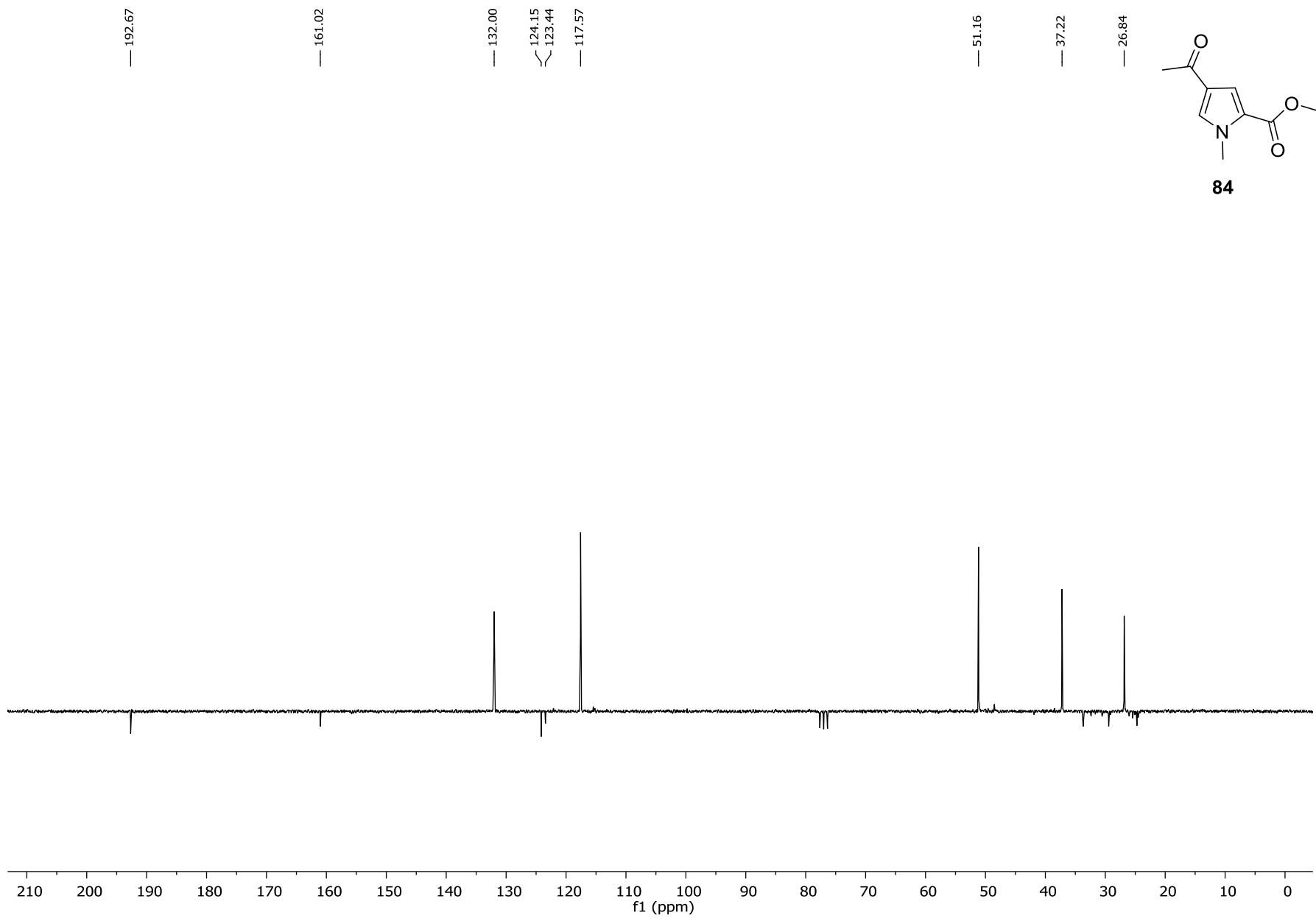
**83**

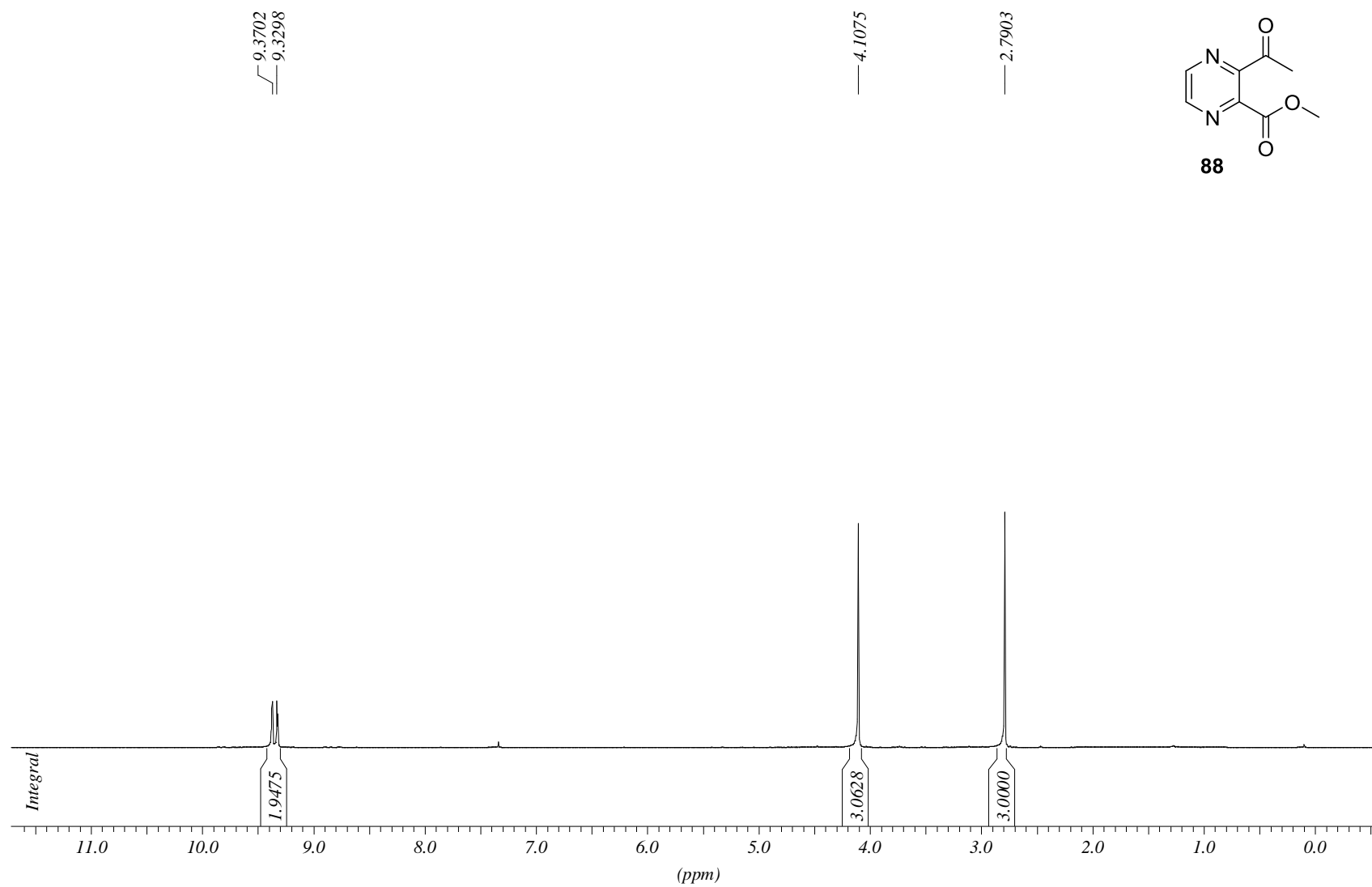
[MS Spectrum]



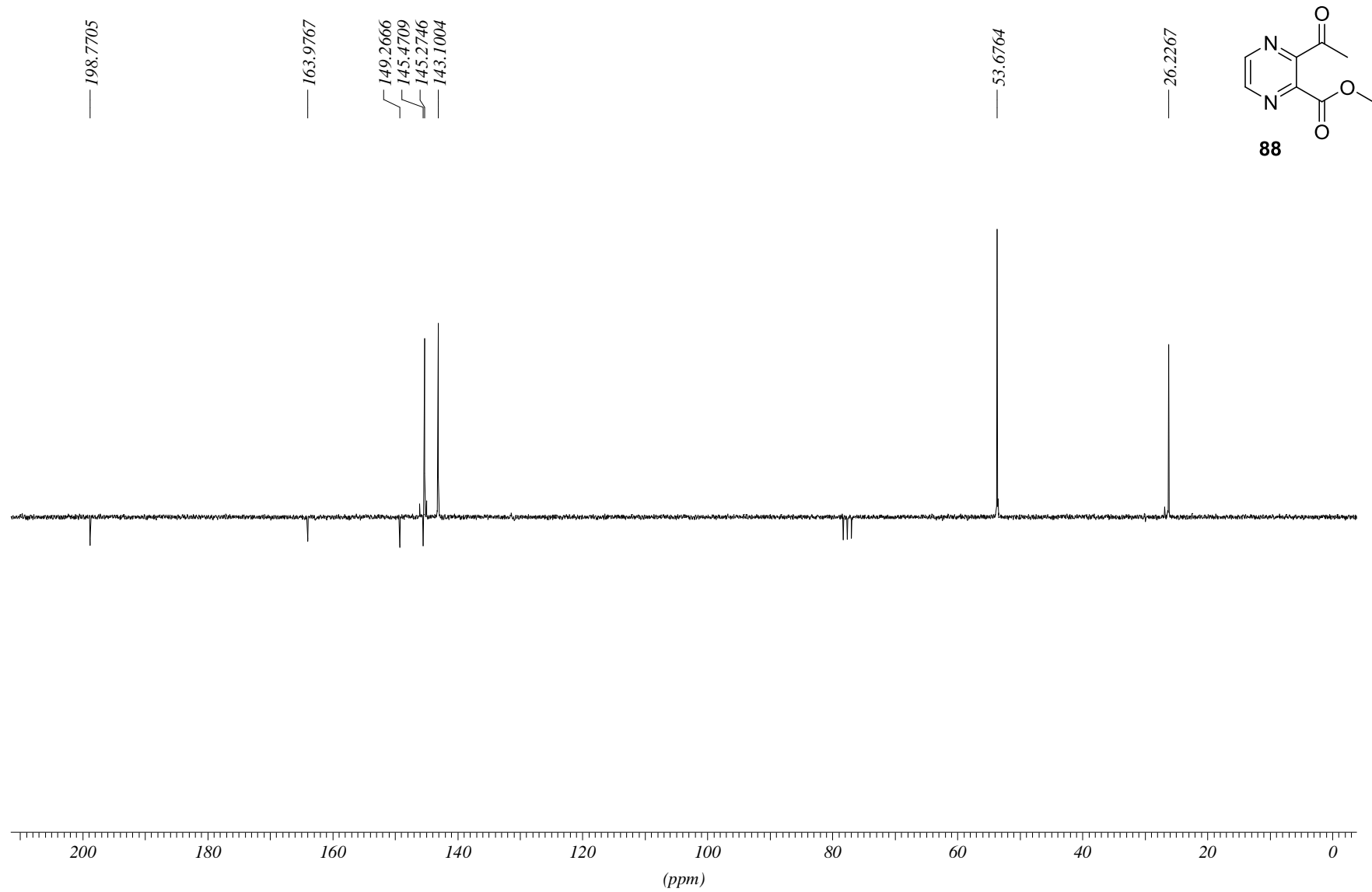
83

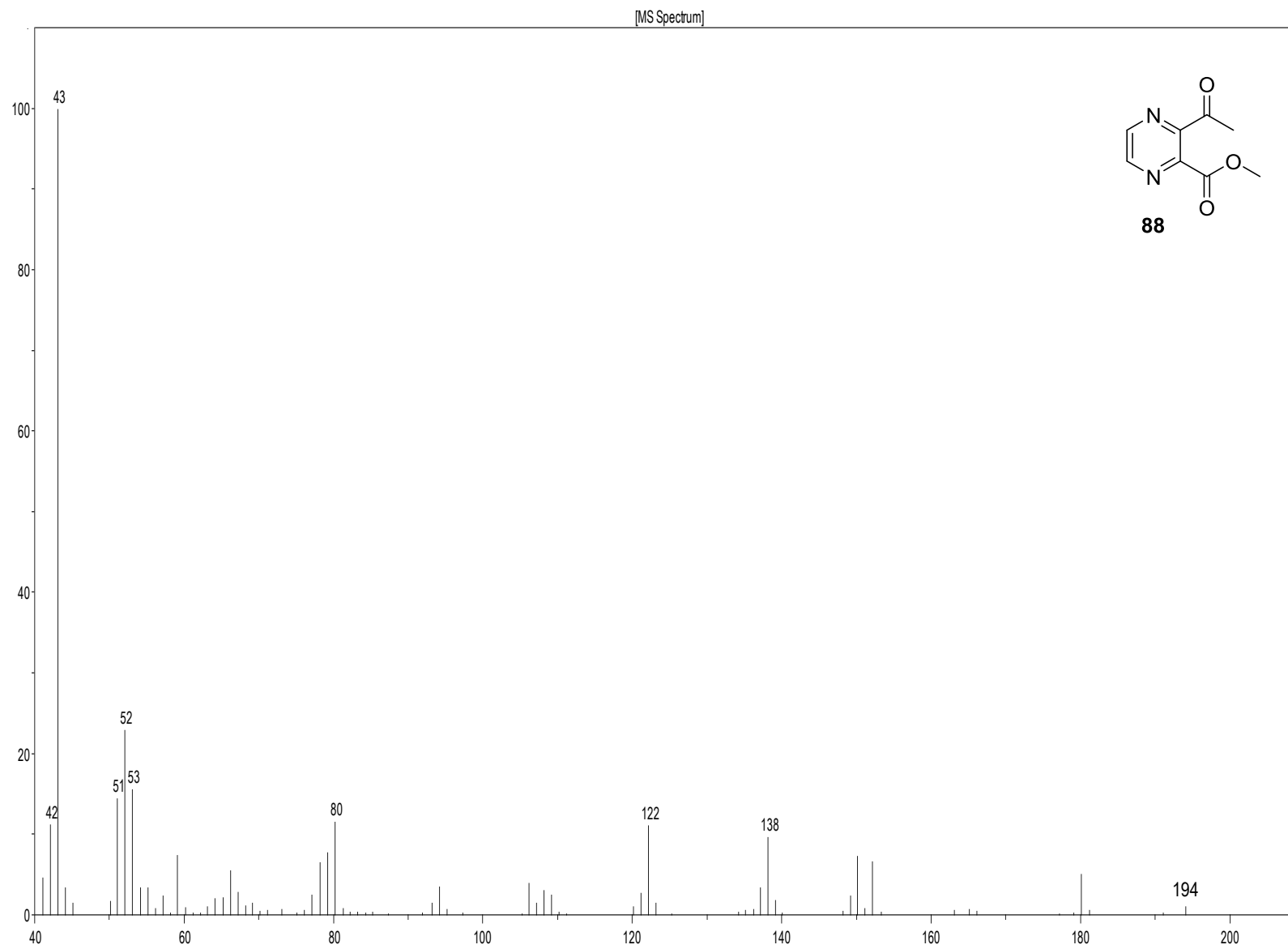
**84**



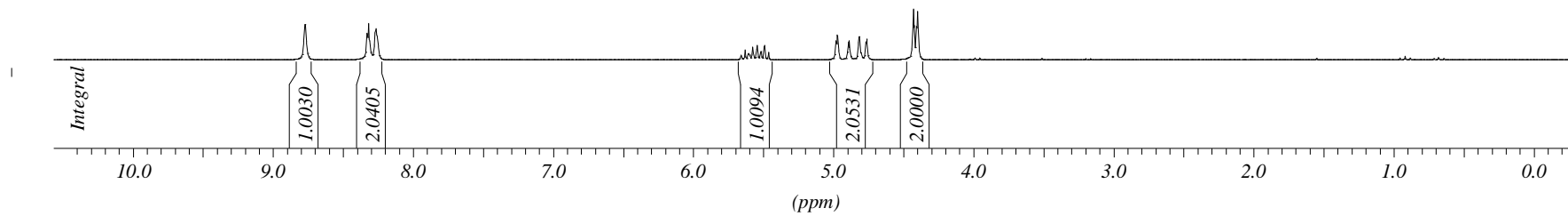
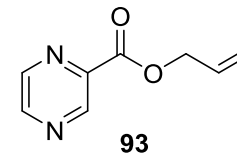
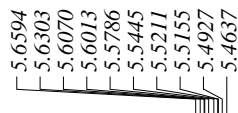
PROTON CDCl₃ opt/xwinmr neudorfer 1

C13APT CDCl3 opt/xwinnmr neudorfer 52

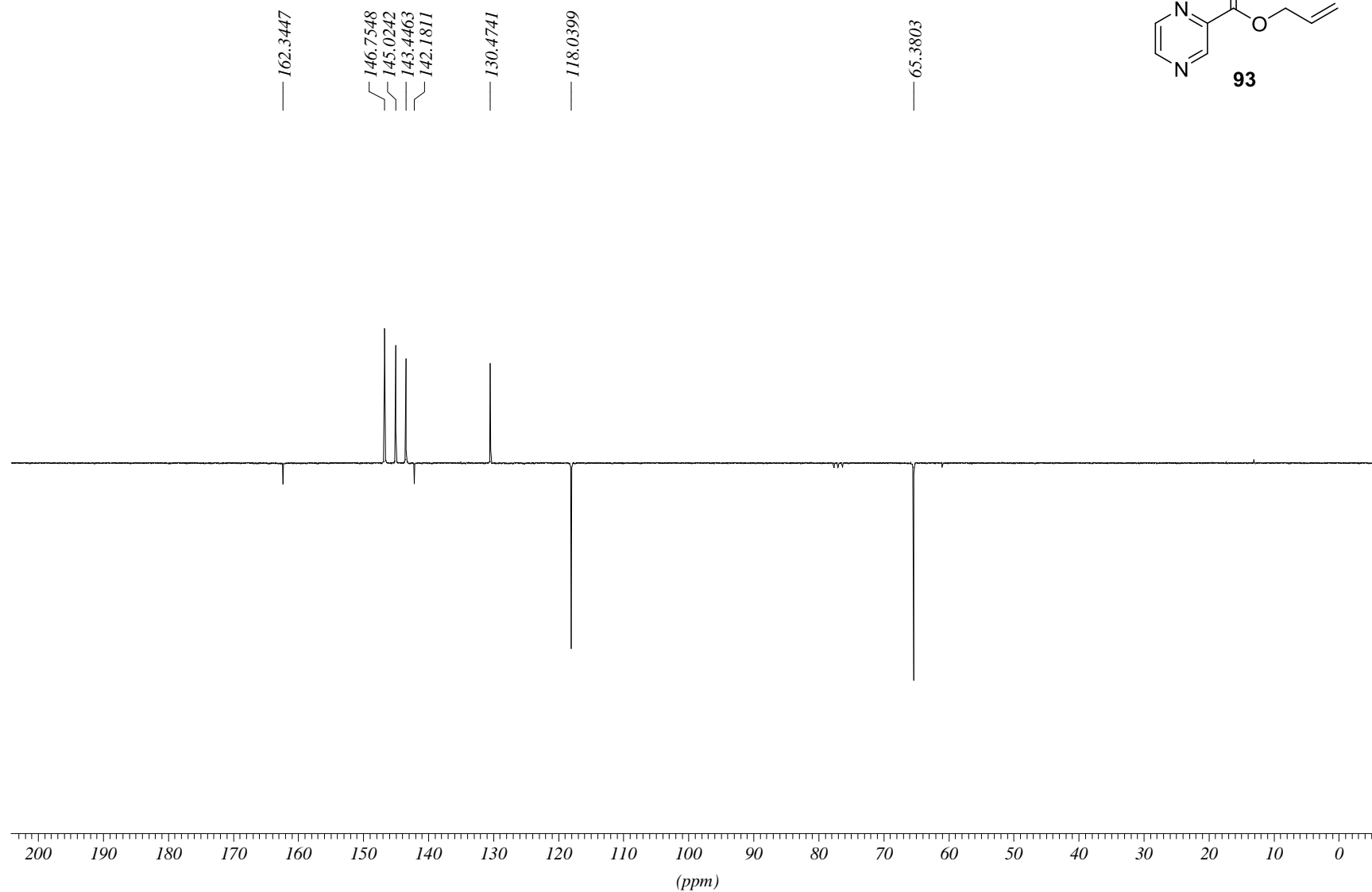




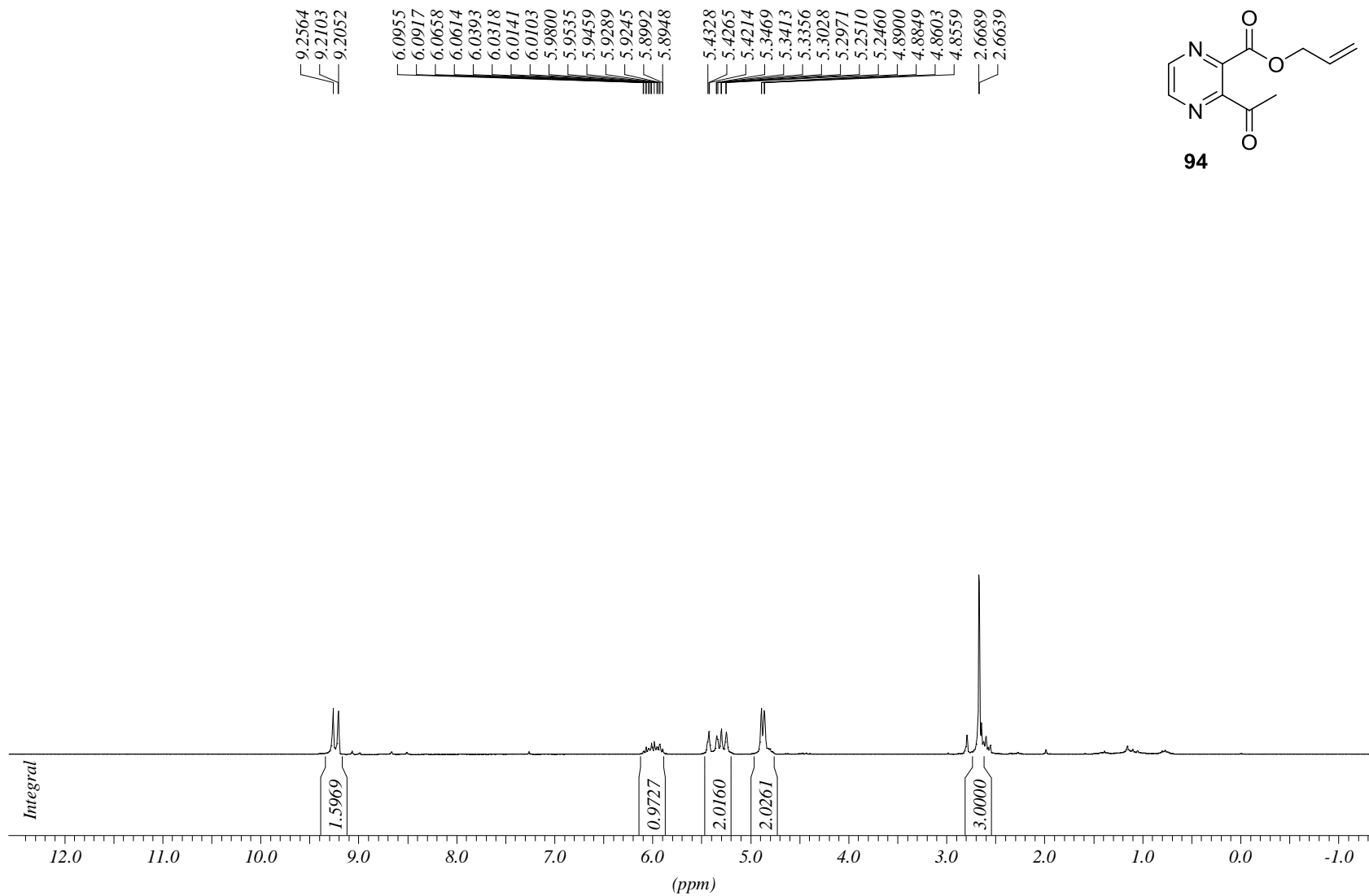
PROTON CDCl₃ opt/xwinmr neudorfer 40



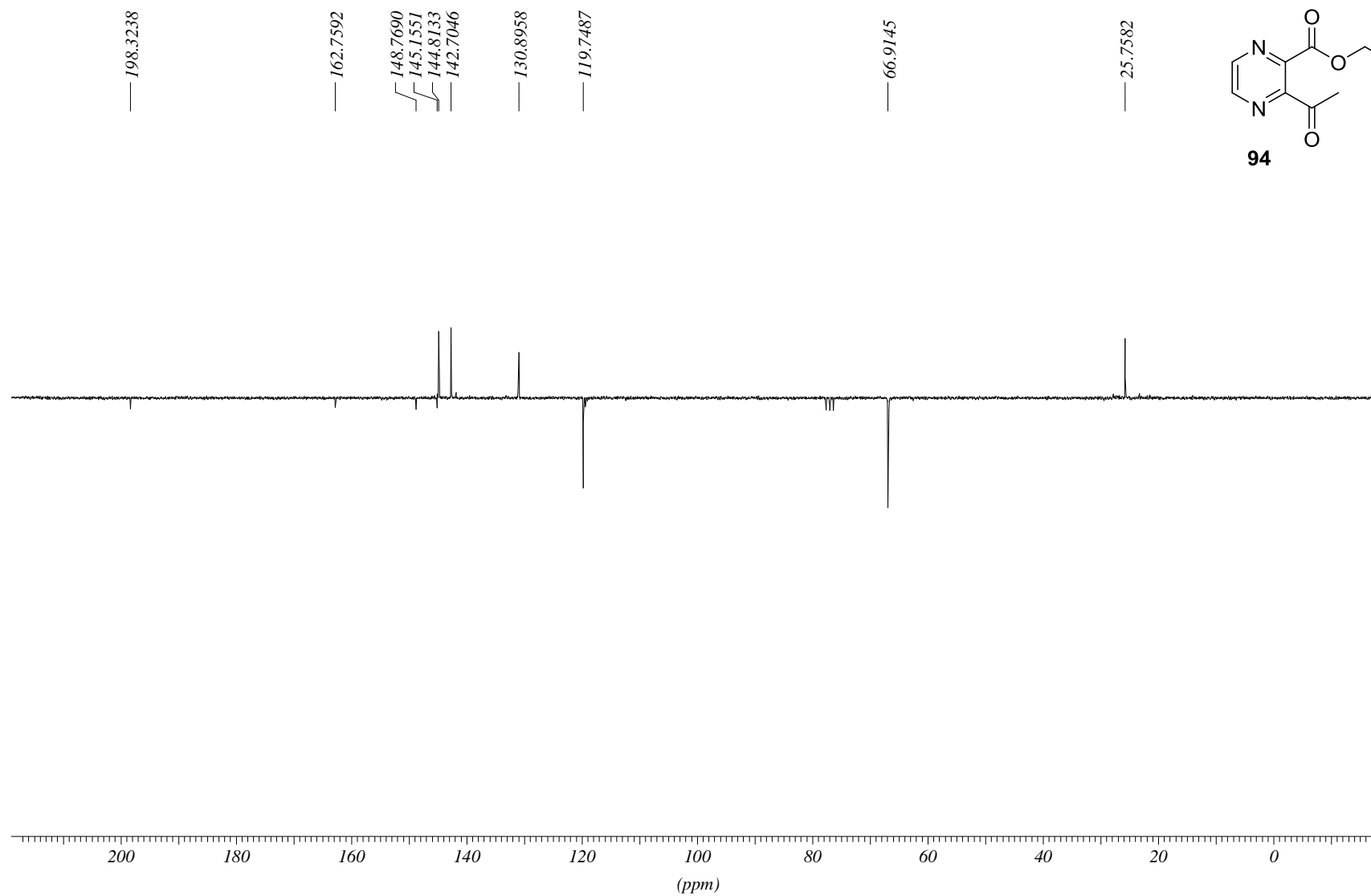
C13APT CDCl3 opt/xwinmr neudorfer 40



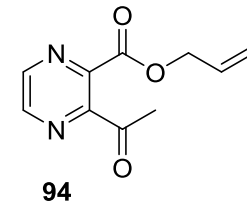
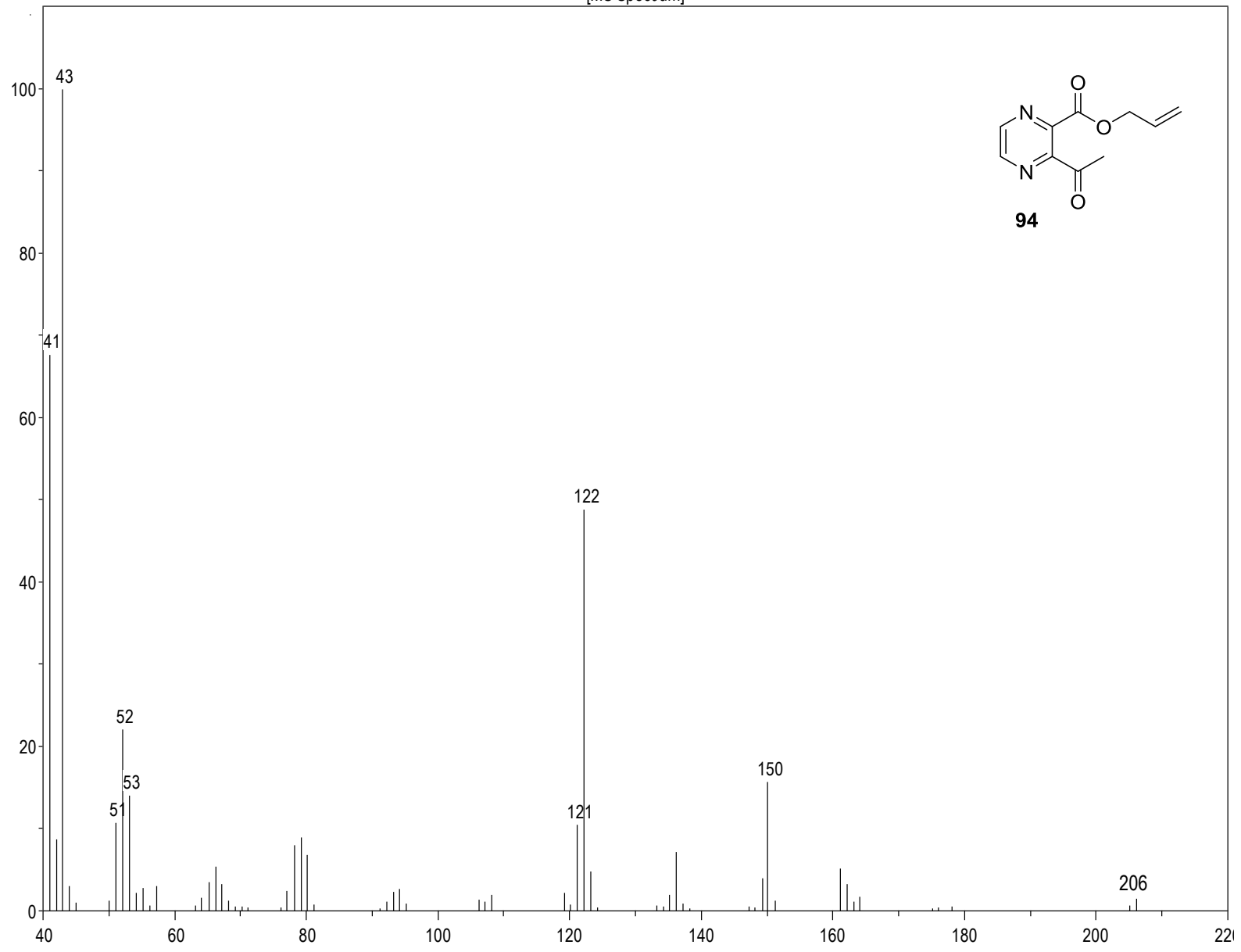
PROTON CDCl3 opt/xwinmr neudorfer 59

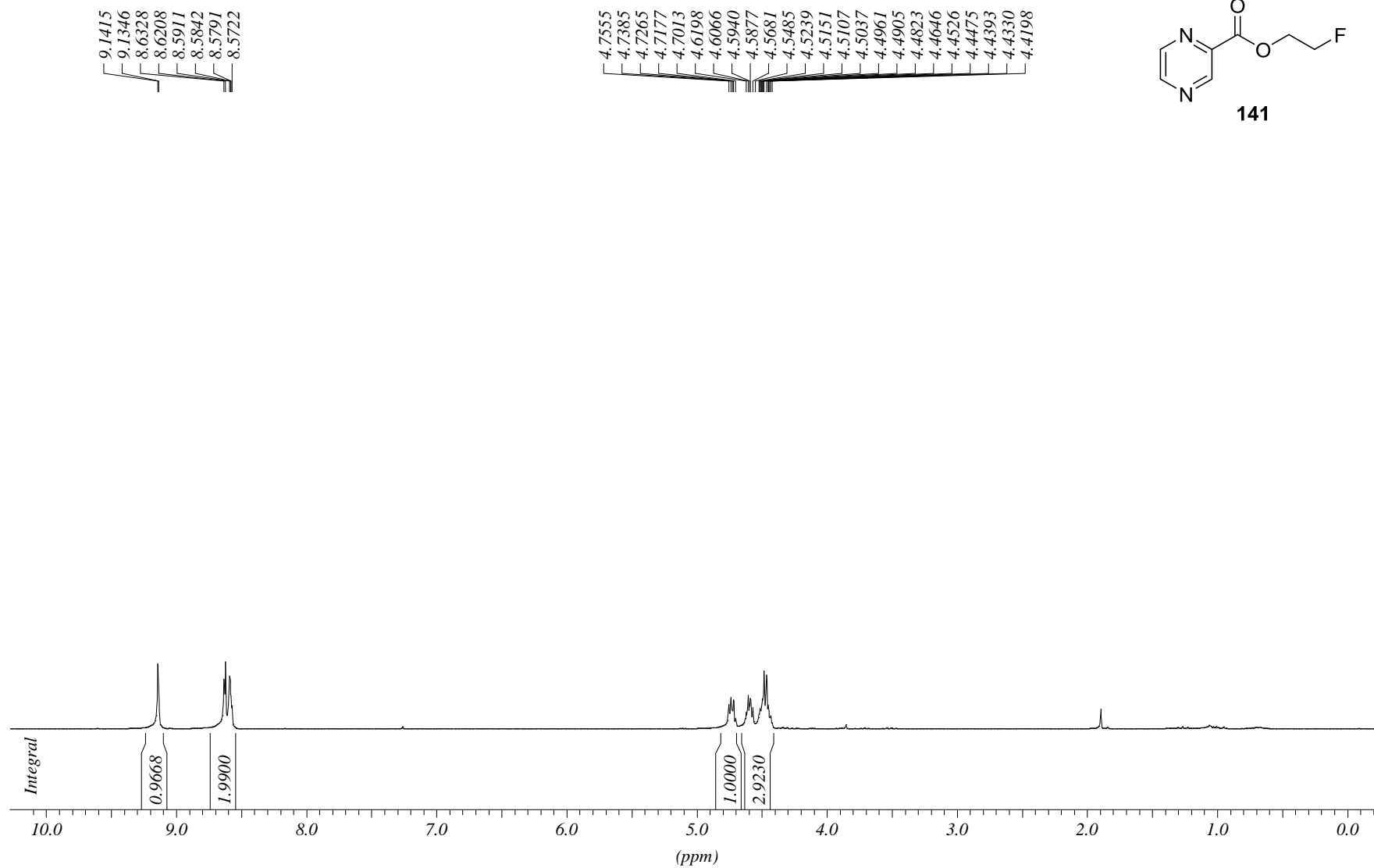


C13APT CDCl3 opt/xwinmr neudorfer 59

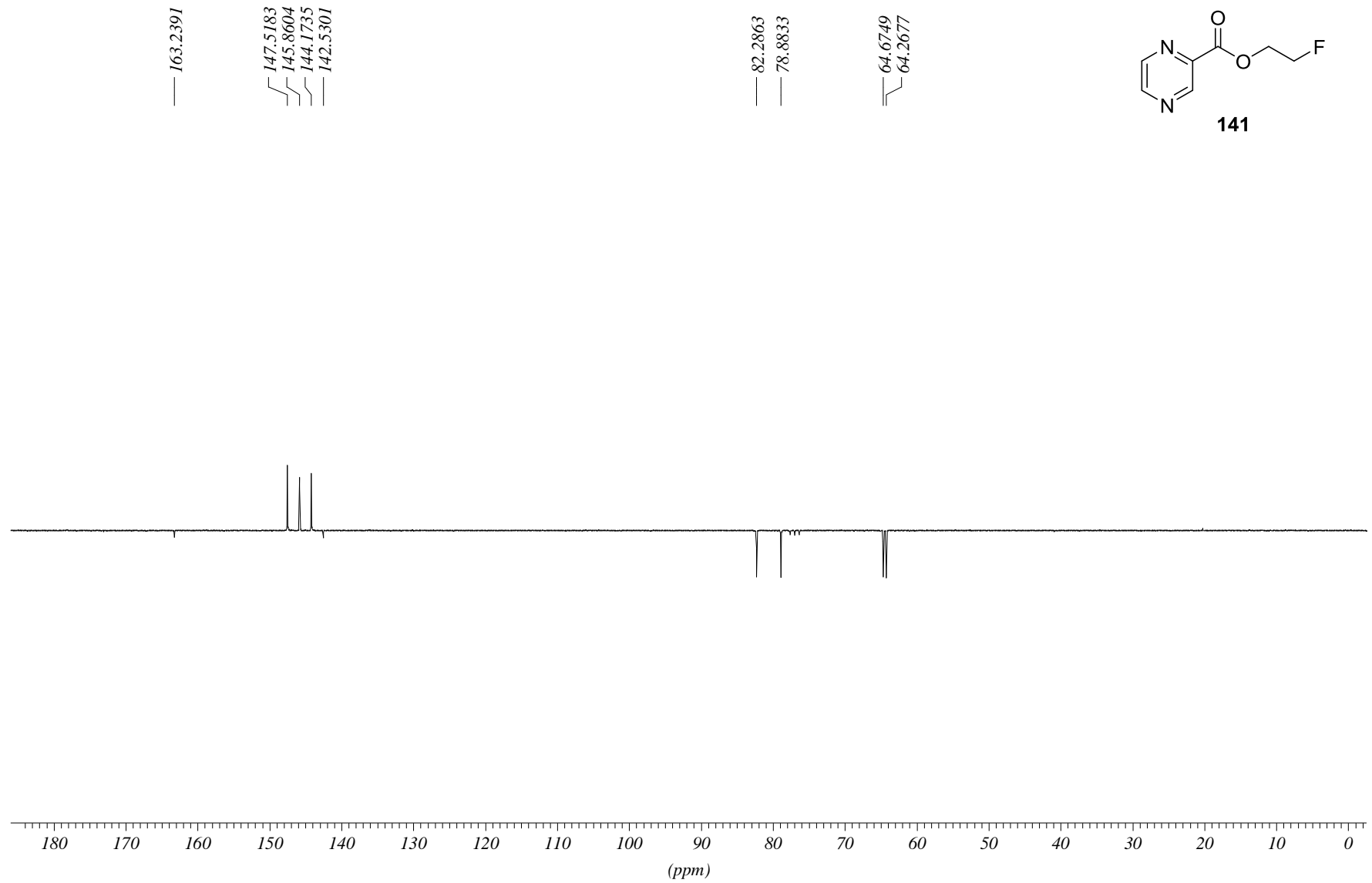


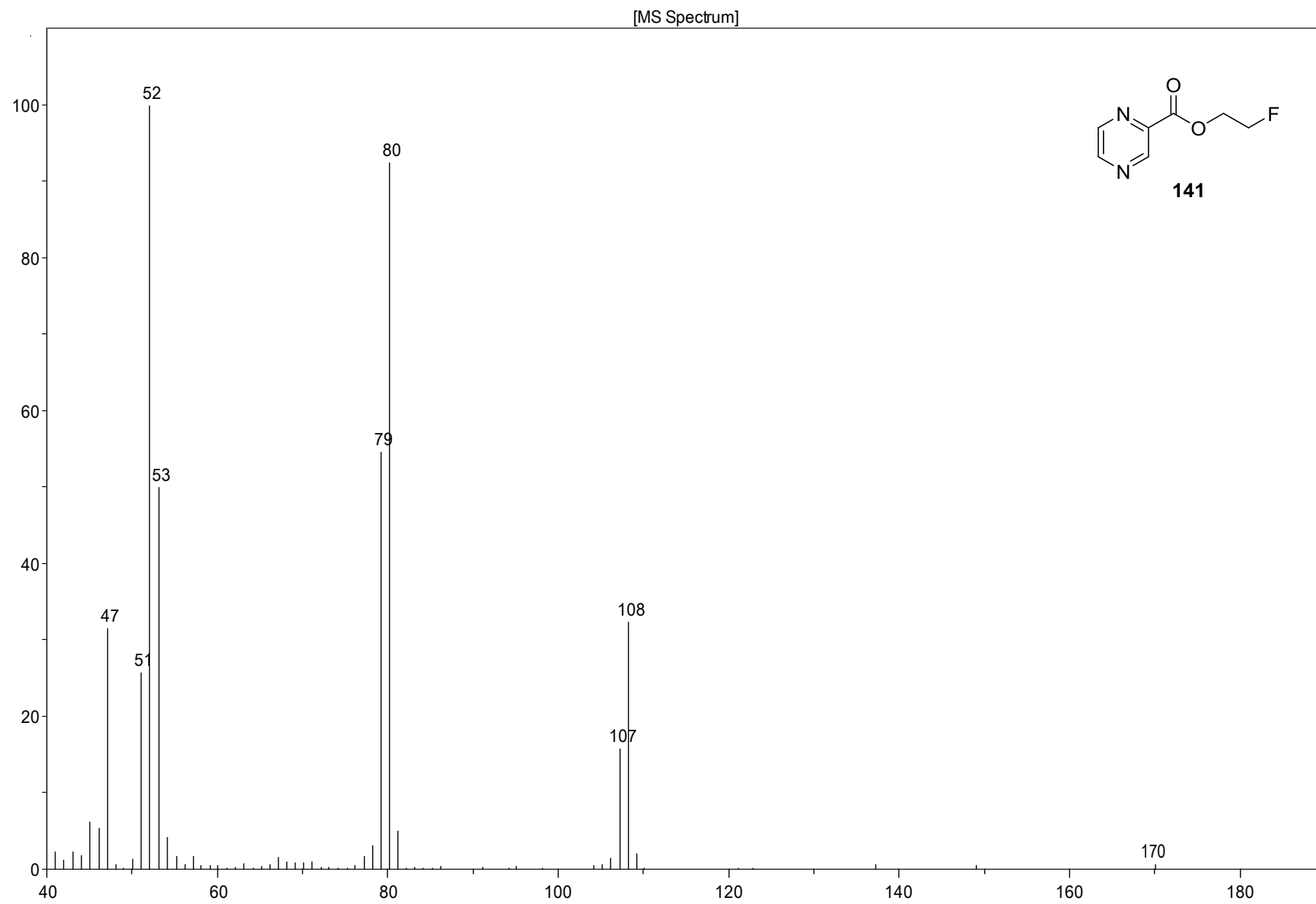
[MS Spectrum]



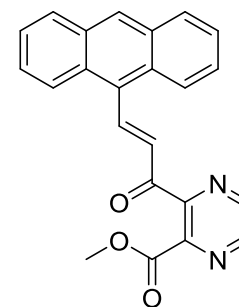
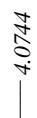
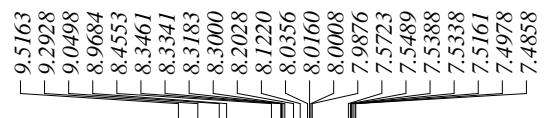
PROTON CDCl₃ opt/xwinmr neudorfer 30

C13APT CDCl3 opt/xwinmr neudorfer 30

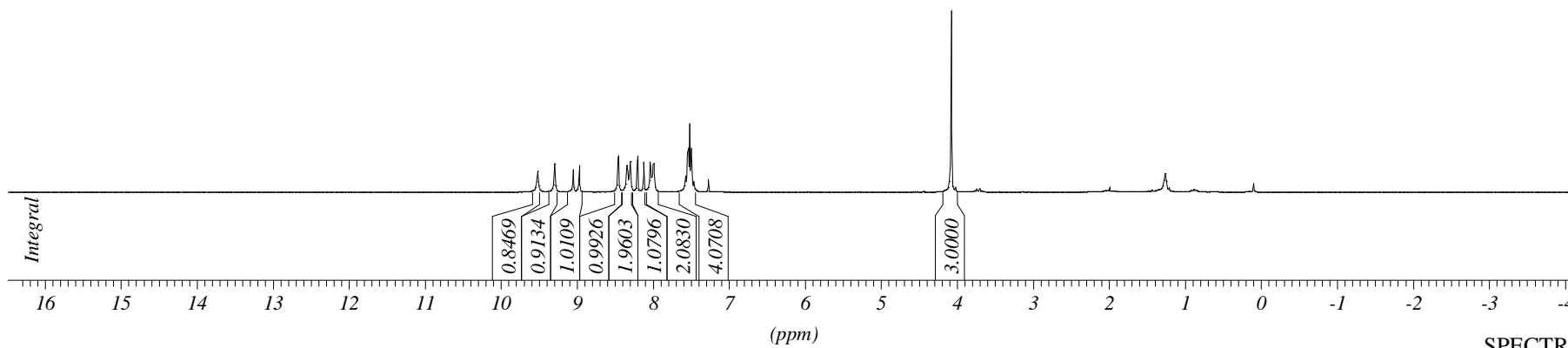


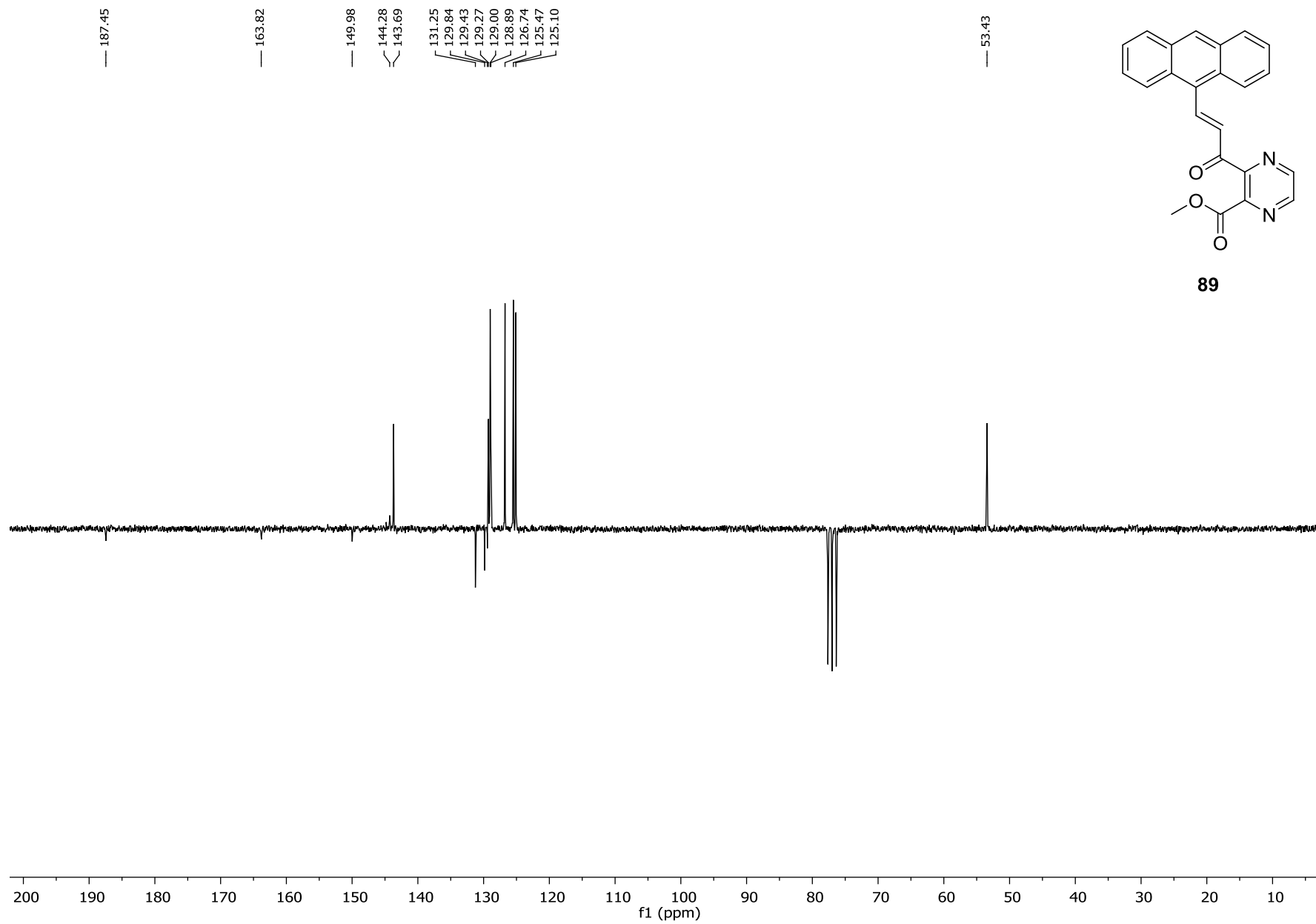


PROTON CDCl3 opt/xwinmmr neudorfer 58

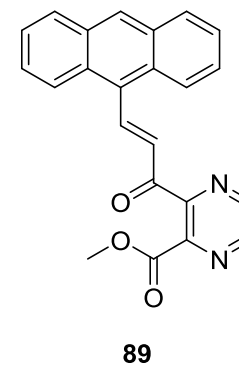
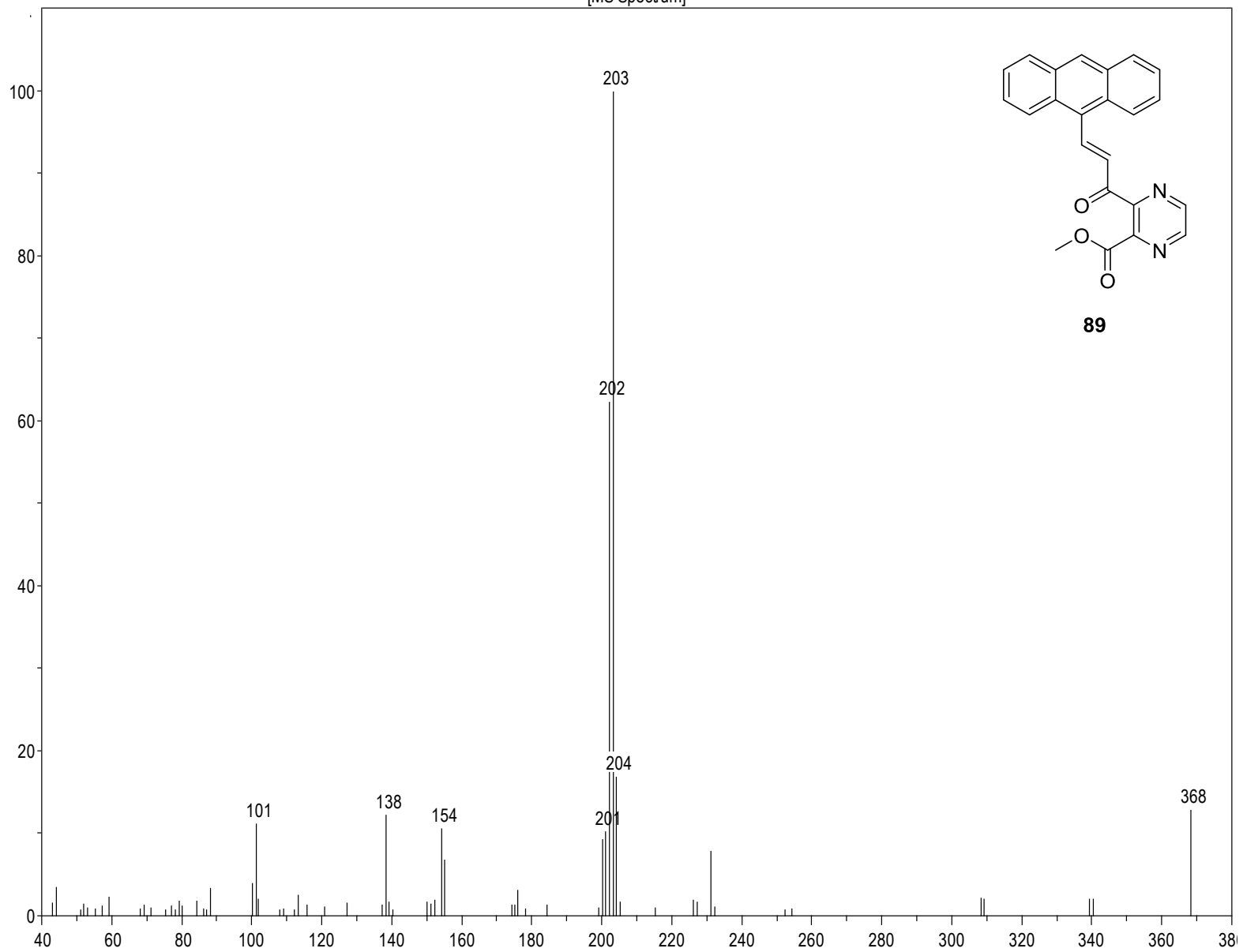


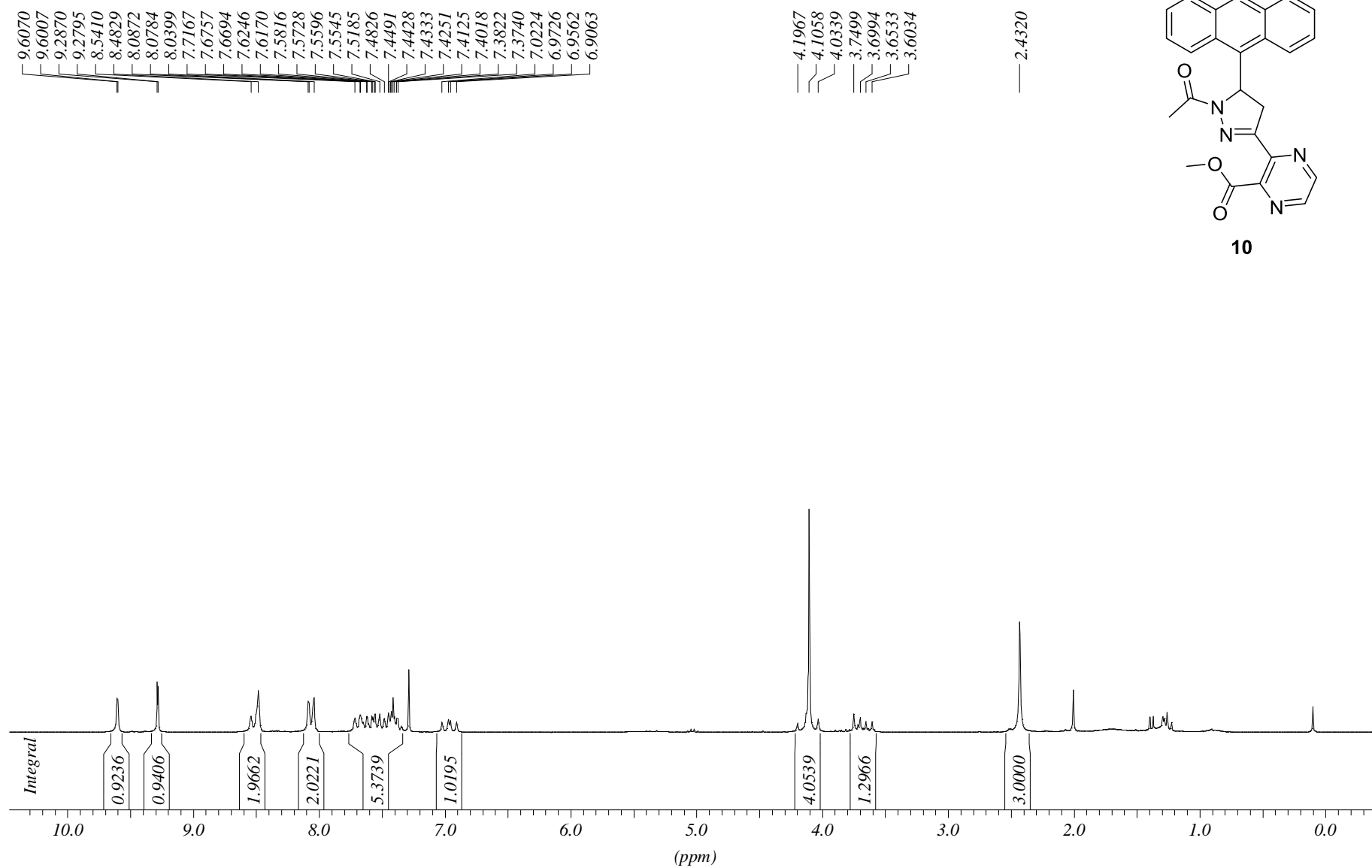
89

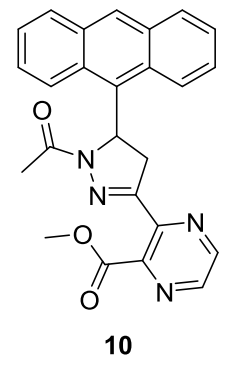
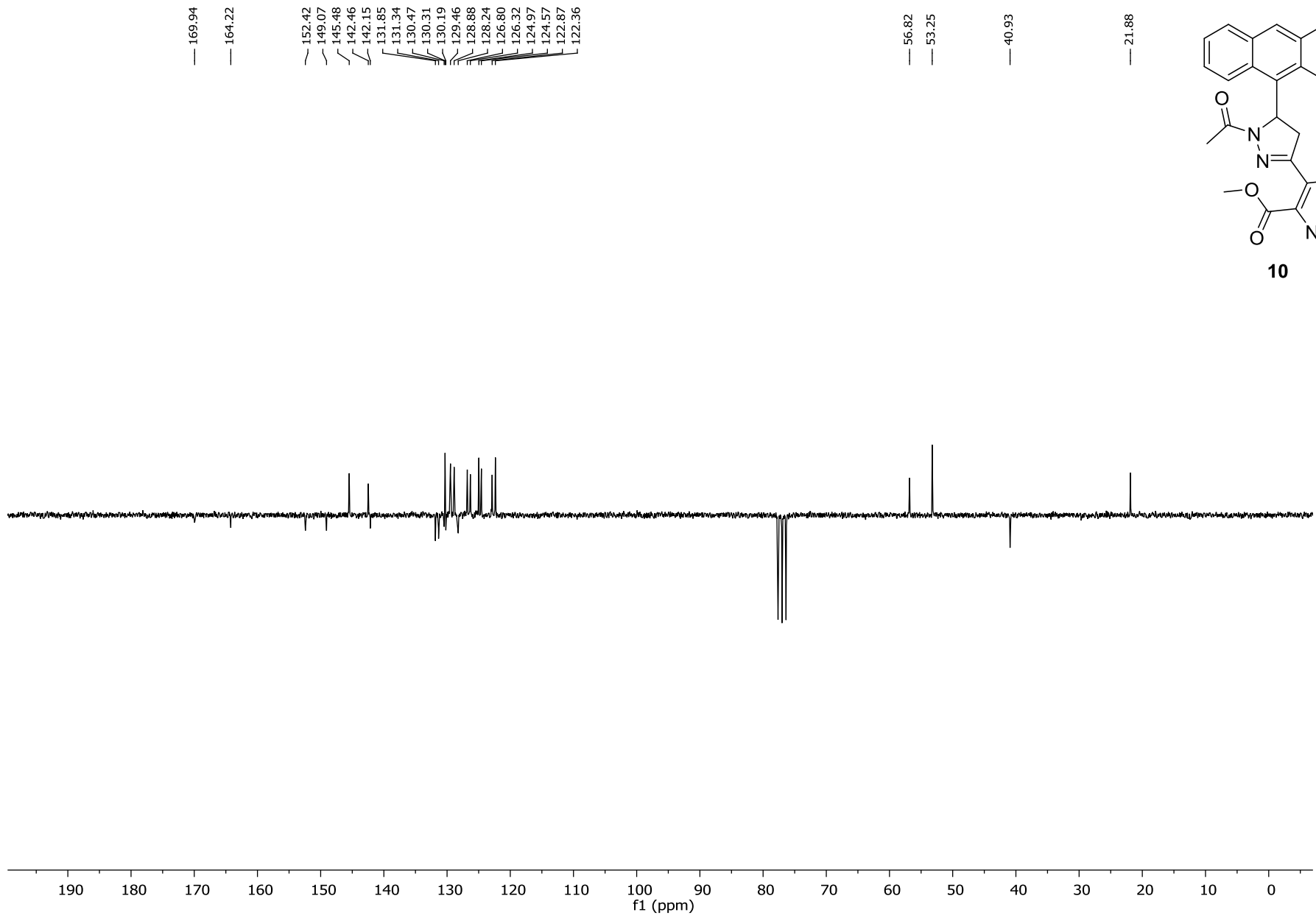




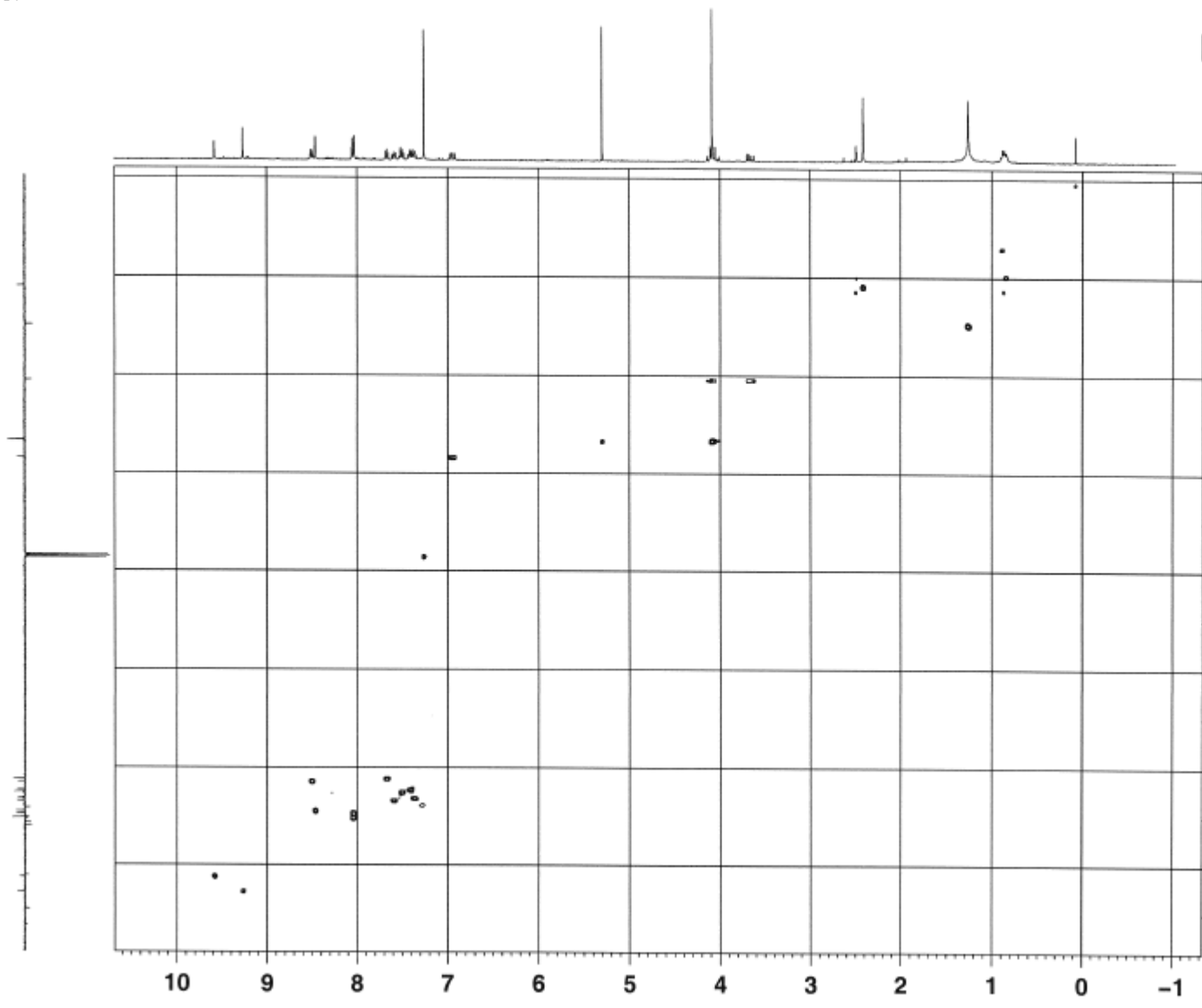
[MS Spectrum]



PROTON CDCl₃ opt/xwinnmr neudorfer 41



pyraz/CDCl3/HSQC



```

Current Data Parameters
NAME      02_pyraz1
EXPNO    1
PROCNO   1

F2 - Acquisition Parameters
Date_    20180111
Time     21.55
INSTRUM  spect
PROBHD   5 mm PABBO BB/
PULPROG  zgpg30p12
TD       1324
SOLVENT  CDCl3
NS       2
DS       32
SWH      4887.432 Hz
FIDRES   4.455612 Hz
AQ       0.186446 sec
RG       203
CW       164.308 usec
DE       10.00 usec
TE       297.3 K
CHFT2    145.860000
CHFT17   -0.320000
DS       0.000000 sec
DL       2.000000 sec
D4       0.0017414 sec
DL1      0.000000 sec
DL4      0.000000 sec
D24      0.000000 sec
IN1      0.000000 sec

***** CHANNEL F1 *****
NUC1      1H
P1       12.50 usec
P2       15.00 usec
D21      1000.00 usec
PLW1     14.0000000 W
SFO1     400.2318228 MHz

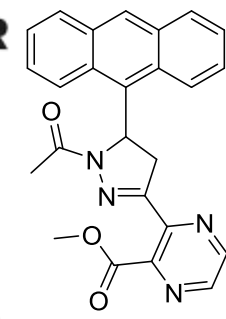
***** CHANNEL F2 *****
CPDPRG2  zgpg
NUC2      13C
P3       8.50 usec
P14      500.00 usec
D24      2000.00 usec
PCPD2    75.00 usec
PLW2     64.0000000 W
PLW13    0.42204002 W
SFO2     100.627038 MHz
SFOHAK3  Crp50.8.5.20.1
SFOAL3   0.500
SFOFF3   0 Hz
SFO3     7.86488902 W
SFOHAK7  Crp40comp.4
SFOAL7   0.500
SFOFF7   0 Hz
SFO7     7.86503006 W

***** GRADIENT CHANNEL *****
SFOHAK1  SH5010.180
SFOHAK2  SH5010.180
SFOHAK3  SH5010.180
SFOHAK4  SH5010.180
GDEL1   90.00 %
GDEL2   20.10 %
GDEL3   11.80 %
GDEL4   -5.00 %
P19     1000.00 usec
P19     600.00 usec

F1 - Acquisition Parameters
SD       288
SFO1     100.627038 MHz
FIDRES   62.803691 Hz
SW       140.000 ppm
PULPROG  echo-antico

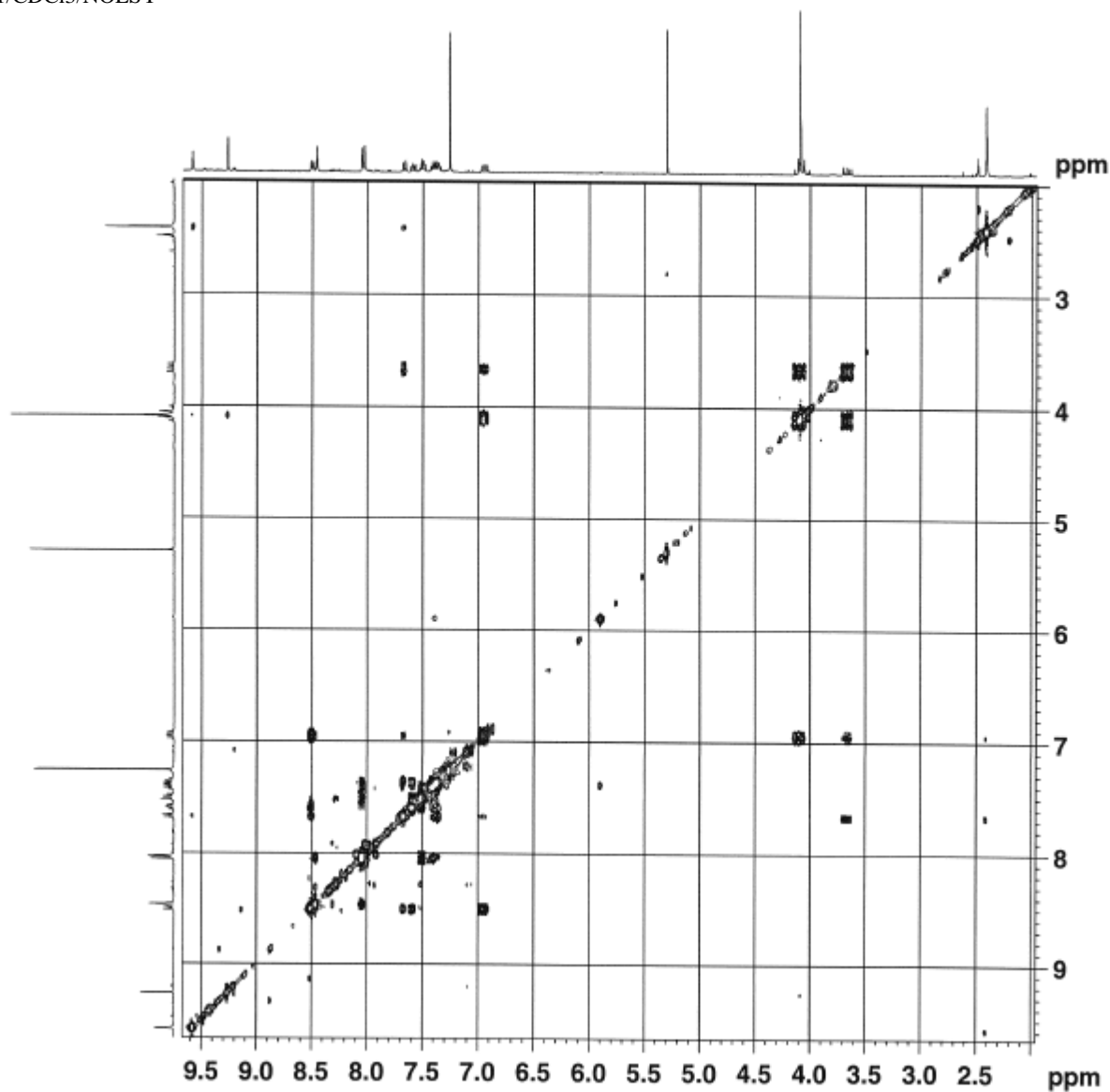
F2 - Processing parameters
SI       1024
SF       400.231818 MHz
WDW      EM
SSB      0 Hz
GB       0
PC       1.00

F1 - Processing parameters
SI       1024
SF       echo-antico
SF       140.6379165 MHz
WDW      States-TPP1
SSB      0 Hz
GB       0
PC       0
    
```



10

pyraz1/CDC13/NOESY



Current Data Parameters
NAME KN_pyraz1
EXPNO 5
PROCNO 1

F2 - Acquisition Parameters
Date_ 20140111
Time 23.43
INSTRUM spect
PROBHD 5 mm PABBO BB/
FULPROG noesypph
TD 2048
SOLVENT CDC13
NS 8
DS 8
SWH 4000.000 Hz
FIDRES 1.953125 Hz
AQ 0.2560500 sec
RG 161
DW 125.000 usec
DE 10.00 usec
TE 297.3 K
DO 0.00010901 sec
D1 2.00000000 sec
D8 0.80000001 sec
D16 0.00020000 sec
IND 0.00024985 sec

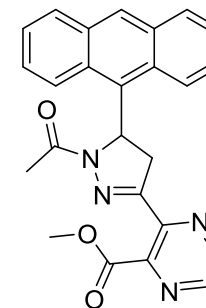
----- CHANNEL f1 -----
NUC1 1H
P1 12.50 usec
P2 25.00 usec
PLW1 16.00000000 W
SFO1 400.2318629 MHz

----- GRADIENT CHANNEL -----
GPMW1 SMSQ10.100
GPE1 40.00 %
P16 1000.00 usec

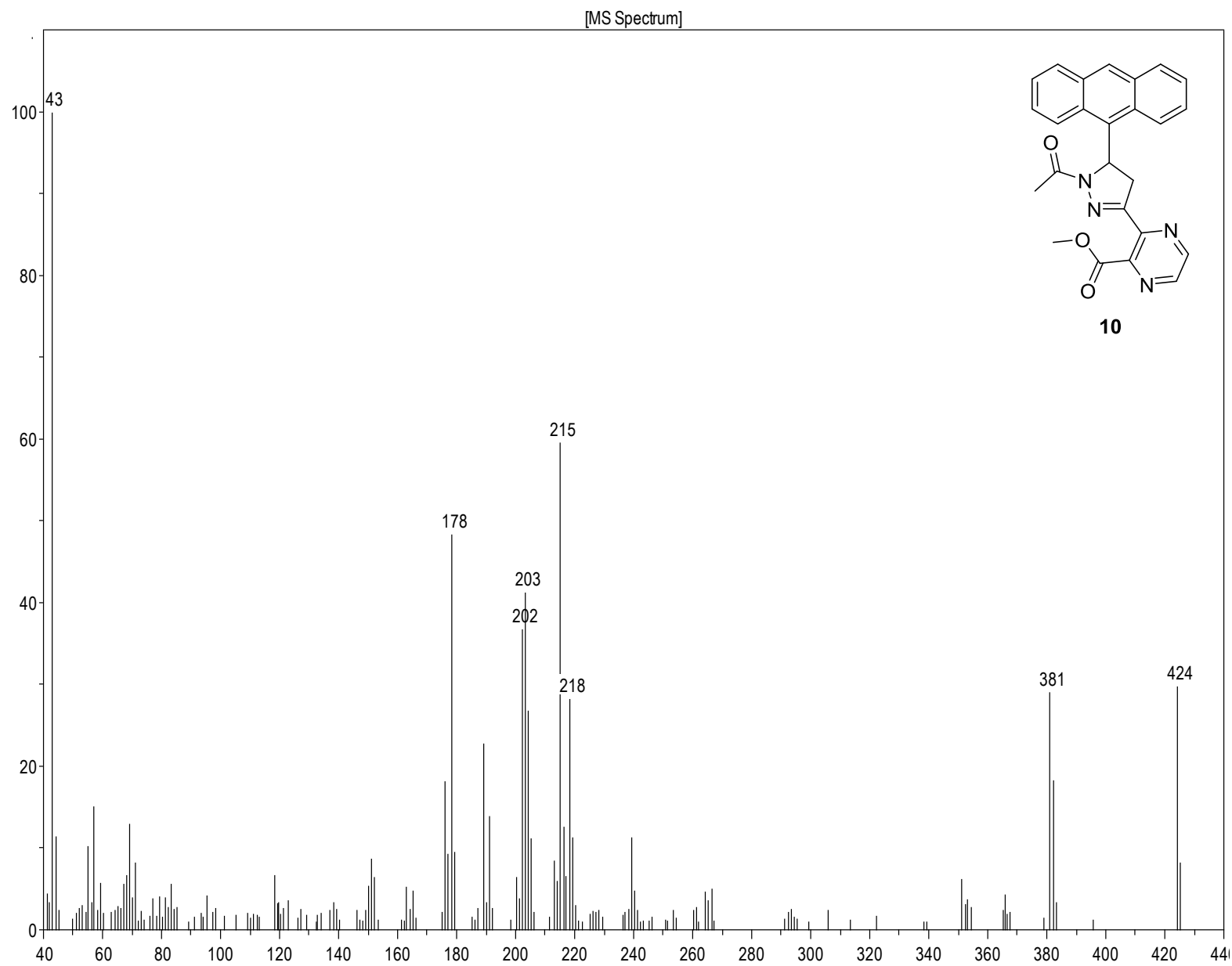
F1 - Acquisition parameters
TD 256
SFO1 400.2319 MHz
FIDRES 15.634058 Hz
SW 10.000 ppm
PnMODE States-TPPI

F2 - Processing parameters
SI 2048
SF 400.2300118 MHz
WDW QSINE
SSB 2
LB 0 Hz
GB 0
PC 1.00

F1 - Processing parameters
SI 2048
MC2 States-TPPI
SF 400.2300118 MHz
WDW States-TPPI
SSB 2
LB 0 Hz
GB 0



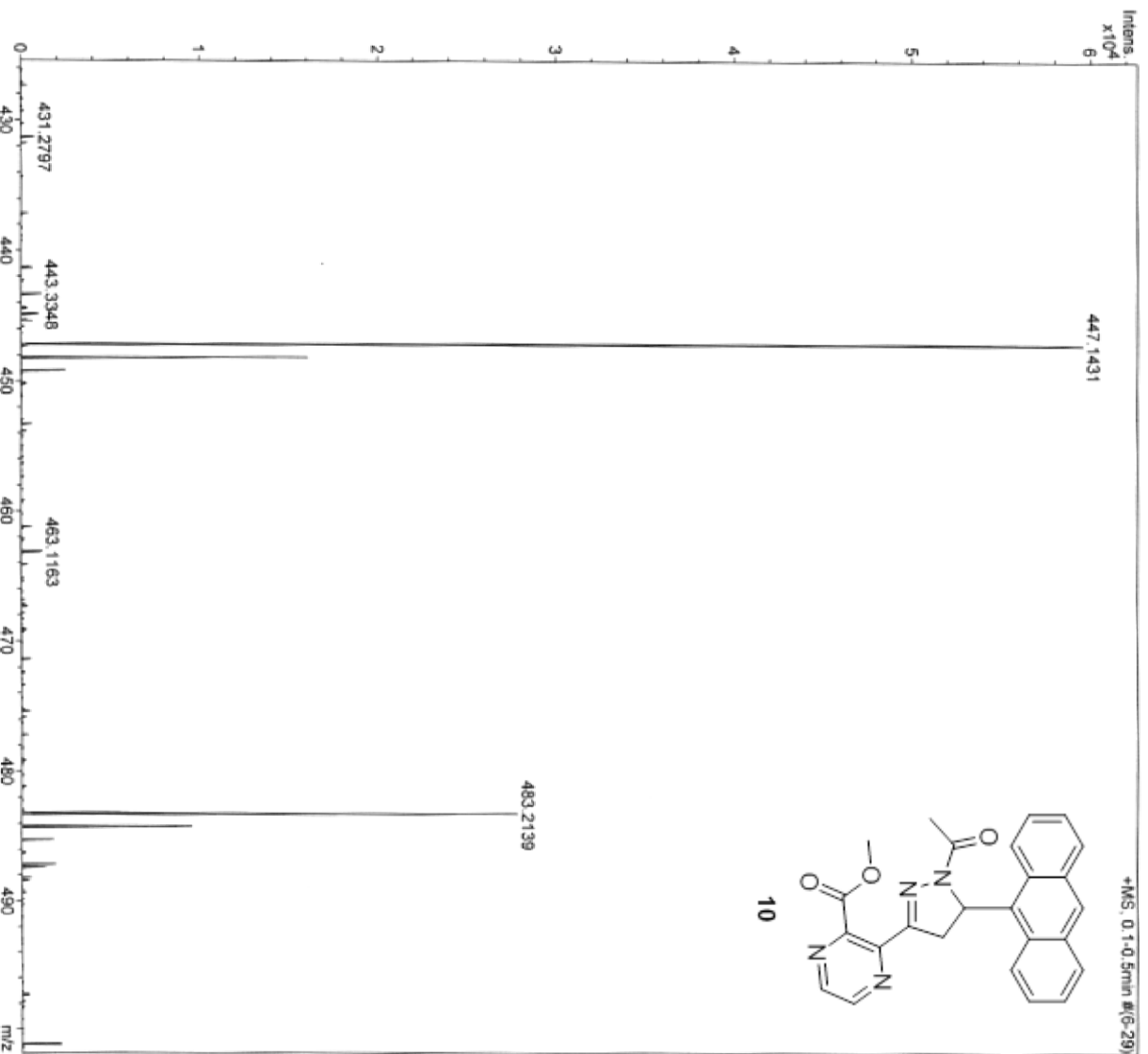
10



MassenspektrometrieZentrum FakultätChemieUniWien

Analysis Info
Analysis Name D:\Data\MS_MessService\39199000002.d
Method tune_low_nach_Quadropol.m
Sample Name pyrac 7
Auftragneber/Com Neudorfer/Spreitzer
Ergebnis: +/-5 ppm
ACN/MeOH

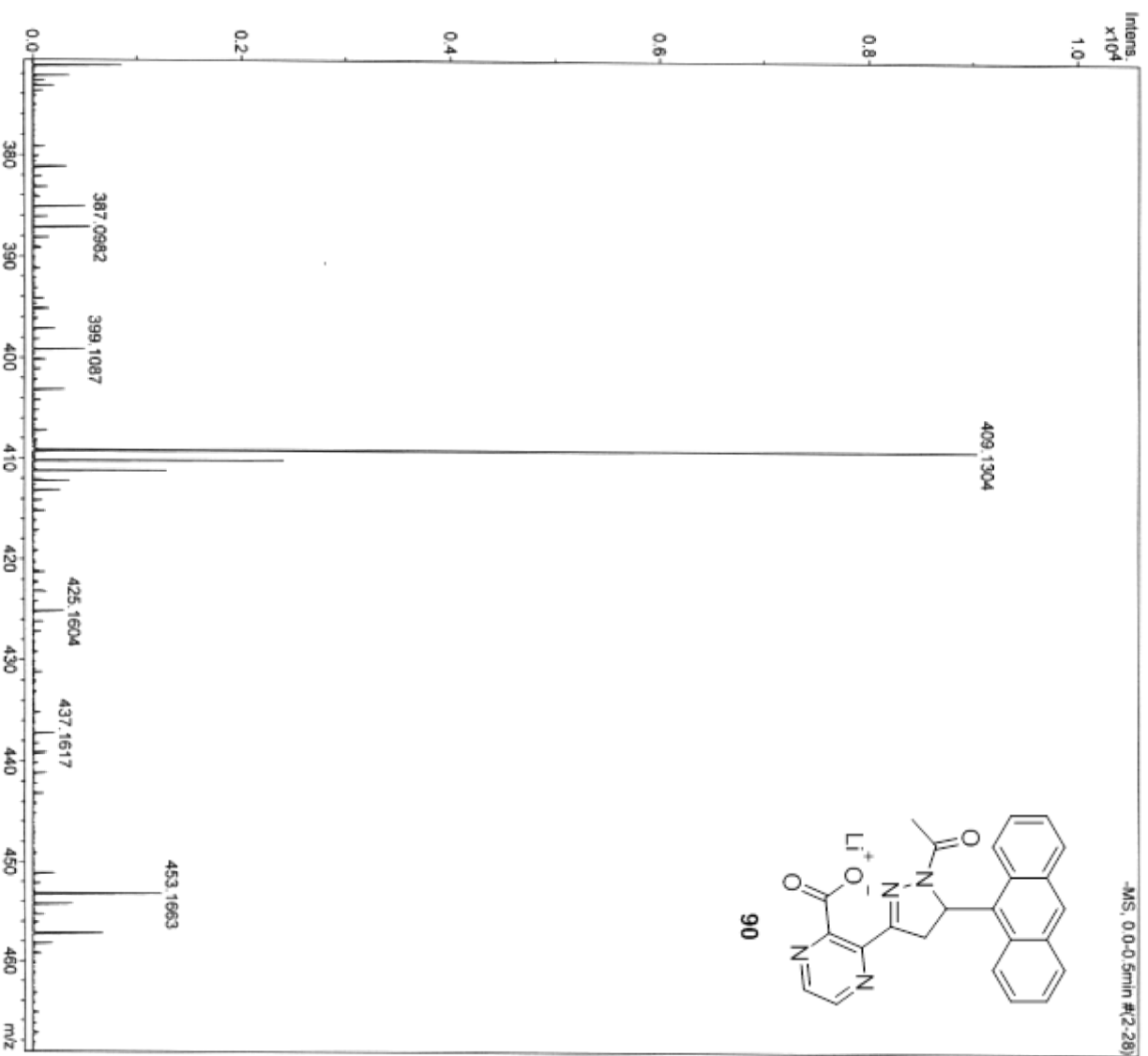
Acquisition Date 1/16/2013 2:50:30 PM
Operator phu
Instrument maxis

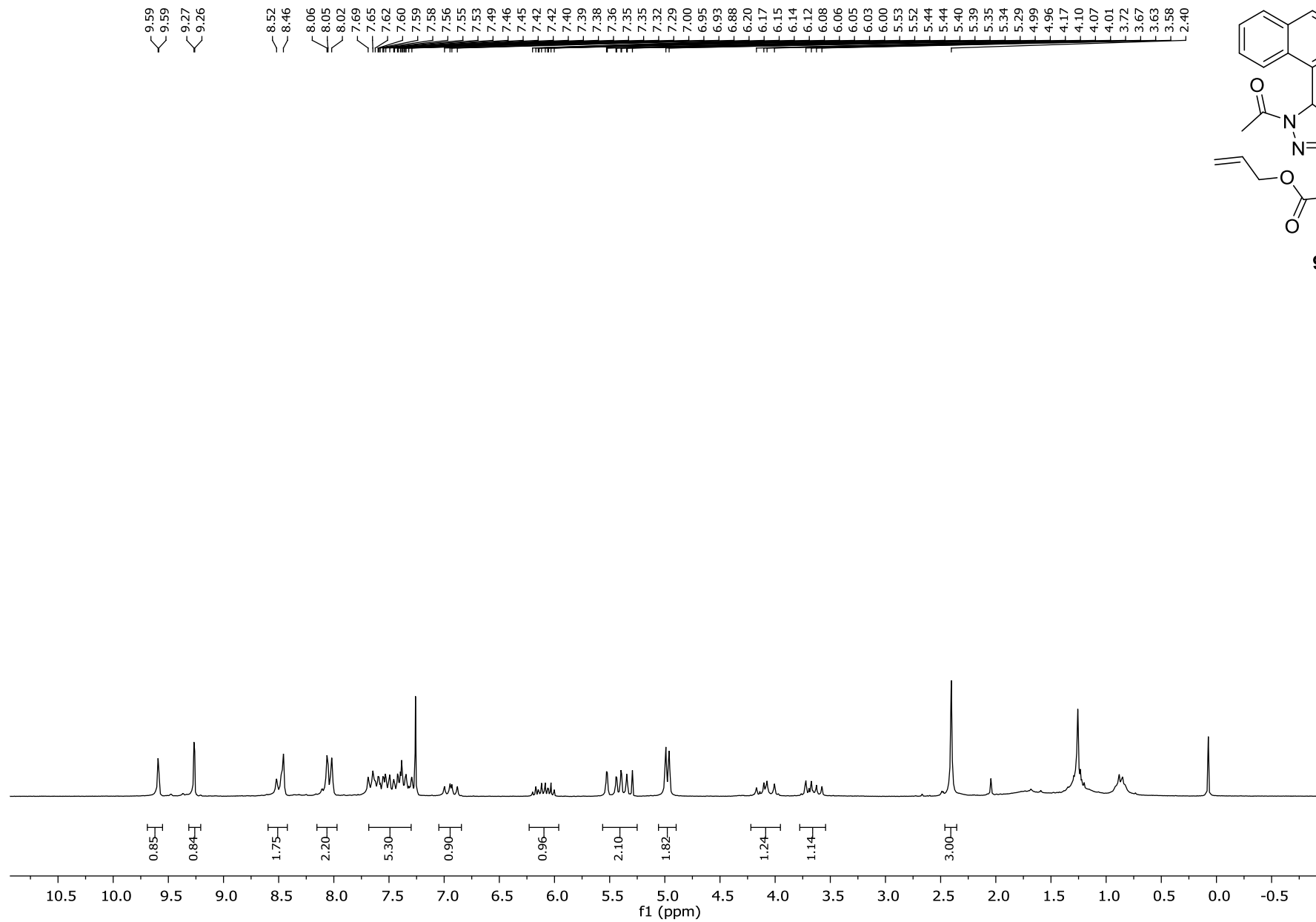
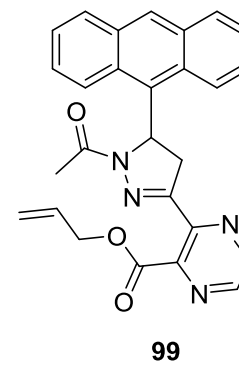


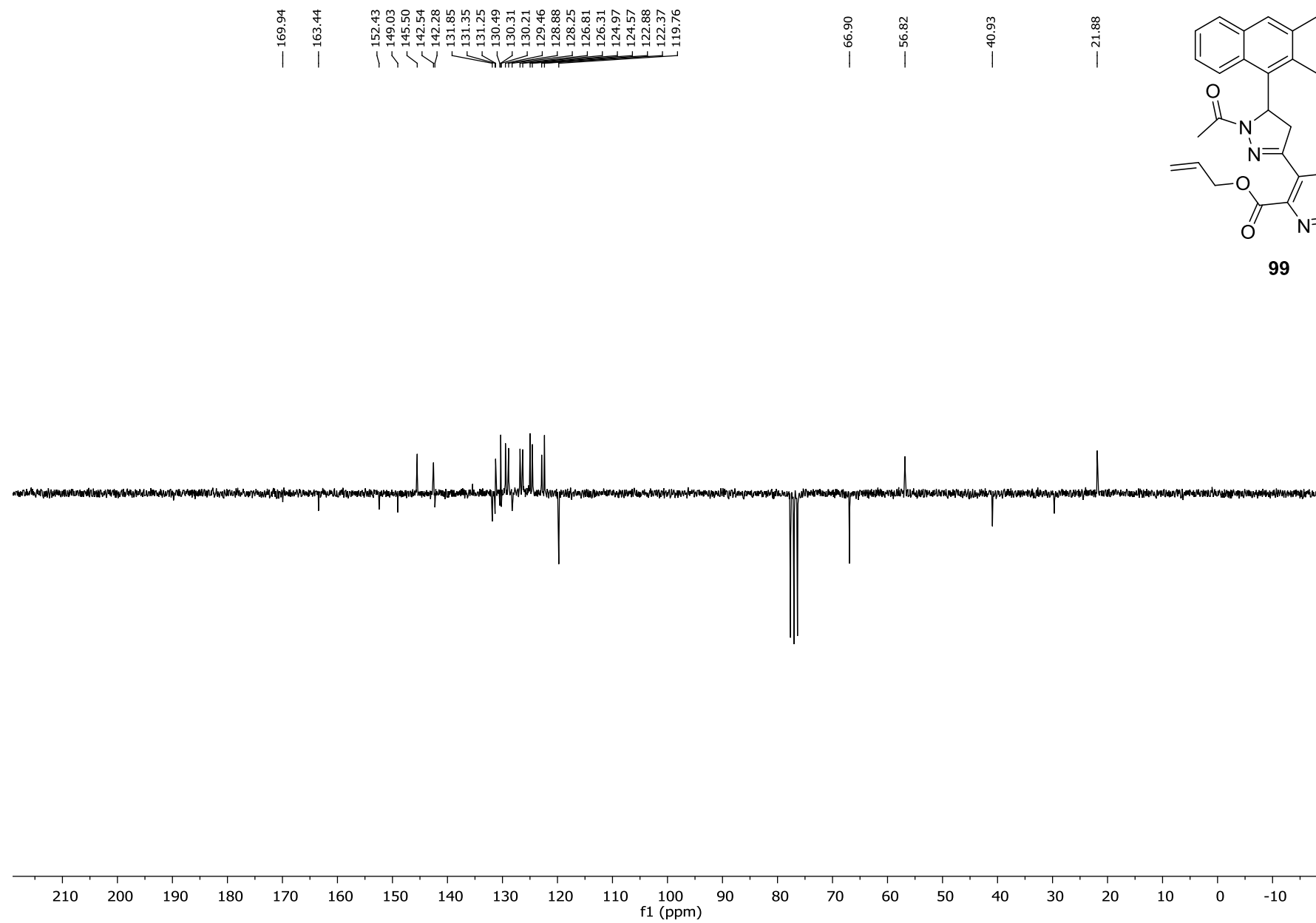
MassenspektrometrieZentrum FakultätChemieUniWien

Analysis Info
 Analysis Name D:\Data\MS_MessService\394040000001.d
 Method tune_low_MS_Service_03_13.m
 Sample Name PyraCS1
 Auftraggeber/Com Neudorfer/Spreitzer
 Ergebnis: +/-5 ppm
 ACN\MeOH 1% H2O

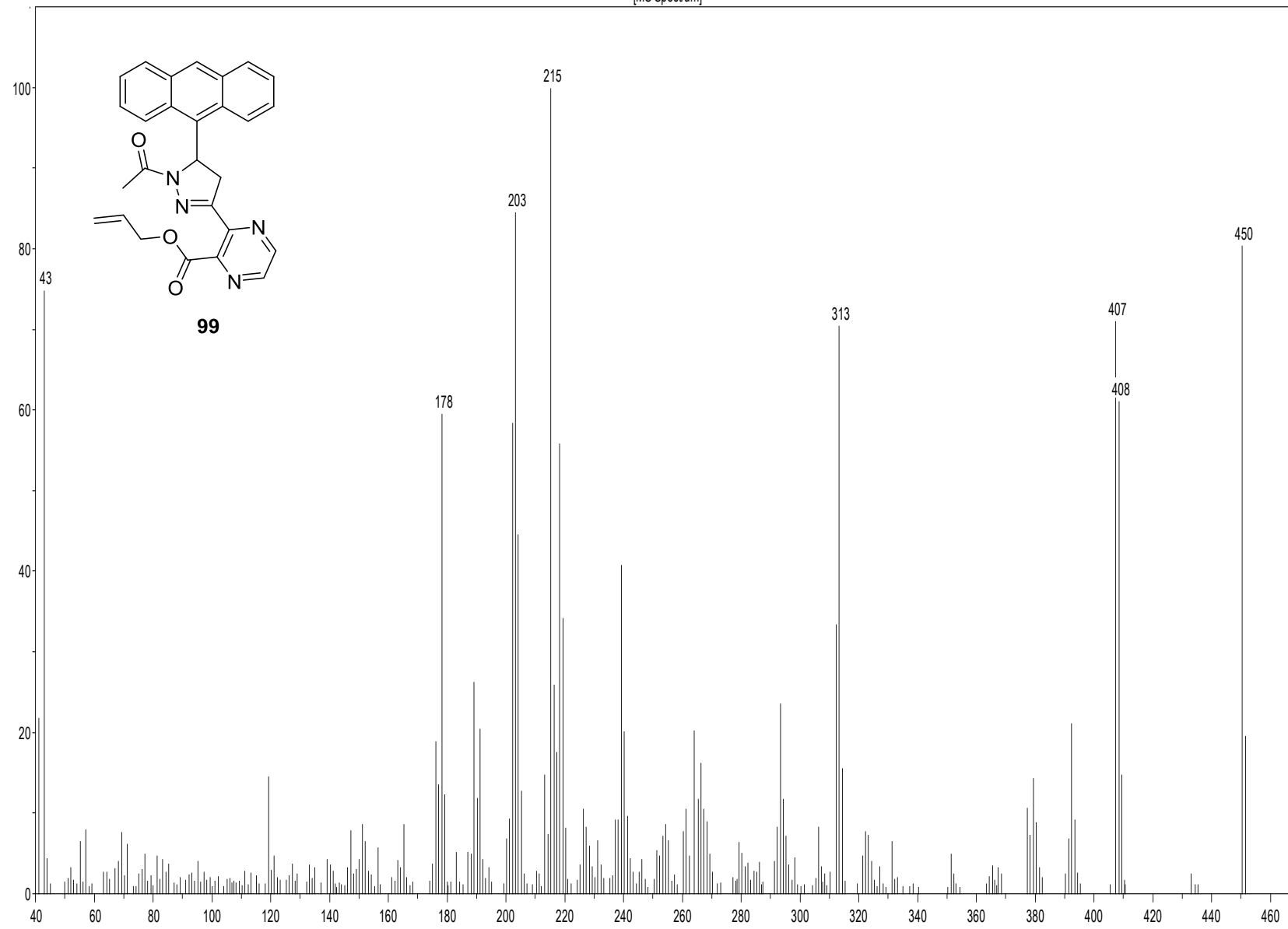
Acquisition Date 3/15/2013 2:04:50 PM
 Operator phu
 Instrument maxis







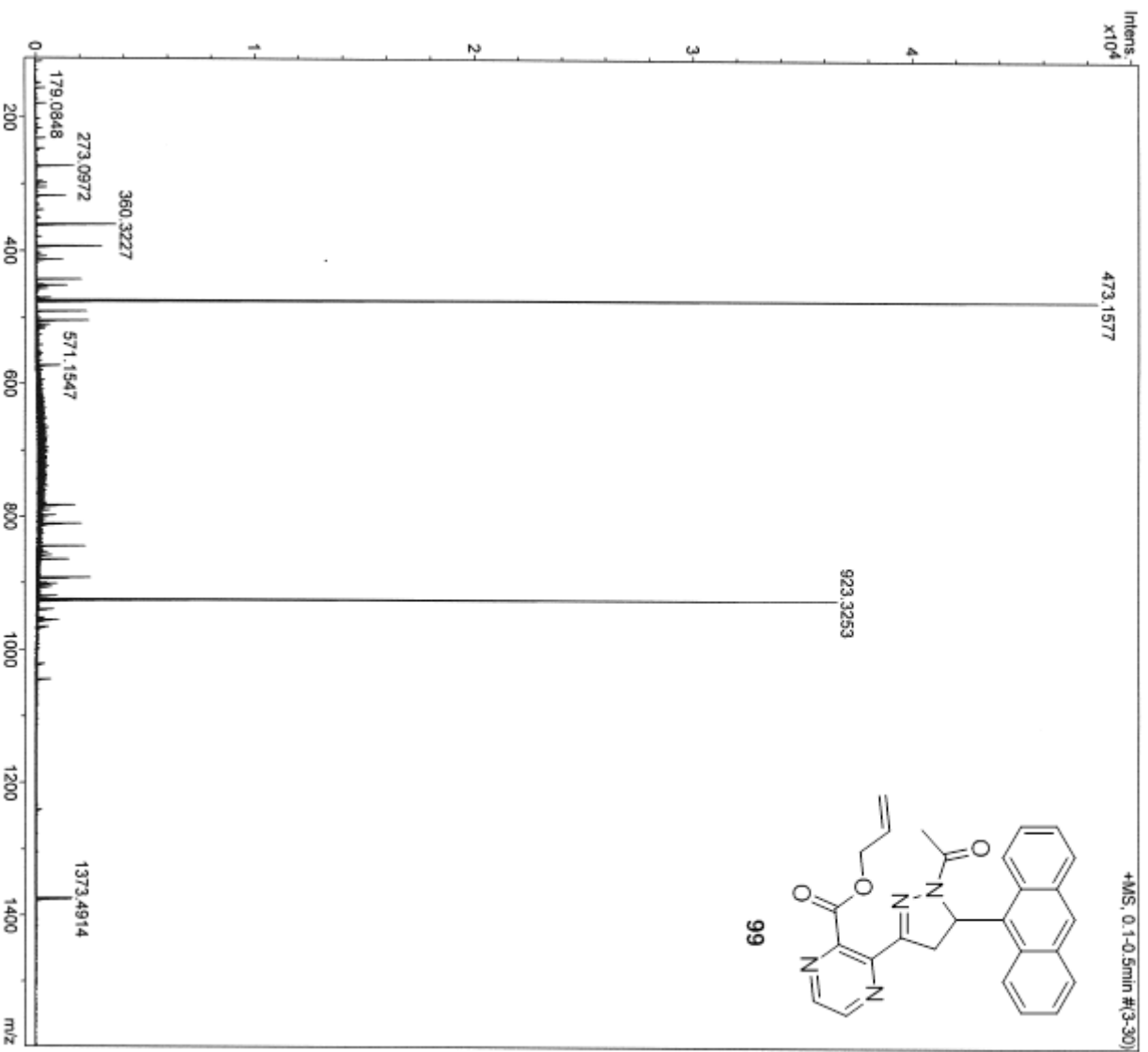
[MS Spectrum]

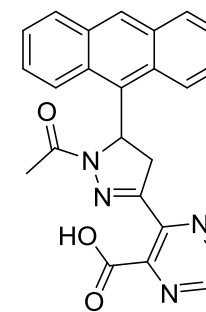
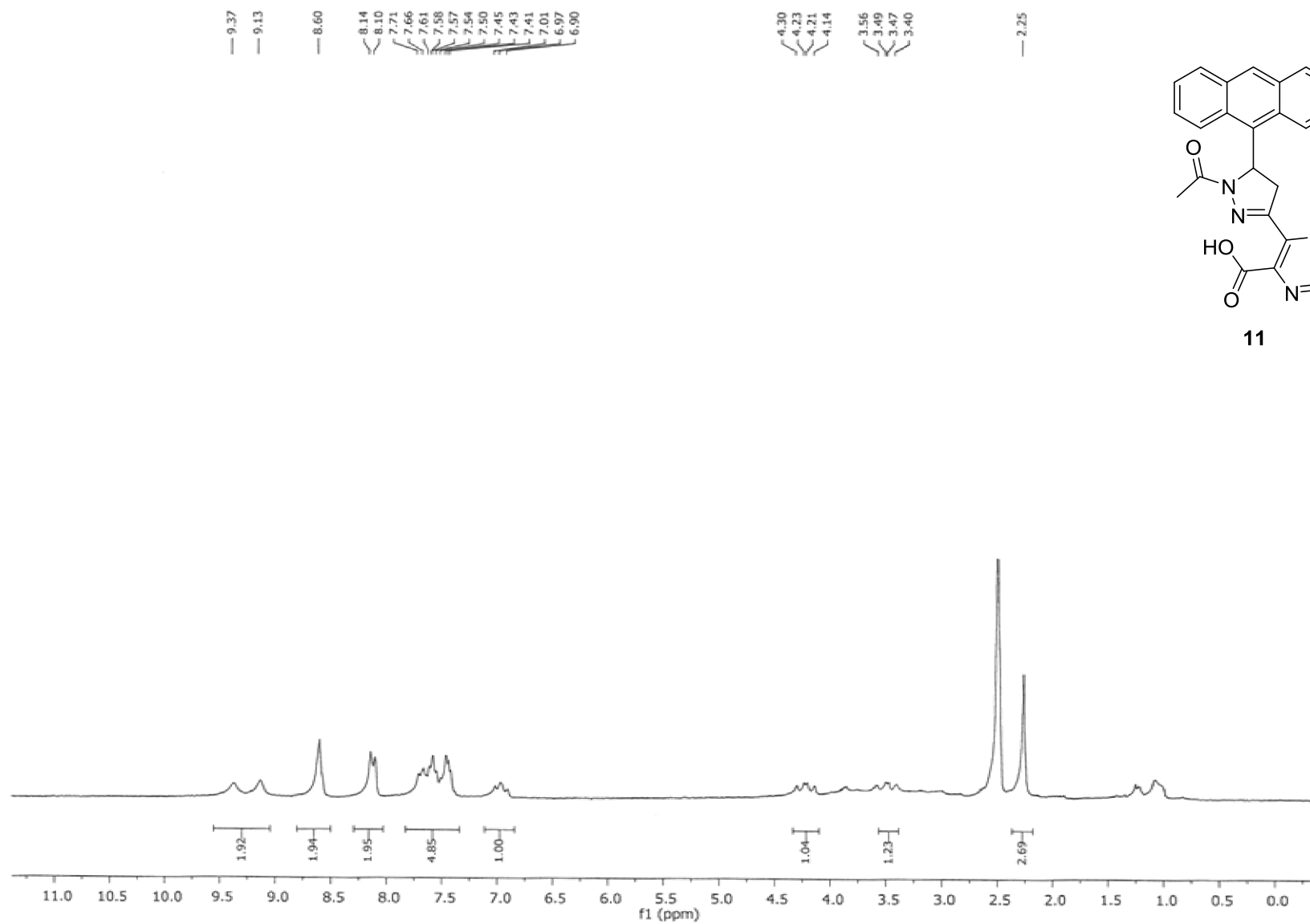


MassenspektrometrieZentrum FakultätChemieUniWien

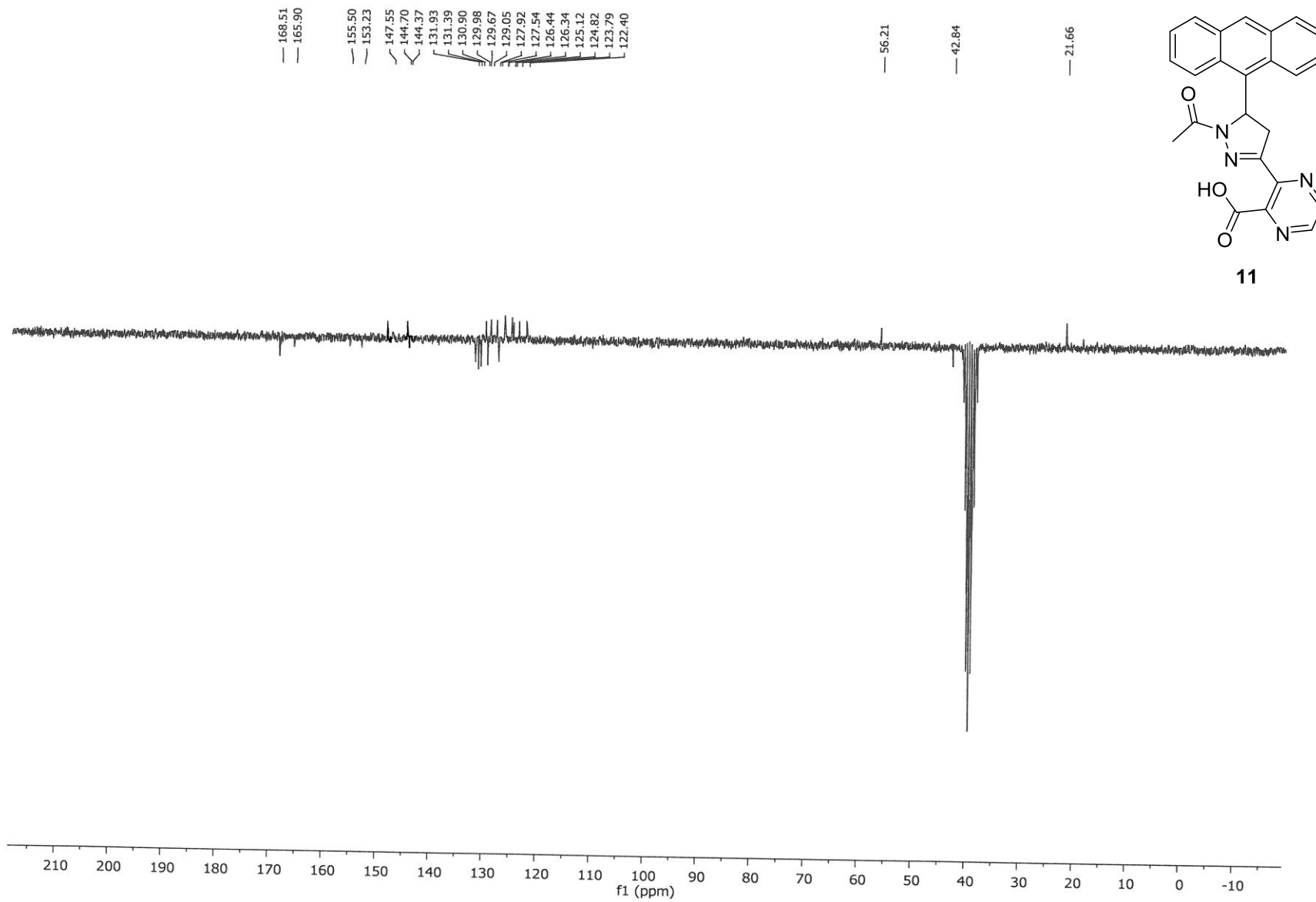
Analysis Info
 Analysis Name D:\Data\MS_MessService\401250000001.d
 Method tune_low_MS_Service_12_13.m
 Sample Name C.J002
 Auftraggeber/Com Neudorfer/Pharm
 Ergebnis: +/- 5ppm
 ACN/MeOH 0.1%/H2O

Acquisition Date 11/25/2013 8:42:28 AM
 Operator phu
 Instrument maxis





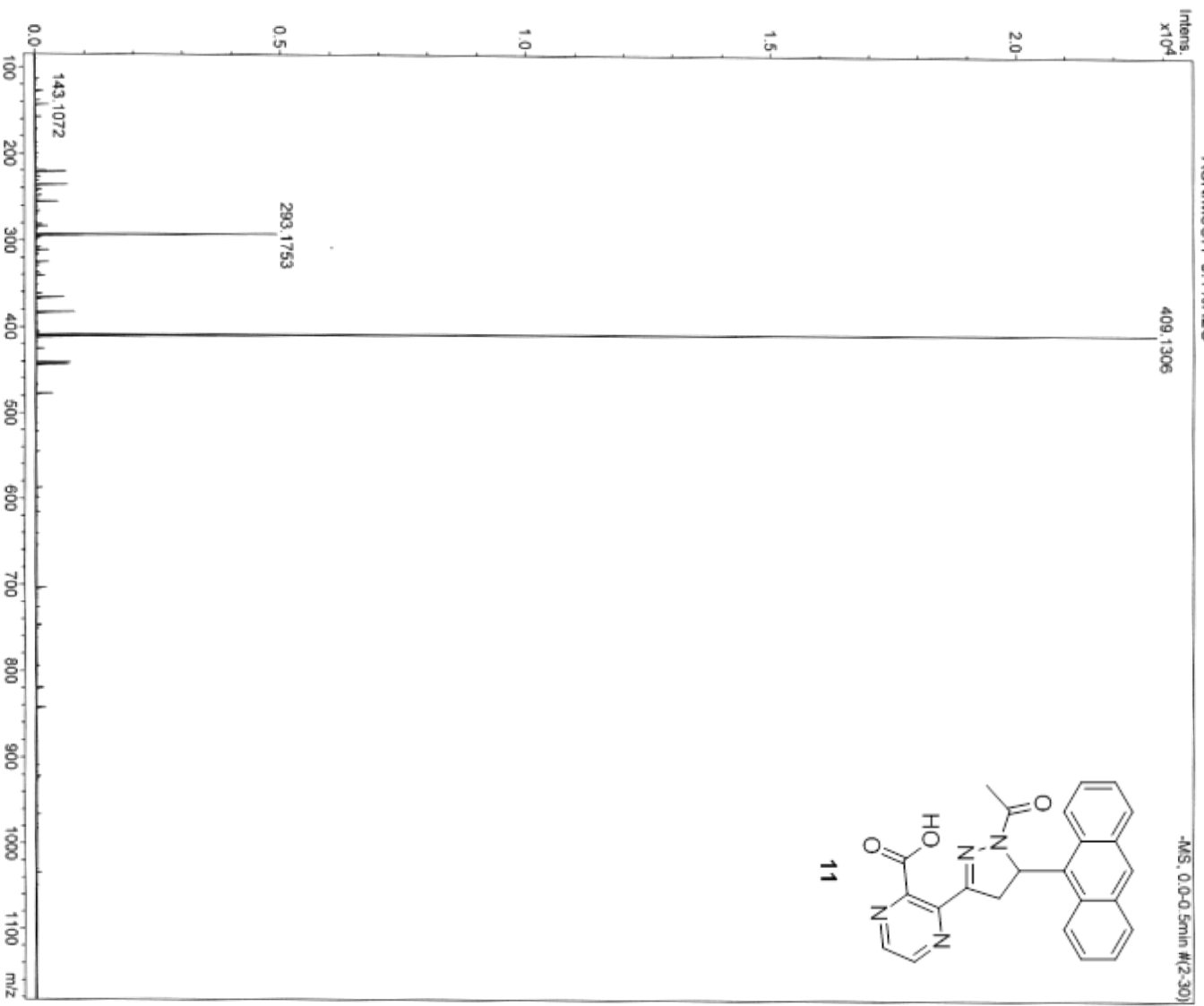
11

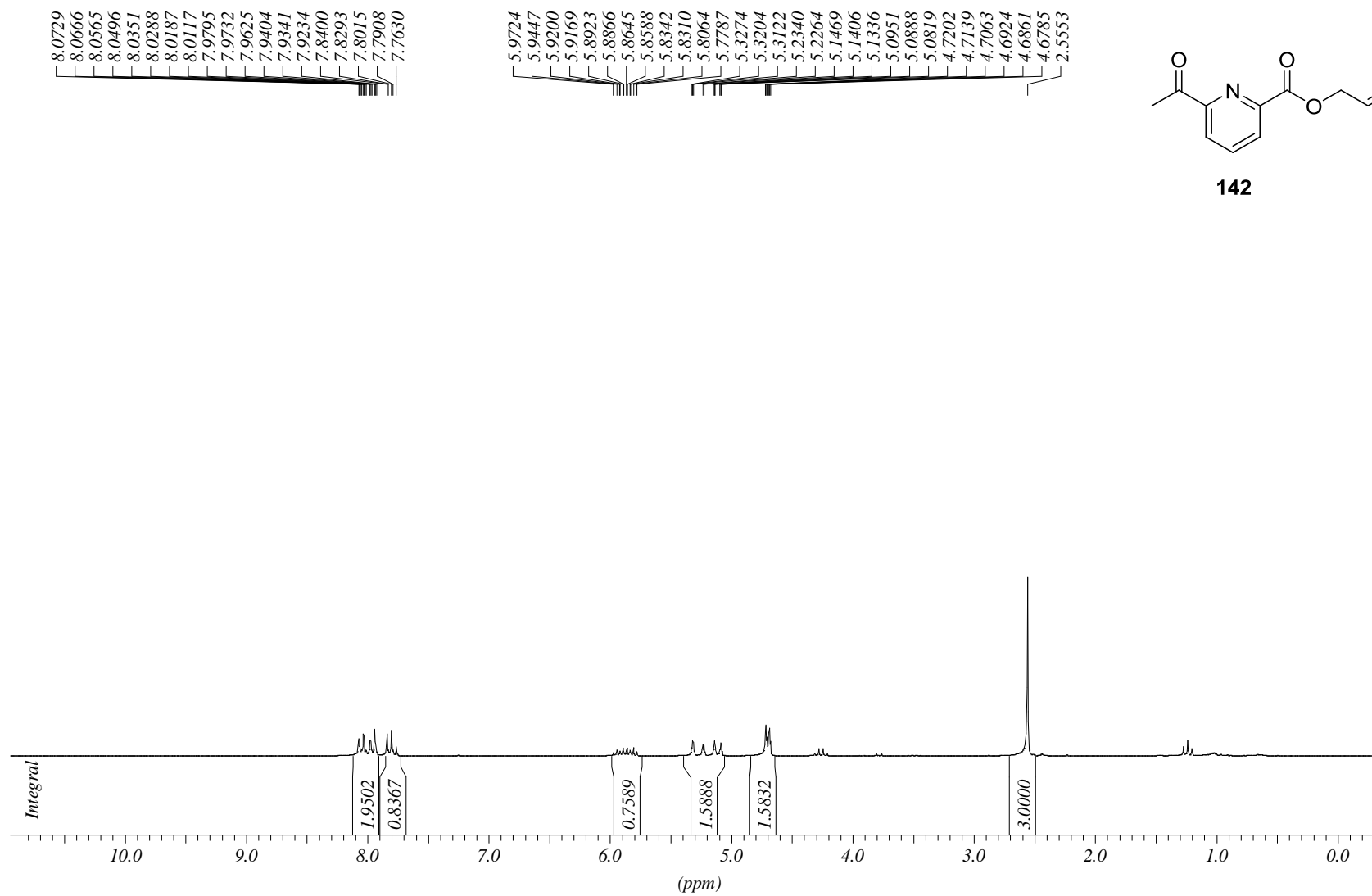


MassenspektrometrieZentrum FakultätChemieUniWien

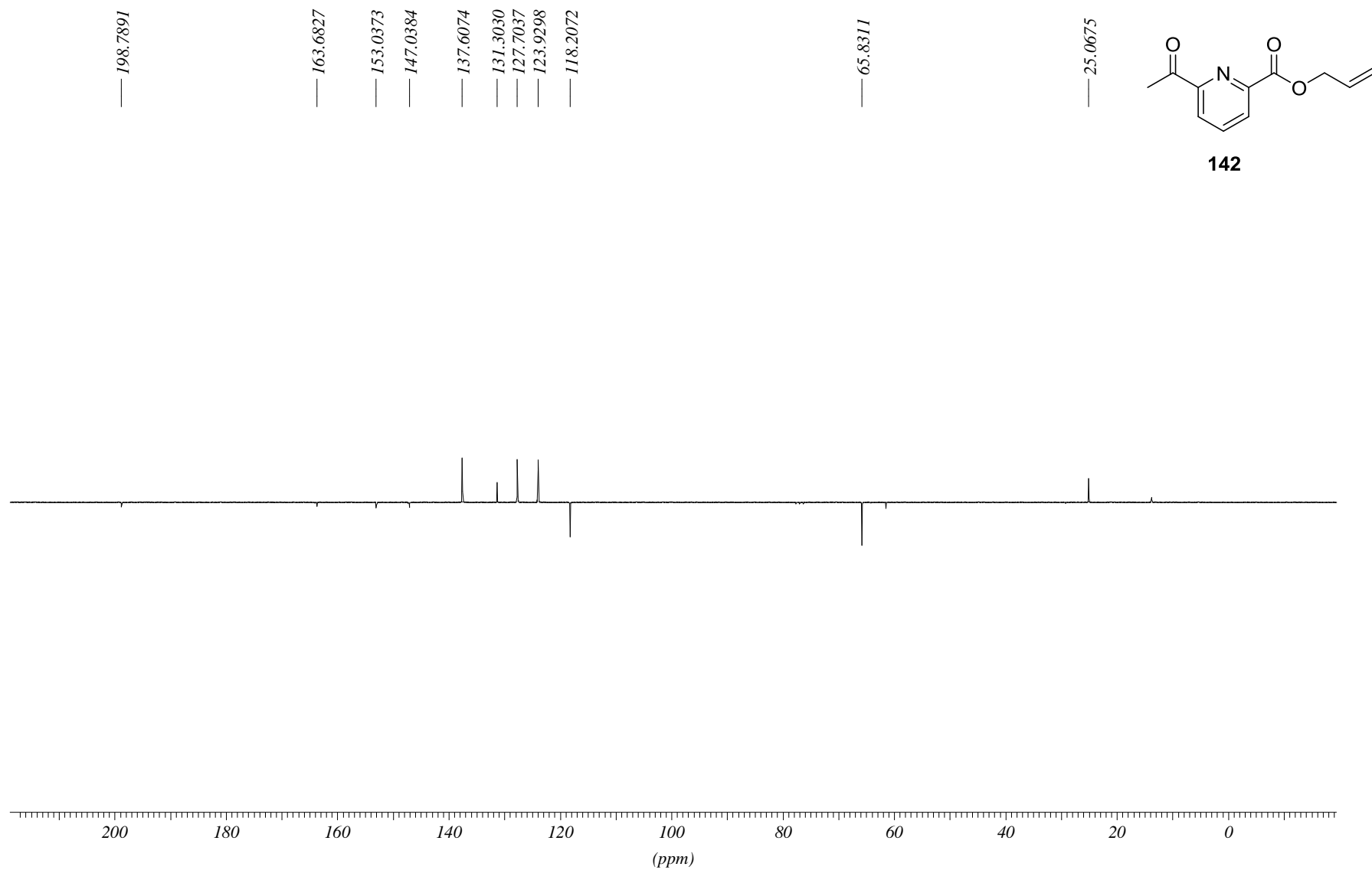
Analysis Info
Analysis Name D:\Data\MS_MessService\40291000002.d
Method tune_low_MS_Service_01_14.m
Sample Name q1014
Auftragneber/Com Neudorfer/Pharm
ACN/MeOH 0.1% H_2O

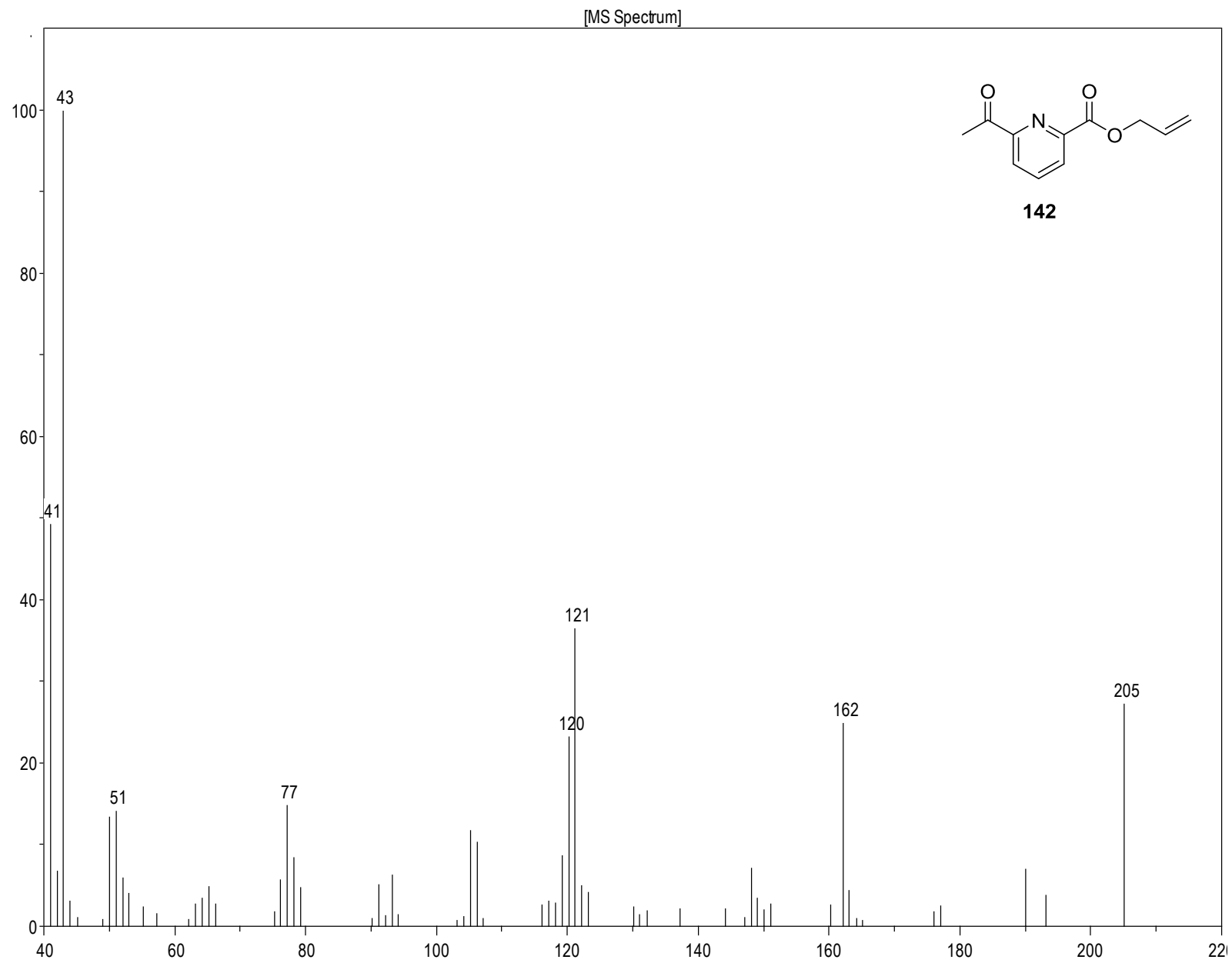
Acquisition Date 1/28/2014 7:54:41 AM
Operator phu
Instrument maxis



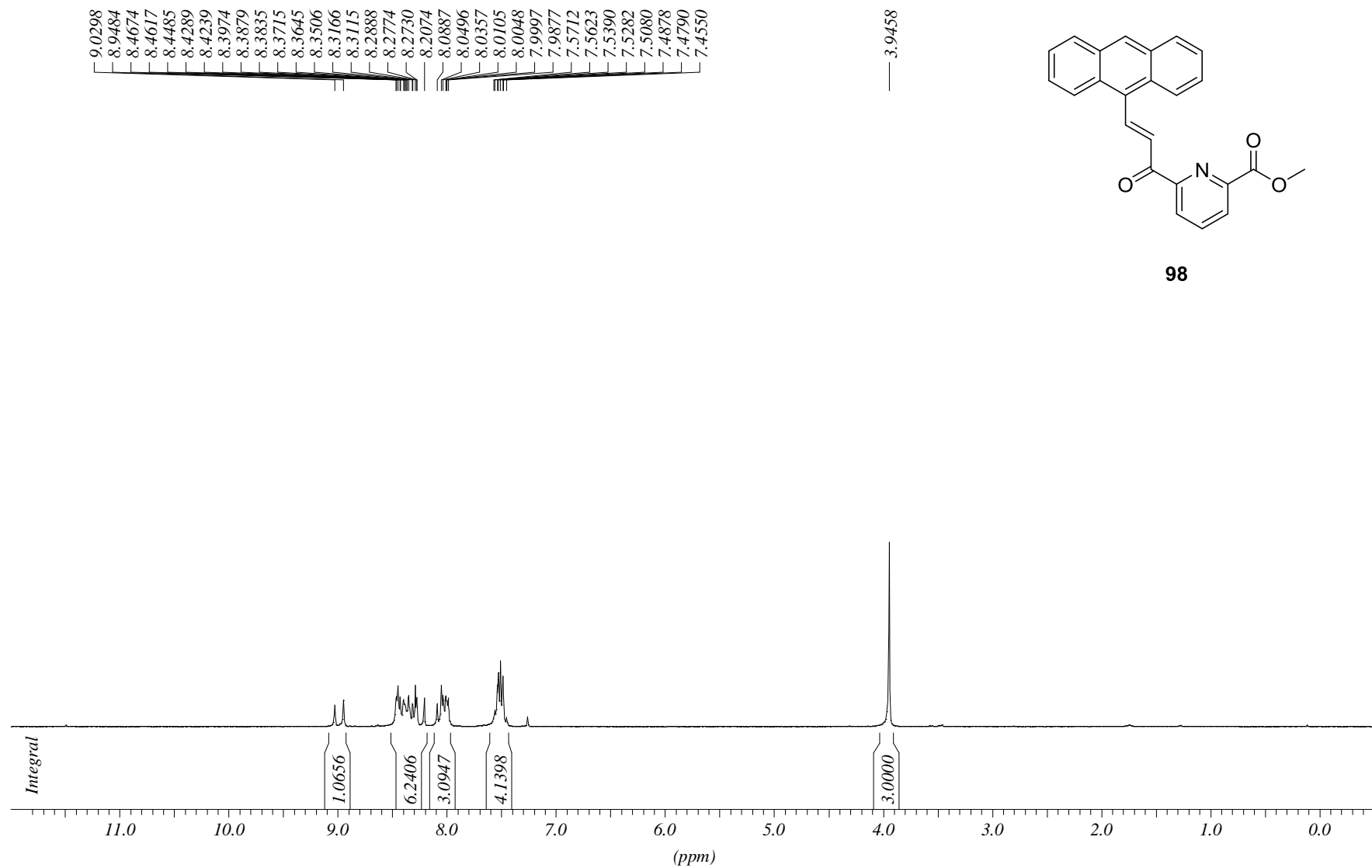
PROTON CDCl₃ opt/xwinmr neudorfer 16

C13APT CDCl3 opt/xwinmr neudorfer 16

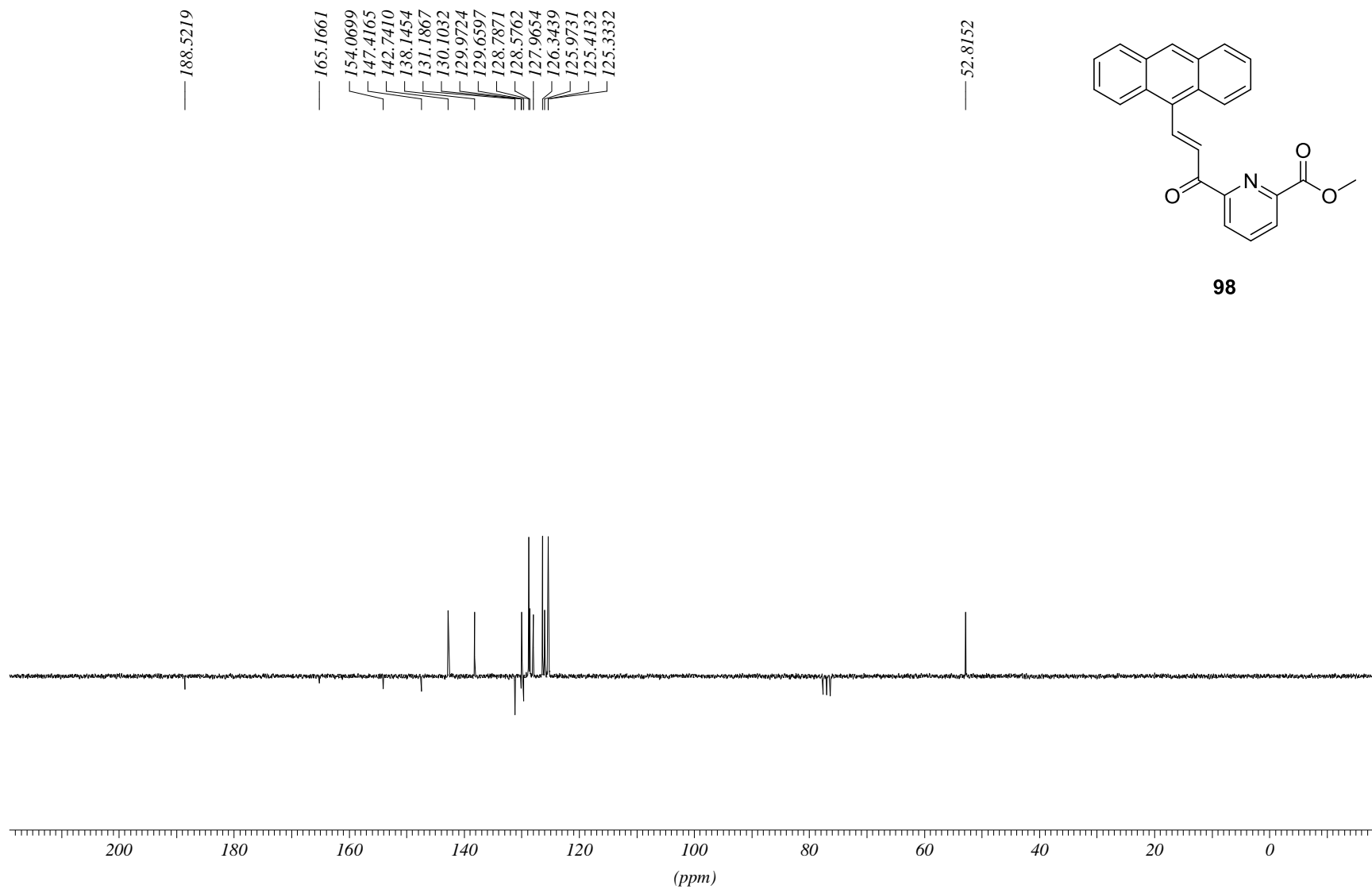




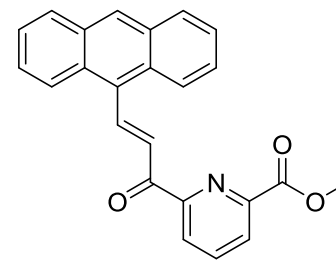
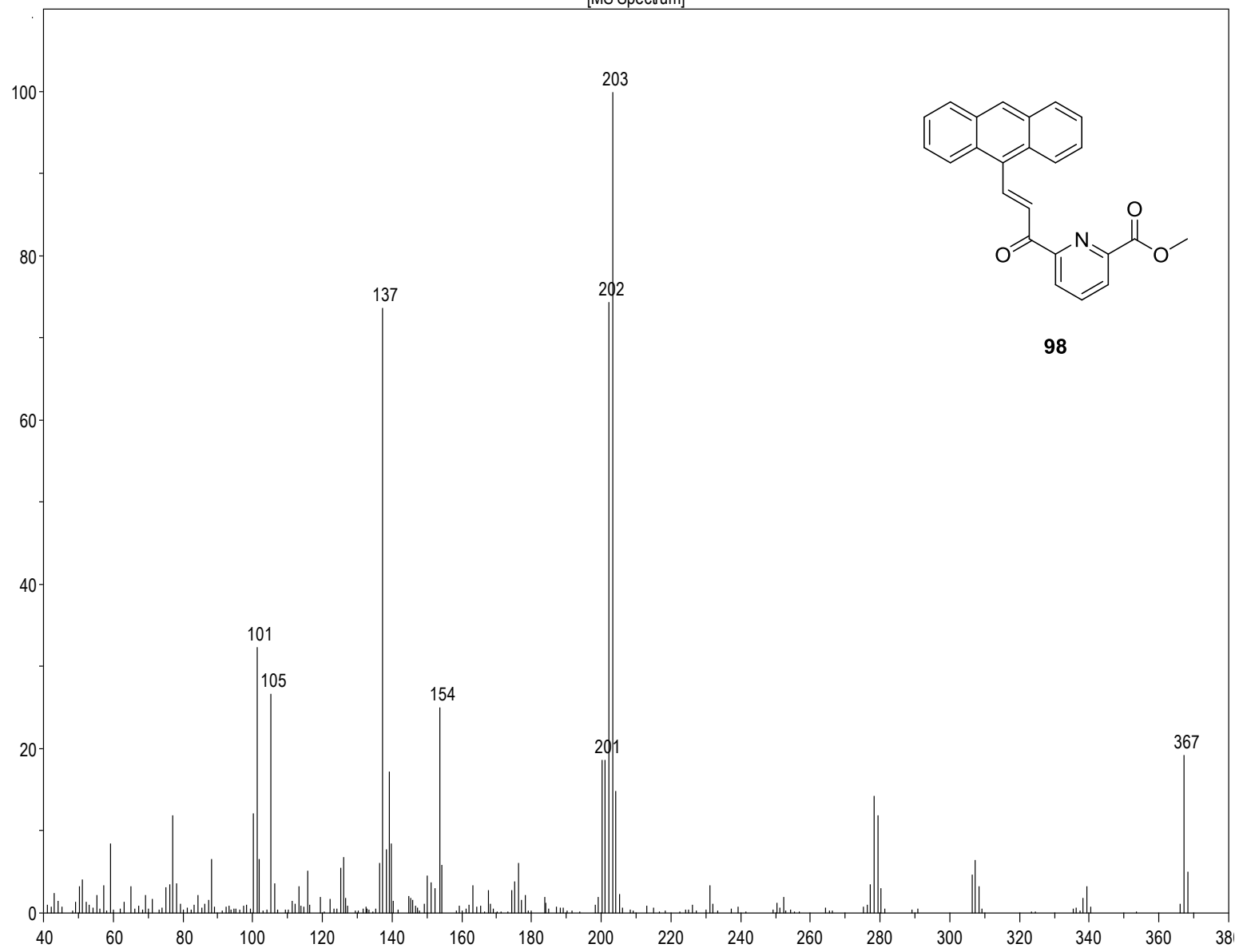
PROTON CDCl₃ opt/xwinmr neudorfer 15



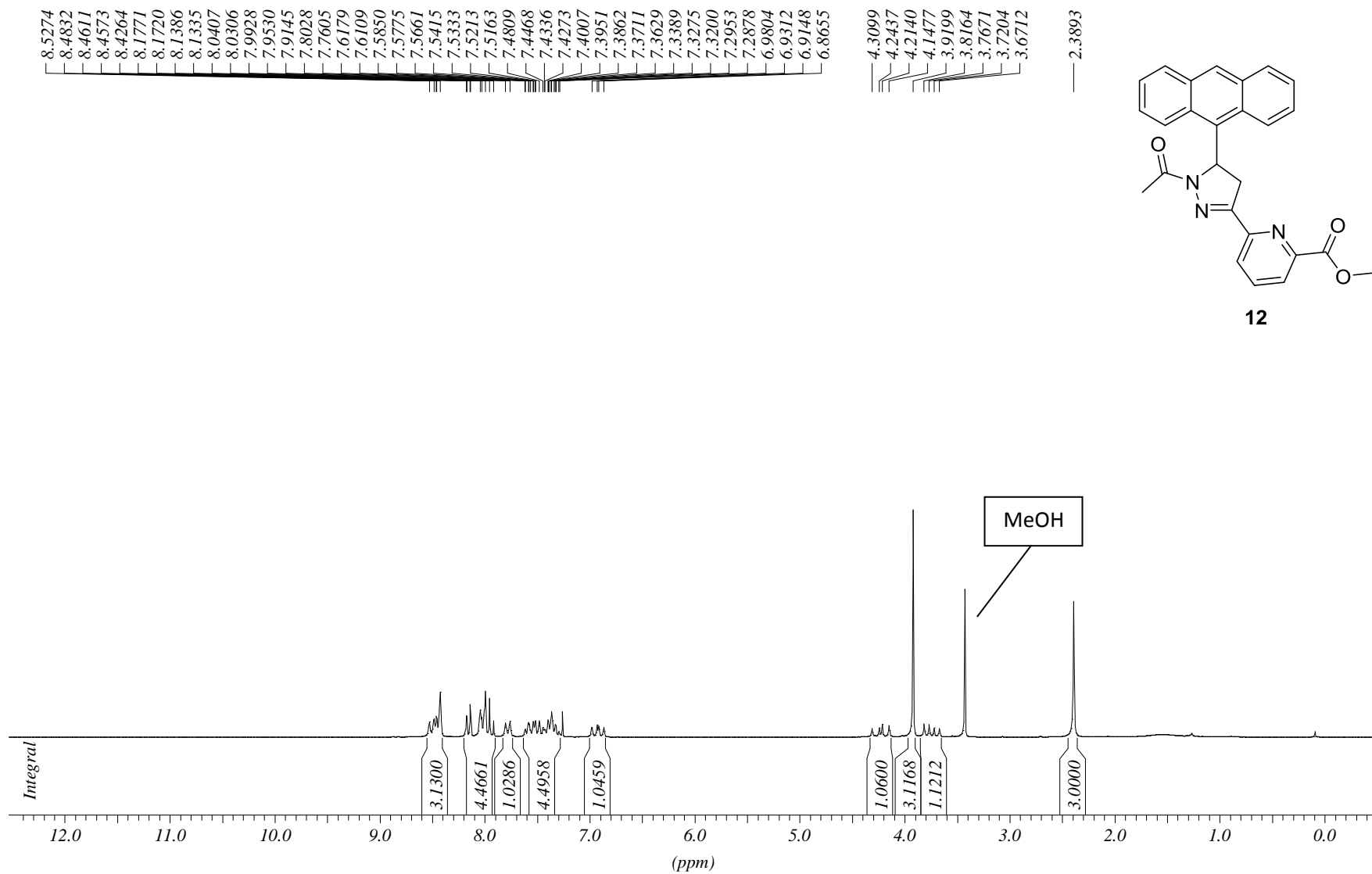
C13APT CDCl3 opt/xwinmr neudorfer 15



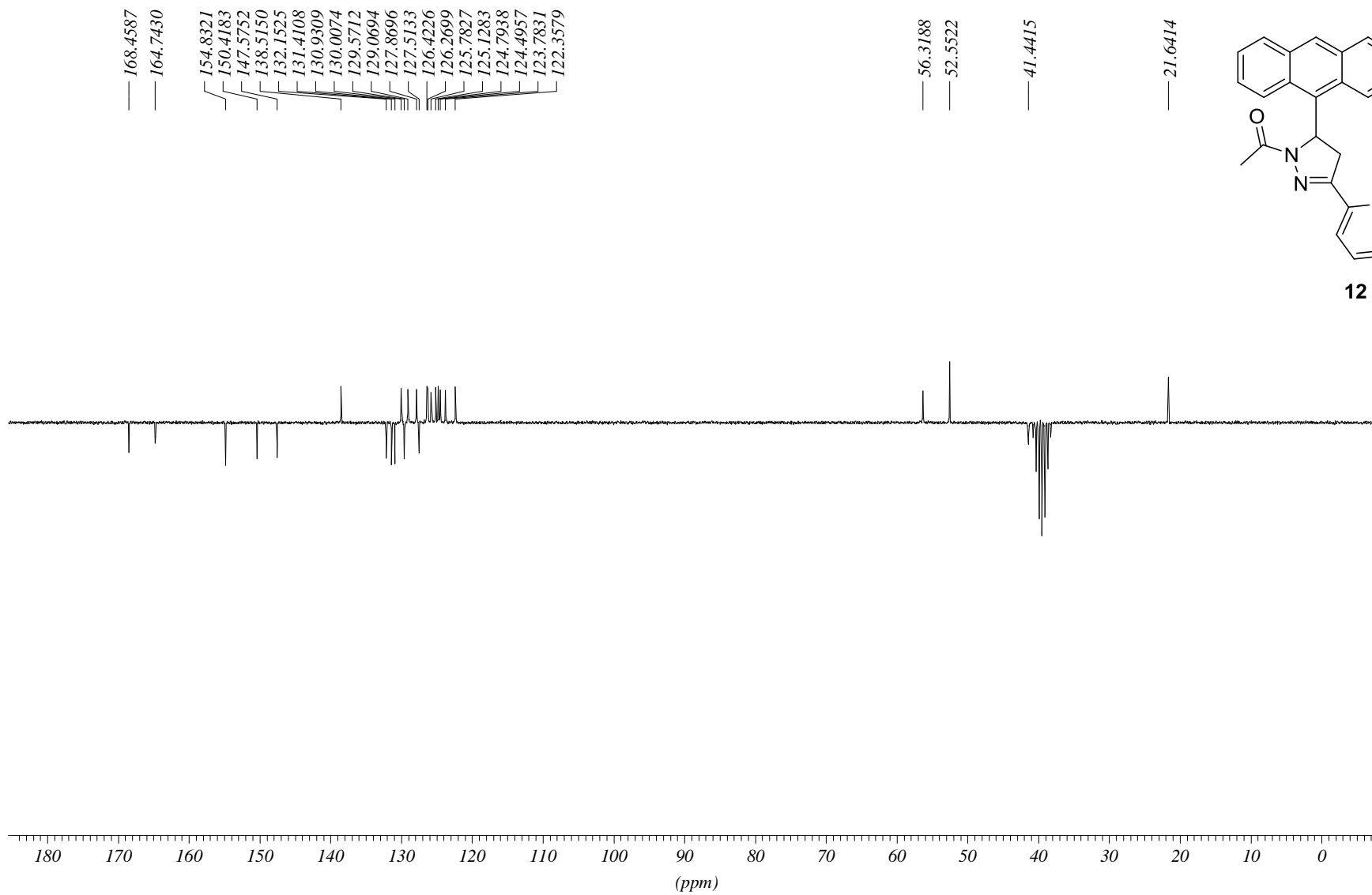
[MS Spectrum]



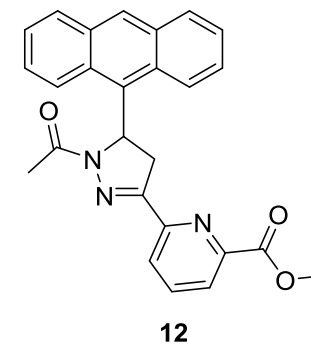
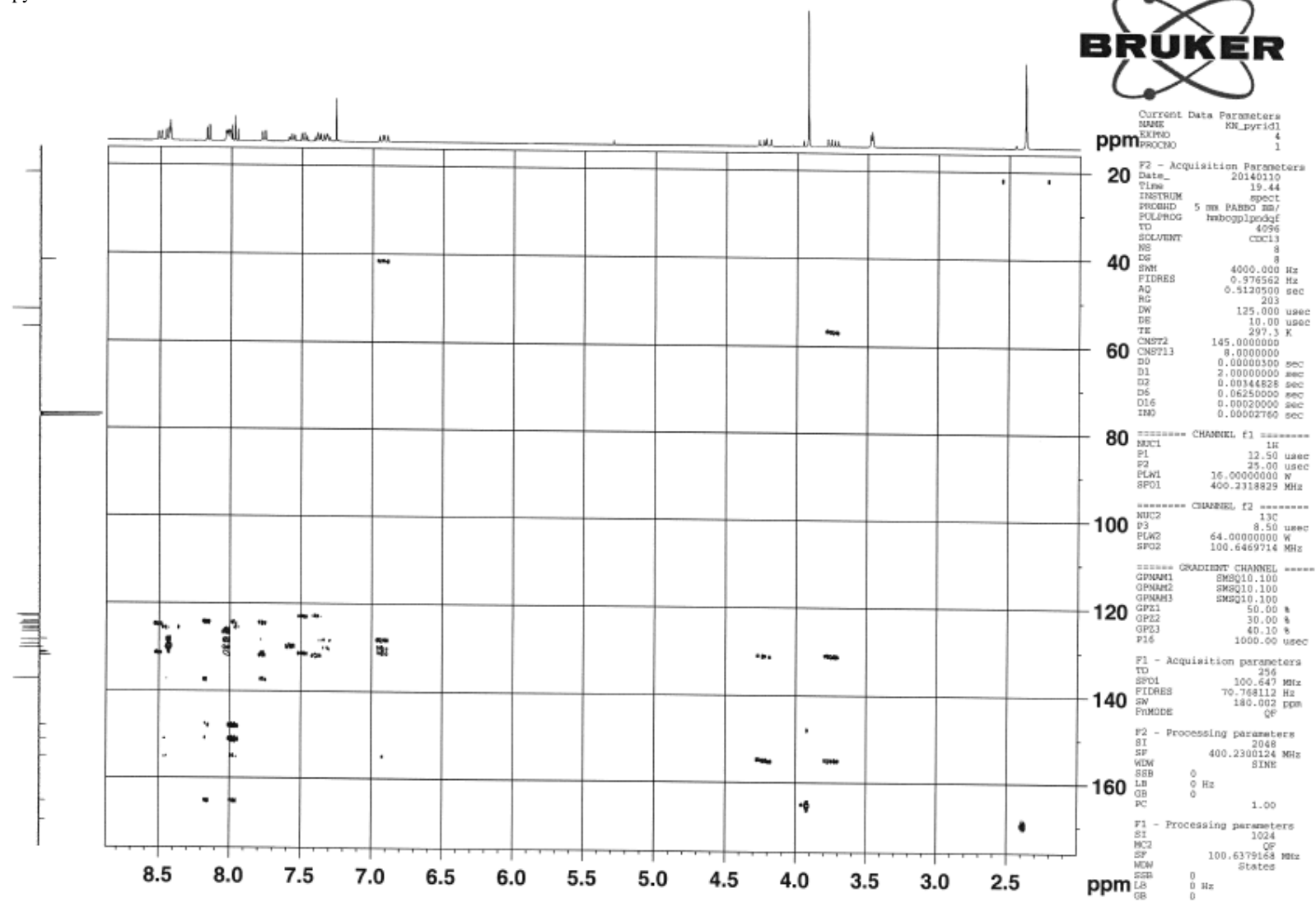
98

PROTON CDCl₃ opt/xwimmr neudorfer 19

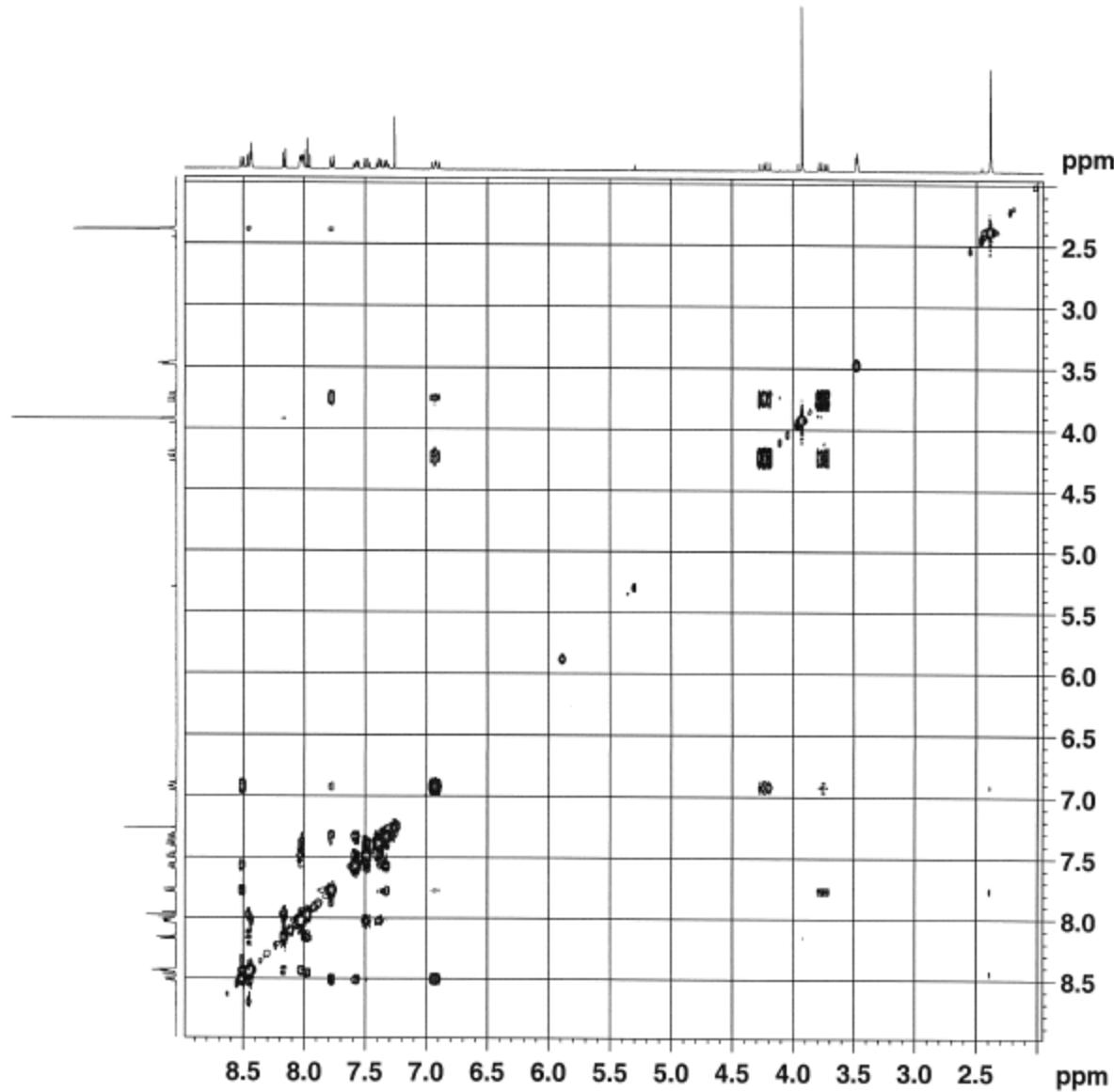
C13APT DMSO opt/xwinnmr neudorfer 30



pyrid1/CDCI3/HMBC



pyrid1/CDC13/NOESY



Current Data Parameters
NAME KM_pyrid1
EXPNO 5
PROCNO 1

F2 - Acquisition Parameters
Date_ 20140110
Time 21.14
INSTRUM spect
PROBHD 5 mm PABBO BB/
PULPROG noesygpph
TD 2048
SOLVENT CDCl3
NS 8
DS 8
SMH 4000.000 Hz
FIDRES 1.953125 Hz
AQ 0.2560500 sec
RG 128
DW 125.000 usec
DE 10.00 usec
TE 297.3 K
D0 0.00010901 sec
D1 2.00000000 sec
D8 0.80000001 sec
D16 0.00020000 sec
IN0 0.00024985 sec

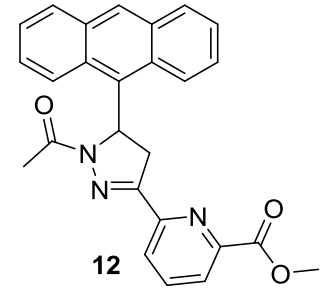
----- CHANNEL f1 -----
NUC1 1H
P1 12.50 usec
P2 25.00 usec
PLW1 16.00000000 W
SF01 400.231829 MHz

----- GRADIENT CHANNEL -----
GPNAM1 SMSQ10.100
GPZ1 40.00 %
P16 1000.00 usec

F1 - Acquisition parameters
TD 256
SF01 400.2319 MHz
FIDRES 15.634058 Hz
SW 10.000 ppm
FhMODE States-TPPI

F2 - Processing parameters
SI 2048
SF 400.2300124 MHz
WDW QSINE
SSB 2
LB 0 Hz
GB 0
PC 1.00

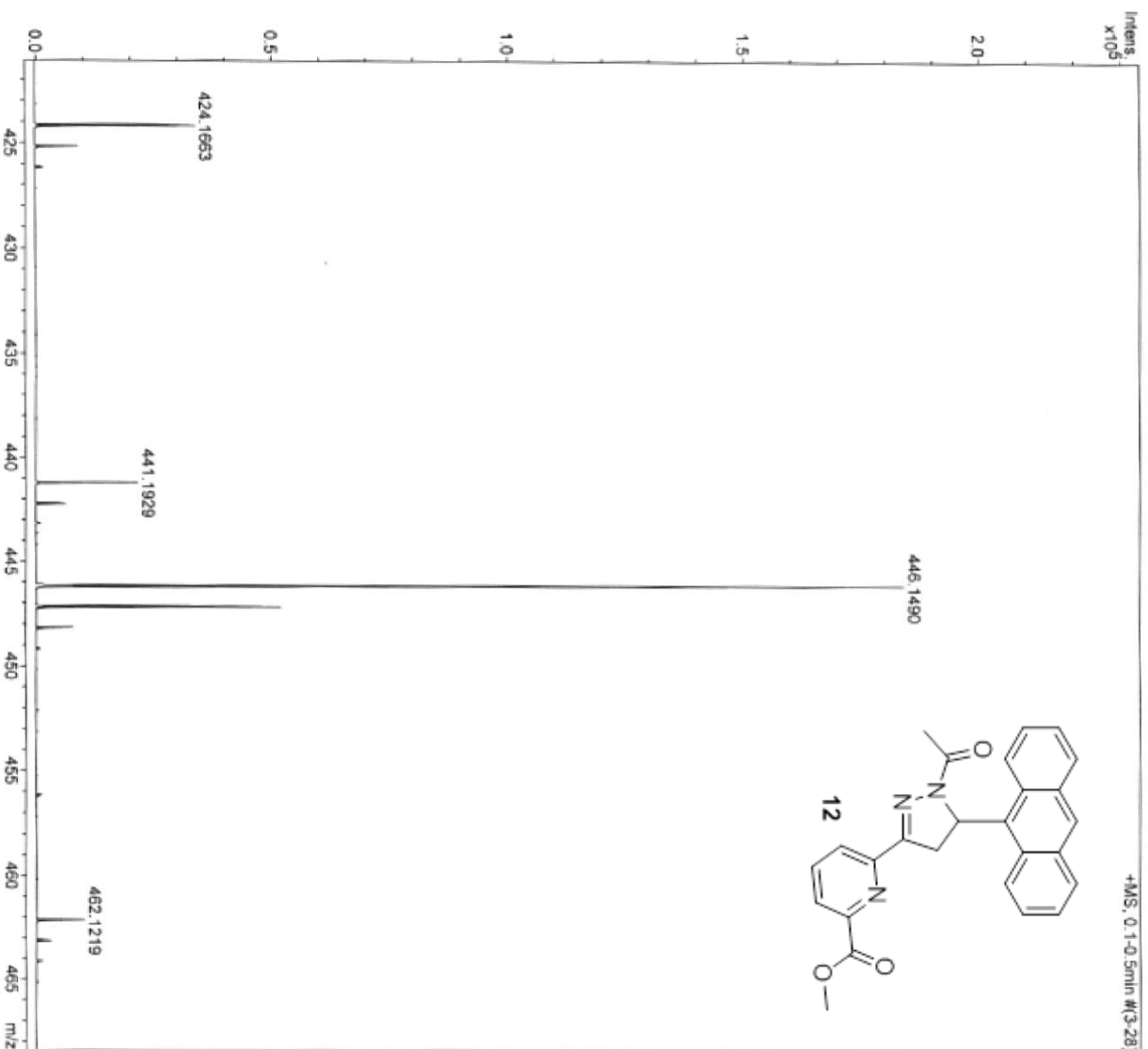
F1 - Processing parameters
SI 2048
MC2 States-TPPI
SF 400.2300124 MHz
WDW States-TPPI
SSB 2
LB 0 Hz
GB 0

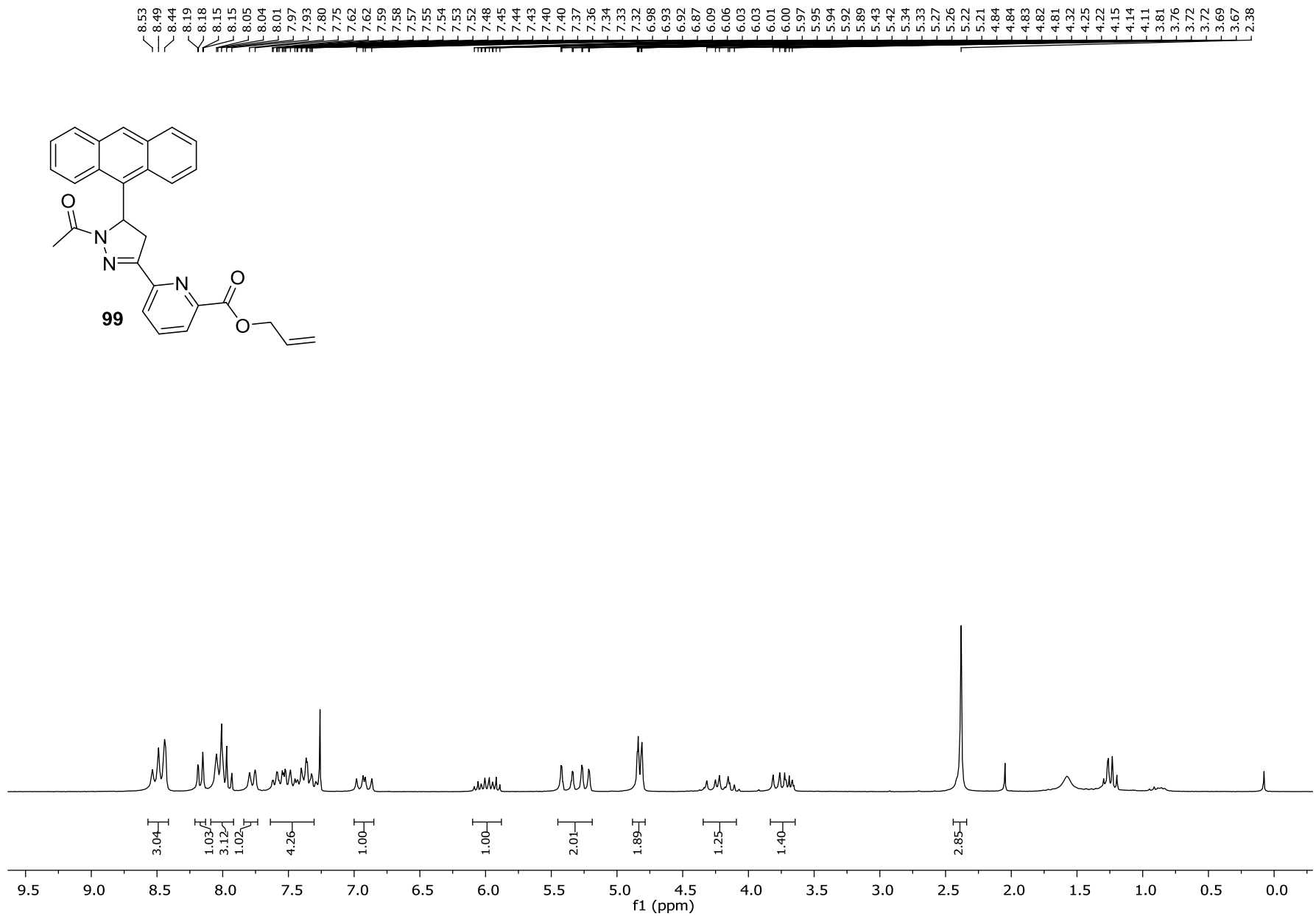
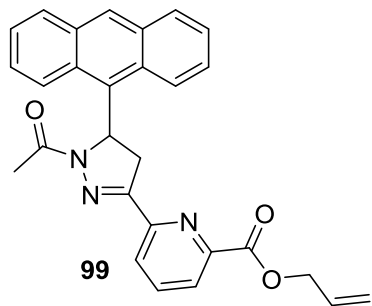


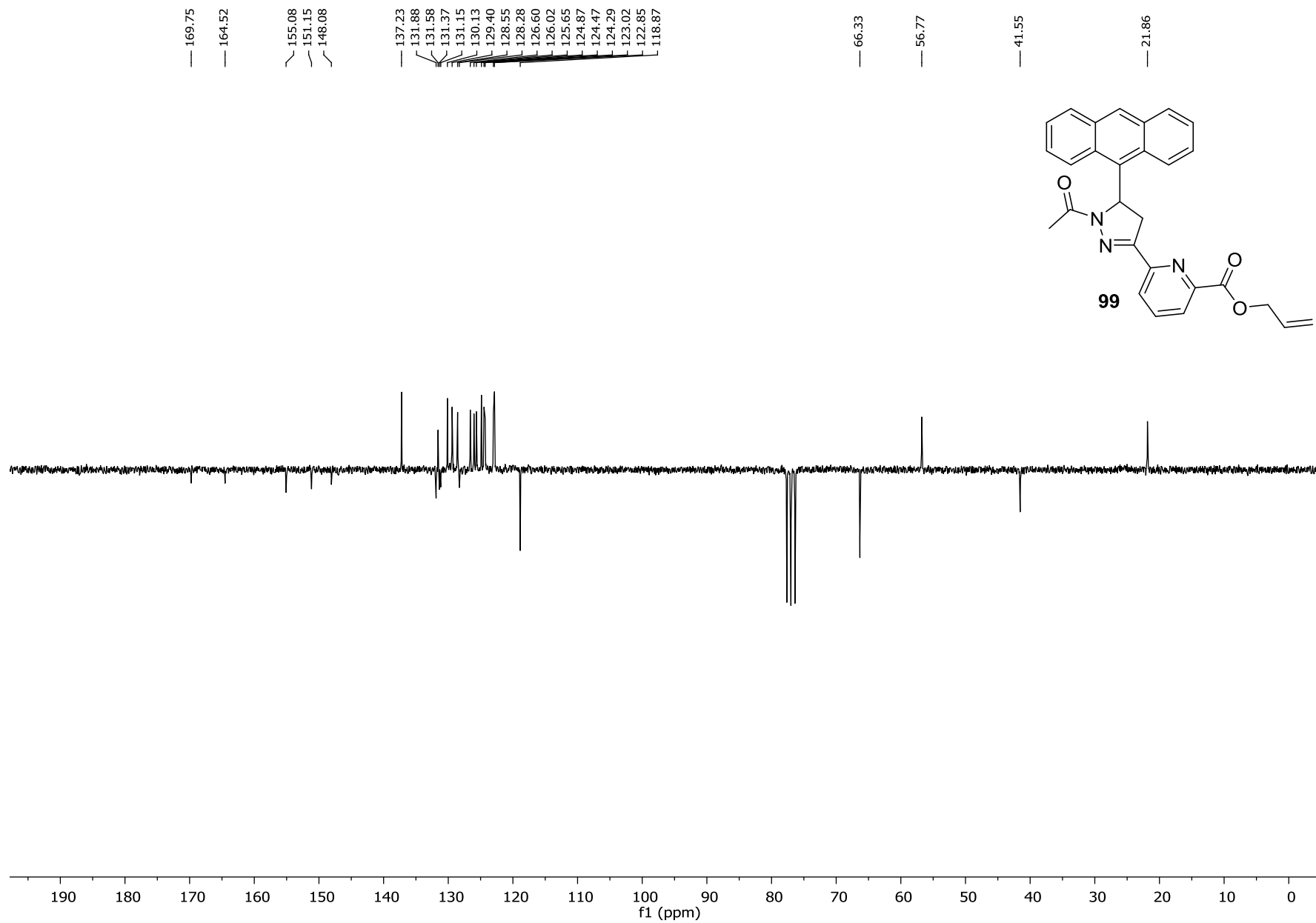
MassenspektrometrieZentrum FakultätChemieUniWien

Analysis Info
Analysis Name D:\Data\MS_MessService\39606000001.d
Method tune_low_MS_Service_06_13.m
Sample Name cypcy5
Auftraggeber/Com Neudorfer/Spreitzer
Ergebnis: +/- 5ppm
ACN/MeOH 1%/H2O

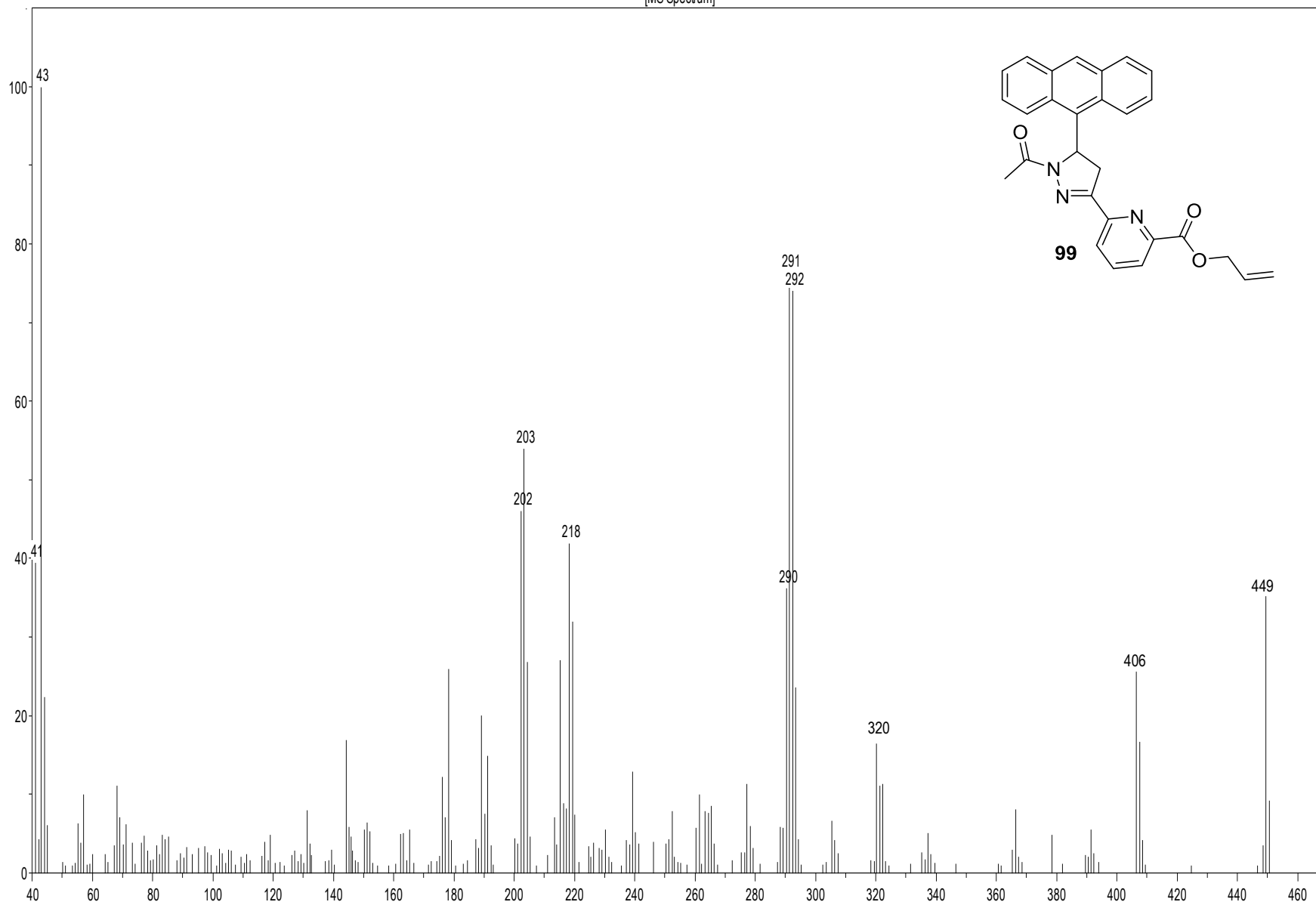
Acquisition Date 6/7/2013 9:02:27 AM
Operator phu
Instrument maxis







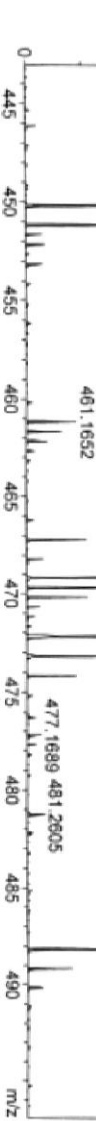
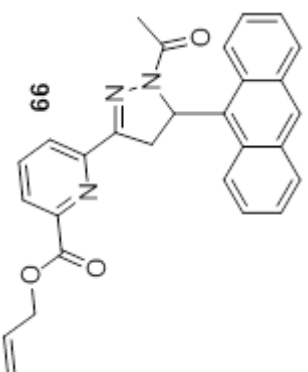
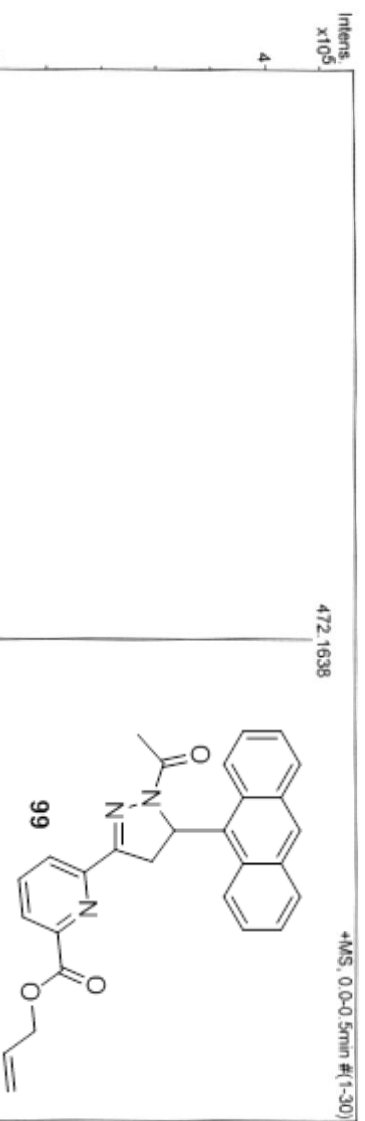
[MS Spectrum]

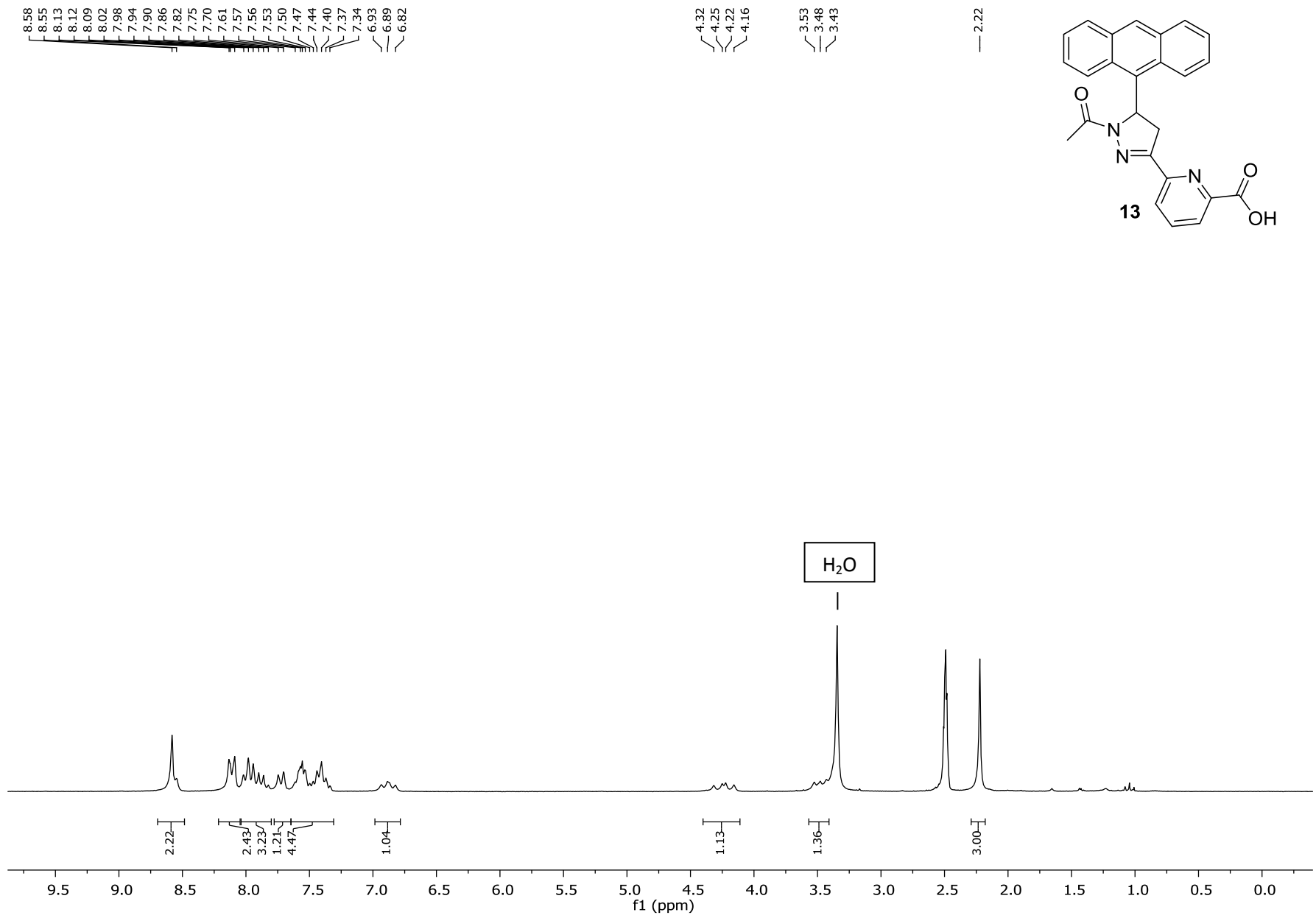


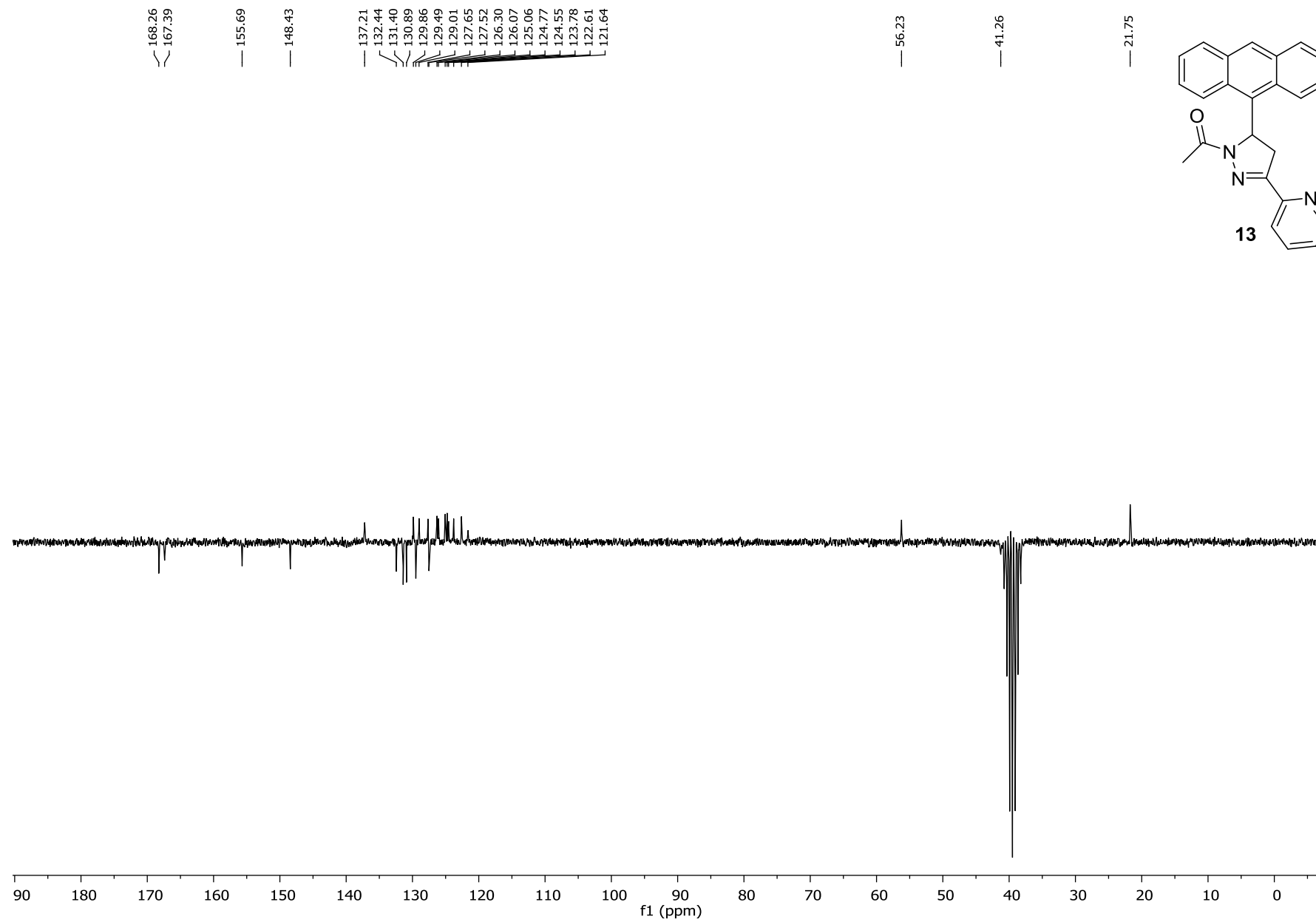
MassenspektrometrieZentrum FakultätChemieUniWien

Analysis Info
 Analysis Name D:\Data\MS_MessService\398894000001.d
 Method Nanomate Intuition MS-Service.im
 Sample Name ~~paesigle~~
 Auftraggeber/Com Neudorfer/Spreitzer/Pharm
 Ergebnis: +/- 5ppm
 ACN/MeOH 1%/H2O Sample: pyraliz

Acquisition Date 9/9/2013 2:07:30 PM
 Operator phu
 Instrument maxis



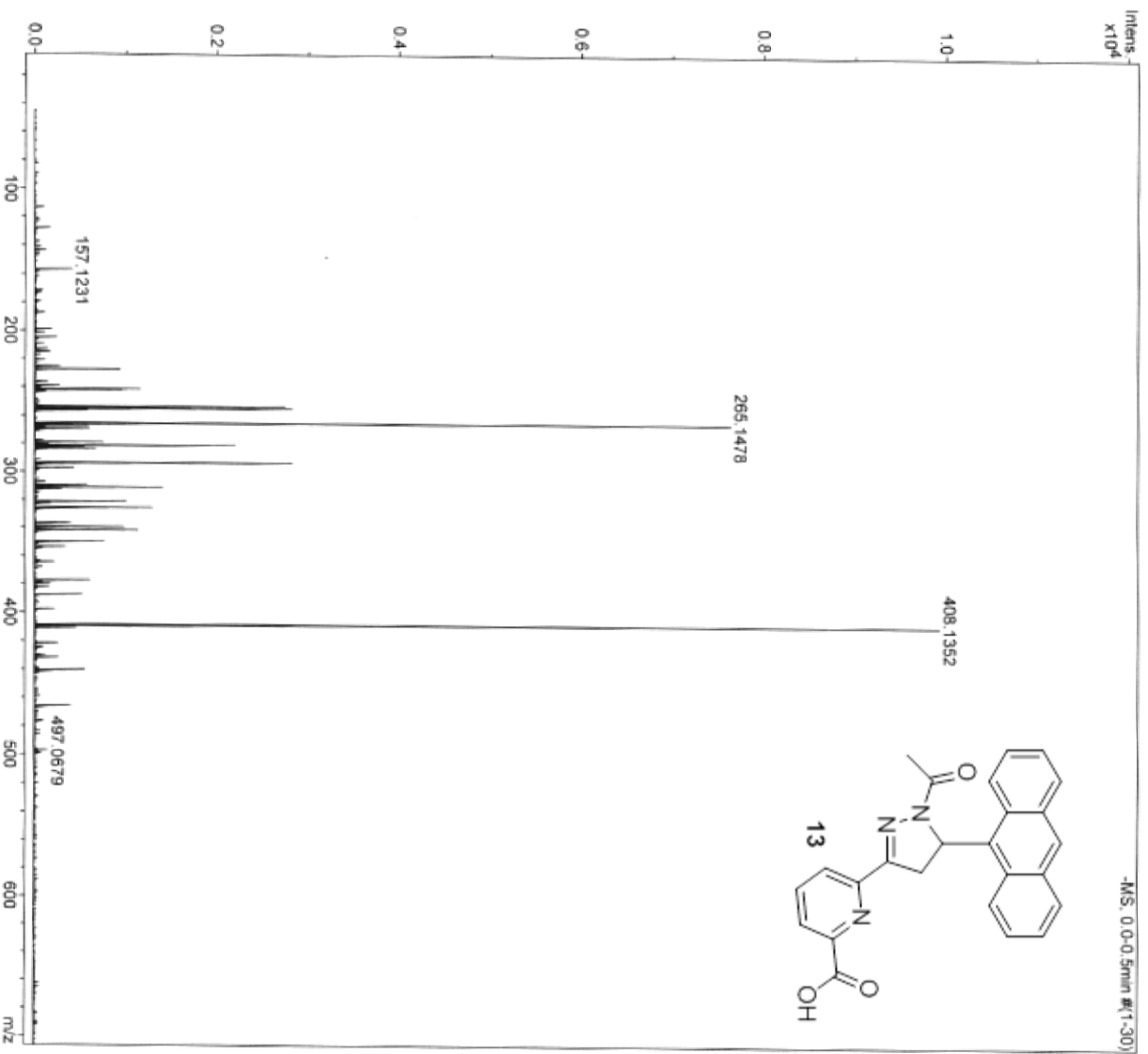


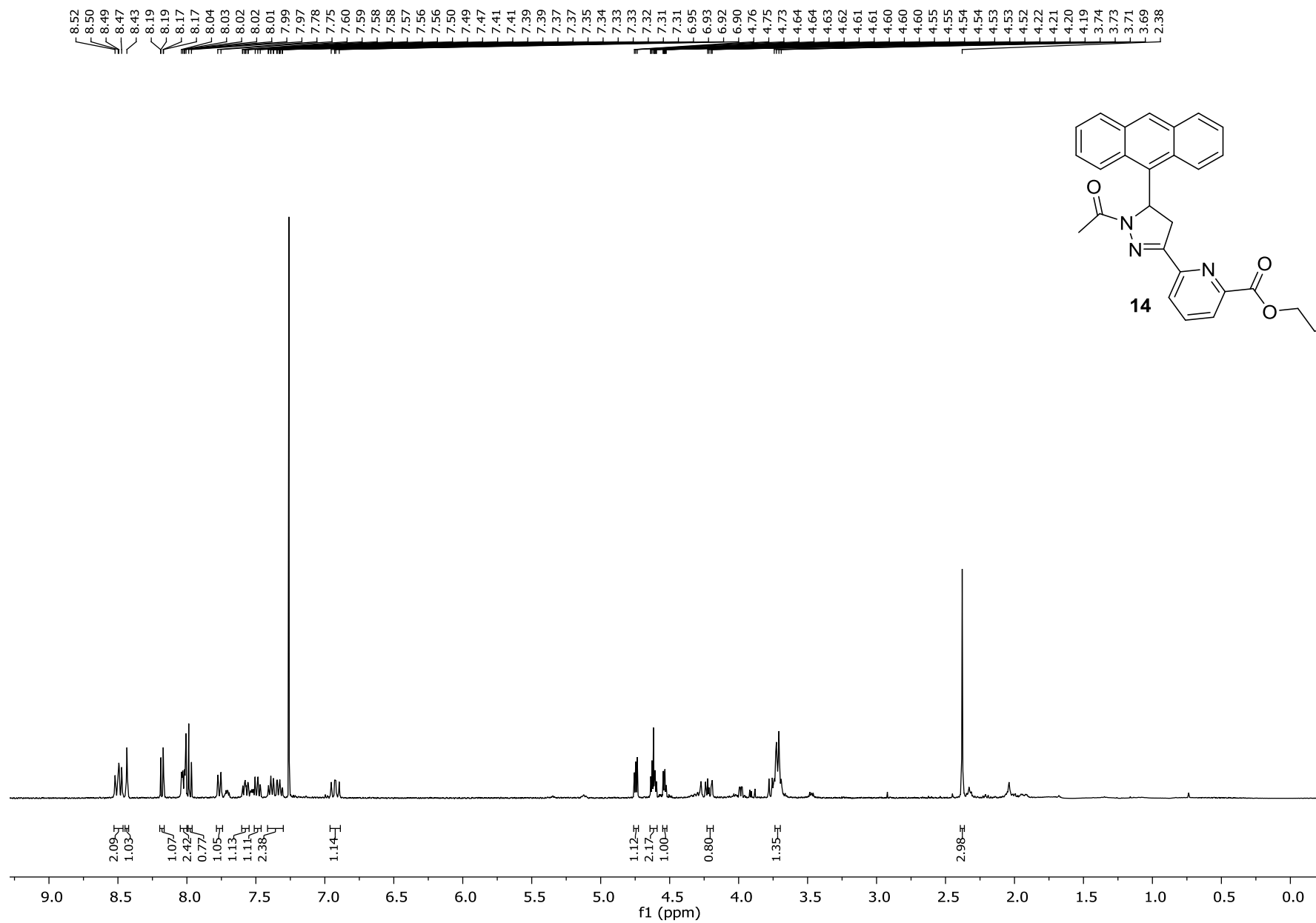


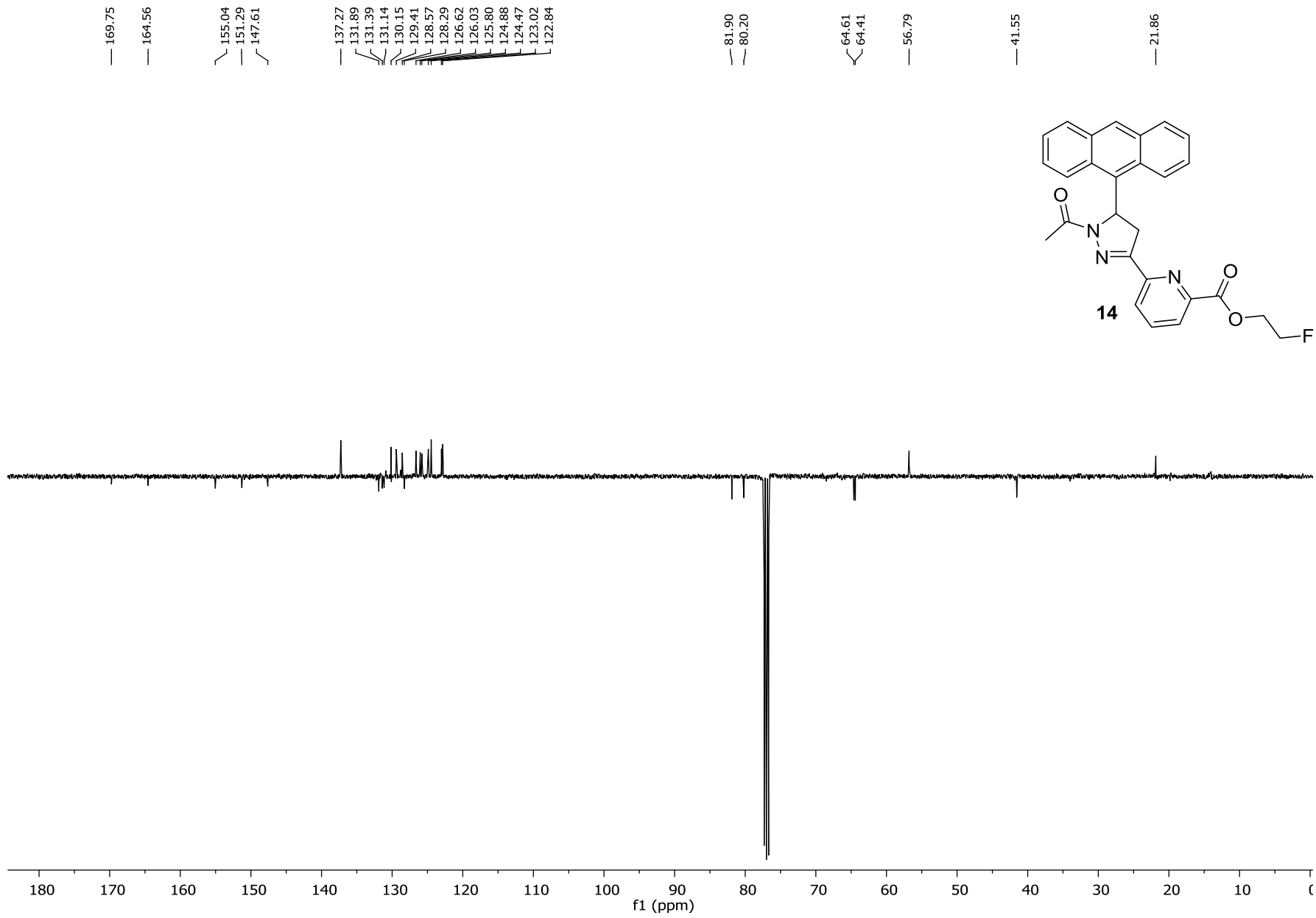
MassenspektrometrieZentrum FakultätChemieUniWien

Analysis Info
Analysis Name D:\Data\MS_MessService\39930000001.d
Method Tune_Low_Neg_27_02_12.m
Sample Name pystore2
Auftraggeber/Com Neudorfer/Spreitzer/Pharm
Ergebnis: +/- 5ppm
ACN/MeOH 1%/H2O

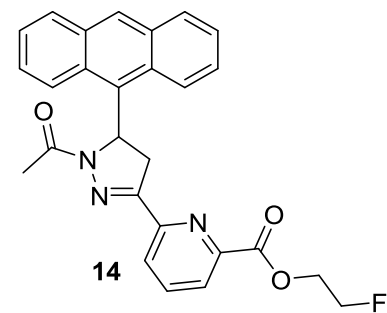
Acquisition Date 10/7/2013 11:45:40 AM
Operator phu
Instrument maxis



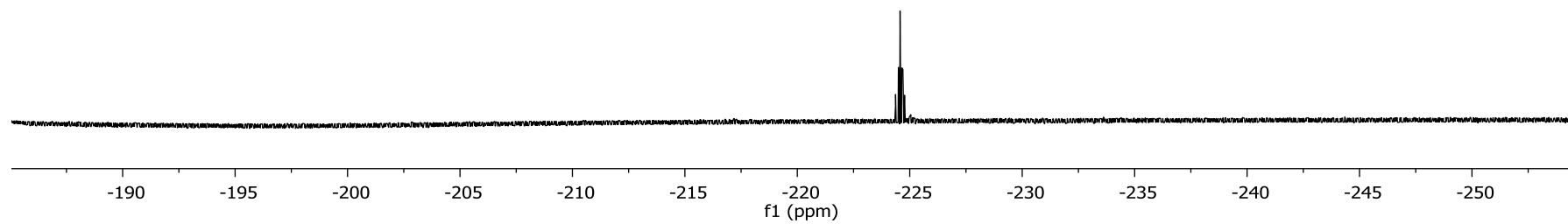




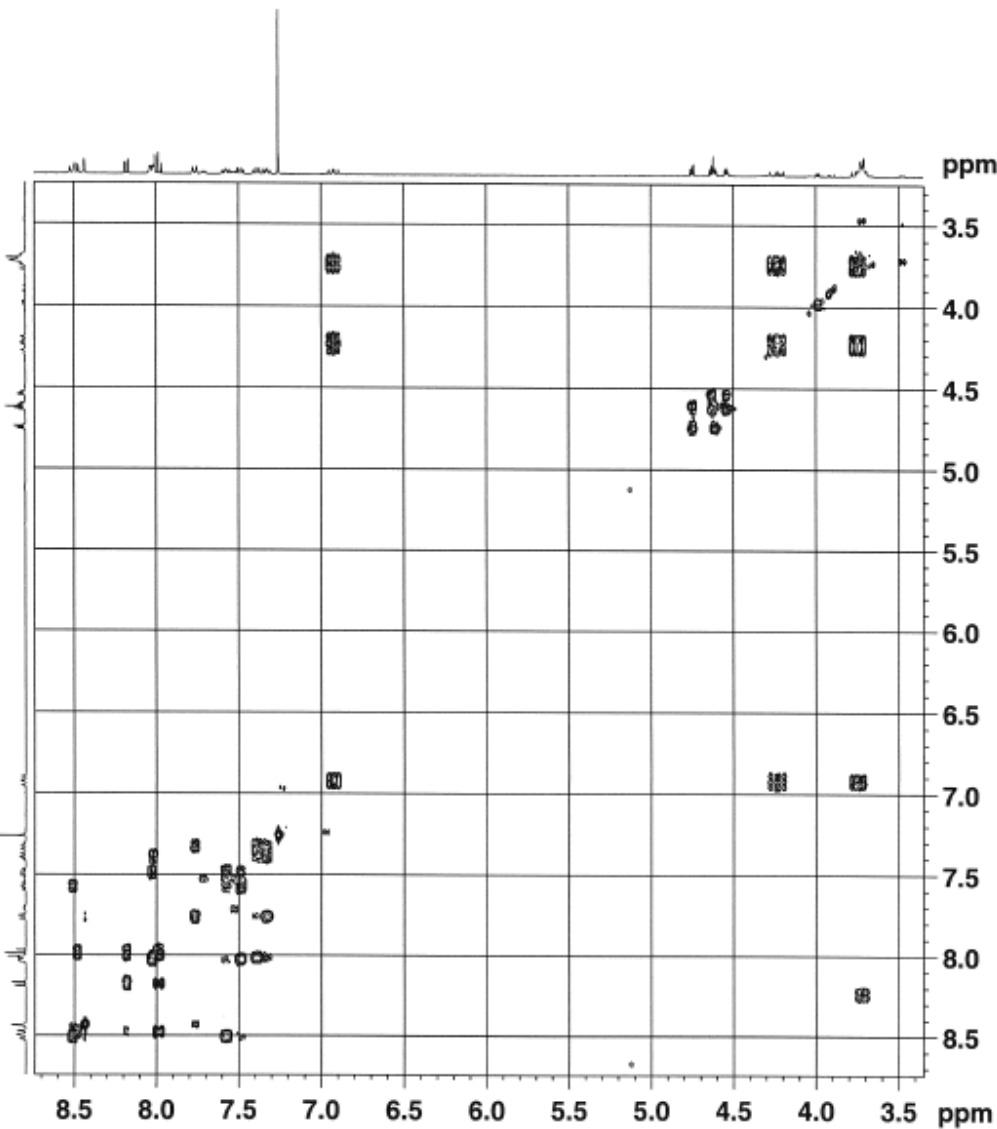
-224.37
-224.44
-224.49
-224.57
-224.64
-224.70
-224.77



14



pyrf12/CDC13/COSY



Current Data Parameters
NAME KN_pyrf112
EXFNO 7
PROCNO 1

F2 - Acquisition Parameters
Date_ 20131201
Time 6:57
INSTRUM spect
PROBHD 5 mm PABBO BB/
PULPROG cosypppqf
TD 2048
SOLVENT CDCl3
NS 4
DS 8
SWH 2802.691 Hz
FIDRES 1.368501 Hz
AQ 0.3654132 sec
RG 287
DW 178.400 usec
DE 10.00 usec
TE 297.3 K
D0 0.00000300 sec
D1 2.00000000 sec
D11 0.03000000 sec
D12 0.00002000 sec
D13 0.00000400 sec
D16 0.00020000 sec
IN0 0.00035695 sec

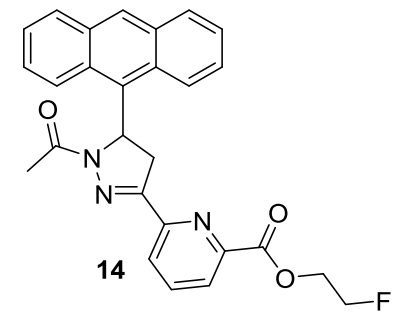
===== CHANNEL f1 =====
NUC1 1H
P0 12.50 usec
P1 12.50 usec
P17 2500.00 usec
PLM1 16.00000000 W
PLM10 2.60150003 W
SPO1 400.2324014 MHz

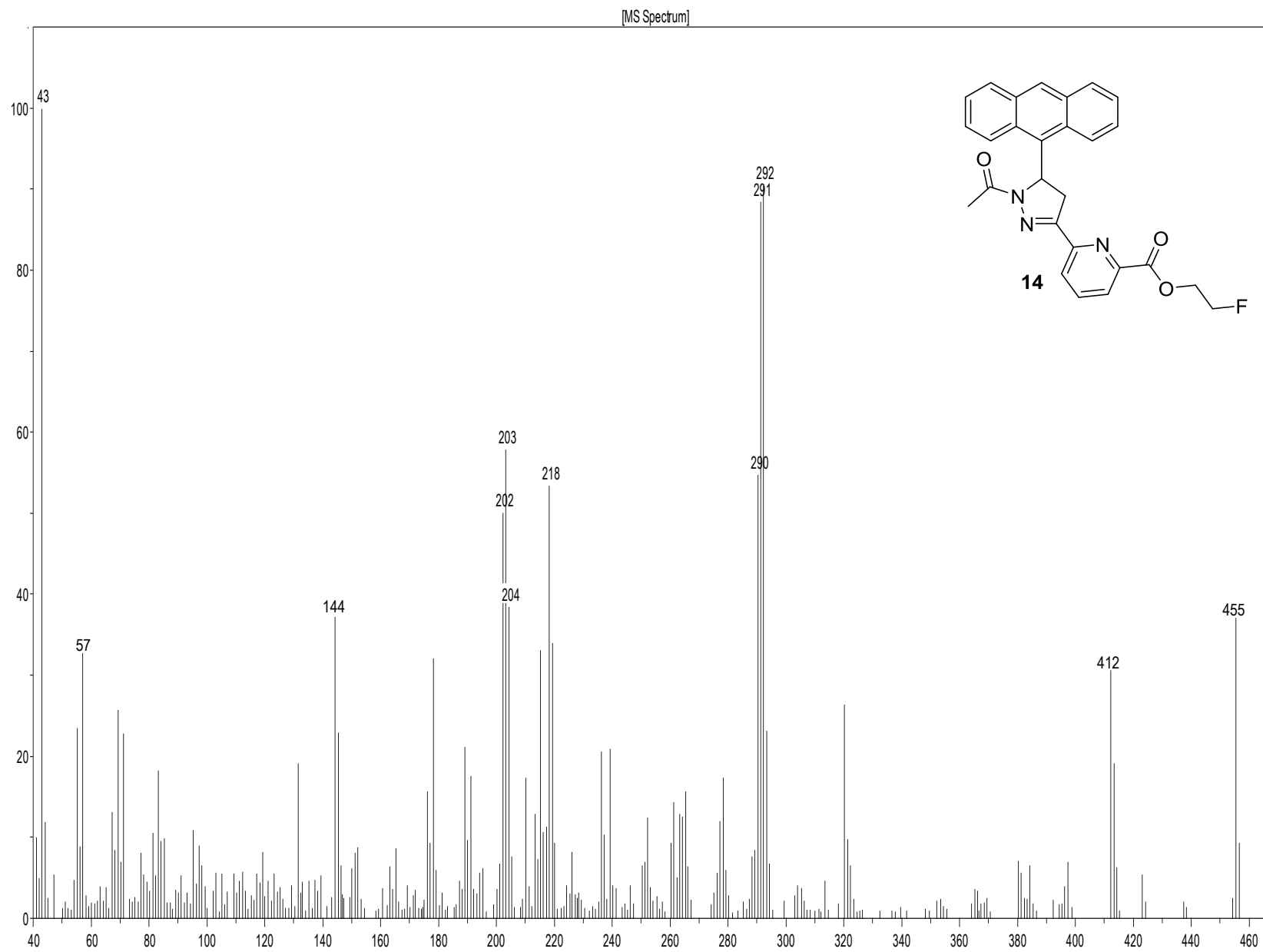
===== GRADIENT CHANNEL =====
GPNAM1 SMSQ10.100
GP21 20.00 %
P16 1000.00 usec

F1 - Acquisition parameters
TD 256
SPO1 400.2324 MHz
FIDRES 10.943841 Hz
SW 7.000 ppa
FnMODE QF

F2 - Processing parameters
SI 1024
SF 400.2300123 MHz
MDW QSIINE
SBB 0
LB 0 Hz
GB 0
PC 1.00

F1 - Processing parameters
SI 1024
MC2 QF
SF 400.2300123 MHz
MDW States-TPPI
SBB 0
LB 0 Hz
GB 0





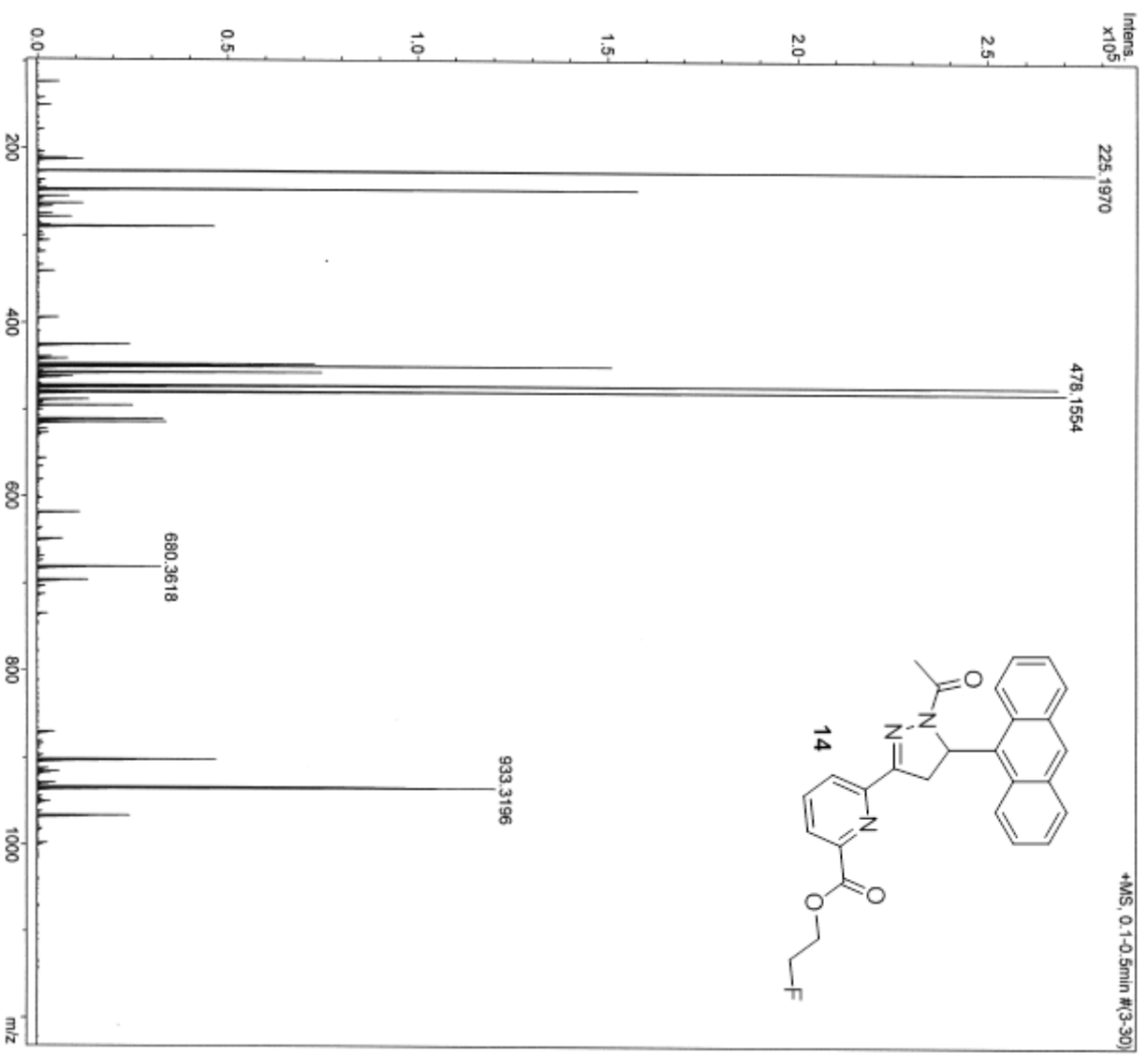
MassenspektrometrieZentrum FakultätChemieUniWien

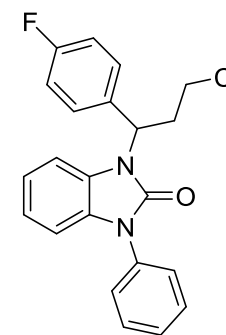
Analysis Info

Analysis Name D:\Data\MS_MessService\40089000004.d
Method tune_low_MS_Service_11_13.m
Sample Name pyrfl 11
Auftraggeber/Com Neudorfer/Farm
Ergebnis: +/- 5ppm
ACN/MeOH 0.1%/H2O

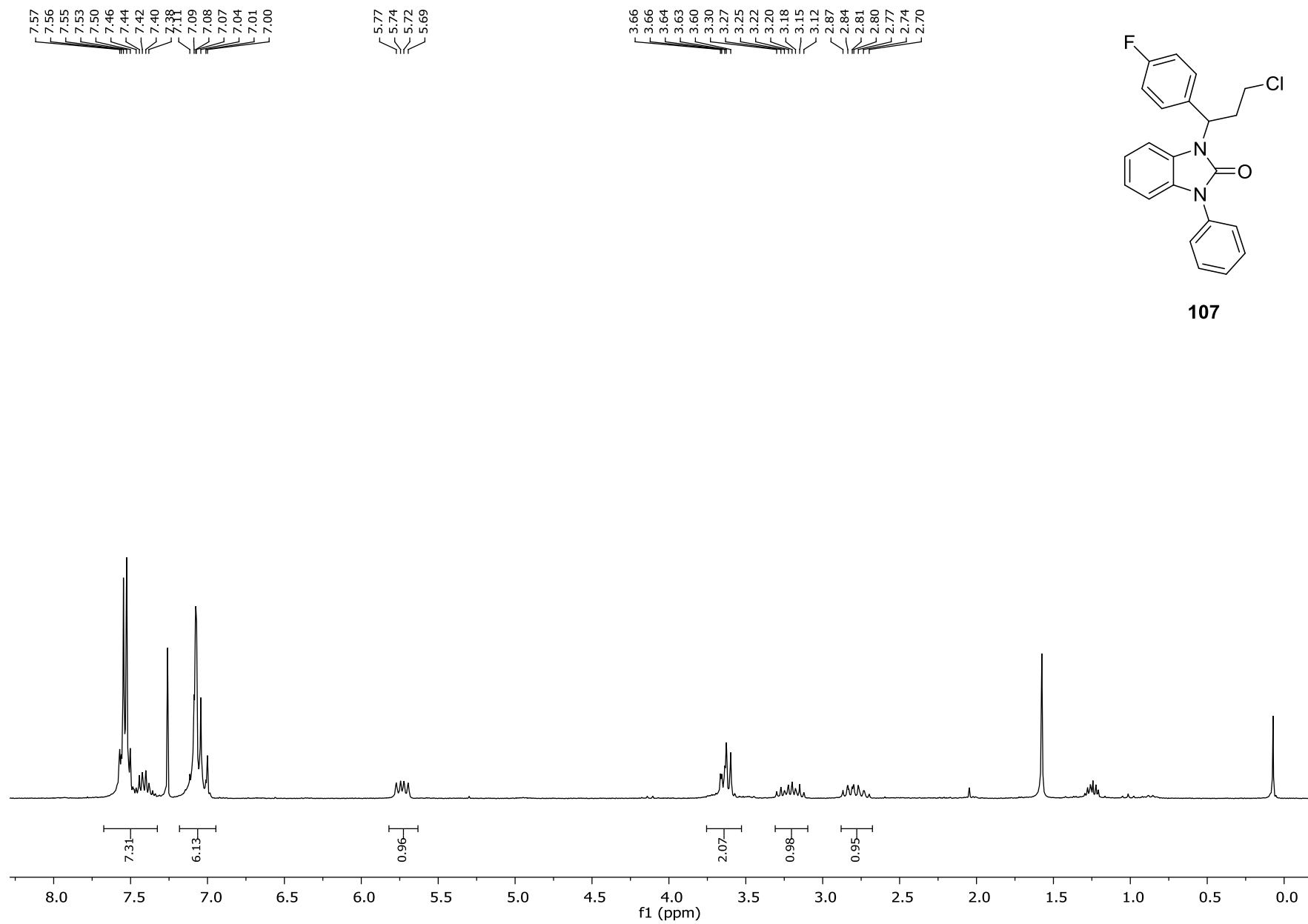
Acquisition Date 11/14/2013 2:13:11 PM

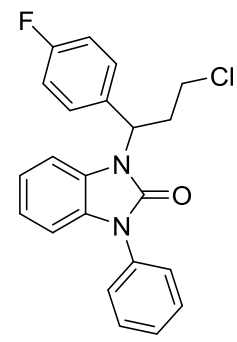
Operator phu
Instrument maxis



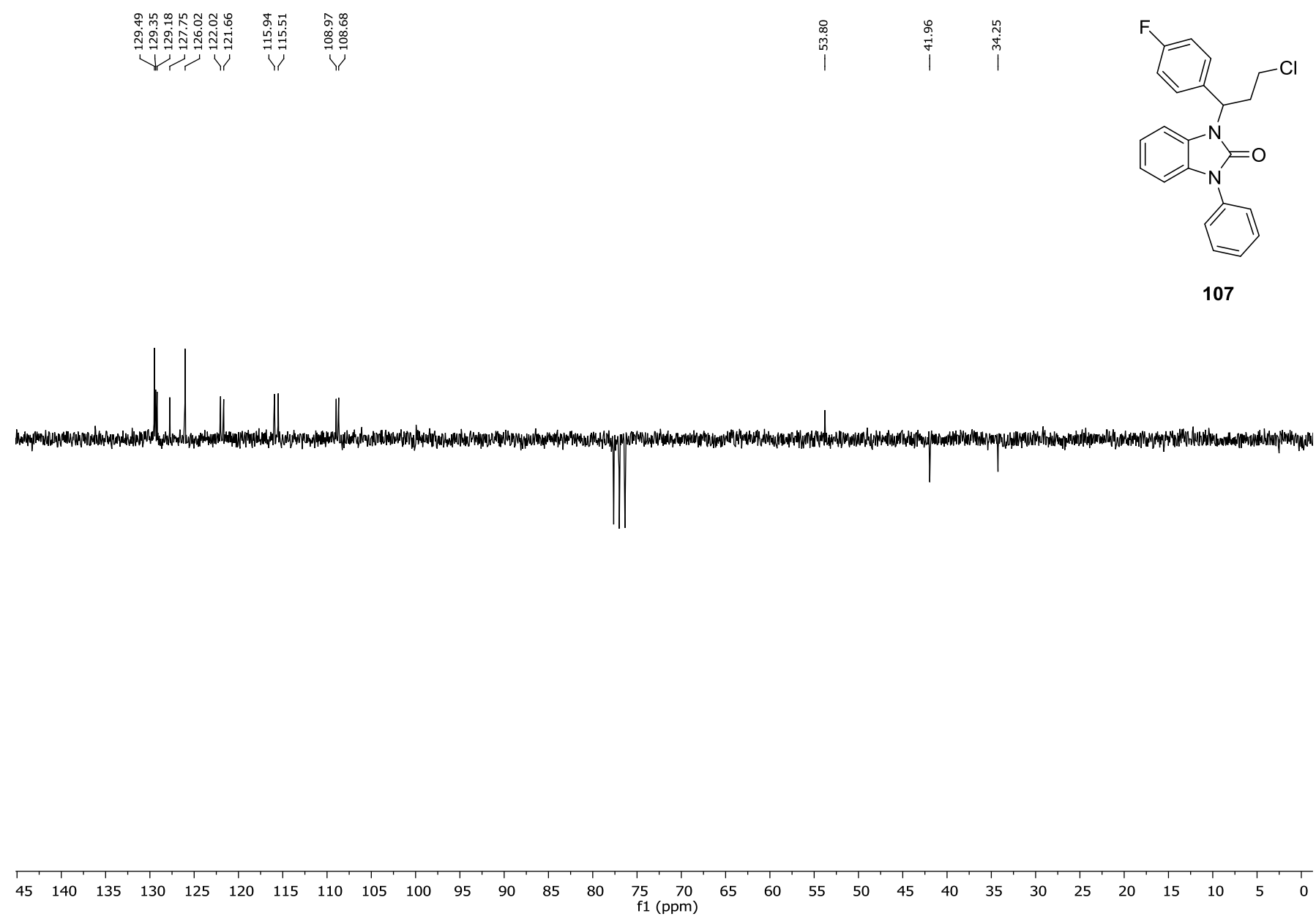


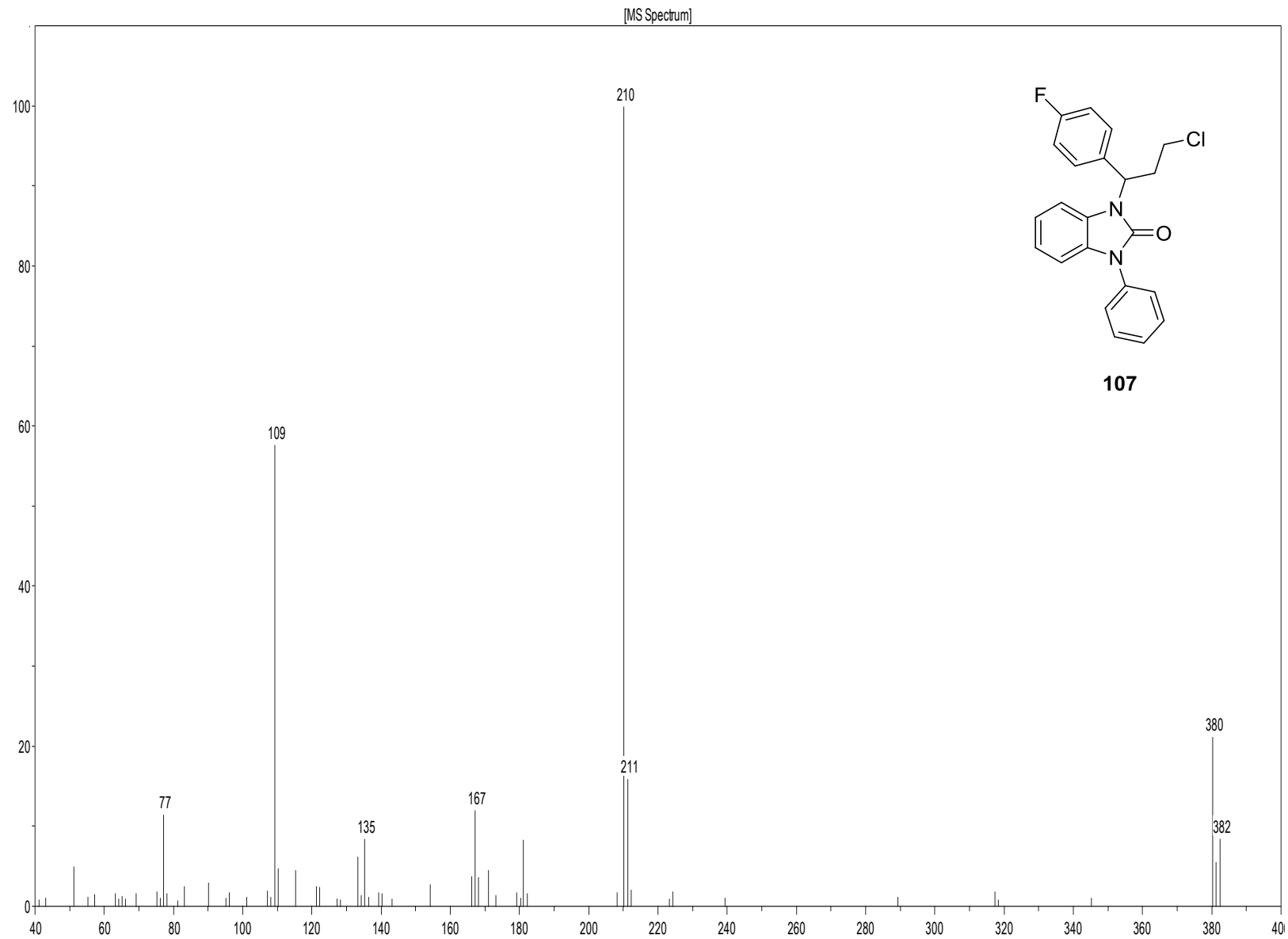
107





107

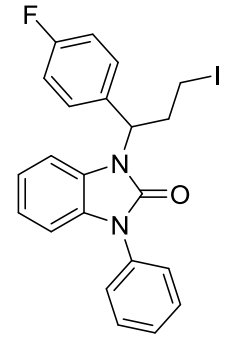




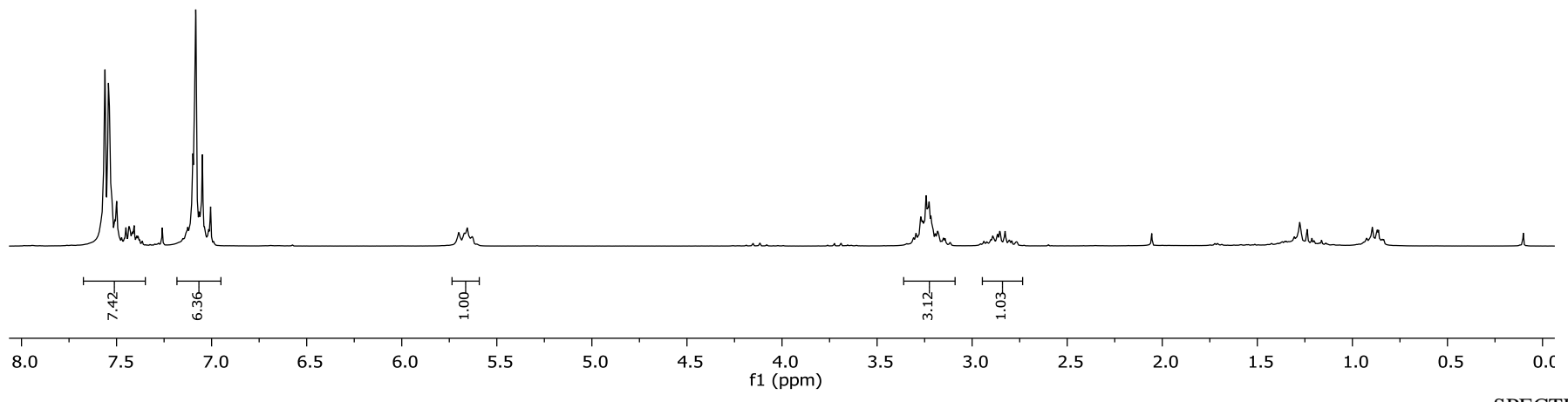
7.56
7.54
7.54
7.53
7.50
7.47
7.45
7.44
7.43
7.42
7.42
7.41
7.39
7.39
7.38
7.36
7.10
7.08
7.07
7.05
7.02
7.01

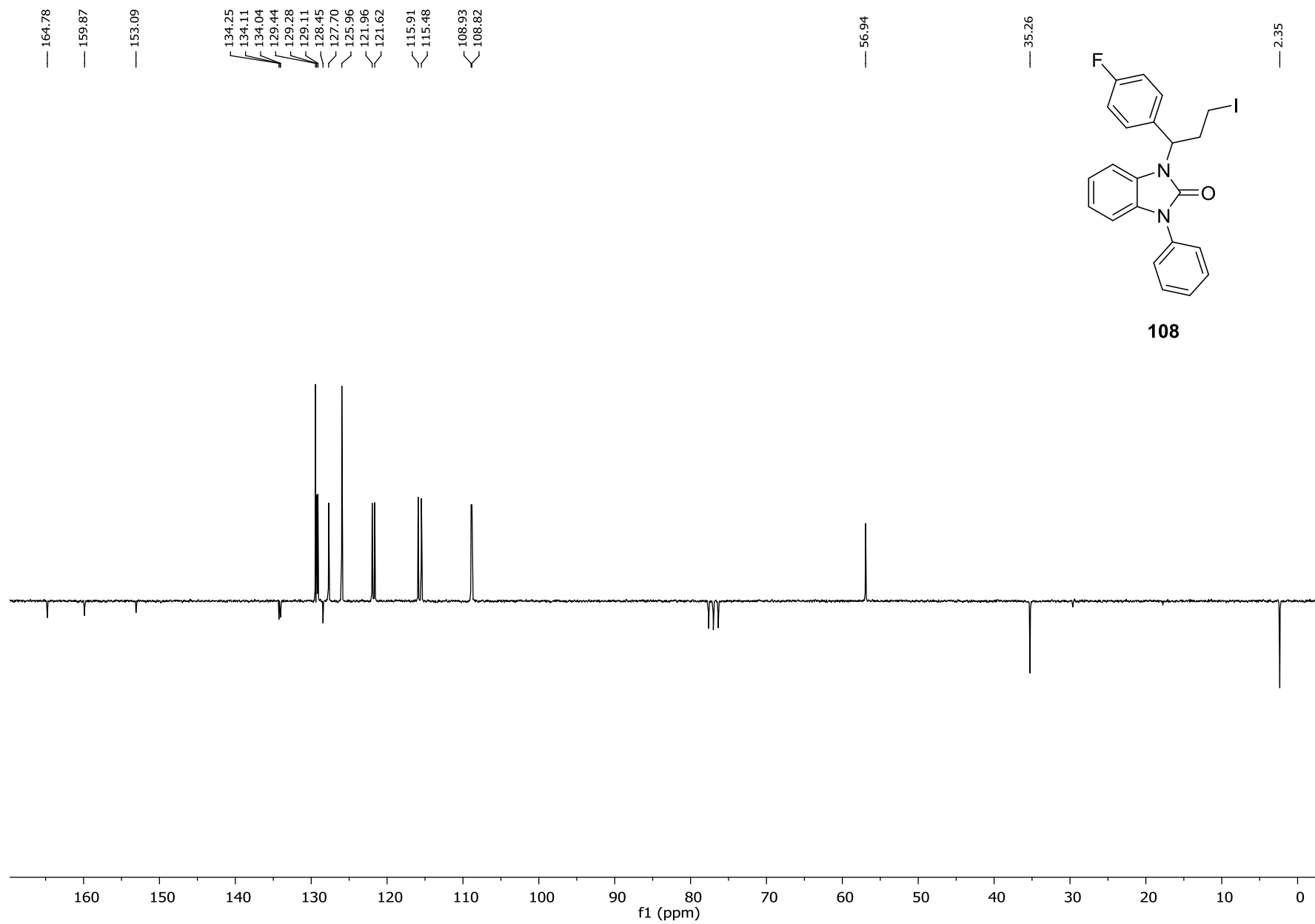
5.70
5.67
5.66
5.63

3.31
3.30
3.27
3.26
3.25
3.24
3.23
3.23
3.22
3.19
3.18
3.16
3.15
3.14
3.12
2.94
2.92
2.90
2.89
2.87
2.85
2.83
2.80
2.79
2.77

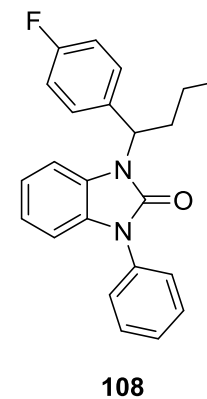
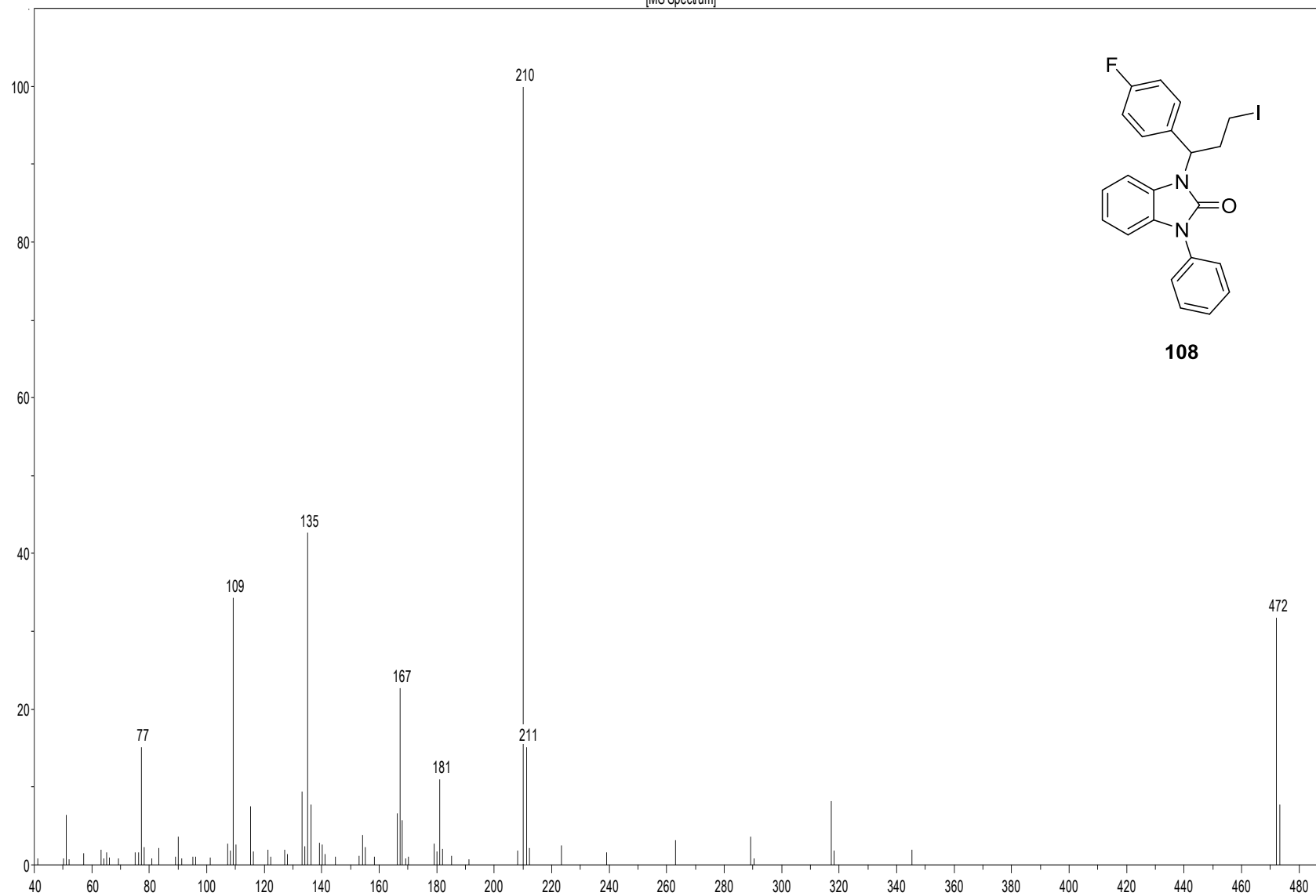


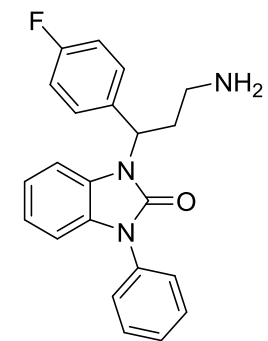
108



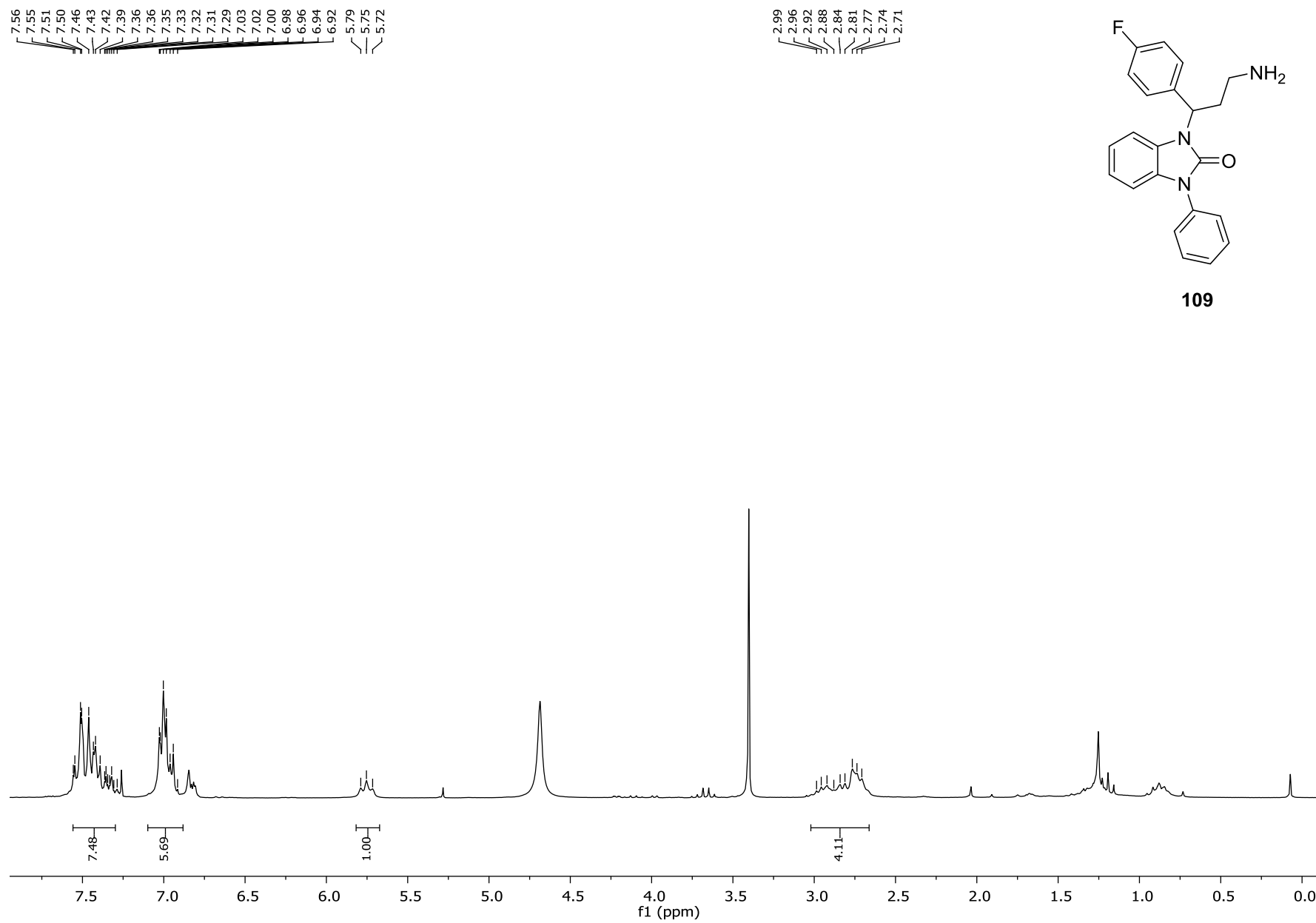


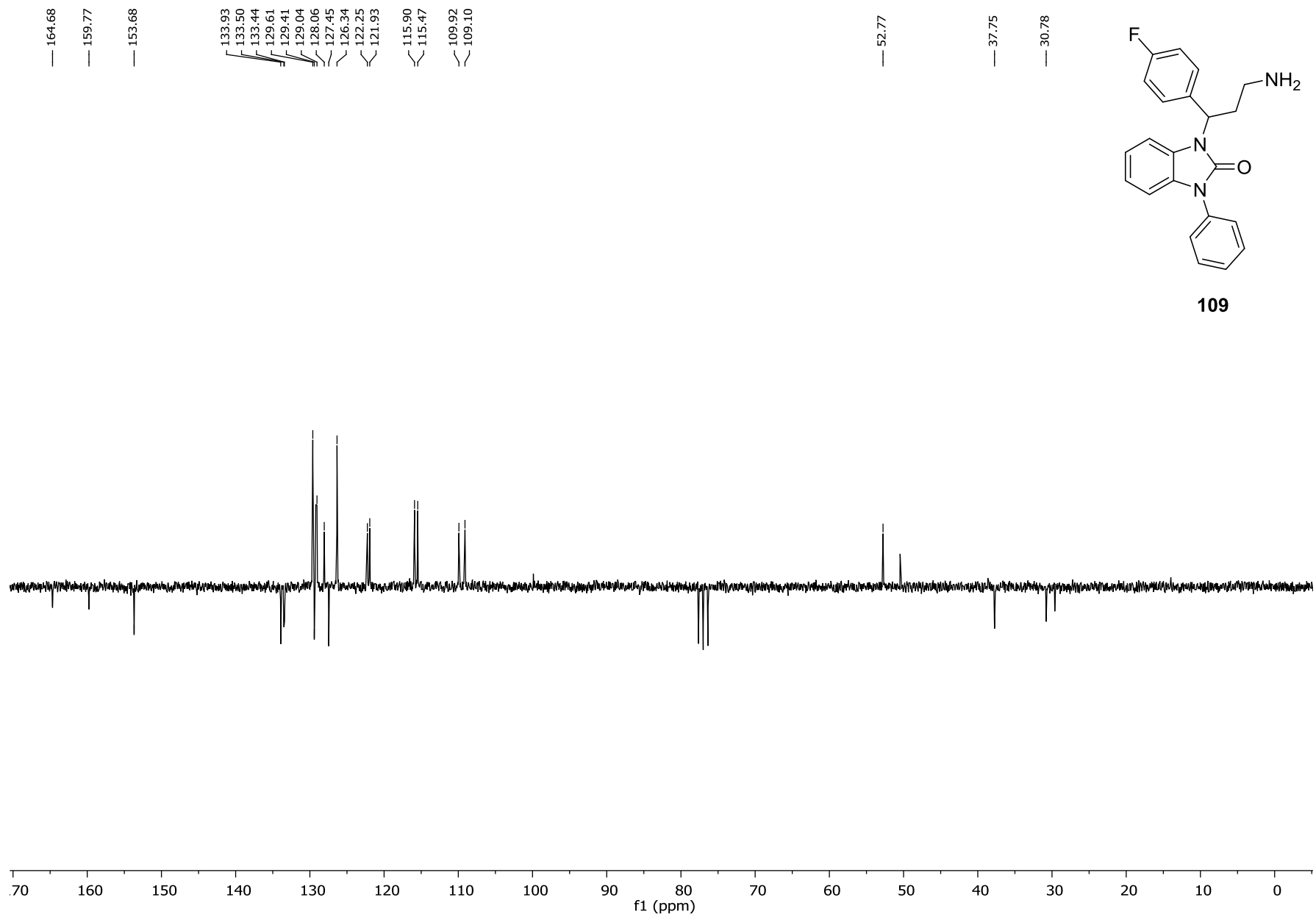
[MS Spectrum]

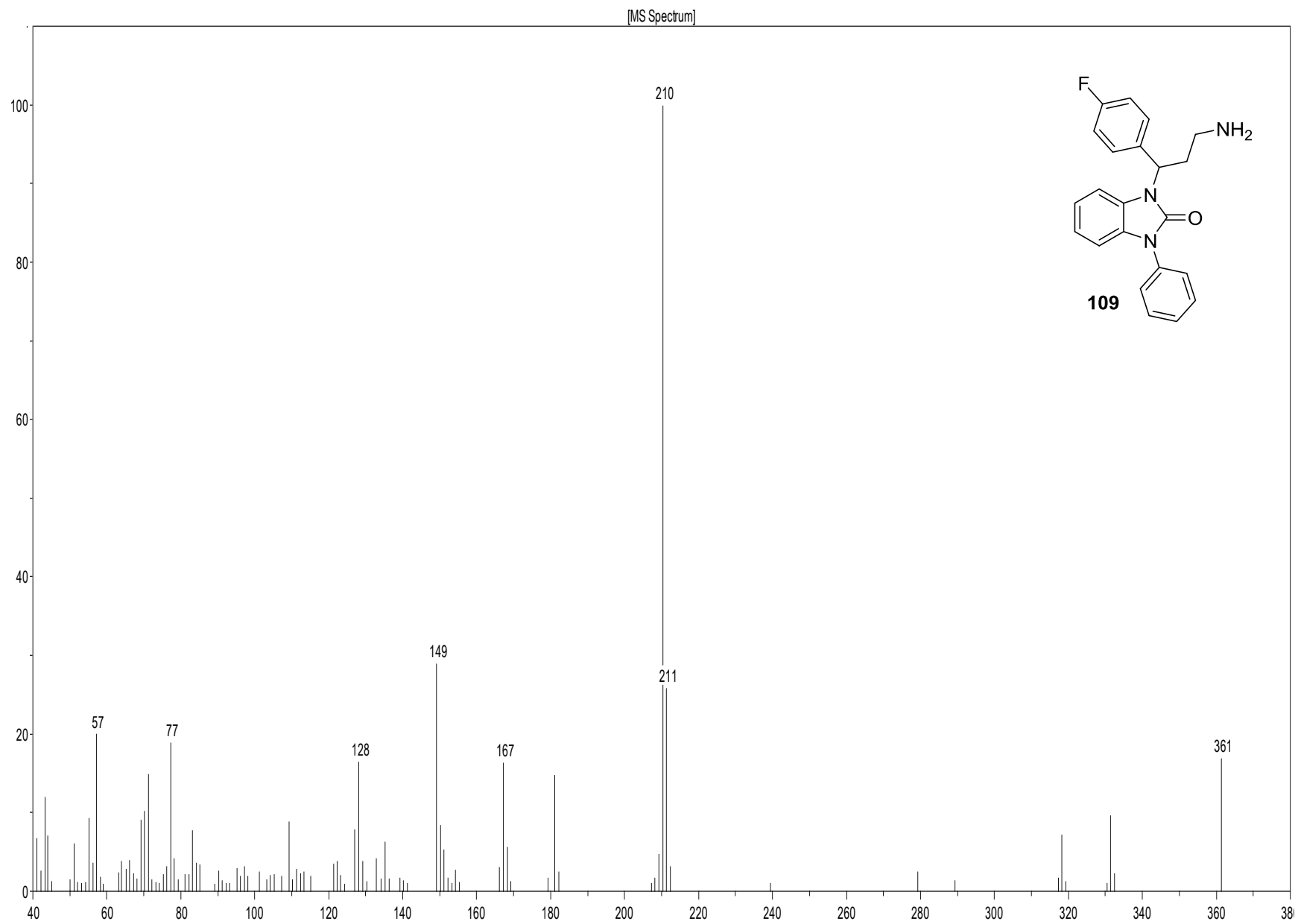




109

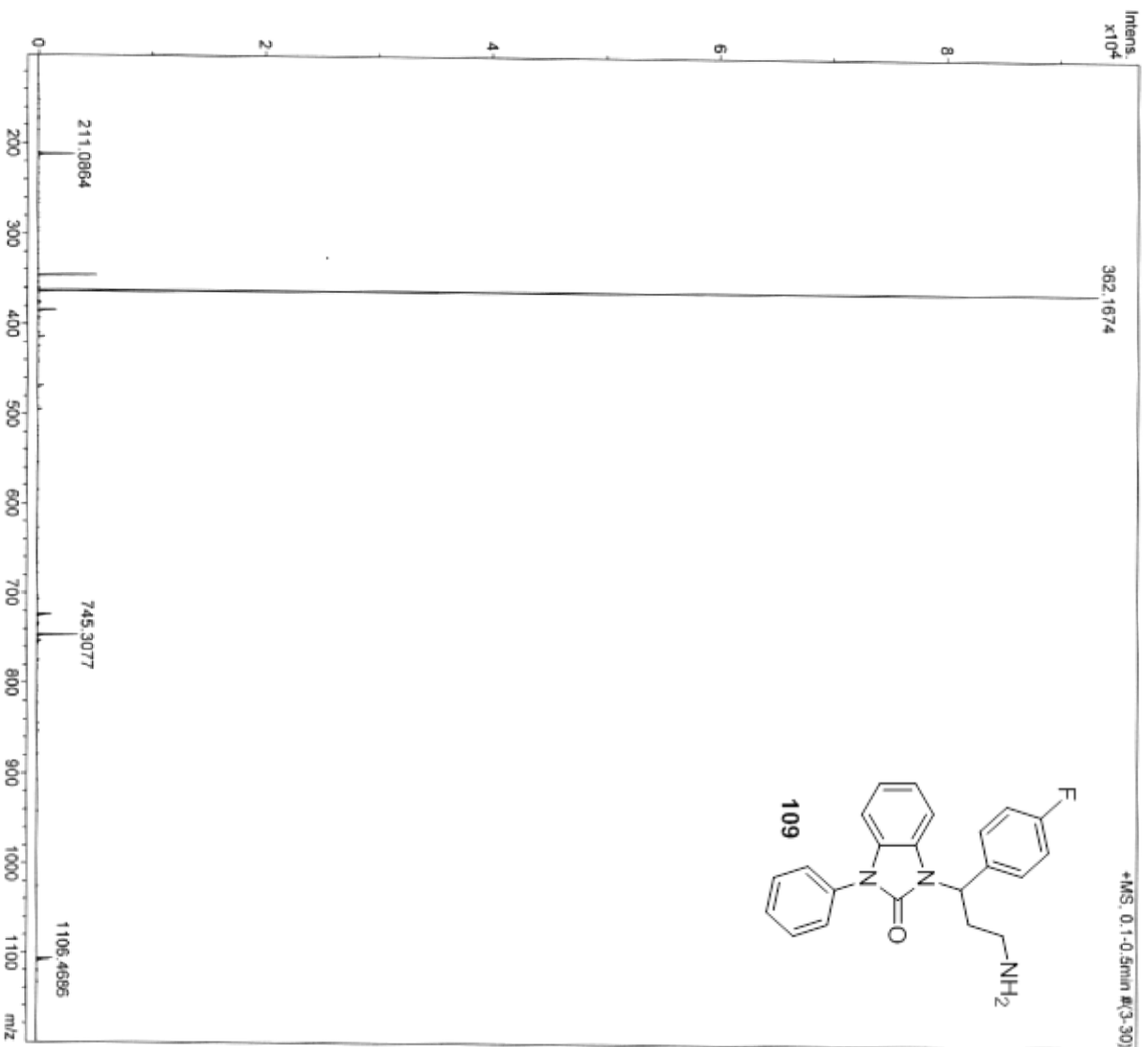


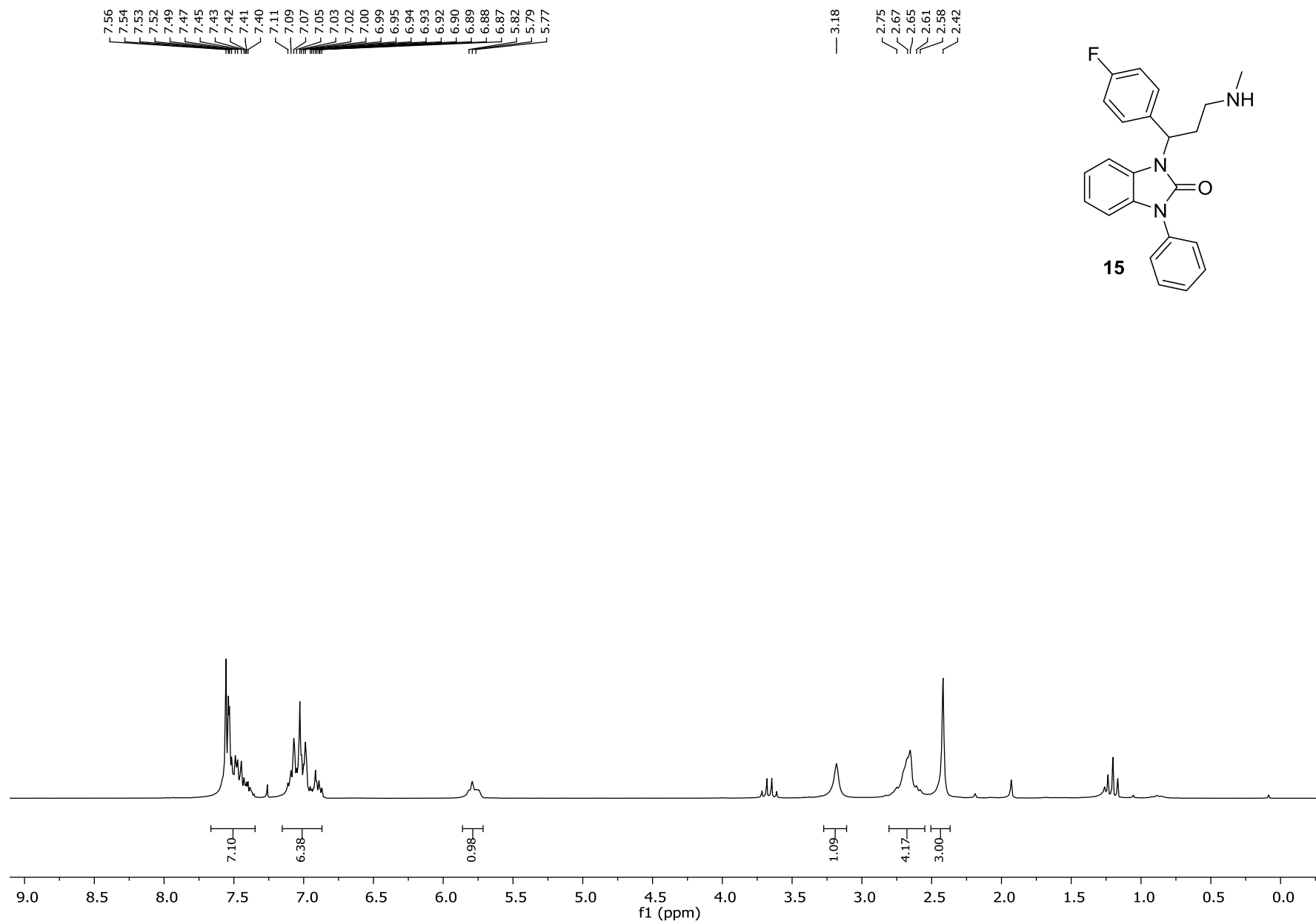


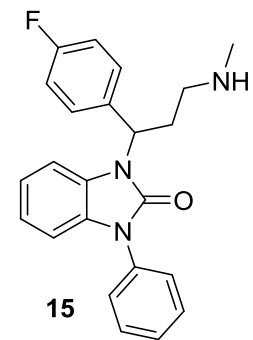
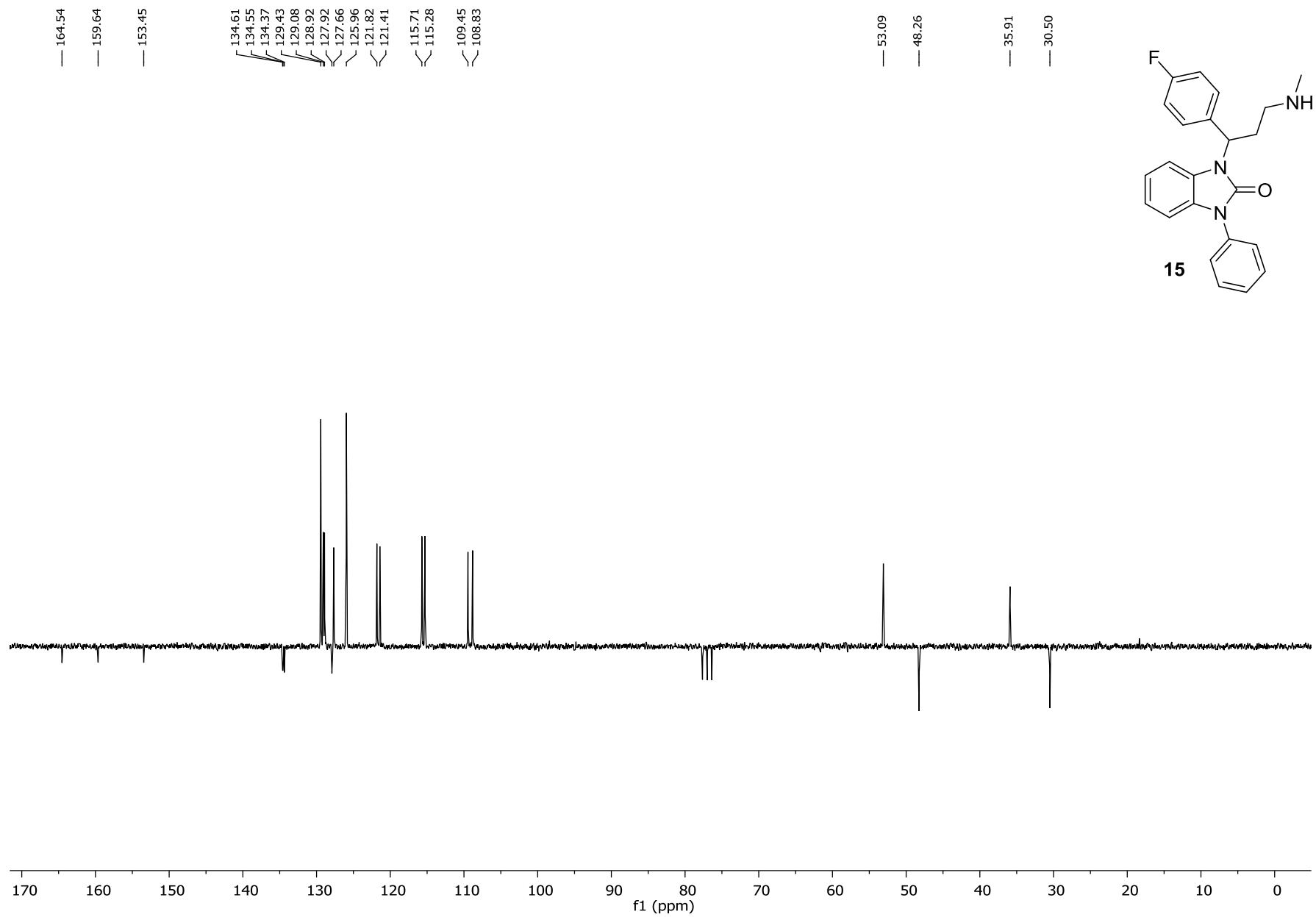


MassenspektrometrieZentrum FakultätChemieUniWien

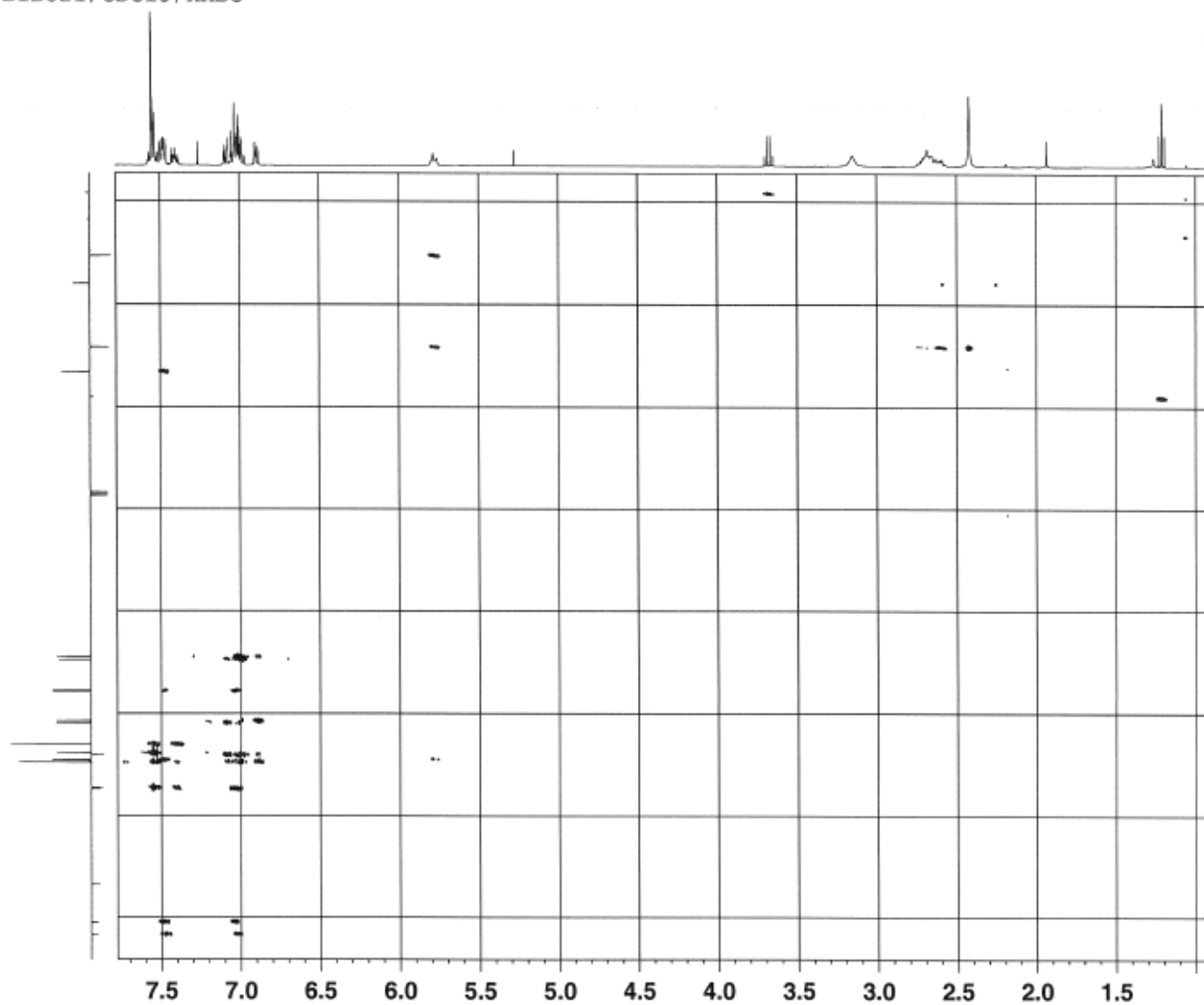
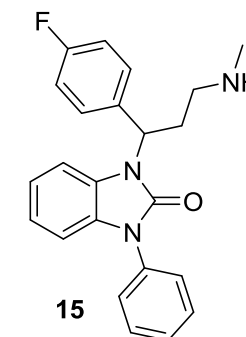
Analysis Info
Analysis Name D:\Data\MS_MessService\39919000002.d Acquisition Date 9/26/2013 8:25:23 AM
Method tune_low_MS_Service_09_13.m Operator phu
Sample Name BB361 Instrument maxis
Auftraggeber/Com Bornatowicz/Spreitzer
Ergebnis: +/- 5ppm
ACN/MeOH 1%/H2O







BIBO21/CDC13/HMBC



Current Data Parameters
 NAME BIBO21
 EXPNO 4
 PROCNO 1

F2 - Acquisition Parameters
 Date_ 20131005
 Time 16.39
 INSTRUM spect
 PROBNM 5 mm PASPO BB/
 PULPROG hbhcgplpndgpf
 TD 4096
 SOLVENT CDC13
 NS 4
 DS 8
 SWH 4000.000 Hz
 FIDRES 0.978962 Hz
 AQ 0.5120500 sec
 RE 203
 DN 125.000 usec
 DE 10.00 usec
 TE 297.3 K
 CBST2 145.000000
 CBST13 8.0000000
 D0 0.00000100 sec
 D1 2.00000000 sec
 D2 0.00344828 sec
 D6 0.06250000 sec
 DL6 0.00020000 sec
 IM1 0.00002615 sec

===== CHANNEL f1 =====
 NUC1 1H
 P1 12.50 usec
 P2 25.00 usec
 PLW1 16.00000000 W
 SFO1 400.231829 MHz

===== CHANNEL f2 =====
 NUC2 13C
 P3 8.50 usec
 PLW2 64.00000000 W
 SFO2 100.6474746 MHz

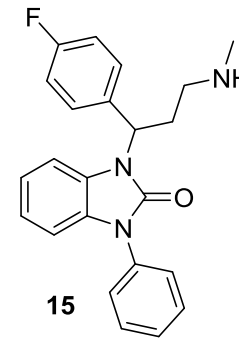
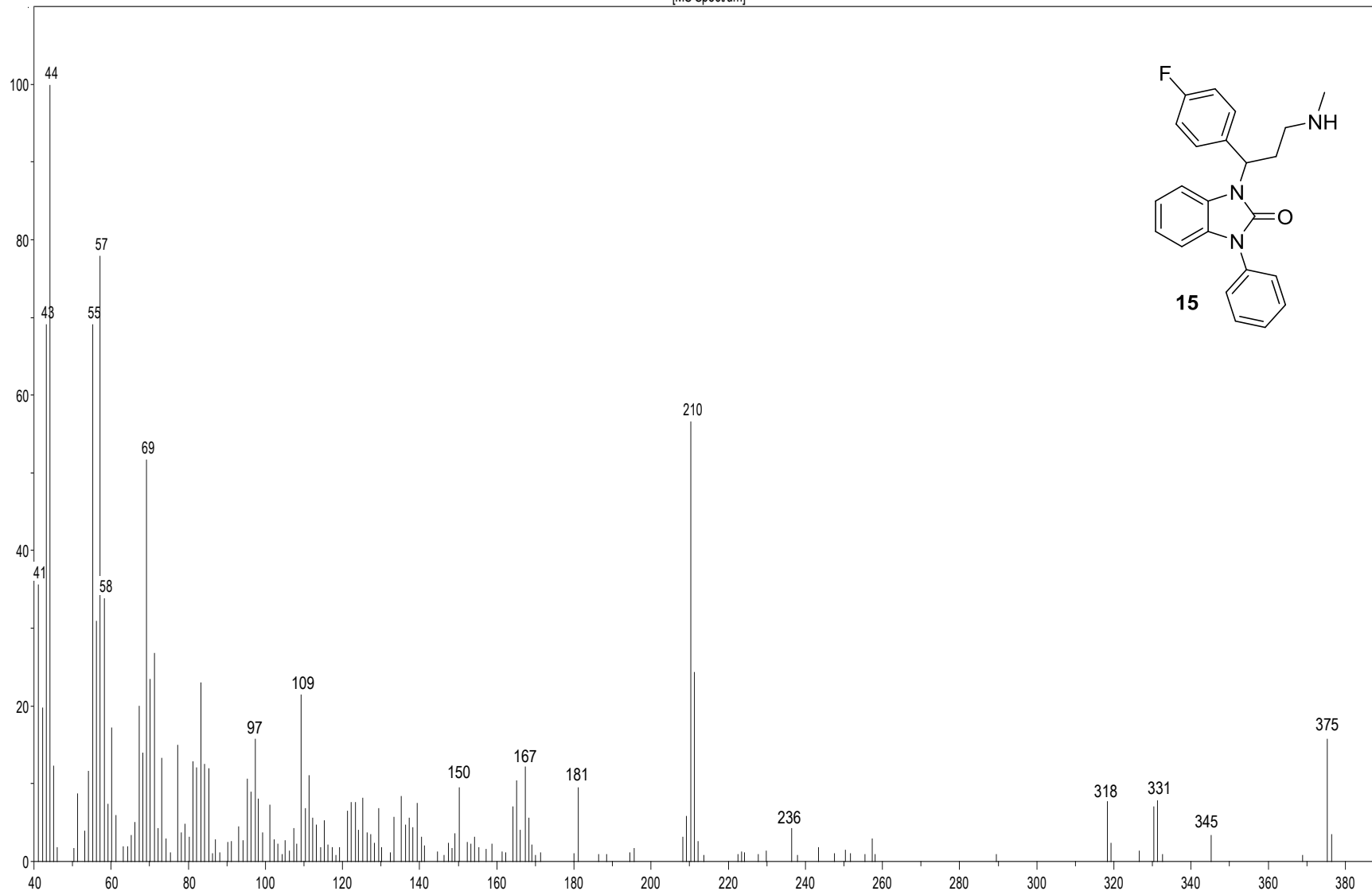
===== GRADIENT CHANNEL =====
 GPMAM1 SMSG10.100
 GPMAM2 SMSG10.100
 GPMAM3 SMSG10.100
 GP21 50.00 %
 GP22 30.00 %
 GP23 40.10 %
 P16 1000.00 usec

F1 - Acquisition parameters
 TD 512
 SFO1 100.6475 MHz
 FIDRES 37.349834 Hz
 SW 190.001 ppm
 PRMODE QF

F2 - Processing parameters
 SI 2048
 SF 400.2500117 MHz
 MEM 8192
 SSB 0
 LB 0 Hz
 GB 0
 PC 1.00

F1 - Processing parameters
 SI 1024
 MC2 QF
 SF 100.6379239 MHz
 MEM States
 SSB 0
 LB 0 Hz
 GB 0

[MS Spectrum]



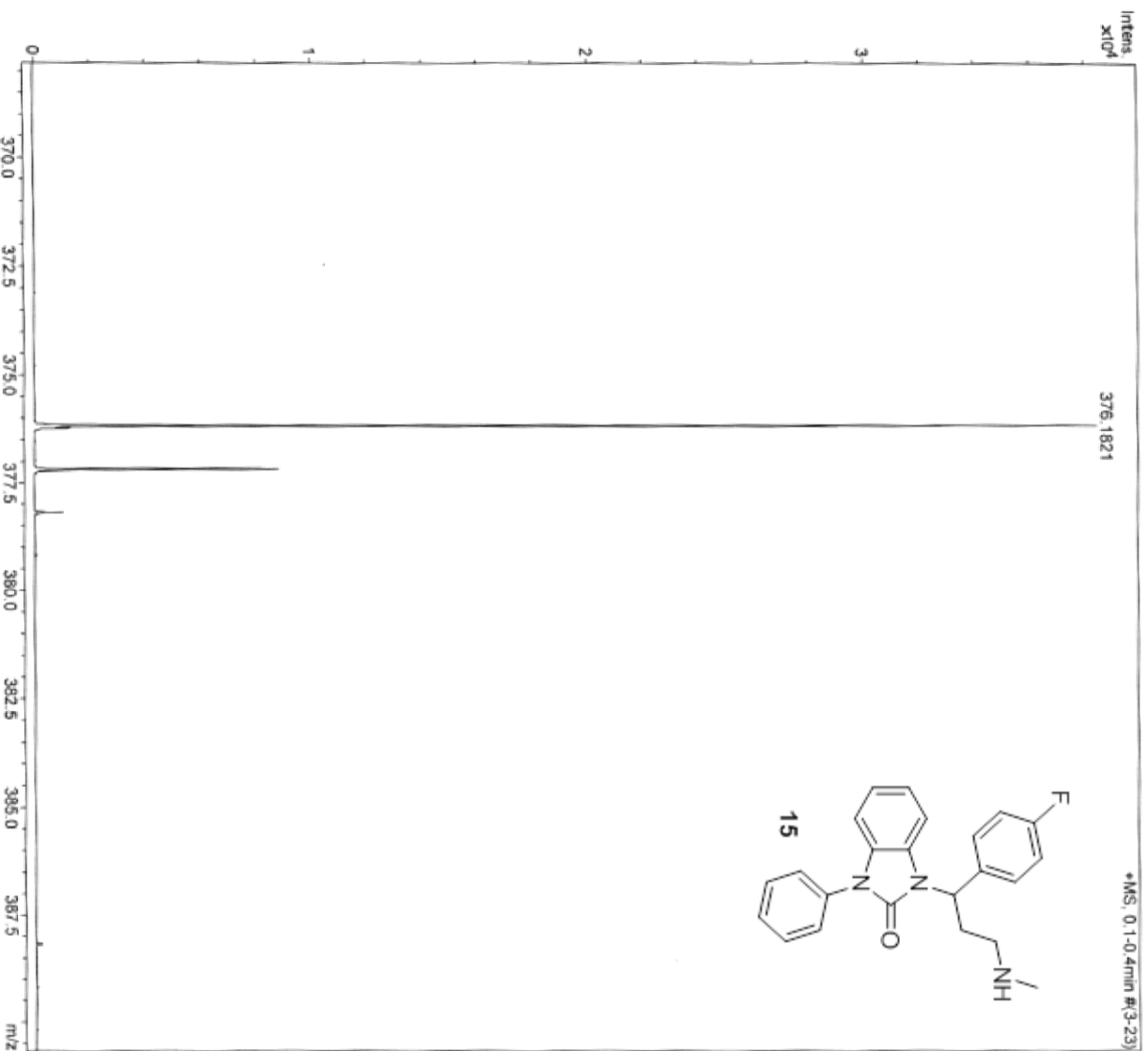
MassenspektrometrieZentrum FakultätChemieUniWien

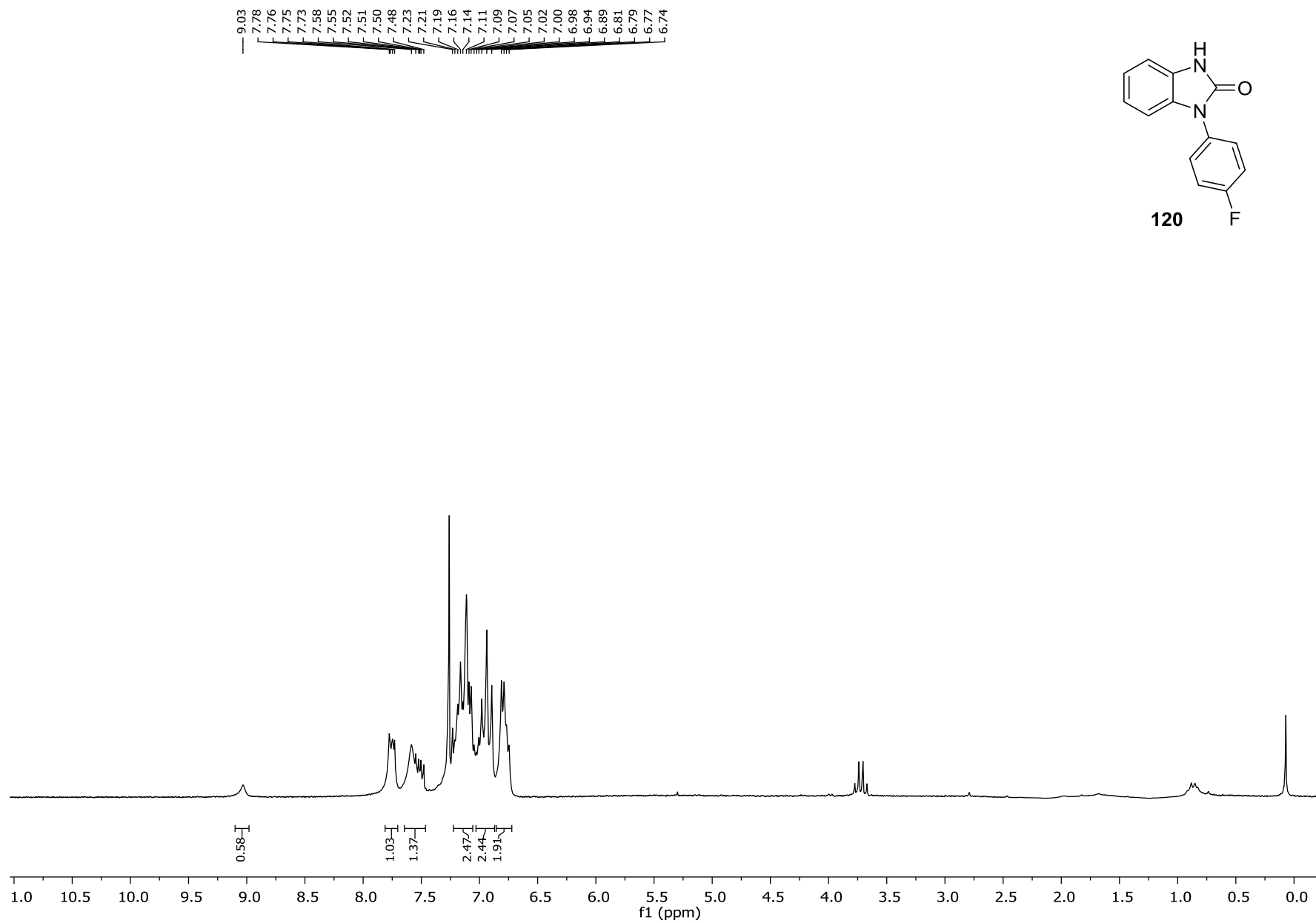
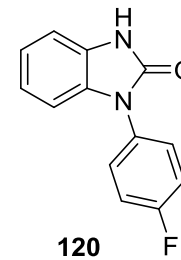
Analysis Info

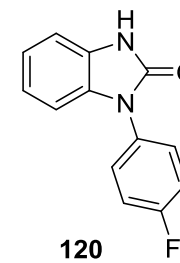
Analysis Name D:\Data\MS_MessService\39918000002.d
Method tune_low_MS_Service_09_13.m
Sample Name b 3
Auftragneber/Com Neudorfer/Spreitzer
Ergebnis: +/- 5ppm
ACN/MeOH 1%/H2O

Acquisition Date 9/26/2013 8:13:57 AM

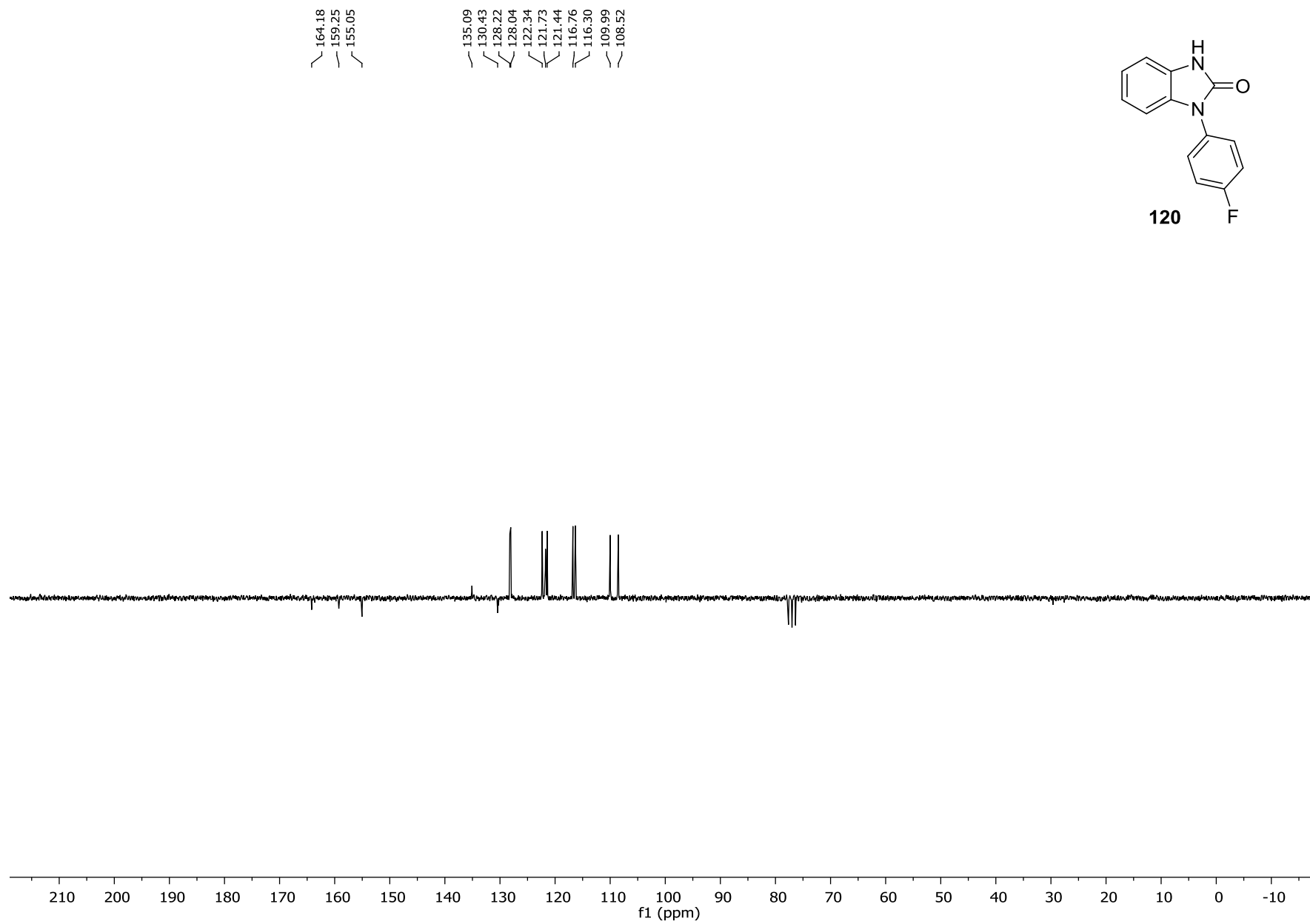
Operator phu
Instrument maxis



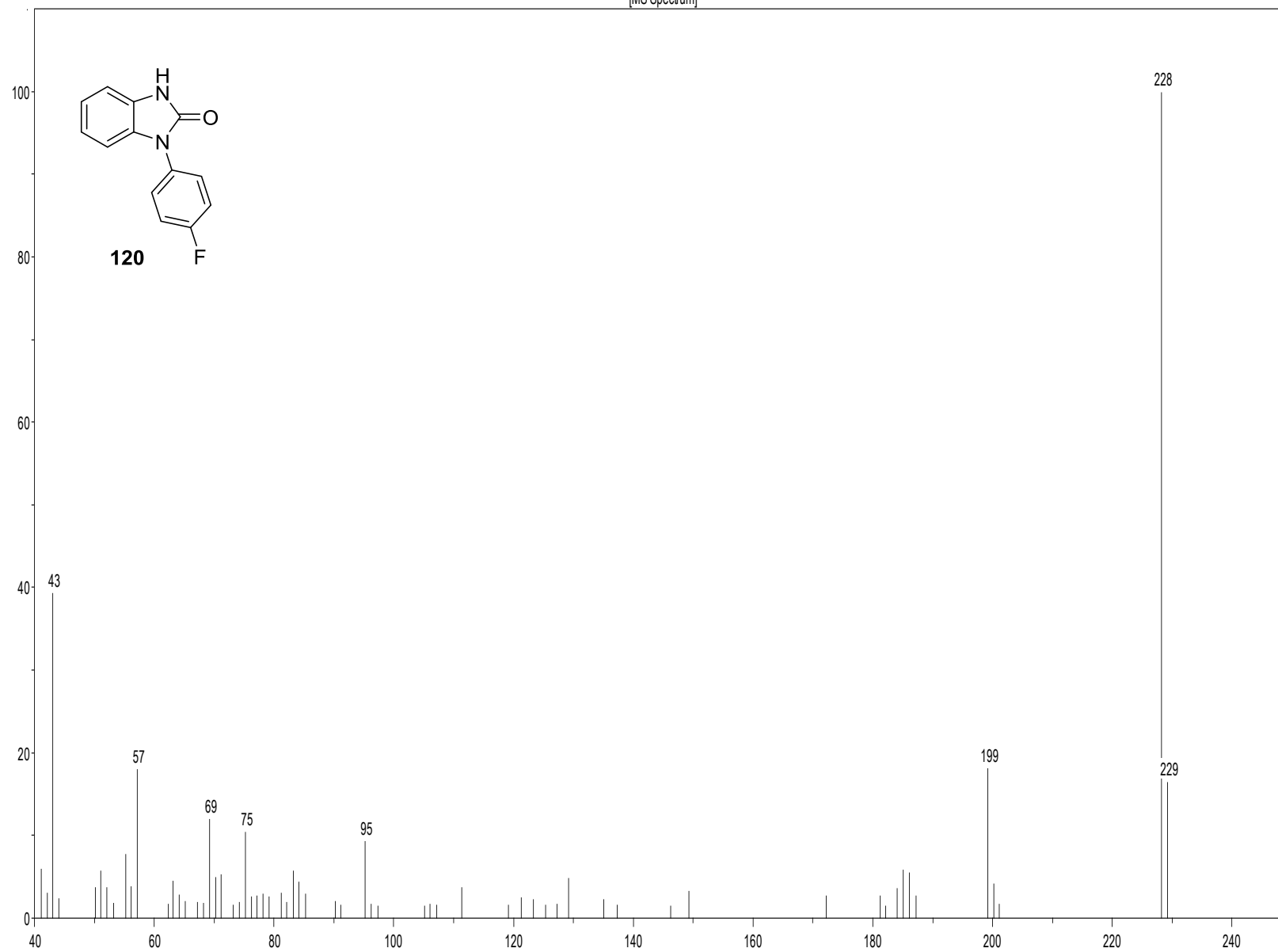


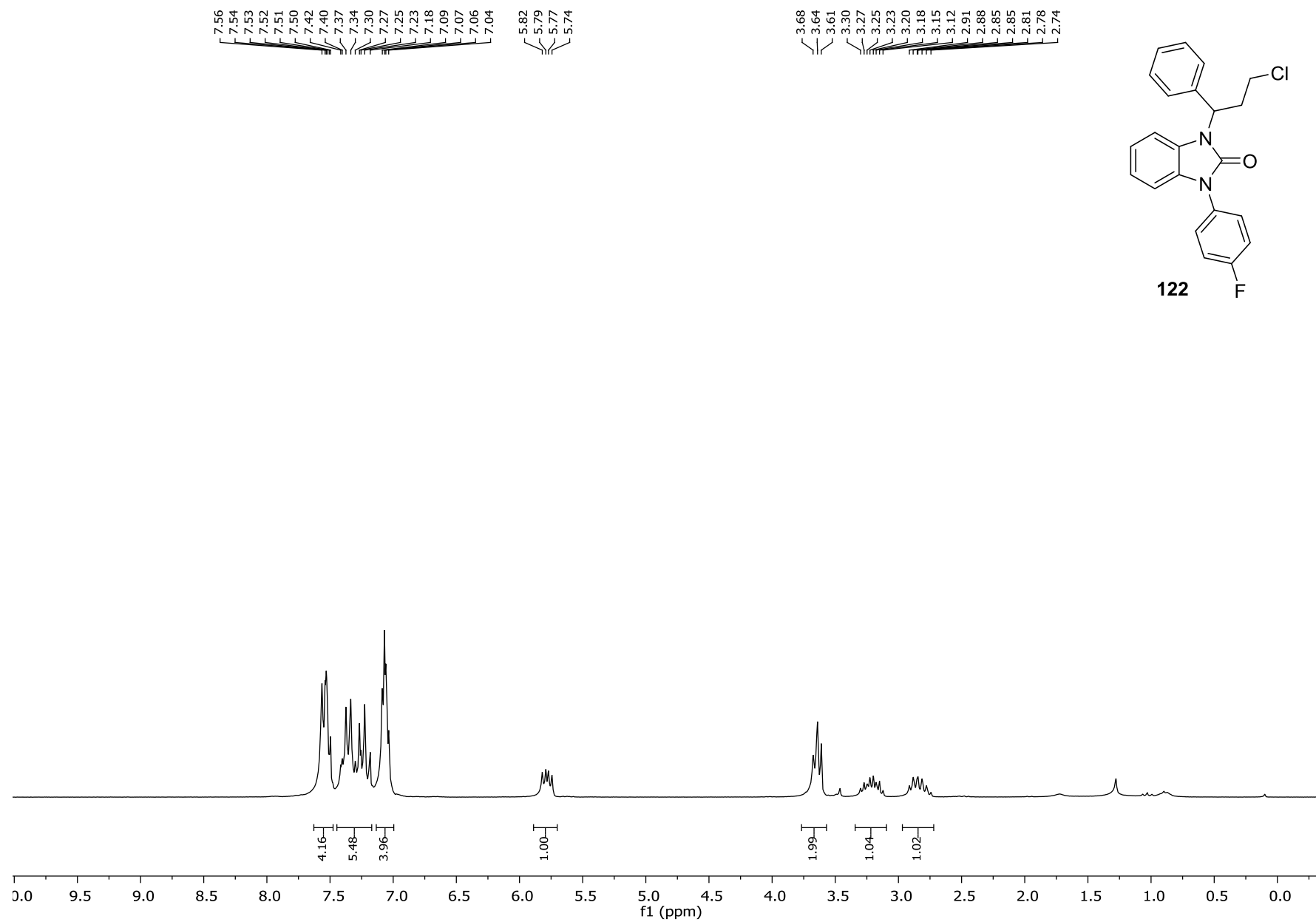


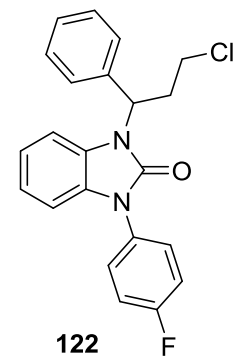
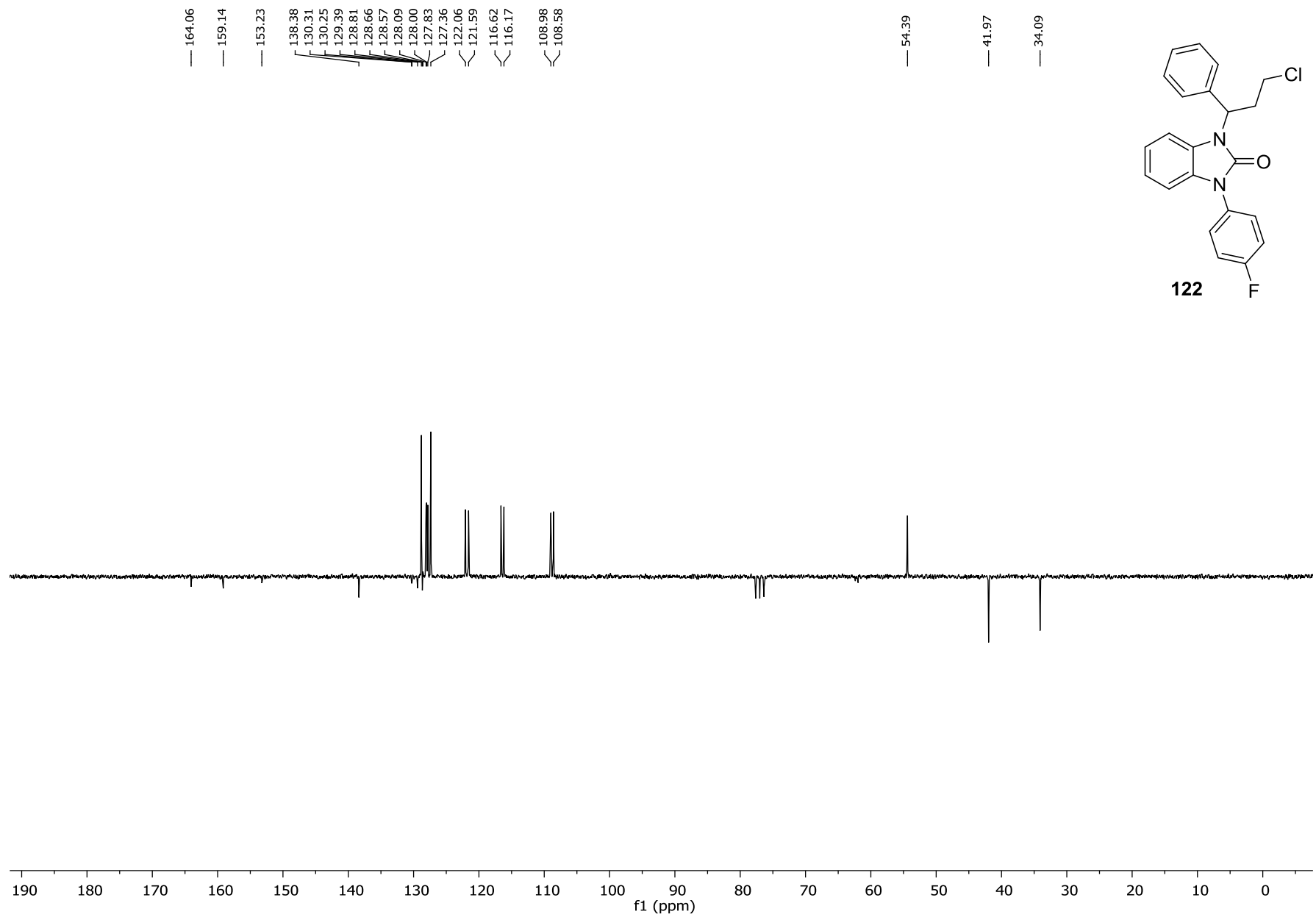
120

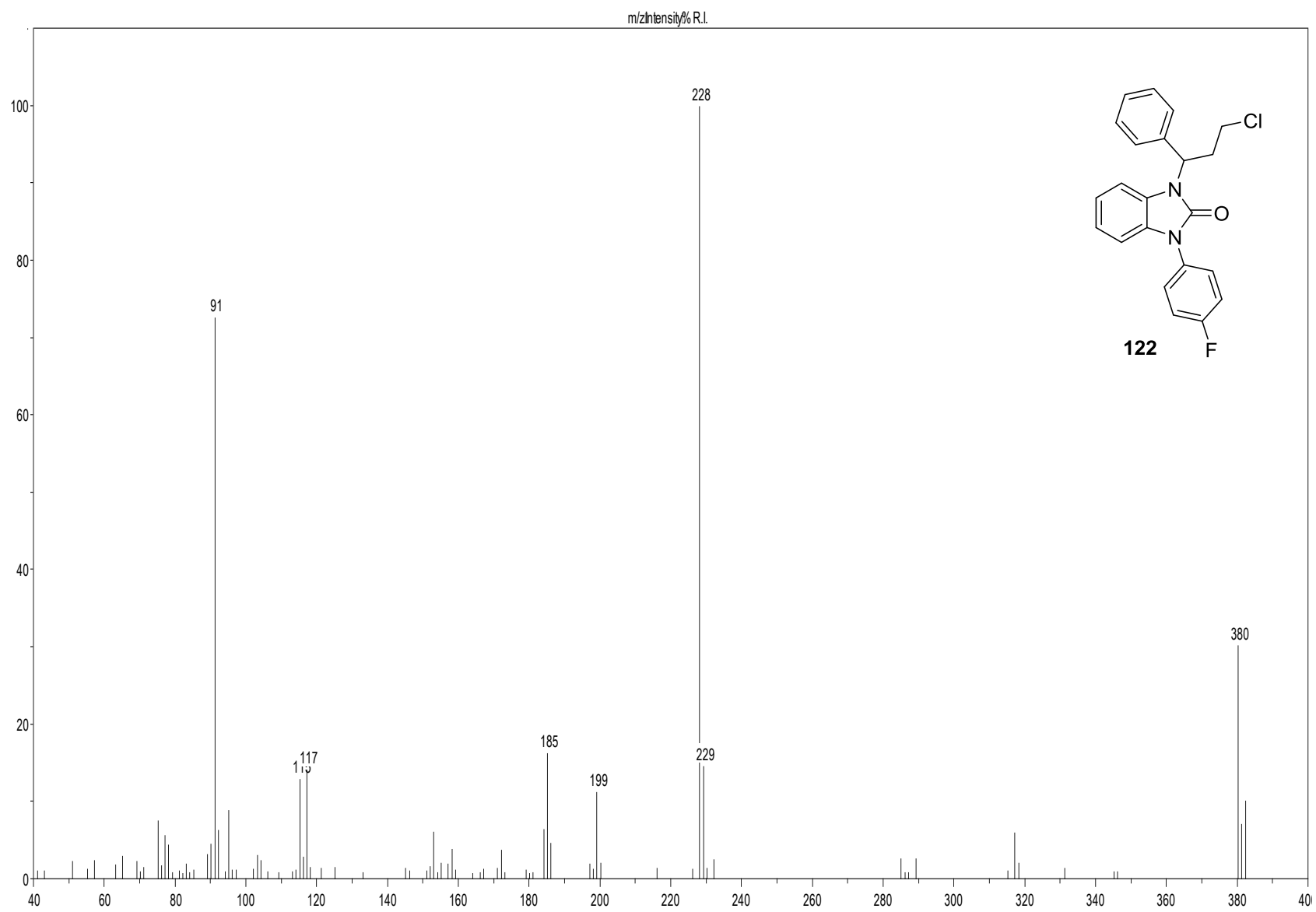


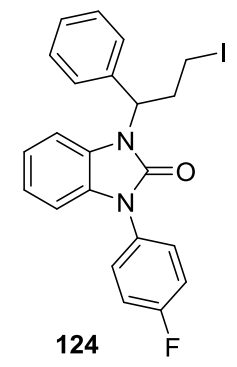
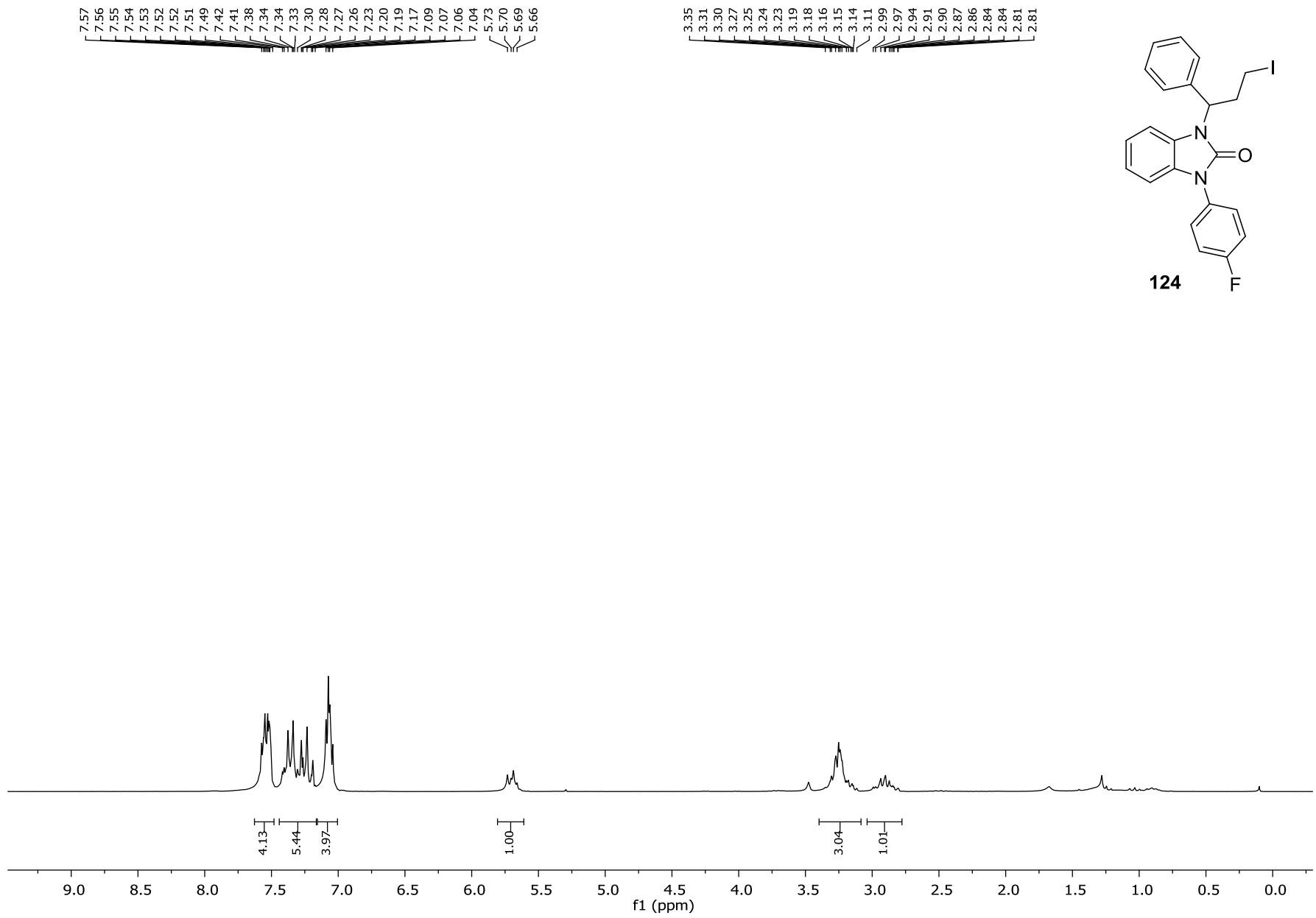
[MS Spectrum]

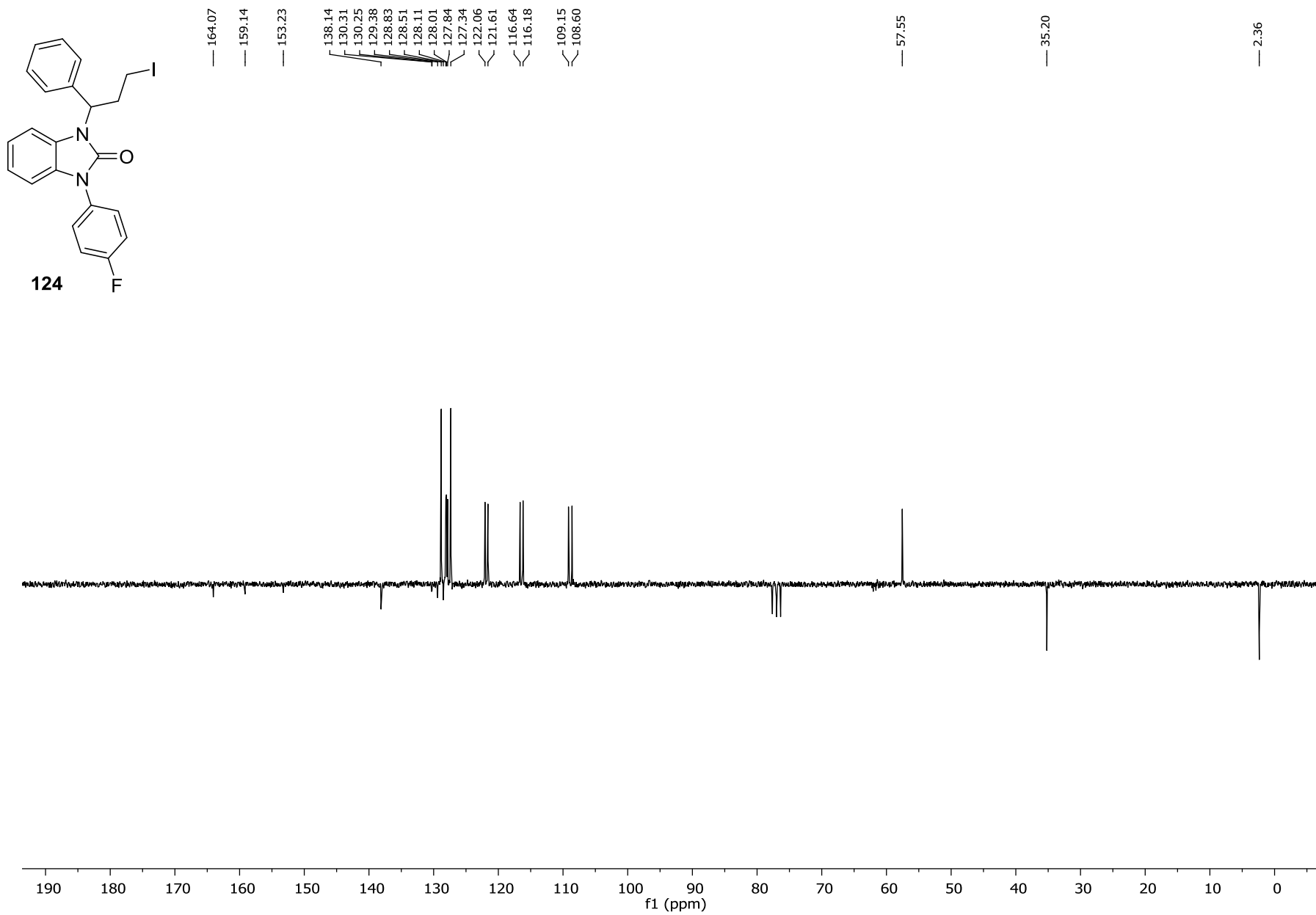




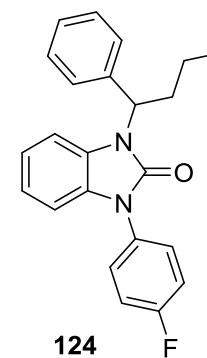
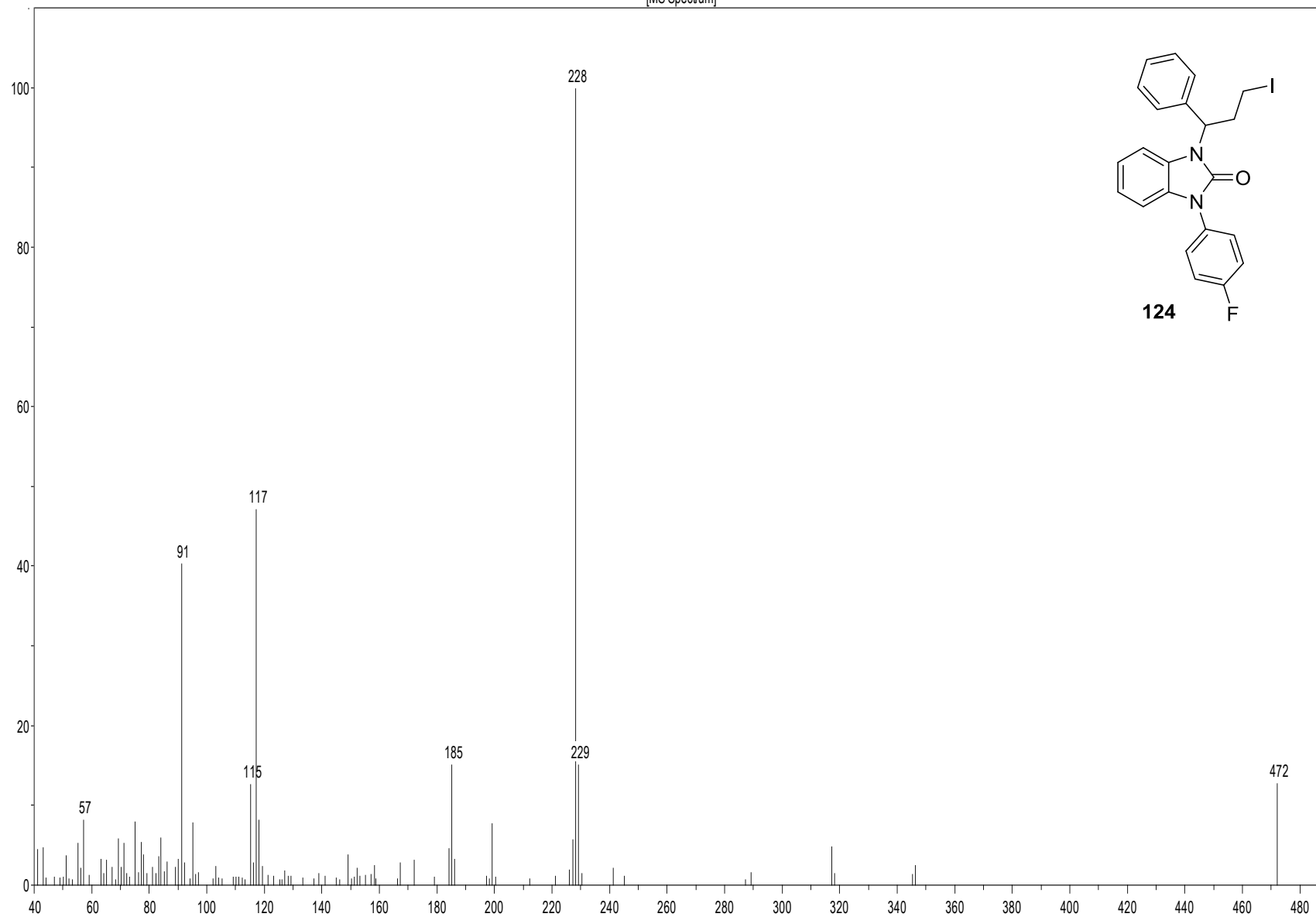


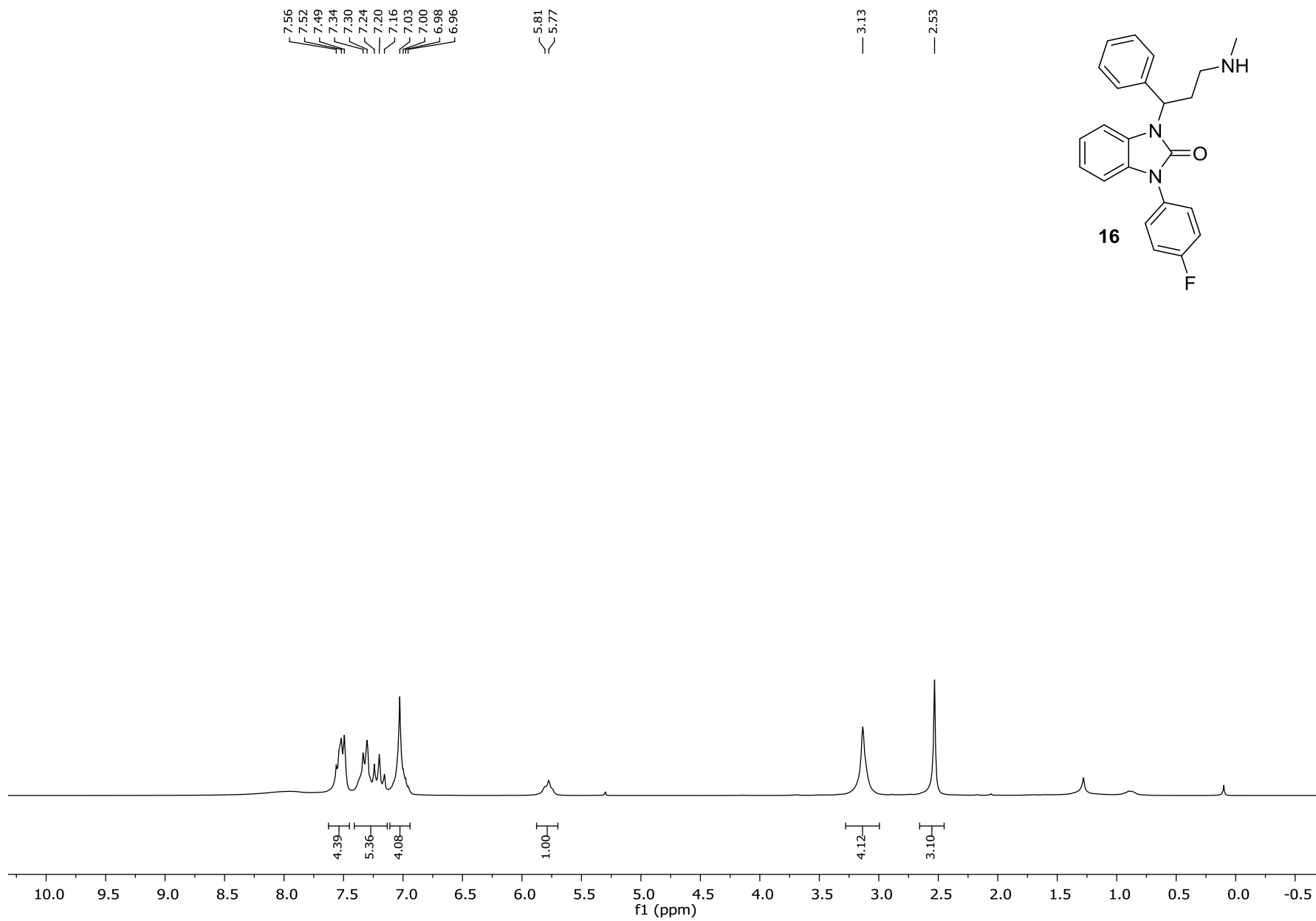


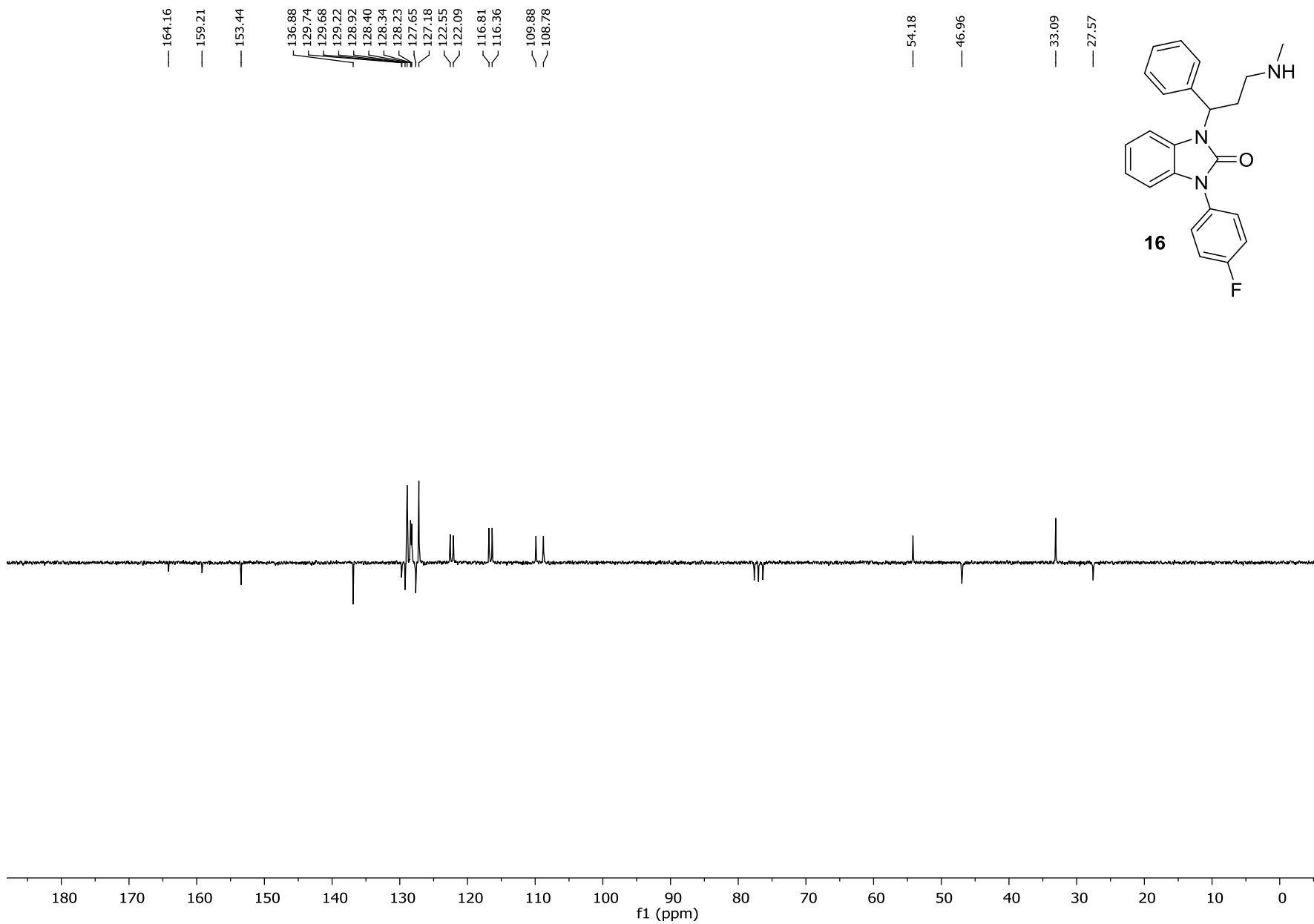


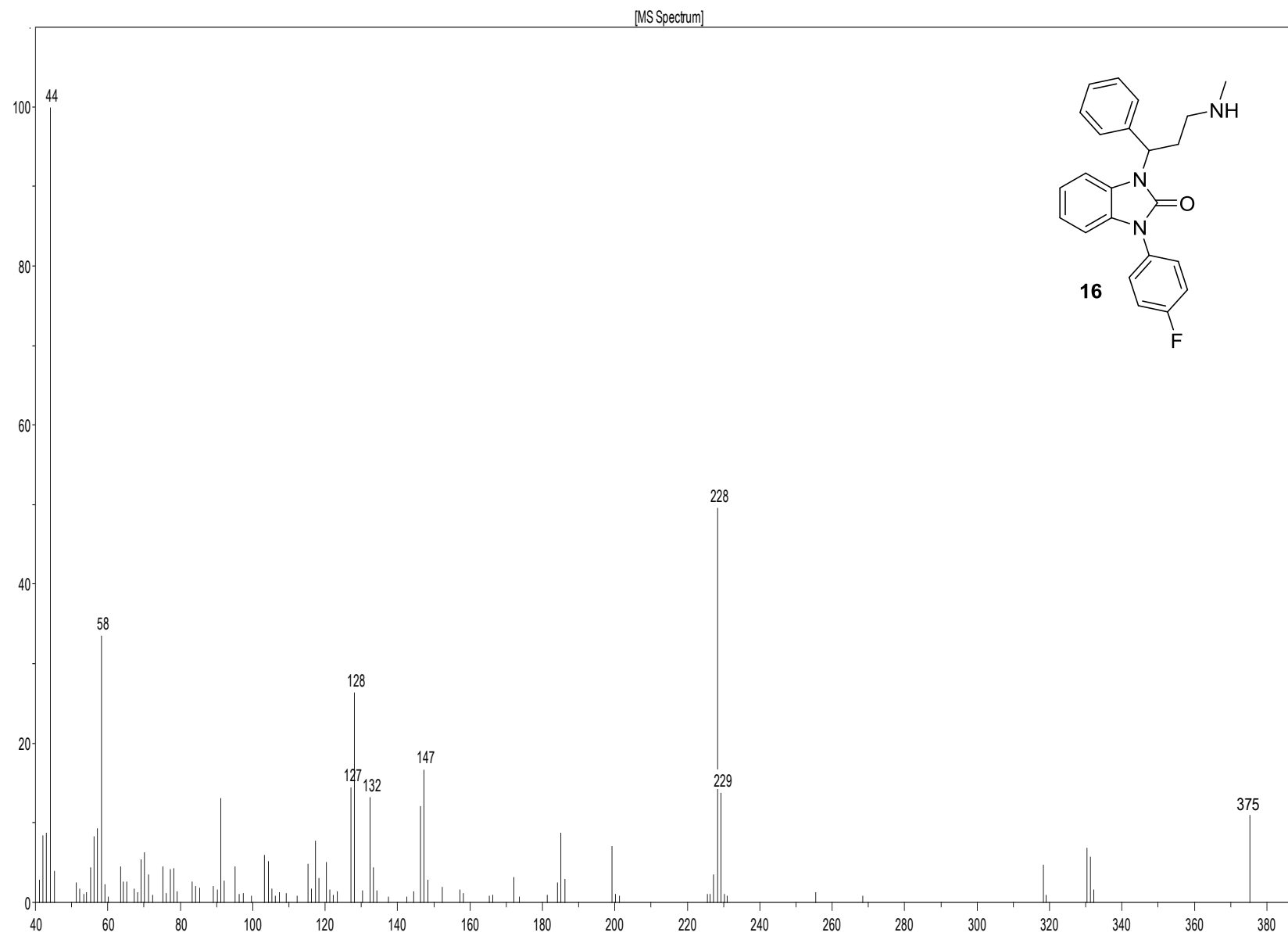


[MS Spectrum]









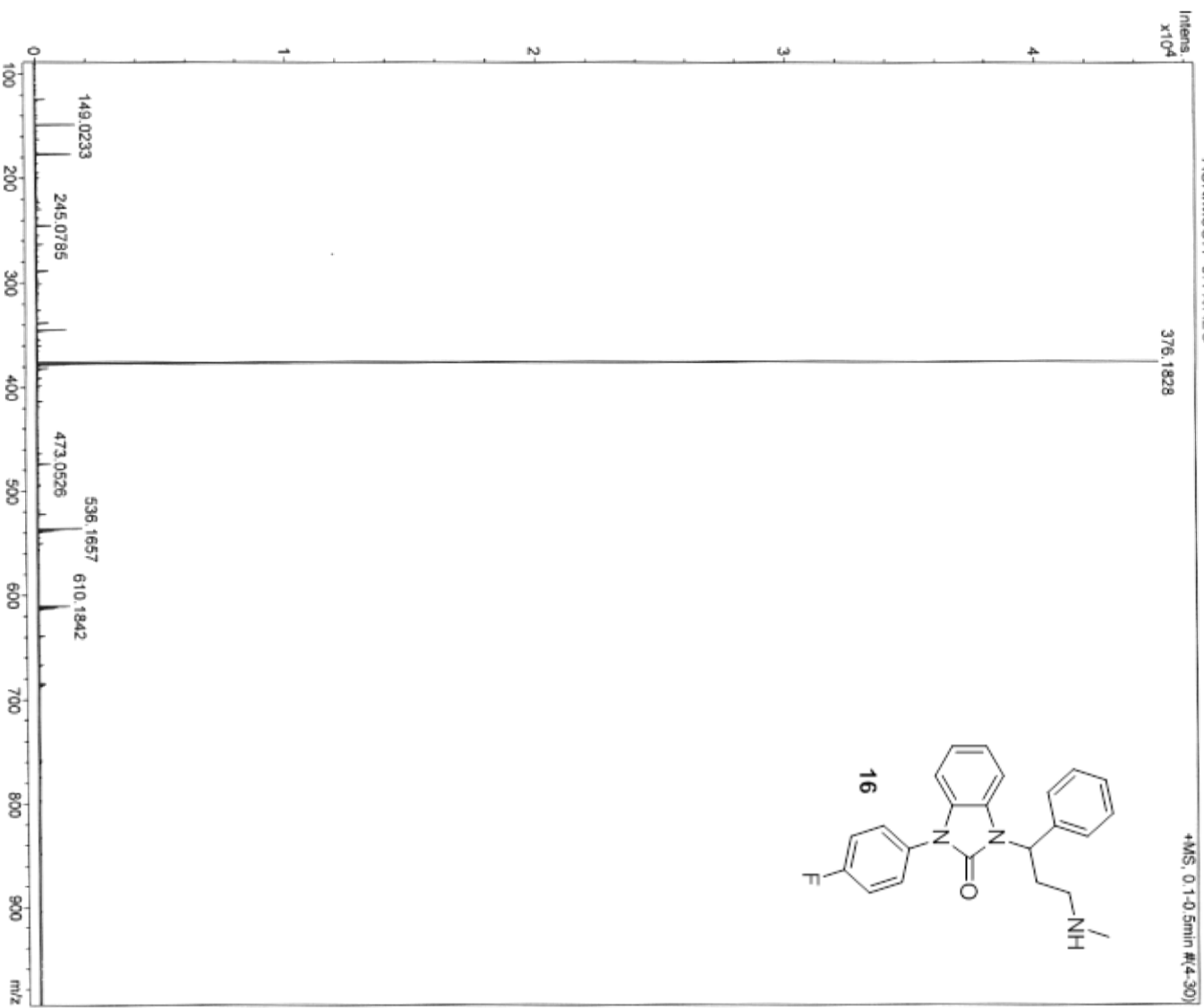
MassenspektrometrieZentrum FakultätChemieUniWien

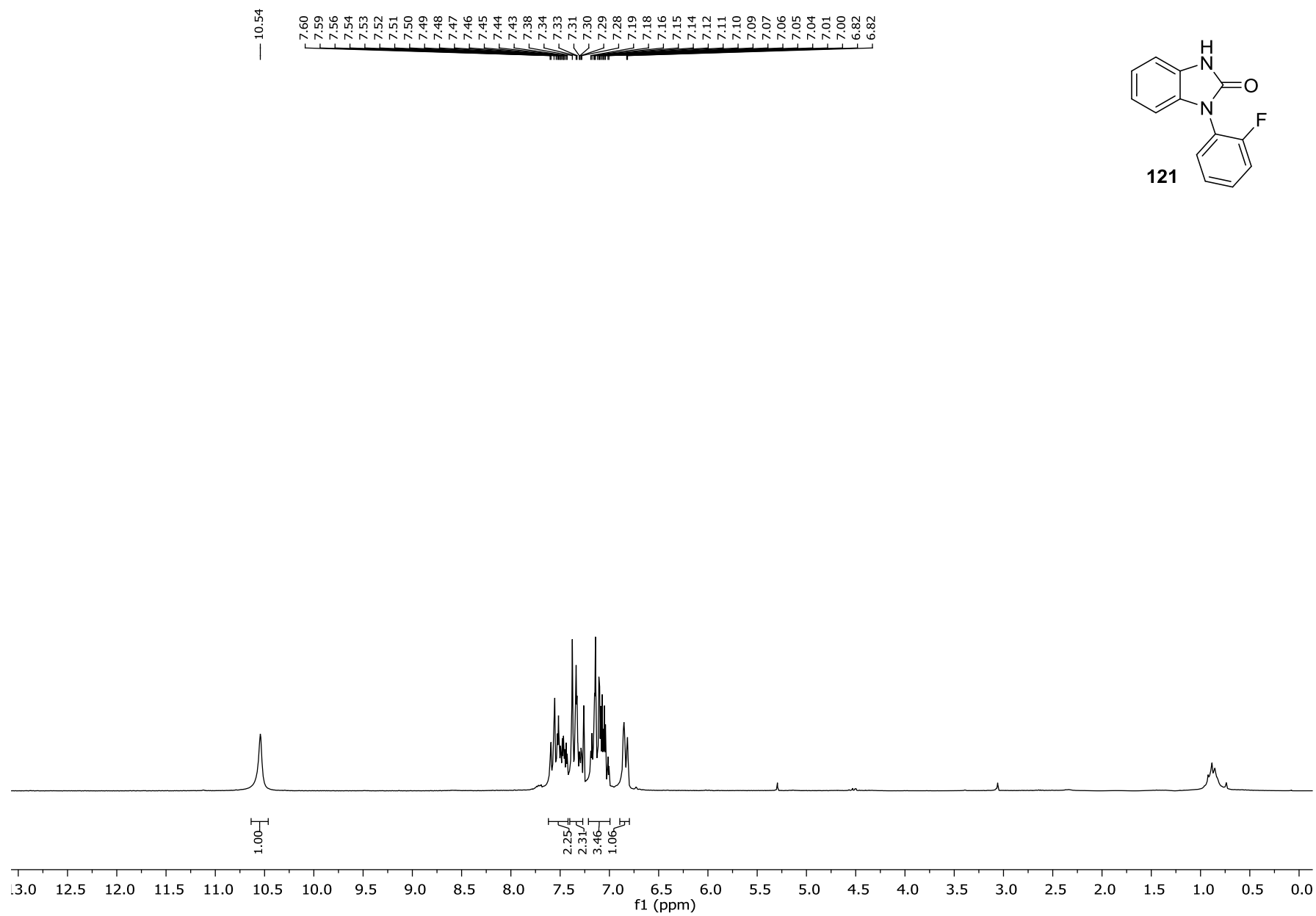
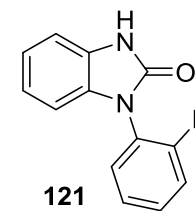
Analysis Info

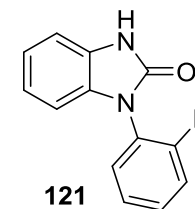
Analysis Name D:\Data\MS_MessService\40297000002.d
Method tune_low_MS_Service_01_14.m
Sample Name PI
Auftraggeber/Com Neudorfer/Pharm
ACN/MeOH 0.1%/H2O

Acquisition Date 1/28/2014 8:40:32 AM

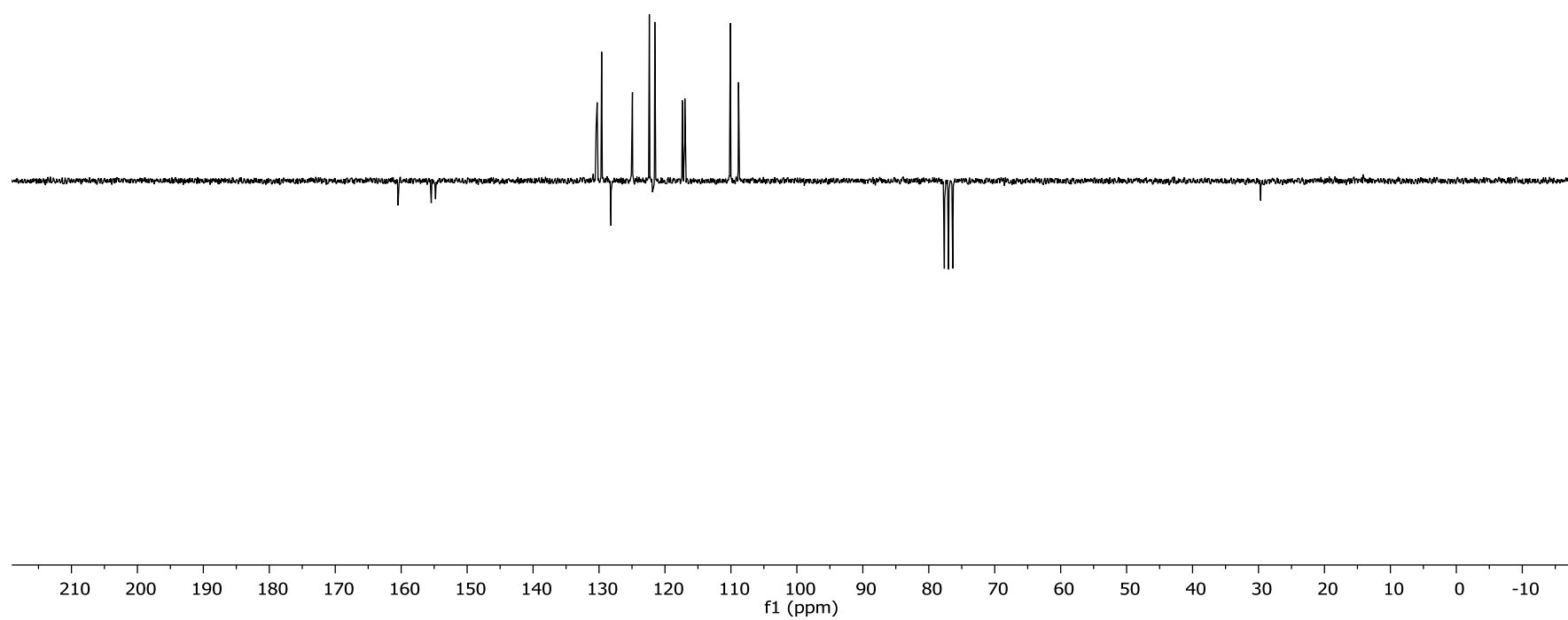
Operator phu
Instrument maxIs

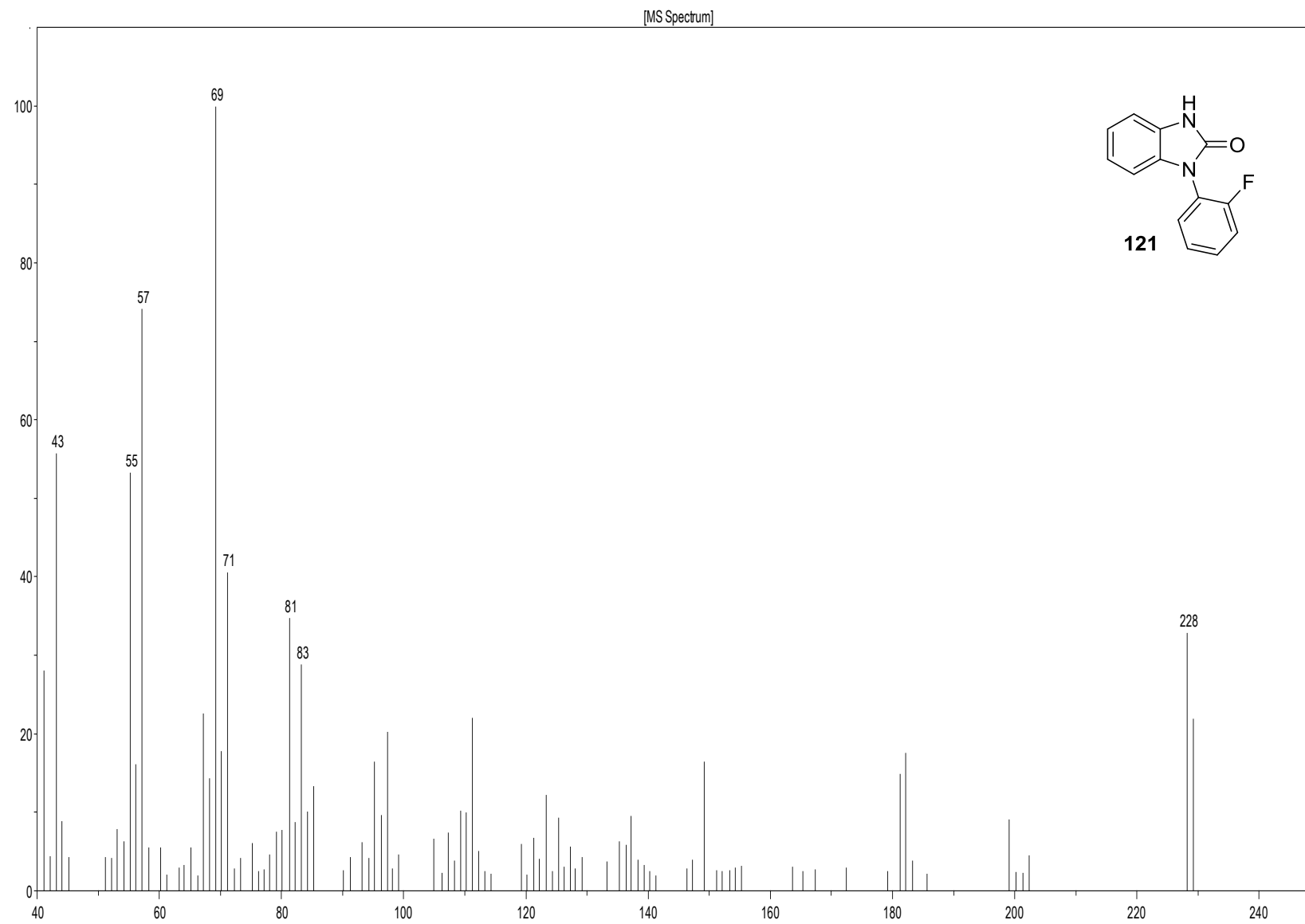






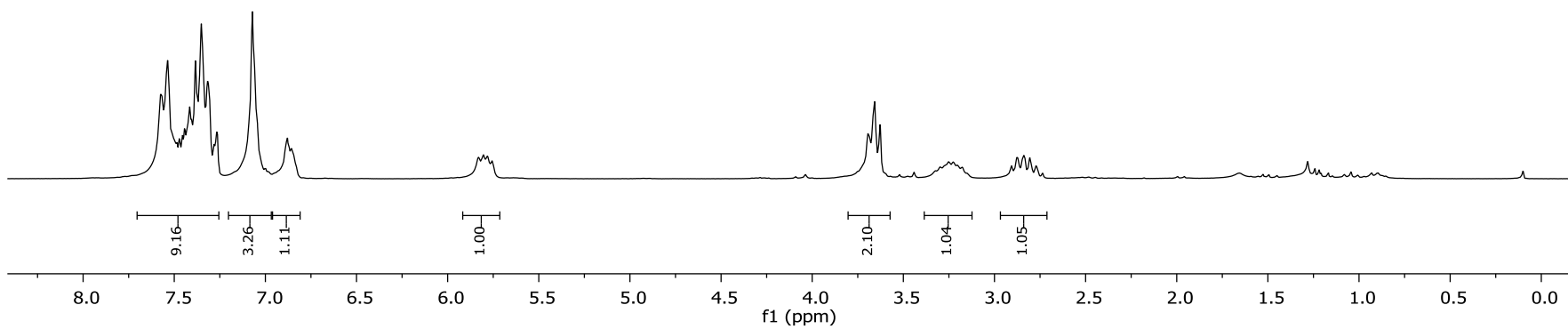
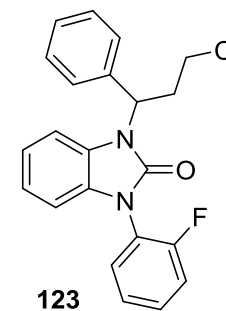
160.48
155.44
154.80
130.44
129.61
128.19
125.01
124.93
122.37
121.89
121.54
117.38
116.99
110.08
108.85

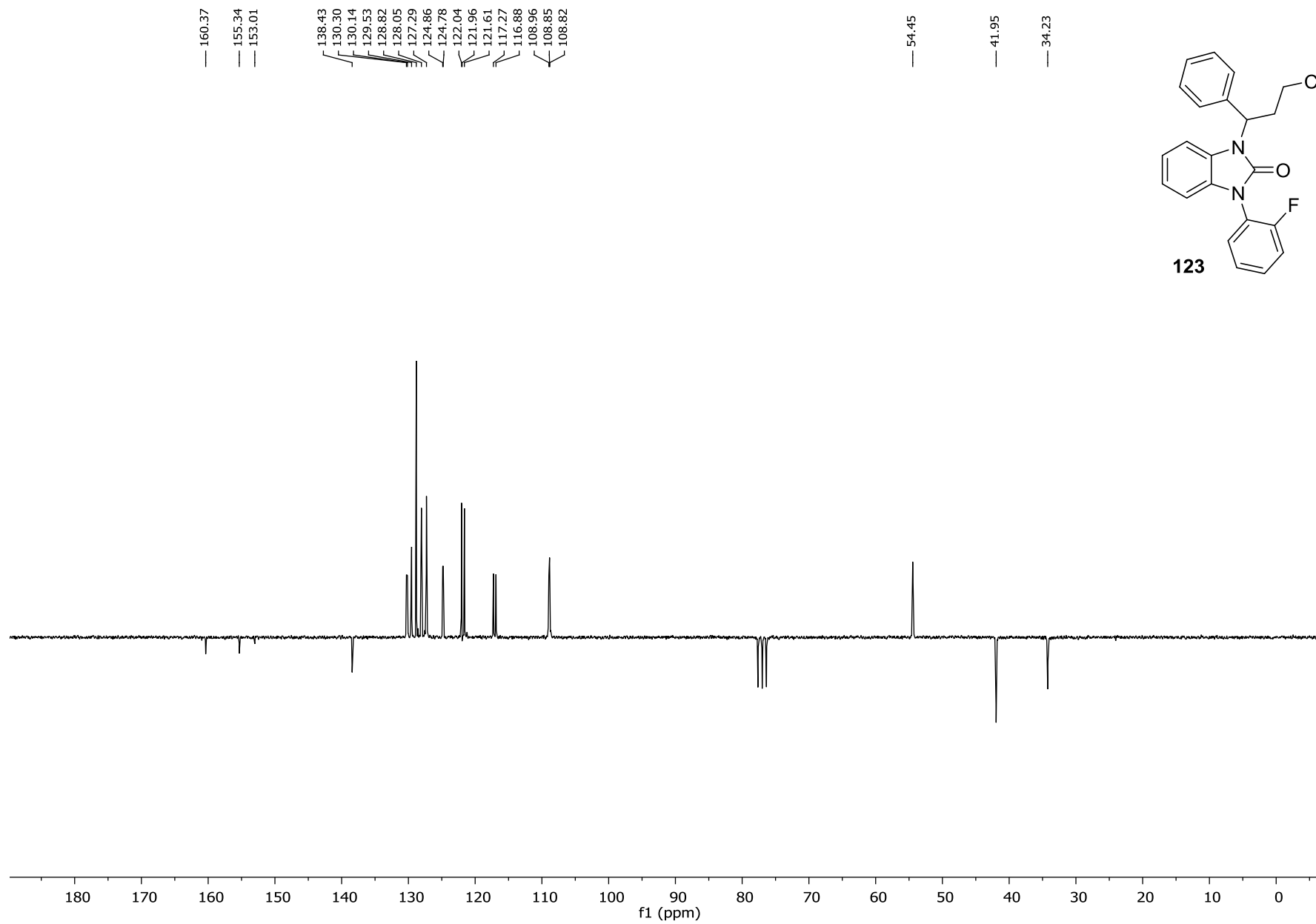


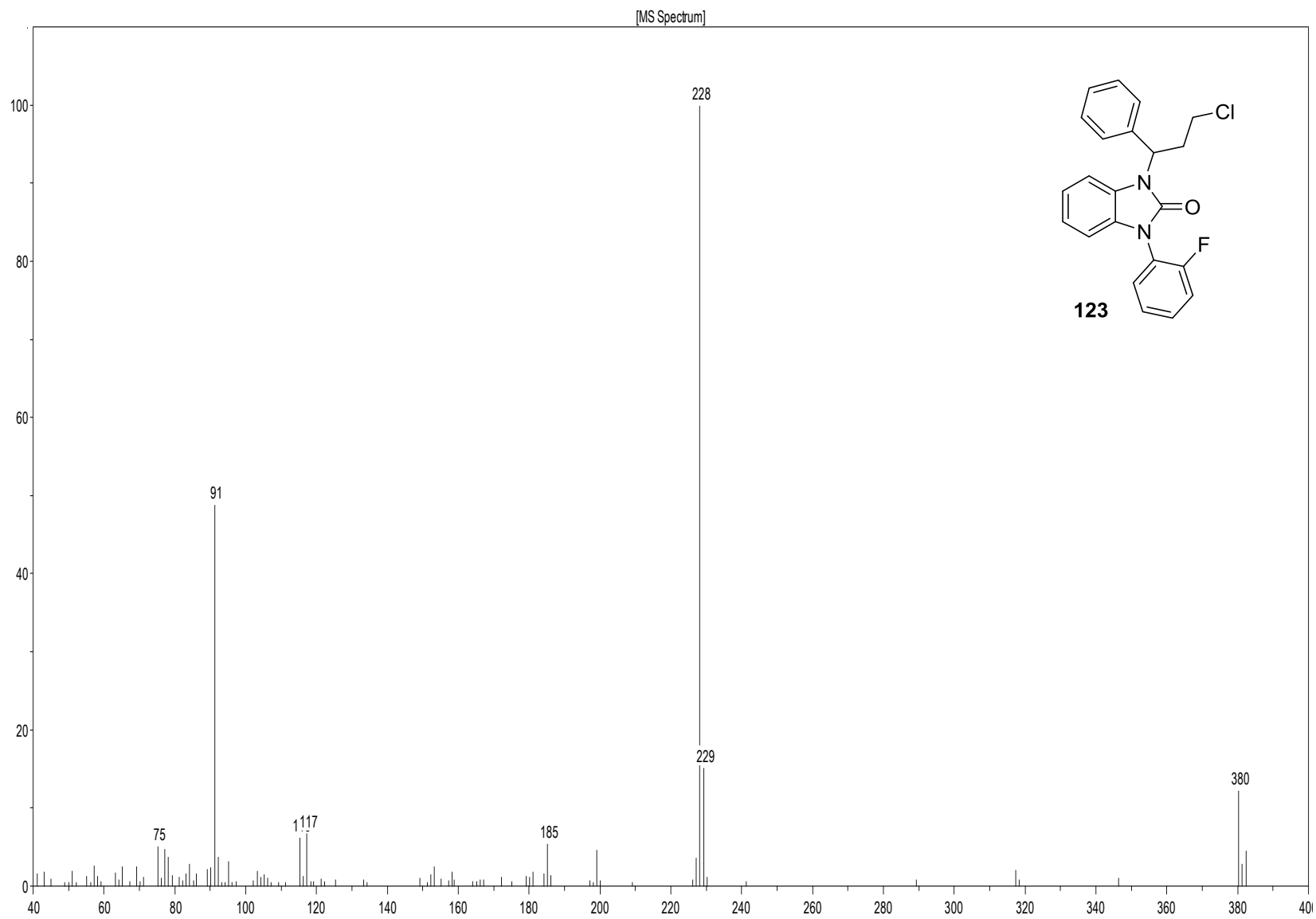


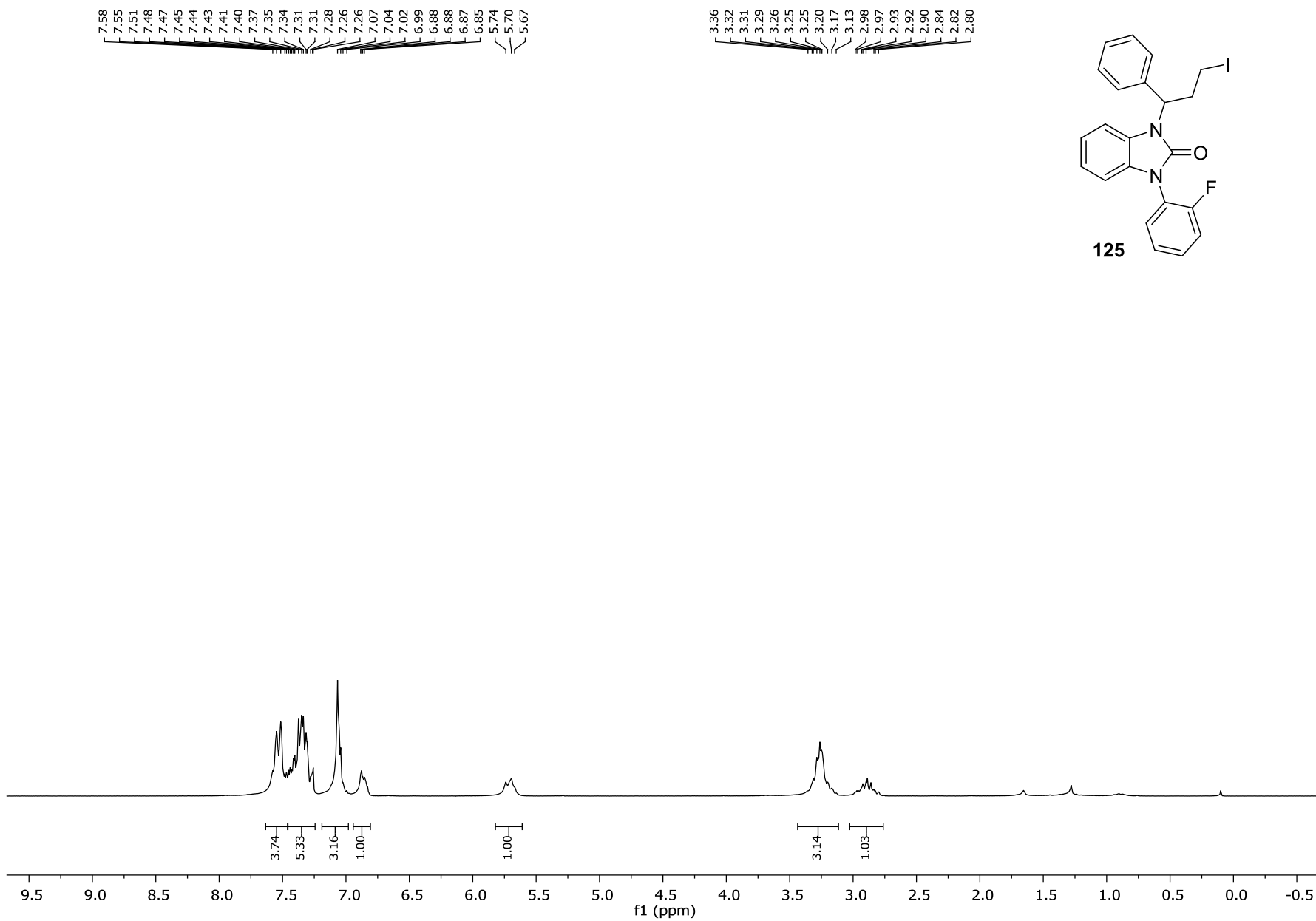
7.57
7.54
7.48
7.47
7.47
7.45
7.44
7.44
7.43
7.42
7.40
7.38
7.37
7.35
7.32
7.31
7.28
7.27
7.26
7.07
7.05
6.88
6.87
6.86
5.83
5.80
5.78
5.76

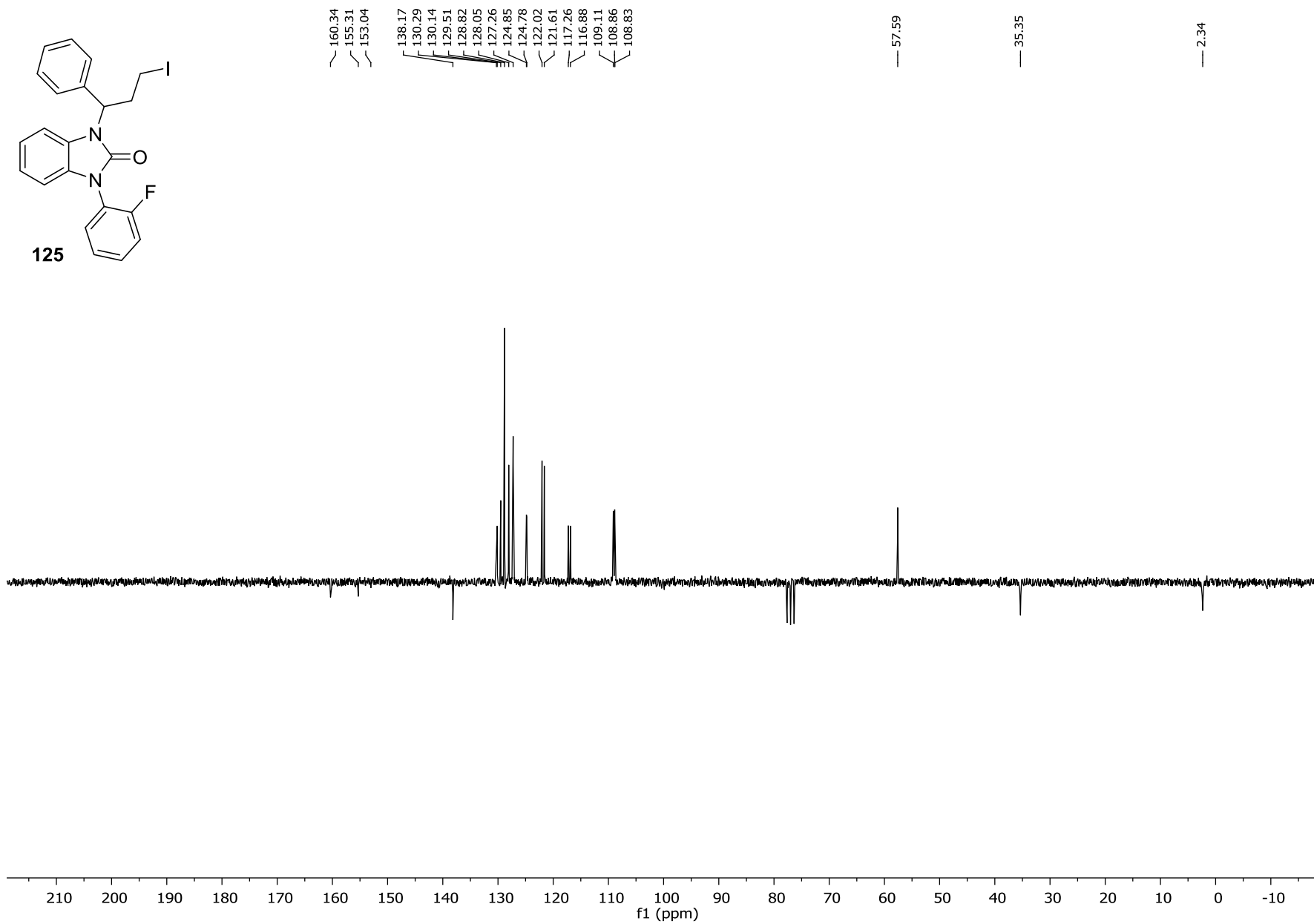
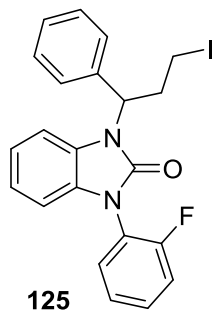
3.69
3.66
3.63
3.32
3.30
3.27
3.25
3.23
3.20
3.18
3.15
2.91
2.88
2.87
2.84
2.84
2.81
2.77
2.74

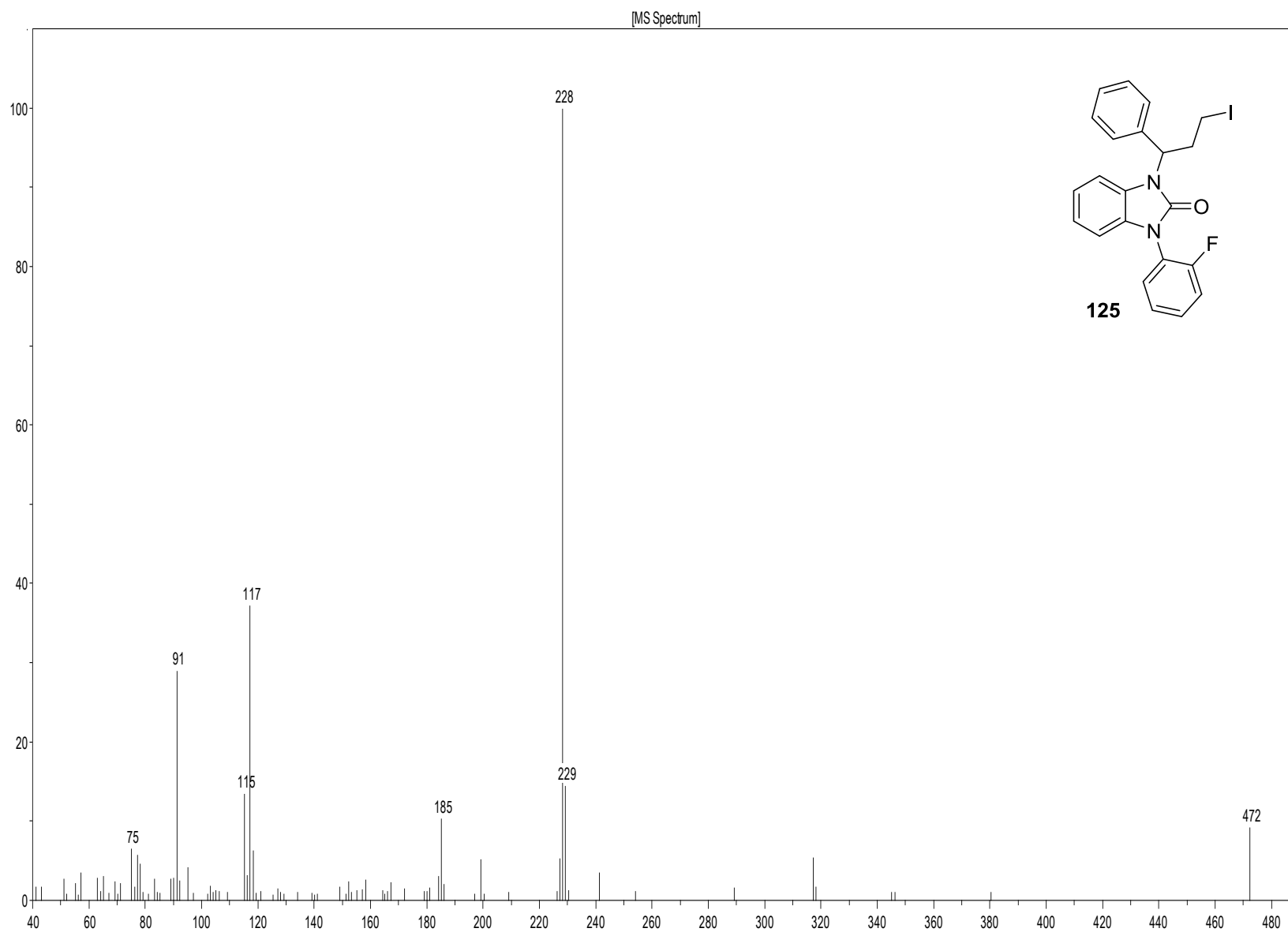


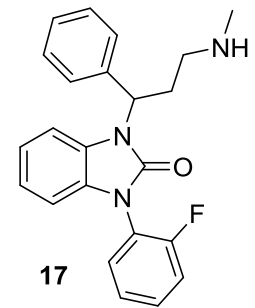
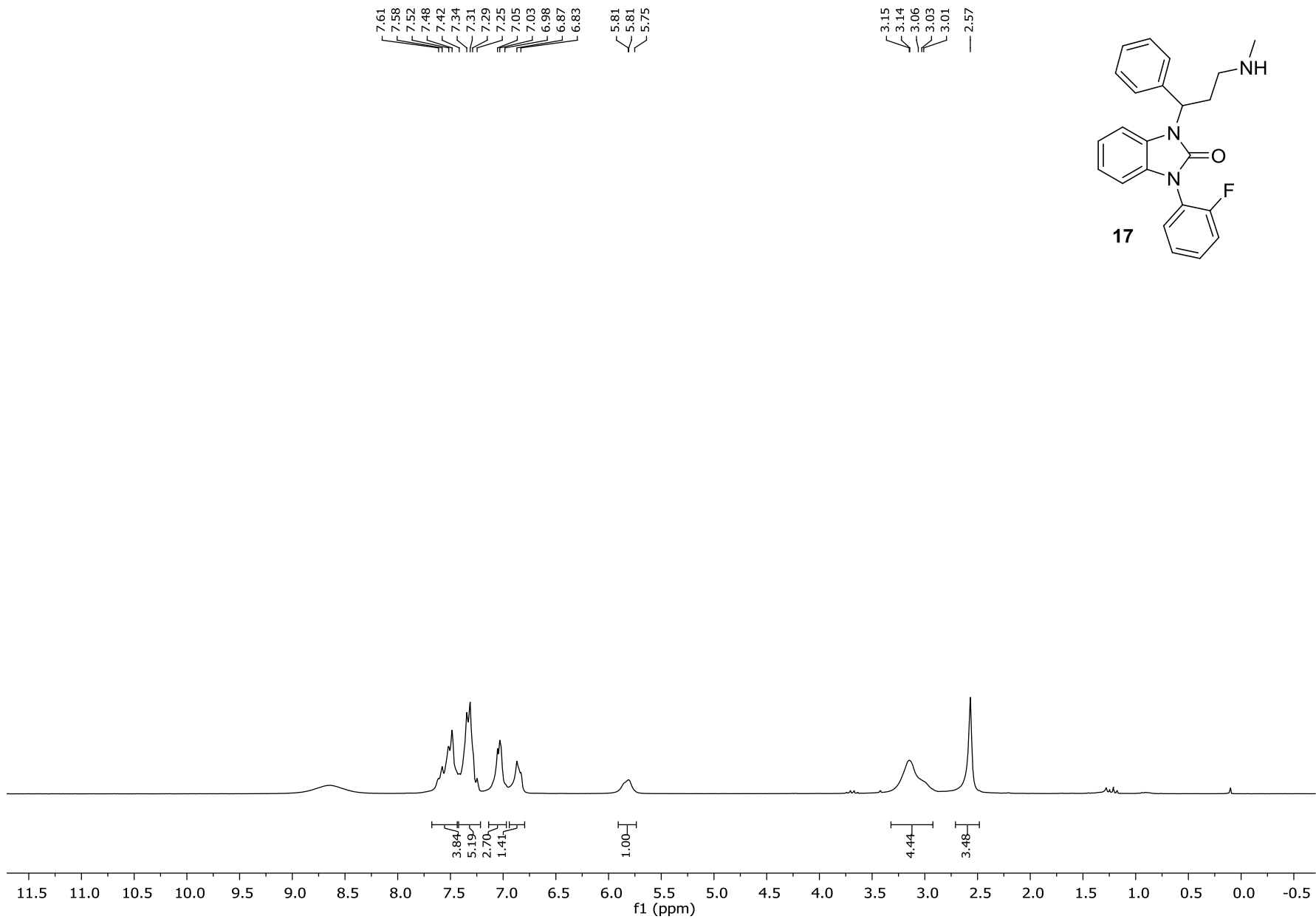


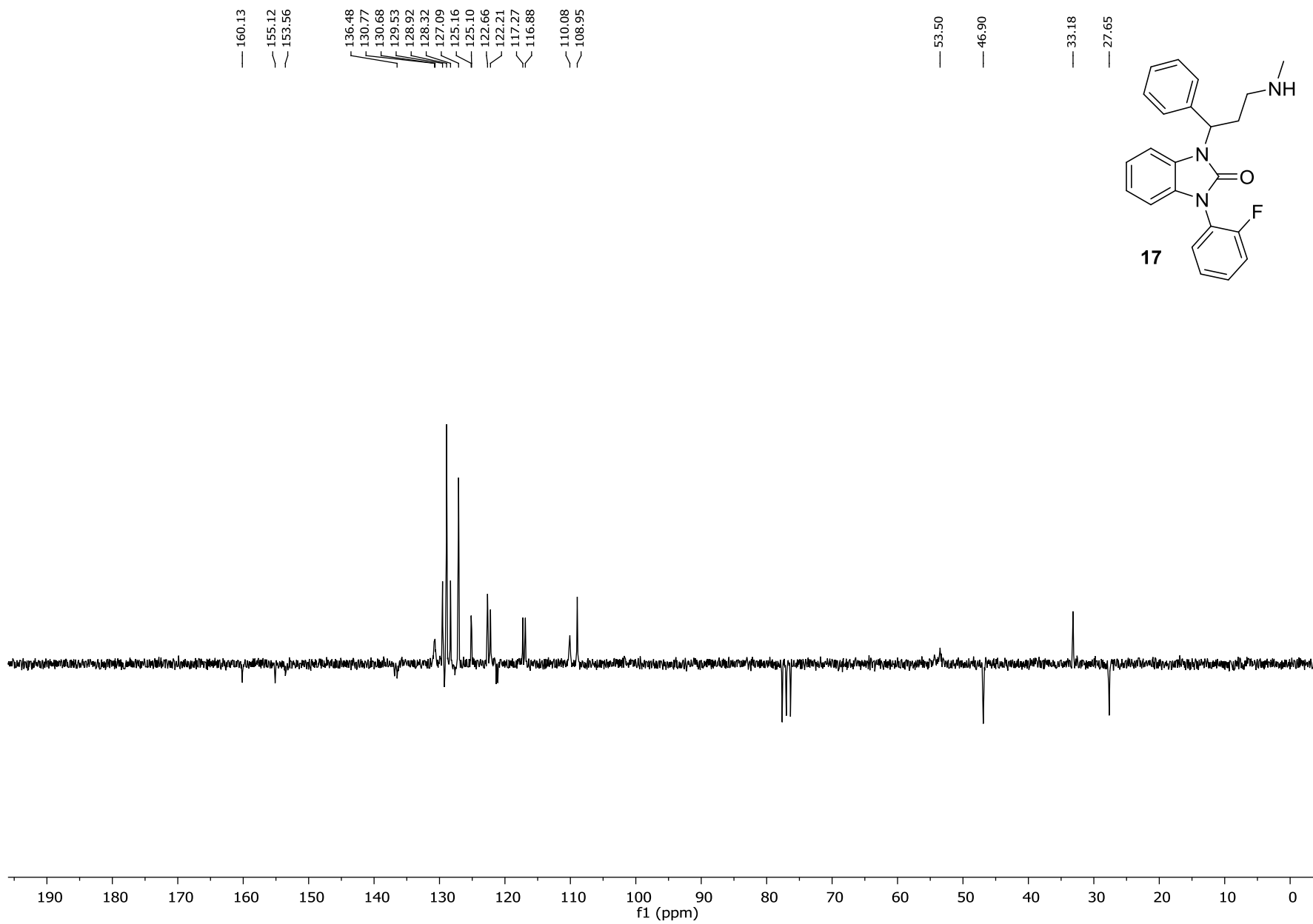




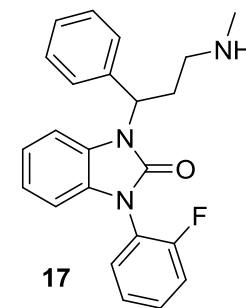
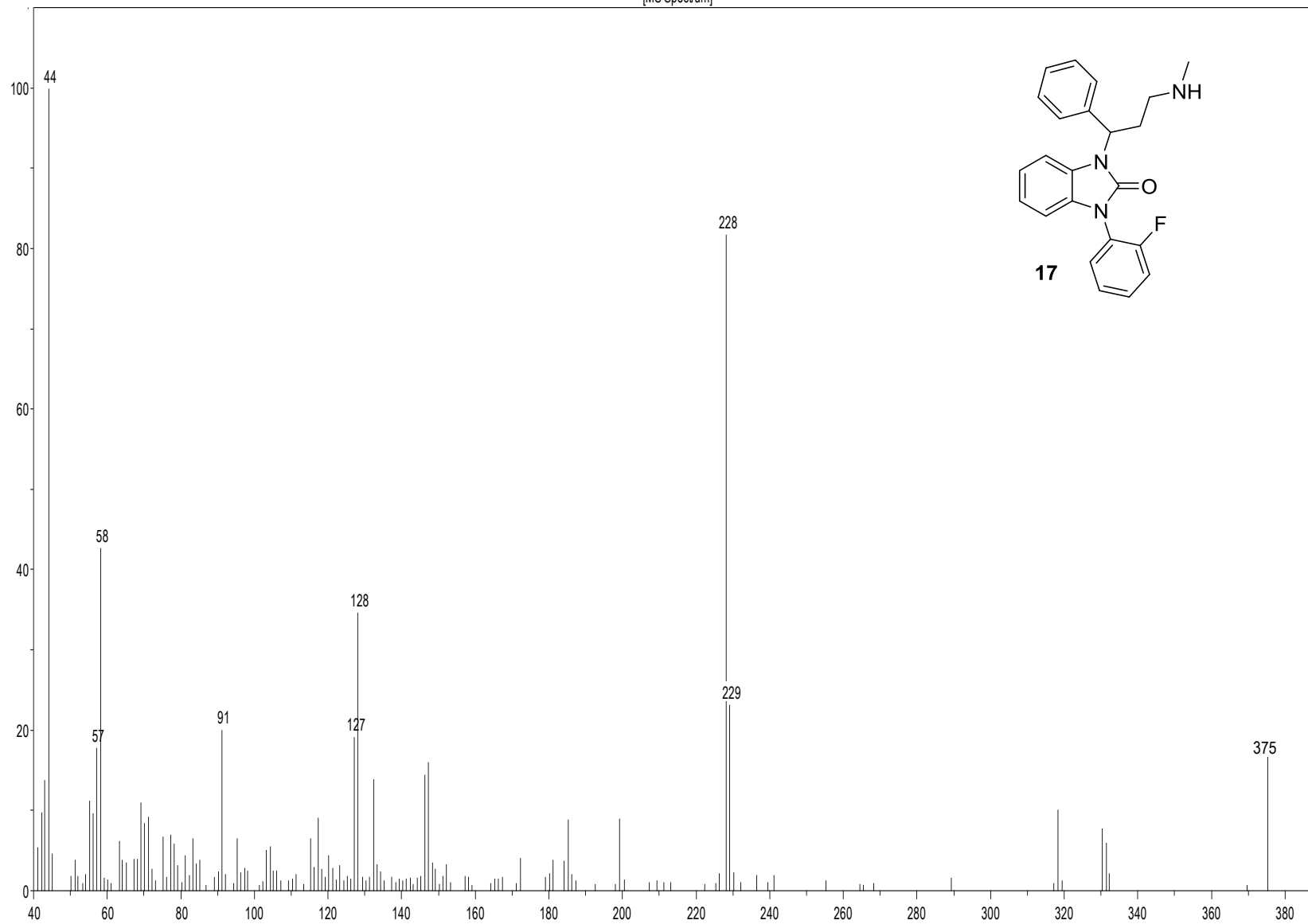








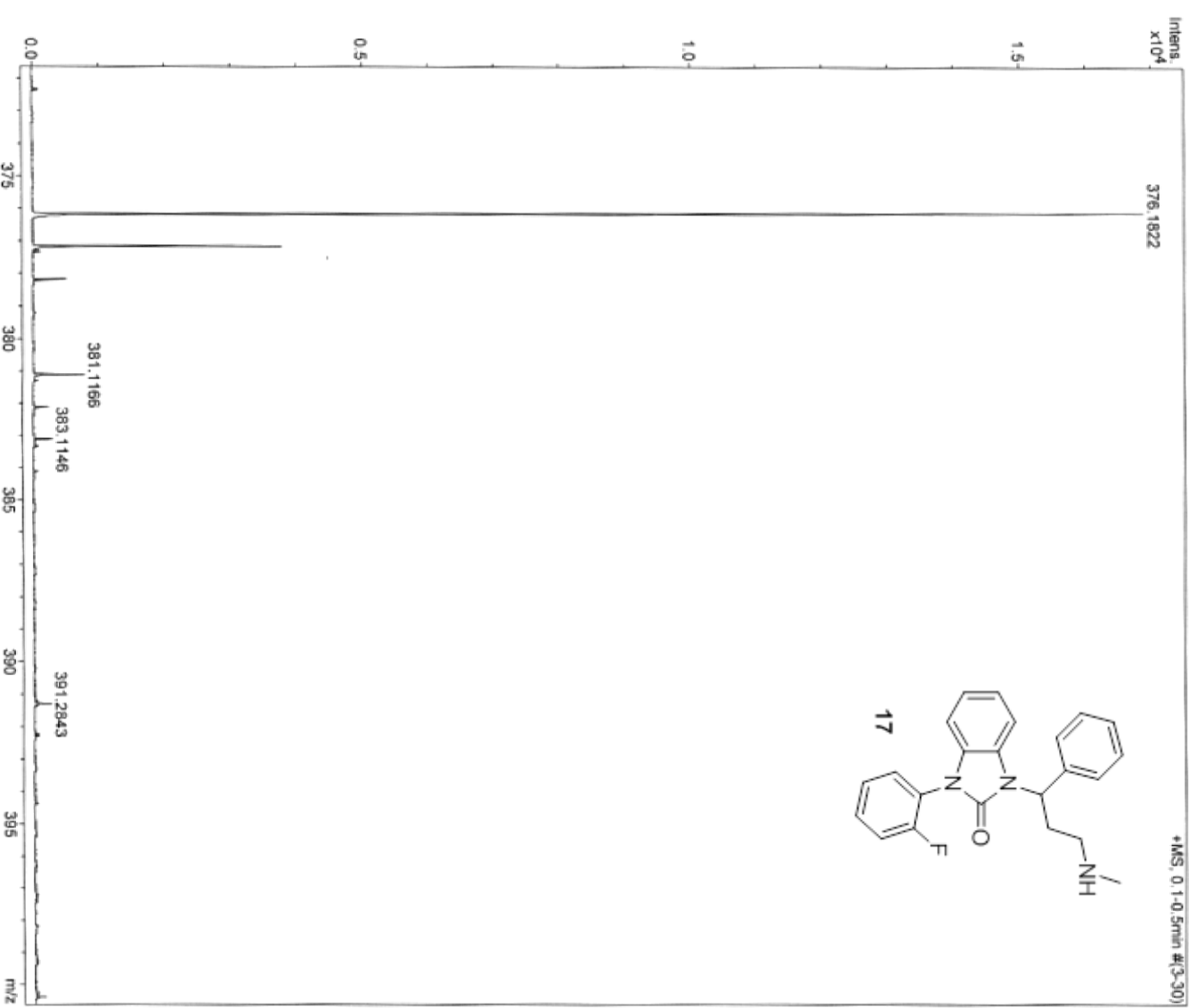
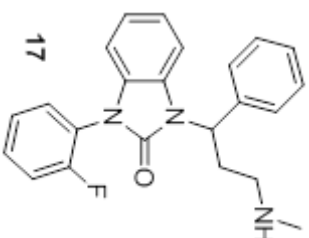
[MS Spectrum]

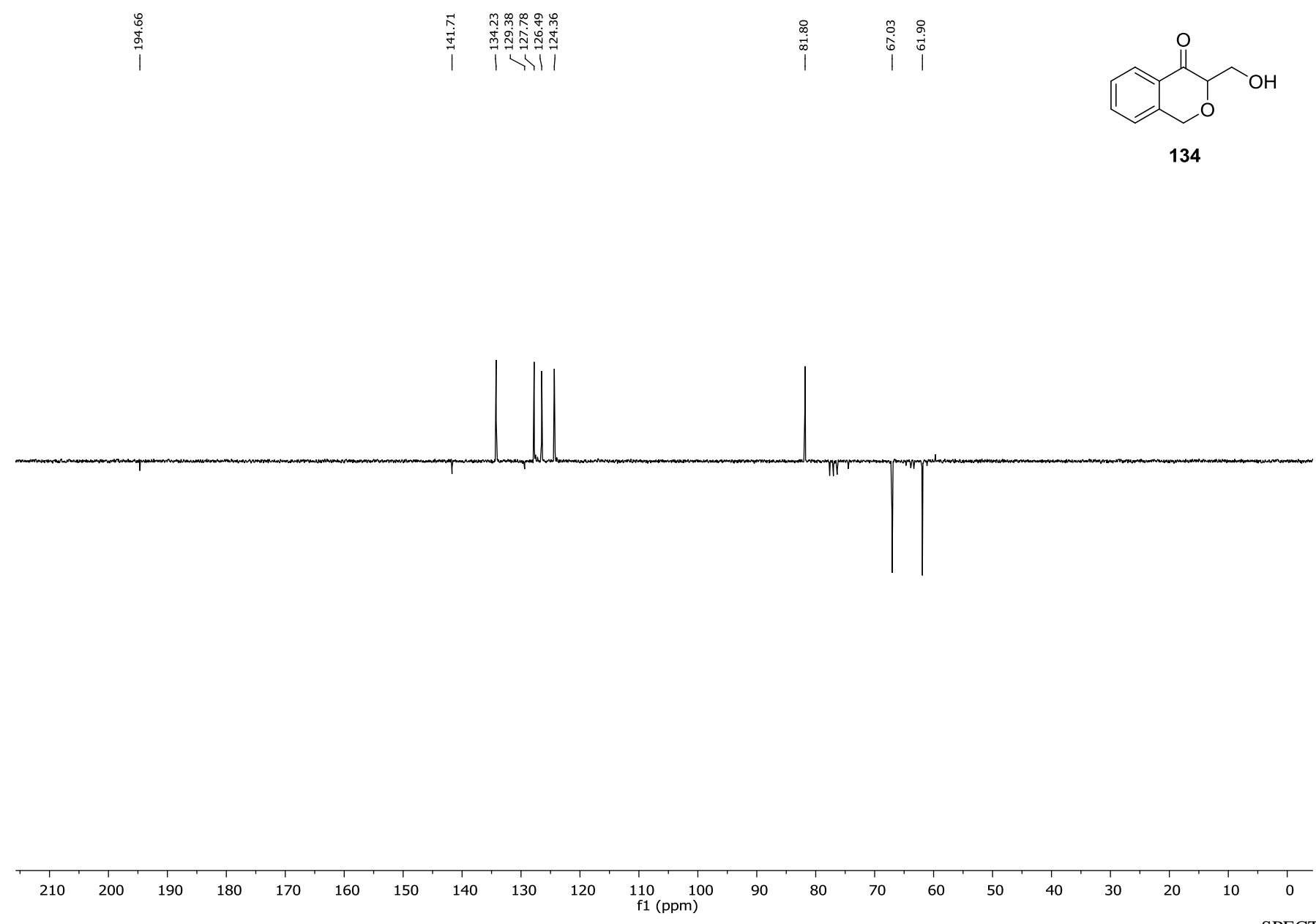
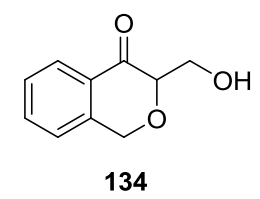


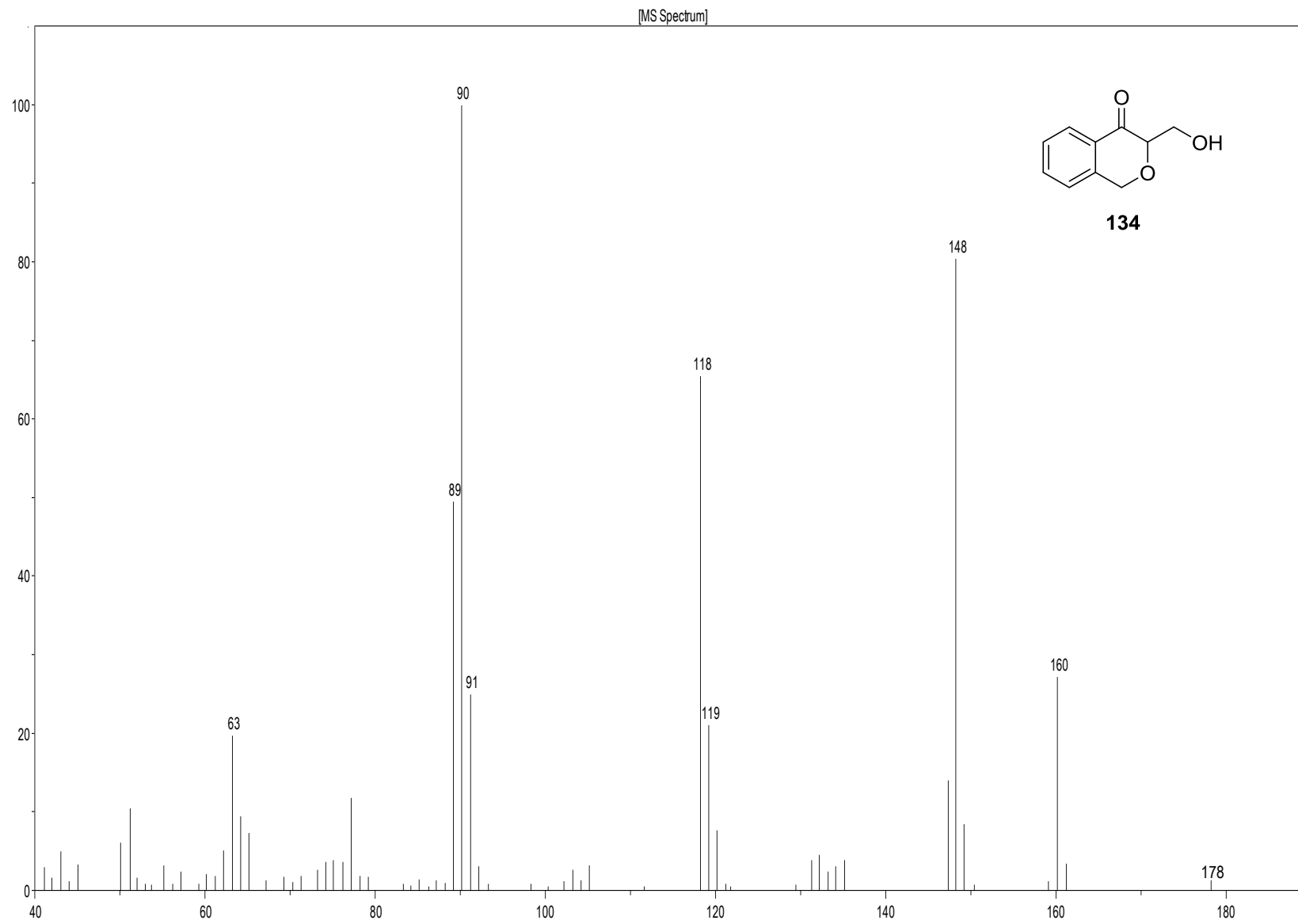
MassenspektrometrieZentrum FakultätChemieUniWien

Analysis Info
Analysis Name D:\Data\MS_MessService\402980000002.d
Method tune_low_MS_Service_01_14.m
Sample Name P11
Auftrageber/Com Neudorfer/Pharm.
ACN/MeOH 0.1% H_2O

Acquisition Date 1/28/2014 8:44:34 AM
Operator phu
Instrument maxis

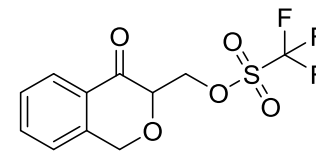




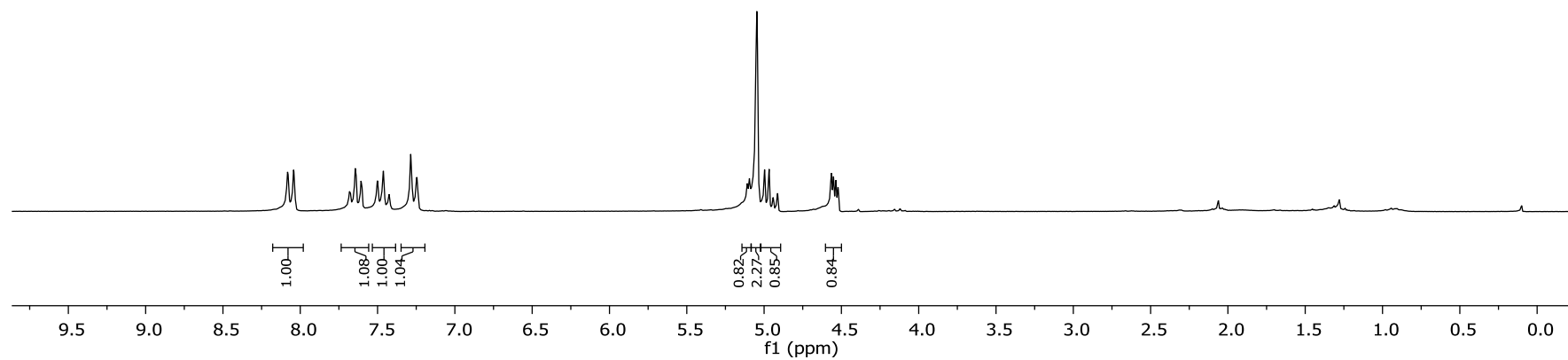


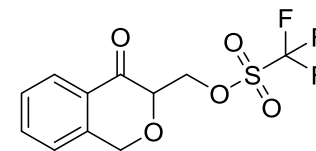
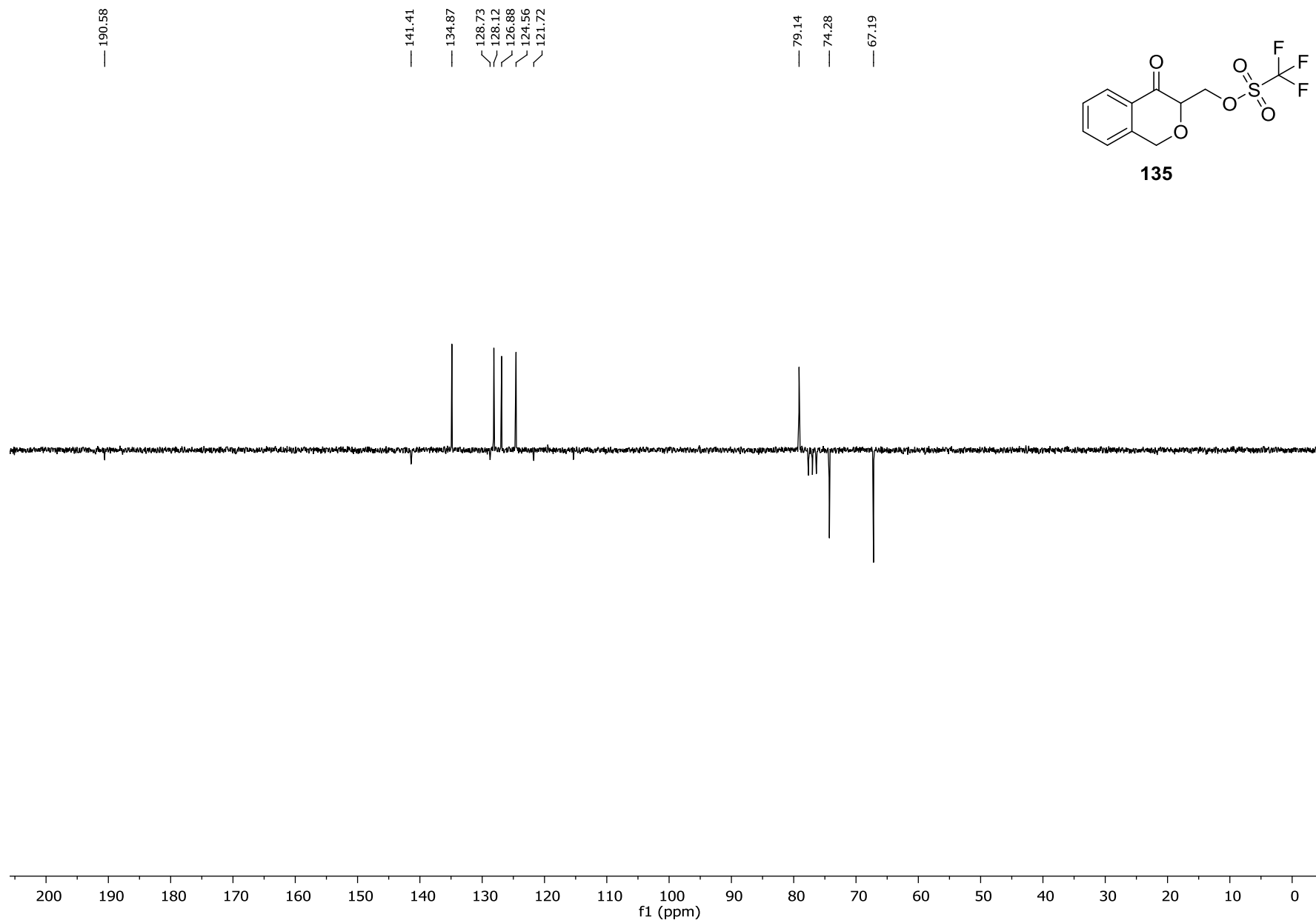
8.08
8.04
7.68
7.64
7.64
7.61
7.60
7.50
7.46
7.43
7.29
7.25

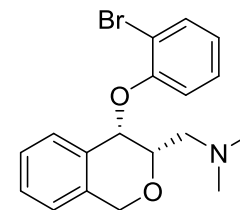
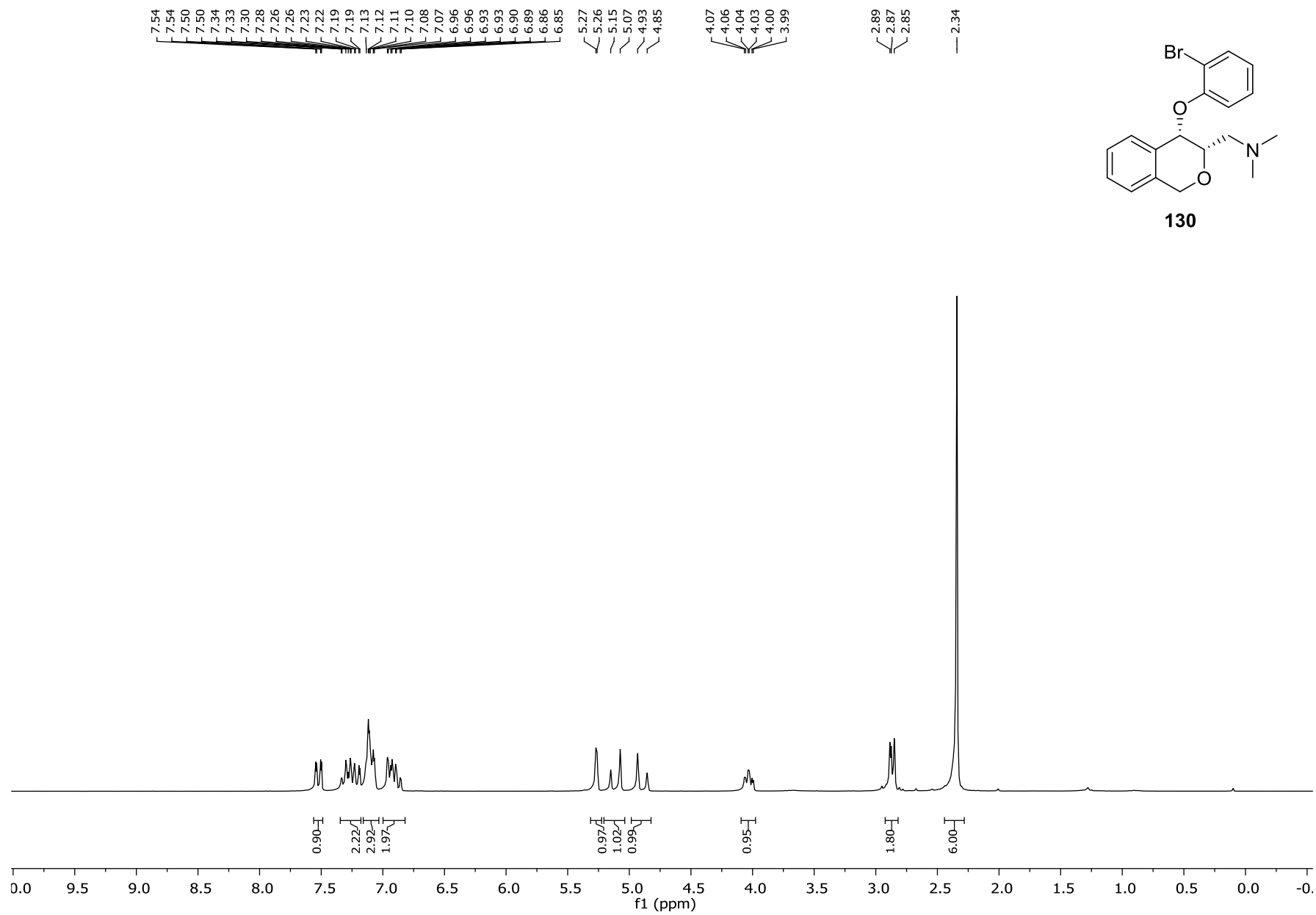
5.11
5.09
5.05
5.00
4.97
4.94
4.91
4.56
4.55
4.53
4.52



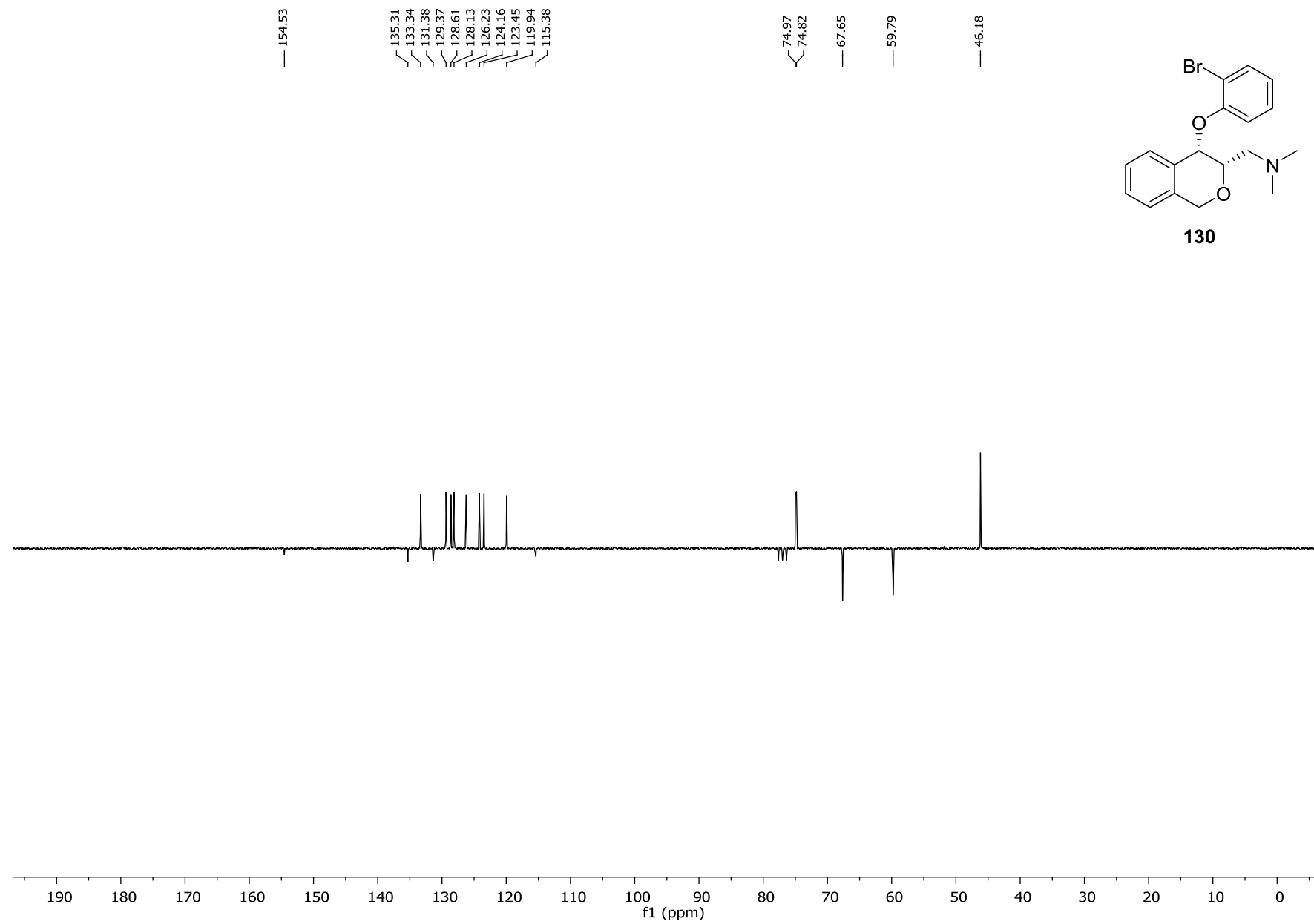
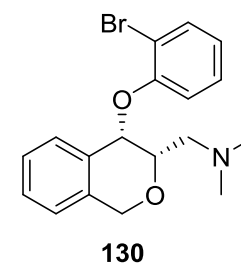
135



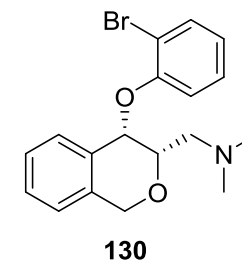
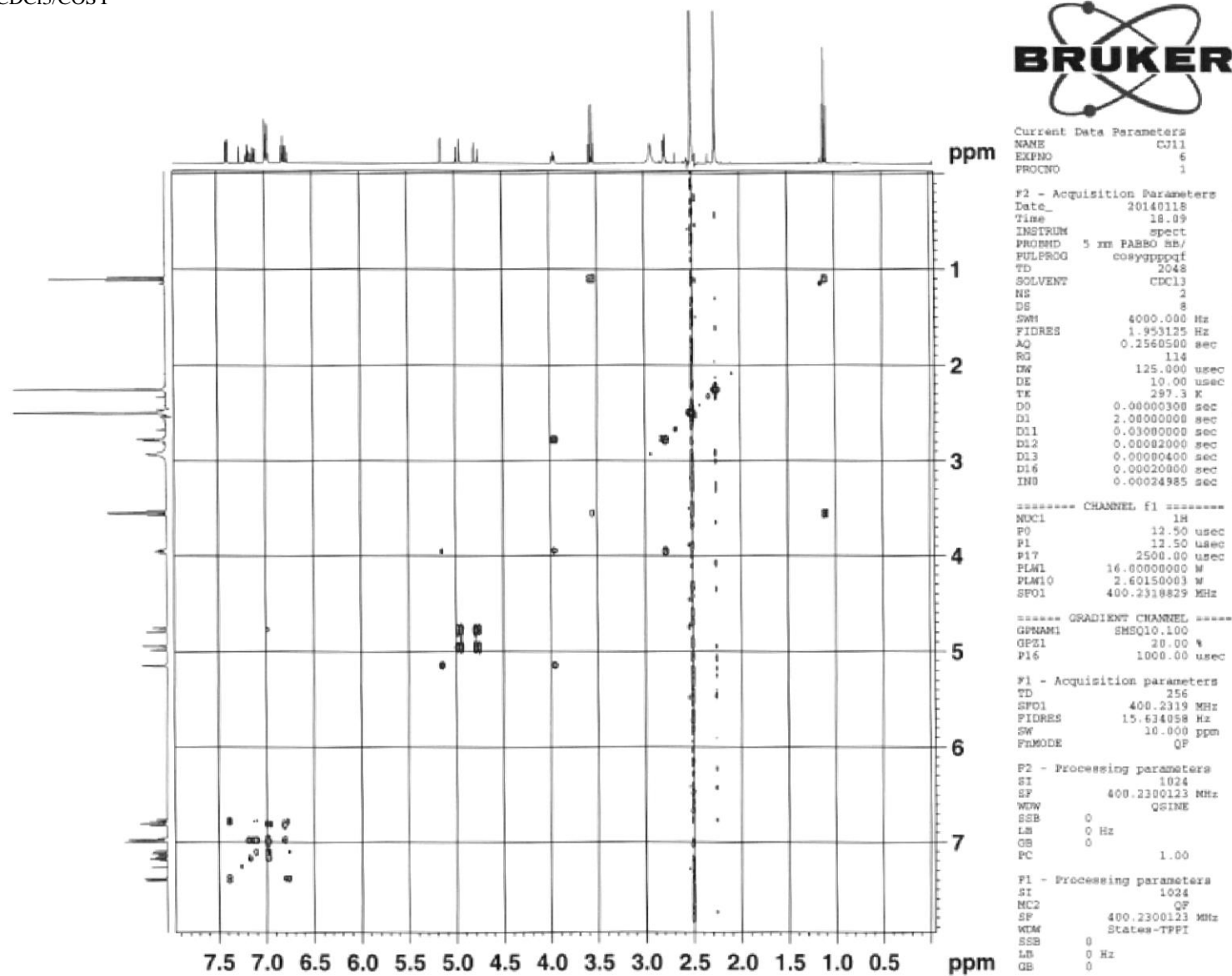
**135**

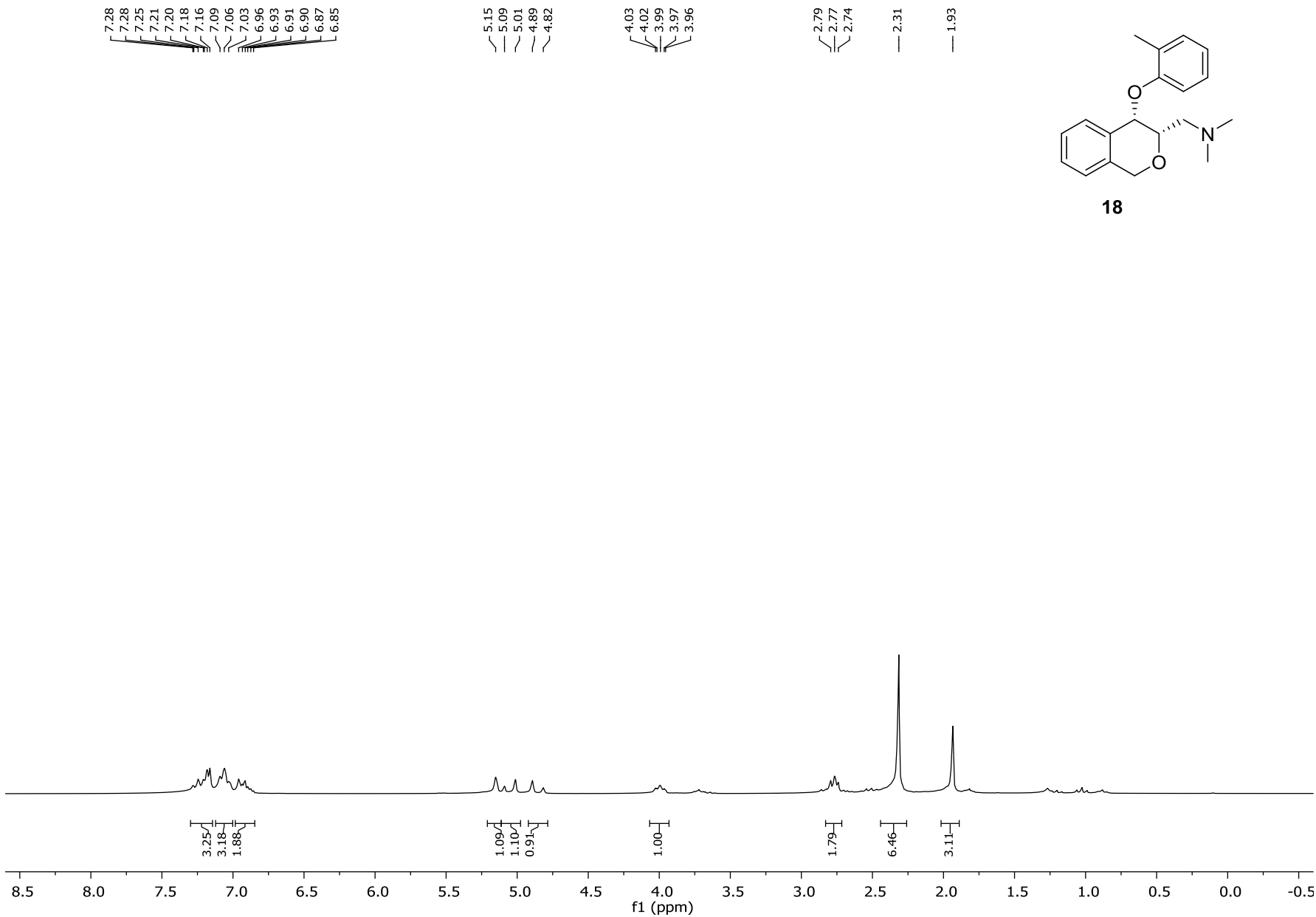


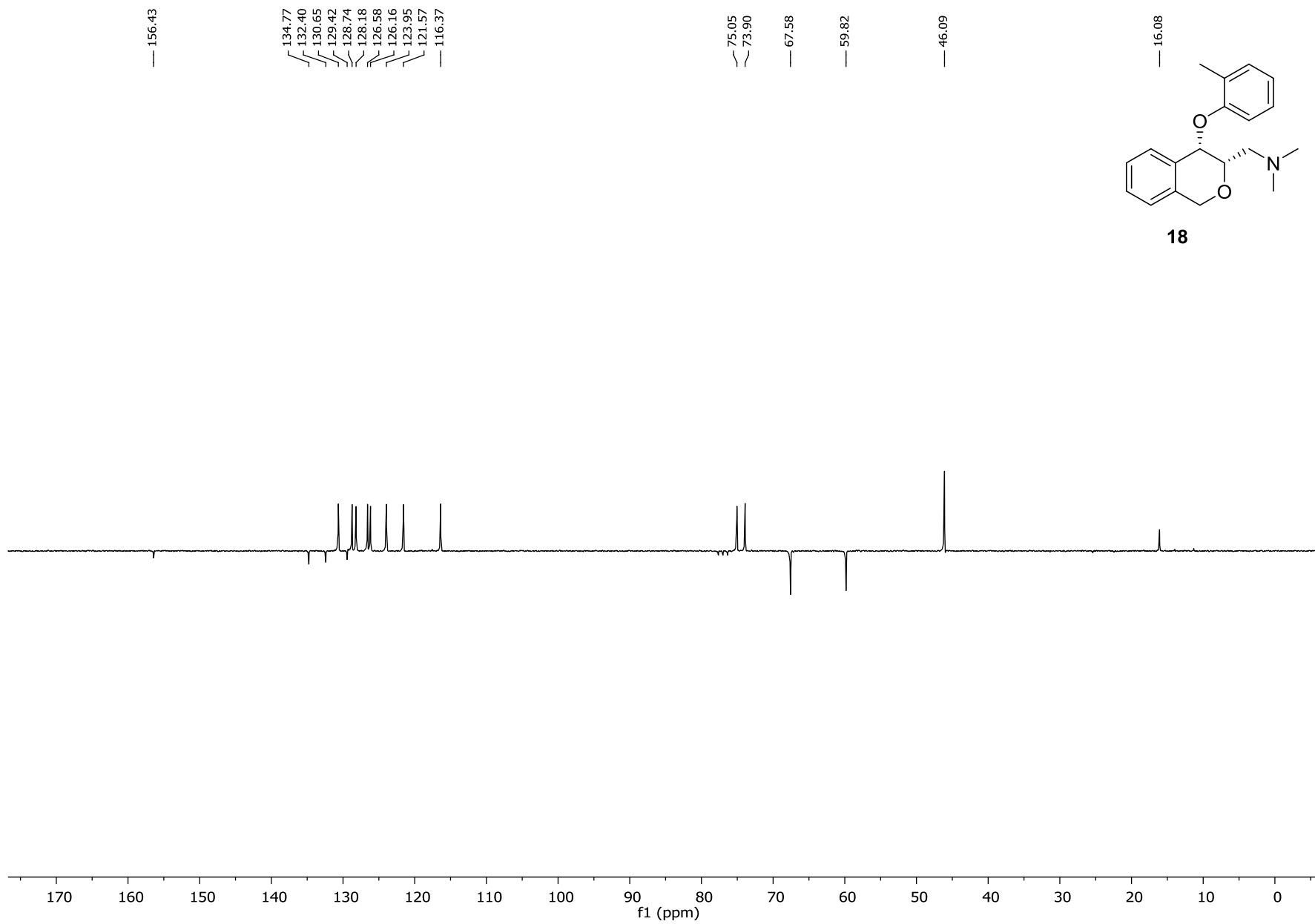
130



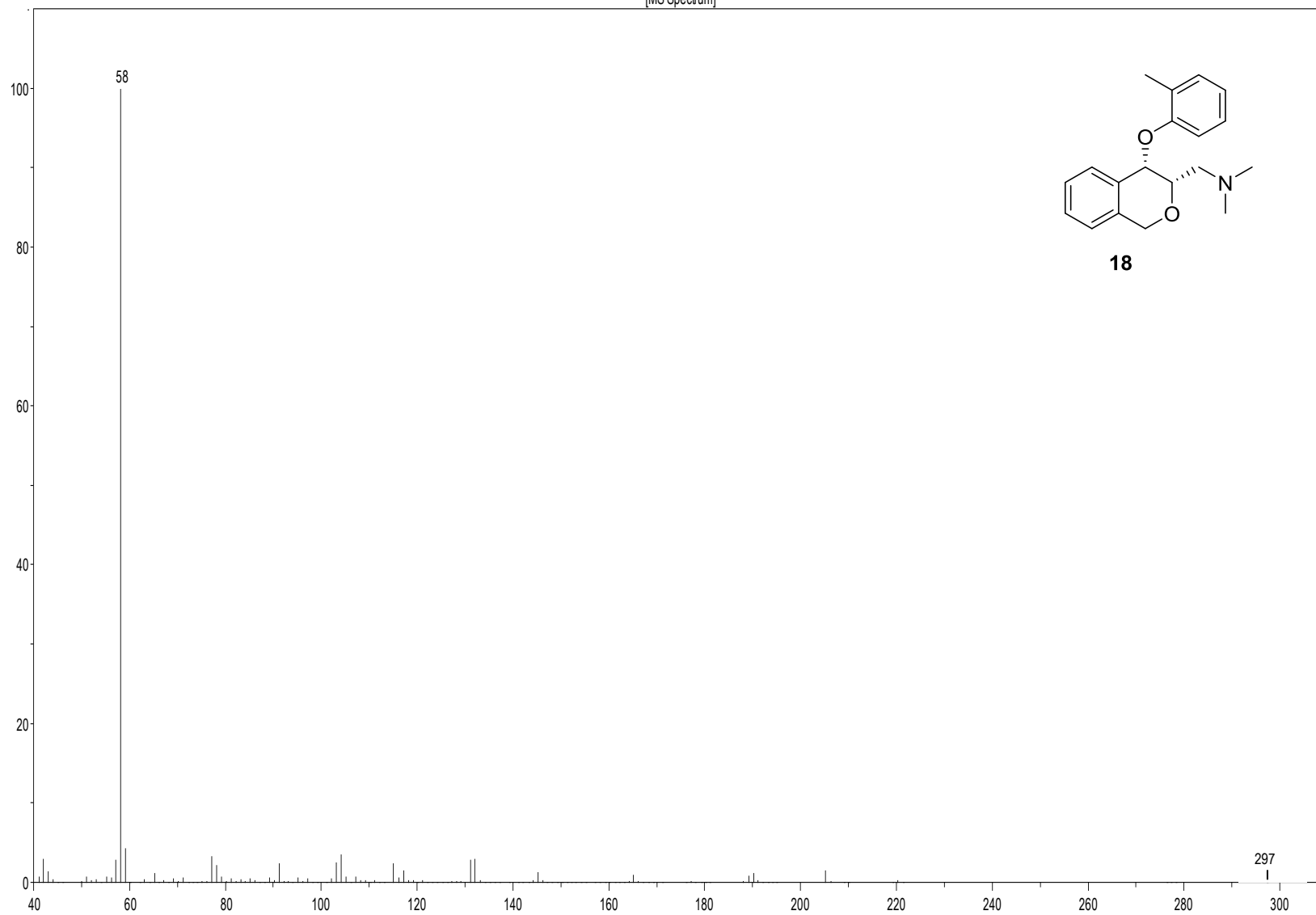
CJ11/CDC13/COSY







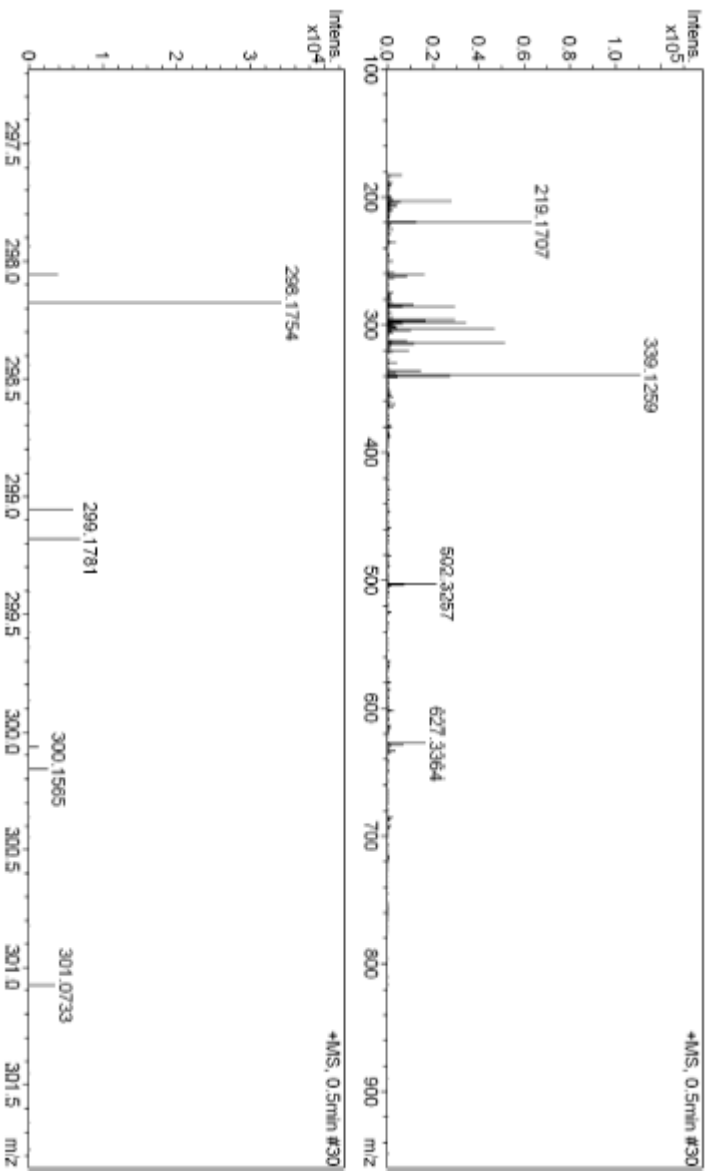
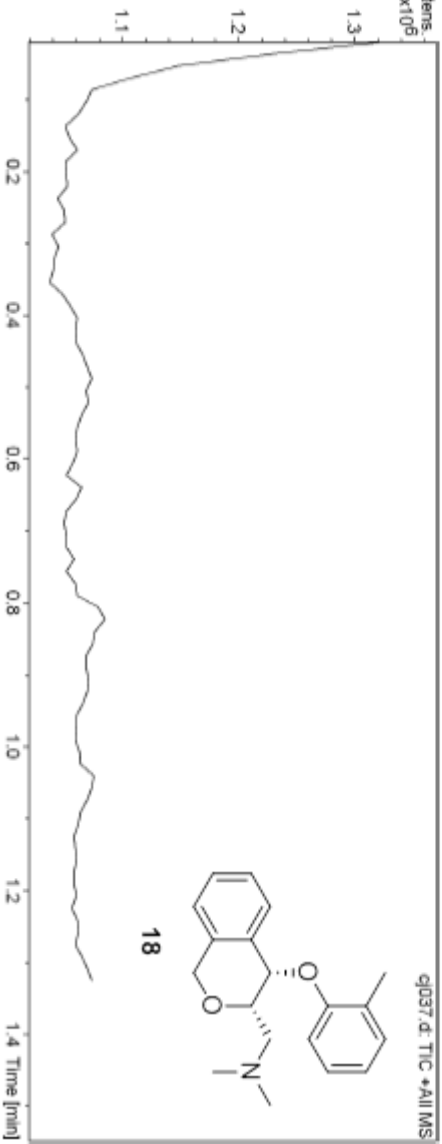
[MS Spectrum]

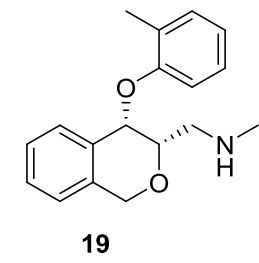
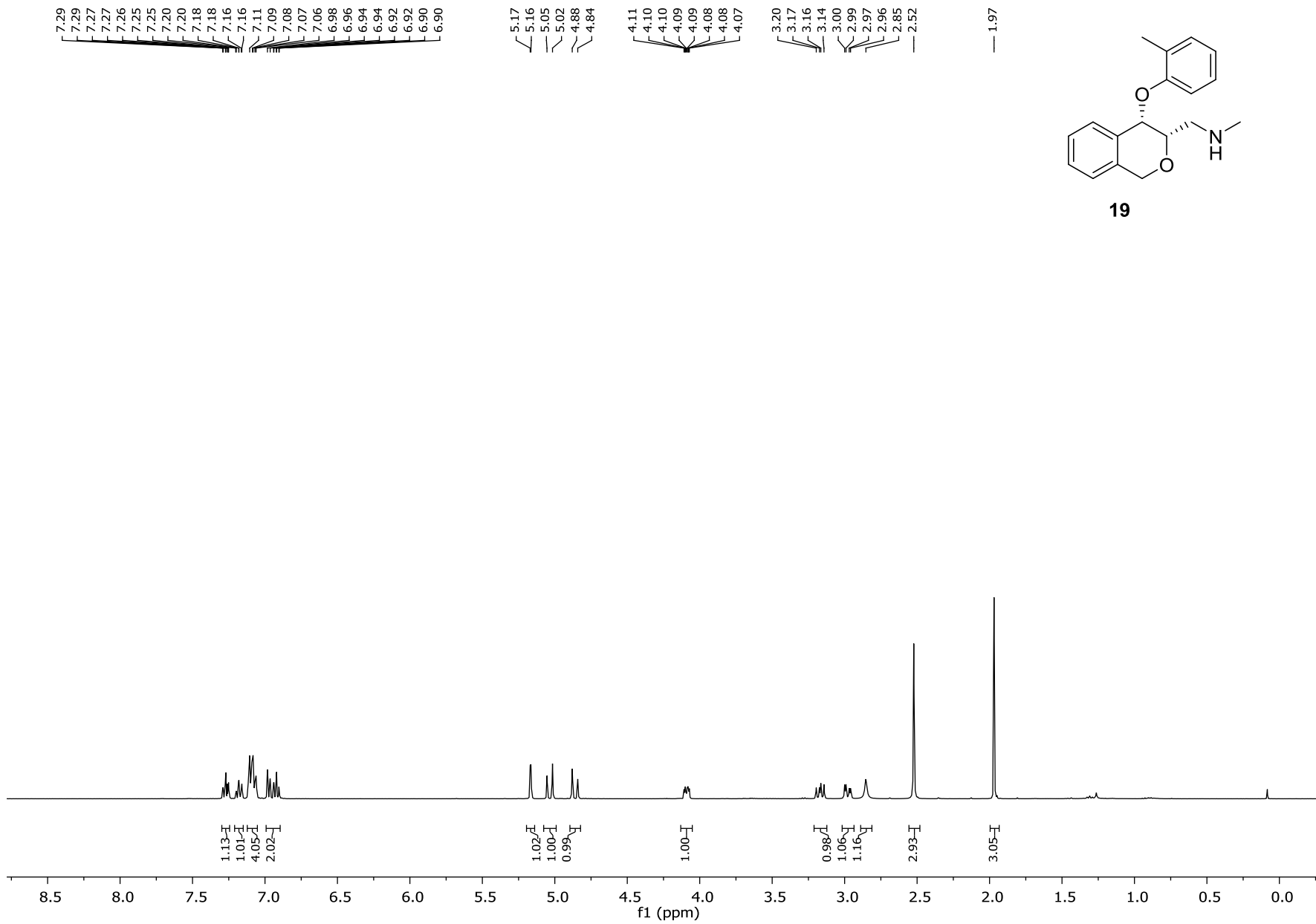


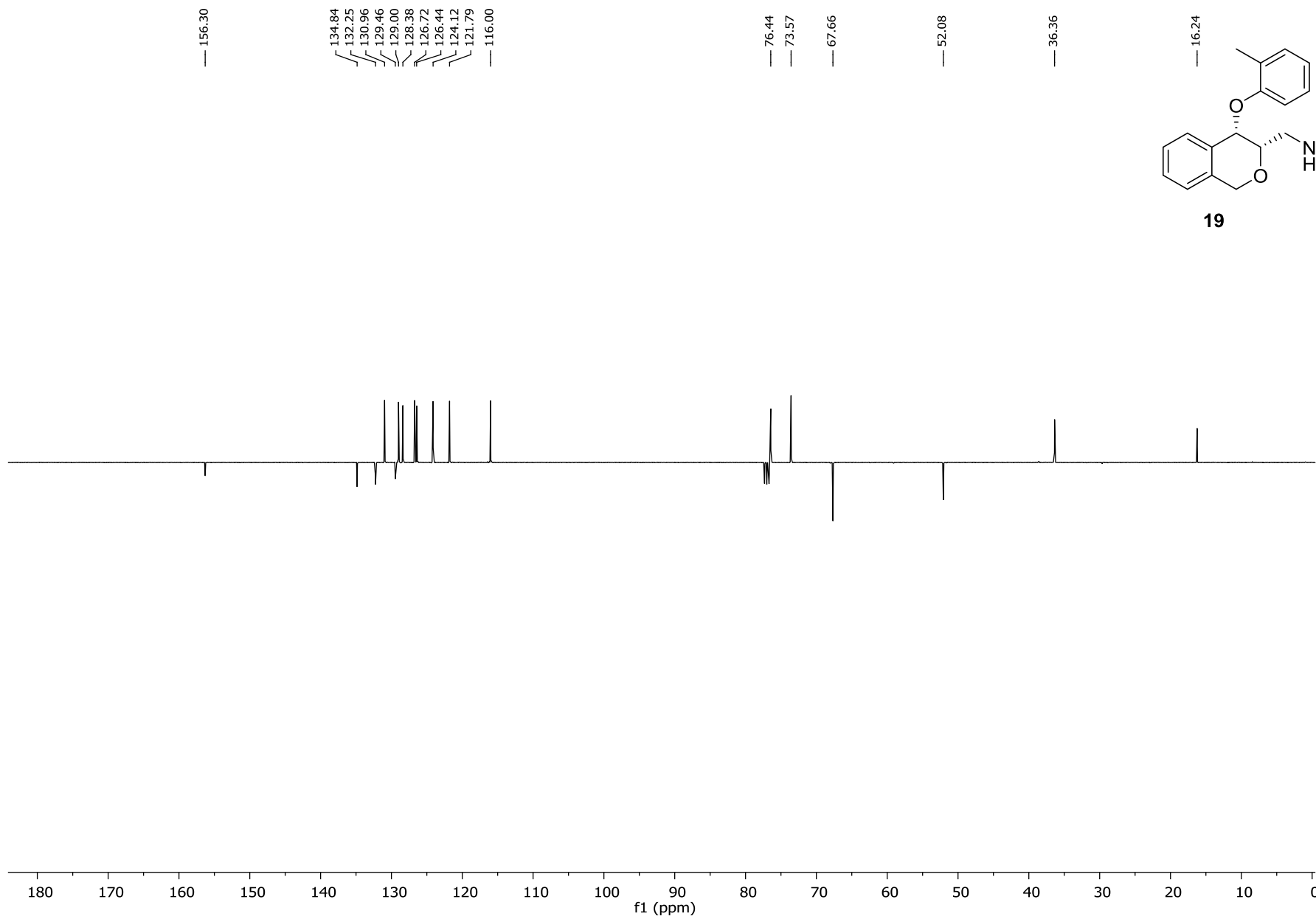
Display Report

Analysis Info	Acquisition Date 6/24/2014 11:34:22 AM
Analysis Name D:\Data\Externe Messungen\qj037.d	Operator JFI
Method CN_24062014.m	Instrument microTOF-Q II 10240
Sample Name qj037	Comment

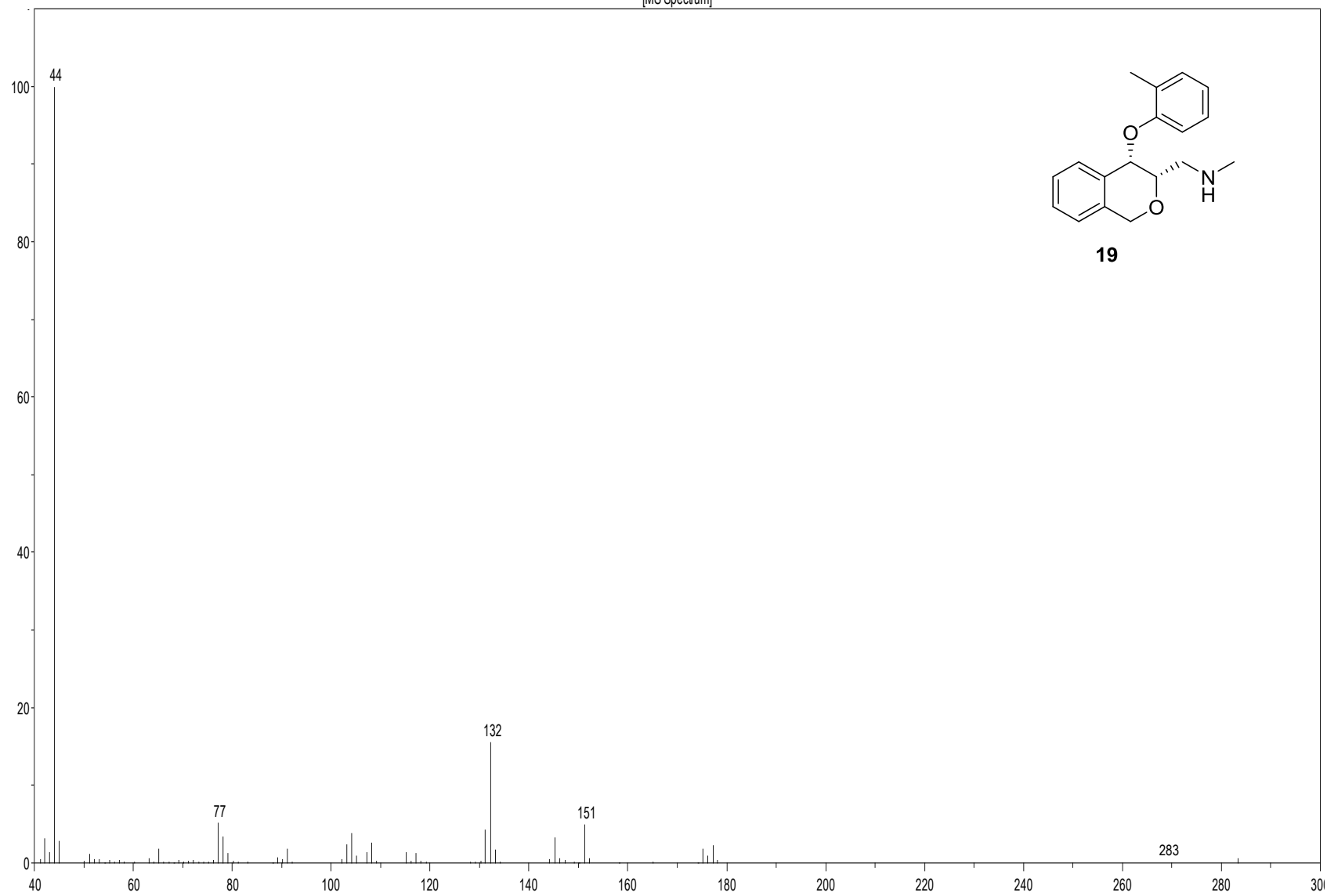
Acquisition Parameter			
Source Type ESI	Ion Polarity Positive	Set Nebulizer 0.4 Bar	
Focus Active	Set Capillary 4500 V	Set Dry Heater 180 °C	
Scan Begin 100 m/z	Set End Plate Offset -500 V	Set Dry Gas 4.0 l/min	
Scan End 1000 m/z	Set Collision Cell RF 350.0 Vpp	Set Divert Valve Waste	







[MS Spectrum]



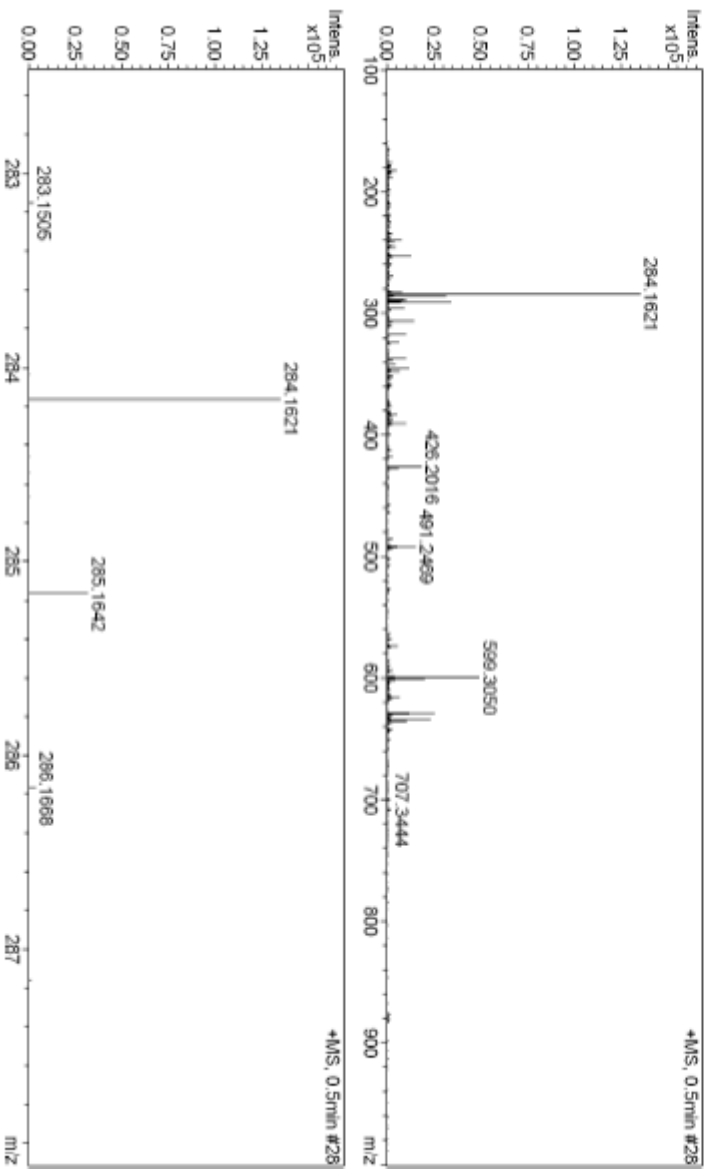
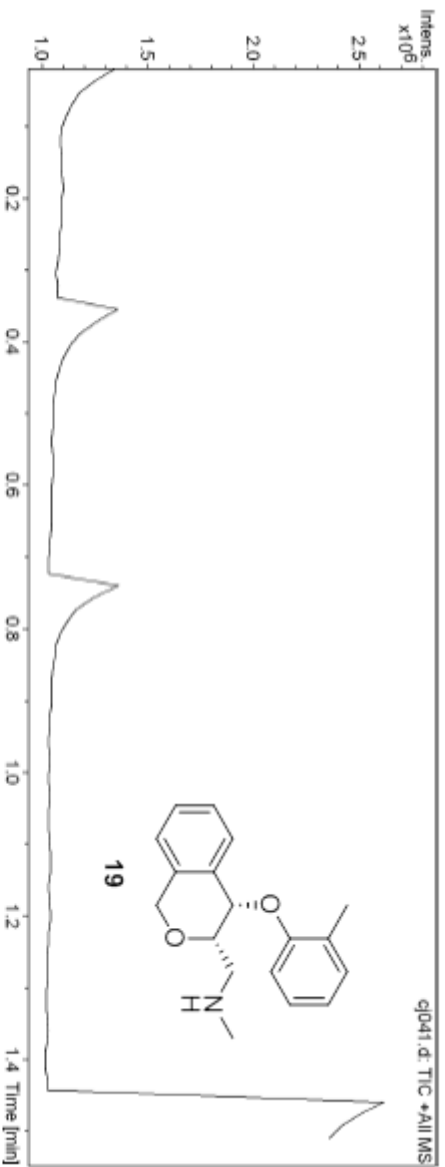
Display Report

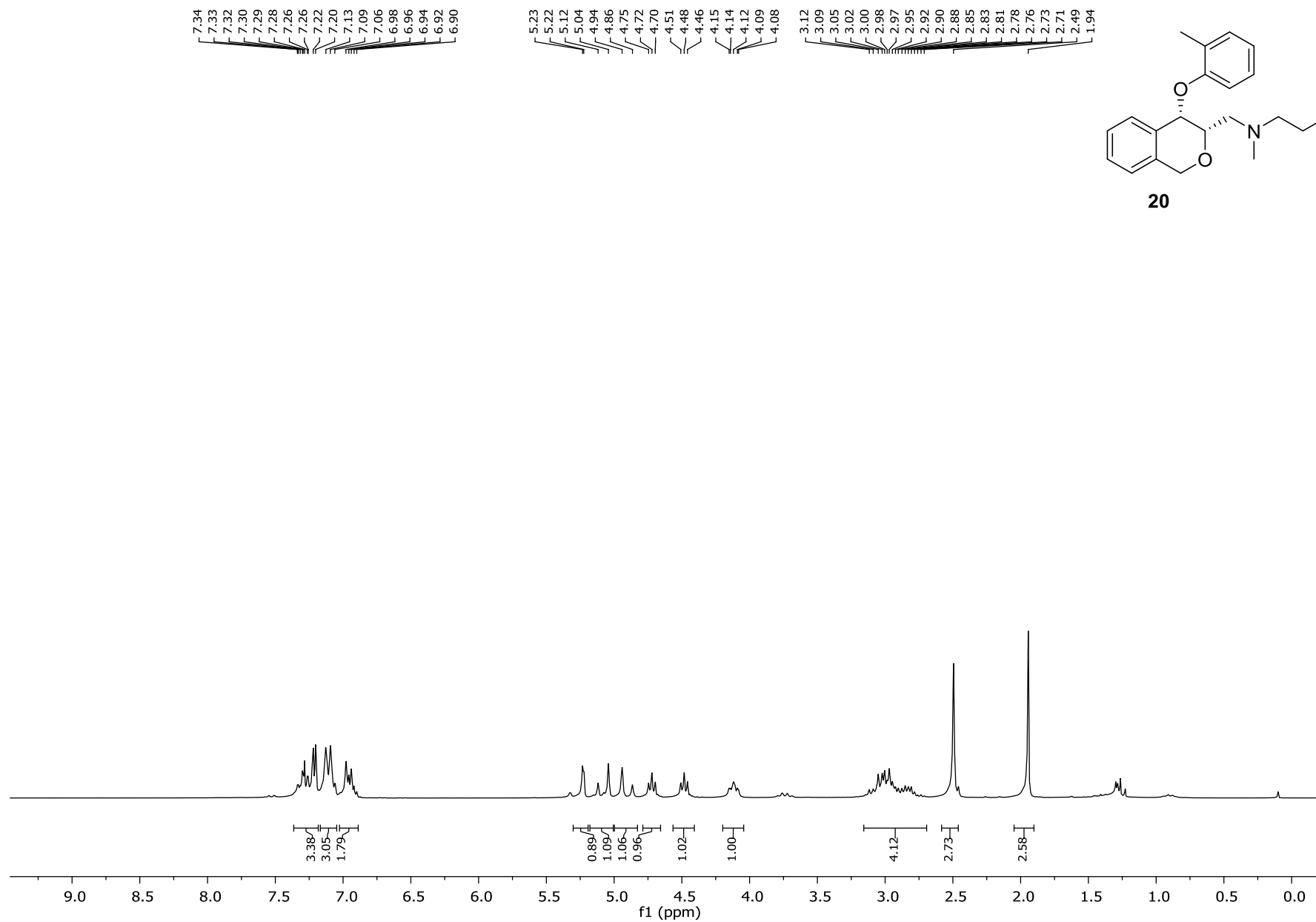
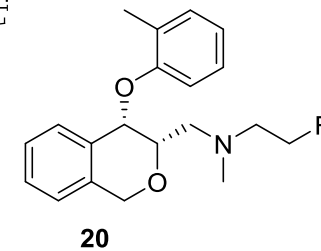
Analysis Info

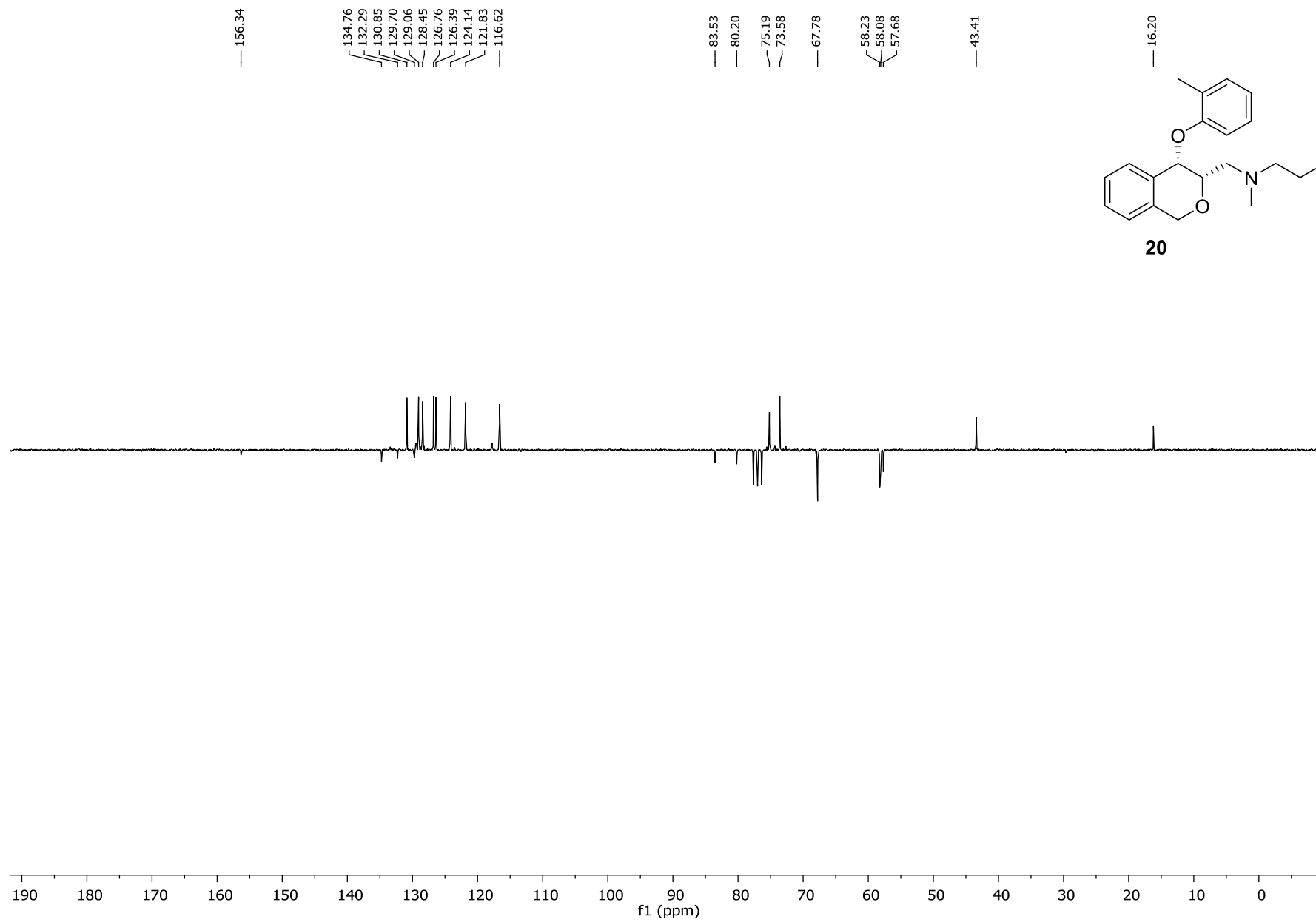
Analysis Name D:\Data\Externe Messungen\cj041.d Acquisition Date 6/24/2014 11:28:56 AM
 Method CN_24062014.m Operator JFI
 Sample Name cj041 Instrument micrOTOF-Q II 10240
 Comment

Acquisition Parameter

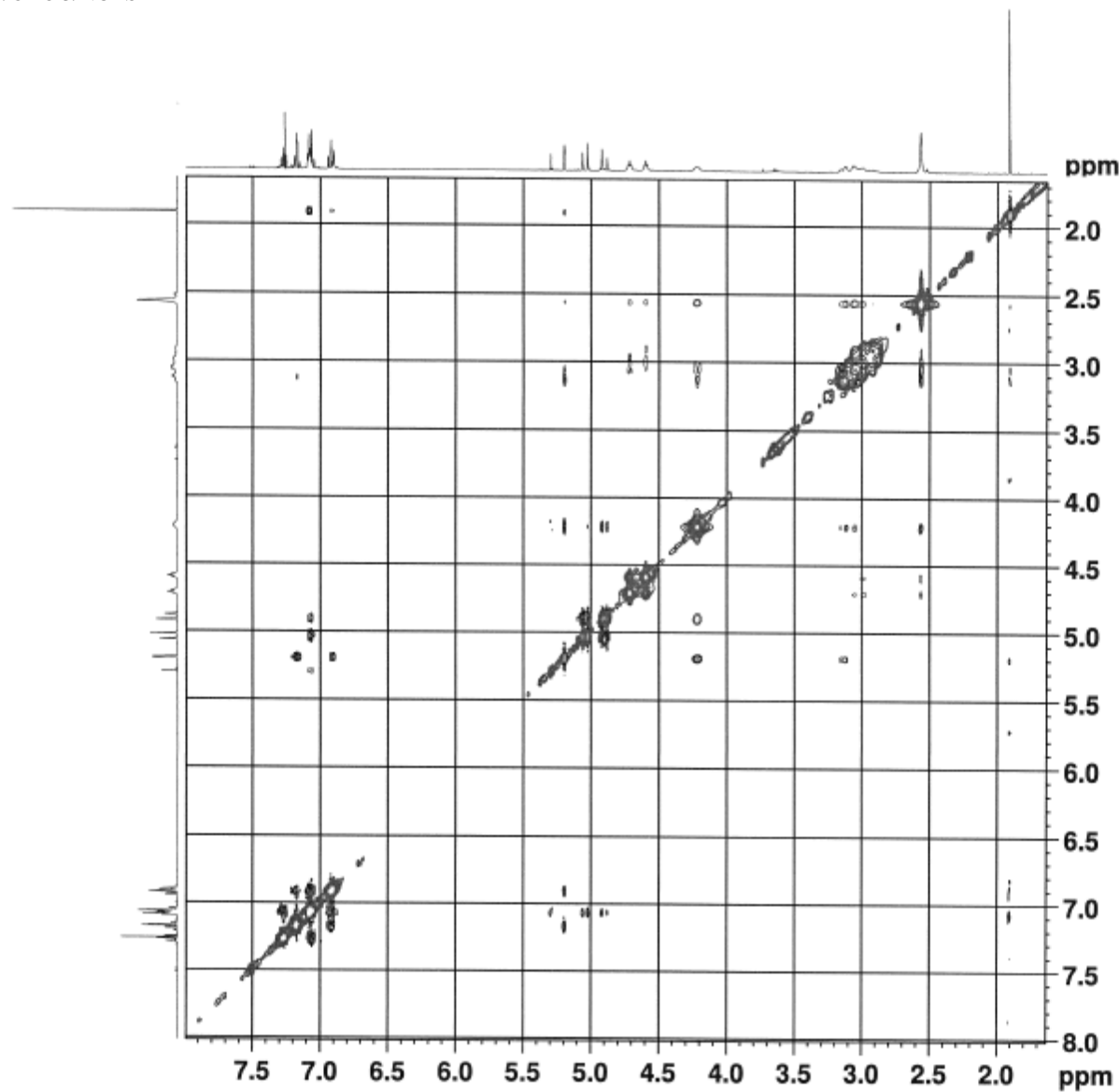
Source Type	ESI	Ion Polarity	Positive	Set Nebulizer	0.4 Bar
Focus	Active	Set Capillary	4500 V	Set Dry Heater	190 °C
Scan Begin	100 m/z	Set End Plate Offset	-500 V	Set Dry Gas	4.0 l/min
Scan End	1000 m/z	Set Collision Cell RF	300.0 Vpp	Set Divert Valve	Waste







sp055/CDCI3/NOESY



Current Data Parameters
NAME KN_sp055
EXPNO 5
PROCNO 1

F2 - Acquisition Parameters
Date_ 20140612
Time 4.22
INSTRUM spect
PROBHD 5 mm PABBO BB/
PULPROG noesygpph
TD 2048
SOLVENT CDCl3
NS 4
DS 8
SWH 4000.000 Hz
FIDRES 1.953125 Hz
AQ 0.2560000 sec
RG 181
DW 125.000 usec
DE 10.00 usec
TE 297.3 K
D0 0.00010898 sec
D1 2.00000000 sec
D8 0.80000001 sec
D16 0.00020000 sec
IN0 0.00024980 sec

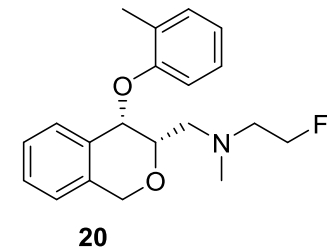
----- CHANNEL f1 -----
SF01 400.2318829 MHz
NUC1 1H
P1 12.50 usec
P2 25.00 usec
PLW1 16.00000000 W

----- GRADIENT CHANNEL -----
GPHAM[1] SMSQ10.100
GP21 40.00 %
P16 1000.00 usec

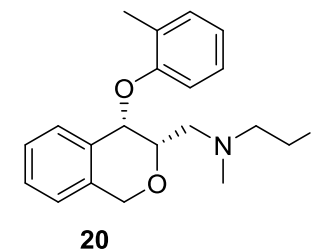
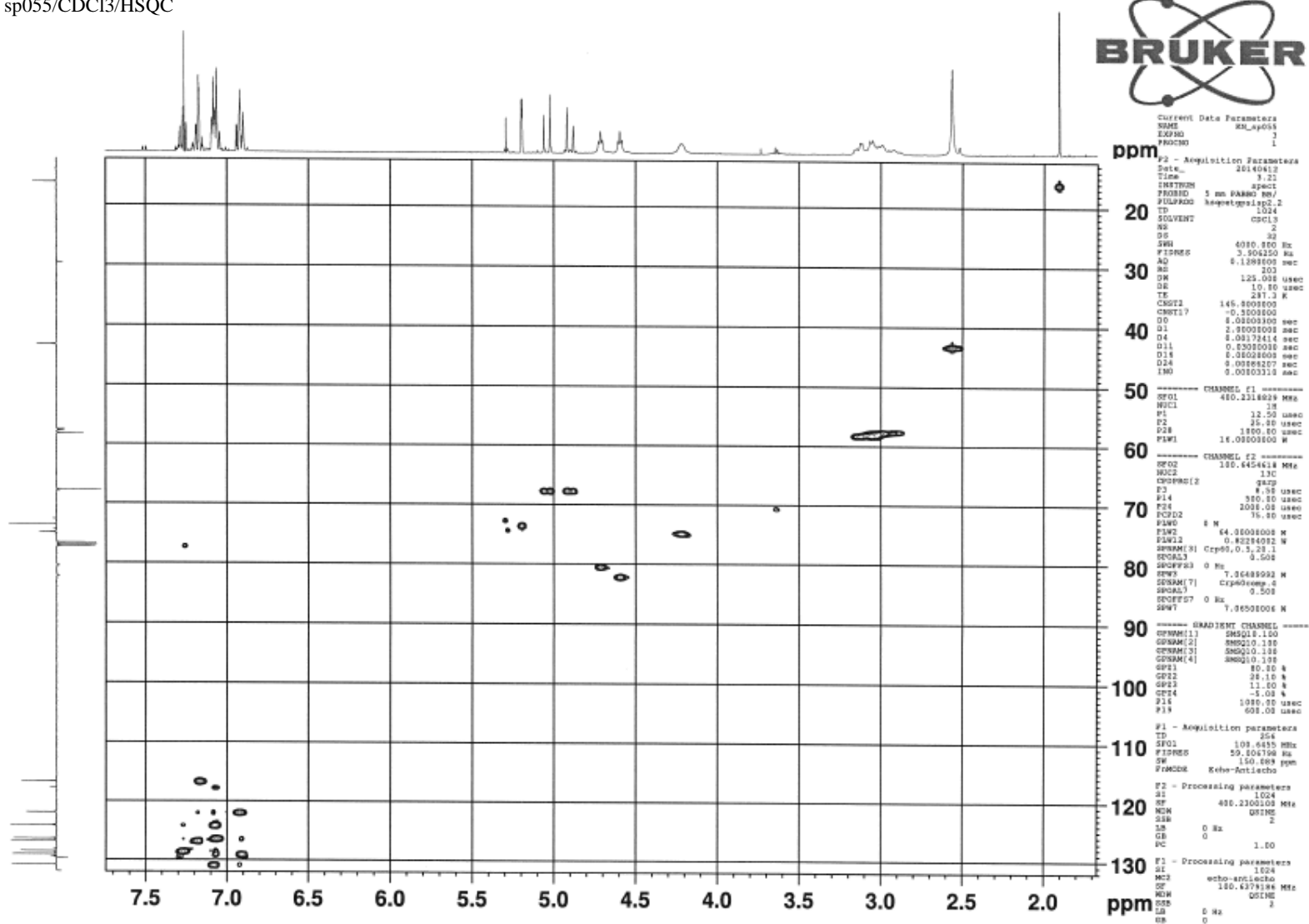
F1 - Acquisition parameters
TD 256
SF01 400.2319 MHz
FIDRES 15.637510 Hz
SW 10.002 ppm
FnMODE States-TPPI

F2 - Processing parameters
SI 2048
SF 400.2300100 MHz
WDW QSINE
SSB 2
LB 0 Hz
GB 0
PC 1.00

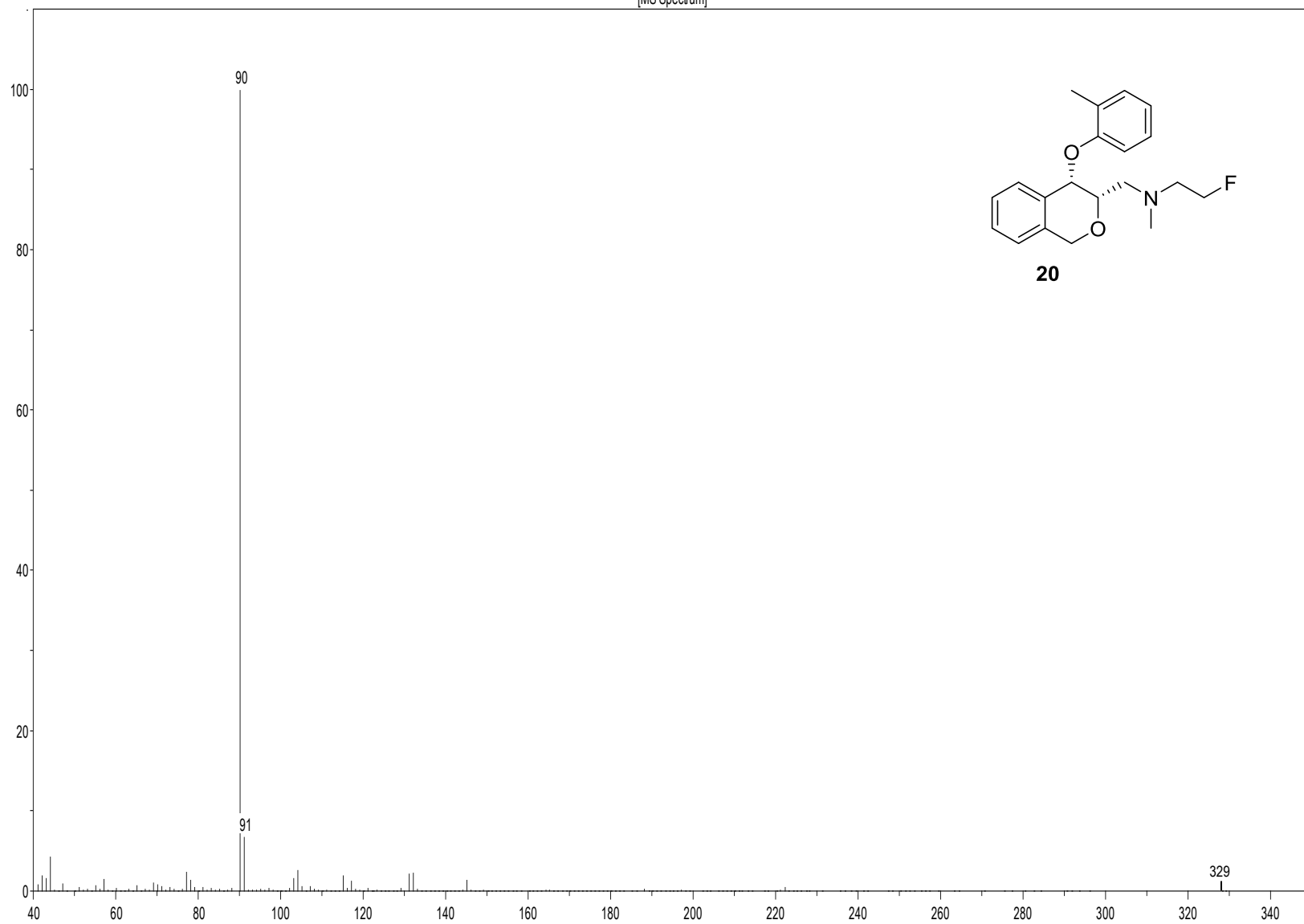
F1 - Processing parameters
SI 2048
MC2 States-TPPI
SF 400.2300100 MHz
WDW QSINE
SSB 2
LB 0 Hz
GB 0



sp055/CDC13/HSQC



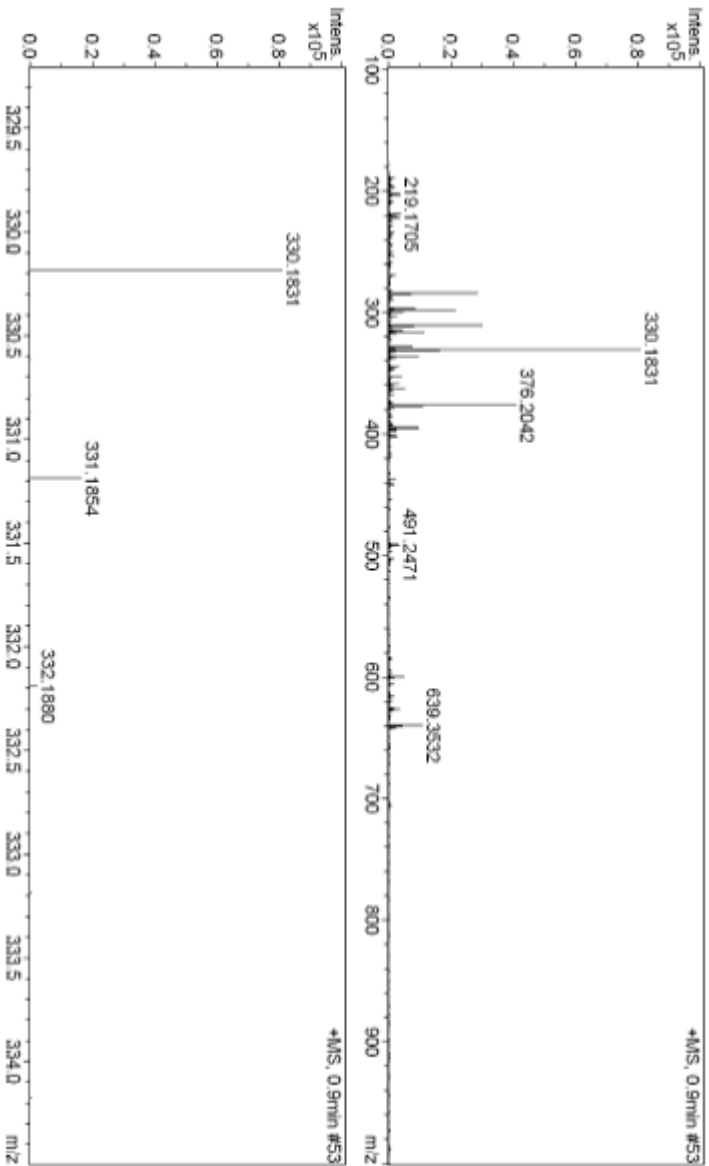
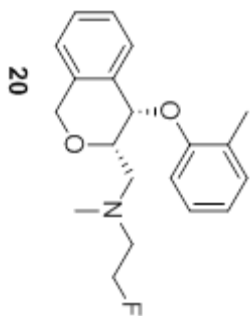
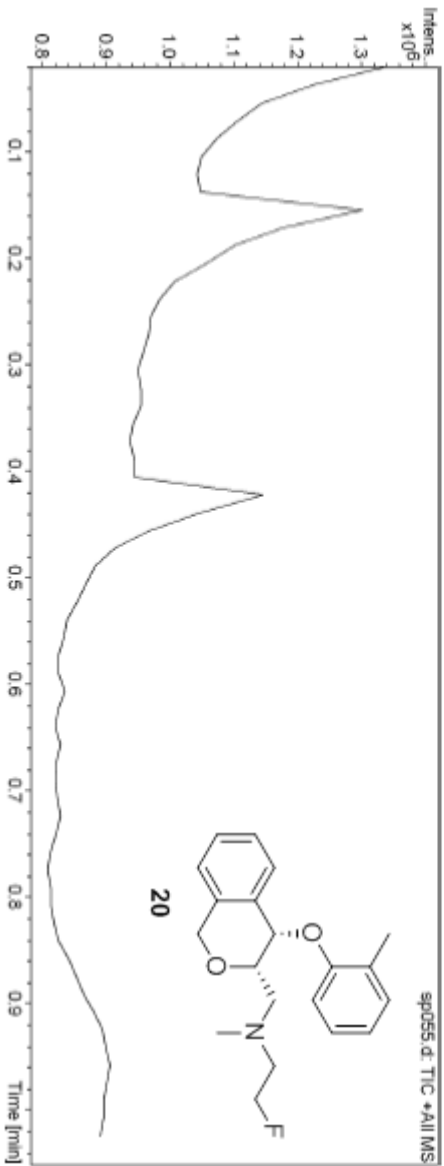
[MS Spectrum]

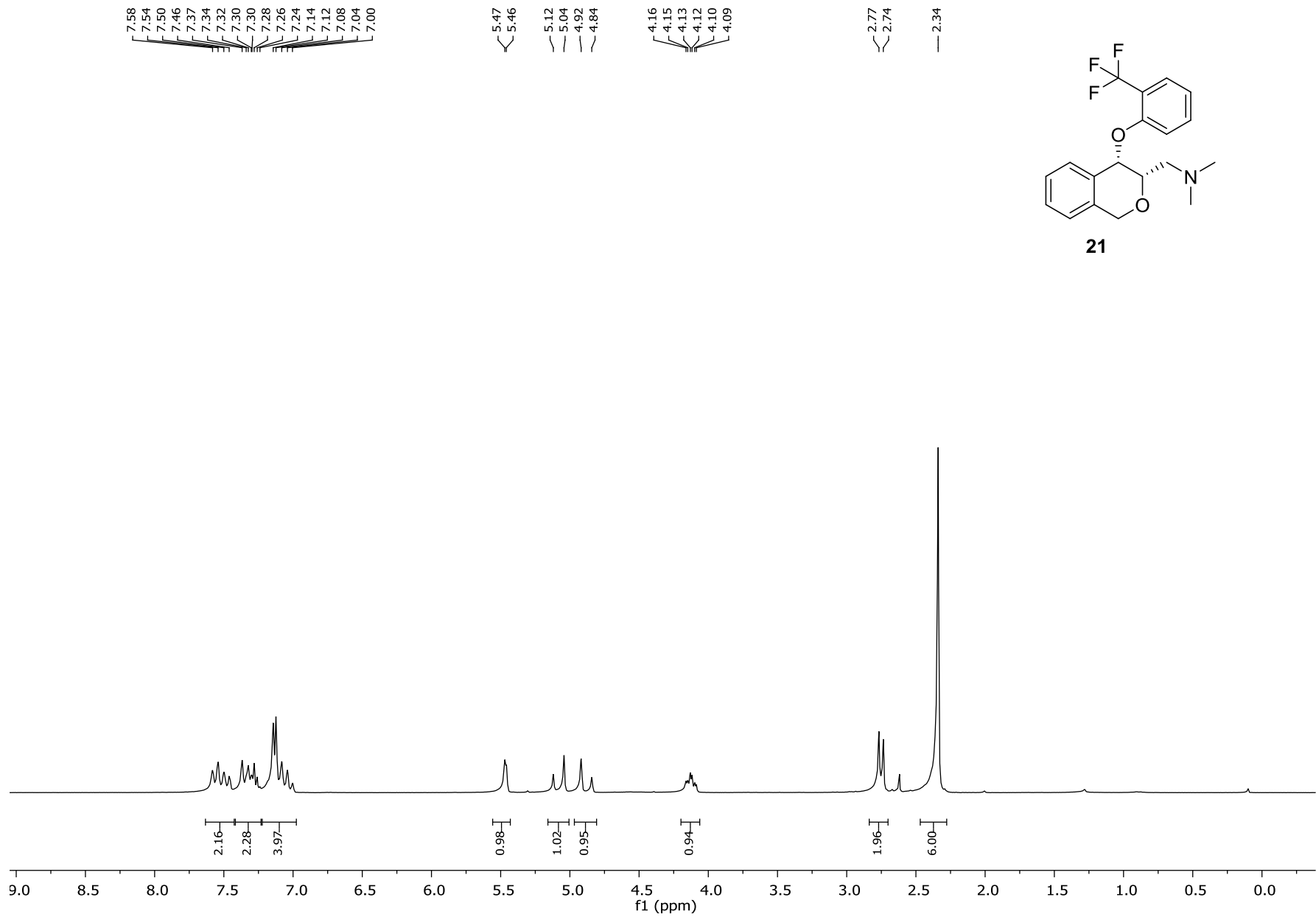


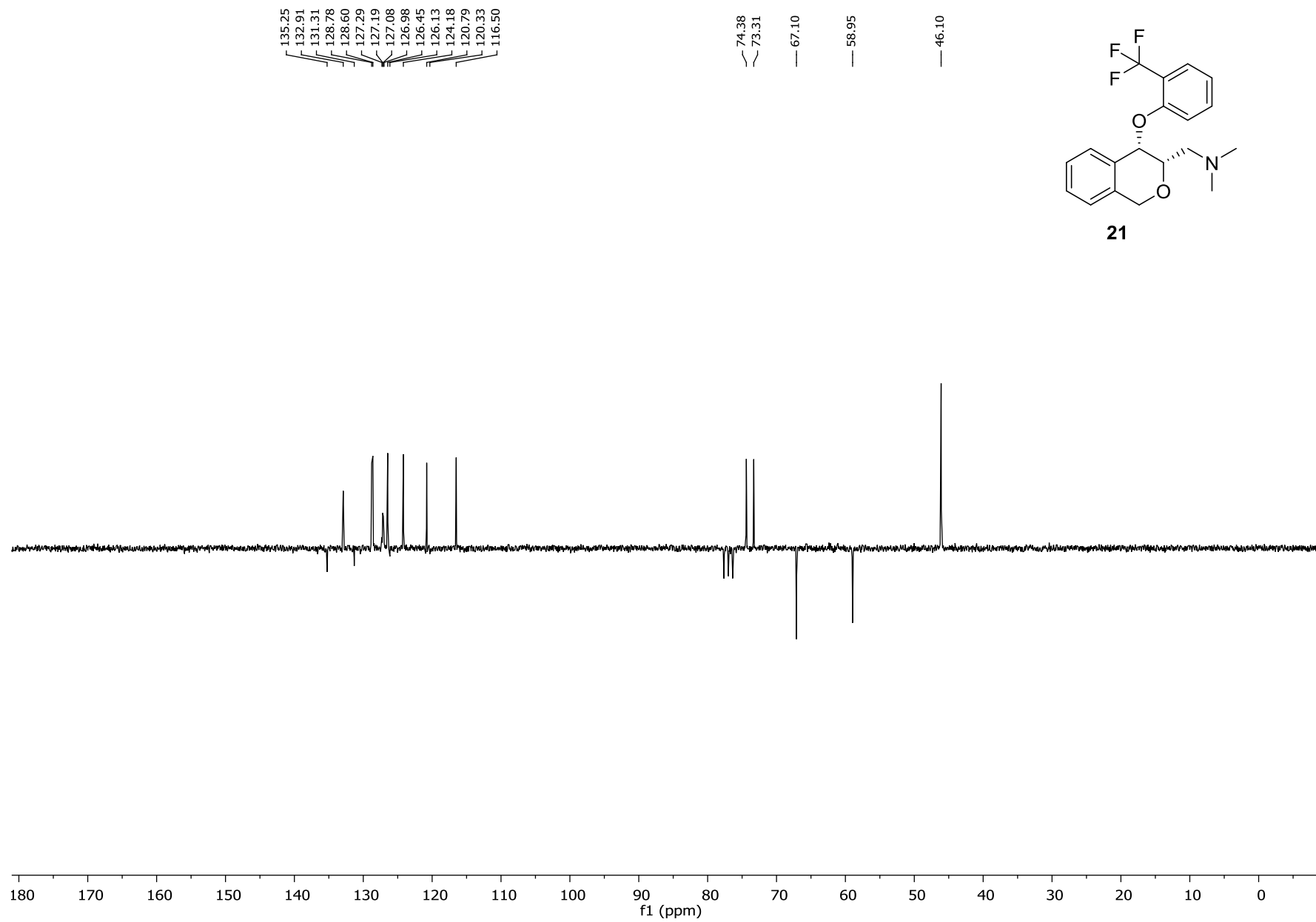
Display Report

Analysis Info		Acquisition Date	6/24/2014 11:38:03 AM
Analysis Name	D:\Data\Externe Messungen\sp055.d	Operator	JFI
Method	CN_24062014.m	Instrument	microTOF-Q II 10240
Sample Name	sp055	Comment	

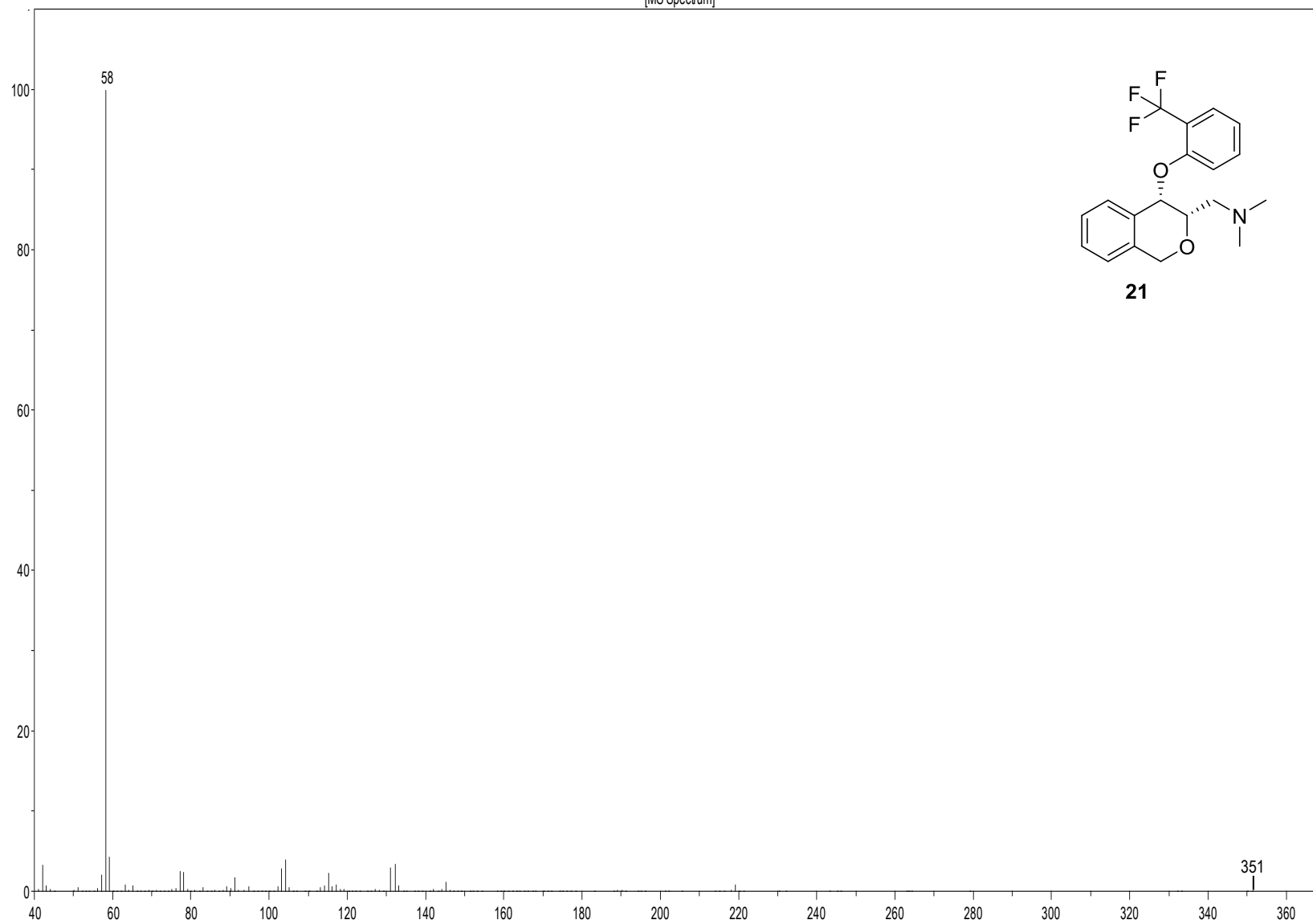
Acquisition Parameter	
Source Type	ESI
Focus	Active
Scan Begin	100 m/z
Scan End	1000 m/z
Ion Polarity	Positive
Set Capillary	4500 V
Set End Plate Offset	-500 V
Set Collision Cell RF	350.0 Vpp
Set Nebulizer	0.4 Bar
Set Dry Heater	180 °C
Set Dry Gas	4.0 l/min
Set Divert Valve	Waste







[MS Spectrum]



Display Report

Analysis Info

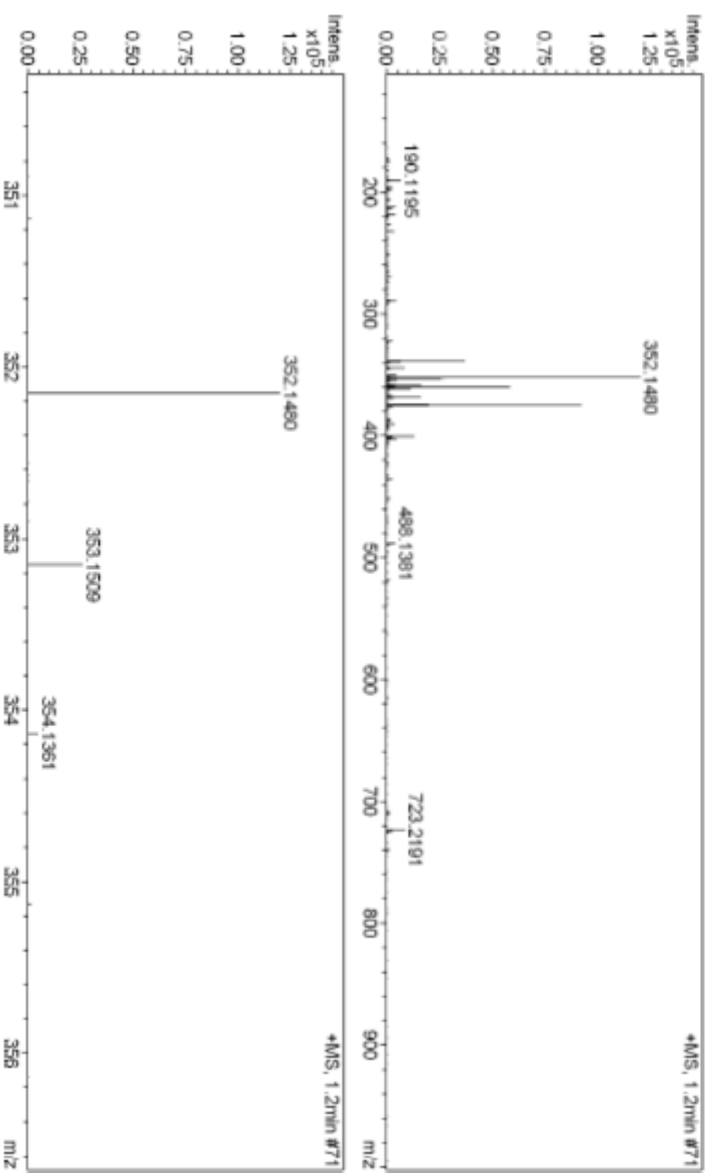
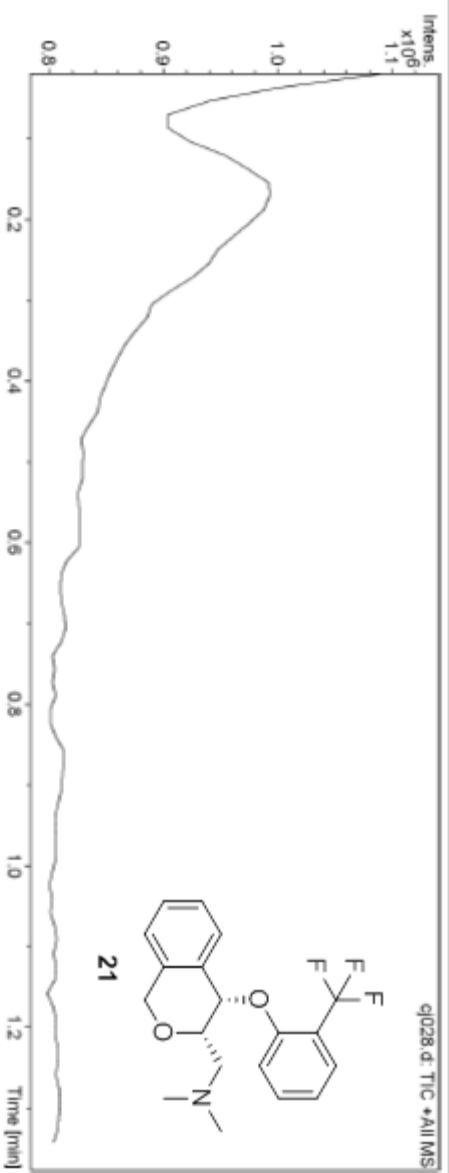
Analysis Name D:\Data\Externe Messungen\qj028.d
 Method CN_24062014.m
 Sample Name qj028
 Comment

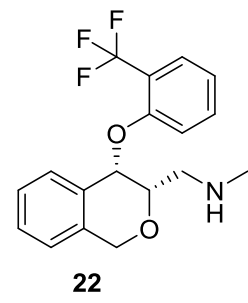
Acquisition Date 6/24/2014 11:47:31 AM

Operator JFI
 Instrument micrOTOF-Q II 10240

Acquisition Parameter

Source Type	ESI	Ion Polarity	Positive	Set Nebulizer	0.4 Bar
Focus	Active	Set Capillary	4500 V	Set Dry Heater	150 °C
Scan Begin	100 m/z	Set End Plate Offset	-500 V	Set Dry Gas	4.0 l/min
Scan End	1000 m/z	Set Collision Cell RF	300.0 Vpp	Set Divert Valve	Waste



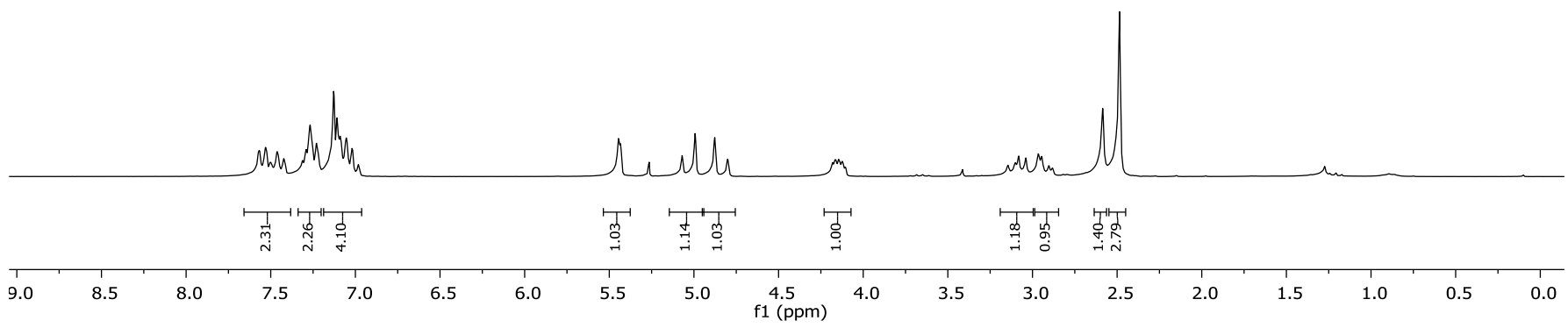


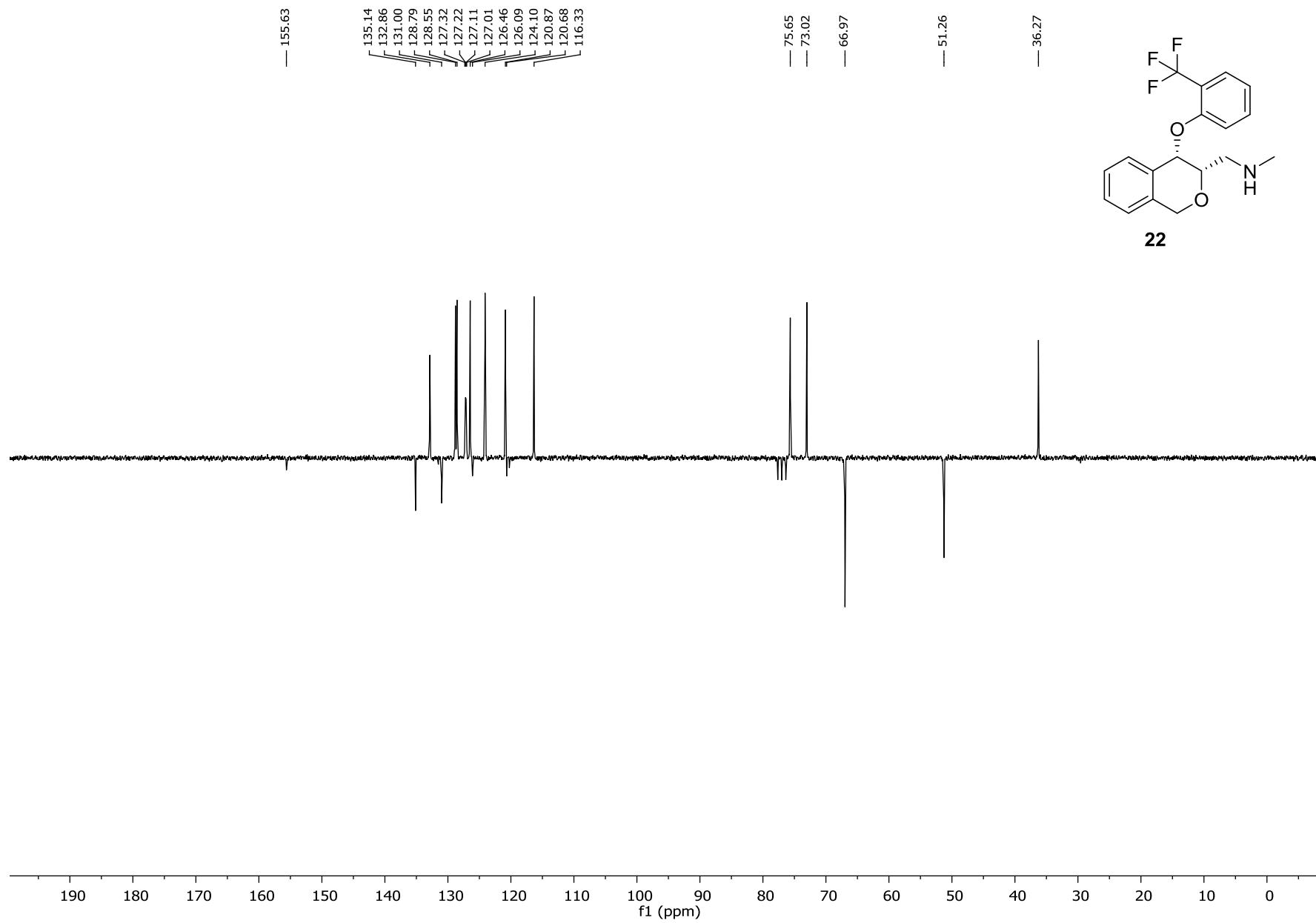
7.57
7.53
7.50
7.46
7.42
7.31
7.29
7.27
7.23
7.13
7.11
7.09
7.05
7.02
6.98

5.45
5.43
5.07
4.99
4.88
4.80

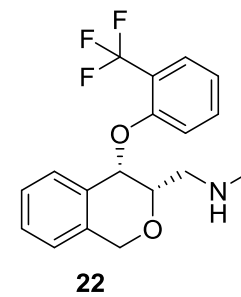
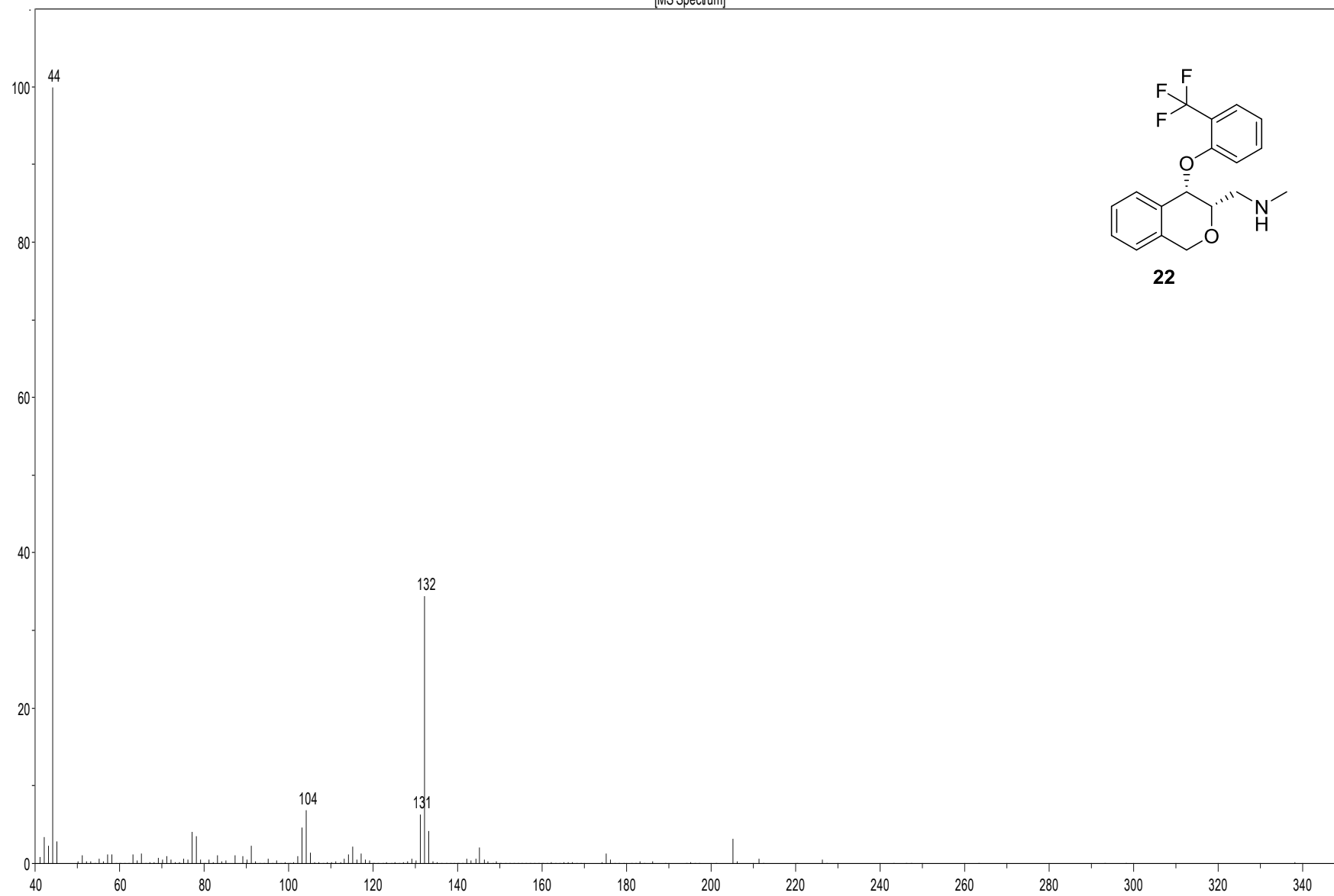
4.18
4.17
4.14
4.12
4.11

3.14
3.10
3.08
3.04
2.97
2.95
2.90
2.88
2.59
2.49





[MS Spectrum]



Display Report

337

Analysis Info

Analysis Name D:\Data\Extreme Messungen\sp050.d
 Method CN_24082014.m
 Sample Name sp050
 Comment

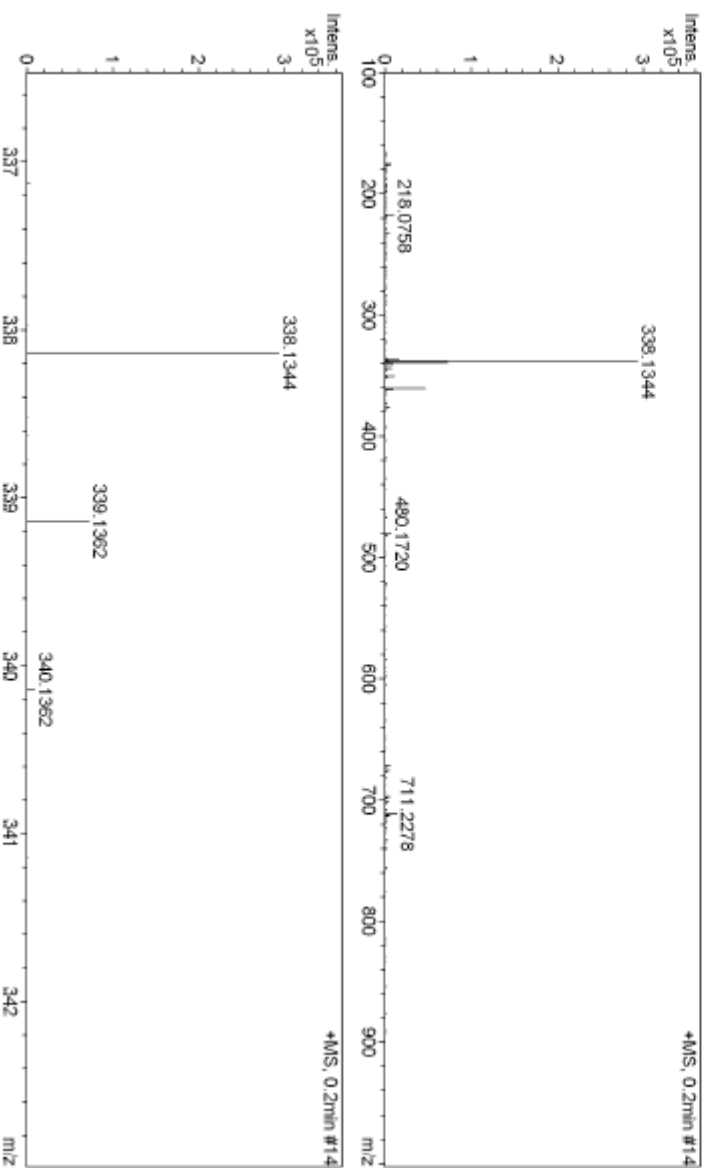
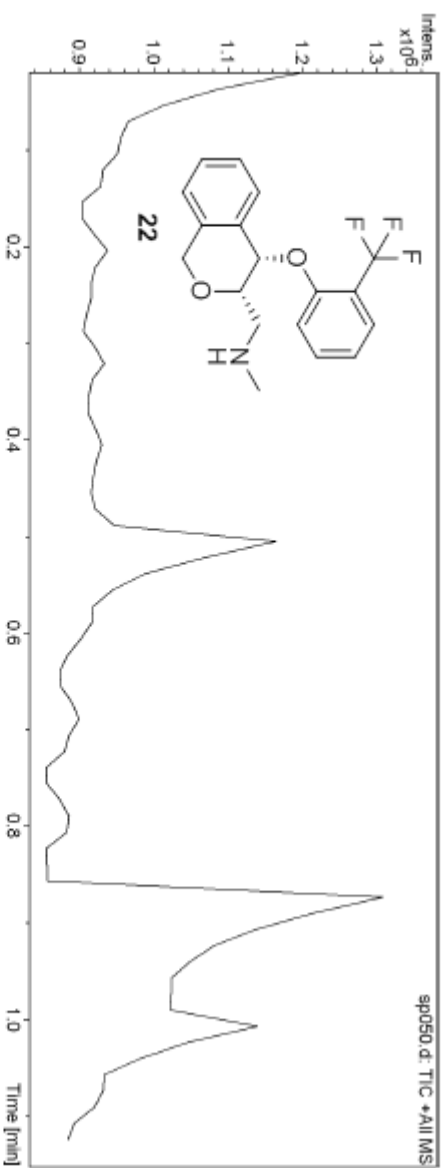
Acquisition Date 6/24/2014 11:44:21 AM
 Operator JFI
 Instrument micrOTOF-Q II 10240

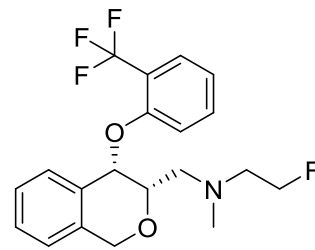
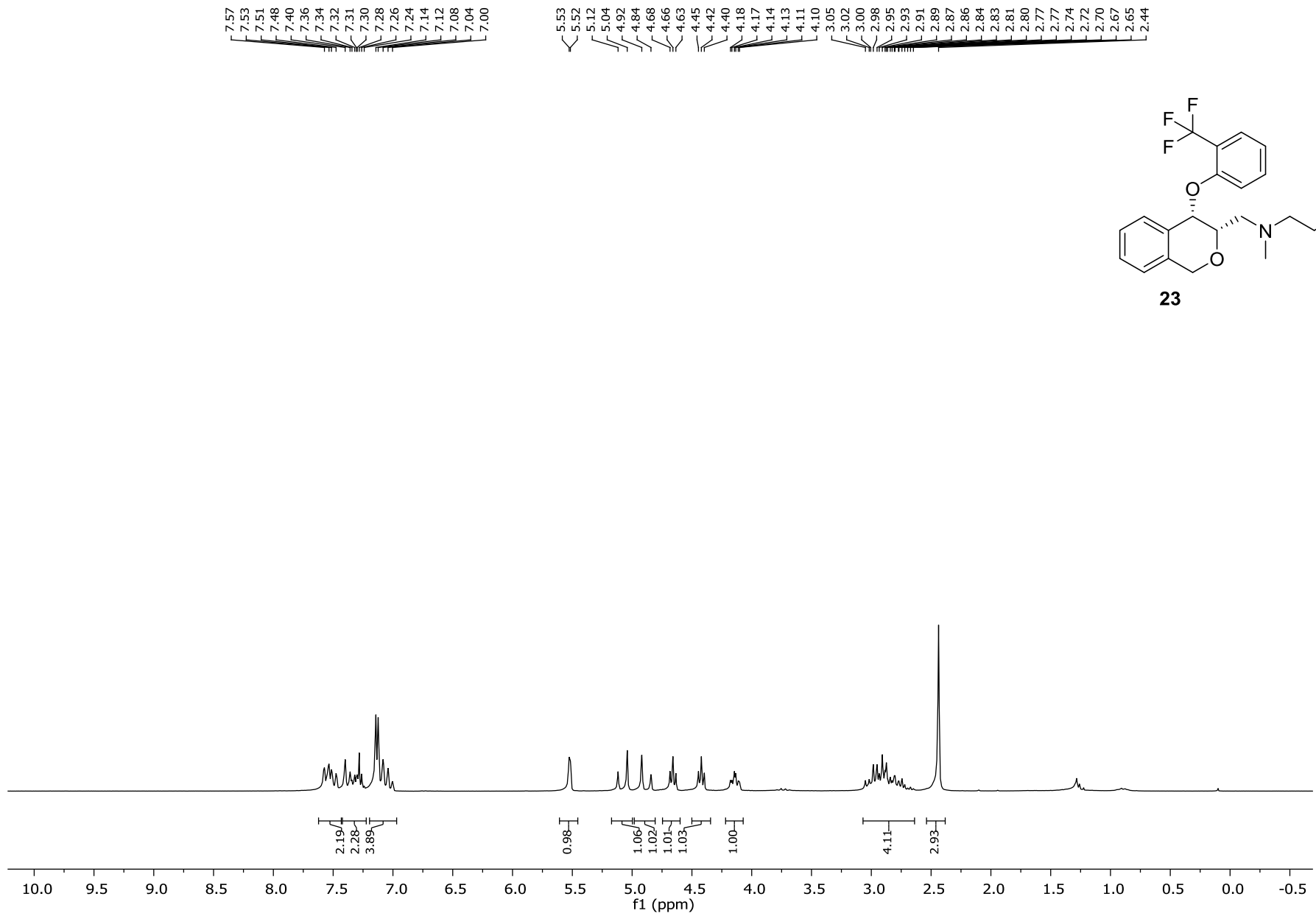
Acquisition Parameter

Source Type ESI
 Focus Active
 Scan Begin 100 m/z
 Scan End 1000 m/z

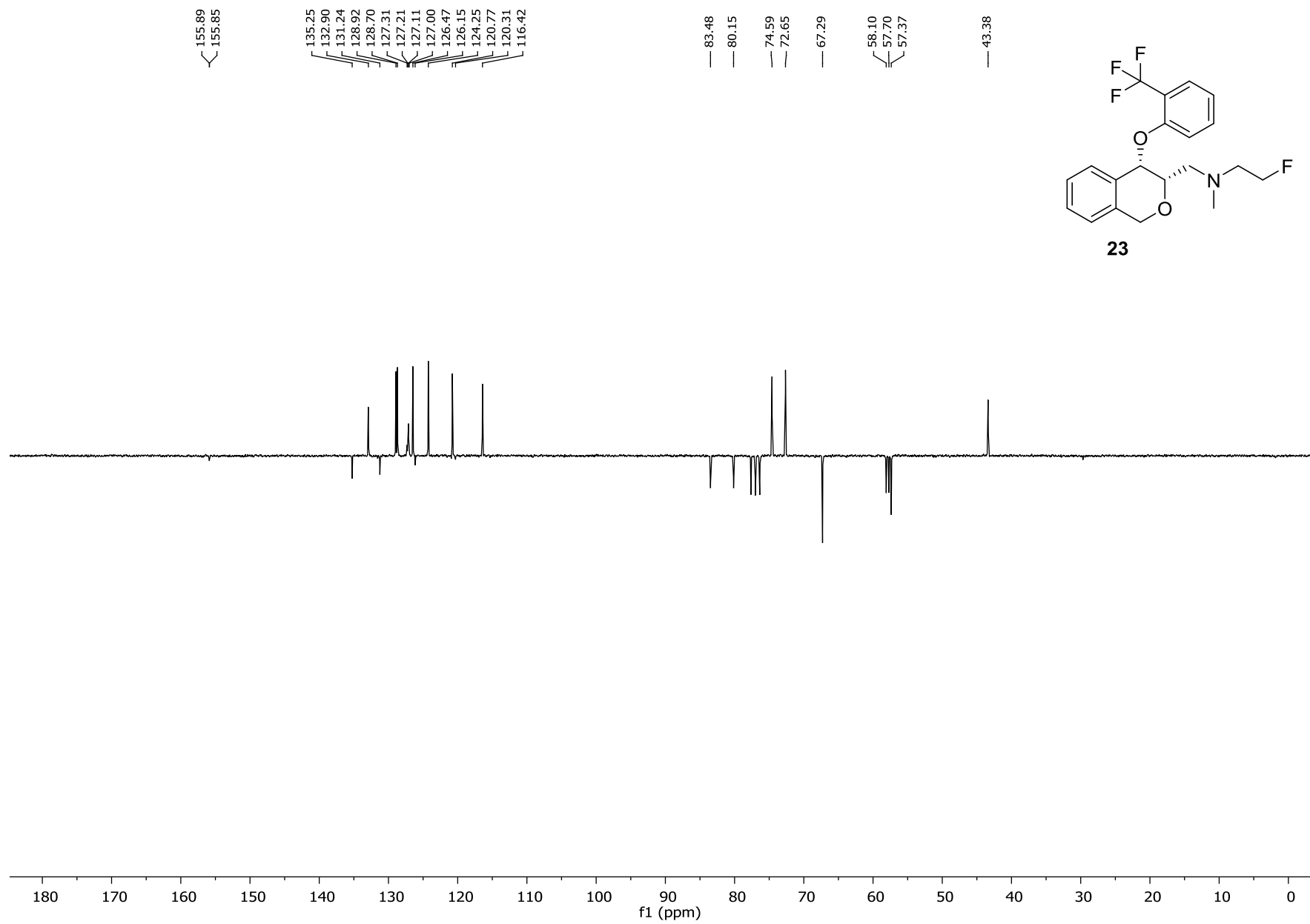
Ion Polarity Positive
 Set Capillary 4500 V
 Set End Plate Offset -500 V
 Set Collision Cell RF 300.0 Vpp

Set Nebulizer 0.4 Bar
 Set Dry Heater 180 °C
 Set Dry Gas 4.0 l/min
 Set Divert Valve Waste

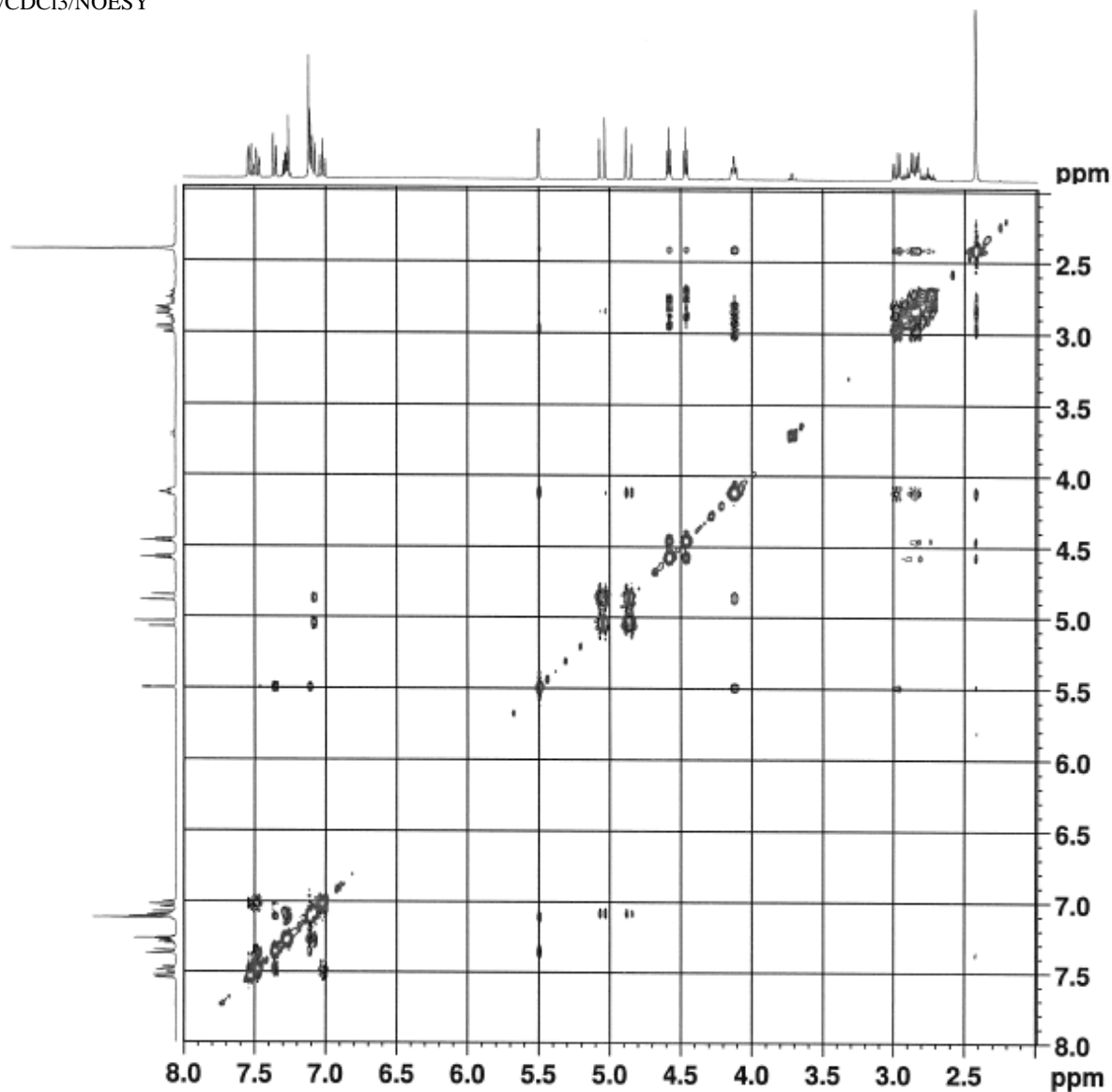




23



sp053/CDCl3/NOESY



Current Data Parameters
NAME KN_sp053
EXPNO 5
PROCNO 1

F2 - Acquisition Parameters
Date_ 20140605
Time 2.42
INSTRUM spect
PROBHD 5 mm PABBO BB/
PULPROG noesygpph
TD 2048
SOLVENT CDCl3
NS 4
DS 8
SWH 4000.000 Hz
FIDRES 1.953125 Hz
AQ 0.2560000 sec
RG 181
DM 125.000 usec
DE 10.00 usec
IE 297.3 K
DO 0.00010898 sec
D1 2.00000000 sec
D8 0.80000001 sec
D16 0.00020000 sec
IN0 0.00024980 sec

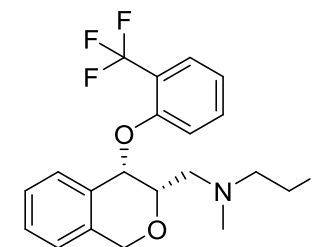
----- CHANNEL f1 -----
SFO1 400.2318829 MHz
NUC1 1H
P1 12.50 usec
P2 25.00 usec
PLW1 16.00000000 W

----- GRADIENT CHANNEL -----
GENAM[1] SMSQ10.100
GFZ1 40.00 %
P16 1000.00 usec

F1 - Acquisition parameters
TD 256
SFO1 400.2319 MHz
FIDRES 15.637510 Hz
SW 10.002 ppm
PRMODE States-TPFI

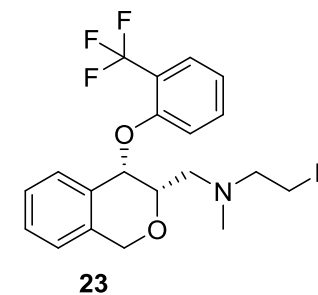
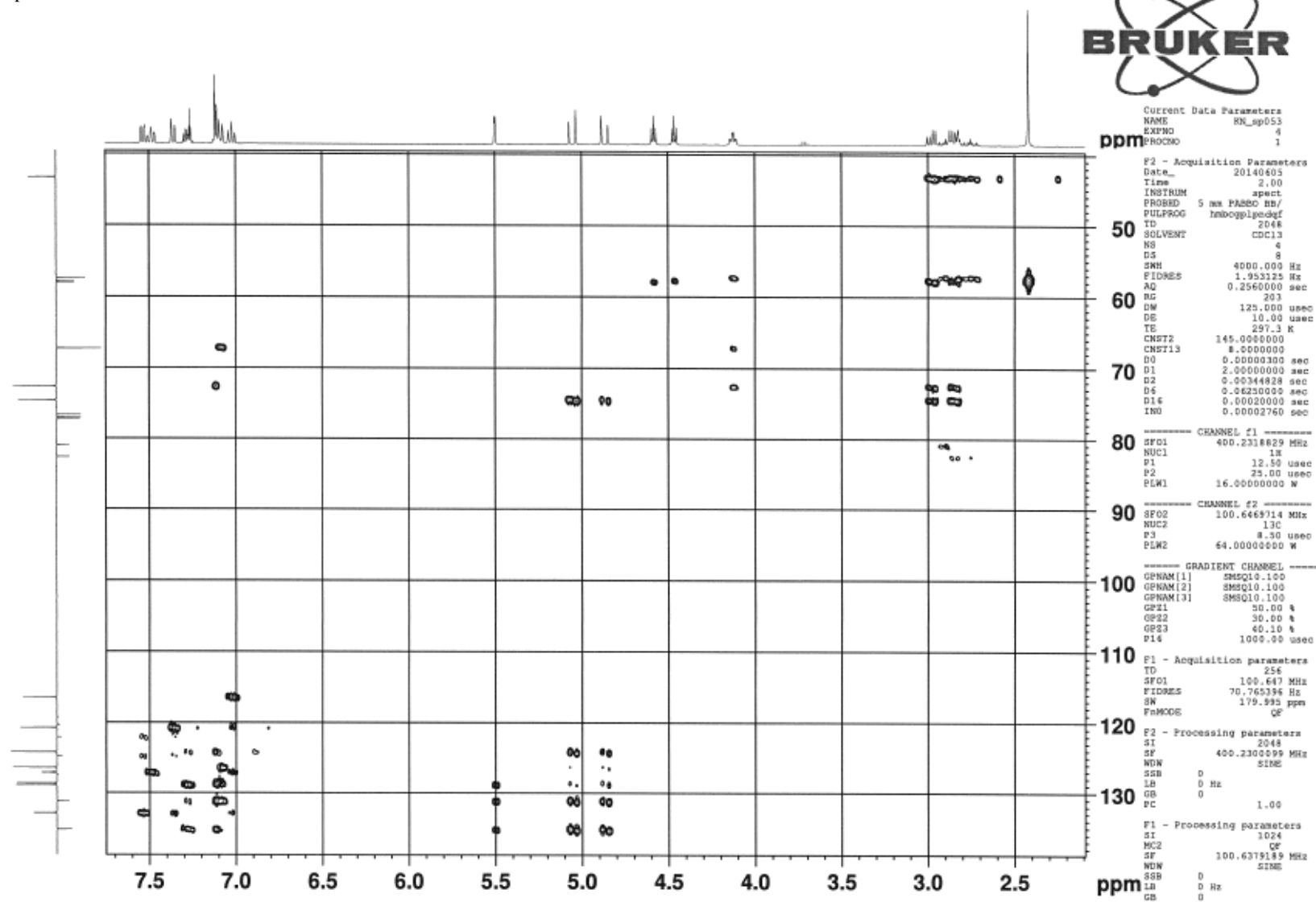
F2 - Processing parameters
SI 2048
SF 400.230099 MHz
WDW QSI
SSB 2
LB 0 Hz
GB 0
PC 1.00

F1 - Processing parameters
SI 2048
MC2 States-TPFI
SF 400.230099 MHz
WDW QSI
SSB 2
LB 0 Hz
GB 0

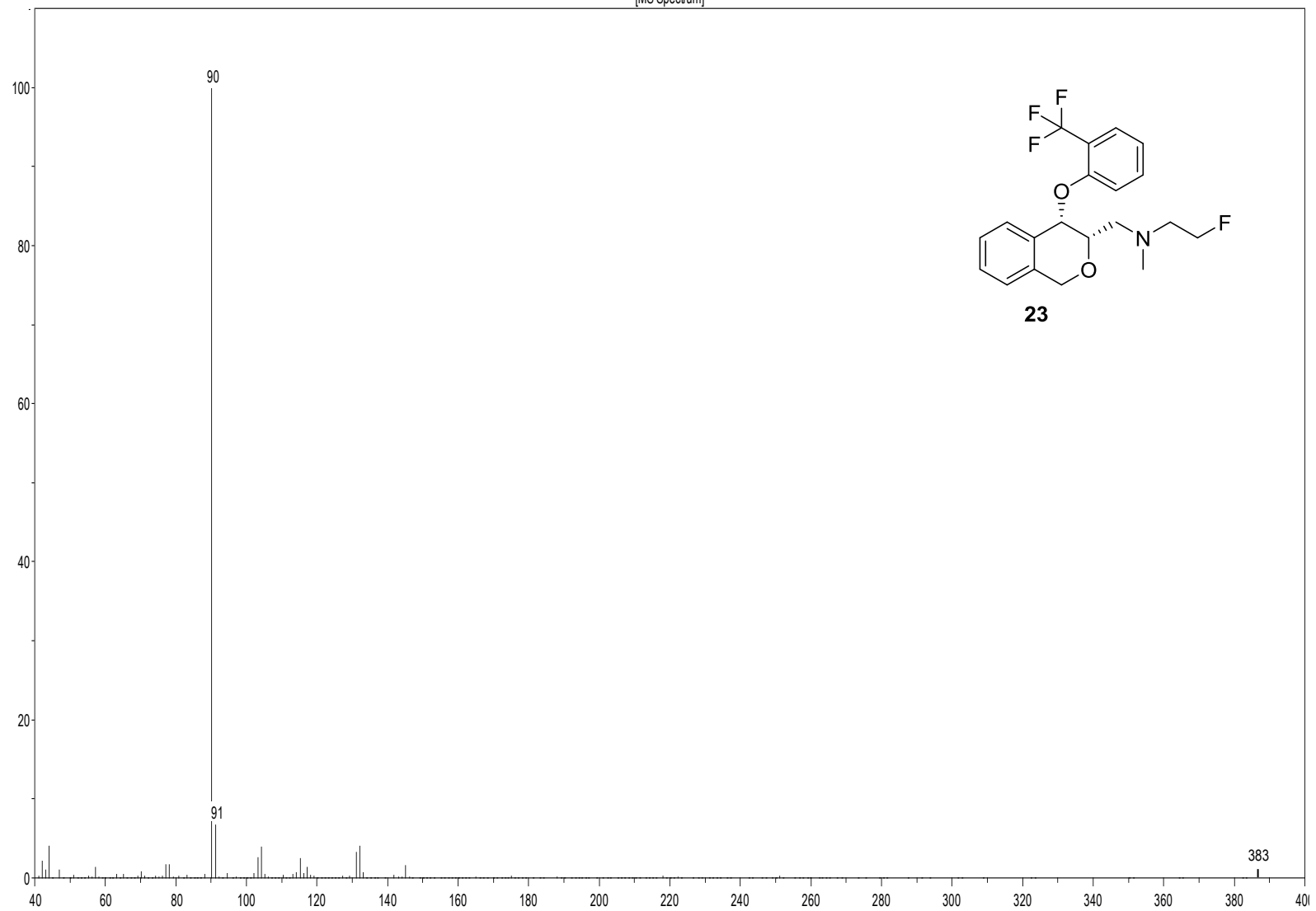


23

sp053/CDCl3/HMBC



[MS Spectrum]

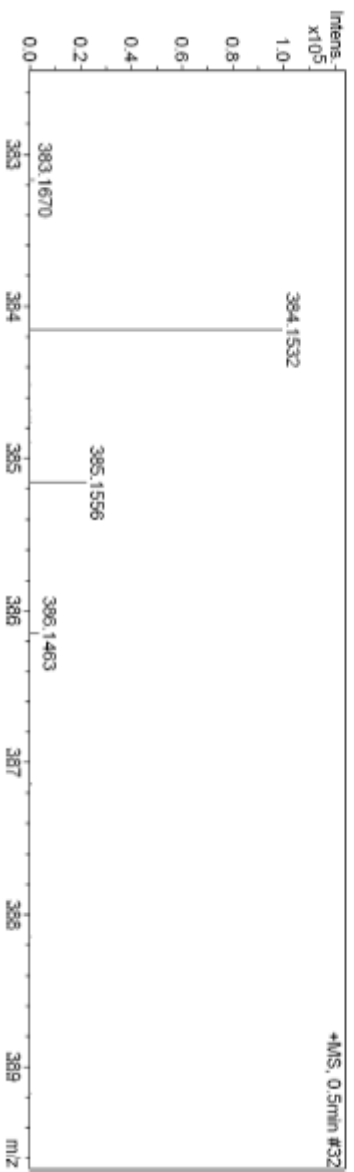
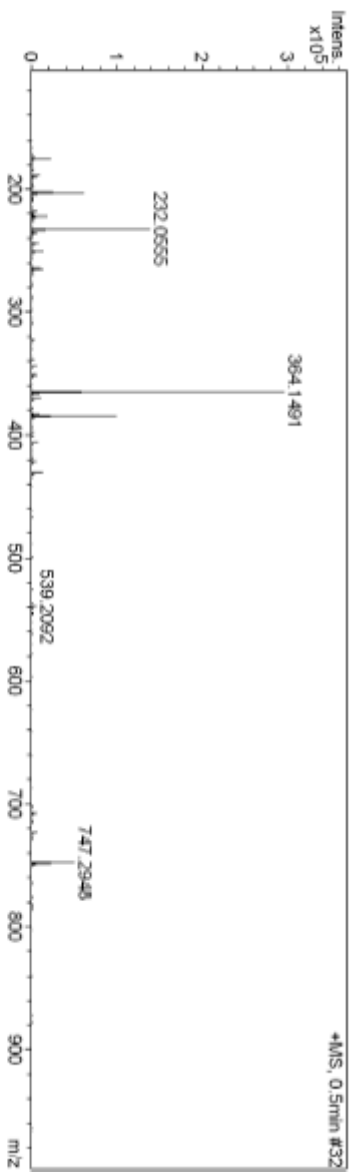
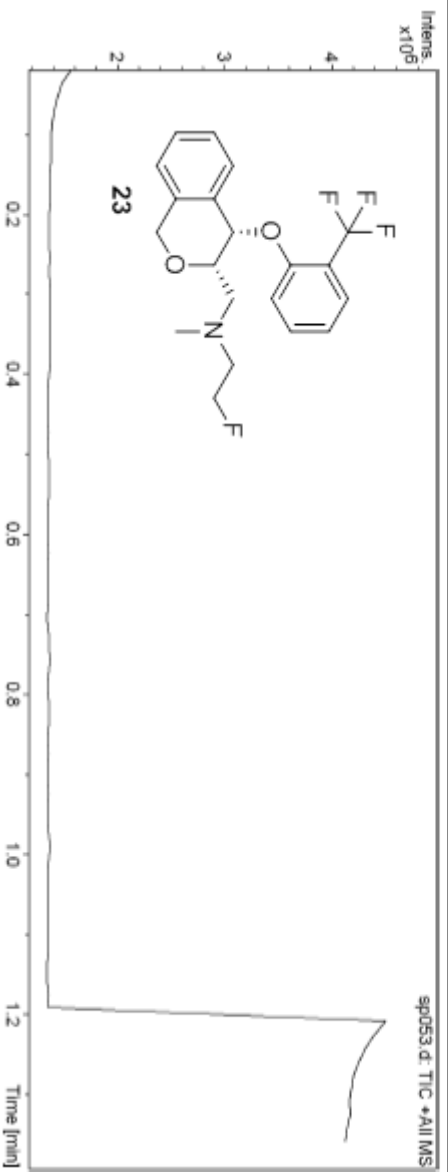


Display Report

Analysis Info	Acquisition Date 6/24/2014 11:53:30 AM
Analysis Name D:\Data\Externe Messungen\sp053.d	Operator JFI
Method CN_24062014.m	Instrument microTOF-Q II 10240
Sample Name sp053	Comment

Acquisition Parameter

Source Type ESI	Ion Polarity Positive
Focus Active	Set Capillary 4500 V
Scan Begin 100 m/z	Set End Plate Offset -500 V
Scan End 1000 m/z	Set Collision Cell RF 300.0 Vpp
	Set Nebulizer 0.4 Bar
	Set Dry Heater 180 °C
	Set Dry Gas 4.0 l/min
	Set Divert Valve Waste



5.4 PUBLICATIONS

5.4.1 MAO-B



Contents lists available at ScienceDirect

Bioorganic & Medicinal Chemistry Letters

journal homepage: www.elsevier.com/locate/bmcl

Development of potential selective and reversible pyrazoline based MAO-B inhibitors as MAO-B PET tracer precursors and reference substances for the early detection of Alzheimer's disease



Catharina Neudorfer^{a,b,*}, Karem Shanab^{a,b}, Andreas Jurik^c, Veronika Schreiber^d, Carolina Neudorfer^b, Chrysoula Vraka^{a,e}, Eva Schirmer^b, Wolfgang Holzer^b, Gerhard Ecker^c, Markus Mitterhauser^a, Wolfgang Wadsak^a, Helmut Spreitzer^{b,*}

^a Medical University of Vienna, Department of Biomedical Imaging and Image-guided Therapy, Division of Nuclear Medicine, Waehringer Guertel 18-20, 1090 Vienna, Austria

^b University of Vienna, Faculty of Life Sciences, Department of Pharmaceutical Chemistry, Division of Drug Synthesis, Althanstraße 14, 1090 Vienna, Austria

^c University of Vienna, Faculty of Life Sciences, Department of Pharmaceutical Chemistry Division of Drug Design and Medicinal Chemistry, Althanstraße 14, 1090 Vienna, Austria

^d University of Vienna, Faculty of Life Sciences, Division of Clinical Pharmacy and Diagnostics, Althanstraße 14, 1090 Vienna, Austria

^e University of Vienna, Department of Nutritional Sciences, Althanstraße 14, 1090 Vienna, Austria

ARTICLE INFO

Article history:

Received 13 June 2014

Revised 25 July 2014

Accepted 30 July 2014

Available online 7 August 2014

Keywords:

MAO-B

Alzheimer's disease

PET

Pyrazoline derivatives

Molecular imaging

ABSTRACT

Since high MAO-B levels are present in early stages of AD, the MAO-B system can be designated as an appropriate and prospective tracer target of molecular imaging biomarkers for the detection of early AD. According to the preceding investigations of Mishra et al. the aim of this work was the development of a compound library of selective and reversible MAO-B inhibitors by performing bioisosteric modifications of the core structure of 3-(anthracen-9-yl)-5-phenyl-4,5-dihydro-1H-pyrazoles. In conclusion, 13 new pyrazoline based derivatives have been prepared, which will serve as precursor substances for future radiolabeling as well as reference compounds for the investigation of increased MAO-B levels in AD.

© 2014 Elsevier Ltd. All rights reserved.

Currently, two distinct enzymatic isoforms of MAO (monoamine oxidase) have been characterized, namely MAO-A and MAO-B. Although they share a high sequence similarity of about 70%, they differ in their tissue distribution, substrate specificity and inhibitor selectivity.¹ MAO-B is prevalent in lymphocytes and platelets and displays high concentration levels in the human brain, mostly predominant in serotonergic and histaminergic neurons, as well as in astrocytes. Since MAO-B plays a pivotal role as degradation enzyme in the human brain, it is involved in a variety of neurological diseases, such as attention deficit hyperactivity disorder (ADHD), Tourette's syndrome, amyotrophic lateral sclerosis (ALS), Huntington's disease and age-related neurological disorders like Parkinson's disease (PD) and Alzheimer's disease (AD).²

As a chronic, progressive neurodegenerative disorder, AD affects millions of people worldwide, causing loss of mental and physical functions.^{3,4} Since increased MAO-B levels are measured even in

* Corresponding authors. Tel.: +43 4277 55629; fax: +43 4277 855629 (C.N.); tel.: +43 4277 55621; fax: +43 4277 855621 (H.S.).

E-mail addresses: catharina.neudorfer@gmail.com (C. Neudorfer), helmut.spreitzer@univie.ac.at (H. Spreitzer).

early stages of AD,^{5–10} the MAO-B system exhibits a promising and prospective tracer target for molecular imaging of AD and especially early stage AD.^{10–12} The state of the art method for the visualization and quantification of receptor and enzyme systems in vivo is PET (positron emission tomography), a technique which allows to quantify in vivo processes non-invasively. In the context of developing new PET radioligands for the detection of MAO-B in AD, their precursors for radiolabeling, and reference compounds for preclinical testing, first needed to be prepared.

According to the results of Mishra et al.¹³ 5-(anthracen-9-yl)-3-phenyl-4,5-dihydro-1H-pyrazoles (Fig. 1) represent highly selective and extremely potent, reversible MAO-B inhibitors. They do not only display a superior affinity towards MAO-B, but also provide a high MAO-B versus MAO-A selectivity ratio. Additionally, these compounds display docking scores superior > –12.5 and predicted K_i values in nanomolar ranges, what makes them at least 100 times more potent than the positive control, selegiline.¹³ It should be noted that the chemical structure in the original article of Mishra et al.¹³ depicts the double bond of the pyrazoline ring in the false position. Figure 1 shows the correct chemical structure, which is expected according to the preceding synthesis.

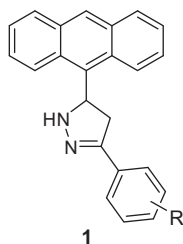


Figure 1. Chemical structure of the highly potent, selective and reversible MAO-B inhibitor 5-(anthracen-9-yl)-3-phenyl-4,5-dihydro-1H-pyrazole.

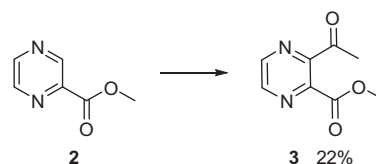
This Letter aims at the synthesis and docking studies of a compound library of selective and reversible methyl- and fluoroethyl-substituted 5-(anthracen-9-yl)-4,5-dihydro-1H-pyrazole MAO-B inhibitors (**16–20** and **28–32**) (Scheme 4) by applying bioisosteric principles to 5-(anthracen-9-yl)-3-phenyl-4,5-dihydro-1H-pyrazoles, which have been proven extremely potent towards MAO-B. Additionally, precursor compounds (**23–27**) (Scheme 4) for future radiolabeling were prepared within the scope of this work. Due to stability issues, the core structure (Fig. 1) had to be modified by inserting an additional acetyl moiety or thiocarbamoyl moiety, respectively, at position 1 of the pyrazoline ring. All bioisosteric methyl- and fluoroethyl-substituted pyrazoline derivatives (**16–20** and **28–32**) (Scheme 4) will be subjected to affinity-, selectivity-, and lipophilicity studies towards MAO-B as well as blood brain barrier penetration measurements at the General Hospital of Vienna. The most promising MAO-B ligands will then be selected for the development of new, selective and reversible PET-tracers for the MAO-B system.

Scheme 1 is giving a general overview of the envisaged synthetic pathway. The preparation of methyl- and fluoroethyl-substituted reference compounds (**16–20**, **32** and **33**) as well as precursor substances (**23–27**) for ^{11}C and ^{18}F radiolabeling started from

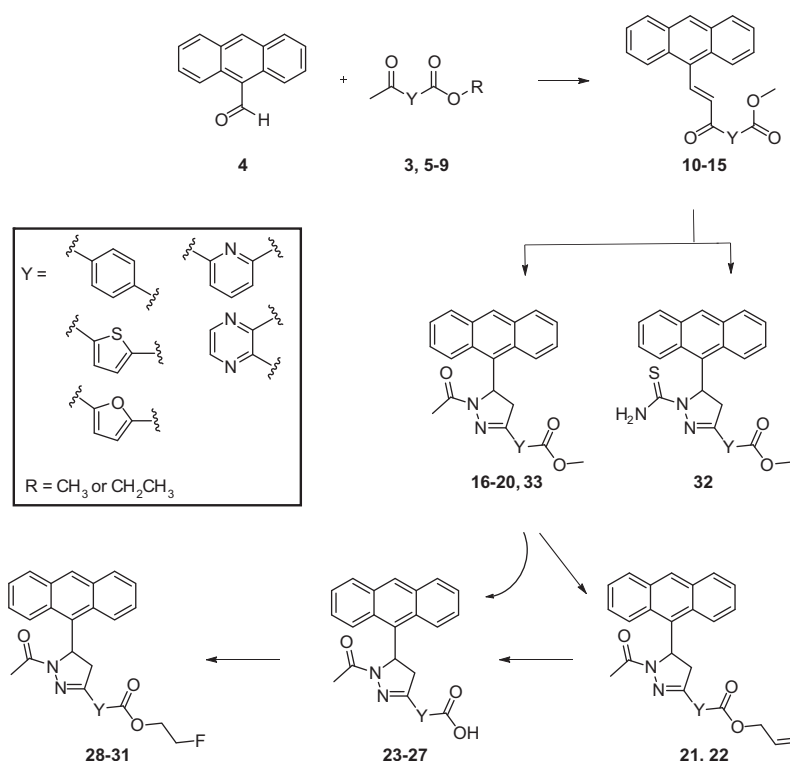
anthracene-9-carbaldehyde **4**. A variety of esters **3**, **5–9** was reacted with anthracene-9-carbaldehyde **4** in order to prepare the respective chalcones **10–15**. Cyclization of the respective chalcone with hydrazine hydrate gave methyl esters **16–20** and **33**, which were either directly converted into the free carboxylic acids **23–27** or reacted into the corresponding allyl esters. All prepared allyl esters represent intermediate compounds for the further conversion into the free carboxylic acids. The free carboxylic acids were transformed into the respective fluoroethyl esters **28–31**, which will be subjected to preclinical experiments and serve as reference compounds for the ^{18}F radiolabeled analogs. All reactions are discussed in detail in the following paragraphs.

Since aldol condensation reactions could not be realized with molecules bearing a free carboxylic acid moiety, methyl esters **3**, **5**, **7–9** and ethyl ester **6** served as starting materials, to conduct the condensation reaction with anthracene-9-carbaldehyde **4**. The preparation of **3** is depicted in Scheme 2 and could be achieved by a Minisci reaction with *tert*-BuO₂H, FeSO₄·7H₂O, sulfuric acid and acetic acid.¹⁴ The reaction was completed by the reduction of excess *tert*-BuO₂H with Na₂SO₃.

The base catalyzed aldol condensation was performed in methanol under the same reaction conditions for acetyl esters **3**, **5** and **7–9** with anthracene-9-carbaldehyde **4** to yield compounds **10** and **12–15** (Scheme 3). Thereby, conversion of **4** with methyl



Scheme 2. Synthesis of methyl 3-acetylpyrazine-2-carboxylate (**3**), reagents and conditions: acetaldehyde, H₂SO₄ (50%), AcOH (99%), $-5\text{ }^{\circ}\text{C}$ → *tert*-BuO₂H (70%), FeSO₄·7H₂O → 2 h → rt, Na₂SO₃.

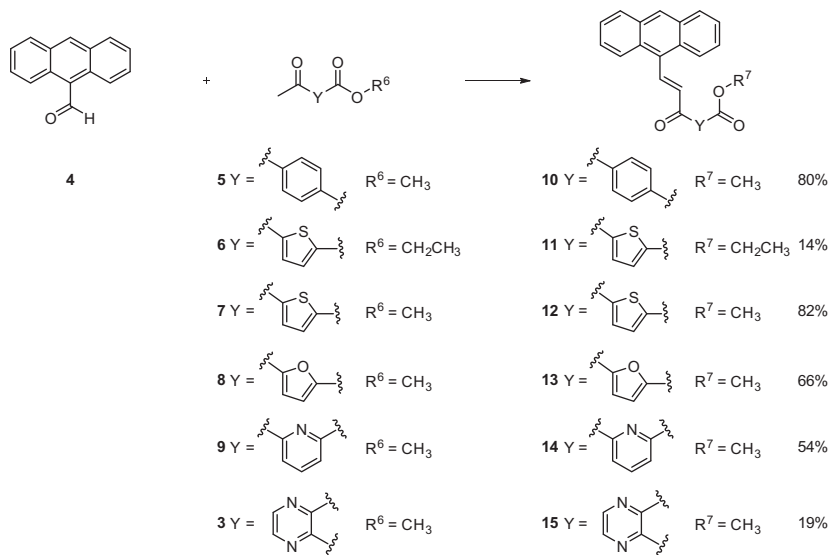


Scheme 1. General synthesis plan for the preparation of methyl- and fluoroethyl-substituted reference compounds as well as precursor substances.

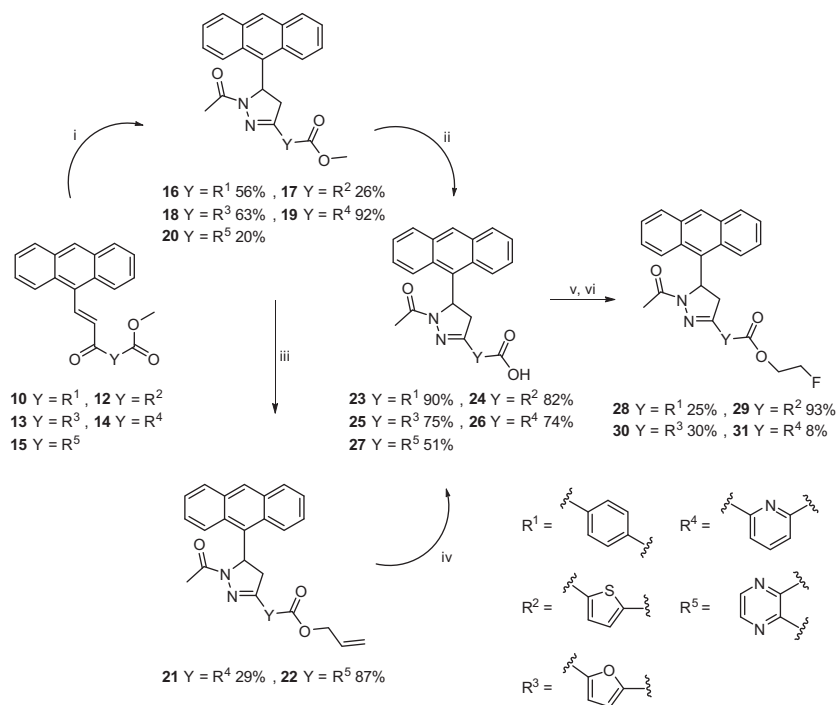
4-acetylbenzoate (**5**) or electron-rich heteroaromatic methyl esters (**7** and **8**) into the respective chalcone resulted in better yields than the same reaction of **4** with electron-deficient heteroaromatic methyl esters (**3** and **9**). Aldol condensation of **4** with ethyl ester **6** was carried out in a similar way as described for **3**, **5** and **7–9**, by using ethanol as the solvent and sodium hydroxide as base to yield compound **11**.

Chalcones (**10–15**) had to be converted rapidly into the corresponding cyclization product, due to decomposition under atmospheric oxygen. Since non-substituted dihydropyrazoles (Fig. 1)

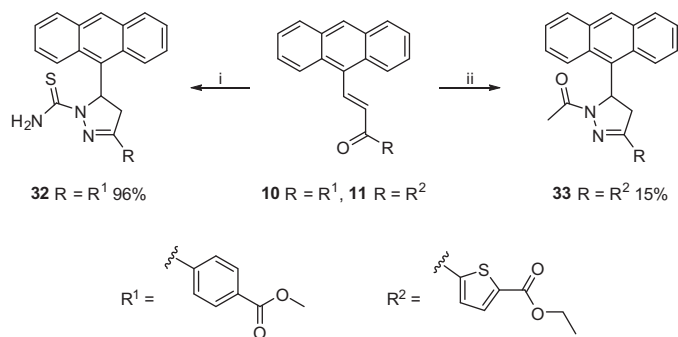
had exhibited instability, the pyrazoline ring was substituted with an additional acetyl moiety (see compounds **16–20** and **33**). Several authors^{15,16} discussed pyrazoline derivatives, substituted with an acetyl moiety as stable and even demonstrated superior MAO-B inhibitory activity of those compounds. Ring closure of compounds **10–15** (Scheme 4) was achieved under microwave assisted reaction conditions in an acidic medium. Methyl esters **16–18** then underwent alkaline hydrolysis in the presence of lithium hydroxide monohydrate to give the corresponding acids (**23–25**). Methyl esters **19** and **20** had to be first converted into the respective allyl



Scheme 3. Synthesis of aldol condensation products **10–15**: reactions and conditions for **10** and **12–15**: methanol, 85% KOH solution, 0 °C → 48 h → rt; reactions and conditions for **11**: ethanol, NaOH, 0 °C → 48 h → rt; % values refer to yields.



Scheme 4. Reactions and conditions: (i) for the reaction of **10–15** into **16–20**: hydrazine monohydrate, CH₃COOH, H₂SO₄, microwave oven at 700 W and 85 °C, (ii) for the reaction of **16–18** into **23–25**: THF/H₂O/MeOH, lithium hydroxide monohydrate, 50 °C, (iii) for the reaction of **19** and **20** into **21** and **22**: toluene, 2-propen-1-ol, NaOMe, 80 °C, 24 h, (iv) for the reaction of **21** and **22** into **26** and **27**: THF, (PPh₃)₄Pd, morpholine, room temperature, 2 h, (v) for the reaction of **23–25** into **28–30**: fluoroethanol, DCC, DMAP, abs. CH₂Cl₂, room temperature, overnight, (vi) for the reaction of **26** into **31**: CH₂Cl₂, 0 °C, oxalyl chloride, DMF, room temperature, overnight → CH₂Cl₂, fluoroethanol, 24 h, room temperature.



Scheme 5. Reactions and conditions: (i) thiosemicarbazide, 1,5,7-triazabicyclo[4.4.0]dec-5-ene, anhydrous acetonitrile, 24 h, 60 °C, (ii) hydrazine monohydrate, CH₃COOH, H₂SO₄, microwave oven at 700 W and 85 °C.

esters (**21** and **22**), in order to obtain free carboxylic acids **26** and **27**. The transesterification of methyl esters into allyl esters was performed in toluene using sodium methoxide as catalyst. Formed methanol was removed by distillation, in order to shift the reaction equilibrium towards the product (**21** and **22**), and thus achieving better yields. Since this transesterification method gave the desired products **21** and **22** only in poor yields, a method of Ilankumaran et al.¹⁷ was adapted for the transesterification of **20** into **22**, using the catalyst 2,8,9-trimethyl-2,5,8,9-tetraaza-1-phosphabi-cyclo [3.3.3]undecane. By employing this method, not only the reaction could be carried out under milder conditions in regard to the temperature, but also the yield could be improved by 54%.

Cleavage of the allyl moiety of **21** and **22** with tetrakis(triphenylphosphine)palladium and morpholine as the nucleophile was performed selectively due to the high sensitivity of the allyl ester function towards transition metals. Resulting acids **23–25** as well as acid **26** were subjected to an esterification reaction with fluoroethanol. Compounds **28–30** were synthesized under mild reaction conditions, using dicyclohexylcarbodiimide and dimethylamino-pyridine. To obtain fluoroethyl ester **31**, the reaction of **26** into the corresponding acid chloride was required, which was subsequently converted into the desired product **31** with fluoroethanol. Following the synthesis protocol of compound **31**, carboxylic acid **27** was also transformed into the corresponding acid chloride to

obtain the desired fluoroethyl ester by reaction with fluoroethanol. Unfortunately, **27** could not be converted into the respective fluoroethyl ester and it is unclear whether the reaction procedure was unsuccessful or the desired target product could not be isolated due to instability of the molecule.

Since it was reported that not only pyrazoline based compounds, containing an acetyl moiety showed enhanced MAO-B inhibitory activity, but also pyrazoline derivatives substituted with a thiocarbamoyl moiety,^{18–20} compound **32** was prepared as well. As depicted in **Scheme 5**, excellent yields of **32** were achieved by cyclization of chalcone **10** with thiosemicarbazide and the catalyst 1,5,7-triazabicyclo[4.4.0]dec-5-ene. However, preliminary log*P* evaluations of **32** were rather discouraging as a log*P* value of 5.66 for substance **32** was determined. Thus, synthesis of this substance class was discontinued.

In the course of finding an ideal cyclization method for compounds **16–20**, compound **33** was also synthesized (**Scheme 5**). The cyclization procedure in acetic acid with hydrazine monohydrate ameliorated product stability, due to substitution of the pyrazoline ring with an acetyl moiety, which additionally improved the yield of **33**. Since good results were achieved by employing this approach, compounds **16–20** were prepared in the same manner.

For selected compounds full and unambiguous assignment of all ¹H, ¹³C, ¹⁵N and ¹⁹F NMR resonances was achieved by combining standard NMR techniques,²¹ such as fully ¹H-coupled ¹³C NMR spectra, APT, gs-HSQC, gs-HMBC, COSY, TOCSY and NOESY experiments.

For model compound **17** the crucial HMBC correlations (left) as well as some important NOEs (right) are displayed in **Figure 2**, unambiguously confirming the given structure. The location of the *N*-acetyl group and thus the position of the C=N double bond in the dihydropyrazole system is supported by HMBC correlations between pyrazole H-4 and H-4' to anthranyl C-9, from pyrazole H-5 to anthranyl C-8a, C-9 and C-9a and from thiophene H-4 to pyrazole C-3. An interesting phenomenon was observed for the 9-anthranyl system, in which corresponding positions 1 and 8, 2 and 7, 3 and 6, 8a and 9a, etc. were found to be non-equivalent. A possible explanation for this phenomenon would be restricted rotation of the anthranyl system around the pyrazole C-5–anthranyl C-9 single bond. Thus, for instance, protons of the pyrazole system show different through-space interactions to corresponding protons of the anthranyl system: whereas a stronger NOE between

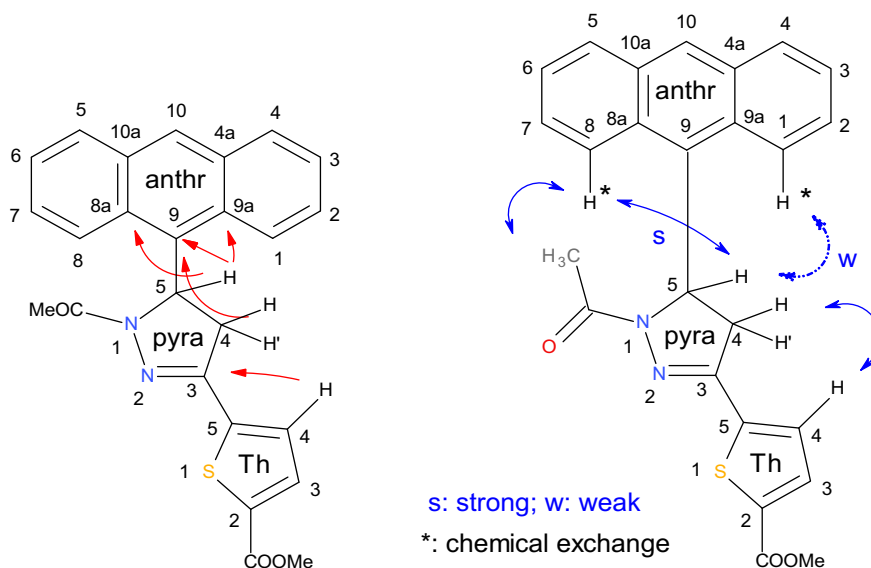


Figure 2. Atom numbering, important HMBC correlations (left) and NOEs (right) of compound **17** (in CDCl₃ solution).

pyrazole H-5 (6.88 ppm) and anthranil H-8 (7.73 ppm) is detected, the appropriate effect is considerably smaller between pyrazole H-5 and anthranil H-1 (8.47 ppm). Moreover, a distinct NOE between the acetyl-H protons and anthranil H-8 is evident, in contrast, the interaction between acetyl protons and anthranil H-1 is very small. The relatively large chemical shift difference between accordant anthranil protons H-1 (8.47 ppm) and H-8 (7.73 ppm) can be explained by the magnetic anisotropy effect of the acetyl C=O group which obviously influences H-1 considerably more than H-8 in the preferred rotameric status at hand. In the NOESY spectrum of **17** the signals due to anthranil H-1 and H-8 exhibit a characteristic cross peak resulting from chemical exchange (different phase property compared to the cross peaks originating from NOEs), thus giving a hint to a slow rotation of the anthranil unit compared to the NMR timescale.

In order to estimate the binding affinity of the synthesized compounds, they were docked into the crystal structure of the human MAO-B in complex with FAD and noncovalently bound *p*-nitro-benzylamine (PDB code 2C70).

Compounds **16–20** and **28–31**, as well as reference compounds **34** and **35**, being the most active substances in Mishra and Sasmal,¹³ were prepared for a physiological pH using LigPrep (LigPrep, version 2.5, Schrödinger, LLC, New York, NY, 2012).

As the acetyl- or thiocarbamoyl substituents on the pyrazoline moiety had to be accommodated within a relatively narrow binding pocket, side chains of the residues in the hydrophobic pocket (I198 and Y435) were allowed to take possible rotamer orientations defined within the GOLD docking software.²² A maximum of ten poses per ligand was allowed, primarily ranked by the default scoring function, ChemPLP.²³ In order to reduce strain energies caused by the placement algorithm, the complexes were energy minimized using a stepwise relaxation protocol within the MOE software package (Molecular Operating Environment (MOE) version 2013.0801, Chemical Computing Group, Montreal, Canada). Subsequently, the binding free energy of the minimized complexes was estimated by external rescoring using X-Score,²⁴ as the original scoring values of ChemPLP are per se dimensionless. K_i values were further calculated from ΔG values of the best scored pose per ligand, using Eq. 1.

$$K_i = \exp\left(\frac{\Delta G}{R \cdot T}\right)$$

$$R = 8.3144621 \text{ J/mol} \cdot \text{K}; T = 298.15 \text{ Kelvin} \quad (1)$$

Analysis of the docking results indicates that the novel compounds are able to be accommodated in a similar way as described for the reference compounds **34** and **35**. As expected, introduction of bulky groups on the central heteroaromatic linker enforced a slightly different orientation of the synthesized compounds. Figure 3 shows the most prominent interaction among the observed poses, a pi stacking interaction between Y435 and ring A or C of the anthracene moiety. Simultaneously, the phenolic hydroxy group of the aromatic side chain was frequently observed to stabilize the substituted heteroaromatic linker (acetyl or thiocarbamoyl moiety). Potentially less favorable side chain orientations caused by the bulky substituents hence could be compensated. In analogy to the nitro group of compound **34**, the carbonyl oxygen of the distal ester function among the investigated molecules sporadically acted as hydrogen bond acceptor for the side chain of Y326. Due to the absence of an acceptor atom in the corresponding position, reference compound **35** is unable to form this particular interaction, which could be an explanation for the inferior experimentally determined K_i value. In general, the calculated K_i values were about an order of magnitude larger than the literature values of **34** and **35**. However, as demonstrated in Table 1, it can be assumed that the activity of compounds **16–20**

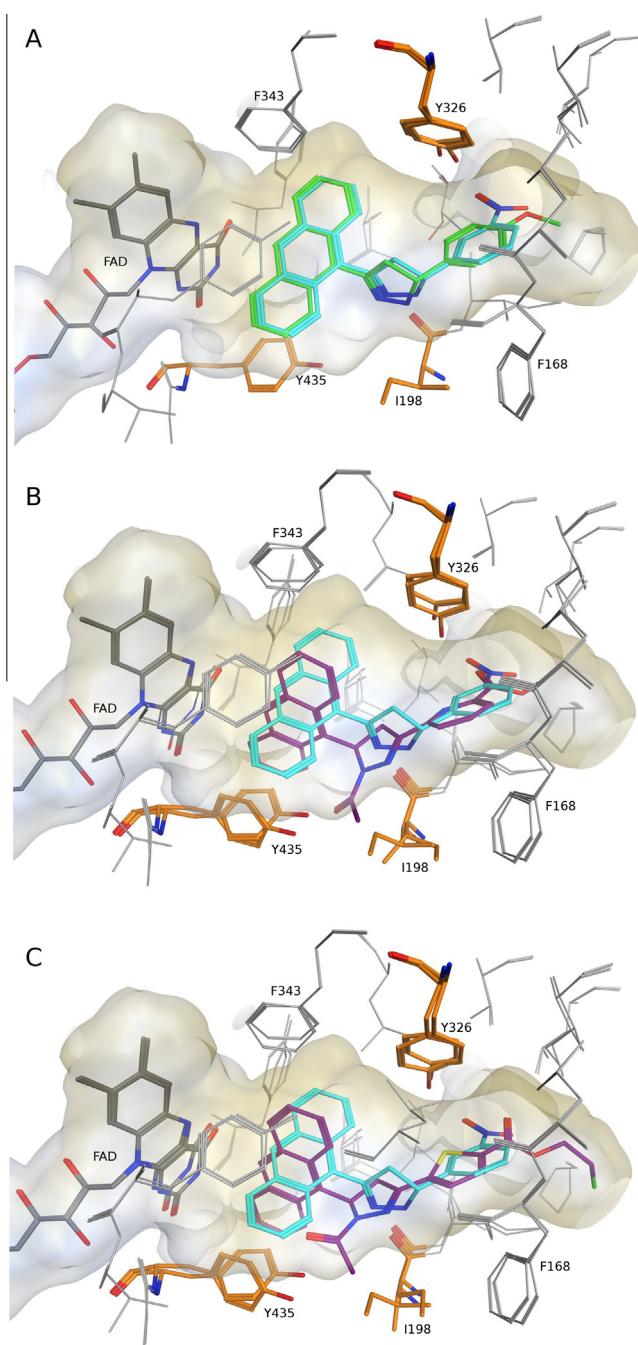


Figure 3. MAO-B binding pocket in complex with reference compounds and exemplary docking poses of methyl- and fluoroethyl ester derivatives. Key residues are highlighted in orange. (A) Reference compounds **34** (cyan) and **35** (green) in superposition. (B) Docking poses of **34** (cyan) and **19** (purple). (C) Docked complexes of **34** (cyan) and **29** (purple).

and **28–31** is in the range of the reference compounds (**34** and **35**). As the significant activity difference between **34** and **35** was at least indicated by the calculated ΔG values, the energy estimates could as well be used for prioritizing new members of this compound class prior to in vitro testing (Fig. 4).

Taken together, thirteen new target compounds have been prepared within the scope of this work, which aimed at the development of new, selective and reversible PET tracer precursors and reference compounds for the imaging of the MAO-B system via PET. Substitution of the pyrazoline ring with an additional acetyl moiety at position 1 of the pyrazoline ring has been proven

Table 1
Molecular weight, yield, melting point and calculated K_i value of methyl esters (**16–20** and **32**) and fluorethyl esters (**28–31**) as well as reference compounds (**34** and **35**)

Compound	MW	Y (%)	Mp (°C)	Calcd K_i (nM)
16	422.48	58	279–281	2.44
17	428.51	26	266–267	4.96
18	412.44	63	201–203	5.58
19	423.47	92	154–155	2.79
20	424.46	20	244–246	7.06
28	454.50	25	214–215	3.36
29	460.52	93	130–132	4.26
30	444.46	30	157–158	9.73
31	455.49	8	–	5.97
32	439.53	96	295–296	2.48
34	367.41	–	110	4.19
35	352.44	–	107	7.18

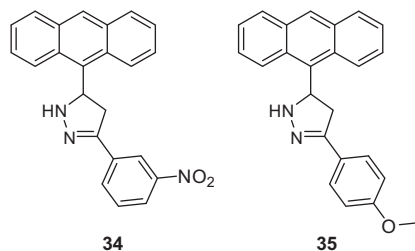


Figure 4. Chemical structure of 5-(anthracen-9-yl)-3-(3-nitrophenyl)-4,5-dihydro-1H-pyrazole (**34**) and 5-(anthracen-9-yl)-3-(4-methoxyphenyl)-4,5-dihydro-1H-pyrazole (**35**).

beneficial for the stability of compounds **16–31** in contrast to non-stable 5-(anthracen-9-yl)-3-phenyl-4,5-dihydro-1H-pyrazole derivatives. Additionally, compound **32** has been prepared by inserting an additional thiocarbamoyl moiety. As preliminary investigations showed rather unsatisfactory results, regarding the $\log P$ value, the synthesis of the substance class containing a thiocarbamoyl moiety, was not continued. Methyl esters **16–20** and fluorethyl esters **28–31** serve as reference compounds and will be evaluated for affinity and selectivity towards MAO-B. Docking studies indicate that methyl esters **16–20** and fluorethyl esters **28–31** might bind in an analogous way than the reference compounds **34** and **35**¹³ and thus are promising candidates for biological testing. The most promising compounds regarding their suitability as MAO-B ligands, will then be selected for the further development of new, selective and reversible PET-tracers for the MAO-B system. Therefore, free carboxylic acids **23–27** will serve as starting materials for the preparation of radiolabeled ¹¹C and ¹⁸F pyrazoline based MAO-B PET tracers. Hence, it is

conclusive to assume that ¹¹C and ¹⁸F labeled pyrazoline based MAO-B PET tracers may serve as promising molecular imaging biomarkers for the detection of increased MAO-B levels in early AD. The results of ongoing studies on affinity, selectivity and lipophilicity of the discussed compounds, will be published in the following paper.

Supplementary data

Supplementary data associated with this article can be found, in the online version, at <http://dx.doi.org/10.1016/j.bmcl.2014.07.085>.

References and notes

- Shih, J. C.; Chen, K.; Ridd, M. J. *Annu. Rev. Neurosci.* **1999**, *22*, 197.
- Bortolato, M.; Chen, K.; Shih, J. C. *Adv. Drug Delivery Rev.* **2008**, *60*, 1527.
- Brookmeyer, R.; Johnson, E.; Ziegler-Graham, K.; Arrighi, H. M. *Alzheimers Dement.* **2007**, *3*, 186.
- Lendon, C. L.; Ashall, F.; Goate, A. M. *JAMA* **1997**, *277*, 825.
- Gulyás, B.; Pavlova, E.; Kása, P.; Gulya, K.; Bakota, L.; Várszegi, S.; Keller, É.; Horváth, M. C.; Nag, S.; Hermecz, I.; Magyar, K.; Halldin, C. *Neurochem. Int.* **2011**, *58*, 60.
- Kennedy, B. P.; Ziegler, M. G.; Alford, M.; Hansen, L. A.; Thal, L. J.; Masliah, E. J. *Neural Transm.* **2003**, *110*, 789.
- Nakamura, S.; Kawamata, T.; Akiyoshi, I.; Kameyama, M.; Nakamura, N.; Kimura, H. *Acta Neuropathol.* **1990**, *80*, 419.
- Saura, J.; Luque, J. M.; Cesura, A. M.; Da Prada, M.; Chan-Palay, V.; Huber, G.; Löffler, J.; Richards, J. G. *Neuroscience* **1994**, *62*, 15.
- Mück-Seler, D.; Presecki, P.; Mimica, N.; Mustapic, M.; Pivac, N.; Babic, A.; Nedic, G.; Folnegovic-Smalc, V. *Prog. Neuropsychopharmacol. Biol. Psychiat.* **2009**, *33*, 1226.
- Mimica, N.; Mück-Seler, D.; Pivac, N.; Mustapic, M.; Dezeljin, M.; Stipcevic, T.; Presecki, P.; Radonic, E.; Folnegovic-Smalc, V. *Coll. Antropol.* **2008**, *32*, 119.
- Pugliese, M.; Rodriguez, M. J.; Gimeno-Bayon, J.; Pujadas, L.; Billett, E. E.; Wells, C.; Mahy, N. J. *Neurosci. Res.* **2010**, *88*, 2588.
- Zellner, M.; Baureder, M.; Rappold, E.; Buger, P.; Kotzailias, N.; Babeluk, R.; Baumgartner, R.; Attems, J.; Gerner, C.; Jellinger, K.; Roth, E.; Oehler, R.; Umlauf, E. J. *Proteom.* **2012**, *75*, 2080.
- Mishra, N.; Sasmal, D. *Bioorg. Med. Chem. Lett.* **2011**, *21*, 1969.
- Houminer, Y.; Southwick, E. W.; Williams, D. L. *J. Org. Chem.* **1989**, *54*, 640.
- Lévai, A.; Jeko, J.; Brahmabhatt, D. I. *J. Heterocycl. Chem.* **2005**, *42*, 1231.
- Lévai, A.; Jeko, J. *J. Heterocycl. Chem.* **2006**, *43*, 111.
- Ilankumaran, P.; Verkade, J. G. *J. Org. Chem.* **1999**, *64*, 3086.
- Ucar, G.; Gokhan, N.; Yesilada, A.; Bilgin, A. A. *Neurosci. Lett.* **2005**, *382*, 327.
- Gökhan-Kelekcı, N.; Yabanoglu, S.; Küpeli, E.; Salgin, U.; Özgen, Ö.; Ucar, G.; Yesilada, E.; Kendi, E.; Yesilada, A.; Bilgin, A. A. *Bioorg. Med. Chem.* **2005**, *15*, 5775.
- Gökhan, N.; Yesilada, A.; Ucar, G.; Erol, K.; Bilgin, A. A. *Arch. Pharm.* **2003**, *336*, 362.
- Braun, S.; Kalinowski, O. O.; Berger, S. *150 and More Basic NMR Experiments: A Practical Course*, 2nd expanded ed.; Wiley-VCH: Weinheim, 1998.
- Verdonk, M. L.; Cole, J. C.; Hartshorn, M. J.; Murray, C. W.; Taylor, R. D. *Proteins* **2003**, *52*, 609.
- Korb, O.; Stützel, T.; Exner, T. E. *J. Chem. Inf. Model.* **2009**, *49*, 84.
- Wang, R.; Lai, L.; Wang, S. J. *Comput. Aided Mol. Des.* **2002**, *16*, 11.

5.4.2 NET

Article

Synthesis and *in silico* evaluation of novel compounds for PET based investigations of the norepinephrine transporter

Catharina Neudorfer ^{1,2,*}, Amir Seddik ³, Karem Shanab ^{1,2}, Andreas Jurik ³, Christina Rami-Mark ¹, Wolfgang Holzer ², Gerhard Ecker ³, Markus Mitterhauser ¹, Wolfgang Wadsak ¹, Helmut Spreitzer ^{2,*}

¹ Medical University of Vienna, Department of Biomedical Imaging and Image-guided Therapy, Division of Nuclear Medicine, Waehringer Guertel 18-20, 1090 Vienna, Austria

² University of Vienna, Faculty of Life Sciences, Department of Pharmaceutical Chemistry, Division of Drug Synthesis, Althanstraße 14, 1090 Vienna, Austria

³ University of Vienna, Faculty of Life Sciences, Department of Pharmaceutical Chemistry, Division of Drug Design and Medicinal Chemistry, Althanstraße 14, 1090 Vienna, Austria

* Author to whom correspondence should be addressed; E-Mail: catharina.neudorfer@gmail.com; Tel.: +43-4277-55629; Fax: +43-4277-855629 (C. Neudorfer). E-Mail: helmut.spreitzer@univie.ac.at; Tel.: +43-4277-55621; Fax: +43-4277-855621 (H. Spreitzer).

Received: / Accepted: / Published:

Abstract: Since the NET is involved in a variety of diseases, the investigation of underlying dysregulation-mechanisms of the NE system is of major interest. Based on the previously described highly potent and selective NET ligand 1-(3-(methylamino)-1-phenylpropyl)-3-phenyl-1,3-dihydro-2H-benzimidazol-2-one (Me@APPI), this paper aims at the development of several fluorinated methylamine based analogs of this compound. The newly synthesized compounds were computationally evaluated for their interactions with the monoamine transporters and represent reference compounds for PET based investigation of the NET.

Keywords: NET; ADHD; Cocaine dependence; BAT; PET; FAPPI

1. Introduction

Abnormal regulation of the norepinephrine transporter (NET) or NET dysfunction, respectively, cause either increased or decreased levels of norepinephrine (NE) in the synaptic cleft. Since NE is a fundamental neurochemical messenger, its accurate regulation is of major importance. Thus, the NET, responsible for NE equilibrium in the synaptic cleft, is representing the reuptake site and considered to be involved in a variety of neurological/psychiatric disorders,^{1,2} but also plays a pivotal role in cardiovascular^{1,2,3} and metabolic diseases.³⁻⁵ Reduced NET levels go along with neurological disorders like major depression,^{6,7} Parkinson's disease (PD), Alzheimer's disease (AD)⁸⁻¹⁸, and cardiovascular diseases such as hypertension, cardiomyopathy, and heart failure.^{5,13} Furthermore, a dysfunction of the NE system was reported in Attention Deficit Hyperactivity Disorder (ADHD),^{9,17,19} suicide,^{1,12,20} substance abuse (cocaine dependence),¹⁶ and schizophrenia.¹⁰ A more recent discovery is the involvement of the NET in diseases like diabetes and obesity, due to its presence in brown adipose tissue (BAT) and the proposed activation thereof via NE.^{4,5,21}

Based on the fact that the NET is involved in such a variety of diseases, the investigation of the underlying dysregulation-mechanism of the NE system is of major interest. For this purpose, information about the transporter abundance and density in healthy and pathological living human brains is required. The most suitable and accurate technique to gain this information is positron emission tomography (PET). As a non-invasive molecular imaging technique, it represents a suitable approach towards the collection of missing data in the living organism and direct quantification of receptor/transporter densities *in vivo*. To fully gain insight in the molecular changes of the noradrenergic system *via* PET, however, prior development of suitable NET PET radioligands is required.

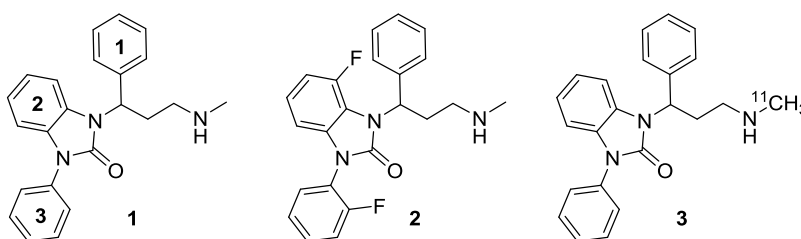
So far, radiolabeled NET binding reboxetine analogs [¹¹C]MeNER, [¹¹C]MRB, ((*S,S*)-2-(α -(2-[¹¹C]methoxyphenoxy)benzyl) morpholine) and [¹⁸F]FMeNER-D₂ ((*S,S*)-2-(α -(2-[¹⁸F]Fluoro[²H₂]methoxyphenoxy)benzyl) morpholine) have been described, which however display certain limitations such as metabolic stability, complex radiosynthesis, or late equilibrium.²²⁻²⁶

Recently, Zhang *et al*²⁶ evaluated a series of benzimidazolone based propanamines with *in vitro* inhibitory activity on the human norepinephrine transporter (hNET). The results of these investigations suggested that compounds containing a phenyl moiety directly at the benzimidazolone ring (e.g. **1**) (figure 1) were the most potent, representing a half maximal inhibitory concentration (IC₅₀) below 10 nM (IC₅₀ < 10 nM). Furthermore, hNET selectivity over hSERT (human serotonin transporter) turned out (> 300-fold) superior to those of reboxetine and atomoxetine (16- and 81-fold).²⁶ Fluorination at position 2 of the phenyl moiety, attached to the benzimidazolone ring (e.g. **2**) (figure 1), indicated similar hNET potency, comparable to its non-fluorinated analogs (e.g. **1**) and additionally exhibited hNET selectivity over hSERT (80-fold) similar to atomoxetine.²⁶

Both benzimidazolone derived propanamines with a phenyl moiety (**1**), as well as a fluorinated phenyl moiety (**2**) indicated excellent hNET selectivity over hDAT (human dopamine transporter) with < 50% inhibition of the cocaine analog [³H]WIN-35,428, binding to hDAT at a concentration of 10 μ M.²⁶

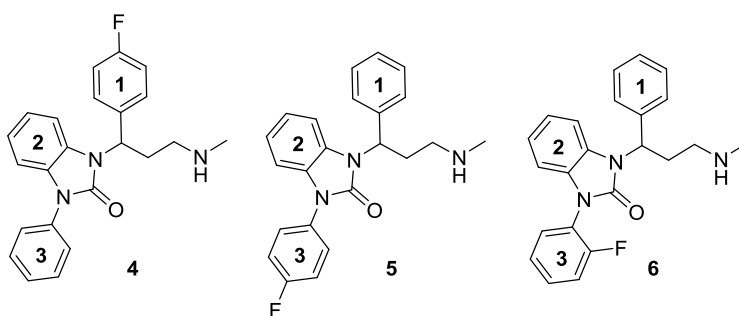
Given those findings, both described benzimidazolone based propanamines (**1** and **2**) represent excellent candidates for selective and potent NET inhibition with high affinity and low unspecific binding. Thus, on the basis of the results of Zhang *et al.*²⁶ the methylamino moiety of core compound **1** has been radiolabeled with ¹¹C and tested by our research group.²⁷ All investigated preclinical parameters, such as affinity, blood brain barrier penetration, lipophilicity, metabolic degradation, and selectivity showed excellent results, thus suggesting suitability of ¹¹C radiolabeled 1-(3-(methylamino)-1-phenylpropyl)-3-phenyl-1,3-dihydro-2H-benzimidazole-2-one (¹¹C]Me@APPI) (**3**) (figure 1) as a NET radioligand for the employment in PET.

Figure 1. Chemical structure of the highly potent and selective NET ligands 1-(3-(methylamino)-1-phenylpropyl)-3-phenyl-1,3-dihydro-2H-benzimidazol-2-one (Me@APPI) (**1**) and 4-fluoro-1-(2-fluorophenyl)-3-(3-(methylamino)-1-phenylpropyl)-1,3-dihydro-2H-benzimidazol-2-one (**2**) as well as radiolabeled analog [¹¹C]Me@APPI (**3**).



Due to successful preclinical testing of [¹¹C]Me@APPI (**3**) and given the excellent *in vitro* results of compound **2**, shown by Zhang *et al.*,²⁶ the aim of this paper is the synthesis and docking studies of several fluorinated analogs (**4-6**) of compound **1** (figure 2) as reference compounds for their later prepared radioactive analogs. All methylamine derived benzimidazolone derivatives (**4-6**) will be subjected to affinity, selectivity, and lipophilicity studies towards the NET as well as blood brain barrier penetration experiments at the Medical University of Vienna. The most promising NET ligands will then be selected for the development of new, selective PET tracers for the NET. Thereby, radiolabeling with both, ¹¹C and ¹⁸F will be subject of further experiments.

Figure 2. Chemical structure of envisaged reference compounds **4-6** (FAPPI: 1-3).



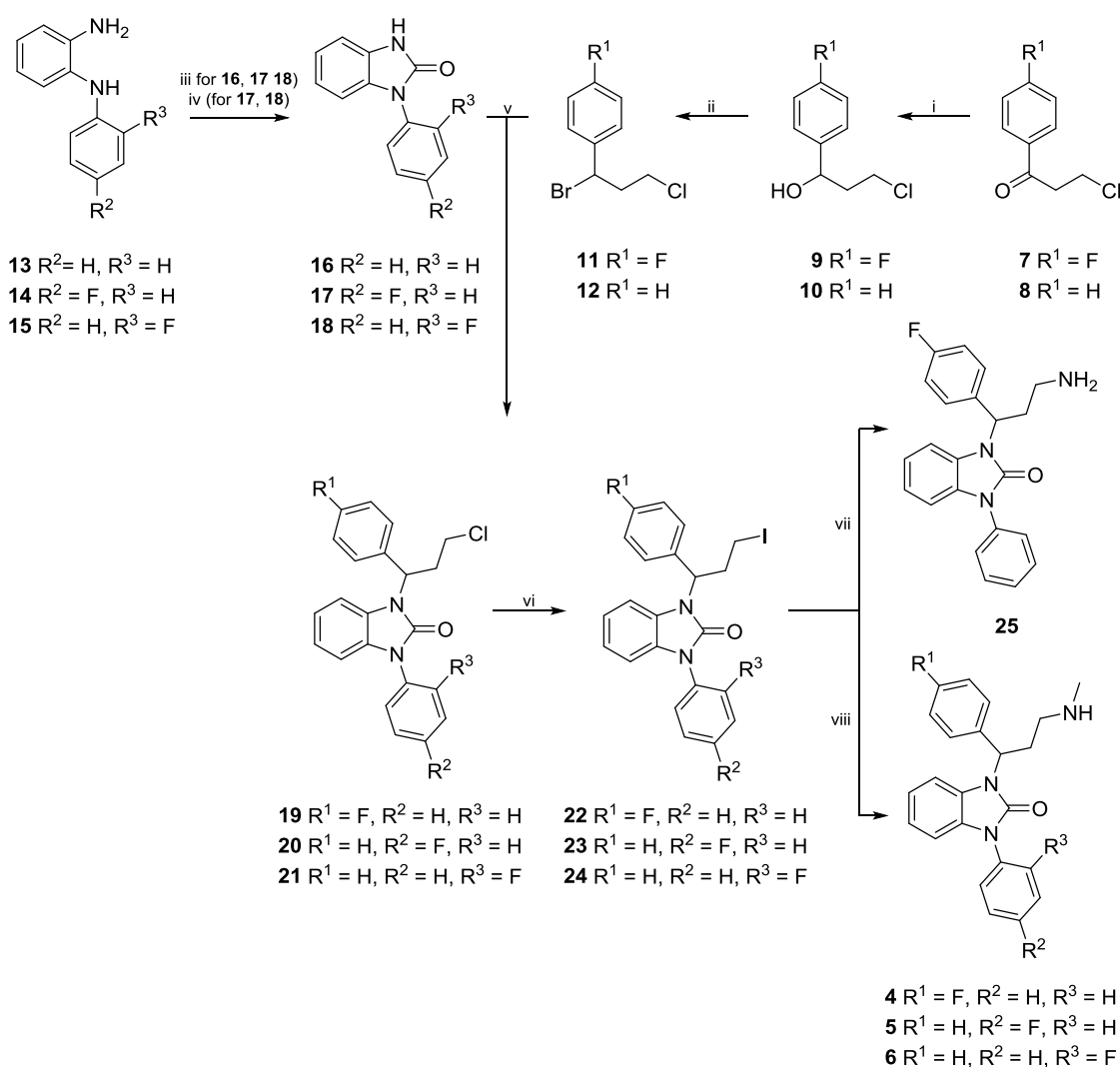
2. Results and Discussion

The synthesis of reference compounds **4-6** first required the preparation of side chains **11** and **12**, as well as core compounds **16-18**. After successful preparation, side chain **11** was merged in a

condensation reaction with core compound **16**, whereas side chain **12** was reacted with core compounds **17** and **18**, prior to halogen exchange and substitution with methylamine (scheme 1).

For the synthesis of side chains **11** and **12**, the keto group of commercially available compounds **7** and **8** was reduced with sodium borohydride, in order to obtain intermediate alcohols **9** and **10**. Subsequent bromination of **9** and **10** with aqueous hydrogen bromide led to the formation of products **11** and **12**, respectively.

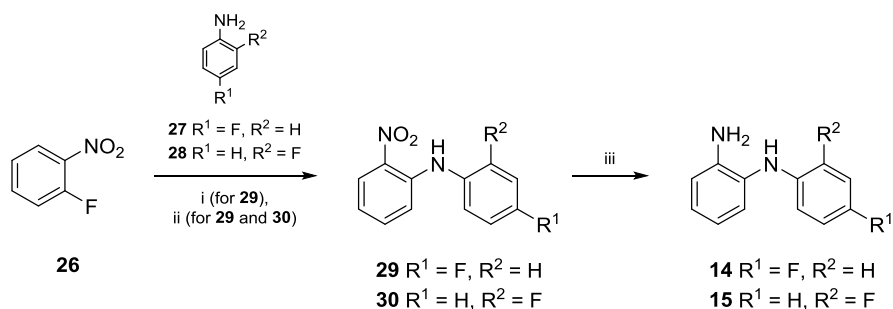
Scheme 1. Reactions and conditions for: (i) THF, EtOH, NaBH₄, -10°C → -5°C, 10 min, yields for **9**: 95%, **10**: 100%; (ii) aqu. HBr, rt, 3 h, yields for **11**: 64%, **12**: 86%; (iii) 1,1'-carbonyldiimidazol, anhyd. THF, rt, overnight, yields for **16**: 74%, **17**: 61%, **18**: 69%; (iv) 1,1'-carbonyldiimidazol, anhyd. DMF, 90°C, 2 h, yields for **17**: 80%, **18**: 80%; (v) K₂CO₃, DMF, rt, 30 min → addition of **11** and **12** → rt, 30 min, yields for **19**: 32%, **20**: 63%, **21**: 55%; (vi) NaI, acetone, reflux, 24 h, yields for **22**: 82%, **23**: 76%, **24**: 53%; (vii) NH₃ in isopropanol, 80°C, 3 h, yield for **25**: 50%; (viii) methylamine in EtOH, 80°C, 3 h, yields for **4**: 48%, **5**: 29%, **6**: 30%.



Core compound **16** was prepared by the reaction of commercially available *N*-phenylbenzene-1,2-diamine (**13**) with 1,1'-carbonyldiimidazole. For the preparation of **17** and **18** however, **14** and **15** first

had to be made accessible (scheme 2). Thus, 1-fluoro-2-nitrobenzene (**26**) reacted with commercially available fluoroanilines **27** and **28**, respectively, to obtain disubstituted amines **29** and **30**. Therefore, two different methods were applied (scheme 2): The first method (i) was conducted by heating **26** and **27** with anhydrous potassium fluoride and potassium carbonate in a microwave oven. Since an alternative method -conventional heating at 180 °C- gave compound **29** in higher yields, this approach (ii) was chosen for the large scale synthesis of **29** as well as for the preparation of **30**.

Scheme 2. Reactions and conditions for (i) anhyd. KF, K₂CO₃, microwave oven, 900 W, 10 min, yields for **29**: 58%; (ii) anhyd. KF, K₂CO₃, 180°C, 2 d, yields for **29**: 68%, **30**: 52%; (iii) Zn, AcOH, 0°C → rt, 2 h, yields for **14**: 93%, **15**: n.d.



In the next reaction step, the nitro groups of both disubstituted amines (**29** and **30**) were reduced. For this purpose **29** or **30** were added to a mixture of zinc/acetic acid. The resulting amines **14** or **15** were obtained in excellent yields (scheme 2).

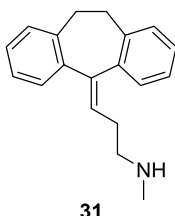
Freshly prepared intermediates **14** and **15** were then subjected to a cyclization reaction with 1,1'-carbonyldiimidazol in DMF under anhydrous conditions (scheme 1). DMF was preferred over THF in order to ensure higher yields and shorter reaction times.

Condensation reactions of benzimidazolones **16**, **17**, and **18** with side chains **11** and **12**, respectively were performed under basic conditions (scheme 1). After purification, the chloro substituted derivatives **19-21** were converted into the iodo compounds (**22-24**) in a Finkelstein reaction. Target compounds **4-6** (FAPPI:1-3) were then made accessible by heating derivatives **22-24** in a solution of methylamine in ethanol in a sealed tube for 3 h. Additionally to reference compounds **4-6**, free amine **25** was synthesized by dissolving **22** in a solution of ammonia in isopropanol and heating the resulting mixture in a sealed tube for 3 h. As compound **25** features a free amine moiety, it can be considered a precursor for radiosynthesis.

Since compounds **4** and **5** comprise a novel fluoro substitution, a computational docking study was performed to assess if these compounds still would fit in the binding site of the NET. Furthermore, we aimed at creating a binding mode hypothesis which allows gaining insights into the molecular basis of binding and selectivity towards the monoamine transporters. As the basic scaffold has been shown to act in an enantioselective manner, the respective (*R*) enantiomers were used throughout the docking studies.²⁶ The ligands were docked in the substrate binding site (S1) of the outward-open conformation of the transporter models (see Experimental Section for details), since related inhibitors, such as nortriptyline, sertraline, mazindol, etc. were also shown to fit in the S1 of the *Drosophila* DAT (dDAT) and the "SERT"-ized leucine transporter ("LeuBAT") in the same protein conformation.^{28,29}

Interestingly, the co-crystallized ligand in dDAT, nortriptyline (**31**), has the same ranking of human NET, SERT and DAT activity as reference compound **1**, i.e. 4.4, 18 and 1149 nM K_D vs. 9, 2995 and >10000 nM IC_{50} , respectively.^{26,30} Additionally, nortriptyline shares important structural features with the benzimidazolones, i.e. two aromatic moieties and an *N*-methyl-ethylenamine side chain. Therefore their binding mode can be expected to be similar.

Figure 3. Chemical structure of nortriptyline (co-crystallized ligand from the template (PDB code 4M48)).²⁸



Common scaffold clustering³¹ revealed two binding hypotheses (see Experimental Section) which indicated that compounds **4-6** fit in the S1 of all three transporters. Hence, additional fluorination does not seem to cause steric clashes. In both hypotheses, the most prominent protein-ligand interaction was the cationic nitrogen atom placed in the A sub pocket,³² located between the central Asp75/98/79 side chain as a salt-bridge and the Phe72/95/76 side chain as a cation-*pi* interaction in NET/SERT/DAT, respectively. This is well in accordance with the X-ray structures of the templates. Additional *pi-pi* stacking interactions with Phe152/176/156 and Phe323/355/341 further promote the binding in both hypotheses obtained.

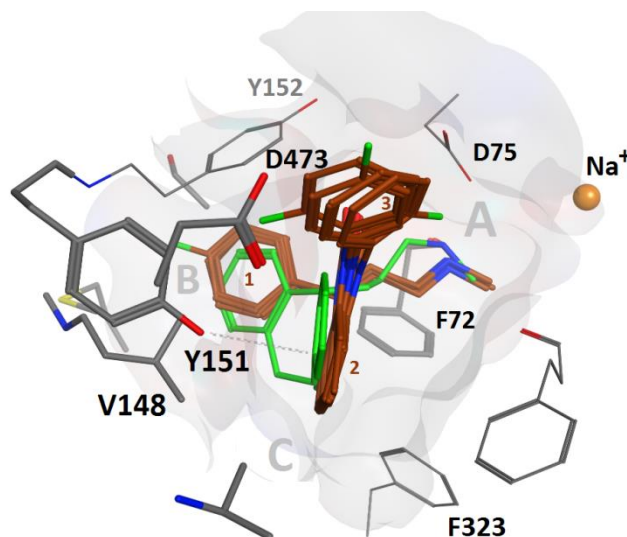
Hypothesis 1: the benzimidazolone heterocycle (ring 2) is placed in the B sub pocket and ring 3 in the C pocket, whereas ring 1 is solvent exposed (see figure in Experimental Section).

Hypothesis 2: Ligand ring 1 is placed in the B pocket whereas ring 2 is placed at the same height (measured from the membrane-water interface) and overlap with the rings of nortriptyline (**31**). The solvent exposed Tyr151/Tyr175/Phe155 in NET/SERT/DAT, resp. T-stacks with ring 2 whereas ring 3 points extracellularly (Table 1, Figure 4).

Table 1. Sequence alignment of all distinct monoamine transporter residues located in sub sites (reference **32**) in the vicinity of the docked compounds. Red: hydrophilic side chain, green: lipophilic side chain, bold: bulkier side chain.

	B site				C site			Outer site		
hNET	S420	M424	G149	V148	A145	F72	D473	Y151	A477	
hSERT	T439	L443	A173	I172	A177	Y95	E493	Y175	T497	
hDAT	A423	M427	G153	V152	S149	F76	D476	F155	A480	

Figure 4. Overlay of compounds **1**, **2**, and **4-6** (maroon) in binding hypothesis 2 in hNET showing agreement with the co-crystal pose of nortriptyline (**31**) (green). Val148 and Asp473 allow more space than Ile172 and Glu439 in hSERT, resp., whereas Tyr151 might induce a more potent stacking interaction as compared to Phe155 in hDAT. The angle between ligand ring 2 and 3 is almost 90° in all poses. The extracellular space is located above.



As binding hypothesis 2 is in close agreement with the co-crystallized ligands in dDAT and LeuBAT, we focus further analysis on this proposed binding mode.

Binding hypothesis 2 indicates why the investigated compounds (**4-6**) show weaker affinity to SERT and DAT than to NET: lower SERT affinity may be due to Ile172 and Glu439, allowing less space for the ligand to be accommodated as compared to in NET, that comprises a valine and an aspartate at the homologous positions, respectively. Lower DAT affinity could be ascribed to weaker T stacking interactions of Phe155 as compared to Tyr151 in NET, based on previous findings that a Tyr-Phe pair has a stronger binding energy than a Phe-Phe pair.³⁴

3. Experimental Section

3.1. General

The NMR spectra were recorded from CDCl₃ or DMSO-*d*₆ solutions on a Bruker DPX200 spectrometer (200 MHz for ¹H, 50 MHz for ¹³C) or on a Bruker Avance III 400 spectrometer (400 MHz for ¹H, 100 MHz for ¹³C, 40 MHz for ¹⁵N, 376 MHz for ¹⁹F) at 25 °C. The center of the solvent (residual) signal was used as an internal standard which was related to TMS with δ 7.26 ppm (¹H in CDCl₃), δ 2.49 ppm (¹H in DMSO-*d*₆), δ 77.0 ppm (¹³C in CDCl₃) and δ 39.5 ppm (¹³C in DMSO-*d*₆). ¹⁵N NMR spectra (gs-HMBC, gs-HSQC) were referenced against neat, external nitromethane, ¹⁹F NMR spectra by absolute referencing via \mathcal{E} ratio. Digital resolutions were 0.25 Hz/data point in the ¹H and 0.3 Hz/data point in the ¹³C-NMR spectra. Coupling constants (*J*) are quoted in Hz. The following abbreviations were used to show the multiplicities: s: singlet, d: doublet, t: triplet, q: quadruplet, dd: doublet of doublet, m: multiplet. Mass spectra were obtained on a Shimadzu QP 1000 instrument (EI, 70 eV), high-resolution mass spectrometry was carried out on a Finnigan MAT 8230 (EI, 10 eV) or

Finnigan MAT 900 S (ESI, 4 kV, 3 μ A, CH₃CN/MeOH) electrospray ionization mass spectrometer with a micro-TOF analyzer. Microwave experiments were carried out in a Synthos 3000 microwave oven (Anton Paar, SXQ80 rotor) with an internal temperature probe.

3.2. Syntheses

Compound purity: All compounds synthesized featured a purity of at least 95%.

General procedure for the synthesis of 9 and 10

Starting materials **7** or **8**, respectively (1 mmol) was dissolved in THF (1 ml) and EtOH (1 ml) was added. The mixture was cooled to -10°C and NaBH₄ (1.05 mmol) was slowly added at this temperature. The solution was stirred at -5°C for 10 min and thereafter, poured into a mixture of saturated aqueous ammonium chloride (3 ml) in ice (1.5 g). The product was extracted with diethyl ether, dried over Na₂SO₄ and evaporated to dryness. The crude product was employed directly in the subsequent reaction step without further purification.

3-Chloro-1-(4-fluorophenyl)propan-1-ol (9) Yield: 4.78 g (95%), pale yellow oil, analytical data are in complete accordance with literature values.³⁵

3-Chloro-1-phenylpropan-1-ol (10) Yield: 4.61 g (99%), light yellow oil, analytical data are in complete accordance with literature values.³⁶

General procedure for the synthesis of 11 and 12

To starting material **5** or **6**, respectively (1 mmol) was added 48% aqueous HBr (3 ml) and the mixture was stirred for 3h at room temperature. Thereafter, the solution was poured into a mixture of K₂CO₃ (1 g) in ice (5.5 g) and additional solid K₂CO₃ was added for neutralization (pH 7). The crude reaction product was extracted with diethyl ether, the combined organic layers were dried with MgSO₄ and evaporated to dryness. The crude product was employed directly in the subsequent reaction step without further purification.

1-(1-Bromo-3-chloropropyl)-4-fluorobenzene (11) Yield: 64%, pale yellow oil, analytical data are in complete accordance with literature values.³⁷

(1-Bromo-3-chloropropyl)benzene (12) Yield: 5.64 g (86%), yellow oil, analytical data are in complete accordance with literature values.³⁶

General procedure for the synthesis of 29 and 30

4-Fluoroaniline or 2-fluoroaniline, respectively (1 mmol), anhydrous KF (1 mmol), and K₂CO₃ (1 mmol) were well powdered with a mortar and a pestle, then 1-fluoro-2-nitrobenzene (1 mmol) was added and the mixture was stirred for 2 days at 180°C. Thereafter, water (5 ml) and CH₂Cl₂ (5 ml) were added and the organic layer was washed with 10% HCl (5 ml) and brine (5 ml). The combined

organic layers were dried over Na_2SO_4 and evaporated to dryness prior to purification by column chromatography.

***N*-(4-Fluorophenyl)-2-nitroaniline (29)** Yield: 68%, dark orange crystals, mp. 82°C-83°C, purification: silica gel 60, petrol ether/ethyl acetate 9:1 and RP-18 silica gel, methanol/water 7:3, analytical data are in complete accordance with literature values.³⁸

2-Fluoro-*N*-(2-nitrophenyl)aniline (30) Yield: 52%, orange crystals, mp. 79°C-80°C, purification: silica gel 60, petrol ether/ethyl acetate 9:1, analytical data are in complete accordance with literature values.³⁹

Alternative procedure for the synthesis of 29

4-Fluoroaniline (7.89 g, 70.87 mmol), anhydrous KF (4.13 g, 70.87 mmol), and K_2CO_3 (9.81 g, 70.87 mmol) were well powdered with a mortar and a pestle, then 1-fluoro-2-nitrobenzene (10.00 g, 70.87 mmol) was added and the mixture was irradiated in the microwave (900 W, 10 min). Thereafter, water and CH_2Cl_2 were added and the organic layer was washed with 10% HCl and brine. The combined organic layers were dried over Na_2SO_4 and evaporated to dryness prior to purification by column chromatography (silica gel 60, petrol ether/ethyl acetate 9.5:0.5). Yield: 9.51 g (58%), dark orange crystals, mp. 82°C-83°C

General procedure for the synthesis of 14 and 15

To a solution of Zn^0 (13.8 mmol) in glacial acetic acid (1 ml) was added starting material **28** or **29** (1 mmol) at 0°C under argon atmosphere. After the addition, the mixture was allowed to warm to room temperature and was stirred for 2 h. Zn^0 was filtered off and the pH of the solution was adjusted to pH 9 with 2N NaOH. Thereafter, the aqueous layer was extracted three times with CH_2Cl_2 , the combined organic layers were dried over MgSO_4 and evaporated to dryness.

***N*-(4-Fluorophenyl)benzene-1,2-diamine (14)** Yield: 93%, dark orange-reddish oil, purification: silica gel 60, petrol ether/ethyl acetate 9:1, analytical data are in complete accordance with literature values.⁴⁰

***N*-(2-Fluorophenyl)benzene-1,2-diamine (15)** The crude reaction product was subjected to the next reaction step without further purification.

General procedure for the synthesis of 16-18

To a solution of starting materials **13**, **14**, or **15** (1 mmol) in THF was added 1,1'-carbonyldiimidazole (1.4 mmol) under argon atmosphere and the mixture was stirred at room temperature overnight. Thereafter, the crude reaction product was purified by column chromatography.

1-Phenyl-1,3-dihydro-2H-benzimidazol-2-one (16) Yield: 0.85 g (74%), pink crystals, mp. 201°C–202°C, THF: 10 ml, purification: silica gel 60, petrol ether/ethyl acetate 1:1, analytical data are in complete accordance with literature values.⁴¹

1-(4-Fluorophenyl)-1,3-dihydro-2H-benzimidazol-2-one (17) Yield: 61%, brown resin, THF: 25 ml, purification: silica gel 60, petrol ether/ethyl acetate 9:1, ¹H-NMR (200 MHz, CDCl₃): δ (ppm) 6.74–6.81 (m, 2H), 6.89–7.11 (m, 2H), 7.14–7.23 (m, 2H), 7.48–7.59 (m, 1H), 7.73–7.78 (m, 1H), 9.03 (br s, 1H), ¹³C-NMR (50 MHz, CDCl₃): δ (ppm) 108.5, 110.0, 116.3, 116.8, 121.4, 121.7, 122.3, 128.0, 128.2, 130.4, 135.1, 155.1, 159.3, 164.2, **MS**: m/z (%) 228 (M⁺, 100), 199 (31), 172 (8), 114 (9), 95 (10), 75 (17), 51 (10), **HRMS**: m/z calculated for C₁₃H₁₀FN₂O [M + H]⁺: 229.0772. Found: 229.0769.

1-(2-Fluorophenyl)-1,3-dihydro-2H-benzimidazol-2-one (18) Yield: 69%, brown resin, THF: 20 ml, purification: silica gel 60, petrol ether/ethyl acetate 9:1, ¹H-NMR (200 MHz, CDCl₃): δ (ppm) 6.82–6.85 (m, 1H), 7.00–7.19 (m, 3H), 7.26–7.88 (m, 2H), 7.43–7.60 (m, 2H), 10.54 (br s, 1H), ¹³C-NMR (50 MHz, CDCl₃): δ (ppm) 108.9, 110.1, 117.0, 117.4, 121.5, 121.9, 122.4, 124.9, 125.0, 128.2, 129.6, 130.4, 154.8, 155.4, 160.5, **MS**: m/z (%) 228 (M⁺, 33), 199 (9), 181 (15), 149 (17), 111 (22), 97 (20), 71 (41), 69 (100), 55 (53), 43 (56), **HRMS**: m/z calculated for C₁₃H₉FN₂NaO [M + Na]⁺: 251.0597. Found: 251.0592.

Alternative procedure for the synthesis of 17 and 18

A solution of 1,1'-carbonyldiimidazole (1.4 mmol) in DMF (4 ml) was slowly added to a mixture of **14** or **15** (1 mmol) in DMF (4 ml) under argon atmosphere. The resulting solution was stirred at 90°C for 2 h. After completion of the reaction, the solvent was evaporated *in vacuo*, the slurry was taken up in water, filtered and dried.

1-(4-Fluorophenyl)-1,3-dihydro-2H-benzimidazol-2-one (17) Yield: 80%, brown resin

1-(2-Fluorophenyl)-1,3-dihydro-2H-benzimidazol-2-one (18) Yield: 80%, brown resin

General procedure for the synthesis of 19–21

Starting materials **16–18** (1 mmol) and K₂CO₃ (2 mmol) were suspended in DMF (1.8 ml) and stirred at 25°C for 30 min. **11** and **12**, respectively (1.5 mmol) were added after 30 min and the solution was stirred at room temperature overnight. To the mixture was added ethyl acetate (5 ml) and water (5 ml). The aqueous layer was extracted several times with ethyl acetate and the combined organic layers were washed with brine, dried over MgSO₄ and evaporated to dryness.

1-(3-Chloro-1-(4-fluorophenyl)propyl)-3-phenyl-1,3-dihydro-2H-benzimidazol-2-one (19) Yield: 32%, white oil, purification: silica gel 60, petrol ether/ethyl acetate 8:2, ¹H-NMR (200 MHz, CDCl₃): δ (ppm) 2.70–2.87 (m, 1H), 3.12–3.30 (m, 1H), 3.60–3.66 (m, 2H), 5.73 (m, 1H), 7.00–7.11 (m, 6H), 7.38–7.57 (m, 7H), ¹³C-NMR (50 MHz, CDCl₃): δ (ppm) 34.3, 42.0, 53.8, 108.7, 109.0, 115.5,

115.9, 121.7, 122.0, 126.0, 127.8, 129.2, 129.4, 129.5, **MS**: m/z (%) 380 (M^+ , 21), 210 (100), 181 (8), 167 (12), 135 (9), 115 (5), 109 (58), 77 (12), **HRMS**: m/z calculated for $C_{22}H_{18}ClFN_2ONa [M + Na]^+$: 403.0989. Found: 403.0989.

1-(3-chloro-1-phenylpropyl)-3-(4-fluorophenyl)-1,3-dihydro-2H-benzimidazol-2-one (20)

Yield: 63%, dark orange resin, purification: silica gel 60, petrol ether/ethyl acetate 9:1 and RP-18 silica gel, methanol, **1H -NMR** (400 MHz, $CDCl_3$): δ (ppm) 2.80-2.88 (m, 1H, 2'- $\underline{CH_2}$), 3.17-3.26 (m, 1H, 2'- $\underline{CH_2}$), 3.62-3.70 (m, 2H, 3'- $\underline{CH_2}$), 5.79 (dd, $J = 10.0$ Hz and 5.6 Hz, 1H, 1'- \underline{CH}), 7.04-7.09 (m, 4H, benzim 4- \underline{CH} , benzim 5- \underline{CH} , benzim 6- \underline{CH} , benzim 7- \underline{CH}), 7.21-7.26 (m, 2H, f-phen 3- \underline{CH} , f-phen 5- \underline{CH}), 7.31-7.33 (m, 1H, phen 4- \underline{CH}), 7.36-7.40 (m, 2H, phen 3- \underline{CH} , phen 5- \underline{CH}), 7.52-7.56 (m, 4H, f-phen 2- \underline{CH} , f-phen 6- \underline{CH} , phen 2- \underline{CH} , phen 6- \underline{CH}), **^{13}C -NMR** (100 MHz, $CDCl_3$): δ (ppm) 34.1 (2'- $\underline{CH_2}$), 42.0 (3'- $\underline{CH_2}$), 54.4 (1'- \underline{CH}), 108.6 (benzim 4- \underline{CH}), 109.0 (benzim 7- \underline{CH}), 116.4 (d, $J = 22.9$ Hz, f-phen 3- \underline{CH}), 116.4 (d, $J = 22.9$ Hz, f-phen 5- \underline{CH}), 121.6 (benzim 5- \underline{CH}), 122.1 (benzim 6- \underline{CH}), 127.4 (phen 2- \underline{CH}), 127.4 (phen 6- \underline{CH}), 127.9 (d, $J = 8.6$ Hz, f-phen 2- \underline{CH}), 127.9 (d, $J = 8.6$ Hz, f-phen 6- \underline{CH}), 128.1 (phen 4- \underline{CH}), 128.7 (benzim 7a-C), 128.8 (phen 3- \underline{CH}), 128.8 (phen 5- \underline{CH}), 129.4 (benzim 3a-C), 130.3 (d, $J = 3.1$ Hz, f-phen 1-C), 138.4 (phen 1-C), 153.2 (benzim 2- \underline{CO}), 161.6 (d, $J = 247.7$ Hz, f-phen 4- \underline{CF}), **^{19}F -NMR** (471 MHz, $CDCl_3$): δ (ppm) -113.31 (m, 5- \underline{CF}), **MS**: m/z (%) 380 (M^+ , 2), 228 (100), 199 (11), 185 (16), 153 (6), 117 (14), 91 (73), 75 (8), **HRMS**: m/z calculated for $C_{22}H_{19}ClFN_2O [M + H]^+$: 381.1170. Found: 381.1176.

1-(3-chloro-1-phenylpropyl)-3-(2-fluorophenyl)-1,3-dihydro-2H-benzimidazol-2-one (21)

Yield: 55%, orange resin, purification: silica gel 60, petrol ether/ethyl acetate 9:1, **1H -NMR** (400 MHz, $CDCl_3$): δ (ppm) 2.78-2.86 (m, 1H, 2'- $\underline{CH_2}$), 3.23 (br s, 1H, 2'- $\underline{CH_2}$), 3.64-3.68 (m, 2H, 3'- $\underline{CH_2}$), 5.79 (br s, 1H, 1'- \underline{CH}), 6.85-6.87 (m, 1H, benzim 4- \underline{CH}), 7.05-7.06 (m, 3H, benzim 5- \underline{CH} , benzim 6- \underline{CH} , benzim 7- \underline{CH}), 7.28-7.40 (m, 5H, f-phen 3- \underline{CH} , f-phen 6- \underline{CH} , phen 3- \underline{CH} , phen 4- \underline{CH} , phen 5- \underline{CH}), 7.43-7.48 (m, 1H, f-phen 4- \underline{CH}), 7.52-7.56 (m, 3H, f-phen 5- \underline{CH} , phen 2- \underline{CH} , phen 6- \underline{CH}), **^{13}C -NMR** (100 MHz, $CDCl_3$): δ (ppm) 34.2 (2'- $\underline{CH_2}$), 41.9 (3'- $\underline{CH_2}$), 54.5 (1'- \underline{CH}), 108.8 (d, $J = 1.7$ Hz, benzim 4- \underline{CH}), 109.0 (benzim 7- \underline{CH}), 117.1 (d, $J = 19.5$ Hz, f-phen 3- \underline{CH}), 121.6 (benzim 5- \underline{CH}), 121.9 (f-phen 1-C), 122.0 (benzim 6- \underline{CH}), 124.8 (d, $J = 3.9$ Hz, f-phen 6- \underline{CH}), 127.3 (phen 2- \underline{CH}), 127.3 (phen 6- \underline{CH}), 128.1 (phen 4- \underline{CH}), 128.8 (phen 3- \underline{CH}), 128.8 (phen 5- \underline{CH}), 129.4 (benzim 3a-C), 129.5 (f-phen 5- \underline{CH}), 130.2 (d, $J = 7.8$ Hz, f-phen 4- \underline{CH}), 138.4 (phen 1-C), 153.0 (benzim 2- \underline{CO}), 157.9 (d, $J = 253.2$ Hz, f-phen 2- \underline{CF}), due to limited resolution of the measuring apparatus, quaternary carbon benzim 7a-C could not be detected, **^{19}F -NMR** (471 MHz, $CDCl_3$): δ (ppm) -118.39 (m, f-phen 2- \underline{CF}), **MS**: m/z (%) 380 (M^+ , 12), 228 (100), 199 (5), 153 (3), 117 (7), 91 (49), 75 (5), **HRMS**: m/z calculated for $C_{22}H_{19}ClFN_2O [M + H]^+$: 381.1170. Found: 381.1164.

General procedure for the synthesis of 22-24

A solution of starting materials **19**, **20**, or **21** (1 mmol) and NaI (1.03 g, 6.89 mmol) in acetone (7 ml) was refluxed for 24 h. The precipitate formed was filtered and the solvent was removed *in vacuo*.

1-(1-(4-Fluorophenyl)-3-iodopropyl)-3-phenyl-1,3-dihydro-2H-benzimidazol-2-one (22) Yield: 82%, yellow resin, $^1\text{H-NMR}$ (200 MHz, CDCl_3): δ (ppm) 2.77-2.92 (m, 1H), 3.14-3.31 (m, 3H), 5.63-5.70 (m, 1H), 7.01-7.10 (m, 6H), 7.36-7.56 (m, 7H), $^{13}\text{C-NMR}$ (50 MHz, CDCl_3): δ (ppm) 2.3, 35.3, 57.0, 108.8, 108.9, 115.5, 115.9, 121.6, 122.0, 126.0, 127.7, 128.5, 129.1, 129.3, 129.4, 134.0, 134.1, 134.3, 153.0, 159.9, 164.8, **MS**: m/z (%) 472 (M^+ , 32), 317 (8), 210 (100), 181 (11), 167 (23), 140 (3), 135 (43), 115 (8), 109 (34), 77 (15), 51 (7), **HRMS**: m/z calculated for $\text{C}_{22}\text{H}_{18}\text{FIN}_2\text{ONa}$ [$\text{M} + \text{Na}$] $^+$: 495.0346. Found: 495.0353.

1-(4-fluorophenyl)-3-(3-iodo-1-phenylpropyl)-1,3-dihydro-2H-benzimidazol-2-one (23) Yield: 76%, yellow crystals, mp. 39°C-41°C, purification: silica gel 60, petrol ether/ethyl acetate 9:1, $^1\text{H-NMR}$ (200 MHz, CDCl_3): δ (ppm) 2.81-2.99 (m, 1H, 2'- CH_2), 3.11-3.35 (m, 3H, 2'- CH_2 , 3'- CH_2), 5.70 (dd, $J = 6$ Hz and 2 Hz, 1H, 1'- CH), 7.04-7.09 (m, 4H, benzim 4- CH , benzim 5- CH , benzim 6- CH , benzim 7- CH), 7.17-7.42 (m, 5H, f-phen 3- CH , f-phen 5- CH , phen 4- CH , phen 2- CH , phen 5- CH), 7.51-7.57 (m, 4H, f-phen 2- CH , f-phen 6- CH , phen 2- CH , phen 6- CH), $^{13}\text{C-NMR}$ (50 MHz, CDCl_3): δ (ppm) 2.4 (2'- CH_2), 35.2 (3'- CH_2), 57.6 (1'- CH), 108.6 (benzim 4- CH), 109.2 (benzim 7- CH), 116.4 (d, $J = 23$ Hz, f-phen 3- CH), 116.4 (d, $J = 23$ Hz, f-phen 5- CH), 121.6 (benzim 5- CH), 122.1 (benzim 6- CH), 127.3 (phen 2- CH), 127.3 (phen 6- CH), 127.8 (phen 4- CH), 128.1 (d, $J = 5$ Hz, f-phen 2- CH), 128.1 (d, $J = 5$ Hz, f-phen 6- CH), 128.5 (benzim 7a-C), 128.8 (phen 3- CH), 128.8 (phen 5- CH), 129.4 (benzim 3a-C), 130.3 (d, $J = 3$ Hz, f-phen 1-C), 138.1 (phen 1-C), 153.2 (benzim 2- CO), 161.6 (d, $J = 247$ Hz, f-phen 4- CF), **MS**: m/z (%) 472 (M^+ , 13), 317 (5), 228 (100), 185 (15), 117 (47), 103 (2), 91 (40), 75 (8), 55 (5), **HRMS**: m/z calculated for $\text{C}_{22}\text{H}_{19}\text{FIN}_2\text{O}$ [$\text{M} + \text{H}$] $^+$: 473.0526. Found: 473.0506.

1-(2-fluorophenyl)-3-(3-iodo-1-phenylpropyl)-1,3-dihydro-2H-benzimidazol-2-one (24) Yield: 53%, yellow crystals, mp. 38°C-39°C, purification: silica gel 60, petrol ether/ethyl acetate 9:1, $^1\text{H-NMR}$ (200 MHz, CDCl_3): δ (ppm) 2.80-2.98 (m, 1H, 2'- CH_2), 3.13-3.36 (m, 3H, 2'- CH_2 , 3'- CH_2), 5.67-5.74 (m, 1H, 1'- CH), 6.85-6.88 (m, 1H, benzim 4- CH) 6.99-7.07 (m, 3H, benzim 5- CH , benzim 6- CH , benzim 7- CH), 7.26-7.45 (m, 5H, f-phen 3- CH , f-phen 6- CH , phen 3- CH , phen 4- CH , phen 5- CH), 7.47-7.58 (m, 4 H, f-phen 4- CH , f-phen 5- CH , phen 2- CH , phen 6- CH), $^{13}\text{C-NMR}$ (50 MHz, CDCl_3): δ (ppm) 2.3 (2'- CH_2), 35.4 (3'- CH_2), 57.6 (1'- CH), 108.9 (d, $J = 1.5$ Hz, benzim 4- CH), 109.1 (benzim 7- CH), 117.1 (d, $J = 19$ Hz, f-phen 3- CH), 121.6 (benzim 5- CH), 121.9 (f-phen 1-C), 122.0 (benzim 6- CH), 124.8 (d, $J = 3.5$ Hz, f-phen 6- CH), 127.3 (phen 2- CH), 127.3 (phen 6- CH), 128.1 (phen 4- CH), 128.8 (phen 3- CH), 128.8 (phen 5- CH), 129.5 (f-phen 5- CH), 130.2 (d, $J = 8$ Hz, f-phen 4- CH), 138.2 (phen 1-C), 153.0 (benzim 2- CO), 157.8 (d, $J = 251.5$ Hz, f-phen 2- CF), **MS**: m/z (%) 472 (M^+ , 9), 317 (5), 241 (4), 228 (100), 199 (5), 185 (10), 117 (37), 91 (29), 75 (7), **HRMS**: m/z calculated for $\text{C}_{22}\text{H}_{19}\text{FIN}_2\text{O}$ [$\text{M} + \text{H}$] $^+$: 473.0526. Found: 473.0532.

General procedure for the synthesis of 1-(3-Amino-1-(4-fluorophenyl)propyl)-3-phenyl-1,3-dihydro-2H-benzimidazol-2-one (25)

1-(1-(4-fluorophenyl)-3-iodopropyl)-3-phenyl-1,3-dihydro-2H-benzimidazol-2-one (0.26 g, 0.55 mmol) and a solution of NH_3 in isopropanol (2 M, 22 ml) were heated in a sealed tube for 3 h at 80°C.

After evaporation of the solvent, the crude product was purified by column chromatography (silica gel 60, CH₂Cl₂/MeOH 9:1). Yield: 0.10 g (50%), light brown crystals, mp. 87°C-88°C

¹H-NMR (400 MHz, CDCl₃): δ (ppm) 2.74-2.84 (m, 3H, 2'-CH₂, 3'-CH₂), 2.98-3.04 (m, 1H, 3'-CH₂), 5.74-5.78 (m, 1H, 1'-CH), 6.79-6.81 (m, 1H, benzim 7-CH), 6.96-7.01 (m, 5H, benzim 4-CH, benzim 5-CH, benzim 6-CH, f-phen 3-CH, f-phen 5-CH), 7.30-7.33 (m, 1H, phen 4-CH), 7.40-7.48 (m, 4H, f-phen 2-CH, f-phen 6-CH, phen 3-CH, phen 5-CH), 7.52-7.54 (m, 2H, phen 2-CH, phen 6-CH), due to limited resolution of the measuring apparatus, protons NH₂ could not be detected, **¹³C-NMR** (100 MHz, CDCl₃): δ (ppm) 30.3 (2'-CH₂), 37.8 (3'-CH₂), 52.7 (1'-CH), 109.2 (benzim 4-CH), 110.0 (benzim 7-CH), 115.7 (d, *J* = 21.5 Hz, f-phen 3-CH), 115.7 (d, *J* = 8.2 Hz, f-phen 5-CH), 122.0 (benzim 5-CH), 122.3 (benzim 6-CH), 126.4 (phen 2-CH), 126.4 (phen 6-CH), 127.5 (benzim 7a-C), 128.1 (phen 4-CH), 129.2 (d, *J* = 8.2 Hz, f-phen 2-CH), 129.2 (d, *J* = 8.2 Hz, f-phen 6-CH), 129.5 (benzim 3a-C), 129.7 (phen 3-CH), 129.7 (phen 5-CH), 133.3 (d, *J* = 3.2 Hz, f-phen 1-C), 134.0 (phen 1-CH), 153.8 (benzim 2-CO), 162.3 (d, *J* = 247.4 Hz, f-phen 4-CF), **¹⁹F-NMR** (471 MHz, CDCl₃): δ (ppm) -113.68 (m, f-phen CF), **MS**: m/z (%) 361 (M⁺, 17), 331 (10), 210 (100), 181 (15), 167 (16), 149 (29), 128 (17), 77 (19), 57 (20), 43 (12), **HRMS**: m/z calculated for C₂₂H₂₁FN₃O [M + H]⁺: 362.1669. Found: 362.1674.

General procedure for the synthesis of 4-6

Starting materials **18**, **19** or **20** (1 mmol) and a solution of methylamine in EtOH (12.5 ml, 8 M) were heated in a sealed tube for 3 h at 80°C. After evaporation of the solvent, the crude reaction product was purified by column chromatography.

1-(1-(4-Fluorophenyl)-3-(methylamino)propyl)-3-phenyl-1,3-dihydro-2H-benzimidazol-2-one (4) Yield: 48%, light orange resin, purification: silica gel 60, dichloromethane/methanol 9:1 and dichloromethane/ethyl acetate/methanol 7:2:1, **¹H-NMR** (400 MHz, CDCl₃): δ (ppm) 2.42 (s, 3H, NHCH₃), 2.57-2.74 (m, 4H, 2'-CH₂, 3'-CH₂), 3.15 (br s, 1H, NHCH₃), 5.76-5.79 (m, 1H, 1'-CH), 6.88-6.90 (m, 1H, benzim 7-CH), 6.97-7.05 (m, 4H, benzim 5-CH, benzim 6-CH, f-phen 3-CH, f-phen 5-CH), 7.07-7.10 (m, 1H, benzim 4-CH), 7.39-7.43 (m, 1H, phen 4-CH), 7.46-7.57 (m, 6H, f-phen 2-CH, f-phen 6-CH, phen 2-CH, phen 3-CH, phen 5-CH, phen 6-CH), **¹³C-NMR** (100 MHz, CDCl₃): δ (ppm) 30.6 (2'-CH₂), 35.9 (NHCH₃), 48.3 (3'-CH₂), 53.1 (1'-CH), 108.9 (benzim 4-CH), 109.5 (benzim 7-CH), 115.5 (d, *J* = 21.5 Hz, f-phen 3-CH), 115.5 (d, *J* = 21.5 Hz, f-phen 5-CH), 121.4 (benzim 5-CH), 121.8 (benzim 6-CH), 126.0 (phen 2-CH), 126.0 (phen 6-CH), 127.7 (phen 4-CH), 128.0 (benzim 7a-C), 129.0 (d, *J* = 8.1 Hz, f-phen 2-CH), 129.0 (d, *J* = 8.1 Hz, f-phen 6-CH), 129.4 (benzim 3a-C), 129.5 (phen 3-CH), 129.5 (phen 5-CH), 134.4 (phen 1-CH), 134.6 (d, *J* = 3.4 Hz, f-phen 1-CH), 153.5 (benzim 2-CO), 162.1 (d, *J* = 246.7 Hz, f-phen 4-CF), **¹⁹F-NMR** (471 MHz, CDCl₃): δ (ppm) -114.36 (m, f-phen 4-CF), **MS**: m/z (%) 375 (M⁺, 16), 210 (57), 181 (10), 167 (12), 150 (10), 109 (22), 97 (16), 71 (27), 57 (78), 44 (100), **HRMS**: m/z calculated for C₂₃H₂₃FN₃O [M + H]⁺: 376.1825. Found: 376.1821.

1-(4-fluorophenyl)-3-(3-(methylamino)-1-phenylpropyl)-1,3-dihydro-2H-benzimidazol-2-one

(5) Yield: 29%, light yellow crystals, mp. 100°C-102°C, purification: silica gel 60, dichloromethane/methanol 9:1 and RP-18 silica gel methanol/water 9:1 and 7:3, $^1\text{H-NMR}$ (200 MHz, CDCl_3): δ (ppm) 2.53 (s, 3H, NHCH_3), 3.13 (br s, 4H, $2'\text{-CH}_2$, $3'\text{-CH}_2$), 5.77-5.81 (m, 1H, $1'\text{-CH}$), 6.96-7.03 (m, 4H, benzim 4- CH , benzim 5- CH , benzim 6- CH , benzim 7- CH), 7.16-7.34 (5H, f-phen 3- CH , f-phen 5- CH , phen 4- CH , phen 2- CH , phen 5- CH), 7.49-7.56 (m, 4H, f-phen 2- CH , f-phen 6- CH , phen 2- CH , phen 6- CH), due to limited resolution of the measuring apparatus, proton NH could not be detected, $^{13}\text{C-NMR}$ (50 MHz, CDCl_3): δ (ppm) 27.6 ($2'\text{-CH}_2$), 33.1 (NHCH_3), 47.0 ($3'\text{-CH}_2$), 54.2 ($1'\text{-CH}$), 108.8 (benzim 4- CH), 109.9 (benzim 7- CH), 116.6 (d, $J = 23$ Hz, f-phen 3- CH), 116.6 (d, $J = 23$ Hz, f-phen 5- CH), 122.1 (benzim 5- CH), 122.6 (benzim 6- CH), 127.2 (phen 2- CH), 127.2 (phen 6- CH), 127.7 (phen 4- CH), 128.3 (d, $J = 6$ Hz, f-phen 2- CH), 128.3 (d, $J = 6$ Hz, f-phen 6- CH), 128.4 (benzim 7a-C), 128.9 (phen 3- CH), 128.9 (phen 5- CH), 129.2 (benzim 3a-C), 129.7 (d, $J = 3$ Hz, f-phen 1-C), 136.9 (phen 1-C), 153.4 (benzim 2- CO), 161.7 (d, $J = 248$ Hz, f-phen 4- CF), **MS**: m/z (%) 375 (M^+ , 11), 330 (7), 228 (50), 199 (7), 185 (9), 147 (17), 128 (26), 117 (8), 91 (13), 58 (34), 44 (100), **HRMS**: m/z calculated for $\text{C}_{23}\text{H}_{23}\text{FN}_3\text{O}$ [$\text{M} + \text{H}$] $^+$: 376.1825. Found: 376.1828.

1-(2-fluorophenyl)-3-(3-(methylamino)-1-phenylpropyl)-1,3-dihydro-2H-benzimidazol-2-one

(6) Yield: 30%, yellow crystals, mp. 92°C-93°C, purification: silica gel 60, dichloromethane/methanol 9:1 and RP-18 silica gel methanol/water 9:1 and 7:3, $^1\text{H-NMR}$ (200 MHz, CDCl_3): δ (ppm) 2.57 (s, 3H, NHCH_3), 3.01-3.15 (m, 4H, $2'\text{-CH}_2$, $3'\text{-CH}_2$), 5.75-5.86 (m, 1H, $1'\text{-CH}$), 6.83-6.87 (m, 1H, benzim 4- CH) 6.98-7.05 (m, 3H, benzim 5- CH , benzim 6- CH , benzim 7- CH), 7.25-7.42 (m, 5H, f-phen 3- CH , f-phen 6- CH , phen 3- CH , phen 4- CH , phen 5- CH), 7.48-7.61 (m, 4 H, f-phen 4- CH , f-phen 5- CH , phen 2- CH , phen 6- CH), due to limited resolution of the measuring apparatus, proton NHCH_3 could not be detected, $^{13}\text{C-NMR}$ (50 MHz, CDCl_3): δ (ppm) 27.7 ($2'\text{-CH}_2$), 33.2 (NHCH_3), 46.9 ($3'\text{-CH}_2$), 53.5 ($1'\text{-CH}$), 109.0 (benzim 4- CH), 110.1 (benzim 7- CH), 117.1 (d, $J = 19.5$ Hz, f-phen 3- CH), 122.2 (benzim 5- CH), 122.7 (benzim 6- CH), 125.1 (d, $J = 3.0$ Hz, f-phen 6- CH), 127.3 (phen 2- CH), 127.1 (phen 6- CH), 128.3 (phen 4- CH), 128.9 (phen 3- CH), 128.9 (phen 5- CH), 129.5 (f-phen 5- CH), 130.7 (d, $J = 4.5$ Hz, f-phen 4- CH), 136.5 (phen 1-C), 153.6 (benzim 2- CO), 157.6 (d, $J = 250.5$ Hz, f-phen 2- CF), due to limited resolution of the measuring apparatus, quaternary carbon f-phen 1-C could not be detected, **MS**: m/z (%) 375 (M^+ , 17), 318 (10), 228 (82), 199 (9), 185 (9), 147 (16), 128 (35), 117 (9), 91 (20), 58 (43), 44 (100), **HRMS**: m/z calculated for $\text{C}_{23}\text{H}_{23}\text{FN}_3\text{O}$ [$\text{M} + \text{H}$] $^+$: 376.1825. Found: 376.1822.

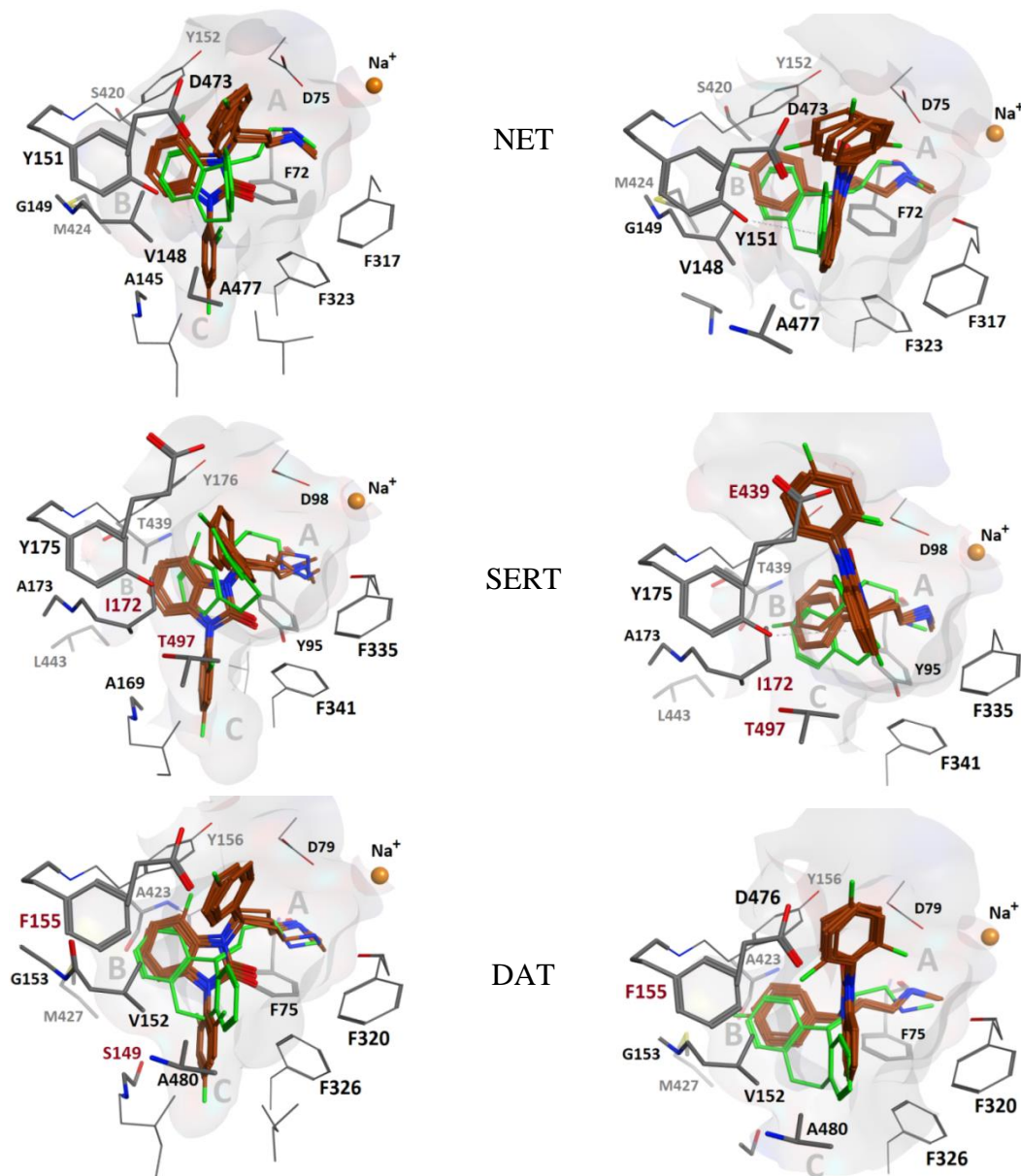
3.3. Computational Methods

The ligand structures were built in the protonated form using Molecular Operating Environment (MOE) 2013.⁴² Homology models of human NET, SERT and DAT were obtained from the *Drosophila* dopamine transporter template (dDAT_{cryst}, PDB id 4M48⁴³), by selecting the model with the most favorable Discrete Optimized Protein Energy (DOPE) of 250 generated by Modeller 9.11.⁴⁴ The co-crystallized inhibitor nortriptyline was retained during model generation and the compounds were docked in the same site using Genetic Optimization for Ligand Docking (GOLD) 5.2.⁴⁵ One hundred

poses per ligand (i.e. five hundred poses per protein target) were generated based on the GoldScore scoring function, while keeping the ligand flexible and the protein rigid.

The common chemical scaffold, i.e. the reference compound, was extracted from the resulting poses, analogous to the methods of our previous study.⁴⁶ Cluster analysis was performed based on Euclidian distance and complete linkage of the root-mean square deviation of the ligand's heavy atoms matrix using XLStat.⁴⁷ The dendrogram was cut at eight clusters and the ones containing all five ligands were selected.

Figure 5. *Left column:* Overlay of compounds **1**, **2**, and **4-6** (maroon) in binding hypothesis 1 and comparison with the co-crystal pose of nortriptyline (**31**) (green). In NET, V148 allows more space than I172 in SERT. The angle between ligand ring 2 and 3 is ca. 60° in all poses. *Right column:* Overlay of compounds **1**, **2**, and **4-6** (maroon) in binding hypothesis 2. In NET, V148 still allows more space than in hSERT, whereas E439 might disrupt ligand ring 3. DAT lacks a more potent stacking interaction due to F155 as compared to NET[Y151] and SERT[Y175]. Binding mode 2 poses are more in agreement with the co-crystal pose. The angle between ligand ring 2 and 3 is almost 90° in all poses.



4. Conclusions

In conclusion, four new final compounds have been synthesized within the scope of this work, which aimed at the development of new, selective, high affinity references for the imaging of the NET system *via* PET. Whilst methylamines **4-6** (FAPPI:1-3) represent reference compounds for their later prepared radioactive analogs, additionally prepared free amine **25** (APPI:1) will serve as precursor for radiolabeling. Compounds **4-6** will be evaluated for affinity and selectivity towards the NET and additionally will be subject of lipophilicity and blood brain barrier penetration experiments at the Medical University of Vienna. Docking studies indicate that fluorinated methyl amines **4-6** (FAPPI:1-3) bind in an analogous way to the NET as reference compound **1**. Thus these compounds (**4-6**) are promising candidates for biological evaluation. The most promising derivatives regarding their suitability as NET ligands will then be selected for the further development of new and selective PET tracers for the NET, which will comprise either a [¹¹C]methylamine, [¹⁸F]fluoroalkyl amine or [¹⁸F]fluorobenzene radiolabel, respectively. The results of ongoing studies on affinity, selectivity and lipophilicity of the discussed compounds, will be published in a following paper.

Acknowledgments

AS, AJ, and GFE acknowledge financial support provided by the Austrian Science Fund, grants AW/0123221 and F3502.

Conflicts of Interest

The authors declare no conflict of interest.

References and Notes

1. Sung, U.; Apparsundram, S.; Galli, A.; Kahlig, K. M.; Savchenko, V.; Schroeter, S.; Quick, M. W.; Blakely, R. D. *J. Neurosci.*, **2003**, *23*, 1697.
2. Kim, C. H.; Hahn, M. K.; Joung, Y.; Anderson, S. L.; Steele, A. H.; Mazei-Robinson, M. S.; Gizer, I.; Teicher, M. H.; Cohen, B. M.; Robertson, D.; Walman, I. D.; Blakely, R. D.; Kim, K. S. *PNAS*, **2006**, *103*, 19164.
3. Hahn, M. K.; Robertson, D.; Blakely, R. D. *J. Neurosci.*, **2003**, *23*, 4470.
4. Mirbolooki, M. R.; Upadhyay, S. K.; Constantinescu, C. C.; Pan, M. L.; Mukherjee, J. *Nucl. Med. Biol.*, **2014**, *41*, 10.
5. Lin, S. L.; Fan, X.; Yeckel, C. W.; Weinzimmer, D.; Mulnix, T.; Gallezot, J. D.; Carson, R. E.; Sherwin, R. S.; Ding, Y. S. *Nuc. Med. Biol.*, **2012**, *39*, 1081.
6. Stöber, G.; Nöthen, M. M.; Pörzgen, P.; Brüß, M.; Bönisch, H.; Knapp, M.; Beckmann, H.; Propping, P. *American Journal of Medical Genetics (Neuropsychiatric Genetics)*, **1996**, *67*, 523.
7. Young, J. B.; Landsberg, L. *Catecholamines and the adrenal medulla*. In: Williams Textbook of Endocrinology, 9th Ed., Wilson, J. D., Foster, D. W. (Eds.) W. B. Saunders Co., Philadelphia, **1998**, 680.
8. Tellioglu, T.; Robertson, D. *Exp. Rev. Mol. Med.*, **2001**, *1*.
9. Blakely, R. D.; Bauman, A. L., *Curr. Opin. Neurobiol.*, **2000**, *10*, 328.

10. Zhu, M. Y.; Shamburger, S.; Li, J.; Ordway, G. A. *Journal of Pharmacology and Experimental Therapeutics*, **2000**, 295, 951.
11. Moron, J. A.; Grockington, A.; Wise, R. A.; Rocha, B. A.; Hope, B. T. *J. Neurosci.*, **2002**, 22, 386.
12. Schroeter, S.; Apparsundaram, S.; Wiley, R. G.; Miner, L. H.; Sesack, S. R.; Blakely, R. D. *The Journal of comparative neurology*, **2000**, 420, 211.
13. Torres, G. E.; Gainetdinov, R. R.; Caron, M. G. *Nature Reviews Neuroscience*, **2003**, 4, 13.
14. Ordway, G. A.; Stockmeier, C. A.; Cason, G. W.; Klimek, V. *J. Neurosci.*, **1997**, 17, 1710.
15. Smith, H. R.; Beveridge, T. J. R.; Porrino, L. J. *Neuroscience*, **2006**, 138, 703.
16. Zhou, J. *Drugs Future*, **2004**, 29, 1235.
17. Curatolo, P.; D'Agati, E.; Moavero, R. *Ital. J. Pediatr.*, **2010**, 36, 79.
18. Mash, D. C.; Ouyang, Q.; Qin, Y.; Pablo, J. *Neurosci. Methods*, **2005**, 143, 79.
19. Barr, C. L.; Kroft, J.; Feng, Y.; Wigg, K.; Roberts, W.; Malone, M.; Ickowicz, A.; Schachar, R.; Tannock, R.; Kennedy, J. L. *American Journal of Medical Genetics (Neuropsychiatric Genetics)*, **2002**, 114, 255.
20. Klimek, V.; Stockmeier, C.; Overholser, J.; Meltzer, H. Y.; Kalka, S.; Dilley, G.; Ordway, G. A. *J. Neurosci.*, **1997**, 17, 8451.
21. Nedergaard, J.; Cannon, B. *Cell Metabolism*, **2010**, 11, 268.
22. Gulyas, B.; Brockschneider, D.; Nag, S.; Pavlova, E.; Kasa, P.; Beliczai, Z.; Legradi, A.; Gulya, K.; Thiele, A.; Dyrks, T.; Halldin, C. *Neurochem Int* 56, 789-798.
23. Wilson, A. A.; Johnson, D. P.; Mozley, D.; Hussey, D.; Ginovart, N.; Nobrega, J.; Garcia, A.; Meyer, J.; Houle, S. *Nucl Med Biol.*, **2003**, 30, 85.
24. Takano, A.; Gulyas, B.; Varrone, A.; Halldin, C. *Eur. J. Nucl. Med. Mol. Imaging*, **2009**, 36, 1885.
25. Schou, M.; Zoghbi, S. S.; Shetty, H. U.; Shchukin, E.; Liow, J. S.; Hong, J.; Andrée, B. A.; Gulyás, B.; Farde, L.; Innis, R. B.; Pike, V. W.; Halldin, C. *Mol Imaging Biol.* **2009**, 11, 23.
26. Zhang, P.; Terefenko, E. A.; McComas, C. C.; Mahaney, P. E.; Vu, A.; Trybulski, E.; Koury, E.; Johnston, G.; Bray, J.; Deecher, D. *Bioorg. Med. Chem. Lett.*, **2008**, 18, 6067.
27. Mark, C.; Bornatowicz, B.; Mitterhauser, M.; Hendl, M.; Nics, L.; Haeusler, D.; Lanzenberger, R.; Berger, M. L.; Spreitzer, H.; Wadsak, W. *Nucl. Med. Biol.*, **2013**, 40, 295.
28. Penmatsa, A.; Wang, K. H.; Gouaux, E. *Nature*, **2013**, 503, 85.
29. Wang, H.; Goehring, A.; Wang, K. H.; Penmatsa, A.; Ressler, R.; Gouaux, E. *Nature*, **2013**, 503, 141.
30. Tatsumi, M.; Groshan, K.; Blakely, R. D.; Richelson, E. *European Journal of Pharmacology*, **1997**, 340, 249.
31. Richter, L.; de Graaf, C.; Sieghart, W.; Varagic, Z.; Morzinger, M.; de Esch, I. J.; Ecker, G. F.; Ernst, M., *Nature chemical biology*, **2012**, 8, 455-64.
32. Andersen, J.; Olsen, L.; Hansen, K. B.; Taboureau, O.; Jorgensen, F. S.; Jorgensen, A. M.; Bang-Andersen, B.; Egebjerg, J.; Stromgaard, K.; Kristensen, A. S. *The Journal of biological chemistry*, **2010**, 285, 2051.
33. Bissantz, C.; Kuhn, B.; Stahl, M. *J. Med. Chem.*, **2010**, 53, 5061.
34. Chelli, R.; Gervasio, F. L.; Procacci, P.; Schettino, V. *J. Am. Chem. Soc.*, **2002**, 124, 6133.
35. Yu, F.; Zhou, J. N.; Zhang, X. C.; Sui, Y. Z.; Wu, F. F.; Xie, L. J.; Chan, A. S. C.; Wu, J. *Chemistry - A European Journal*, **2011**, 17, 14234.

36. Varney, M. D.; Romines, W. H.; Boritzki, T.; Margosiak, S. A.; Barlett, C.; Howland, E. J. *J. Heterocyclic Chem.*, **1995**, 32, 1493.
37. La Regina, G.; Diodata D'Auria, F.; Tafi, A.; Piscitelli, F.; Olla, S.; Caporuscio, F.; Nencioni, L.; Cirilli, R.; La Torre, F.; Rodrigues De Melo, N.; Kelly, S. L.; Lamb, D. C.; Artico, M.; Botta, M.; Palamara, A. T.; Silvestri, R. *J. Med. Chem.*, **2008**, 51, 3841.
38. Xu, Z. B.; Lu, Y.; Guo, Z. R. *Synlett*, **2003**, 4, 564.
39. Panagopoulos, A. M.; Steinman, D.; Goncharenko, A.; Geary, K.; Schleisman, C.; Spaargaren, E.; Zeller, M.; Becker, D. P. *JOC*, **2013**, 78, 3532.
40. Wang, X. J.; Xi, M. Y.; Fu, J. H.; Zhang, F. R.; Cheng, G. F.; Yin, D. L.; You, Q. D. *Chinese Chemical Letters*, **2012**, 23, 707.
41. Liu, P.; Wang, Z.; Hu, X. *European Journal of Organic Chemistry*, **2012**, 10, 1994.
42. Molecular Operating Environment (MOE), C. C. G. I., 1010 Sherbooke St. West, Suite #910, Montreal, QC, Canada, H3A 2R7, **2013**.
43. Penmatsa, A.; Wang, K. H.; Gouaux, E. *Nature*, **2013**, 503, 85.
44. Sali, A.; Potterton, L.; Yuan, F.; van Vlijmen, H.; Karplus, M. *Proteins*, **1995**, 23, 318.
45. Jones, G.; Willett, P.; Glen, R. C.; Leach, A. R.; Taylor, R. *Journal of Molecular Biology*, **1997**, 267, 727.
46. Richter, L.; de Graaf, C.; Sieghart, W.; Varagic, Z.; Morzinger, M.; de Esch, I. J.; Ecker, G. F.; Ernst, M. *Nature Chemical Biology*, **2012**, 8, 455.
47. Addinsoft Inc., N. Y., NY. USA.

Sample Availability: Samples of the compounds **4-6**, **9-25**, and **29** and **30** are available from the authors.

© 2014 by the authors; licensee MDPI, Basel, Switzerland. This article is an open access article distributed under the terms and conditions of the Creative Commons Attribution license (<http://creativecommons.org/licenses/by/4.0/>).

5.5 Curriculum Vitae

Personal:

Name: Catharina Neudorfer
 Date and place of birth: 31.03.1988, Vienna, Austria
 Parents: Dipl.-Ing. Wolfgang Neudorfer
 Judith Neudorfer, née Polzer
 Siblings: Dr. med. Clemens Neudorfer, 07.04.1989
 Cand. med. Carolina Neudorfer, 05.12.1991
 Christoph Neudorfer, 13.08.1998
 Citizenship: Austria
 Marital status: Single

Education:

Oct 2011 - present **University of Vienna, Austria:** Undergraduate study of Social and Cultural Anthropology
 May 2011 - present **University of Vienna, Austria:** PhD at the Department of Drug and Natural Product Synthesis in cooperation with the Department of Nuclear Medicine (Medical University of Vienna)
 Jul. 2010 - Nov. 2010 Diploma thesis at the **Department of Drug and Natural Product Synthesis** under the supervision of Prof. Spreitzer, University of Vienna "Syntheses of new adenosine A3 receptor antagonists"
 Oct. 2006 - Dec. 2010 **University of Vienna, Austria:** Undergraduate study of Pharmacy (merit scholarship in 2009 and 2010)
 Sept. 1998 - Jun. 2006 **High School:** Gymnasium Sacré - Coeur (Vienna/Austria)

Employment:

May 2013 - present **University of Vienna, Austria:** Research associate (Universitäts - Assistentin)
 Dec. 2012 - present **Fachhochschule FH Campus Vienna:** Organic chemistry lab teaching assistant
 Mar. 2011 - present **University of Vienna, Austria:** Teaching assistant, supervision, tutoring and grading of students in the field of synthetic organic chemistry
 Jan. - Dec. 2011 Custom syntheses for **Agepha Pharmaceuticals**
 Oct. 2010, Oct. 2009 **University of Vienna, Austria:** Tutor in practical courses of general microbiology at the Department of Pharmacognosy
 Jul. 2009 - Sep. 2009 **University of Vienna, Austria:** Research assistant under the supervision of Prof. Spreitzer
 Jul. 2006 **Pharmacy:** Apotheke zum Weinstock, Vienna, Austria: Internship

Languages:

German: mother tongue

English: spoken - excellent, written - excellent, comprehension - excellent

French: spoken - advanced, written - advanced, comprehension - advanced (B1)

Italian: spoken - advanced, written - advanced, comprehension - advanced (B1)

Presentations:

Reversible pyrazoline based MAO-B inhibitors as MAO-B PET tracer precursors and reference compounds for the early detection of Alzheimer's disease, **Catharina Neudorfer**, Karem Shanab, Andreas Jurik, Gerhard Ecker, Markus Mitterhauser, Wolfgang Wadsak, Wolfgang Holzer, Helmut Spreitzer, EFMC-ISM 2014 - XXIII International Symposium on Medicinal Chemistry, Lisbon, Portugal, 7.-11.9. **2014**

Synthesis of Reference Compounds of Novel PET Tracers for the Investigation of the Norepinephrine Transporter (NET), **Catharina Neudorfer**, Karem Shanab, Christina Rami-Mark, Markus Mitterhauser, Wolfgang Wadsak, Wolfgang Holzer, Helmut Spreitzer. RICT 2014 - Interfacing Chemical Biology and Drug Discovery, Rouen, France, 2.-4.7. **2014**

One-Step Microwave-assisted Preparation of SUPPY:0 Derivatives, **C. Neudorfer**, K. Shanab, L. K. Mien, D. Haeusler, E. Schirmer, H. Spreitzer, R. Lanzenberger, K. Kletter, M. Mitterhauser, W. Wadsak. PACCON 2010 - Pure and Applied Organic Chemistry, Ubon Ratchathani, Thailand 21.-23.1. **2010**

Synthesis of Novel MCH receptor PET tracer precursors, E. Schirmer, M. Mitterhauser, C. Philippe, E. Lehner, W. Wadsak, L.-K. Mien, K. Shanab, **C. Neudorfer**, W. Holzer, B. Datterl, M. Kratzel, H. Spreitzer. PACCON 2010 - Pure and Applied Organic Chemistry, Ubon Ratchathani, Thailand 21.-23.1. **2010**

"O/S - regioselective [¹⁸F]fluoroethylations", K. Shanab, L.-K. Mien, D. Haeusler, E. Schirmer, **C. Neudorfer**, H. Spreitzer, R. Lanzenberger, H. Viernstein, R. Dudczak, K. Kletter, M. Mitterhauser, W. Wadsak, PACCON 2010 - Pure and Applied Organic Chemistry, Ubon Ratchathani, Thailand, 21.-23.1. **2010**

Publications:

Synthesis and *in silico* evaluation of novel compounds for PET based investigations of the norepinephrine transporter, **Catharina Neudorfer**, Amir Seddik, Karem Shanab, Andreas Jurik, Christina Rami-Mark, Wolfgang Holzer, Gerhard Ecker, Markus Mitterhauser, Wolfgang Wadsak, Helmut Spreitzer, *Molecules*, **2014**, accepted

Development of potential selective and reversible pyrazoline based MAO-B inhibitors as MAO-B PET tracer precursors and reference substances for the early detection of Alzheimer's disease, **Catharina Neudorfer**, Karem Shanab, Andreas Jurik, Veronika Schreiber, Carolina Neudorfer, Chrysoula Vraka, Eva Schirmer, Wolfgang Holzer, Gerhard Ecker, Markus Mitterhauser, Wolfgang Wadsak, Helmut Spreitzer, *Bioorg. & Med. Chem. Lett.*, **2014**, 24, 4490-4495

Synthesis and antiproliferative activity of new cytotoxic 5H-pyrido[3,4-b]carbazole-5,11(10H)-dione derivatives, Shanab K., Schirmer E., **Neudorfer C.**, Leber S., Shahabi M., Leepasert T., Holzer W., Spreitzer H., Schmidt P., Aicher B., Müller G., Günther E., *Bioorg. & Med. Chem. Lett.*, **2014**, submitted

Impact of Co-administered Drugs on Drug Monitoring of Capecitabine in Patients with Advanced Colorectal Cancer, Veronika Schreiber, Marie Kitzmüller, Martina Poxhofer, Stefanie Gintersdorfer, **Catharina Neudorfer**, Maria Lichtneckert, Christian Dittrich, Martin Czejka, *ANTICANCER RESEARCH*, **2014**, 34, 3371-3376

A One-Step Microwave-Assisted Synthetic Method for an O/S-Chemoselective Route to Derivatives of the First Adenosine A3 PET Radiotracer, **Catharina Neudorfer**, Karem Shanab, Wolfgang Holzer, Markus Mitterhauser, Wolfgang Wadsak, Helmut Spreitzer, *Molecules*, **2014**, 19 (4), 4076-4082

Syntheses of Precursors and Reference Compounds of the Melanin-Concentrating Hormone Receptor 1 (MCHR1) Tracers [¹¹C]SNAP-7941 and [¹⁸F]FE@SNAP for Positron Emission Tomography, Eva Schirmer, Karem Shanab, Barbara Datterl, **Catharina Neudorfer**, Markus Mitterhauser, Wolfgang Wadsak, Cécile Philippe, Helmut Spreitzer, *Molecules*, **2013**, 18 (10), 12119-12143

Green Solvents in Organic Synthesis: An Overview, K. Shanab, **C. Neudorfer**, E. Schirmer, H. Spreitzer, *Current Organic Chemistry*, **2013**, 17, 1179-1187